

Vers une viticulture sans pesticide : analyse du microbiome de la vigne et des sols viticoles pour développer le biocontrôle microbien du mildiou

Paola Fournier

▶ **To cite this version:**

Paola Fournier. Vers une viticulture sans pesticide : analyse du microbiome de la vigne et des sols viticoles pour développer le biocontrôle microbien du mildiou. Sciences et techniques de l'agriculture. Université de Bordeaux, 2024. Français. ⟨NNT : 2024BORD0306⟩. ⟨tel-04988536⟩

HAL Id: tel-04988536

https://theses.hal.science/tel-04988536v1

Submitted on 12 Mar 2025

HAL is a multi-disciplinary open access archive for the deposit and dissemination of scientific research documents, whether they are published or not. The documents may come from teaching and research institutions in France or abroad, or from public or private research centers.

L'archive ouverte pluridisciplinaire **HAL**, est destinée au dépôt et à la diffusion de documents scientifiques de niveau recherche, publiés ou non, émanant des établissements d'enseignement et de recherche français ou étrangers, des laboratoires publics ou privés.



HAL Authorization

université de BORDEAUX

THÈSE PRÉSENTÉE POUR OBTENIR

LE GRADE DE

DOCTEURE DE

L'UNIVERSITÉ DE BORDEAUX

ÉCOLE DOCTORALE n° 304 Sciences et Environnements

SPÉCIALITÉ Écologie évolutive, fonctionnelle et des communautés

Par Paola FOURNIER

Vers une viticulture sans pesticide: analyse du microbiome de la vigne et des sols viticoles pour développer le biocontrôle microbien du mildiou

Towards pesticide-free viticulture: analysing the microbiome of grapevines and vineyard soils to develop microbial biocontrol of downy mildew

Sous la direction de : Corinne Vacher et Patrice This

Soutenue le 02/12/2024

Membres du jury :

Mme Vacher Corinne, DR, INRAE	Directrice de thèse
M. This Patrice, DR, INRAE	Directeur de thèse
Mme Mony Cendrine, Pr, Université de Rennes 1	Rapportrice
M. Sarniguet Alain, DR, IRHS	Rapporteur
Mme Adrian Marielle, Pr, Université de Bourgogne	Examinatrice
Mme Cluzet Stéphanie, Pr, Université de Bordeaux	Examinatrice
M. Courty Pierre-Emmanuel, DR, INRAE	Examinateur

Vers une viticulture sans pesticide: analyse du microbiome de la vigne et des sols viticoles pour développer le biocontrôle microbien du mildiou

Résumé de la thèse

Les vignes et les sols viticoles hébergent une grande diversité de micro-organismes, qui forment collectivement le microbiote. Certains micro-organismes sont des agents pathogènes, comme l'oomycète *Plasmopara viticola*, responsable du mildiou. D'autres, tels que les promoteurs de croissance et les antagonistes des pathogènes, ont une influence positive sur la santé de la vigne. Ces interactions plante-microbe et microbe-microbe ont fait l'objet d'une attention accrue ces dernières années car leur compréhension pourrait constituer une piste pour sortir des pesticides. Le programme de recherche VITAE (2020-26) combine plusieurs approches de gestion innovantes pour réduire l'utilisation des fongicides en viticulture. L'une de ces approches est la gestion du microbiote de la vigne et des sols viticoles pour contrôler les maladies foliaires, dont le mildiou. L'objectif de cette thèse est d'identifier des micro-organismes, qu'il s'agisse de bactéries ou de champignons, susceptibles de contribuer au biocontrôle du mildiou. Le premier chapitre est une synthèse bibliographique sur la dynamique des interactions entre la vigne et son microbiote, au cours de l'histoire évolutive et au cours de la vie de la plante. Le deuxième chapitre compare le microbiote de tissus foliaires asymptomatiques avec le microbiote associé aux lésions du mildiou. Il montre que les lésions du mildiou hébergent des levures basidiomycètes (*Sporobolomyces patagonicus*, *S. roseus*, *Cryptococcus laurentii* et *Udeniomyces pyricola*) et des bactéries (*Bacillales*, *Streptomycetales*), la plupart connues pour leurs propriétés de biocontrôle. En revanche, les tissus foliaires asymptomatiques sont plutôt associés à d'autres agents pathogènes aériens (oïdium, botrytis). Ces résultats suggèrent que la feuille recrute localement certains taxons microbiens ayant une activité de biocontrôle lors de l'infection par le mildiou. Le troisième chapitre analyse le microbiote foliaire et le microbiote du sol superficiel dans des parcelles choisies en fonction de relevés épidémiologiques. Il montre que certains taxons microbiens fongiques (par exemple, *Buckleyzyma aurantiaca*, *Bullera alba*, *Trichoderma virens* et *Trichoderma hamatum*) et bactériens (par exemple, les genres *Streptomyces* et *Bacillus*) sont systématiquement plus abondants dans les parcelles historiquement moins sensibles au mildiou. Ces taxons sont nombreux dans la couche superficielle du sol, où les oospores (forme dormante du pathogène) passent l'hiver, et ils sont présents dans la phyllosphère, où les zoospores (spores biflagellées, forme responsable de l'infection) infectent les feuilles. En revanche, l'endosphère foliaire, où se développe le mycélium du pathogène, contient peu de taxons microbiens liés aux données épidémiologiques. Ce troisième chapitre montre aussi que la composition du microbiote du sol superficiel permet de prédire la sensibilité d'une parcelle au mildiou. Le quatrième chapitre explore le rôle du microbiote foliaire dans la résistance au mildiou de deux espèces de vigne américaines (*Vitis aestivalis* et *V. labrusca*). Ce chapitre s'appuie sur une campagne

d’échantillonnage menée sur la côte est des États-Unis. Les données sont en cours d’analyse. En conclusion, la thèse a révélé l'existence de consortia microbiens naturellement présents dans les vignobles, qui constituent des candidats prometteurs pour le biocontrôle du mildiou. Ces micro-organismes sont présents dans la phyllosphère et dans le sol superficiel en début de saison végétative et semblent ensuite augmenter en abondance dans les lésions de la maladie. Les perspectives majeures sont : (i) l'isolement des candidats microbiens et l'évaluation expérimentale de leur activité de biocontrôle, seuls ou combinés en communautés synthétiques, (ii) l’identification des pratiques agronomiques favorisant les consortia microbiens identifiés et (iii) le développement d’outils de prédiction de la sensibilité au mildiou basés sur le microbiote.

Mots-clés : Microbiome, écologie microbienne, agroécologie, biocontrôle, métagénomique environnementale, vigne

Towards pesticide-free viticulture: analysing the microbiome of grapevines and vineyard soils to develop microbial biocontrol of downy mildew

Abstract

Grapevines and viticultural soils host a great diversity of microorganisms that collectively form the microbiota. Some microorganisms are pathogens, such as the oomycete *Plasmopara viticola*, which causes downy mildew. Others, such as growth promoters and pathogen antagonists, are beneficial to grapevine health. These plant-microbe and microbe-microbe interactions have received increased attention in recent years because understanding them could provide a way to reduce the use of pesticides. The VITAE research program (2020-26) combines several innovative management approaches to reduce fungicide use in viticulture. One of these approaches is the management of vine and vineyard soils microbiota to control foliar diseases, including downy mildew. The aim of this thesis is to identify microorganisms, whether bacteria or fungi, that may contribute to the biocontrol of downy mildew. The first chapter is a literature review on the dynamics of interactions between the vine and its microbiota throughout the evolutionary history and life of the plant. The second chapter compares the microbiota of asymptomatic leaf tissues with the microbiota associated with downy mildew lesions. It shows that downy mildew lesions harbor basidiomycete yeasts (*Sporobolomyces patagonicus*, *S. roseus*, *Cryptococcus laurentii*, and *Udeniomyces pyricola*) and bacteria (*Bacillales*, *Streptomycetales*), most of which are known for their biocontrol properties. In contrast, asymptomatic leaf tissues are more associated with other aerial pathogens (powdery mildew, botrytis). These results suggest that the leaf locally recruits certain microbial taxa with biocontrol activity during downy mildew infection. The third chapter analyses the leaf and surface soil microbiota in plots selected on the basis of long term epidemiological surveys. It shows that certain fungal microbial taxa (for example, *Buckleyzyma aurantiaca*, *Bullera alba*, *Trichoderma virens*, and *Trichoderma hamatum*) and bacterial taxa (for example, the genera *Streptomyces* and *Bacillus*) are systematically more abundant in historically less downy mildew-susceptible plots. These taxa are abundant in the soil surface layer, where the oospores (the dormant form of the pathogen) overwinter, and in the phyllosphere, where the zoospores (flagellated spores, the form responsible for infection) infect the leaves. In contrast, the leaf endosphere, where the pathogen's mycelium develops, contains few microbial taxa linked to epidemiological data. This third chapter also shows that

the composition of the surface soil microbiota allows for the prediction of a plot's susceptibility to downy mildew. The fourth chapter examines the role of leaf microbiota in downy mildew resistance of two American grapevine species (*Vitis aestivalis* and *V. labrusca*). This chapter is based on a sampling campaign carried out on the east coast of the United States. The data are currently being analysed. In conclusion, the thesis revealed the existence of microbial consortia naturally present in vineyards, which are promising candidates for the biocontrol of downy mildew. These microorganisms are present in the phyllosphere and in the surface soil at the beginning of the growing season and then seem to increase in abundance in the disease lesions. The main perspectives are: (i) the isolation of microbial candidates and the experimental evaluation of their biocontrol activity, either alone or combined in synthetic communities, (ii) the identification of agronomic practices that favour the identified microbial consortia, and (iii) the development of microbiota-based predictive tools for downy mildew susceptibility.

Keywords: Microbiome, microbial ecology, agroecology, biocontrol, environmental metagenomics, grapevine

REMERCIEMENTS

La rédaction de cette thèse marque l'aboutissement de trois années de travail, d'apprentissage et de persévérance. Ce chemin n'aurait pas été possible sans le soutien et l'accompagnement de nombreuses personnes, auxquelles je souhaite exprimer ma profonde gratitude.

Je tiens à remercier toutes les personnes qui ont encadré les différents stages de recherche que j'ai réalisés au cours de mon parcours. C'est lors de mon premier stage en DUT que mon intérêt pour la recherche et l'idée de faire une thèse sont nés. Les trois stages suivants ont confirmé cette passion un par un. Chacun, à sa manière, m'a transmis le goût de la recherche et a cru en mon potentiel pour continuer : Fabienne Rajas, Marine Silva, Marine Mommert, Claire Ricono, Cendrine Mony et Philippe Vandenkoornhuyse.

Ensuite, je souhaite remercier les membres de mon jury pour le temps consacré à l'évaluation de mes travaux de thèse. Merci à vous Cendrine Mony et Alain Sarniguet d'avoir évalué mon travail en tant que rapporteurs ainsi qu'à vous Marielle Adrian, Stéphanie Cluzet et Pierre-Emmanuel Courty de l'avoir évalué en tant qu'examinateur. Merci à vous tous d'avoir fait le déplacement pour assister à ma soutenance, en ce jour pluvieux du mois de décembre 2024, et pour la discussion qui s'en est suivie. Cendrine je voudrais t'adresser un mot en particulier, tu m'as suivie dès mon stage de M1 et j'ai beaucoup appris à tes côtés, merci pour ta rigueur scientifique, ta gentillesse et tes encouragements.

Mes remerciements s'adressent ensuite naturellement à vous Corinne et Patrice, mes encadrants. Merci pour avoir si bien réfléchi le projet en amont, m'épargnant ainsi d'avoir à l'inventer de toutes pièces. Merci pour votre entente, cette collaboration qui m'a semblé facile, bien que vous ne vous connaissiez pas avant ma thèse. Merci d'avoir toujours voulu le mieux pour moi, en m'encourageant à présenter mon travail au travers de divers congrès et en me proposant différentes formations.

Patrice, je tiens ici à te réaffirmer toute ma gratitude. Malgré un emploi du temps chargé et la distance, tu as toujours maintenu et priorisé nos réunions hebdomadaires. Merci de m'avoir permis de rencontrer les membres de ton équipe de recherche et m'avoir fait connaître auprès d'eux. Grâce à toi, j'ai eu de nombreuses occasions d'échanger et d'enrichir mes connaissances avec des experts du domaine de la vigne, que ce soit lors des journées du groupe vigne, de l'école d'été vigne et vin, ou encore du séminaire international organisé par la KIM Vine & Wine Sciences, sans oublier cette semaine de juillet 2024 à Logroño. Merci aussi pour ton regard extérieur, toujours critique et constructif, sur les figures que je te présentais (« *mais du coup, un point, ça représente quoi… ?* »), ainsi que sur mon travail de manière générale. Je te suis particulièrement reconnaissante pour ton accompagnement dans l'expérience qui, à l'avance, m'a sans doute le plus terrorisée de ma vie : voyager aux États-Unis. Merci de m'avoir permis de me reposer entièrement sur toi lors des deux premières semaines de cette mobilité, et de m'avoir donné l'opportunité de rencontrer et de travailler avec Lance et son équipe. Cette expérience, bien que redoutée, restera gravée en moi tant elle a été enrichissante et apaisante.

Corinne, merci pour ton encadrement au quotidien. En particulier, j'ai pu pleinement bénéficier de ton expérience dans la réflexion et la mise en œuvre d'une campagne d'échantillonnage de terrain. J'ai ainsi découvert qu'une campagne de terrain et le traitement des échantillons qui suivent ne s'improvisent pas, mais que ces étapes nécessitent des protocoles rigoureusement testés et validés bien avant le jour J. Merci pour ta motivation et ton enthousiasme sans faille. Chaque réunion avec toi me reboostait. Merci d'avoir accueilli mes incertitudes et mon stress avec bienveillance, et d'avoir su adapter tes réponses pour me faire rebondir à chaque fois. Je te suis reconnaissante pour tes grandes compétences scientifiques, tes félicitations, la reconnaissance que tu m'accordes et tes encouragements quotidiens. Et enfin, merci pour l'opportunité que tu m'offres avec ce post-doc juste après ma thèse. Je suis ravie de poursuivre cette aventure à SAVE, dans un environnement où je me sens bien et pleinement intégrée.

Je n'aurais pas pu rêver meilleur encadrement que celui que vous m'avez offert à deux. Pour cela, je vous remercie infiniment.

Un grand merci aux quatre membres de mon comité de thèse : Chloé Delmas, Charlotte Tollenaere, Pere Mestre et Christophe Mougel. À deux reprises, vous avez pris votre mission très au sérieux, consacrant deux demi-journées à vous plonger dans mon projet, à y réfléchir avec attention, à m'apporter des conseils et des réponses précieuses. Tout a été pris en compte.

Je veux aussi remercier toutes celles et ceux qui font partie de la team microbiote, qui n'existait pas à mon arrivée en thèse et qui s'est construite petit à petit tout au long de ces trois ans. Un immense merci à Lucile Pellan, Aarti Jaswa, Jessica Vallance, Olivier Fabreguettes, Manon Chargy, Marie Ancelle, Marie-Cécile Dufour, Valérie Martin et Corinne Vacher. Merci pour ces réunions et discussions sereines, où chacun sait écouter et laisser la place aux autres, pour vos conseils avisés et votre bienveillance.

Je remercie également tous les membres du WP1 de VITAE. À plusieurs reprises, j'ai eu l'opportunité de vous présenter mon travail et, grâce à ces échanges, j'ai appris à voir les présentations orales autrement : non plus comme un exercice d'évaluation face à des experts plus qualifiés que moi, mais comme un véritable dialogue d'égal à égal. Cet apprentissage m'a fait découvrir que cet exercice avait comme but le partage et a été le point de départ de mon gout pour les présentations orales. Merci pour vos apports respectifs à mon travail : Simon Labarthe, Thierry Candresse, Armelle Marais-Colombel, Guilherme Martins, Isabelle Masneuf-Pomarède, Chantal Faure, Isabelle Demeaux et Laurent Delière.

Un mot aussi sur le projet VITAE, qui a entièrement financé ma thèse et dont l'objectif m'a toujours tenu particulièrement à cœur : identifier une combinaison de leviers permettant la culture de la vigne sans pesticides d'ici 2030-2040 (Je ne compte même plus le nombre de fois où j'ai énoncé cet objectif lors de mes présentations !). Je suis ravie d'y avoir contribué, en

explorant le levier du pilotage du microbiote. Un immense merci aux coordinateurs du projet : François Delmotte, Marielle Adrian et Hervé Hannin.

Trois ans, c'est long, mais ce n'est pas un long fleuve tranquille. Il y a eu des périodes de rush, des doutes, de l'ennui, des moments qu'on préfère oublier - adieu les échantillonnages, l'odeur de la javel, les soirées passées sous la hotte jusqu'à 21h, l'alarme du labo qui hurle dans les oreilles et fait battre la chamade au cœur, adieu la phase terminale de rédaction et de préparation de la soutenance, adieu les crises de larmes et de stress, adieu les cigarettes - et puis, il y a eu l'été 2023 passé dans la petite ville de Geneva (Etat de New York). Une parenthèse hors du temps, une retraite paisible, quelques mois suspendus. Loin de l'agitation, du bruit, de ce besoin de vigilance. On traverse le jardin pour se rendre au labo, et on laisse l'herbe caresser les pieds déchaussés le soir au retour, on ne loupe aucune des balades digestives dans la nuit après le dîner, on mange une glace sur le perron aussi souvent qu'on en a envie, on découvre l'Amérique et ses habitants, leurs habitudes …

J'adresse ma plus grande gratitude à mes collègues américains, pour cette qualité qui les définit si bien : leur sens de l'accueil. Leur envie sincère de mettre à l'aise chaque nouvel arrivant, leur bienveillance, leur disponibilité, leur enthousiasme contagieux. Merci pour votre patience face à mon anglais hésitant (mauvais même !).

Merci en particulier Erin, pour ces deux semaines de prospection à travers les Etats de la côte Est des Etats-Unis, pour avoir été notre guide en Amérique, et pour ton aide précieuse lors des échantillonnages de la collection. Anna, merci pour tout le travail que tu as fourni sur la conservation et le traitement de mes échantillons, pour tes enseignements, pour ces moments partagés et l'intérêt que tu m'as porté. Amy, merci pour les manips réalisées pour moi, et pour avoir tout fait pour que je sois dans les meilleures conditions de travail. Enfin, Lance, merci pour ton enthousiasme quotidien, ton excitation pour chaque idée et cette volonté de m'aider autant que tu le peux dans la réalisation de mon projet. Merci pour ce petit déjeuner au *Water Street Cafe*, le prêt in extremis de ta voiture pour les échantillonnage à Fredonia et pour avoir toujours fait en sorte que je me sente bien.

Cette expérience n'aurai pas eu la même saveur si elle n'avait pas été partagée avec vous, l'équipe d'international people : Leocir du Brésil, Aafreen du Cachemire, Nana de Géorgie, 임동준 de Corée du Sud, et Masoume d'Iran. Merci, car si j'ai amélioré mon anglais, c'est entièrement grâce à vous. Merci pour les longues discussions : à la *Yellow* et la *Blue house*, les sessions cuisine, shopping et tourisme. De nombreux souvenirs resteront gravés dans ma mémoire, comme la journée d'échantillonnage à Fredonia, les levers de soleil sur le Seneka *lake* et les petits déjeuners au *Water Street Cafe*, ces cours d'anglais qu'on a rapidement déserté. Merci pour tous ces échanges scientifiques et personnels... Merci Aafreen pour tous ces moments partagés, merci de m'avoir nourri et ouvert la voie à la cuisine du Cachemire, j'aime toujours autant cuisiner les *fungi* (et pas les *mushrooms*), merci pour nos moments

d'errance dans le *Wegmans*, ces essais culinaires de produits américains et cet état d'esprit de soutien quotidien.

Merci au personnel de l'UMT SEVEN, en particulier Christian Debord et Marc Raynal pour m'avoir mis à disposition la base de données Epicure, celle contenant les relevés de symptômes des TNT et qui a servi de fondement au second chapitre de ma thèse, lui-même le fondement de ma thèse.

Merci à toutes les personnes qui ont contribué à la production des données que ce soit en participant activement aux échantillonnages et manip au laboratoire pour une journée ou sur un temps plus long, en partageant leurs protocoles, en répondant à mes innombrables questions: Olivier Bonnard, Olivier Nefti, Cyril Condomines, Alexandre Chataigner, Fanny Pinoteau, Camille Grosgeorge, Erwan Guichoux, Émilie Chancerel, Zoé Delporte, Zachary Allouche, Eva Courchinoux, Thierry Leste-Lassere, Sylvain Santoni, Charlotte Poeydebat. Et un remerciement spécial à toi, Alexandre, qui m'as véritablement soulagée en prenant en charge la fin des manips de BM du chapitre 2 de ma thèse et l'entièreté des manips du chapitre 4 ! Emilie merci à toi pour la formation extraction d'ADN/PCR dispensée dans les locaux de la PGTB.

Marine Cambon et Julie Aubert, merci pour votre aide précieuse en analyse de données, merci d'avoir pris le temps de me partager vos script R et de m'avoir expliqué les méthodes du Random Forest et de l'analyse de réseaux sous PLN.

Un grand merci également à Maureen Pellan et Léa Cabrol-Froget pour vos contributions significatives et de dernière minute à la confection des schémas de mon manuscrit ! Merci Olivier et Benoît pour m'avoir fourni une figure et la légende associée, qui ont été intégrées directement dans l'introduction de ma thèse.

Je n'ai jamais pu envisager de travailler quelques part sans y nouer de vraies amitiés. À chaque étape de mes études et de mes stages, j'ai toujours cherché à tisser des liens avec mes collègues. Aujourd'hui, je veux remercier les membres de *The Paola's Crew* : Ninon, Sylvie, Julie et Lucile. Merci pour ces rires du quotidien, pour ces innombrables discussions à la salle café ou entre deux portes, pour avoir accueilli mes pleurs, mes inquiétudes, mes excitations, mes secrets. Vous rencontrer et vous avoir à mes côtés tout au long de cette thèse a été une chance inestimable. Ninon, je ne veux jamais oublier tous ces soirs où, après le départ de Martha, je venais m'installer dans *ta chambre* (oui, je sais, le plus gros lapsus du thésard lorsqu'il parle de son bureau…) pour bosser avec toi – enfin, soyons honnêtes, je te racontais surtout ma vie pendant que tu travaillais. Je veux garder en mémoire comment, après, on fonçait sur nos bécanes rouillées en direction du bar. Je ne veux pas oublier notre semaine à Ithaca pour le GiESCO 2023, ni notre super voyage à Logroño, méticuleusement organisé et réalisé dans la plus grande des légalités. Sylvie, merci pour nos échanges quotidiens et pour tous ces défis (sportifs ou non !) dans lesquels tu m'as embarquée. Merci d'avoir été ma mère pendant ces quelques semaines d'avril 2022 et encore parfois depuis. Merci de m'avoir aidée à grandir. Je

veux continuer à venir te voir aussi souvent que j'ai envie d'aller aux toilettes. À nos pauses innombrables thé/café passées et futures ! Julie, aka Jul, que dis-je, Carmen ! Partager mon premier bureau avec toi a été une merveilleuse expérience. Je me souviens encore de notre rencontre, le jour de mon arrivée en thèse, où tu n'as pas répondu au « Bonjour » de Corinne et moi quand nous sommes rentrées dans la pièce, et où j'ai compris que tu n'étais pas du genre facile à amadouer. Merci pour cet inestimable nombre de délires au labo... Bon, je vais éviter d'en dire trop ici, parce que franchement, j'assume moyen nos sujets de rigolade ! Mais juste, merci. Merci pour ton écoute, ta franchise et ta sensibilité. Lucile, je t'ai longtemps considérée comme une encadrante à part entière. Merci infiniment de m'avoir fait bénéficier de ton expérience de la thèse, de ton sens de l'organisation et de l'anticipation. Tu as été, et restes à ce jour, ma plus grande source d'inspiration, tant sur le plan professionnel que personnel. Merci d'avoir été ma binôme. Je veux garder en mémoire nos journée passées ensemble dans le laboratoire confiné de la PGTB, ton sens de l'humour, l'accent chantant que tu prends à chaque fois que tu imite quelqu'un, l'odeur des Philippes Moris le matin, les cafés au soleil (ou sous la pluie !), les câlins et tous nos tête à tête à la cantine.

Et parce que j'aime aller butiner à toutes les fleurs, merci à toutes les autres fleurs de l'UMR SAVE ! Oui, parce que je peux le dire : j'ai eu une relation privilégiée avec presque chacun de vous (ça fait beaucoup de relations privilégiées quand on est 80 !), et je me suis toujours sentie bien ici, sans jamais redouter de parler à qui que ce soit. Un grand merci en particulier à la team du Stag – en vrac : Arthur, Thomas, Lucas, Olivier, Sarah, Clémence, Paige. Nos rendez-vous hebdomadaires pas si réguliers au Stag-and-Loar, un bar que je déteste, n'auront finalement pas été si anecdotiques ! Sarah, merci pour les défis sportifs. À notre futur marathon, prévu le 10 mai pour ceux qui voudraient venir nous encourager ! Merci à vous de m'avoir offert un petit goût de vacances au cœur de mon dernier été de thésarde. Merci pour ce week-end du 15 août à Rochefort-du-Gard, entre plongeons dans la piscine, sorties trail dans la garrigue, discussions animées et politisées et… rédaction de l'article ! Merci pour la sortie aux lacs d'Ayous, ça m'aura permis d'aller voir les Pyrénées au moins une fois en trois ans ! Arthur, merci pour ces nombreux films plus ou moins barbants à l'Utopia (RIP Godland), ces litres de bières, ces fameuses parties de fléchettes et évidemment pour ces enseignement sur la stratégie R. Quand tu veux je te donne un cours sur ggplot3 !

À mes parents, qui m'ont toujours soutenu dans mon rêve de faire une thèse, tant financièrement que moralement, merci. Merci de m'avoir soutenu tout au long de mon parcours scolaire et professionnel, me permettant d'en être là aujourd'hui, de m'avoir laissée faire mes choix, de m'avoir accompagnée dans ma vie d'adulte, et de m'avoir laissée m'envoler quand j'étais prête, sans jamais ni me pousser ni me retenir.

Estelle, tu es mon phare dans l'océan, ce mât du bateau qui ne cède pas malgré la tempête. Toujours présente, droite et solide, tu es celle à qui je peux m'accrocher pour traverser toutes les épreuves, quelles qu'elles soient. Tu as tout suivi de loin, tout su – et il s'en est passé, des choses, pendant ces trois ans, et pas seulement sur le plan professionnel. Merci pour tout ce

qu'on a vécu, et pour tout ce qu'on vivra encore. Pour les discussion quotidiennes, les rires et les gue-bla. Enfin bref, *tu vois c'que j'veud*.

Je termine cette sessions de remerciements en m'adressant à vous, les membres de la Villa 151 : Aurore, Pauline et Ginkgo. Vivre avec vous c'est recevoir une vague de bonheur chaque jour dans la figure. C'est comme se sentir bien tout le temps. C'est grandir aussi. Alors merci. Merci pour nos innombrables sessions jardinage, nettoyage de la terrasse au jet d'eau, apéros *everywhere* (terrasse, parc Sacré-Cœur, bar), marathon de séries, ateliers cuisine, sorties improvisées jusqu'au bout de la *noche*. Merci d'avoir su dealer avec mes phases de stress, d'avoir accepté, d'avoir essayé de comprendre. Merci pour votre soutien, en particulier dans les derniers jours qui ont été redoutables. Merci à toi mon Ginkgo. Pour tous les câlins quand ça n'allait pas. Pour cet enthousiasme avec lequel tu m'accueilles chaque jour.

Merci le jasmin, le chèvrefeuille, la glycine, les ipomées, les roses trémières, la passiflore de donner à la ville cette saveur. Merci au jasmin de parfumer la pluie.

AVANT PROPOS

Cette thèse en Écologie évolutive, fonctionnelle et des communautés de l'Ecole Doctorale n° 304 Sciences et Environnements de l'Université de Bordeaux, d'une durée de trois ans, a été financée par le projet VITAE « Cultiver la vigne sans pesticides : vers des socio- écosystèmes viticoles agroécologiques » coordonné par François Delmotte (Institut des Sciences de la Vigne et du Vin à Bordeaux), Hervé Hannin (Institut Agro Montpellier à Montpellier) et Marielle Adrian (Institut Universitaire de la Vigne et du Vin à Dijon). Ce projet, lauréat de l'appel à projets du Programme Prioritaire de Recherche (PPR) « Cultiver et protéger autrement », a été financé par le gouvernement français. Le travail de recherche exposé dans cette thèse a principalement été mené au sein de l'Unité Mixte de Recherche 1065 "Santé et Agro-écologie du Vignoble" de l'INRAE à Bordeaux. Les expérimentations du chapitre 3 ont été effectuées à la Plateforme Génomique Transcriptomique de Bordeaux (PGTB). Un séjour de 4 mois a été réalisé à l'université de Cornell (Geneva, NY, United States of America) en collaboration avec le Dr Cadle-Davidson (Grape Genetics Research Unit, USDA, ARS, Geneva, NY, USA), pour la réalisation des travaux présentés dans le chapitre 4.

Au cours de cette thèse, mes recherches ont fait l'objet de diverses communications écrites et orales. Les communications orales auxquelles j'ai contribué en tant que coauteure, ne sont cependant pas mentionnées ici.

Publications

- Publié

Fournier, P. and Pellan, L., Barroso-Bergadà, D., Bohan, D. A., Candresse, T., Delmotte, F., ... & Vacher, C. (2022). *Chapter Two - The functional microbiome of grapevine throughout plant evolutionary history and lifetime. In*: Bohan, D.A., Dumbrell, A. (Eds.), *Advances in Ecological Research, Functional Microbiome*s. Academic Press, pp. 27–99 (Chapitre 1)

- Soumis

Fournier, P., Pellan, L., Jaswa, A., Cambon, M., Chataigner, A., Bonnard, O., ... & Vacher, C. *Revealing microbial consortia that interfere with grapevine downy mildew through microbiome epidemiology. Submitted to Microbiome in September 2024*. (Chapitre 3)

- En préparation

Fournier, P., Pellan, L., Aubert, J., This, P., & Vacher, C. *A new scenario of pathogen-microbiota interactions for the oomycete Plasmopara viticola. In preparation*. (Chapitre 2)

Fournier, P., Chataigner, A., Galarneau, E., Underhill, A., Mestre, P., Petit, E., ... & This, P. *Is the microbiome of American Vitis species involved in their resistance to grapevine downy mildew? In preparation*. (Chapitre 4)

- Posters

Fournier, P., Raynal, M., Debord, C., Delmotte, F., Deliere, L., This, P. & Vacher, C. (2022). Plan d'expérience pour identifier des antagonistes microbiens de *Plasmopara viticola*, un agent pathogène foliaire majeur de la vigne cultivée (*Vitis vinifera* L.). 13èmes Rencontres de Phytopathologie - Mycologie d'Aussois 2022, Sep 2022, Aussois, France. (Annexe n°1)

Fournier, P., Jaswa, A., Pellan, L., Vallance, J., Chancerel, E., Bonnard, O., ... & Vacher, C. (2023). *Towards microbiota-based disease management: analysis of grapevine microbiota in plots with contrasted levels of downy mildew infection. 22nd GiESCO (Group of international Experts for Cooperation on Vitivinicultural Systems) 2023, Jul 2023, Ithaca, United States.* (Annexe n°2A)

Pellan, L., Mercier, L., Fournier, P., Chancerel, E., Vallance, J., Delmotte F., & Vacher, C. (2023). Recherche de Bioindicateurs Microbiens de la Résilience de la Vigne en Champagne. La microbiologie du sol au service d'une agriculture durable : diagnostics et solutions innovantes 27 et 28 juin 2023 Biocitech, Romainville-Grand Paris, Amphithéâtre Pasteur. (Annexe n°3)

- *Proceedings*

Fournier, P. Jaswa, A., Pellan, L., Vallance, J., Chancerel, E., Bonnard, O., ... & Vacher, C. (2023). *Towards microbiota-based disease management: analysis of grapevine microbiota in plots with contrasted levels of downy mildew* infection. *IVES Conference Series, GiESCO 2023*. (Annexe n°2B)

Pellan, L., Fournier, P., Brevot, M., Chancerel, E., Guichoux, E., Delmotte, F., ... & Vacher, C. (2024). *Arbuscular mycorrhizal fungi as biomarkers of vineyard yield in Champagne.* 45e édition du Congrès mondial de l'Organisation internationale de la Vigne et du Vin (OIV), du 14 au 18 octobre 2024, Dijon, France. (Annexe n°4)

- Communications orales

Fournier, P., Pellan, L., Chancerel, E., Guichoux, E., Delmotte, F., This, P., & Vacher, C. (2023). *Mining microbiome data to identify antagonists of grapevine downy mildew (Plasmopara viticola)*. INRAE Genomics 2023 du 13 au 15 Novembre 2023, Bordeaux, France.

Fournier, P., Pellan, L., Guichoux, E., Chancerel, E., Raynal, M., Debord, C., ... & Vacher, C. (2024). Vers un biocontrôle microbien du mildiou de la vigne : étude comparative du microbiote de parcelles inégalement sensibles à l'agent pathogène *Plasmopara viticola*. Jean-Chevaugeon (JJC) - Rencontres de Phytopathologie - Mycologie : du 15 au 19 janvier 2024 (Aussois). (Annexe n°5)

Fournier, P., Jaswa, A., Pellan, L., Vallance, J., Chancerel, E., Bonnard, O., ... & Vacher, C. (2024). Exploitation des données du microbiote pour identifier les antagonistes du mildiou de la vigne (*Plasmopara viticola*). Rencontres à destination des équipes techniques des crus du Médoc et de Sauterne le 05 Mars 2024, Château Lagrange, Saint-Julien, France. Rencontres organisé par Inn'ovin en partenariat avec le Conseil des Grands Crus Classés en 1855.

Fournier, P., Pellan, L., Jaswa, A., Vallance, J., Chancerel, E., Bonnard, O., ... & Vacher, C. (2024). *Mining microbiome data to identify antagonists of grapevine downy mildew (Plasmopara viticola). Open International Conference on Grapevine Physiology and Biotechnology (Open-GPB2024), Logroño – La rioja, Spain, July 7-11 2024*.

Table des matières

Introduction générale....1
Cultiver et protéger autrement pour réduire l'usage des pesticides : un défi à relever....1
Le modèle d'étude : le pathosystème *Vitis vinifera* / *Plasmopara viticola*....2
Les interactions entre le microbiote des plantes et les oomycètes pathogènes....17
Objectifs et structure de la thèse....21
Chapitre 1 : Le microbiome fonctionnel de la vigne au cours de l'histoire évolutive de la plante et de son cycle de vie....25
Abstract....26
Keywords....26
Introduction....26
The grapevine functional microbiome THROUGHOUT evolutionary history....27
The grapevine functional microbiome THROUGHOUT plant lifetime....35
Let's make the grapevine microbiome more functional....50
Chapitre 2 : Un nouveau scénario d'interactions pathogène-microbiote pour l'oomycète *Plasmopara viticola*....63
Abstract....65
Introduction....65
Materials and methods....68
Results....74
Discussion....85
Supplementary figures....90
Supplementary tables....99
Chapitre 3 : Révéler les consortia microbiens qui interfèrent avec le mildiou de la vigne grâce à l'épidémiologie du microbiome....103
Abstract....105
Keywords....105
Background....106
Materials and methods....109
Results....120
Discussion....135

Conclusion and perspectives 141
Supplementary methods 142
Supplementary figures 145
Supplementary tables 171
Chapitre 4 : Le microbiome des espèces américaines de *Vitis* est-il impliqué dans leur résistance au mildiou de la vigne ? 181
Introduction 183
Material and methods 185
Results 191
Supplementary figures 196
Supplementary tables 202
Discussion générale 215
Conclusion et perspectives 229
References 231
Annexes 287

Introduction générale

Cultiver et protéger autrement pour réduire l'usage des pesticides : un défi à relever

La France est le premier pays producteur de produits agricoles en Europe (INSEE, 2018), le troisième exportateur européen et le 6e exportateur mondial de produits agricoles et agroalimentaires (FranceAgriMer, 2024). Cependant, elle figure aussi parmi les plus gros consommateurs de produits phytosanitaires, occupant la deuxième place en Europe après l'Espagne en 2021[1]. Ces produits phytosanitaires incluent des produits phytosanitaires conventionnels, issues de la synthèse chimique, et des produits phytosanitaires de biocontrôle qui peuvent être à base de micro-organismes, de médiateurs chimiques ou de substances naturelles[2]. Les produits phytosanitaires conventionnels représentaient, en 2020, environ deux-tiers des substances actives vendues[3]. Cet usage massif de pesticides chimiques de synthèse est préoccupant car ils contribue à la contamination des sols, de l'eau et de l'air, avec des impacts négatifs considérables sur la santé humaine et le fonctionnement des écosystèmes (Hassaan & El Nemr, 2020; Rani *et al.*, 2021; Panis *et al.*, 2022). De plus, la sélection de résistances aux molécules actives dans les populations d'organismes cibles compromet l'efficacité de ces pesticides sur le long terme (Massi *et al.*, 2021; Walsh *et al.*, 2022).

Face à cette situation, le gouvernement français a lancé plusieurs initiatives pour réduire l'usage des pesticides conventionnels, dont le plan Ecophyto, lancé en 2008 à la suite du Grenelle de l'Environnement (2007). Ce plan visait une réduction de 50 % de l'utilisation des produits phytosanitaires conventionnels dans un délai de dix ans. Cet objectif, réaffirmé dans le cadre des plans Ecophyto II en 2015 et Ecophyto II+ en 2018, reflète la volonté du gouvernement français d'investir dans la recherche pour développer des systèmes de production agricole durables, réduisant les effets néfastes des pesticides chimiques sur l'environnement et la santé.

C'est dans ce contexte qu'a été lancé le Programme Prioritaire de Recherche (PPR) « Cultiver et protéger autrement », dont l'objectif est de permettre, à l'horizon 2030-2040, l'émergence d'une agriculture sans pesticides, en mobilisant les principes de prophylaxie et d'agroécologie. Ce PPR, doté d'une enveloppe de 30 millions d'euros, visait à financer des projets de recherche collaborative sur le long terme (jusqu'à six ans). Ces projets doivent permettre des avancées décisives en matière de développement de nouvelles pratiques et de nouveaux systèmes de production agricole n'utilisant pas de pesticides. Le programme concerne l'ensemble de l'agriculture française, de métropole et d'outre-mer, ainsi que l'ensemble des productions

[1] https://www.touteleurope.eu/agriculture-et-peche/quel-pays-europeen-utilise-le-plus-de-pesticides/

[2] https://agriculture.gouv.fr/quest-ce-que-le-biocontrole

[3] https://sante.gouv.fr/IMG/pdf/note_de_suivi_plan_ecophyto_2019-2020.pdf

végétales, annuelles et pérennes. Il est piloté par l'Institut national de recherche pour l'agriculture, l'alimentation et l'environnement (INRAE), qui est chargé de son pilotage scientifique et de son animation, et par l'Agence nationale de la recherche (ANR), qui est chargée de la sélection, du conventionnement et du suivi des projets financés.

Le projet VITAE, « Cultiver la vigne sans pesticides : vers des socio-écosystèmes viticoles agroécologiques », est l'un des 10 lauréats de l'appel à projets de l'ANR présentés le 23 septembre 2020 dans le cadre du PPR « Cultiver et protéger autrement ». Doté d'un financement de 3 millions d'euros sur six ans (2020-2026), le projet VITAE développe des recherches pluridisciplinaires (Fig. 1) centrées sur la filière viticole, un secteur particulièrement concerné par l'usage intensif de pesticides. Il est coordonné par François Delmotte (Institut des Sciences de la Vigne et du Vin à Bordeaux), Hervé Hannin (Institut Agro Montpellier à Montpellier) et Marielle Adrian (Institut Universitaire de la Vigne et du Vin à Dijon). Le projet regroupe une centaine de scientifiques français travaillant sur la vigne et le vin.

VITAE vise à sortir des pesticides en viticulture en combinant l'usage de plusieurs leviers (Fig. 1), souvent à effets partiels, et en passant d'une approche curative à une démarche agroécologique basée sur la prophylaxie, la surveillance et une meilleure résilience des systèmes viticoles. Le projet est structuré autour de plusieurs axes de travail (Fig. 1), appelés *work packages*, qui comprennent: la gestion du microbiote, le développement du biocontrôle, la résistance génétique de la vigne, l'exploitation de la biodiversité, la reconception des systèmes de culture, la valorisation et les incitations socio-économiques. Le premier *work package* (WP1), intitulé « Gestion du microbiote », a pour objectif d'identifier des consortia microbiens qui interfèrent avec les principaux pathogènes de la vigne, en combinant des approches de génomique environnementale, de culturomique et de modélisation des communautés microbiennes. Plus spécifiquement, il vise à assembler des consortia microbiens ayant une activité antagoniste contre le mildiou et l'oïdium de la vigne, car ces deux maladies aériennes sont la cible de la majorité des traitements fongicides. Ce *work package* est coordonné par Corinne Vacher (UMR Santé et Agroécologie du Vignoble, INRAE-Bordeaux Sciences Agro) et Simon Labarthe (équipe PLEIADE, INRAE-INRIA). Ce travail de thèse s'inscrit dans le WP1 du projet VITAE.

Le modèle d'étude : le pathosystème *Vitis vinifera* / *Plasmopara viticola*

La vigne, une plante avec une place majeure dans l'économie française

Vitis vinifera L., communément appelée la vigne ou vigne cultivée, est une espèce de plante dicotylédone appartenant à la famille des *Vitaceae* et au genre *Vitis*. Il s'agit d'une liane qui s'accroche à son support grâce à des vrilles, et dont les tiges peuvent atteindre jusqu'à six mètres de long. Le genre *Vitis* regroupe plus de 60 espèces interfertiles (This *et al.*, 2006), présentes principalement dans l'hémisphère nord.

Le genre *Vitis* se divise généralement en deux sous-genres : *Muscadinia* et *Vitis* (ou *EuVitis*), comprenant respectivement 3 et 108 espèces reconnues (Olien, 1990). Parmi ces espèces, *Vitis*

vinifera est la seule à avoir acquis une importance économique significative (This et al., 2006). En tant qu'espèce principale de vigne cultivée en Europe et dans le monde, *Vitis vinifera* possède une grande diversité génétique, qui se matérialise par plusieurs milliers de variétés, utilisés aussi bien pour la production de raisins dits de cuves utilisés pour le vin (avec les cépages Cabernet-Sauvignon, Merlot, Pinot, Sauvignon, etc.) que pour la production de raisin de table (Italia, Muscat de Hambourg, …). D'autres espèces du genre *Vitis*, notamment les espèces nord-américaines *V. rupestris*, *V. labrusca* ou *V. riparia* ont été utilisées dans la création des porte-greffes ou d'hybrides interspécifiques résistants aux maladies, en raison de leur résistance à des pathogènes de la vigne tels que le phylloxéra, l'oïdium et le mildiou (Alleweldt & Possingham, 1988; This *et al.*, 2006; Merdinoglu *et al.*, 2018). On trouve les vignes sauvages nord-américaines à l'état naturel en bord de route ou dans les sous-bois (Fig. 2) ainsi qu'à l'état cultivé dans les collections ampélographiques, qui servent à préserver le patrimoine génétique de la vigne (Lacombe, 2023).

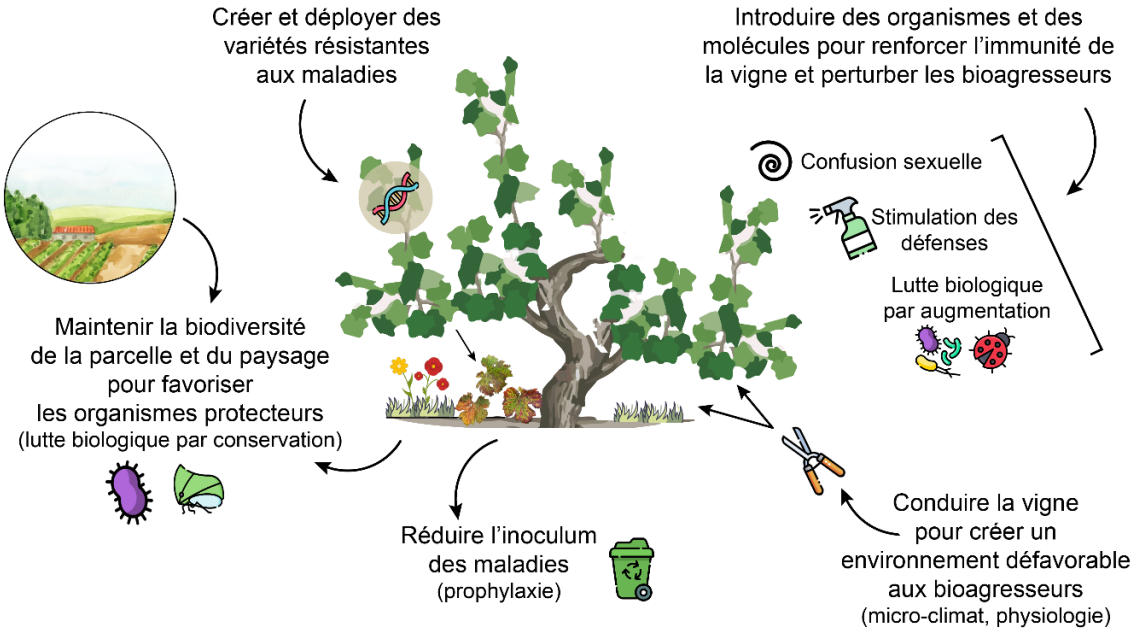


Figure 1 : Différents leviers étudiés dans le projet VITAE « Cultiver la vigne sans pesticides : vers des socio-écosystèmes viticoles agroécologiques ».
Les stratégies à combiner pour atteindre une viticulture « zéro-pesticide » incluent la création et le déploiement de variétés résistantes aux maladies, la réduction de l'inoculum primaire des agents pathogènes par des méthodes prophylactiques, la gestion de la biodiversité à l'échelle de la parcelle et du paysage pour favoriser les organismes protecteurs des cultures, l'inoculation de substances actives d'origine naturelle, de microorganismes ou de macroorganismes pour perturber les cycles de vie des agents pathogènes et des ravageurs et renforcer les défenses de la vigne, et la mise en place de modes de conduite qui rendent le micro-environnement défavorable aux agents pathogènes et ravageurs. Source : Léa Cabrol-Froget, Paola Fournier et comité de pilotage de VITAE.

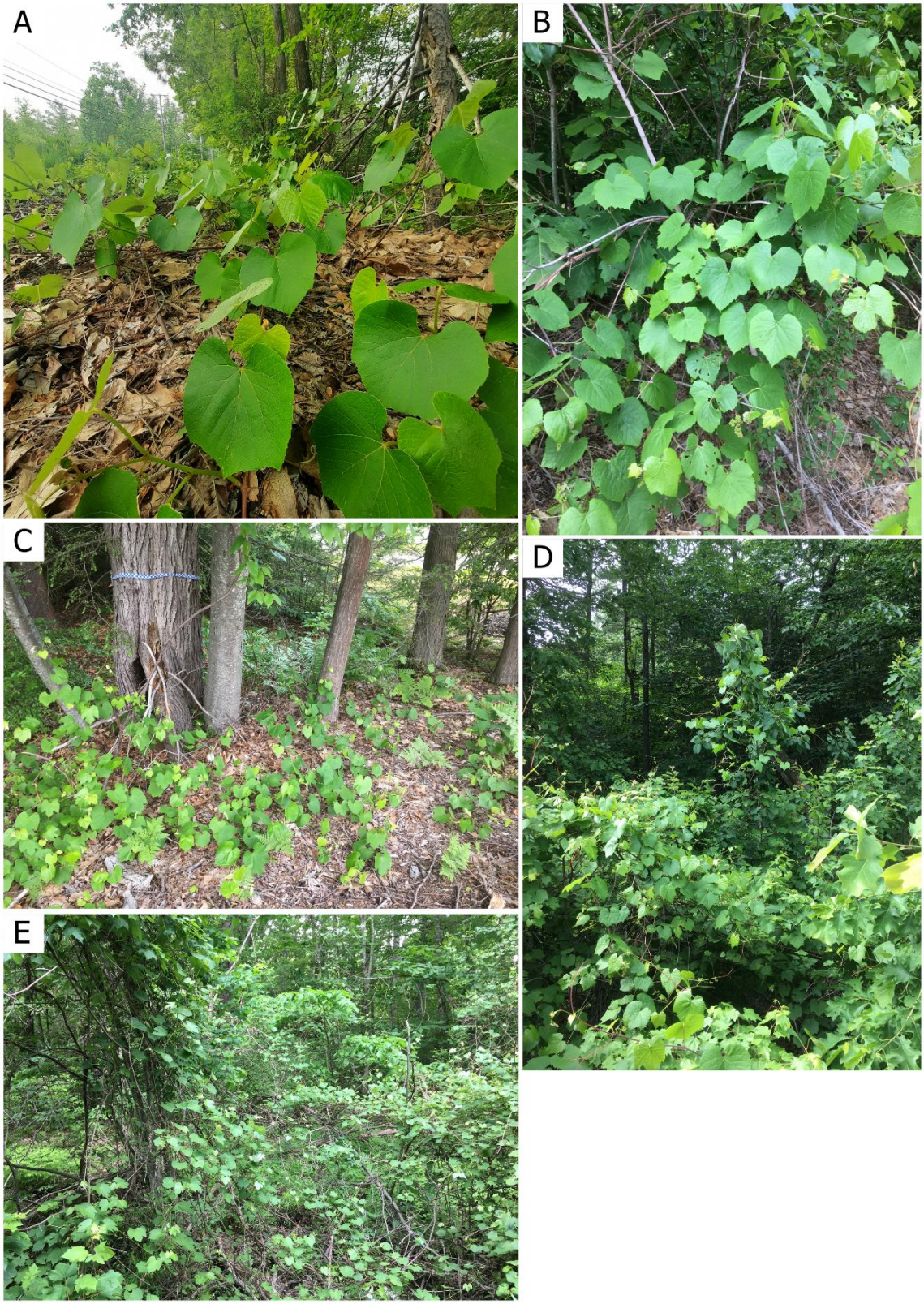


Figure 2: Photos de vignes sauvages américaines dans leur habitat naturel.
Photographies de *Vitis labrusca* (A, C, E) et *Vitis aestivalis* (B - D) poussant en bordure de route, s'étendant sur divers supports tels que le sol, des haies et les arbres. Ces images ont été prises au cours de l'été 2023, durant une campagne d'échantillonnage menée au cours de la thèse dans plusieurs États du nord-est des États-Unis (chapitre 4). Source : P. Fournier (UMR SAVE, INRAE) et P. THIS (UMR AGAP, INRAE).

Aujourd'hui, l'origine de la domestication de la vigne cultivée (*Vitis vinifera*) reste un sujet de grande controverse. Le lieu exact de cette domestication ainsi que la question d'une ou plusieurs domestications indépendantes font l'objet de nombreux débats scientifiques (Wang et al., 2024). Plusieurs études se sont penchées sur cette question, et la plus récente soutient un scénario selon lequel la domestication de la vigne aurait eu lieu il y a environ 11 000 ans en Asie occidentale et dans la région du Caucase, par le biais de deux événements de domestication indépendants (Dong et al., 2023), à partir de son ancêtre sauvage, *Vitis vinifera ssp. sylvestris*. Les formes cultivées se seraient ensuite répandues au Proche-Orient, au Moyen-Orient, puis en Europe centrale. Bien que l'Europe soit traditionnellement considérée comme le berceau de la viticulture, la culture de la vigne s'est aujourd'hui étendue à tous les continents, à l'exception de l'Antarctique.

La vigne occupe une place majeure dans l'économie agricole mondiale. Elle est principalement cultivée pour la production de raisin de cuve, essentiel à l'industrie viticole, qui génère des milliards d'euros chaque année. Le vin, produit phare issu de cette culture, représente un marché mondial de plus de 340 milliards d'euros (OIV, 2023), avec des régions viticoles célèbres comme la France, l'Italie, l'Espagne et les États-Unis dominant la production. Outre le vin, la vigne est également importante pour la production de raisin de table et de raisins secs, utilisés aussi bien pour la consommation directe que dans l'industrie alimentaire. La culture de la vigne soutient des millions d'emplois dans le monde, allant des vignerons aux travailleurs de la production, de la distribution et du commerce. De plus, des sous-produits comme l'huile de pépins de raisin, la gelée, ou encore le vinaigre de vin, contribuent à la diversification des revenus dans ce secteur. Enfin, la viticulture est souvent liée au développement touristique, notamment dans les régions réputées pour leurs vins, où l'œnotourisme attire chaque année des millions de visiteurs.

Il convient de noter que le commerce mondial du vin a connu un déclin en 2023 (OIV, 2023). La récolte, qui a été la plus faible depuis 1961, ainsi que le commerce et la consommation, ont tous diminué par rapport à l'année précédente. La superficie des vignobles a enregistré une baisse de 0,5 %, atteignant ainsi 7,2 millions d'hectares, chiffre qui inclut également les raisins de table. La production de vin a atteint 237 millions d'hectolitres, représentant une diminution de 10 % par rapport à 2022. Les conditions climatiques extrêmes, telles que les gelées précoces, les fortes pluies et la sécheresse, ainsi que la pression pathogène élevée et la baisse de la consommation pour la troisième année consécutive, sont autant de facteurs responsables de cette situation.

Dans ce contexte, la culture de la vigne fait face à de nombreux défis pour son maintien, notamment l'adaptation au changement climatique (van Leeuwen *et al.*, 2024), la lutte contre dépérissement des ceps[4] et la lutte contre de nombreux agents pathogènes (Bois et al., 2017) tout en réduisant l'usage des pesticides chimiques. En 2019, l'Indicateur de Fréquence de

[4] https://www.plan-deperissement-vigne.fr/

Traitement (IFT) moyen en viticulture était de 12,4 en France (7,9 à 19 selon les bassins), avec un indice de fréquence de traitement fongicide de 10,1 au niveau national (5,3 à 15,7 selon les bassins) et de 12,4 dans la région de Bordeaux (Agreste, 2023). Cette fréquence de traitements dépasse de loin celle de nombreuses autres cultures (Agreste, 2023). L'essentiel des traitements concerne la lutte contre les maladies « fongiques » (82 % de l'IFT total), et particulièrement le mildiou et l'oïdium respectivement causés par *Plasmopara viticola* et *Erysiphe necator*.

Ces agents pathogènes originaires d'Amérique du Nord ont atteint l'Europe à la fin du 19ème siècle, causant de graves dommages à l'espèce *Vitis vinifera,* très sensible car ayant évolué en leur absence (Gessler *et al.*, 2011). Il est désormais impératif de trouver des alternatives aux fongicides utilisés contre ces deux maladies majeures, d'autant plus que la pression épidémique augmente, notamment dans le cas du mildiou. En effet, si les modèles prédisant les pressions épidémiques futures en fonction des différents scénarios climatiques ne proposent pas de résultats concordants à l'échelle nationale (Francesca *et al.*, 2006; Salinari *et al.*, 2007; Angelotti *et al.*, 2017; Zito *et al.*, 2018), des données récentes (2010-2024) issues d'observations annuelles sur un réseau national français de parcelles traitées (~250 parcelles) et non traitées (~250 parcelles) montrent une évolution récente vers des épidémies de mildiou plus précoces et de plus fortes intensités (Fig. 3).

Le mildiou de la vigne, un oomycète pathogène originaire d'Amérique du Nord

Plasmopara viticola (Berk. & M.A. Curtis) Berl. & De Toni est un oomycète parasite biotrophe et obligatoire appartenant à la classe des oomycètes et à la famille des *Peronosporaceae*. Il est l'agent pathogène responsable du mildiou de la vigne, une maladie majeure, très destructrice dans les climats tempérés. Cet agent pathogène, originaire du Nord-Est des Etats-Unis, a été introduit en Europe au milieu du 19e siècle (Fig. 4). En raison de la sensibilité de la vigne cultivée *Vitis vinifera*, cette introduction a provoqué une destruction massive des vignobles européens. Les populations européennes de mildiou ont servi de source pour des introductions secondaires dans d'autres régions viticoles du monde, notamment en Chine, en Afrique du Sud et en Australie (Fontaine *et al.*, 2021) (Fig. 4). Plus tard, une troisième introduction a propagé la maladie de l'Australie à l'Argentine (Fontaine *et al.*, 2021) (Fig. 4). Cette maladie est désormais signalée dans la plupart des régions viticoles du monde (Bois *et al.*, 2017; Fontaine *et al.*, 2021) et a un impact économique considérable sur l'industrie viticole (Taylor & Cook, 2018).

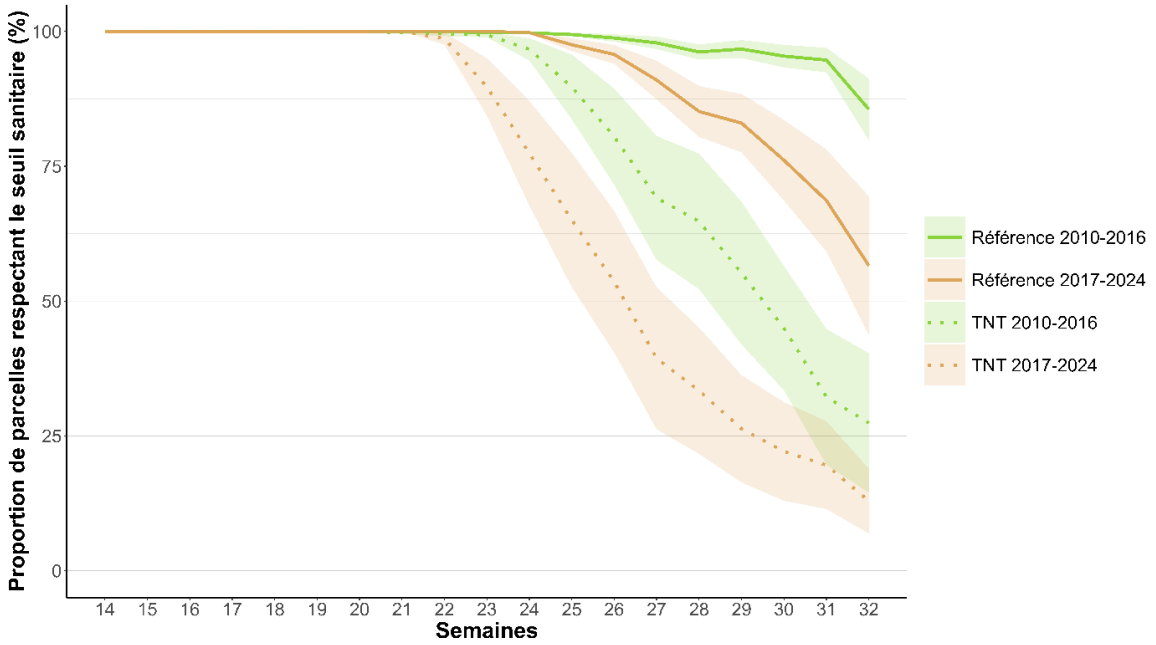


Figure 3 : Suivi épidémiologique du mildiou de la vigne sur les périodes 2010-2016 et 2017-2024. Les relevés épidémiologiques ont été effectués sur un réseau de parcelles suivi par l'Institut Français de la Vigne et du Vin (IFV), s'étendant dans les régions Sud-Ouest, Aquitaine, Val de Loire, Charentes, Bourgogne et Corse. Les parcelles non traitées pendant la saison épidémique sont désignées comme TNT (Témoins Non Traités), tandis que les parcelles traitées servent de référence. Cette figure montre le pourcentage de parcelles du réseau qui atteignent ou dépasse le seuil sanitaire de 20% d'incidence des symptômes sur les baies et à quel moment de la saison. Source des données : Institut Français de la Vigne et du Vin (IFV).

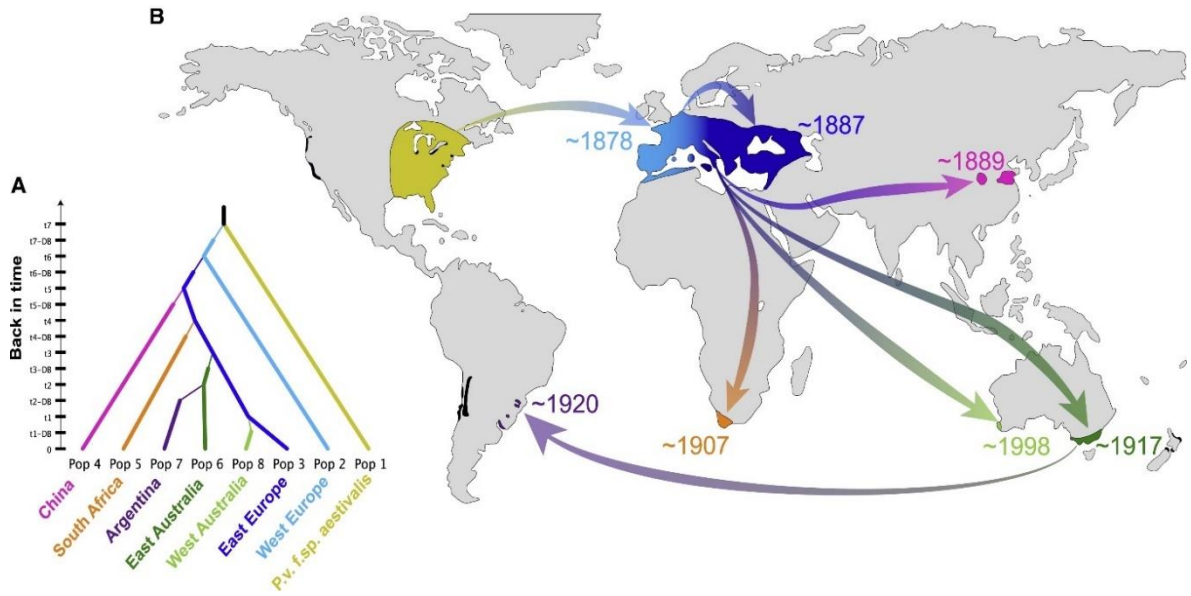


Figure 4 : Histoire de l'invasion mondiale de *Plasmopara viticola*.
(A) : Arbre phylogénétique montrant la divergence des populations invasives au cours du temps, de Pop 1 (la population à l'origine de l'invasion de l'Europe de l'Ouest vers 1878) à Pop 8 (la population ayant envahi l'ouest de l'Australie vers 1998). (B) : Carte mondiale retraçant les mouvements de ces populations depuis l'Amérique du Nord, avec des flèches indiquant les dates approximatives d'introduction dans diverses régions du monde, comme l'Europe de l'Ouest (~1878), l'Afrique du Sud (~1907), et l'Australie (~1917, 1998). Source : Fontaine et al., 2021.

Le cycle biologique de *P. viticola* est complexe (Fig. 5). A l'automne, la diminution de la température et de la photopériode favorise la formation d'oospores dans les feuilles par le biais de la reproduction sexuée, impliquant la fécondation d'une oogone par un spermatocyste. Les oospores issues passent l'hiver dans la litière de feuilles et dans le sol. Au début du printemps suivant, lorsque la température dépasse 10 ºC, que l'humidité relative atteint plus de 95 % et que la fréquence des pluies augmente, les oospores peuvent germer, à condition qu'une pellicule d'eau subsiste autour d'elles pendant au moins 24 heures. La germination des oospores conduit à la production de sporanges, qui libèrent des zoospores biflagellées. Ces zoospores, dispersées par l'eau de pluie et le vent, se déposent sur les tissus verts de la vigne, tels que les jeunes feuilles à peine déployées et les vrilles (Fig. 5). Elles nagent dans la pellicule d'eau à la surface de la feuille jusqu'à atteindre les stomates, où elles s'enkystent, germent et pénètrent dans les tissus via les stomates (Fig. 6). Une fois dans la cavité sous-stomatique, les zoospores forment une vésicule à partir de laquelle les hyphes se ramifient et colonisent les cellules du mésophylle, produisant des haustoria qui absorbent les nutriments des cellules hôtes (Fröbel & Zyprian, 2019) (Fig. 6). Après quelques jours, une coloration en « tache d'huile » apparaît sur la face supérieure des feuilles infectées. Finalement, l'émission par les stomates de sporangiophores (Fig. 6) portant les sporanges se produit lorsque la température dépasse 13 ºC, que l'humidité relative est supérieure à 95 %, et qu'il y a au moins 4 heures d'obscurité, marquant ainsi la fin de la période de latence de la maladie. Cette dernière dure entre 7 et 10 jours après le début de l'infection, en fonction des conditions météorologiques, de la sensibilité de l'hôte, de l'organe infecté et de la résistance ontogénique, qui se renforce à mesure que l'organe vieillit (Agrios, 2005; Kortekamp, 2005; Steimetz *et al.*, 2012; Caffi *et al.*, 2013; Buonassisi *et al.*, 2017). Cette sporulation forme un feutrage blanc sur la face inférieure des feuilles. Les sporangiophores, par le biais de la reproduction asexuée, libèrent de nouvelles zoospores qui constituent l'inoculum secondaire. Ces zoospores, dispersées par le vent et la pluie, provoquent à leur tour des infections secondaires sur d'autres tissus verts de la vigne non encore infectés, initiant de nouveaux cycles d'infections secondaires (Yin *et al.*, 2017). Comme les infections de mildiou ont lieu dans tous les tissus photosynthétiques de la plante (Bitsadze *et al.*, 2014; Fröbel & Zyprian, 2019), les inflorescences et les jeunes baies peuvent être infectées quand elles apparaissent, plus tard au cours de la saison (Fröbel & Zyprian, 2019). Au cours de la saison végétative, les cycles d'infections primaires, causées par l'inoculum primaire dérivé des oospores, et secondaires se déroulent en parallèle, contribuant tous deux à l'entretien de l'épidémie (Gobbin *et al.*, 2005; Boso *et al.*, 2019; Hong *et al.*, 2020; Sargolzaei *et al.*, 2020; Santos *et al.*, 2020a; Maddalena *et al.*, 2021).

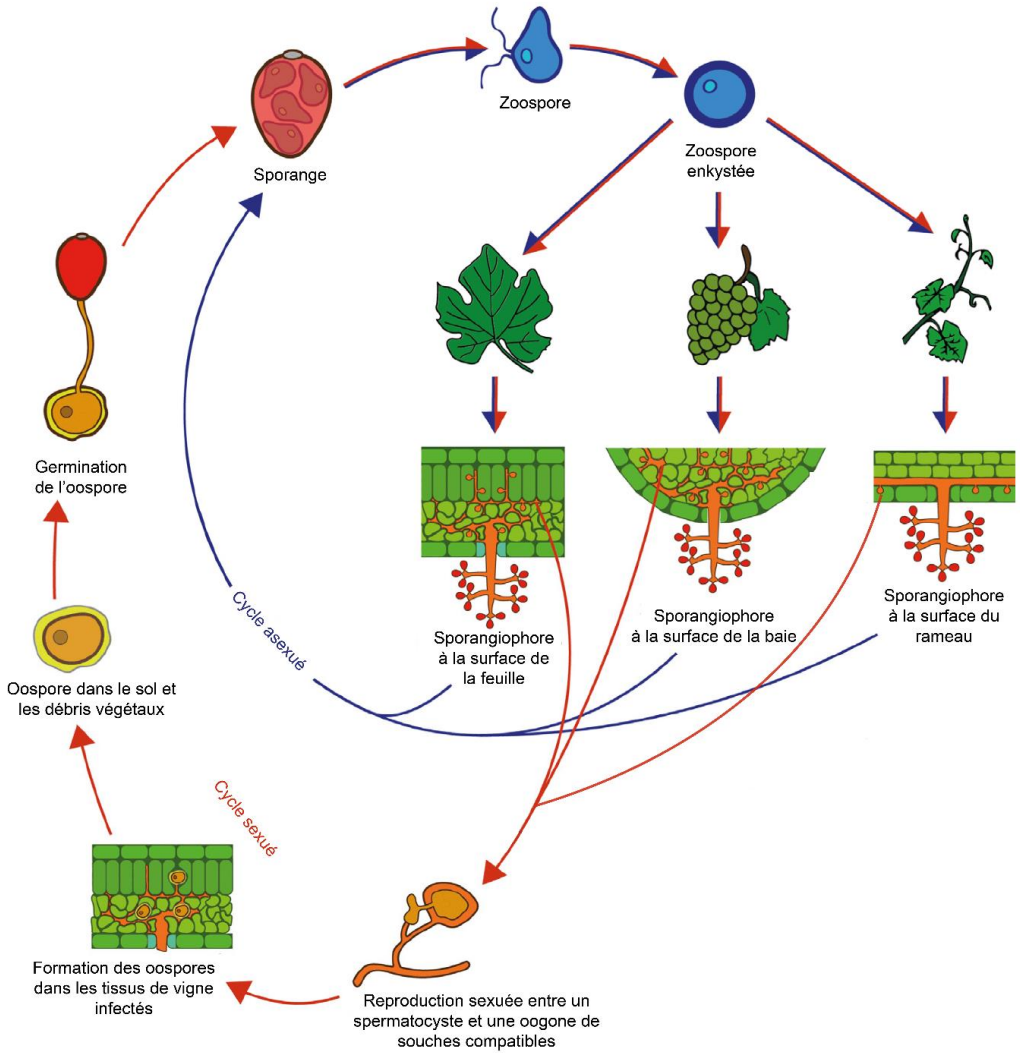


Figure 5 : Cycle de vie de l'oomycète *Plasmopara viticola*, responsable du mildiou de la vigne. Les flèches rouges représentent le cycle sexué tandis que les flèches bleues représentent le cycle asexué. Adapté de Velasquez-Camacho et al. (2023).

La lutte chimique est la principale méthode utilisée pour contrôler le mildiou, avec des produits chimiques systémiques ou de contact tels que le cuivre, fortement utilisé en viticulture biologique. Quelques produits de biocontrôle existent également[5] (Table 1), dont un seul à base de micro-organisme, le Taegro. L'utilisation de ce produit contre le mildiou est autorisée, via une autorisation de mise sur le marché (AMM)[6], mais elle n'est pas revendiquée par le fabriquant[7], probablement à cause d'une faible efficacité du produit.

[5] https://www.vignevin.com/wp-content/uploads/2023/04/fiche_biocontrole_vigne_mars_2023v2.pdf

[6] https://www.vignevin.com/article/liste-des-produits-de-bio-controle-homologues-en-viticulture-2023/

[7] https://www.syngenta.fr/biocontrole/vigne/dossier-taegro

Noms commerciaux (1)	type (3)	Principe actif	Mode d'action	UAB	faible risque
Mildiou (Plasmopara viticola)					
LBG-01F34 / Etonan / Pertinan / Alucinan / Facinan	sb nat	Phosphonate de potassium	Fongicide et SDP		
Phytosarcan/ Kerala / Boing / Tenrok	sb nat	Phosphonate de potassium	Fongicide et SDP		
Fosika	sb nat	Phosphonate de potassium	Fongicide et SDP		
Savial Forte / Mikonos Evo	sb nat	Phosphonate de potassium	Fongicide et SDP		
Ceraxel / BCPC358FC	sb nat	Phosphonate de disodium	Fongicide et SDP		
Redeli / Sirius / Fructial	sb nat	Phosphonate de disodium	Fongicide et SDP		
Messager/ Blason / Bastid / Bstim	sb nat	COS-OGA	Stimulateur des défenses (SDP)	AB	
Fytosave /Esdéaine	sb nat	COS-OGA	Stimulateur des défenses (SDP)	AB	oui
Romeo / Actileaf	sb nat	Cerevisane (parois de levures)	Stimulateur des défenses (SDP)	AB	oui
Essen'ciel/ Limocide/Auran'ciel /Limoil	sb nat	Huile essentielle d'orange	Fongicide	AB	
Orocide / PrevAM ultra / Prev-AM plus / Oro-quin/Sinala	sb nat	Huile essentielle d'orange	Fongicide	AB	
Taegro ¥	microrg	Bacillus amyloliquefaciens s. FZB24	Antibiose et SDP	AB	oui

Table 1 – Liste des produits de biocontrôle disponibles en 2023 pour lutter contre le mildiou de la vigne.
Tous les produits sont basés sur des substances naturelles (sb nat) sauf un, le Taegro, qui est basé sur un microorganisme. La moitié des produits sont utilisables en agriculture biologique (UAB) et trois produits possèdent un faible risque selon la commission européenne. Source: Institut Français de la Vigne et du Vin (https://www.vignevin.com/article/liste-des-produits-de-bio-controle-homologues-en-viticulture-2023/).

Des variétés de vignes résistantes au mildiou ont également été développées (Merdinoglu *et al.*, 2018), en s'appuyant sur les gènes de résistance identifiés dans le génome des vignes sauvages nord-américaines et asiatiques. Les gènes ou loci de résistance sont désigné Rpv pour *Resistance to P. viticola* et confèrent différents degrés de résistance à la maladie (Dry *et al.*, 2019). Les principaux gènes sont Rpv1, Rpv2, Rpv3, Rpv8, Rpv12 et Rpv15. Ils ont été identifiés chez *Muscadinia rotundifolia*, *V. labrusca*, *V. amurensis* et *V. piasezkii* et confèrent une résistance partielle à totale à l'infection par le mildiou (Merdinoglu *et al.*, 2003; Bellin *et al.*, 2009; Blasi *et al.*, 2011; Di Gaspero *et al.*, 2012; Venuti *et al.*, 2013; Feechan *et al.*, 2013; Welter *et al.*, 2017). Les autres gènes de résistance sont considérés comme mineurs car ils confèrent un faibles degré de résistance et ils ne sont utiles que lorsqu'ils sont combinés à des gènes majeurs (Sargolzaei *et al.*, 2021). Étant donné la capacité des oomycètes pathogènes, comme *Plasmopara viticola*, à développer des résistances aux traitements chimiques et à contourner les gènes de résistance des plantes (Kamoun *et al.*, 2015; Derevnina *et al.*, 2016), il est essentiel d'adopter une approche de lutte intégrée. Cette approche doit intervenir à différents stades du cycle de vie de *Plasmopara viticola* et combiner plusieurs leviers, en associant des actions préventives et curatives.

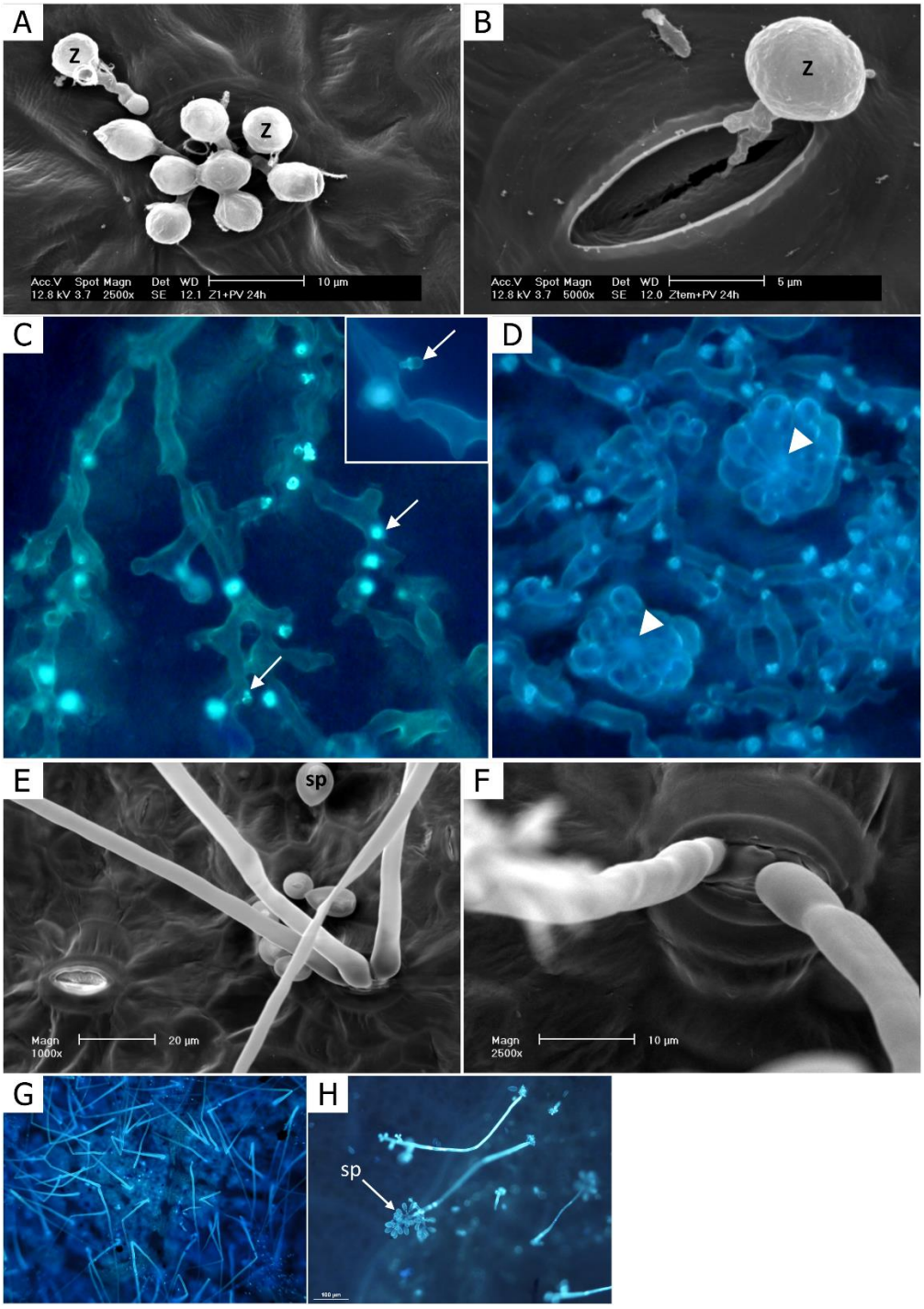


Figure 6 : Photographies illustrant les étapes de l'infection d'une feuille de vigne par l'agent pathogène *Plasmopara viticola*.

A-B : enkystement des zoospores en bordure de stomate et pénétration par l'ostiole. C-D : colonisation interne du limbe avec développement des hyphes entre les cellules de parenchyme, mise en place d'haustoria (flèches et encarta) nourriciers puis, 5 à 6 jours post-inoculation, regroupement d'hyphes dans la chambre sous-stomatique (tête de flèche) indiquant une phase de pré-sporulation. E-H : sporulation asexuée en surface de limbe avec sortie des sporangiophores, portant de nombreux sporanges, par les stomates. Ces illustrations ont été prises soit en microscopie électronique à balayage (A-B et E-F), soit en microscopie optique à épifluorescence après coloration au bleu d'aniline (C-D et G-H). z : zoospore, sp : sporange. Source : S. Trouvelot (UMR Agroécologie).

Gérer le microbiote pour protéger les plantes contre les pathogènes

La plante : un holobionte

Les plantes vivent en étroite association avec diverses communautés de micro-organismes qui collectivement forment le microbiote végétal. Ces communautés microbiennes sont constituées principalement de bactéries et, dans une moindre mesure, de champignons, mais aussi de groupes moins étudiés tels que les archées, les protistes et les virus (Compant *et al.*, 2024) (Fig. 7). De nombreuses études ont fait état d'un large éventail d'effets bénéfiques des membres du microbiote sur la santé et la croissance des plantes. Ces effets bénéfiques incluent la protection contre les maladies (Mendes *et al.*, 2013; Ritpitakphong *et al.*, 2016), via notamment l'activation du système immunitaire de la plante , l'amélioration de la nutrition (van der Heijden *et al.*, 2016), via notamment l'établissement d'associations mycorhiziennes (Garbaye, 1994), et enfin l'augmentation de la tolérance aux stress abiotiques (Rolli *et al.*, 2015) et plus généralement aux variations environnementales (Haney *et al.*, 2015). Bien que ce soient les effets du microbiote sur la plante qui sont le plus souvent étudiés, il faut noter que les interactions entre la plante et son microbiote ne sont pas unidirectionnelles. La plante hôte fournit des ressources métaboliques à ses associés microbiens, ce qui conduit à l'adaptation de microbes spécialisés dans une niche, qui peuvent avoir un impact positif (mutualiste), neutre (commensaliste) ou délétère (pathogène) sur la santé de la plante (Thrall *et al.*, 2007). Par exemple, l'association symbiotique entre les plantes et les champignons mycorhiziens améliore la captation de nutriments minéraux essentiels par les plantes, tandis que les plantes allouent en retour des composés carbonés aux champignons (Smith & Read, 2010). A l'inverse, certains micro-organismes pathogènes, tels que *P. viticola,* exploitent la plante pour se nourrir ou se reproduire, causant des symptômes allant de la défoliation à la mort (Armijo *et al.*, 2016).

Ainsi, les phénotypes de la plante et des micro-organismes associés résultent des interactions, nombreuses et bi-directionnelles, entre la plante et les micro-organismes et entre les micro-organismes, dans un environnement spécifique à un moment donné (Vorholt *et al.*, 2017). Par conséquent, une plante (ou tout autre macro-organisme) ne doit plus être perçue comme un individu isolé, mais plutôt comme le produit d'interactions complexes avec son microbiote (Zilber-Rosenberg & Rosenberg, 2008). Un concept actuel propose de considérer l'hôte multicellulaire et son microbiote comme une entité fonctionnelle, appelée « holobionte », au sein de laquelle des pression de sélection s'exercent entre l'hôte et les microbes, mais aussi au sein des différentes communautés microbiennes associées à l'hôte (Vandenkoornhuyse *et al.*, 2015; Hassani *et al.*, 2018; Teixeira *et al.*, 2019).

Chaque organe de la plante possède son propre microbiote

Les micro-organismes colonisent tous les organes végétaux (Fig. 7), tant le système racinaire (Bulgarelli *et al.*, 2015), que les parties aériennes, c'est-à-dire les tiges (Wang *et al.*, 2016), les feuilles (Behrens & Fischer, 2022a), les fleurs (Aleklett *et al.*, 2014), les fruits, et les graines en formation sur la plante (Simonin *et al.*, 2022). Les fruits et les graines tombent ensuite au sol,

emmenant avec eux une communauté microbienne aérienne qui se mélange avec les communautés microbiennes souterraines (Rochefort *et al.*, 2021). De manière générale, la diversité microbienne diminue des parties souterraines vers les parties aériennes de la plante (feuilles, fleurs, graines et fruits) (Dong *et al.*, 2019; Sun *et al.*, 2021a; Xie *et al.*, 2024), avec un changement progressif de la composition des communautés microbiennes (Zarraonaindia *et al.*, 2015a; Leach *et al.*, 2017; Sun *et al.*, 2021a; Xie *et al.*, 2024).

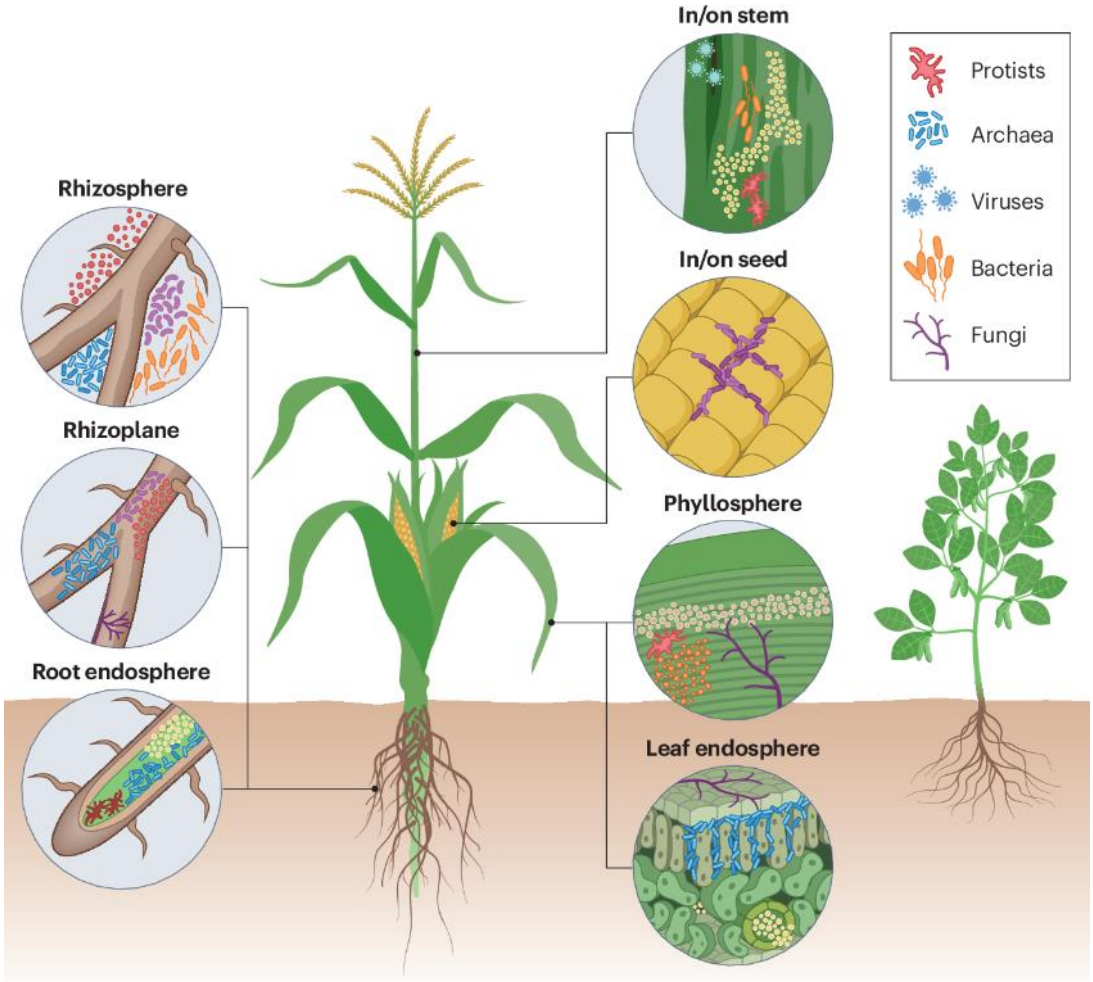


Figure 7 : Habitats microbiens principaux sur et dans une plante, notamment la rhizosphère, le rhizoplan, l'endosphère racinaire, la phyllosphère. Source : Compant et al. (2024).

Les micro-organismes épiphytes vivent à la surface des tissus (Andrews & Harris, 2000) tandis que les micro-organismes endophytes vivent à l'intérieur des tissus (Hardoim *et al.*, 2015; Compant *et al.*, 2021). Cette séparation est un peu arbitraire car de nombreuses espèces, comme les oïdiums et les mildious, peuvent être à la fois épiphytes et endophytes, colonisant à la fois la surface et l'intérieur des feuilles au cours de leur cycle de vie (Glawe, 2008; Castrillo-Sequeira *et al.*, 2023). L'intérieur des tissus est généralement appelé endosphère, tandis que de nombreux termes sont employés dans la littérature pour qualifier les habitats des épiphytes. Par exemple, les termes anglais *ectosphere* (Vandenkoornhuyse *et al.*, 2015) et *episphere* (Compant *et al.*, 2024) peuvent être utilisés pour désigner l'ensemble des surfaces d'une plante. La surface de chaque organe est un habitat microbien particulier (Fig. 7). Ainsi le rhizoplan désigne la surface des racines, tandis que la rhizosphère désigne la fine couche de

sol adhérant aux racines (Berendsen *et al.*, 2012; Mendes *et al.*, 2013). Les autres surfaces sont généralement appelées phylloplan ou phyllosphere (surface des feuilles), cauloplan ou caulosphere (surface des tiges), anthoplan ou anthosphere (surface des fleurs) et carpoplan ou carposphere (surface des fruits) (Vacher *et al.*, 2016a; Lemanceau *et al.*, 2017). La fine couche de sol influencée par l'activité de la graine en germination est appelée spermosphère (Nelson, 2004, p. 200). Le terme phyllosphère est parfois utilisé utilisé pour désigner l'ensemble des parties aériennes des plantes (Lindow & Brandl, 2003; Vorholt, 2012). Dans cette thèse, nous adopterons la définition la plus stricte, celle de la surface des feuilles (Vacher *et al.*, 2016a).

La surface foliaire terrestre estimée à plus de 1 × 10^9 km² (Vorholt, 2012), soit environ deux fois la superficie des continents. Cet habitat unique et dynamique est soumis à des fluctuations irrégulières et parfois importantes de température, de rayonnement UV, de disponibilité en nutriments, ainsi que d'humidité relative (Lindow & Brandl, 2003), fournissant ainsi un environnement éphémère et instable pour les micro-organismes qui l'habitent (Vorholt, 2012). Malgré ces contraintes environnementales, de nombreux micro-organismes parviennent à prospérer à la surface des feuilles. Si des champignons et des archées colonisent la phyllosphère, les bactéries y sont de loin les plus abondantes (Andrews & Harris, 2000; Lindow & Brandl, 2003). Ces microorganismes peuvent avoir des effets délétères ou bénéfiques sur leurs plantes hôtes, en agissant comme des agents pathogènes ou en empêchant la colonisation des feuilles par des agents pathogènes (Kishore et al., 2005). Des études conduites sur *Arabidopsis* (Horton *et al.*, 2014; Ritpitakphong *et al.*, 2016; Chen *et al.*, 2020b), le maïs (Balint-Kurti *et al.*, 2010; Manching *et al.*, 2014; Wallace *et al.*, 2018; Wagner *et al.*, 2020) et l'olivier (Hladnik *et al.*, 2023) et récemment sur la vigne (Wicaksono *et al.*, 2023) suggèrent l'existence d'une relation entre les communautés microbiennes de la phyllosphère et la sensibilité de la plante hôte aux agents pathogènes foliaires. Ces communautés jouent également un rôle dans le cycle des nutriments, notamment par la fixation de l'azote atmosphérique (JONES, 1970; Freiberg, 1998). La composition des communautés microbiennes de la phyllosphère varie entre les espèces de plante du fait de la sélection exercée par des traits phénotypiques foliaires tels que la morphologie des feuilles (Hunter *et al.*, 2010; Kusstatscher *et al.*, 2020), la composition de la cuticule (Bodenhausen *et al.*, 2014; Ritpitakphong *et al.*, 2016) ou encore l'émission de signaux volatils et hormonaux (Vorholt, 2012). Des facteurs environnementaux tels que l'anthropisation du milieu (Laforest-Lapointe *et al.*, 2017), les pratiques de gestion des cultures (Chen *et al.*, 2021c) et la saison (Rastogi *et al.*, 2012) ont également un impact important sur le microbiote de la phyllosphère.

La plante recrute son microbiote dans les réservoirs environnementaux, notamment le sol

La première source d'inoculum pour le microbiote de la plantule sont la graine et le sol qui entoure la graine au moment de sa germination (Barret *et al.*, 2015). Ce microbiote initial peut avoir des impacts à long terme sur l'établissement des cultures en favorisant l'établissement de micro-organismes du sol bénéfiques pour les plantes (Ridout *et al.*, 2019) ou en limitant l'incidence des agents pathogènes des plantes transmis par le sol (Matsumoto *et al.*, 2021). La graine en formation sur la plante peut acquérir son microbiote de deux manières,

horizontalement à partir de divers environnements (par exemple, l'air, l'eau, les insectes, le traitement des semences), ou bien verticalement à partir de la plante mère (Fort *et al.*, 2021), rendant possible une transmission sur plusieurs générations (Shahzad *et al.*, 2018; Rodríguez *et al.*, 2020).

Lorsque la plante n'est plus une plantule, le sol devient le réservoir majeur des micro-organismes qui colonisent ses tissus (Zarraonaindia *et al.*, 2015a). La colonisation des parties souterraines par les micro-organismes a pour origine le sol et progresse vers l'endosphère racinaire en passant par la rhizosphère et le rhizoplan (Müller *et al.*, 2016). Certains micro-organismes issus du sol peuvent ensuite se propager ensuite à d'autres habitats microbiens via le xylème (Naveed *et al.*, 2014). Les micro-organismes sont attirés du sol vers la rhizosphère grâce à la sécrétion par les racines de métabolites carbonés complexes, appelés exsudats racinaires. Ces exsudats, composés principalement de sucres, d'acides aminés, d'acides organiques et de polysaccharides (Badri & Vivanco, 2009), permettent à la plante de recruter certains microbes en fonction de ses besoins (Kiers *et al.*, 2011; Vannier *et al.*, 2015)

Les micro-organismes colonisant les parties aériennes de la plante peuvent provenir de diverses sources. En début de saison végétative, dans le cas des plantes pérennes, des micro-organismes peuvent provenir des bourgeons dans lesquels ils ont passé l'hiver (Osono, 2014). L'immigration des micro-organismes sur les feuilles peut aussi se faire via la pluie et les éclaboussures engendrées par les gouttes d'eau (Palmero *et al.*, 2011; Mechan Llontop *et al.*, 2021), comme dans le cas de l'oomycète pathogène *P. viticola* (Castrillo-Sequeira *et al.*, 2023). Les insectes pollinisateurs et herbivores peuvent aussi transporter des micro-organismes (Osono, 2014). Les plantes du voisinage ont également été proposé comme un réservoir microbien des habitats aériens (Vorholt, 2012). Cependant, la source principale des micro-organismes foliaires est l'atmosphère, et plus précisément les bioaérosols qui s'y trouvent et qui contiennent un mélange de micro-organismes issus d'écosystèmes terrestres et aquatiques (Bulgarelli *et al.*, 2013). La pénétration des micro-organismes dans les tissus végétaux aériens peut se faire par des blessures ou par des ouvertures naturelles, telles que les stomates ou le stigmate des fleurs (Xin & He, 2013; Vacher *et al.*, 2016a).

Il convient de souligner que pour contrer les pathogènes ayant réussi à pénétrer à l'intérieur des tissus, les plantes disposent d'un système immunitaire très efficace, en raison de l'absence de cellules immunitaires mobiles (Nishad *et al.*, 2020). Deux formes de systèmes immunitaires existent chez les plantes, selon le type de molécules ciblées : le PTI (*pattern-triggered immunity*) et l'ETI (*effector-triggered immunity*) (Nishad *et al.*, 2020). Le PTI est déclenché par des motifs spécifiques (MAMP/PAMP/DAMP) reconnus par les récepteurs membranaires des plantes (PRRs), motifs généralement présents à la surface des agents pathogènes (Saijo *et al.*, 2018). En revanche, l'ETI, considéré comme un système plus sophistiqué, repose sur la reconnaissance d'effecteurs, tels que des facteurs de virulence exprimés par les pathogènes pour contrer le système de défense de base (ETI) (Jones & Dangl, 2006). Bien que la mise en place de ce système immunitaire soit essentielle pour la lutte contre les pathogènes, elle peut également modifier les assemblages microbiens en général (Hiruma *et al.*, 2016).

Les micro-organismes recrutés interagissent entre eux et avec la plante

Le microbiote peut freiner l'établissement et la propagation des agents pathogènes, soit en inhibant directement leur croissance par des interactions microbiennes antagonistes, soit en atténuant les symptômes en stimulant le système immunitaire de la plante (Hardoim *et al.*, 2015). Les interactions antagonistes peuvent prendre différentes formes.

Le parasitisme se définit comme une interaction où un organisme extrait des nutriments d'un autre en envahissant et en détruisant le mycélium, les spores et les structures de repos des pathogènes fongiques, ainsi que les cellules des pathogènes bactériens (Ghorbanpour *et al.*, 2018). Si l'hôte est également un parasite, comme c'est souvent le cas pour les agents phytopathogènes, cette interaction est qualifiée d'hyperparasitisme, un phénomène fréquemment observé entre différentes espèces de champignons. Parmi les hyperparasites les plus étudiés, on trouve des espèces fongique du genre *Trichoderma*, ainsi que des oomycètes tels que *Pythium*, y compris *Pythium oligandrum*, et des bactéries comme les *Streptomyces*.

La production de composés antimicrobiens, souvent liée à l'antibiose, désigne la synthèse de métabolites secondaires antimicrobiens, tels que des antibiotiques, des enzymes lytiques et d'autres composés antifongiques (Raaijmakers & Mazzola, 2012). Ces substances inhibent la croissance des micro-organismes, diminuent la production de facteurs de virulence ou les détruisent, par exemple en exerçant des effets anti-germination ou en dégradant les parois et membranes cellulaires. Des composés antimicrobiens ont été identifiés dans plusieurs genres microbiens, incluant des champignons tels que les *Trichoderma*, *Cryptococcu*s, *Saccharomyces*, ainsi que des bactéries comme les *Bacillus*, *Pseudomonas* et *Streptomyces* (Abdallah *et al.*, 2018).

Enfin, les micro-organismes peuvent entrer en compétition pour les nutriments lorsqu'ils ont besoin des mêmes ressources, ou en compétition spatiale lorsqu'ils occupent un espace limité (Ghorbanpour *et al.*, 2018). En plus d'interactions directes de type antagonistes, les microbes sont capables de déclencher le système de défense de la plante, induisant une immunité contre les agents pathogènes dans toute la plante (Pieterse *et al.*, 2014). Ce phénomène est désigné sous le nom de résistance systémique induite (ISR). Divers micro-organismes, tels que des membres des genres *Pseudomonas*, *Bacillus* et *Trichoderma*, ainsi que les champignons mycorhiziens à arbuscules (AMF), ont montré qu'ils pouvaient induire une résistance systémique induite (ISR) chez les plantes, offrant ainsi une protection contre une large gamme de pathogènes (Pieterse *et al.*, 2014). Les agents pathogènes peuvent également provoquer une réponse systémique, qui protège d'autres parties de la plante, ce qu'on appelle la résistance systémique acquise (SAR) (Pieterse *et al.*, 2014).

Ces interactions ayant lieu entre microbes-microbes ou microbes-plantes et qui sont bénéfiques pour la santé des plantes ont suscité un intérêt croissant ces dernières années, car elles pourraient constituer une alternative viable à l'utilisation de pesticides (Bakker *et al.*, 2012; Busby *et al.*, 2017; Toju *et al.*, 2018).

Applications au biocontrôle microbien des maladies

Les micro-organismes protégeant les plantes des agents pathogènes sont désignés comme agents de lutte biologique. Ils sont largement répandus dans la nature et incluent des bactéries, des champignons, des virus, des levures et des protozoaires (Raymaekers *et al.*, 2020; Volynchikova & Kim, 2022). Les stratégies de biocontrôle microbien représentent des solutions prometteuses pour améliorer la protection des plantes contre les ravageurs et les maladies tout en réduisant l'utilisation de pesticides chimiques (Syed Ab Rahman *et al.*, 2018; Legein *et al.*, 2020). Ces approches reposent sur l'emploi de micro-organismes ou de leurs sous-produits pour combattre les agents nuisibles, que ce soit à travers des réactions antagonistes comme l'antibiose, la prédation, le parasitisme ou la compétition pour l'espace et les ressources, ou par des interactions indirectes, notamment en modulant l'immunité des plantes (Köhl *et al.*, 2019; Legein *et al.*, 2020).

La lutte biologique par inoculation est une méthode qui consiste à introduire activement et périodiquement des agents de contrôle dans un environnement cible. Ces produits peuvent être formulés à partir d'une seule souche et sont appliqués soit par arrosage du sol pour les micro-organismes vivants dans le sol ou les endophytes, ou encore par pulvérisation foliaire pour les organismes résidant dans la phyllosphère (Sessitsch *et al.*, 2019). L'objectif de cette méthode est de diminuer les populations de ravageurs ou d'agents pathogènes, généralement sur une période limitée, car les organismes inoculés ne s'établissent pas de manière permanente et nécessitent des réintroductions régulières (Bartoli *et al.*, 2020). L'efficacité des inoculants microbiens peut varier considérablement, étant fortement influencée par les conditions de l'environnement récepteur, le génotype de la plante et la méthode d'application (Bartoli *et al.*, 2020). De plus, les principaux défis à l'établissement durable des inoculants dans le microbiote incluent leur faible compétitivité par rapport à un microbiote du sol bien adapté, la prédation, ainsi que les faibles taux de colonisation des plantes (French *et al.*, 2021; Compant *et al.*, 2024).

En 2020, 200 souches microbiennes ont été homologuées au niveau mondial comme agents de biocontrôle contre les agresseurs des plantes (Bartoli *et al.*, 2020), principalement issues des genres bactériens *Bacillus* (par exemple, *B. thuringiensis* et *B. subtilis*), *Pseudomonas* (tels que *P. fluorescens* et *P. putida*), *Streptomyces*, *Mycobacterium*, ainsi que des champignons tels que *Trichoderma* (comme *T. harzianum* et *T. virens*) (van Lenteren *et al.*, 2018).

Les interactions entre le microbiote des plantes et les oomycètes pathogènes

Les oomycètes sont des organismes eucaryotes du règne des Straménopiles qui ressemblent superficiellement à des champignons filamenteux. Les maladies qu'ils provoquent comprennent les brûlures foliaires, la fonte des semis, les pourritures des tiges et des racines, les pourritures des fruits, les mildious, les rouilles blanches, etc. qui entraînent des pertes économiques importantes et de graves dommages aux écosystèmes naturels (Kamoun *et al.*, 2015; Sharma *et al.*, 2021). Les oomycètes les mieux étudiés sont les *Phytophthora*, auxquels appartiennent les espèces les plus connues tel que par exemple *P. infestans*, connue pour avoir

déclenché la famine de la pomme de terre en Irlande (Judelson & Blanco, 2005; Kamoun *et al.*, 2015). Les oomycètes sont remarquablement diversifiés dans leurs modes de vie : biotrophes, nécrotrophes ou hémibiotrophes. Leur cycle de vie comprend plusieurs phases, alternant entre des formes asexuées et sexuées (Sharma *et al.*, 2021). La colonisation de la plante hôte par la majorité des oomycètes commence lorsqu'un sporange asexué libère des zoospores, qui s'enkystent et forment un tube germinatif. Lors des conditions favorables, ils produisent des spores asexuées appelées zoospores, qui se déplacent dans l'eau grâce à leurs flagelles et nagent jusqu'à la surface de la plante, perdent leurs flagelles et s'enkystent, s'attachant fermement à la surface de la plante. Ces zoospores peuvent infecter les plantes et donner naissance à de nouvelles colonies. En cas de conditions défavorables, certains oomycètes forment des structures de survie appelées oospores, qui permettent de résister à des périodes de stress environnemental. La reproduction sexuée se produit lorsque deux gamètes s'unissent pour former des oospores, assurant ainsi la diversité génétique.

Les interactions avec le microbiote résident peuvent agir sur la croissance et la virulence de l'oomycète (Kemen, 2014; Larousse & Galiana, 2017). Dans leur revue Larousse and Galiana (2017) ont proposé différents modes d'action par lesquels les membres du microbiote de l'hôte (plante ou animal) peuvent réguler positivement ou négativement l'infection par un oomycète pathogène : altérer la mobilité des zoospores, leur adhésion à l'hôte, la germination des kystes et l'élongation des hyphes, la pénétration et la croissance invasive dans l'hôte, la dissémination des propagules dans le sol.

Les interactions microbiote-oomycètes pendant le cycle asexué

De nombreux micro-organismes présentent une activité antagoniste contre les oomycètes, en particulier contre les espèces de *Phytophthora* (Volynchikova & Kim, 2022), qui sont les plus étudiées dans ce groupe. Par exemple, la souche *Bacillus licheniformis* BL06 dispose de divers mécanismes inhibiteurs contre *Phytophthora capsici*, notamment la lyse des hyphes et des zoospores, ainsi que l'inhibition du développement des sporanges. De plus, l'application de cette souche a réduit la motilité, la germination et l'allongement du tube germinatif des zoospores, des effets attribués à une protéine antifongique, la carboxypeptidase (Wang *et al.*, 2014). Un autre exemple est celui des filtrats de culture de la souche fongique *Aspergillus flavipes* ATCC24487, un champignon de la rhizosphère, identifiés comme inhibiteurs puissants de la croissance mycélienne de diverses espèces de *Phytophthora*. Ces extraits ont significativement réduit la pathogénicité de *P. parasitica* sur *Nicotiana benthamiana*, en inhibant la croissance mycélienne de l'oomycète et provoquant d'importantes anomalies dans le développement de ses hyphes. De plus, ce champignon empêche la germination, réduit la viabilité des zoospores et freine la production des sporanges (El-Sayed & Ali, 2020).

Chez *Arabidopsis thaliana* et d'autres systèmes végétaux, l'infection par un oomycète induit des modifications significatives du microbiote, que ce soit en favorisant la croissance de certaines bactéries bénéfiques (Berendsen *et al.*, 2018; Vlasselaer *et al.*, 2024) ou en réprimant des populations microbiennes via des composés antimicrobiens (Gómez-Pérez *et al.*, 2023). Par exemple, Berendsen et son équipe (2018) ont signalé la promotion d'un consortium

bactérien composé d'un *Microbacterium*, d'un *Sténotrophomonas* et d'un *Xanthomonas* sp. dans la rhizosphère d'A. thaliana (Stenotrophomonas sp., Xanthomonas sp. et *Microbacterium* sp.) lors d'une infection foliaire par *Hyaloperonospora arabidopsidis*. Lorsqu'elles ont été pré-inoculées en mélange dans des sols cultivant des plantes d'Arabidopsis, ces trois souches ont induit une résistance systémique contre le pathogène et stimulé la croissance des plantes (Berendsen *et al.*, 2018). Ces résultats suggèrent que l'infection foliaire déclenche des signaux systémiques vers les racines, favorisant la croissance d'espèces microbiennes spécifiques et bénéfiques dans la rhizosphère (Berendsen *et al.*, 2018). Dans une autre étude, sur le pathosystème *A. thaliana – Albugo candida*, les auteurs ont montré que le pathogène libère des protéines dans l'apoplaste de la plante hôte, réprimant ainsi les bactéries associées (Gómez-Pérez *et al.*, 2023; Rovenich & Thomma, 2023, p. 202). L'activité antimicrobienne de ces protéines améliore la colonisation de l'hôte par le pathogène , démontrant que l'infection par *A. candida* modifie le microbiote de l'hôte via la sécrétion de composés antimicrobiens (Gómez-Pérez *et al.*, 2023; Rovenich & Thomma, 2023, p. 202). Les auteurs concluent que la manipulation du microbiote est un mécanisme clé pour l'établissement des pathogènes dans leur niche (Gómez-Pérez *et al.*, 2023; Rovenich & Thomma, 2023, p. 202). Enfin, *Albugo laibachii*, a été identifié comme un taxon central du microbiote de la phyllosphère des populations sauvages d'*A. thaliana* (Agler *et al.*, 2016), réduisant considérablement la diversité bactérienne des habitats foliaires épiphytes et endophytes.

À ce jour, aucune étude, à notre connaissance, n'a spécifiquement exploré l'impact de *P. viticola* sur le microbiote naturel de son hôte vigne. Une expérience en laboratoire qui a prélevé et inoculé des microbiotes résidents sur des feuilles de vignes infectés a tout de même montré que l'ensemble de la communauté microbienne de la phyllosphère peut réduire de manière significative la gravité du mildiou (Perazzolli *et al.*, 2014). De nombreux micro-organismes isolés à partir de tissus foliaires de vignes ont été testés individuellement pour leur activité antagoniste contre le mildiou, à la fois sur des feuilles détachées et dans des essais en plein champ. Certains se sont révélés être des candidats prometteurs pour le biocontrôle du stade asexué de *P. viticola* et sont présentés dans des revues (Gessler *et al.*, 2011; Koledenkova *et al.*, 2022; Castrillo-Sequeira *et al.*, 2023; Peng *et al.*, 2024; Nadalini & Puopolo, 2024). En plus d'observer une réduction de la croissance du pathogène, certaines études ont utilisé la microscopie électronique à balayage (SEM) pour explorer les mécanismes sous-jacents et observer directement les dommages infligés aux structures de *P. viticola* (voir Fig. 8). Par exemple, l'examen au microscope a révélé des effets marquants du liquide de fermentation de l'isolat bactérien *Ochrobactrum* SY286 sur la morphologie du mycélium et des sporanges de *P. viticola* (Zang *et al.*, 2020). Des distorsions irrégulières ont été observées dans le mycélium du pathogène, et ses sporanges apparaissaient froissés ou éclatés (Fig. 8E et 8F). De plus, ce liquide de fermentation renfermait divers métabolites, tels que des cellulases, des sidérophores et des protéases, qui pourraient avoir contribué à ces effets observés (Zang *et al.*, 2020).

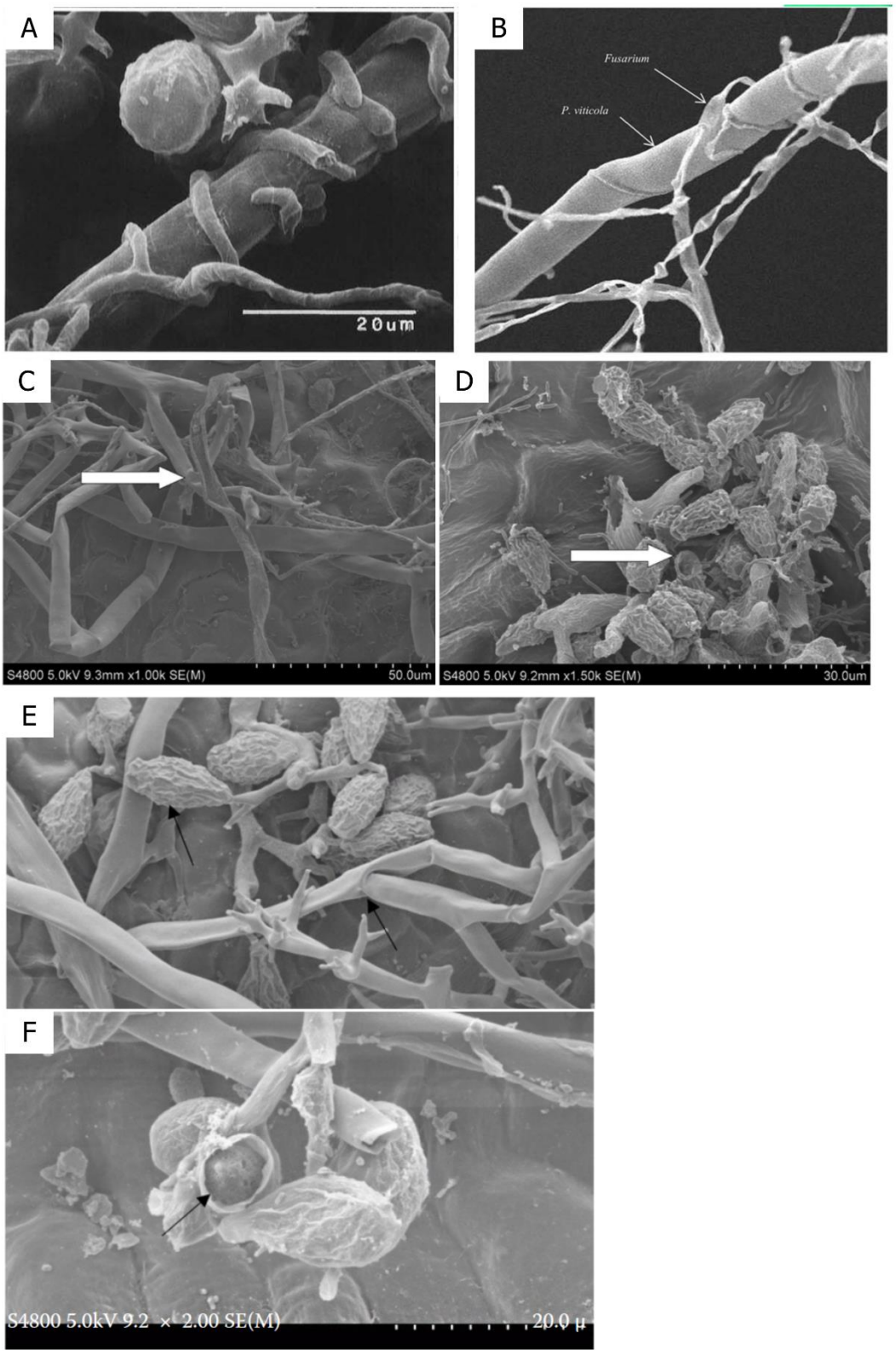


Figure 8 : Photographies illustrant l'antagonisme microbien direct et indirect à l'égard de l'oomycète *Plasmopara viticola*.

(A-B) Hyperparasitisme par une souche fongique de *Fusarium*, enroulée autour d'un sporangiophore de *P. viticola* (source : Falk (1996); Ghule et al. (2018)). **(C-D-E-F)** Antibiose par application d'une liqueur de fermentation produite par une souche bactérienne de *Streptomyces* (**C-D**) et *Ochrobactrum* (**E-F**), provoquant des distorsions irrégulières des mycéliums de *Plasmopara viticola*, ainsi que l'ondulation et la rupture de ses sporanges (source : Liang et al. (2016); Zang et al. (2020)).

Les interactions microbiote-oomycète pendant le cycle sexué

Jusqu'à présent, les recherches sur la relation entre les microbiotes et la forme de conservation hivernale des oomycètes ont été limitées. Pour des raisons évidentes, ces recherches ont été historiquement menées plutôt sur les agents pathogène « tellurique » c'est-à-dire ceux vivant dans le sol et infectant les plantes à travers leurs racines que sur les agent pathogènes des parties aériennes des plantes. Quelques observations au microscope réalisées dans ont tout de même montré que divers taxons bactériens et fongiques provenant de sols naturels peuvent parasiter les oospores de plusieurs espèces d'oomycètes, y compris *Pythium* sp., *Phytophthora* sp. et *Aphanomyces euteiches* (Sneh *et al.*, 1977; Ayers & Lumsden, 1977; Humble & Lockwood, 1981).

Plus récemment une étude de laboratoire a démontré l'activité antagoniste du champignon endophyte *Acremonium byssoides* isolé dans des feuilles sans symptômes de différents cultivars de *Vitis vinifera* contre les oospores de *P. viticola* par le biais de l'hyperparasitisme et de l'antibiose (Conigliaro *et al.*, 2008). Dans une autre étude, des bactéries, des champignons et des levures collectés isolés à partir de matières végétales et du sol de vignobles abandonnés ont efficacement inhibé la germination des oospores hivernant dans des conditions naturelles (Dagostin *et al.*, 2006). Dans cette étude, 5 % des 1 764 micro-organismes avaient une capacité d'inhibition de la germination des oospores et seulement 0,8 % inhibant la production de sporangiophore (Vecchione *et al.*, 2007). Ces résultats suggèrent donc que le sol et les débris végétaux sont un habitat plus propices pour contenir des micro-organismes antagonistes les formes de *P. viticola* contenues dans le sol (les oospores) que des formes produites à la surface des parties aériennes de la vigne (les sporangiophores).

Objectifs et structure de la thèse

L'objectif principal des travaux de cette thèse était de générer des hypothèses sur les interactions entre *Plasmopara viticola* (le pathogène responsable du mildiou de la vigne) et les microbiotes de la vigne et des sols viticoles, dans le but d'identifier des bactéries et des champignons susceptibles d'interférer avec les cycles sexués et asexués du mildiou et de contribuer au développement du biocontrôle microbien du mildiou.

La thèse est divisée en quatre chapitres :

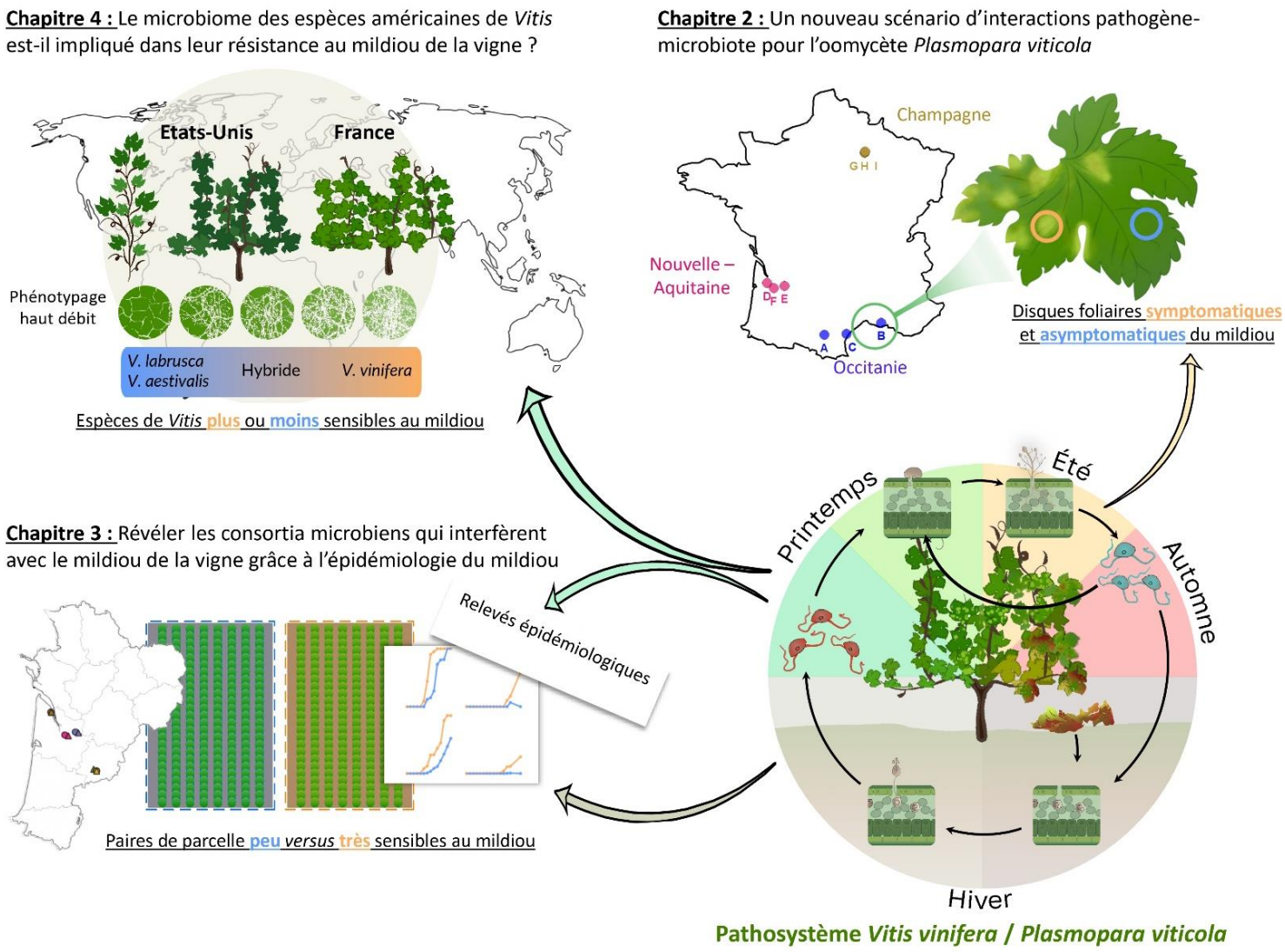
Le premier chapitre est une synthèse bibliographique sur les interactions vigne-microorganismes qui a été publiée en 2022 dans *Advances in Ecological Research* (Fournier, Pellan et al., 2022). Cette synthèse pose les bases conceptuelles et méthodologiques des trois autres chapitres.

Le deuxième chapitre suppose que les tissus foliaires qui restent asymptomatiques pendant une épidémie sont protégés par un microbiote spécifique capable de prévenir ou limiter l'infection. L'objectif était d'identifier les consortia microbiens spécifiques aux tissus foliaires sans symptômes, en comparant leur microbiote à celui des lésions de la maladie. Les données de microbiote ont été collectées en 2018, avant ma thèse, dans neuf parcelles réparties sur

trois grandes régions viticoles françaises, dans un contexte d'épidémie de mildiou. Elles ont été publiées dans un 'papier de données' (Barroso-Bergadà *et al.*, 2023b). J'ai prolongé les analyses statistiques au cours de ma thèse. L'article sera soumis dès que j'aurai terminé les analyses de réseaux d'interactions microbiennes en collaboration avec une équipe de statisticiens de l'Université Paris-Saclay.

Le troisième chapitre suppose que les parcelles historiquement moins sensibles au mildiou, selon les données épidémiologiques de l'IFV, le sont en raison d'un microbiote spécifique capable de prévenir ou limiter l'infection, présent dans le sol ou dans les jeunes feuilles. L'objectif était d'identifier les consortia microbiens propres aux parcelles moins sensibles au mildiou, susceptibles d'interagir avec les phases asexuées et/ou sexuées du pathogène. J'ai collecté les données du microbiote au cours de ma thèse, pendant deux années consécutives (2022 et 2023) et dans dix paires de parcelles, en se concentrant sur trois habitats microbiens (le sol de surface, la phyllosphère, et l'endosphère foliaire, avant l'apparition des premiers symptômes de mildiou). L'article a été soumis à la revue *Microbiome* en septembre 2024.

Le quatrième chapitre analyse le rôle du microbiote foliaire dans la résistance au mildiou de deux espèces de vignes américaines (*Vitis aestivalis* et *Vitis labrusca*), qui sont les hôtes d'origine du mildiou. Les données de microbiote ont été collectées en 2023, dans l'aire d'origine du mildiou (côte Est des Etats-Unis) en collaboration avec une équipe de l'Université de Cornell, ainsi qu'en France dans des collections ampélographiques. Le séquençage du microbiote vient d'être finalisé sur la plateforme de séquençage adossée à AGAP Institut à Montpellier. Les données ont été obtenues le 17 octobre 2024 et n'ont malheureusement pas pu être inclues dans ce document. Elles feront l'objet d'un article de recherche.



Les trois chapitres expérimentaux se distinguent par l'échelle géographique (nationale, régionale, intercontinentale), l'échelle d'étude du microbiote (tissu, parcelle, espèce végétale), les méthodes d'étude du mildiou (phénotypage, relevés épidémiologiques) et les étapes du cycle de vie du mildiou visées.

Chapitre 1 : Le microbiome fonctionnel de la vigne au cours de l'histoire évolutive de la plante et de son cycle de vie

Le premier chapitre de ma thèse est une synthèse bibliographique sur les interactions vigne-microorganismes. Cette synthèse a été co-écrite par 18 auteurs et publiée en 2022 dans *Advances in Ecological Research* (Fournier *et al.*, 2022b). Cette revue bibliographique donne un aperçu des connaissances sur l'évolution du microbiome de la vigne, au cours de la domestication de la plante, chez les différentes espèces de *Vitis* et de l'influence des routes migratoire des pathogènes de la vigne (section 2), puis elle décrit la dynamique du microbiome au cours de la vie de la plante, depuis le stade de la greffe en pépinière jusqu'à l'éventuel dépérissement dans le vignoble (section 3). Dans ces deux sections, nous mettons spécifiquement en évidence les micro-organismes et les virus qui ont une influence démontrée, positive ou négative, sur la performance de l'holobionte-vigne (santé, croissance et qualité des baies). Sur la base de cet état de l'art, nous des approches expérimentales et théoriques qui pourraient conduire à une meilleure compréhension des fonctions du microbiome de la vigne sont suggérées (section 4).

La rédaction de cette synthèse a été coordonnée par Corinne Vacher (UMR SAVE). J'ai réalisé les recherches bibliographiques et l'écriture de la section 2 intitulée « The grapevine functional microbiome throughout evolutionary history », avec l'aide de Patrice This (AGAP Institut). En collaboration avec Lucile Pellan (UMR SAVE, co-premier auteur), j'ai aussi fortement contribué à la synthèse des connaissances sur le microbiome et sur le virome (qui sont rarement étudiés ensemble) présentée dans la section 3. J'ai contribué aux relectures finales et à la mise en forme des références bibliographiques. La section 2 que j'ai rédigée est structurée en trois sous-parties : 2*.1. Microbiome evolution during grapevine domestication and breeding*, *2.2. Microbial interactions in the center of origin of major grapevine pathogens*, *2.3. Microbial dispersal across geographic regions and Vitis species*. Je suis l'autrice des deux figures de cette section (Figures 3 et 4 présentées ci-après). Cette section est le point de départ de ma réflexion sur le chapitre 4 de ma thèse, dont l'échantillonnage a été réalisé aux Etats-Unis en collaboration avec l'équipe de Lance Cadle-Davidson (Université de Cornell, USA).

Chapitre 1

The functional microbiome of grapevine throughout plant evolutionary history and lifetime

Paola Fournier (*), Lucile Pellan (*), Didac Barroso-Bergadà, David A. Bohan, Thierry Candresse, François Delmotte, Marie-Cécile Dufour, Virginie Lauvergeat, Claire Le Marrec, Armelle Marais, Guilherme Martins, Isabelle Masneuf-Pomarède, Patrice Rey, David Sherman, Patrice This, Clémence Frioux, Simon Labarthe, Corinne Vacher

(*) Co-first authors

Published in *Advances in Ecological Research*

Abstract

European grapevine is a complex holobiont composed of two plant genomes, that of the scion (*Vitis vinifera* L.) and the rootstock (*Vitis* spp.), and a multitude of microbial genomes that collectively form the microbiome. The grapevine microbiome has been extensively described over the last decade, primarily using metabarcoding approaches. Unfortunately, metabarcoding data alone provide little information on microbial functions and outcomes of plant-microbe interactions. Here we review knowledge about the microorganisms that have a demonstrated influence, positive or negative, on the performance of the grapevine holobiont. Our review encompasses bacteria, filamentous fungi, yeasts, oomycetes and viruses. It covers aboveground and belowground microorganisms, including arbuscular mycorrhizal and ectomycorrhizal fungi. We focus on taxa and functions that protect the plant against pathogens and pests, promote growth, increase tolerance to abiotic stresses and highlight those involved in disease and decline. As the outcomes of plant-microbe interactions are labile, we examine the dynamics and functions of grapevine-microbiome interactions over both the plant lifetime and the plant evolutionary history, beginning with plant domestication. Based on the knowledge and gaps we identify, we suggest field sampling designs, culture-based experiments, molecular tools and theoretical analysis methods, including shotgun metagenomics and network models, that could be used in future research to uncover and leverage the full functional potential of the grapevine microbiome.

Keywords

plant-microbe interaction, biogeography, coevolution, *Vitis*, bacteria, fungi, oomycete, virus, metagenomics, microbial network

Introduction

European cultivated grapevine is a complex and dynamic system of plant-microbe interactions that has been shaped by humankind to produce grapes and wine. Each plant individual is typically composed of two plant genomes, that of the rootstock (*Vitis* spp.) and the scion (*Vitis vinifera* L.), onto which are linked a multitude of microbial and viral genomes. The set of microbial genomes forms the microbiome (Berg et al., 2020; Compant et al., 2019; Saikkonen

et al., 2020), while the set of viral genomes forms the virome (Roossinck, 2010). The whole, including the plant genomes, forms the hologenome (Bettenfeld et al., 2021; Zilber-Rosenberg and Rosenberg, 2008; Theis et al., 2016). This concept of each grapevine individual as being a complex and dynamic system of plant-microbe interactions (i.e. an holobiont; Bettenfeld et al., 2021; Vandenkoornhuyse et al., 2015) has not been necessary, for most of human history, to grow vines and produce wine. It could provide solutions in the future, however, to maintain grapevine cultivation in a context of climate change (Gambetta *et al.*, 2020) and pesticide-free agriculture (Jacquet et al., 2022; Pertot et al., 2017).

The objective of this chapter is to present the state of art about the dynamics of grapevine-microbiome interactions, from the evolutionary time scale to the seasonal scale, and to propose some research avenues to increase knowledge on the functions of the grapevine microbiome. The chapter first gives an overview of the evolution of the grapevine microbiome, starting with grapevine domestication (Section 1), and then describes the microbiome dynamics during the lifetime of each plant, from the grafting stage in the nursery through to decline in the vineyard (Section 2). In both sections, we specifically highlight those microorganisms and viruses that have a demonstrated influence, positive or negative, on the performance of the grapevine holobiont (health, growth and berry quality). Based on this state of art, we suggest experimental and theoretical approaches that could lead to a better understanding of the functions of the grapevine microbiome (Section 3). We propose some experiments to identify the microbial taxa and functions that play a key role in grapevine performance under drought conditions and in agro-ecological settings. We describe how to decipher the microbial interaction networks to which these key taxa belong, to understand how they maintain in the system and regulate grapevine performance. We also provide recommendations about the biogeographic regions that could be explored in the future to isolate beneficial microbial taxa, which could then be inoculated to drive the system.

The grapevine functional microbiome THROUGHOUT evolutionary history

This section reviews the knowledge and gaps regarding microbiome evolution during grapevine domestication and breeding, as well as the microbiome dynamics triggered by microbial dispersal across geographic regions and between members of the *Vitis* genus. Based on this state of art we hypothesize which geographic regions and plant genetic material are most likely to be associated with beneficial microbial taxa and functions (Fig. 1 and 2).

Microbiome evolution during grapevine domestication and breeding

The Transcaucasus (i.e. the geographic region between Black and Caucasian Sea, which today corresponds to Armenia, Georgia, and Azerbaijan) is the cradle of viticulture (Fig. 1). It is the most probable region of domestication of grapevine 6.000 to 8.000 years ago (Zohary & Hopf, 1993; This *et al.*, 2006), even if secondary domestication probably occurred later in western Europe (Arroyo-García *et al.*, 2006; Terral *et al.*, 2010; Sivan *et al.*, 2021). *Vitis vinifera* subsp. *vinifera*, is nowadays the main *Vitis* species used for the production of wine, table grapes and raisins worldwide. It was domesticated from a wild ancestor, *Vitis vinifera* subsp. *sylvestris*

(hereafter referred to as sylvestris), which naturally occurs in Mediterranean Europe (Fig. 1) and southwestern Asia (Di Vecchi-Staraz *et al.*, 2009). In the wild, sylvestris is a liana that climbs trees, and has very small, black and acidic berries produced by dioecious flowers. During domestication, the grape has undergone marked changes, the most important being the evolution of sex (from dioecious to hermaphroditic flowers), the increase in size of berries and bunches, and changes in berry chemical composition (This *et al.*, 2006).

From the Transcaucasus, cultivated grape spread to Europe, first to the Mediterranean region following the main civilizations (Greeks, Romans, Etruscans, Egyptians), then to northern Europe following the arrival of Christianity. At the beginning, cultivars experienced introgressions from local wild grapes (Myles *et al.*, 2011). Genetic flows in the other direction, from cultivated grapes to wild populations, also occurred (Di Vecchi-Staraz *et al.*, 2009). From the medieval period onwards, cultivars evolved by crossings within *Vitis vinifera* subsp. *vinifera*, most likely in a fortuitous way at the beginning (Bowers *et al.*, 1999), then in a more controlled manner, particularly after the emergence of mildews and phylloxera in Europe (Section 1.2). Nowadays *Vitis vinifera* genetic diversity is huge, with 6,000 to 7,000 cultivars in the world. However, the total number of cultivars commonly used is much lower, given that half the worldwide plantings were of just 16 varieties in 2016 (Anderson & Aryal, 2013).

In addition to genetic and phenotypic changes to the plant, grapevine domestication was accompanied by an evolution of fermentative microorganisms, particularly *Saccharomyces cerevisiae*. *S. cerevisiae* is the main agent of wine fermentation and one of the best models for understanding the eukaryotic cell (Botstein & Fink, 2011). It is naturally part of the berry microbiome (Section 2.4) and colonizes many other ecological niches (Schacherer et al., 2009). *S. cerevisiae* strains naturally occurring in cultivated grapevines are often referred to as vineyard yeasts or domesticated yeasts. The comparison of vineyard and non-vineyard *S. cerevisiae* strains revealed that the oldest lineages and greatest genetic variability are found in the non-vineyard strains (Fay & Benavides, 2005). This is consistent with the hypothesis that *S. cerevisiae* originated in natural environments and was subsequently domesticated by humans. Molecular analyses revealed that domesticated *S. cerevisiae* strains have a single origin. The initial domestication event probably occurred in Mesopotamia, concomitantly with the grapevine domestication event (Legras *et al.*, 2007). Domestication was followed by a marked phenotypic divergence between vineyard and non-vineyard yeasts. For instance, vineyard yeasts show greater resistance to copper sulfate (Fay *et al.*, 2004; Warringer *et al.*, 2011), a chemical compound used as a fungicide against downy mildew since the 1880s, strongly suggesting that vineyard yeast populations have evolved in response to agricultural practices.

How has the microbiome of European cultivated grapevine, *Vitis vinifera* subsp. *vinifera*, evolved during grape domestication? Little is known for many species apart from *S. cerevisiae* (reviewed above). Several studies have suggested that grapevine domestication caused a decrease in microbiome diversity and a change in microbiome functions. Wild sylvestris grapes are inhabited by a greater diversity of endophytic bacteria, epiphytic yeasts and arbuscular mycorrhizae than domesticated grapes (Ocete *et al.*, 2015; Campisano *et al.*, 2015a; Cordero-

Bueso *et al.*, 2017). Moreover, microbial communities of wild and domesticated grapes differ in their potential for pathogen biocontrol and plant growth promotion (Campisano *et al.*, 2015a; Cordero-Bueso *et al.*, 2017). Finally, microorganisms generally associated with humans may have been integrated into the grapevine microbiome during domestication (Campisano et al.; 2014; Youssaf et al. 2014). After the initial domestication event, the grapevine microbiome kept evolving as new varieties were created. Molecular analysis of parental relationships among grapevine varieties identified Heunisch weiss, Pinot noir N and Riesling B as the oldest and least evolved varieties, and also the main progenitors of other varieties (Lacombe *et al.*, 2013). Microbiome taxonomic composition of Pinot and Riesling grape varieties has been compared to that of more recent varieties (Zhang *et al.*, 2020; Bao *et al.*, 2022). The results suggested that the compositions of rhizosphere microbial communities of Pinot and Riesling varieties were more similar to one another than those of more recent grape varieties (Bao *et al.*, 2022). Moreover, the bacterial genera *Pseudomonas* and *Rhizobium*, which include plant growth-promoting strains (Section 2.2), were significantly enriched in the rhizosphere of Pinot noir (Bao *et al.*, 2022). Some bacterial genera (*Bacillus*, *Turicibacter* and *Romboutsia*) were also enriched in the leaf microbiome of Pinot noir (Zhang *et al.*, 2020).

Several studies have hypothesized that wild populations of *V. vinifera* subsp. *sylvestris* constitute a reservoir of useful microbial strains, because wild plants often harbor beneficial endophytes that are absent, or less abundant, in domesticated plants (Ofek-Lalzar *et al.*, 2016; Sun *et al.*, 2020). They explored the microbiome of sylvestris and obtained promising results. For instance, the analysis of the root microbiome showed that sylvestris roots were colonized by ectomycorrhizal fungi and that fungal pathogens were completely absent from roots colonized by these fungi (Radić *et al.*, 2021). The analysis of the berry microbiome of sylvestris revealed a high diversity of yeasts, with some of them having promising prospects for use in oenology (Puig-Pujol *et al.*, 2016; Cordero-Bueso *et al.*, 2017, 2022). Yeast strains belonging to four species (*Meyerozyma guilliermondii, Hanseniaspora uvarum, H. clermontiae, and Pichia kluyveri*), all isolated from sylvestris, reduced growth of molds caused by *Botrytis cinerea, Aspergillus carbonarius*, and *Penicillium expansum* (Cordero-Bueso *et al.*, 2017). Finally, endophytic bacterial strains with biocontrol properties against several pathogens were isolated from sylvestris (Campisano *et al.*, 2015a), including strains belonging to *Pantoea* spp. and *Pseudomonas* spp. that showed antagonistic activity against crown gall agents (*Agrobacterium tumefaciens* and *Allorhizobium vitis*) (Asghari *et al.*, 2019).

To identify and isolate beneficial microorganisms that may have been lost during the domestication process, future research should continue to explore the microbiome of *Vitis vinifera* subsp. *sylvestris* and that of ancestral grapevine varieties. We would recommend focusing on sylvestris populations in the center of origin of cultivated grapevines (i.e. the Transcaucasus region; Fig. 1), where beneficial microbes may have co-evolved with wild progenitors, before being lost in those plants cultivated in the expanded range of grapevine. Such analysis could allow the isolation of plant growth-promoting bacteria (Gutierrez and Grillo, 2022), that might confer tolerance to abiotic stresses and grapevine pathogens of

Eurasian origin (such as *Botrytis cinerea*). The case of pathogens introduced from North America is different and is discussed hereafter (Section 1.2).

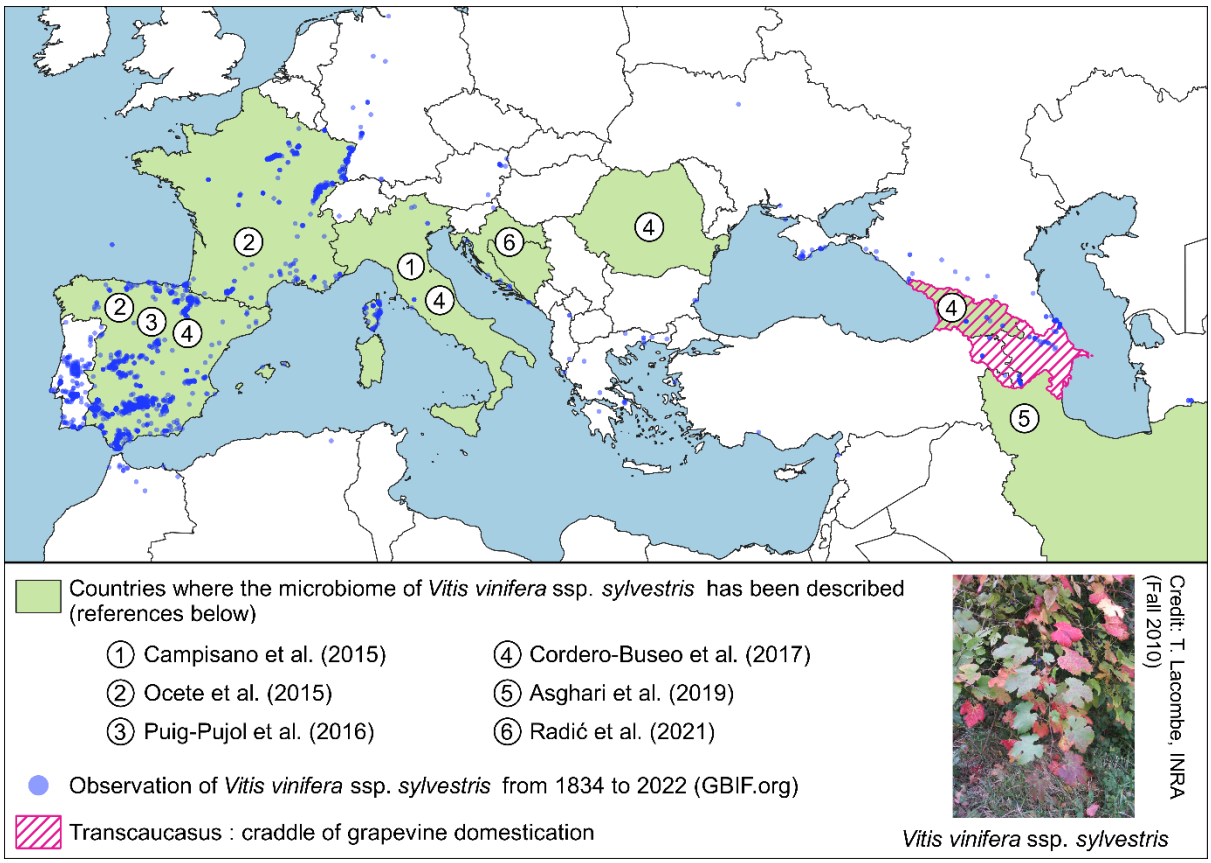


Figure 1: Area of domestication of European cultivated grapevine, Vitis vinifera subsp. vinifera (area hatched in pink), and countries where the microbiome of its wild ancestor, Vitis vinifera subsp. sylvestris, has been described (in green).
Campisano et al. (2015) isolated bacterial endophytes from wild grapevine shoots (1). Ocete et al. (2015) explored taxonomic diversity of arbuscular mycorrhizal fungi in wild grapevine rhizosphere (2). Puig-Pujol et al. (2016) isolated yeast strains at the end of spontaneous fermentations of wild grapes (3). Cordero-Buseo et al. (2017) studied yeasts associated with wild grape berries (4). Asghari et al. (2019) analyzed bacterial endophytes in healthy roots, stems, leaves and fruits of wild grapevines (5). Radić et al. (2021) characterized fungal communities associated with wild grapevine roots with a focus on mycorrhizae (6). For future research, we recommend exploring the center of origin of cultivated grapevines (in pink), studying both the microbiome wild grapevine and that of ancestral grapevine cultivars. Map created using the Free and Open Source QGIS.

Microbial interactions in the center of origin of major grapevine pathogens

In the middle of the 19th century, several fungal pathogen and insect pest species of North American origin crossed the Atlantic and reached Europe, causing the destruction of a large proportion of vineyards (Gessler *et al.*, 2011). These American species included grape phylloxera (introduced in 1863), and the agents of powdery mildew (1848), downy mildew (1878) and black-rot (1885). Phylloxera is caused by the insect *Daktulosphaira vitifoliae*, powdery mildew by the fungi *Erysiphe necator*, downy mildew by the oomycete *Plasmopara viticola*, and black-rot by the fungi *Phyllosticta ampelicida* (asexual stage of *Guignardia bidwellii*). Scientists who established collections of wild American *Vitis* species in botanical

gardens in the early 19th century probably transported these pathogen species to Europe. From there, the diseases spread to other European regions and are now reported in most wine-producing regions of the globe (Bois *et al.*, 2017; Pirrello *et al.*, 2019; Fontaine *et al.*, 2021).

European viticulture was saved by the introduction of native American *Vitis* species (such as *V. riparia*, *V. rupestris* and *V. berlandieri*; Fig. 2) that were resistant to grape phylloxera. Moreover, sulfur, copper and later on, phytosanitary treatments, have been and are still used extensively to protect vines from downy and powdery mildews. The American *Vitis* species were first used to produce rootstocks resistant to phylloxera. Most European cultivated vines, planted since the end of the 19th century, are therefore grafted plants composed of a rootstock tolerant to phylloxera and a scion used to produce berries (Section 2.1). The rootstock and the scion are genetically different and may even belong to different *Vitis* species, which makes European cultivated grapevine an interesting holobiont (Biget *et al.*, submitted). *Vitis* species of American and Asian origin (Fig. 2) have also been used to produce interspecific hybrids cultivated on their own roots (This *et al.*, 2006). More recently, they have been used as sources of disease-resistance genes in breeding programs (Merdinoglu *et al.*, 2018) since they are not only resistant to phylloxera but also to other pests and diseases (Cadle-Davidson et al., 2011; Merdinoglu et al., 2018; Staudt and Kassemeyer, 1995; Villano and Aversano, 2020). However, these new disease-resistant varieties are already threatened by pathogen strains able to overcome resistance genes (for downy mildew: Peressotti et al., 2010, for powdery mildew: Feechan et al., 2015).

As with other plant species, the grapevine microbiome offers tremendous genetic variability that has barely been exploited in breeding programs to date (Gopal & Gupta, 2016). What if American and Asian *Vitis* species still had something to offer to European vineyards? Although this hypothesis has yet to be tested explicitly, the higher resistance of some American *Vitis* accessions to pathogens of North American origin (Fig. 2) could be due to an increased ability of the plant to select a protective microbiome (Gopal & Gupta, 2016; Lyu *et al.*, 2021), in addition to the acquisition of resistance genes in the plant genome. This higher disease-resistance may be the result of a longer coevolution with the pathogens (Jürges *et al.*, 2009a). The resistance of some Asian *Vitis* species (Fig. 2) to mildews is more difficult to explain. The resistance of *V. amurensis* to downy mildew, *Plasmopara viticola,* might be due to the presence in Asia of a related pathogen species, *P. amurensis,* which has similar infection mechanisms (Jürges *et al.*, 2009a). Recent genetic analyses reopened the question of a possible origin of powdery mildew from Asia (Gur *et al.*, 2021), and might account for the resistance of Asian *Vitis* species to powdery mildew.

Several studies have now characterized the microbiome of American and Asian *Vitis* species. They have found a high richness of endophytes (Fan et al., 2020; Kernaghan et al., 2017) and isolated strains with biocontrol properties against pathogens of North-American origin, as well as other pathogens. For instance, *V. amurensis* cv. Shuangyou in China hosted *Alternaria* strains effective against downy mildew (Musetti *et al.*, 2006a). Fungal endophytes isolated from leaves of *V. riparia* in eastern Canada showed high levels of inhibition of gray mold (caused by *Botrytis*

cinerea) and black-foot disease (*Cylindrocarpon destructans*). Fungal strains inhibiting gray mold belonged to *Ramularia pratensis, Phoma aliena* and *Fusarium acuminatum*, while strains inhibiting black-foot belonged to *Ramularia* spp., *Phoma* spp., and *Biscogniauxia mediterranea* (Kernaghan *et al.*, 2017). Similarly, endophytes isolated from *V. labrusca* leaves in Brazil showed *in vitro* antagonistic activity against several grapevine pathogens (Brum *et al.*, 2012; Felber *et al.*, 2016). Isolates of *Flavodon flavus* and *Colletotrichum gloeosporioides* strongly inhibited the root pathogen *Fusarium oxysporum f.* sp *herbemontis* (Brum *et al.*, 2012). Isolates belonging to *Phoma* spp. inhibited the growth of the causal agent of leaf blight (*Alternaria* spp.), isolates of *Fusarium culmorum* regulated anthracnose (*Sphaceloma* spp.) and *Sordariomycetes* isolates controlled ripe rot of grapes (*Glomerella* spp.) (Felber *et al.*, 2016). The fungi *Acaromyces ingoldii*, previously reported for its plant protection functions, was found to be the most abundant taxon in the berry microbiome of muscadine grape (*Muscadinia rotundifolia* Michx.) in China (Sun et al., 2021). In addition, the bacterial genus *Rahnella* was detected in the microbiome of *M. rotundifolia* and might play a role in the biological control of grapevine crown gall, caused by *Agrobacterium vitis* (Chen *et al.*, 2007).

To move toward pesticide-free viticulture, research on the microbial biocontrol of diseases of North American origin (powdery mildew, downy mildew and black-rot) should be fostered. To identify candidate biocontrol agents, we would recommend analyzing the microbiome of American *Vitis* species in their native range (Fig. 2), where they have co-evolved with the pathogens and the rest of the microbiome. It could also be relevant to analyse the microbiome of resistant Asian *Vitis* species (Fig. 2) in areas where they have co-evolved with pathogens related to pathogens of North-American origin. The level of disease-resistance should first be evaluated and the microbiome of all plant compartments colonized by pathogens should be characterized. To highlight microbial taxa that play a role in disease resistance (Section 3.1), the microbiomes of resistant accessions could then be compared to that of sensitive ones in the same geographic region. The inference of microbial interaction networks in resistant *Vitis* species could also generate hypotheses about the microbial taxa or consortia conferring disease resistance (Section 3.3).

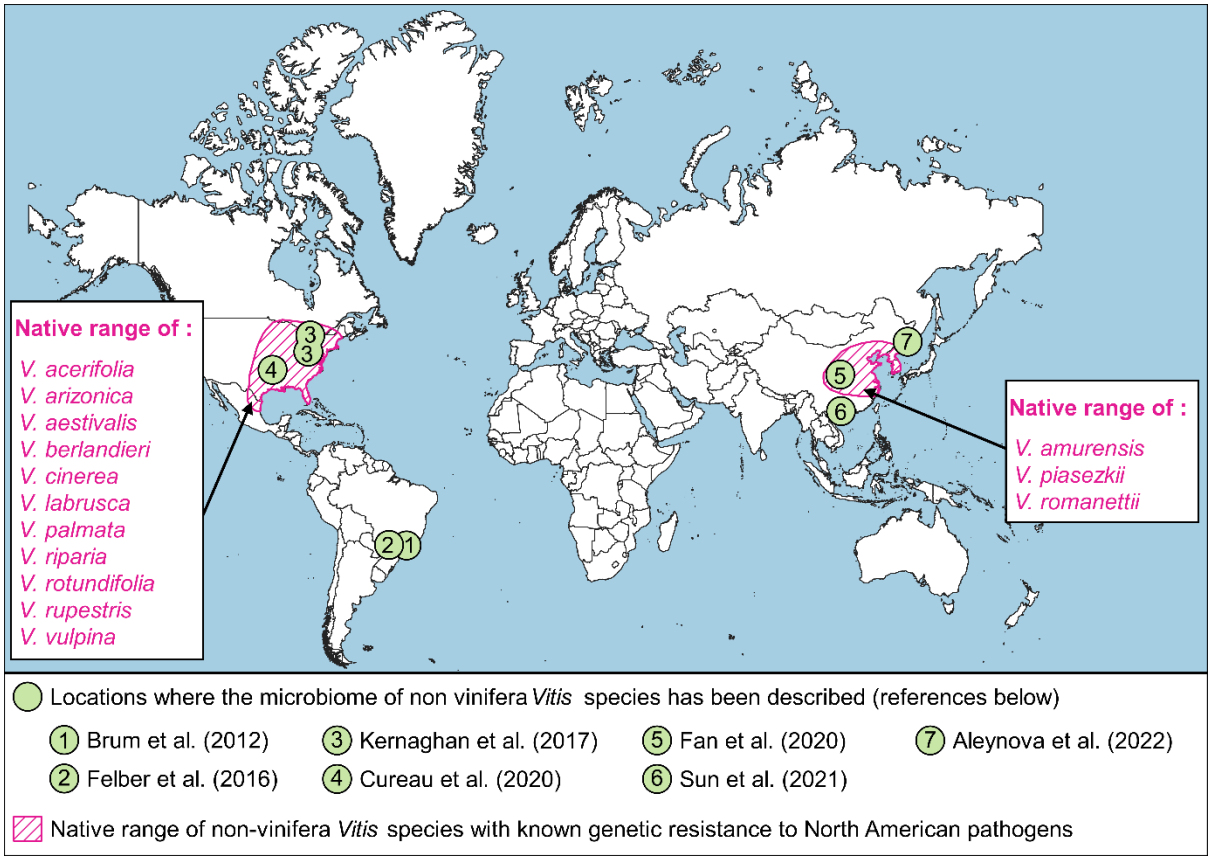


Figure 2: Geographic locations where the microbiome of American and Asian *Vitis* species, partially or totally resistant to pathogens of North American origin (*Plasmopara viticola*, *Erysiphe necator* and *Phyllosticta ampelicida*), has been described (green circles), as well as the native range of these resistant Vitis species (area hatched in pink) (from Wan et al., 2013).

Brum et al. (2012) isolated foliar fungal endophytes from *V. labrusca* cv. Niagara Rosada collected in Brazil (1). Felber et al. (2016) isolated foliar endophytic fungi from grapevine cultivars Bordô and Concord (*V. labrusca*) in Brazil (2). Kernaghan et al. (2017) analyzed foliar fungal endophytes of a cultivated hybrid grape variety (L'Acadie blanc) and one of its native progenitors (*V. riparia*) in eastern Canada (3). Cureau et al. (2021) explored the taxonomic diversity of berry fungal communities in *V. vinifera*, *V. rotundifolia*, *V. aestiva*lis, and in hybrid *Vitis* grape varieties grown in different vineyards in Arkansas (4). Fan et al. (2020) compared endophytic fungi of *V. vinifera* cv. Red Globe (cultivated grape) with those of *V. amurensis* cv. Shuangyou (wild grape) grown in a nursery in China (5). Sun et al. (2021) studied the berry microbiome of six muscadine (*Muscadinia rotundifolia* Michx.) cultivars grown in Guangxi, China (6). Aleynova et al. (2022) compared endophytic bacterial communities of a wild grape population of *V. amurensis* in Russia with those of domesticated *V. vinifera* cultivars from Germany and California (USA) (7). Studies that focused on microorganisms isolated during or at the end of spontaneous grape fermentations are not reported on this map. For future research to identify microbial biocontrol candidates against mildews and black rot, we suggest further exploration of the microbiome of these resistant *Vitis* species in their native range (area hatched in pink), where they have co-evolved with pathogens or with related pathogens. Map created using the Free and Open Source QGIS.

Microbial dispersal across geographic regions and *Vitis* species

As described above, cultivated grapevine is a complex holobiont that incorporates plant and microbial genomes of European, American and Asian origin (Sections 1.1 and 1.2). To understand how this complex system has assembled and evolved since grapevine

domestication (Section 1.1), it is necessary to understand the origin and migratory routes of grapevine-associated microbes. To date, research has focused on the migratory flows of the oenological yeast *Saccharomyces cerevisiae* as well as those of major pathogens of grapevine (*Plasmopara viticola*, in particular).

Molecular evidence for the historical presence of *Saccharomyces cerevisiae* in wine fermentation was obtained from pottery jars hidden in the tomb of King Scorpio I, one of the earliest kings of Egypt, dating back to 3150 BC (Cavalieri *et al.*, 2003). At that time, fermentations were only spontaneous (Marsit & Dequin, 2015), suggesting that *S. cerevisiae* was already an integral part of the berry microbiome. Legras et al. (2007) analyzed migration routes of *S. cerevisiae* and showed that they correspond to the known migration routes of cultivated grapevine (Grassi & De Lorenzis, 2021). From Lebanon, yeast migration may have taken place across the Mediterranean region towards Italy, Spain and France, through three main routes: (1) the Rhône Valley-Burgundy-Alsace and Nantes route that goes along the Rhône and Loire rivers; (2) the Italy-Cognac route; and, (3) the Danube Valley route. This migration of vineyard yeast strains is accounted for, at least in part, by the trade of grape varieties. For instance, the Muscadet grape variety was imported from Burgundy to Nantes during the 15th century, while Ugni blanc, the dominant grape variety in the French Cognac region, originated in Italy. Genetically-distant Austrian yeast strains were domesticated from local wild sylvestris populations (Section 1.1).

Plasmopara viticola is a complex of five species, each with a unique degree of host specialization within the American Vitaceae (Rouxel *et al.*, 2013, 2014; Fontaine *et al.*, 2021). Fontaine et al. (2021, 2013) found that all invasive grapevine downy mildew populations worldwide belonged to the small clade *P. viticola* f. sp. *aestivalis,* which parasitizes *Vitis aestivalis* in Northeast America (Fig. 1). *P. viticola* was first introduced into Western Europe in the middle of the 19th century (Section 1.2), and spread to Central and Eastern Europe. Fontaine et al. (2013) and Gobbin et al. (2006) revealed, using population genetic methods, a low genetic diversity and weak population structure for *P. viticola* across European vineyards, suggesting that the strains initially introduced into Europe came from a single source population of North American origin. European populations of downy mildew then served as a source for secondary introductions into other viticultural regions of the world, including China, South Africa, and Australia. A third introduction event occurred later, that spread the disease from Australia to Argentina.

The migration routes of *Erysiphe necator* and *Phyllosticta ampelicida* have been less studied than those of *Plasmopara viticola*. According to Brewer and Milgroom (2010), populations of *E. necator* in Europe are derived from two separate introductions from the Eastern United States. These initial introductions into Europe were followed by secondary introductions from Europe into the Western United States and Australia. Recently, Gur et al. (2021) proposed an additional non-American (possibly Asian) origin of *E. necator*. There is even less knowledge of the invasion pathways of *P. ampelicida* (Narduzzi-Wicht *et al.*, 2014). Rinaldi et al. (2017) suggested that the pathogen was introduced into Northeastern Italy from Eastern Europe and

that two introductions occurred in Portugal, one from France or Italy, and another from America. Interestingly, these American pathogens not only colonized the European cultivated grapevine *Vitis vinifera* subsp. *vinifera*, but were also incorporated into the microbiome of its wild ancestor *Vitis vinifera* subsp. *sylvestris* (Section 1.1). As a result, the distribution of wild grapevines has been greatly reduced over the last 150 years and it is now considered an endangered plant species in Europe (Arnold *et al.*, 2005).

Future research should continue unravelling the migratory routes of grapevine pathogens and extend these efforts to other member of the functional microbiome (Section 2). This is crucial to identify those geographic locations where grapevine-pathogen-microbiome co-evolution has occurred, as well as the *Vitis* species involved in this coevolutionary process (Fig. 2). This knowledge is necessary to design microbiome studies informed by the biogeography and evolutionary history of grapevine. Microbiome dynamics on a smaller temporal scale should also be considered and is discussed below (Section 2).

The grapevine functional microbiome THROUGHOUT plant lifetime

This section describes how the microbiome assembles, functions and changes over the course of grapevine life. It highlights the plant-microbe interactions that have a proven, direct and significant influence on the grapevine performance (growth, health and berries quality) at every life stage (Fig. 3). The section deals with both the microbiome (bacteria, filamentous fungi, yeasts and oomycetes) and the virome, including phytoviruses (plant-infecting viruses), mycoviruses (fungi-infecting viruses) and phages (bacteria-infecting viruses). It covers both aboveground and belowground microorganisms, including arbuscular mycorrhizal and ectomycorrhizal fungi.

Initial microbiome and virome at the graft stage

The life of cultivated grapevine generally begins in a nursery with a graft (Fig. 3). The two components of the graft, the scion and the rootstock, are produced in nursery “mother” plots. Mother plants produce stems that are pruned during the dormant stage in winter to make cuttings that are then stored in a cold room. The rootstock and scion cuttings and the grafted plants then undergo different treatments depending on the country and the nursery (Gramaje & Armengol, 2011). Most often, immediately after grafting, the scion and the graft zone are dipped in a wax solution, which may contain plant growth regulators (mainly auxins) and fungicides. The grafted plants are then incubated for two to three weeks under controlled temperature (28°C) and high humidity (90%), in order to promote callusing. A second waxing step is then performed, before planting in pots in the greenhouse, or in nursery fields. Potted plants can be shipped directly to winegrowers and planted in the field next autumn, while plants kept in nursery fields are usually shipped as one-year-old, bare-root plants to be planted in spring.

The many steps of the grafting process are critical for assuring the quality of the plants produced. First, the choice of the two plant genomes is crucial. Not accounting losses due to

incompatibility between genotypes (Tedesco *et al.*, 2022), about 50% of the plants produced are unmarketable because of the low quality of the graft (Carrere *et al.*, 2022). Second, it is fundamental for nurseries to produce plants that do not carry diseases (Waite *et al.*, 2015), in particular phytoviruses. Viruses trigger both graft incompatibility and decline of young vines. For instance, the transmission of grapevine leafroll-associated virus 2 (GLRaV-2; Fig. 3) from scion to rootstock results in graft incompatibility (Rowhani et al., 2017). Rootstock susceptibility to infection depends on the genotype, with genotypes 1616 Couderc, Kober 5BB, 1103 Paulsen being the most susceptible rootstocks (Uyemoto *et al.*, 2000, 2001; Alkowni *et al.*, 2011; Rowhani *et al.*, 2017). Reverse incompatibility, where the rootstock is the source of a latent virus, has not been observed in grapevine yet. The decline of young vines triggered by joint infection with GLRaV-2 and grapevine virus B (GVB) infection, or GLRaV-1 and grapevine virus A (GVA), was also observed (Rowhani *et al.*, 2017). The mechanisms underlying such declines have not been clearly determined yet, but they might involve the production of viral small interfering RNAs (vsiRNAs) by the plant cell machinery, which in turn would affect plant gene expression (Smith *et al.*, 2011). Management of these phytoviruses relies primarily on preventive measures (such as the use of clean propagation and planting materials) and robust diagnostics (Martelli, 1999; Maliogka *et al.*, 2015). In addition, hot water treatment (HWT) of the grafted plant (Eichmeier *et al.*, 2018) is sometimes performed to reduce infection by phytoplasmas (flavescence dorée, bois noir, grapevine yellows) and by fungi responsible for grapevine trunk diseases (Section 2.5). *Trichoderma* spp., which are soil microbes with an antagonistic activity against some pathogenic fungi, are sometimes inoculated by nurseries (Eichmeier *et al.*, 2018; Jaarsveld *et al.*, 2021). Finally, mycorrhiza (*Rhizophagus irregularis,* in particular) can also be inoculated at the nursery stage (Fig. 3), to increase grapevine resistance to biotic and abiotic stresses by promoting the structure and development of the root system (Bettenfeld *et al.*, 2021).

All these manipulations and treatments of scions and rootstocks in the nursery can influence the initial grapevine microbiome and its future trajectory of assembly. Gramaje et al. (2022) analyzed the fungal communities associated with rootstocks harvested in two mother plots located 800m appart. No difference in fungal community composition between these two locations was detected, but the fungal communities varied along the grafting process (after cutting from mother plants, after cold storage and hydration, after grafting and callusing, and in dormant grafted plants). The core mycobiome was composed of the genera *Cadophora, Cladosporium, Penicillium* and *Alternaria* in both rootstocks. Numerous genera associated with grapevine trunk diseases (*Cadophora, Dactylonectria, Diaporthe, Diplodia, Ilyonectria, Neofusicoccum, Phaeoacremonium and Phaeomoniella*; Section 2.5) and potential biocontrol activities (*Aureobasidium pullulans*) were identified (Fig. 3). The pathogenic genus *Neofusicoccum* was persistent throughout the propagation process (Fig. 3), confirming the role of rootstock as a primary source of many pathogens. Lade et al. (2022) compared the contribution of nursery, scion variety and rootstock variety to fungal community composition in the graft zone and found that the nurseries (i.e. plant production practices) played a major role, followed by rootstocks and scion varieties.

To better understand and manage the assembly trajectory of the grapevine microbiome, special attention should be paid to the production practices of grafted plants in nurseries. We recommend using the framework of microbial community coalescence (Rillig *et al.*, 2015) to analyze the influence of grafting on the microbiome. The microbiome of the grafted plant would then be considered as a joining of previously separate communities, forming a new entity that is not easily separable and with properties distinct from the progenitor communities (Rillig *et al.*, 2015). At the graft stage, major physiological changes occur (Cookson *et al.*, 2013; Prodhomme *et al.*, 2019), including vascular connection between rootstock and scion that influences sap flow and associated fluxes of microorganisms (Deyett & Rolshausen, 2020). These physiological processes have barely been studied although they could have a significant impact on the initial microbiome of grafted plants and, through priority effects (Zhou and Ning, 2017), on the recruitment of the microbiome after planting (Section 2.2).

Recruitment of the root microbiome from the soil reservoir

Winegrowers usually receive grafted vines (potted or bare-rooted) from nurseries (Section 2.1) for planting in their vineyards. The young plants then begin to recruit microorganisms from the soil (Fig. 3), which is the major reservoir of microorganisms for the plant microbiome (Liu *et al.*, 2019; Swift *et al.*, 2021; Griggs *et al.*, 2021). Recruitment is based on the active release by the roots of a wide range of carbon-containing compounds known as rhizodeposits (Chaparro *et al.*, 2014; Martínez-Diz *et al.*, 2019). The rhizodeposits represent nearly 40% of the photosynthates produced by a plant (Bais *et al.*, 2006). These compounds serve as a substrate for the development of microorganisms and make the rhizosphere (i.e. the transition zone between soil and plant roots) much more attractive for microbes than surrounding soil. The nature and quantity of rhizodeposits depend on the plant genotype and vary across seasons and throughout plant life, allowing the plant to actively shape the composition of rhizosphere microbial communities (Berlanas *et al.*, 2019). Beneficial microorganisms may for instance be recruited under stressful conditions, a mechanism known as the "cry for help" reaction (Rizaludin *et al.*, 2021). Some rhizospheric microorganisms develop physical interactions with the root (case of mycorrhizae, for instance) and some of them can even enter the root endosphere. Once in the root endosphere, some microorganisms colonize the vascular tissues and disseminate in the aerial parts of the plant (Fig. 3), sometimes reaching leaves and berries (Liu *et al.*, 2019; Darriaut *et al.*, 2022). Not all microorganisms can colonize the plant internal tissues from surrounding soil, which creates a decreasing gradient of microbial diversity from the outside of the root towards the inside (Zarraonaindia *et al.*, 2015b; Marasco *et al.*, 2018; Martínez-Diz *et al.*, 2019).

Many studies have examined the taxonomic composition of the grapevine rhizosphere and root microbiome. The same major taxonomic groups are generally represented. Pseudomonadota, Actinomycetota and Acidobacteriota (formerly named Proteobacteria, Actinobacteria and Acidobacteria; Orren and Garrity, 2021) are the dominant bacterial phyla, followed by Bacillota and Bacteroidota (i.e. Firmicutes and Bacteroidetes) (Zarraonaindia *et al.*, 2015b; Novello *et al.*, 2017; Dries *et al.*, 2021; Bettenfeld *et al.*, 2021). Ascomycota, followed

by Basidiomycota, are the dominant fungal phyla (Bettenfeld et al., 2021; Liu and Howell, 2021). At a finer taxonomic scale, the microbiome composition varies with soil physical and chemical features (Bettenfeld et al., 2021; Signorini et al., 2021), geography and climate (Hernandez & Menéndez, 2019; Liu *et al.*, 2019), plant age and rootstock genotype (Berlanas et al., 2019; Ji et al., 2019), and vineyard management practices (Likar *et al.*, 2017) including applications of plant protection products and fertilizers (Canfora *et al.*, 2018; Zaller *et al.*, 2018) and the presence of vegetation cover (Vukicevich *et al.*, 2018).

Root-microbe interactions can foster vine growth and productivity through various mechanisms. Plant Growth-Promoting (PGP) microbes (Fig. 3) can solubilize and make available nutrients to the roots (Darriaut *et al.*, 2022). The mineral elements needed by the plant (phosphorus, nitrogen and phosphate) are naturally present in the soil but cannot be efficiently or directly assimilated by plants because they are complexed with other molecules. Other PGP bacteria produce enzymes (phosphatases) or organic acids (e.g. hydrogen cyanide; Rijavec and Lapanje, 2016) that solubilize inorganic phosphate, while others produce ammonium (NH4+) or convert nitrites (NO2-) to nitrates (NO3-), that are easily absorbed by the plant. Bacteria, including *Bacillus herbersteinensis, Bacillus licheniformis, Micrococcus* spp.*, Pseudomonas* spp., and *Pantoea agglomerans*, can combine these mechanisms (Baldan *et al.*, 2015; Asghari *et al.*, 2020). In the grapevine rhizosphere, the bacterial genera *Pseudomonas, Streptomyces* and *Rhizobia* are those most involved in phosphorus and nitrogen cycles (Bona *et al.*, 2018). Some fungal genera are also involved in phosphate solubilization, such as the genus *Mortierella* (Liu & Howell, 2021; Carbone *et al.*, 2021). Rhizosphere PGP bacteria (Fig. 3) can also produce hormones, such as auxin, which directly stimulates plant growth (Morales-Cedeño *et al.*, 2021). For instance, *Agrococcus baldri* and *Paenibacillus* spp. produce hormones that, even at low concentration, cause root elongation, branching and increase root diameter and density (Baldan *et al.*, 2015). Bacterial species, such as *Bacillus amyloliquefaciens*, can produce microbial siderophores, which bind with iron, and contribute to plant iron nutrition (Mardanov *et al.*, 2019). Other endophytic bacteria associated with root tissues (*Pseudomonas* spp., in particular), produce enzymes (ACC-deaminases) that cleave ACC (1-aminocyclopropane-1-carboxylic acid), which is the immediate precursor of ethylene in plants. This reduces the production of ethylene and limits the damage caused by biotic and abiotic stresses (Saraf *et al.*, 2010; Marasco *et al.*, 2018).

Arbuscular mycorrhizal fungi (AMF) also play an important role in water and nutrient absorption. Belonging mainly to the *Glomeromycota* phylum, these endomycorrhizal fungi establish symbioses with vine roots (Balestrini *et al.*, 2010). Hyphae increase the exchange surface between the vine roots and the soil. They also activate phosphorus and nitrogen transporters in root cortical cells (Trouvelot *et al.*, 2015). AMF are the most abundant mycorrhizae associated with grapevine roots and include species belonging to the genera *Acaulospora, Diversispora, Funneliformis, Glomus* and *Rhizophagus* (Liu & Howell, 2021; Darriaut *et al.*, 2022). They are actively recruited by vine roots during water stress (Carbone *et al.*, 2021).

Grapevine roots are not only colonized by beneficial microorganisms such as PGP and AMF, but also by bacterial, fungal and viral pathogens (Fig. 3). The bacterial pathogen *Allorhizobium vitis,* the causal agent of crown gall, is frequently isolated from diseased plants in the vineyard (Habbadi *et al.*, 2020). The bacteria harbors tumor-inducing plasmids (pTi), part of which integrate into the plant genome (Transfert-DNA, T-DNA) to induce the development of root or crown galls and the synthesis of opines, which the bacteria utilizes as nutrients. The spread of pTI plasmids can be facilitated by bacteria belonging to the *Novosphingobium* genus, which are therefore pathogen stimulants (Gan *et al.*, 2019). Black-foot disease, caused by *Ilyonectria* spp. (*I. liriodendri*, in particular), is responsible for root necrotic lesions, with a reduction in root biomass, besides other symptoms that include reduction of internodes, loss of vigor, patchy foliage and smaller leaves (Bleach *et al.*, 2021). The fungal genus *Ilyonectria* is found in many metabarcoding analyses of vineyard soil because it can persist for several years after the removal of infected vines (Brito *et al.*, 2019; Deyett & Rolshausen, 2020; Liu & Howell, 2021; Rivas *et al.*, 2022). Several fungal genera associated with grapevine trunk diseases (*Botryosphaeria* and *Diplodia*; Section 2.5), Petri disease (*Cadophora, Phaeoacremonium* and *Phaeomoniella*) and Diaporthe dieback (*Diaporthe*) have been detected in asymptomatic root tissues (Martínez-Diz *et al.*, 2019; Deyett & Rolshausen, 2020; Liu & Howell, 2021; Rivas *et al.*, 2022). *Candidatus phytoplasma* spp., the causal agent of bois noir disease, was also detected in healthy root tissues (Marasco *et al.*, 2018), indicating that the root endosphere may be an important reservoir for latent pathogens (Martínez-Diz *et al.*, 2019; Liu & Howell, 2021). Finally, grapevine roots can be infected by phytoviruses, some of which are transmitted by soil nematodes. For instance, grapevine fanleaf virus (GFLV) and arabis mosaic virus (ArMV), the main causal agents of grapevine fanleaf disease, are transmitted by the nematode species *Xiphinema index* and *Xiphinema italiae* in the case of GFLV, and *Xiphinema diversicaudatum* in the case of ArMV (Oliver & Fuchs, 2011). The nematodes feed on the tips of growing roots by pricking them with a stylet. By successively feeding on neighboring vines, they disseminate the virus retained in their esophageal tracts (Maliogka *et al.*, 2015), producing the often patchy distribution of virus-infected plants.

The root microbiome also harbors microorganisms that directly inhibit pathogen growth, through antagonistic microbial interactions, or indirectly limit disease severity or frequency by stimulating the plant immune system or by acting on vector populations (Fig. 3). Microbial interactions responsible for pathogen biocontrol include antibiosis, hyperparasitism, spatial and nutritional competition, interference with pathogen signaling, and disease symptom reduction by degradation of pathogen toxins or virulence factors (Compant *et al.*, 2013). For instance, the biocontrol activity of *Bacillus amyloliquefasciens* mainly relies on antibiosis. This bacteria synthesizes a wide range of antimicrobial compounds (surfactin, plantazolicin, macrolactin, bacillaene, fengycin, difficidin, bacillibactin, and bacilysin) that regulate the growth of several grapevine pathogen species, including *Botrytis cinerea, Phaeoacremonium aleophilum, Phaeomoniella chlamydospora* (Mardanov *et al.*, 2019). Root microbes also stimulate plant defenses, by inducing oxidative bursts, activating signaling pathways (salicylic acid, ethylene/jasmonic acid), and increasing the synthesis of pathogenesis-related (PR)

proteins, lytic enzymes, polyamines and phytoalexins (Héloir *et al.*, 2019). This stimulation increases the capacity of plants to react to ongoing infections, or to future ones by priming the immune system. Bacteria of the *Burkholderia* genus increase the production of PR proteins when inoculated on the roots of grapevine infected with *B. cinerea* (Esmaeel *et al.*, 2020), and the strain *Burkholderia phytofirmans* PsJN can migrate to the aerial parts of grapevine and form biofilms that directly limit the spread of *B. cinerea* (Miotto-Vilanova *et al.*, 2016). Many other root microorganisms have a proven antagonistic effect on grapevine pathogens but their mode of action is not always known. Other bacteria with a biocontrol activity include *Streptomyces* spp, that reduce young grapevine decline and black-foot disease (González-García *et al.*, 2019; Pilar Martínez-Diz *et al.*, 2021), and *Bacillus subtilis*, which directly limits the growth of fungal pathogens related with grapevine trunk diseases (Berlanas *et al.*, 2019). The latter also stimulates plant defenses, similar to *Pseudomonas fluorescens, Pantoea agglomerans, Acinetobacter lwoffii* (Magnin-Robert *et al.*, 2007; Aziz *et al.*, 2016, 2020). Root fungi, in particular AMF, also play a role in disease biocontrol. AMF of the *Glomus* genus and *Rhizophagus irregularis* reduce the severity of black-foot disease (Berlanas et al., 2019; Darriaut et al., 2022). AMF may also protect grapevines from GFLV by inhibiting the proliferation and penetration of its nematode vector (*X. index*) in roots (Hao *et al.*, 2018). In addition, the fungal species *Trichoderma atroviride* and *Aureobasidium pullulans* are antagonists of the fungal pathogens associated with Petri disease (*Phaeomoniella chlamydospora and Phaeoacremonium minimum*), and of *Diplodia seriata* which is associated with Botryosphaeria dieback (Martínez-Diz *et al.*, 2019). *T. atroviride* also fosters plant defenses (Stempien *et al.*, 2020). Finally, the oomycete *Pythium oligandrum* has mostly indirect negative effects on fungal pathogens associated with Petri disease (Yacoub *et al.*, 2016).

This state of art demonstrates that grapevine roots constitute a rich microbial compartment that is quite well understood from a functional point of view. Many microorganisms that have a positive (such as PGP bacteria, AMF and biocontrol agents) or negative (such as *Allorhizobium vitis* or phytoviruses) influence on grapevine have been identified and their mode of action has been described. Shotgun metagenomics and metabolomics associated with metabolic network modeling (Section 3.3) could further advance this understanding by allowing us to build predictive models of the nutritional interactions between grapevine and microbes in the rhizosphere (Jacoby et al. 2017). These models could inform the design of microbial consortia to inoculate to boost plant growth and defense. To optimize soil management, future research should focus on belowground-aboveground microbial interactions in vineyards. They could first assess the effects of soil management on soil microbiome (Bettenfeld et al., 2021; Signorini et al., 2021), and then the cascading effects of the soil microbiome on the root, trunk, leaf and berry microbiomes (Sections 2.3 and 2.4) and their consequences on grapevine health and wine quality.

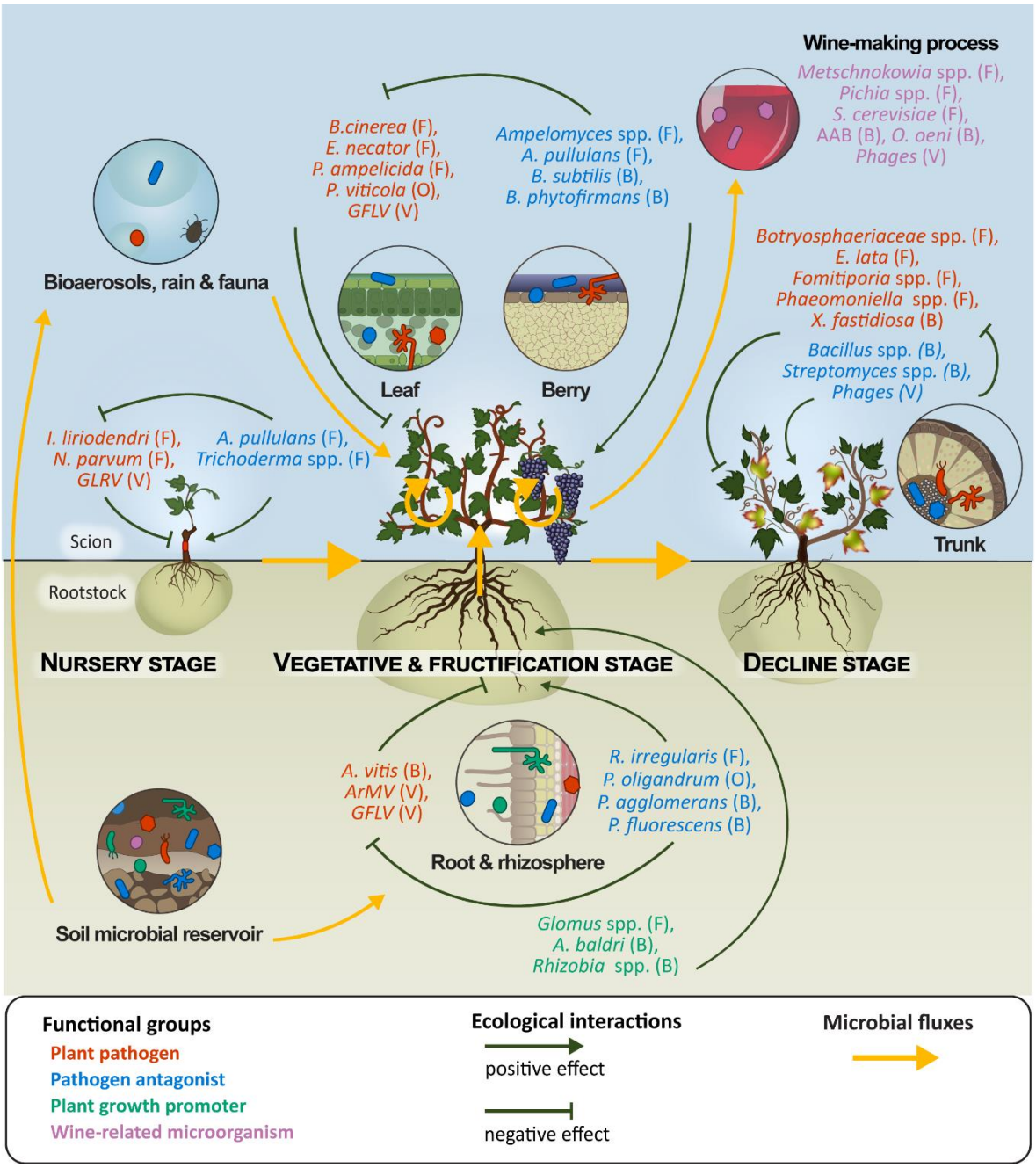


Figure 3: Microbial functional groups that colonize cultivated grapevine from the nursery to plant decline, as well as ecological interactions (black arrows) and microbial fluxes (yellow arrows) that drive the microbiome dynamics during plant lifetime. Plant-microbe-microbe ecological interactions form complex networks (Section 3) that could not be represented here for clarity. Only a few ecological interactions are represented.

For the same reason, we could not represent all the fungal (F), bacterial (B), oomycete (O) species and viruses (V) that significantly influence grapevine performance and wine-making process. We only represented a few well-studied species or species groups. AAB, Acetic Acid Bacteria; GFLV: Grapevine Fanleaf Virus; GLRV, Grapevine Leafroll associated Virus; Other species names: *Agrococcus baldri, Allorhizobium vitis, Aureobasidium pullulans, Bacillus subtilis, Botrytis cinerea, Burkholderia phytofirmans, Candidatus phytoplasma, Erysiphe necator, Eutypa lata, Ilyonectria liriodendri, Neofusicoccum parvum, Oenococcus oeni, Pantoea agglomerans, Phyllosticta ampelicida, Plasmopara viticola, Pseudomonas fluorescens, Pythium oligandrum, Rhizophagus irregularis, Saccharomyces cerevisiae, Xylella fastidiosa.*

Seasonal assembly of the leaf microbiome in interaction with leaf pathogens

The grapevine leaf microbiome is dynamic: it assembles in spring, changes during the vegetative season and then disassembles during leaf senescence. In spring, the buds burst and let the first shoots appear. As vines are lianas, the shoots hang on to the trellis with their tendrils and grow by producing new leaves, at a rate of about one every three days in the Bordeaux area (Calonnec *et al.*, 2008). At a given time, each vine thus displays a mosaic of leaves of different ages. The leaves at the distal end of shoots are the youngest and the leaves near the stock are the oldest (see Fan *et al.*, 2020). As the shoot grows, the young leaves expand, become mature, and are colonized by epiphytic microorganisms (the phyllosphere microbiome *sensu stricto*; Behrens and Fischer, 2022; Vacher et al., 2016a) and endophytic microorganisms (Pacifico *et al.*, 2019) that collectively form the leaf microbiome. The latter is largely dominated by fungi belonging to the Ascomycota and by bacteria belonging to the Actinomycetota, followed by Pseudomonadota and Bacillota (Bettenfeld et al., 2021; Oren and Garrity, 2021; Fort et al., 2016; Singh et al., 2018). The fungal species *Aureobasidium pullulans* was dominant at the end of growing season in several independent metabarcoding studies, representing more than half of the fungal community in old leaves (Grube *et al.*, 2011; Knapp *et al.*, 2021).

Leaf microbiome dynamics depends on many factors, and first and foremost on the specific growth pattern of grapevine (Calonnec *et al.*, 2008, 2018). Indeed, the date at which a leaf emerges determines its morphology and physiology (Majer & Hideg, 2012; Chitwood *et al.*, 2016) and also the microbial fluxes and environmental perturbations to which it will subsequently be exposed. Leaves that emerge first are colonized by microorganisms that overwintered in buds or on woody parts (case of primary infections by the fungal pathogen *Erysiphe necator*, Gadoury et al., 2012), or in senescent leaf debris that remained on the soil (case of primary infections by the oomycete pathogen *Plasmopara viticola*, Burruano, 2000). They are also colonized by microorganisms circulating in the xylem or in the phloem (Fig. 3). These circulating microorganisms may be beneficial, as in the case of the bacterium *Burkholderia phytofirmans* (Compant et al., 2008) or they may be pathogens, like the bacterial pathogen *Xylella fastidiosa* (Deyett and Rolshausen, 2019) and viruses and phytoplasmas (Laimer et al., 2009; Zherdev et al., 2018). Wind and rain disseminate microorganisms from multiple sources (vines, soil, adjacent semi-natural and natural habitats) (Fig. 3) and may also contribute to the initial colonization of the phyllosphere (Abdelfattah *et al.*, 2019; Griggs *et al.*, 2021). By contrast, those leaves that emerge later in the season are in direct contact with other grapevine leaves that already have a more developed microbiome. Leaf-to-leaf transmission of the microbiome (Fig. 3), which may transiently involve the atmosphere or other plant organs, is the dominant microbial colonization pathway in grapevine leaves (Abdelfattah *et al.*, 2019). This transmission is responsible for secondary infection cycles in leaf pathogens. Late-emerging leaves also face greater activity from fauna (arthropods, birds) that are underestimated microbial vectors (Stefanini & Cavalieri, 2018; Griggs *et al.*, 2021). Finally, it should be noted that leaves of different ages do not provide the same habitat for microorganisms. Leaf age

determines the structure of the cuticle and epicuticular waxes, the amount of available nutrients, the concentration of secondary metabolites, all of which regulate the growth of microbial populations (Shakir *et al.*, 2021; Griggs *et al.*, 2021). Leaf age also determines immune status as microbial colonization can stimulate defenses and prime the leaf to be more resistant to subsequent infection (Chaudhry et al., 2021; Shakir et al., 2021; Section 2.2). The effect of leaf age on disease development is well undertsood and is termed ontogenic resistance. It has been demonstrated for several grapevine leaf pathogens (Steimetz *et al.*, 2012; Qiu *et al.*, 2015; Calonnec *et al.*, 2018). All of these factors lead to intra-canopy variation in the composition of the grapevine leaf microbiome (Calonnec *et al.*, 2008; Fan *et al.*, 2020) as well as strong seasonal dynamics. Seasonal dynamics, however, are less pronounced in bacterial communities than in fungal communities, whose diversity decreases markedly over the growing season (Pinto *et al.*, 2014; Fort *et al.*, 2016; Singh *et al.*, 2018; Gobbi *et al.*, 2020; Liu & Howell, 2021).

In addition to seasonal intra-canopy dynamics, the grapevine leaf microbiome exhibits high spatial variability. Its composition changes significantly from one geographical region to another (Oliveira *et al.*, 2018; Singh *et al.*, 2018) and from one vineyard plot to another (Barroso-Bergadà et al., 2021, but see Knapp et al., 2021). These spatial variations are explained by vine-related (scion variety, cultural practices) and environmental factors (climate and microclimate, landscape structure) (Bettenfeld *et al.*, 2021). Several studies have attempted to establish a hierarchy between these factors. For example, variety has a significant effect on leaf microbiome composition (Singh *et al.*, 2018, 2019; Zhang *et al.*, 2020), but its effect is much smaller than that of geographic and climatic factors (Singh *et al.*, 2018). The effect of phytosanitary treatments appears to be less important than seasonal dynamics (Gobbi *et al.*, 2020), in agreement with results demonstrating high resilience of the phyllosphere microbiome to phytosanitary treatments (Perazzolli *et al.*, 2014). The cropping system as a whole, however, has a substantial influence on the diversity and composition of leaf microbiome, with significant differences found between organic and conventional farming (Kernaghan *et al.*, 2017; Castañeda *et al.*, 2018; Miura *et al.*, 2019; Barroso-Bergadà *et al.*, 2021). Finally, several studies investigated whether forest patches or orchards adjacent to grapevine plots structure the grapevine leaf microbiome, with varying results (Fort *et al.*, 2016; Castañeda & Barbosa, 2017; Castañeda *et al.*, 2018; Miura *et al.*, 2019; Chandra *et al.*, 2020).

Among the multitude of microorganisms that colonize grapevine leaves, some affect plant health and growth. Pathogens and their mode of action have been the most studied (Armijo et al., 2016). Powdery and downy mildews (respectively caused by the fungal species *Erysiphe necator* and the oomycete species *Plasmopara viticola*; Fig. 3) are the most important diseases of grapevine (Bois *et al.*, 2017). Black-rot (caused by the fungi *Phyllosticta ampelicida*, Fig. 3) is a foliar disease that is becoming increasingly important in Europe, concomitant with efforts to reduce fungicide use (Molitor & Beyer, 2014). All three pathogens are introduced species of North-American origin (Sections 1.2 and 1.3). When these fungal pathogens colonize the grapevine leaf, they encounter the resident microbiome and virome, which can act as a barrier

to their growth through direct ecological interactions (Hacquard *et al.*, 2017; Chaudhry *et al.*, 2021), such as exploitative competition, interference competition (antibiosis), and hyperparasitism. Once this first barrier is overcome, pathogens are confronted by the plant's immune system, which is itself stimulated by the microbiome, especially the root microbiome (Section 2.2).

Natural antagonists of downy mildew (Fig. 3) have been identified using culture-dependent methods. Several bacterial and fungal species, isolated from grapevine leaves or previously detected in the leaf microbiome, have a negative effect on *Plasmopara viticola* under experimental conditions. For fungi these include *Acremonium byssoides*, *Alternaria alternata*, *Beauveria bassiana*, *Epicoccum nigrum* (Kortekamp, 1997; Musetti *et al.*, 2006a; Burruano *et al.*, 2008, 2016; Zanzotto & Morroni, 2016; Rondot & Reineke, 2019; Taguiam *et al.*, 2021), and several *Fusarium* species (Falk, 1996; Bakshi *et al.*, 2001). The genus *Bacillus*, including *B. subtilis* and *B. pumilus*, predominates among *P. viticola* antagonistic bacteria (Bruisson et al., 2019; Dagostin et al., 2011; Zanzotto and Morroni, 2016; Zhang et al., 2017). Moreover, root colonization by the arbuscular mycorrhizal fungus *Rhizophagus irregularis* (Sections 2.1 and 2.2) increases grapevine resistance to *P. viticola* in leaves (Cruz-Silva *et al.*, 2021). Finally, the virome of *P. viticola* has been analyzed using metatranscriptomics in search for hypovirulence-inducing mycoviruses (Chiapello *et al.*, 2020). However, despite the description of many new mycoviruses (283 new viruses associated with lesions caused by *P. viticola*), the limited availability of phenotypic data on fungal hosts has so far prevented the association of particular viruses with variations in fungal virulence.

Pathogen-microbiome-virome interactions are not well documented for powdery mildew (Panstruga & Kuhn, 2019), but some antagonistic interactions (Fig. 3) have been demonstrated experimentally. Several natural hyperparasites of *Erysiphe necator* have been identified among the *Ampelomyces*, *Lecanicillium*, and *Acremonium* genera (Falk, 1995; Kiss, 2003; Ghule *et al.*, 2019). As with downy mildew, powdery mildew growth is reduced by *B. subtilis* and *B. pumilus* (Crisp *et al.*, 2006; Compant *et al.*, 2013). Network inference (Section 3.3) has suggested an antagonistic interaction between powdery mildew and the yeast *Buckleyzyma aurantiaca* (Pauvert *et al.*, 2020), which remains to be experimentally validated with culture-dependant approaches (Section 3.4). Moreover, as for *Plasmopara viticola*, the virome of *E. necator* has been studied in search of hypovirulence-inducing mycoviruses (Pandey *et al.*, 2018). Mycoviruses have been detected but an effect on fungal virulence and disease development has yet to be been demonstrated.

Future studies should reinforce the searching for members of the resident microbiome and virome that naturally regulate powdery and downy mildews, and identify the biodiversity management practices that favor these natural antagonists. Such results are urgently needed to move toward pesticide-free viticulture (Jacquet *et al.*, 2022), as mildews are currently controlled by chemical pesticides whose use should be drastically reduced to preserve environmental and human health. Based on the co-evolutionary history of *Vitis* spp. and mildew agents (Section 1.2), we recommended exploring the microbiome and the virome of

mildew-resistant *Vitis* species in their native range (Fig. 2) to identify biocontrol candidates. In addition, we would recommend comparing the leaf microbiome of European cultivated grapevines that are rarely *versus* frequenly infected with mildews, according to epidemiological records (Section 3.1). The upper soil and bark microbiomes could also be analyzed as they constitute the overwintering sites of the pathogens. Identifying the microbial taxa that are enriched in the resistance zones and deciphering the microbial interaction networks (Section 3.3) in those zones could provide interesting insights into the natural regulation of mildews.

Dynamics of the berry microbiome to ripening and winemaking

Like the leaf microbiome (Section 2.3), the berry microbiome varies significantly in abundance and composition throughout the season. Population sizes of both fungal and bacterial communities on the berry surface increase with ripening and reach a maximum when the berries become overripe. The community composition varies significantly during the season, with a decrease in *Basidiomycota* (*Aureobasidium, Cryptococcus and Rhodotorula* spp.) and an increase in *Ascomycota* (*Hanseniaspora, Metschnokowia, Pichia* spp.) (Barata *et al.*, 2012). As the season progresses, Gram-negative bacteria (mostly *Pseudomonas spp.*) decrease in abundance whereas Gram-positive communities (mostly *Micrococcus* spp.) increase (Martins *et al.*, 2012). The morphology and chemical composition of berries are major drivers of these seasonal variations in microbiome composition (Liu & Howell, 2021). Indeed, the water activity on grapevine berry skin and the composition of exudates change along the grapevine berry ripening process, with an increase in sugar content, a decrease in pH and acidity (Martins *et al.*, 2014, 2020; Griggs *et al.*, 2021). Other drivers include agricultural practices during the fructification period (phytosanitary treatments, pruning), as well as the climatic conditions from fruit set to harvest (Belessi et al., 2022; Bokulich et al., 2014; Cordero-Bueso et al., 2011a, 2011b; Ding et al., 2021; Martins et al., 2014, 2020; Pinto et al., 2014). In addition to these seasonal variations, the berry microbiome varies markedly in space. Over the last decade, many studies conducted at different spatial scales (world, countries, regions and vineyards) have provided evidence for a biogeographic differentiation of the berry microbiome (Bokulich et al., 2014; Gobbi et al. 2022; Jara et al., 2016; Li et al., 2022; Miura et al., 2017; Vitulo et al., 2019). Based on these findings, these authors have developed the concept of "*microbial* terroir" that proposes a causal relationship between grapevine microbial biogeography and regional wine characteristics.

At the ripening stage, the grapevine berries harbor fermentative microorganisms that will subsequently contribute to the winemaking process and to wine quality (Fig. 3). These microorganisms include *Saccharomyces cerevisiae* (Sections 1.1 and 1.3), non-*Saccharomyces* yeasts and Lactic Acid Bacteria (LAB). *S. cerevisiae* is the species most responsible for alcoholic fermentation. Although its populations reach their highest abundance at berry maturity (10^4 to 10^6 cfu/g), the yeast remains rare at the grapevine berry surface, thus raising questions about its origin (Mortimer and Polsinelli, 1999; Börlin et al., 2020). The abundance and diversity of fermentative yeasts on the grapevine berry surface is impacted by fungicide treatments (Cordero-Bueso et al., 2014) and infection by *Botrytis cinerea*, which modifies sugar availability

(Fleet et al., 2003; Nisiotou and Nychas, 2007). Low numbers (<10^3 cfu/g) of cultivable LAB are also present on sound fruit and end up in must during the early stages of wine processing. Within this group of bacteria, *Oenococcus oeni* (Fig. 3) is responsible for a crucial process called malo-lactic fermentation (MLF), where L-malic acid in wine is converted to softer L-lactic acid. The reduction of acidity, which spontaneously occurs after alcoholic fermentation, is beneficial to the quality of wines made in cool winegrowing regions. Yet, MLF only starts when the *O. oeni* population reaches 10^6 cfu/ml. Understanding the factors reducing the bacterial biomass is crucial, in order to avoid slow or blocked MLF. Phages (Fig. 3) are one of these factors, as they may modulate *O. oeni* population size, and a number of temperate and virulent phages infecting *O. oeni* have been recently isolated from crushed grapes and later winemaking stages (Claisse *et al.*, 2021).

The berry microbiome may also contain microorganisms that alter wine quality, such as Acetic Acid Bacteria (AAB) or fungi that produce off-flavors or mycotoxins. AAB (*Acetobacter* spp., *Gluconobacter* spp.) (Fig. 3) are wine spoilage bacteria that are naturally present in the microbiome of grapevine berries (Fleet, 1993). They cause pre- and post-harvest yield losses and render berries unsuitable for wine production. A relevant example is sour rot of grape (Lleixa et al., 2018), which is a polymicrobial disease requiring the presence of *Drosophila* flies (disease vector), wounded fruits, various yeasts that convert grape sugars to ethanol, and AAB that subsequently oxidize the ethanol to acetic acid. AAB co-exist with phages on ripe berries and a member of the *Tectiviridae* family has been recently characterized (Philippe *et al.*, 2018). The control of AAB is challenging as these bacteria show great capacities to persist during wine making. Phages and their derived enzymes called endolysins may offer new solutions to their control.

Fungi naturally present on ripened grapevine berries can also produce off-flavors, in particular earthy or moldy odors in grape juice and wines. This is the case of *Botrytis cinerea* (Fig. 3), the necrotrophic fungal pathogen responsible for grey mold (Armijo *et al.*, 2016). *B. cinerea* produces cellulases, pectinases, proteases and a *p*-phenol oxygen oxidoreductase able to oxidize phenolics compounds, which is at the origin of severe alteration of wine color. *B. cinerea* also causes an enhancement of phenylpropanoid metabolism, terpenes and fatty acid aroma precursors at the grapevine berry level. It can be associated with *Penicillium expansum*, then leading to the production of geosmin, an earthy off-aroma (La Guerche *et al.*, 2005, 2007). However, *B. cinerea* can also colonize berries under its "noble rot" form which positively develops the berry aroma potential (Thibon *et al.*, 2010, 2011). Natural antagonists of *B. cinerea* have been searched for within the leaf and berry microbiome to develop microbial biocontrol. They include *Aureobasidium pullulans*, which acts against *B. cinerea* through nutritive and spatial competition and antibiosis (Martini *et al.*, 2009, p. 200; Rathnayake *et al.*, 2018; Carmichael *et al.*, 2019). They also include some bacteria (*Bacillus* spp., Actinomycetes) and yeasts (*Metchnikovia* spp., *Pichia* spp.) (Loqman et al., 2009; Raspor et al., 2010; Santos and Marquina, 2004). Mycoviruses infecting *B. cinerea* (Pearson & Bailey, 2013; Ruiz-Padilla *et al.*, 2021) have been searched for to foster biocontrol. Although a rich virome was discovered,

only a few mycoviruses were associated with a reduced virulence of the fungal pathogen (i.e. an hypovirulence phenotype) (Wu *et al.*, 2010; Yu *et al.*, 2015; Khalifa & MacDiarmid, 2021). These mycoviruses belonged to several families, including *Narnaviridae* (single-stranded RNA virus) and *Genomoviridae* (single-stranded DNA virus). An unclassified double-stranded RNA virus was also found. Finally, fungal pathogens producing mycotoxins (*Aspergillus carbonarius*, *Aspergillus niger*) can also develop in mature berries. Mycotoxin contamination can be limited by specific practices (Hocking *et al.*, 2007; Perera *et al.*, 2021), including biocontrol by *A. pullulans* (Bozoudi & Tsaltas, 2018).

Grapevine berries constitute a pivotal microbial compartment because the dynamics of their microbiome depends on the agricultural practices and the climatic conditions in the vineyard, and determines the quality of the end product. Future research should therefore continue investigating the seasonal dynamics of microbial interactions and functions on the grapevine berry surface (Section 3.3), to elucidate their impact on berry quality and wine properties. Significant advances using metabolic networks (Section 3.3) were made made for *Oenococcus oeni* and should be extended the the microbial community level, to understand the interactions between *O. oeni* and other microorganisms (like that *Saccharomyces cerevisiae,* LAB and AAB) that belong to the berry microbiome and are involved in winemaking (Mendoza et al. 2017). Conversely, the impact of the winemaking process on the berry microbiome dynamics could be assessed. Indeed, during winemaking, fermentative microorganisms reach very high population levels in cellars and can be disseminated in the vineyard through CO_2-extraction systems and insect vectors.

Wood microbiome dysbiosis during grapevine aging and decline

Cultivated grapevines are perennial plants that age and are eventually removed when they are no longer productive. Nowadays, a major cause of grapevine decline (Fig. 3) are Grapevine Trunk Diseases (GTDs), a group of diseases which re-emerged in the late 1990s and cause wood degradation and necrosis within the inner structures of mature grapevines (Mugnai *et al.*, 1999; Bruez *et al.*, 2013; Bertsch *et al.*, 2013). GTDs include *Botryosphaeria* dieback, *Diaporthe* dieback, *Eutypa* dieback, *Phomopsis* dieback, Petri disease, black-foot disease and Esca complex diseases. Pathogenic fungi associated with GTDs belong to several genera, including *Phaeomoniella, Phaeoacremonium, Fomitiporia, Eutypa*, and to the *Botryosphaeriaceae* family (Cobos et al., 2022; Fig. 3). However, these fungi have been isolated from both healthy and necrotic wood tissues of both GTD-symptomatic and asymptomatic grapevines. Their role in GTDs has therefore been questioned (Hofstetter *et al.*, 2012) and other microorganisms potentially involved in GTDs have been isolated using culture-dependent methods (Elena *et al.*, 2018; Kraus *et al.*, 2019). Cobos et al. (2022) reported that in 2018, 133 fungal species belonging to 34 genera (mainly ascomycetes and basidiomycetes) had been associated with GTDs worldwide, this number increasing yearly. Bacteria inhabiting grapevine wood have also been isolated, identified and their functions studied. For instance, Bruez et al. (2015) identified 26 bacterial genera inhabiting the various wood tissues, the most abundant being *Bacillus* (34% of the bacterial strains), then *Pantoea* (12%), *Paenibacillus* (9%), and *Enterobacter* (6%).

Bacterial communities differed between anatomical parts (i.e. trunk or cordon) and tissue types (i.e. necrotic or non-necrotic). Functions of bacteria colonizing necrotic and non-necrotic tissues differed, as they metabolized differently the carbon substrates. Over the last decade, next-generation sequencing (Eichmeier *et al.*, 2018; Del Frari *et al.*, 2019; Lade *et al.*, 2022; Gramaje *et al.*, 2022) and metatranscriptomic analyses (Paolinelli *et al.*, 2022; Nerva *et al.*, 2022) have provided a deeper resolution in the grapevine wood fungal and bacterial microbiomes. Depending on the grapevine organs, years, seasons and wood health status (i.e. healthy or necrotic), variations in the wood microbiome composition were observed, for both fungi and bacteria (Bruez *et al.*, 2014, 2020).

Wood necrosis is often observed in mature grapevines (15 to 25-year-old), the difference between healthy and GTDs-plants being the quantity of wood necrosis. White-rot necrotic wood, in particular, is more abundant in diseased plants (Maher *et al.*, 2012; Ouadi *et al.*, 2019, 2021). This observation raised a key question: why does a substantial percentage of wood become necrotic in mature plants? This question has recently been investigated in the case of Esca, the most frequent GTD. Microbiome changes occurring at the onset of Esca were investigated using metabarcoding approaches (Bruez *et al.*, 2020). The results showed a decrease in the diversity of fungal communities in the white-rot of diseased trunks, linked with the tissue colonization by the fungal pathogen *Fomitiporia mediterranea*. Because fungi and bacteria coexist in the wood, the authors hypothesized that fungal-bacteria associations were involved in the wood degradation. In agreement with this hypothesis, associations between GTD-fungal pathogens (*F. mediterranea* and *Phaeomoniella chlamydospora*) and bacterial species (*Sphingomonas* spp. and *Mycobacterium* spp.) were detected in the cordons of young grapevines expressing Esca-foliar symptoms. More recently, Haidar et al. (2021) showed that *F. mediterranea* and a novel species of bacteria isolated from grapevine wood (Haidar et al., submitted) acted synergistically to enhance wood structure degradations associated with Esca.

Plant-microbe and microbe-microbe interactions responsible for other GTDs (*Botryosphaeria* dieback, *Diaporthe* dieback) have also been studied. Several fungal pathogens of the genera *Botryosphaeria*, *Diplodia*, *Lasiodiplodia* and *Neofusicoccum* have been identified as causal agents of *Botryosphaeria* dieback. This complex of xylem-inhabiting fungi can remain latent in the roots before producing phytotoxic compounds and degrading enzymes (xylanases, cellulases, β-glucanases) in stems and symptomatic leaves (Gramaje *et al.*, 2018; Martínez-Diz *et al.*, 2019; Marais *et al.*, 2021). Fungi of the genus *Diaporthe* are responsible for *Diaporthe* dieback, a disease that causes, among others, cane bleaching, swelling arms, trunk cankers, shoots breaking off at the base, loss of vigor, and reduced bunch size (Guarnaccia *et al.*, 2018; Martínez-Diz *et al.*, 2019). These symptoms can allow the implantation of opportunistic microorganisms such as *Didymella negriana*, which is capable of producing mycotoxins (Liu & Howell, 2021; Stranska *et al.*, 2022).

Wood bacteria, fungi and mycoviruses with potential biocontrol activities against fungal pathogens associated GTDs have been investigated (Rezgui *et al.*, 2016; Mondello *et al.*, 2018;

Marais *et al.*, 2021; Haidar *et al.*, 2021). Fotios et al. (2021) analyzed the wood microbiome of asymptomatic and symptomatic plants in three Greek grapevine varieties, using differential abundance analysis (Section 3.1) and network inference methods (Section 3.3). Their results showed that *Bacillus* and *Streptomyces* genera dominated the bacterial microbiome of asymptomatic plants and had a negative co-occurrence pattern with GTD-pathogens belonging to the *Phaeomoniella*, *Phaeoacremonium* and *Seimatosporium* genera. The authors concluded that these bacterial taxa may play a role in the suppression of GTDs. The suppressive role of the wood microbiome was also suggested by Bruez et al. (2016), as they noticed that pathogenic and non-pathogenic fungi reach an equilibrium in the functional tissues of old grapevines. Mycoviruses may also play a role in the suppression of GTDs. For instance, mycoviruses were detected in *Neofusicoccum parvum* isolates from grapevines without symptoms of Esca (Nerva *et al.*, 2019) and in hypovirulent isolates (Marais *et al.*, 2021), suggesting that mycoviruses may reduce the aggressiveness of this *Botryosphaeriaceae* species. It is noteworthy that viruses could also be helpful to fight pathogenic bacteria that colonize xylem vessels, like *Xylella fastidiosa* (Fig. 3), the causal agent of Pierce's Disease, and *Xylophilus ampelinus*, the causal agent of bacterial blight. Biocontrol protocols using virulent phages have been successfully implemented *in planta* in Texas, USA, to control *Xylella fastidiosa* (Das *et al.*, 2015). This approach is promising, especially since the pathogen is vectored by an insect (the glassy-winged sharpshooter, *Homalodisca vitripennis*) (Bhowmick *et al.*, 2016) which has the capacity to uptake *X. fastidiosa* phages (Clavijo-Coppens *et al.*, 2021).

Deciphering plant-microbe-virus interactions occurring in the grapevine wood is crucial for future monitoring and management of GTDs. Specically, tipping points in the wood microbiome dynamics related with the onset of disease symptoms could inform disease-monitoring programs (Section 3.3). For future research, we would recommend analyzing the taxonomy and functions of the wood microbiome, as well as the changes in microbial interactions networks (Section 3.3), just before the appearance of the first Esca-foliar symptoms to answer the following questions: (i) is the onset of the disease marked by an increase in the heterogeneity of the microbiome between grapevines, as stated in the 'Anna Karenina principle' (Zaneveld *et al.*, 2017)? (ii) is the onset of the disease marked by a collapse in microbial interaction networks? (iii) is there a change in the functional composition of the microbiome, marked by an increase in the abundance of pathogenic species?

Answering these questions about the wood microbiome and those raised earlier for the other microbial compartments (roots, leaves and berries) will require the study of the complex microbial communities associated with cultivated grapevines, to identify the environmental drivers of plant-microbe-virus interactions. It will also require the analysis of simpler, synthetic microbial consortia in controlled conditions, to get mechanistic insights into microbial interactions. Both approaches will be linked. Studying natural communities will require dedicated field sampling designs to identify key taxons and functions associated with grapevine performance. These key taxa and functions will then help design culture-based experiments coupled with modeling approaches to leverage omics data and decipher microbial interactions

at the genome scale. These models will be used to optimize the microbial consortia (Busby et al. 2017; Toju et al. 2018) that could ultimately be inoculated to foster grapevine performance under conditions of climate change and reduced pesticide use. Some of the tools to address these challenges and make the grapevine microbiome more functional are described in the next section (Section 3).

Let's make the grapevine microbiome more functional

This section proposes experimental and computational approaches that could help uncover the functioning of the grapevine microbiome, with the goal of integrating it into a more sustainable viticulture. We propose field sampling designs and statistical approaches that exploit what we know of the evolution and dynamics of the grapevine microbiome (Sections 1 and 2) and aim to identify microbial taxa or consortia that may play a role in vine performance and vineyard ecosystem health. We then review the molecular tools and computational approaches that work together to analyze the grapevine holobiont as a dynamic, interactive, and functional system. We emphasize throughout the critical need for culture-dependent approaches to validate the effects of specific microbial taxa and functions on vine performance and vineyard ecosystem functioning. Each subsection sets out research hypotheses or questions about microbiome functioning, describes methodological frameworks that exist or could be developed to address these questions, and finally suggests how to apply them to the grapevine system.

Field sampling designs and statistical approaches to identify beneficial microbial taxa

Grapevine hosts many hundreds of microbial taxa (Knapp et al., 2021; Morgan et al., 2017; Zarraonaindia et al., 2015 and Section 2) of which only a few dozen have known roles and modes of action (Fig. 3). Here we propose field sampling designs and statistical approaches that could be applied to metabarcoding datasets to elucidate the links between the presence or abundance of particular microbial taxa, and functional traits measured at the plant- or ecosystem-scale. In the current context of climate change and need to limit pesticide use (Jacquet *et al.*, 2022), we ask which field sampling designs and statistical approaches are suitable for identifying microorganisms enhancing plant tolerance to drought or providing a barrier effect against microbial pathogens?

Question #1: How to identify microbial taxa enhancing plant tolerance to drought or providing a barrier effect against microbial pathogens from metabarcoding data?

To address this question, the composition of grapevine microbiome samples can be analyzed using metabarcoding approaches and then statistically related to measurements of grapevine physiology or vineyard ecosystem functioning. For example, the microbiome can be related to ecophysiological traits that indicate grapevine tolerance to drought (Gambetta *et al.*, 2020; Vacher *et al.*, in press), or to the frequency and intensity of diseases at the plot level in epidemiological surveys (Chen *et al.*, 2019), or to more integrative agricultural variables such as yield potential. The grapevine microbiome can then be considered as an explanatory factor

of the variation in the functional trait of interest (e.g. drought tolerance, disease resistance, yield). This variation can be analyzed at different temporal and spatial scales (Fig. 4): within the lifetime of a cultivated vine individual (Fig. 3), between vines planted in the same plot (e.g. Darriaut et al., 2021), between vineyard plots, between cultivated vines and their wild ancestors (Section 1.1), or between cultivated vines and disease-resistant *Vitis* species (Section 1.2).

The field sampling design should determine the statistical analyses to be used. One sampling approach is to examine grapevine individuals or vineyard plots along a gradient of a previously measured functional trait of interest. Another would sample pairs of individuals or pairs of plots, of contrasted functional traits (e.g. drought-tolerant vs. drought-sensitive, disease-resistant vs. disease-susceptible, high- vs. low-yielding), other effects being otherwise controlled (same rootstock and scion cultivars, similar plant age, soil type and farming system). These two sampling strategies (Fig. 4) rely on spatial variation in the functional trait of interest. The first maximizes the variation in the trait along the gradient, while the second reduces the environmental heterogeneity within a pair. Longitudinal, time-series surveys (Fig. 4) would complete this picture, and highlight joint temporal variations between the microbiome and the functional trait of interest. This combination is highly relevant for grapevine given the strong dynamics in the microbiome at multiple timescales (Sections 1 and 2).

Several statistical tools can then be applied to metabarcoding data to assess the contribution of microbiome composition to variation in a functional trait, and identify the properties of the microbiome that have explanatory power. These explanatory properties can be the occurrence or abundance of particular microbial taxa or microbial functional groups (Section 3.2), or aggregated properties at the community or network levels such as community alpha-diversity or microbial network connectance (Barroso-Bergadà *et al.*, 2021). The compositional dissimilarity matrix between samples (community beta-diversity) can be converted into explanatory vectors using the method of PCNM eigenvectors, developed for spatial distance matrices (Borcard & Legendre, 2002). The statistical model will have the functional trait of interest as the dependent variable and the microbiome properties and environmental factors as explanatory variables (e.g. Asad et al., 2022 for yield; Cambon et al., 2022 for drought tolerance; Pérez-Valera et al., 2020 for an example of paired samples). When the microbiome contributes significantly to the functional trait of interest, identifying which microbial taxa are the main players can be done using the TITAN2 method (Baker *et al.*, 2015) or differential abundance analysis methods (Nearing et al., 2022; Weiss et al., 2017). Machine learning or deep learning methods can also be applied (Xu *et al.*, 2022); for example, a Random Forest algorithm has been used to identify combinations of microbial taxa indicative of yield (Yergeau *et al.*, 2020). For grapevine, statistical identification of subsets of microbial taxa potentially involved in disease resistance or drought tolerance would be relevant to set up experimental, culture-dependant approaches (Sections 3.4). Finally, to test specific hypotheses on the direct and indirect effects of the explanatory factors (including microbiome) on the functional trait of interest, structural equation models (SEM) have been developed (Jassey *et al.*, 2018). For

grapevine, a descriptive SEM would be highly relevant for assessing the direct and indirect effects (through the microbiome) of variety and environmental factors (drought, agricultural practices) on disease severity and frequency.

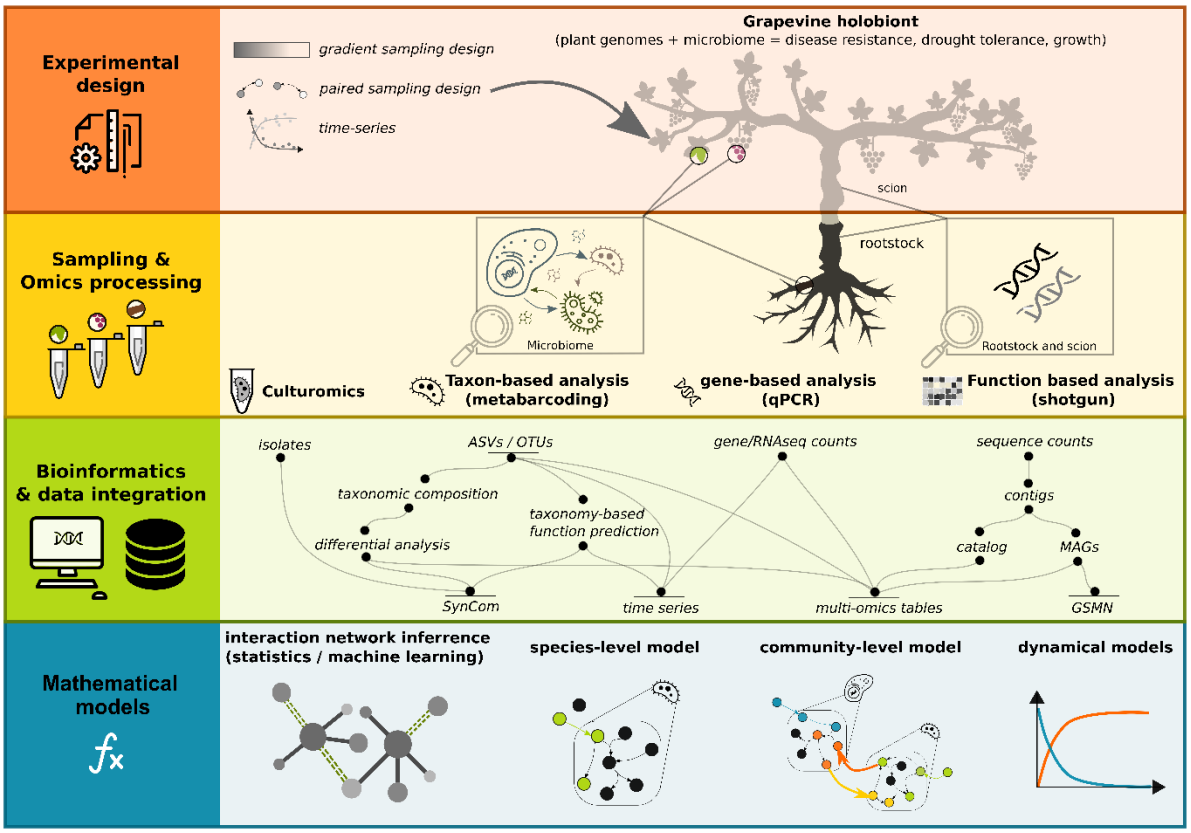


Figure 4: Workflow, from field experiments to mathematical models of omics data, to decipher the complex plant-microbe-microbe interactions forming the grapevine holobiont and to identify beneficial microbial taxa.

The experimental design sets up the sampling plots, hosts, compartments and time-points, according to spatial and temporal variations in a functional trait of interest (e.g. grapevine drought tolerance, disease resistance, yield). Grapevine samples (roots, trunk, leaves or berries) are then collected, cultivated, amplified and sequenced, and omics data are processed. Omics approaches can be culture-based (culturomics), taxon-based (metabarcoding), gene-based (microfluidic qPCR chips, for instance) or function-based (shotgun metagenomics). Bioinformatic analysis and data integration pipelines result in multi-omics tables, time series, SynComs or GSMN construction. This data can be used as input data for interaction network inference, species or community-level models and dynamical systems representing microbial populations' dynamics under various environmental conditions. ASV, Amplicon Sequence Variant; GSNM, Genome-Scale Metabolic Network; MAG, Metagenome-Assembled Genomes; OTU, Operational Taxonomic Unit; SynCom, Synthetic Community.

Molecular tools to uncover the functional potential of the microbiome

Microbiome samples collected from contrasted environments following the field sampling designs described above (Section 3.1) can be further analyzed using culture-independent molecular tools to uncover the microbial genomes present in the sample, analyze the microbial functions they carry, estimate precisely variation in their abundance and link this variation with

plant gene expression patterns. Here, we review the molecular tools that could be used to address the following questions: How to characterize the functional potential of the grapevine microbiome with shotgun metagenomics; and, how to decipher the functional coupling between grapevine and its microbiome with quantitative approaches?

Question #2 : How to characterize the functional potential of the grapevine microbiome with shotgun metagenomics?

Metataxonomics using metabarcoding of amplified marker DNA sequences has been widely used to inventory the microbial taxa present in a sample (Marchesi & Ravel, 2015), including in grapevine (Sections 1 et 2). Bioinformatic tools exploit this data to generate abundance tables of microbial Operational Taxonomic Units (OTUs) or Amplicon Sequence Variants (ASVs) in samples (Schloss *et al.*, 2009; Hildebrand *et al.*, 2014; Callahan *et al.*, 2016, 2017; Pauvert *et al.*, 2019; Estaki *et al.*, 2020). Metabarcoding has strong limitations, however, including primer amplification bias, copy number variation of the target sequence across taxa, and limits to taxonomic resolution, which may prevent the accurate characterization of taxa composition and abundance. Although primarily dedicated to taxonomic characterization, metabarcoding data can nevertheless be used to get insight into the functional potential of a microbiome with taxonomy-based function prediction methods (Louca *et al.*, 2016; Nguyen *et al.*, 2016; Douglas *et al.*, 2020; Wemheuer *et al.*, 2020; Zanne *et al.*, 2020; Belcour *et al.*, 2022). These methods build upon the association of taxonomic clades to known functional guilds, or to metabolic functions or pathways obtained from public databases of annotated genomes (Section 3.3).

In contrast to metabarcoding approaches, shotgun metagenomics (Fig. 4) does not sequence DNA markers but the total DNA material of a sample. Significant data processing is required (Bickhart *et al.*, 2022). Reference-based profiling (Section 3.3) compares these reads to reference genomes. In genome-resolved metagenomics, quality-filtered reads are assembled into contigs (Li *et al.*, 2015; Nurk *et al.*, 2017), which can be parsed into genes that are binned into metagenome-assembled genomes (MAGs) (Wu *et al.*, 2016; Kang *et al.*, 2019; Yue *et al.*, 2020; Borderes *et al.*, 2021). Genomes can be resolved for uncultured bacterial and eukaryotic members of the microbiome, and the precise function carried by a species in the sample can be investigated. The limitations of MAG reconstruction come about as a consequence of the diversity of species found in the same sample (Nayfach *et al.*, 2020; Lemos *et al.*, 2021). Improvements to long-read sequencing such as PacBio or Nanopore technologies lead to better metagenome assembly. They can be combined synergistically with low error rate short reads to accurately retrieve repetitive genome regions (Chen *et al.*, 2021a; Damme *et al.*, 2021). Long reads using the most recent technologies can however suffice alone for reconstructing high-quality MAGs (Sereika *et al.*, 2022). The principal bias in shotgun metagenomics is the taxonomic and functional incompleteness in reference databases that can add noise to the taxonomic assignment and the functional annotation for underrepresented species and functions. In addition to shotgun metagenomics, metabolomics and metatranscriptomics (Paolinelli *et al.*, 2022) approaches identify metabolites or expressed genes, respectively, in the host and the microbiome.

While genome-resolved metagenomics applications to soil and plants are becoming more frequent (Wu *et al.*, 2022a,b), few studies have yet applied it to grapevine. Metagenomics has been used to analyze the microbial composition of grapevine berries and to reconstruct 13 near-complete draft genomes (Salvetti *et al.*, 2016). Azevedo-Silva et al. (2021) discussed the feasibility of applying shotgun metagenomics to grapevine leaf, rhizosphere and soil characterization and proposed a protocol. For grapevine, we recommend using metataxonomics before shotgun metagenomics to first target the environmental samples worthy of deeper sequencing (Fig. 4). We argue that, while metagenomics has some biases, it has fewer than amplicon sequencing and the substantial amount of information it brings makes it worthy of consideration for deeper analyses of the grapevine microbiome.

Question #3 : How to decipher the functional coupling between grapevine and its microbiome with quantitative approaches?

Metabarcoding and metagenomics data are by nature compositional, meaning that we measure the relative abundance of microbial taxa or functions within a sample rather than their absolute abundance. To produce absolute counts requires complementary, quantitative methodologies (Props *et al.*, 2017). Real-time quantitative PCR (RT-qPCR) has developed into a powerful and accurate technique for measuring absolute abundance by assessing quantitative changes in taxonomic or phylogenetic marker genes across spatial and temporal scales (Heid et al., 1996), supplanting the classical colony counting method, which is hindered by the low proportion of cultivable microorganisms (Lou *et al.*, 2018). Development of automated, high-throughput qPCR platforms (Fig. 4) have increased, tenfold, the number of qPCR reactions that can be simultaneously performed on a single instrument. Microfluidic qPCR chips with the Biomark® HD system, for example, can perform 9216 qPCR reactions (96 samples amplified with 96 primer sets) in only 4 hours.

Different microfluidic qPCR chips have been used in pioneer studies of gene expression in grapevines. The NeoVigen chip (Dufour *et al.*, 2016), developed to quantify defense gene expressions in grapevine, quantifies plant genes involved in pathogenesis-related protein synthesis, secondary metabolites synthesis, the indole pathway, the oxidoreduction system, the salicylic acid, ethylene, and jasmonic acid pathways, and cell wall reinforcement. The BioStim chip (Bodin *et al.*, 2020) has extended the gene set by including, among others, genes involved in primary pathways and phytohormones pathways (auxin, cytokinin, gibberellin, abscisic acid). These chips have been used to decipher the mechanisms underlying the effects of biostimulants on grapevine resistance to multiple stresses. The workflow can be adapted to different types of microbial marker genes, whether taxonomic (Kleyer *et al.*, 2017; Dreier *et al.*, 2021) or functional (Crane *et al.*, 2018). The technology could therefore provide simultaneous quantitative snapshots of the microbiome taxonomic and functional composition and of the host response (Zolti *et al.*, 2020; Noman *et al.*, 2021).

To decipher the functional coupling between the grapevine host and its microbiome, we recommend parallel development of microfluidic chips targeting plant genes involved in plant

growth or stress resistance, and chips targeting specific microbial taxa and functions. Considerable progress has been made for the plants (Dufour *et al.*, 2016; Bodin *et al.*, 2020), but a chip has yet to be created for microbiomes. Several challenges must be overcome to choose the most relevant microbial targets, design primer sets, and validate the chip. Target selection must deal with the multitude of microbial taxa colonizing the plant and the multitude of functions they carry (Section 2). Chip validation must use reference species and synthetic microbial communities (Section 3.4) before applying the chip to environmental samples. Once developed, this tool could link microorganisms to plant health biomarkers, for instance to identify beneficial (phyto-probiotic) microbial agents that foster plant health or stimulate plant immunity, or potential antagonists of vine pathogens that are candidates for next-generation biocontrol products.

Computational approaches to understand the grapevine holobiont as a functional and dynamic network

Computational methods exploit the wealth of -omics data produced by high-throughput methods (Sections 3.2) to infer networks of ecological interactions between microbial taxa, unravel the trophic and metabolic relationships that underlie them, and analyze how they drive microbiome dynamics at different time scales (Sections 1 and 2). The various types of –omics data (metataxonomics, shotgun metagenomics, metranscriptomics, metaproteomics, metabolomics) are complementary and can be used to reconstruct ecological networks, metabolic networks, protein-protein interaction networks and gene regulatory networks (Liu et al. 2021). Here we describe the tools to specifically answer the following questions: How to characterize ecological interactions between grapevine-associated microorganisms using metabarcoding data? How to decipher metabolic interactions within the grapevine microbiome using shotgun metagenomics? How to infer the microbial interactions that shape microbiome dynamics from time-series data?

Question #4 : How to identify and characterize ecological interactions between grapevine-associated microorganisms using metabarcoding data?

Microbial ecologists have long used metabarcoding to learn ecological interactions between microbial taxa. They assume that since past or ongoing interactions between microbial taxa may impact their frequencies, patterns in relative shifts in frequency may provide information about the structure of the ecological interaction network (Cobo-Díaz et al., 2022; Jakuschkin et al., 2016; Kerdraon et al., 2019; Poudel et al., 2016; Vacher et al., 2016b). However, this process is not straightforward: metabarcoding data can be biased by amplification and sequencing artifacts, and are always compositional (Gloor et al., 2017; Section 3.2). One of the first tools for inferring interaction networks from relative sequence counts was SparCC (Friedman & Alm, 2012), which avoided the compositional effect by using log-transformation components to obtain correlation. Other tools like SPIEC-EASI (Kurtz *et al.*, 2015) or CCLasso (Fang *et al.*, 2015) refined correlation-based measures. PLN (Chiquet *et al.*, 2019) enhances inference accuracy by exploiting sample covariance, while MPLasso (Lo & Marculescu, 2017)

introduces the use of prior microbiological knowledge through data-mining of external sources of information. HMSC (Ovaskainen *et al.*, 2017) also integrates covariates on samples and taxa and was recently used to infer microbial networks (Abrego *et al.*, 2020; Fort *et al.*, 2021). These tools are extremely robust to noise in experimental data and can be run rapidly on even quite large datasets. Most of them are available in R, which facilitates their use (Dohlman & Shen, 2019; Tikhonov *et al.*, 2020). However, these tools define no clear link between the positive and negative interactions they find, and the ecological mechanisms that may generate them (Röttjers & Faust, 2018).

Explainable machine learning can relate ecological mechanisms to inferred interaction networks (Tamaddoni-Nezhad *et al.*, 2021). Different interaction types, such as competition and mutualism, lead to different changes in species frequencies and patterns (Fig. 4), which can be learned (Derocles *et al.*, 2018; Tshikantwa *et al.*, 2018). Explainable machine learning transcribes these criteria into logical rules that directly infer ecological interactions, with little to no human intervention in the interpretation step (Barroso-Bergada *et al.*, 2022). Hypotheses of ecological interactions between taxa pairs are generated through a process that simultaneously detects interactions and classifies them as competition, mutualism, amensalism or commensalism. This direct approach is particularly valuable for reconstructing microbial networks in previously unstudied ecosystems, where human knowledge for interpretation may effectively be lacking.

For grapevine, this approach was recently applied to microbial communities sampled from symptomatic and asymptomatic leaves of European cultivated grapevine during downy mildew epidemics. After a thorough assessment of the method using simulated datasets (Weiss *et al.*, 2016), preliminary interaction networks were computed and showed potential antagonists of the causal agent *Plasmopara viticola* —some known, some new— constituting options to control mildew development. We expect that this approach will identify sub-networks of interest, centered on pathogen species and their direct antagonists or facilitators, whose subsequent modeling could lead to better understanding of pathogen-microbiome interaction dynamics.

Question #5: How to decipher metabolic interactions within the grapevine microbiome using shotgun metagenomics?

The microbial functions present in a given sample can be assessed from shotgun metagenomic surveys or from metataxonomic data after taxonomy-based function prediction (Section 3.2). An advantage of the former is functional profiling of communities, using assembly-independent reference-based approaches, or de-novo reference-free assembled sequences (Quince *et al.*, 2017). Both approaches delineate microbial species and strains, needed for reconstructing microbial metabolic networks. These networks are then used in mathematical models (kinetic, constraint-based and discrete models) to predict metabolic reactions at the species- or community-level.

Functional profiling of microbial communities using assembly-independent reference-based approaches directly compares reads to reference databases (Beghini *et al.*, 2021) to identify genes and thereby functions. Functions or pathways associated with samples are then compared or used in statistical learning in order to reveal higher level functional patterns between sample groups (Raguideau *et al.*, 2016). Unfortunately, reads cannot be linked to their genome of origin, impeding the interpretation of these patterns in terms of metabolite-mediated trophic interactions between microbial taxa. Moreover, plant and grapevine-associated reference catalogs are less available than, for instance, the gut microbiome. Hence, genome-resolved metagenomics, below, seems to be a better option for grapevine.

Reference-free de novo assembly allows functional annotation of genes (Seemann, 2014; Cantalapiedra *et al.*, 2021), functional characterization of the corresponding organisms, and genome-scale metabolic network (GSMN) reconstructions (Fig. 4). GSMN consist of all biochemical and transport reactions predicted from an individual microbial genome (Gu *et al.*, 2019) and can be reconstructed by different tools (Arkin *et al.*, 2018; Karp *et al.*, 2019; Seaver *et al.*, 2020) or even directly connected to MAG reconstruction (Zorrilla *et al.*, 2021). In most cases, GSMN reconstruction involves manual curation to ensure the quality of the predictions they provide (Karp *et al.*, 2018). GSMN can be associated with mathematical models to predict the metabolism of a species or a community of organisms in an environment. The main difficulty is to achieve high-quality GSMNs, since i) MAGs are frequently incomplete, even worse so when under-studied microbiota are under-represented in the gene annotation databases; and ii) GSMN reconstruction from the MAG can be imperfect. Manually curated GSMNs are best but the number of genomes in a microbiota and limited knowledge about the microorganisms argues in favor of automatisation (Belcour *et al.*, 2020). Fortunately, the multiplication of shotgun sequencing studies of the grapevine microbiome will increase the size and quality of grapevine-related annotated gene catalogs and favor better MAGs-based GSMN automatic reconstruction.

Kinetic modeling uses differential equations models of the kinetics of biochemical reactions throughout the metabolic network of an organism (Ross & McMeekin, 1994), permitting microbial phenotype prediction that accounts for enzyme and metabolite concentration dynamics. While it has been applied to model organisms such as *Escherichia coli*, it is not widely applied due to the need to obtain biochemical measurements to parameterize the models (Khodayari *et al.*, 2014). An alternative are stoichiometric models, also known as constraint-based models. They translate a GSMN into a linear system of constraints for an optimization problem used to predict metabolic fluxes across the GSMN under simplificatory assumptions such as steady state in the system, i.e. the non-accumulation of internal metabolites and their constant concentration over time. Flux Balance Analysis (FBA) or Flux Variability Analysis (FVA) compute the activity rates of metabolic reactions while optimizing an objective function, typically the maximization of the microbial population growth (Orth *et al.*, 2010). FBA models can be coupled with differential equations through dynamic FBA (dFBA) (Mahadevan *et al.*, 2002). These methods have been widely used and extended to the study of microbial

communities (Biggs et al., 2015; Frioux et al., 2020) and to study the metabolism of oenological yeasts (Nidelet *et al.*, 2016; Eder *et al.*, 2020).

Discrete models are an alternative to constraint-based models to capture the metabolic potential of a GSMN, in a nutritional environment ideally characterized by metabolomics. Network expansion (Ebenhöh *et al.*, 2004) computes the set of reachable metabolites from a given set of metabolic seeds and has been used as a building block for screening the metabolism of microbial communities (Belcour *et al.*, 2020). Complexity is reduced by selecting minimal communities that satisfy a metabolic objective, which may take the host metabolism into account (Frioux *et al.*, 2018). Hypotheses arising from these minimal communities can be tested using synthetic communities (SynComs; Marín et al., 2021) selected to provide a targeted function. These approaches can be coupled with dFBA: discrete models are used for systematic screening and selection of SynComs, then dFBA is used on the selected SynComs to decipher the dynamics of the community at a molecular level.

GSMN were used to study soil and rhizosphere microbiome (Jacoby *et al.*, 2017), and to model winemaking process (Mendoza *et al.*, 2017). However, to our knowledge, GSMNs of grapevine phyllosphere or berry microbiomes remain an open challenge, of great potential for improving functional characterization of microbiomes. For grapevine, kinetic modeling would permit, for example, integration of multi-omics data to decipher and validate the dynamical interactions between a microbial pathogen and putative antagonists. Minimal communities identified by discrete modeling, for example to compete against microbial grapevine pathogens, or to promote oenological yeast growth by maintaining a tailored nutritional niche, can be tested with SynComs (Section 3.4).

Question #6: How to infer microbial interactions shaping microbiome dynamics from time-series?

Four fundamental, intrinsically dynamical ecological processes drive microbial communities: evolutionary diversification, selection, dispersal, and ecological drift (Vellend, 2010; Nemergut *et al.*, 2013). The contribution of these deterministic and stochastic processes, complementary to historical contingency and priority effects, can now be evaluated cost-effectively using -omics time-series data (Zhou & Ning, 2017; Ning *et al.*, 2019; Vass *et al.*, 2020). Longitudinal time-series data enable the study of the dynamical interactions that determine selection in the microbial ecosystem.

One increasingly common approach is the use of Generalized Lotka-Volterra models (GLV) to decipher the dynamic interactions shaping community dynamics (Faust *et al.*, 2018). GLV models decompose microbial growth into an intrinsic growth rate that models population fitness and interspecies interactions modeling ecological processes such as competition or parasitism (Fig. 4). These interactions are fitted to reproduce temporal data, which permits an ecological interpretation of the community dynamics. Despite simplifying assumptions such as constant environmental constraints, GLV models are suitable for studying microbiome stability, microbial population persistence and microbial community robustness (Gonze *et al.*, 2018).

They model dynamics that correlation-based methods cannot (Carr *et al.*, 2019). They have been used to study the dynamics of the gut microbiome during primary succession (Marino *et al.*, 2014) and pathogenic infection (Stein *et al.*, 2013), and to identify the assembly rules that determine the long-term composition of synthetic communities (Friedman *et al.*, 2017). Computational tools for inferring GLV interactions have been proposed by Bucci et al. (2016) and Kuntal et al. (2019).

GLV models need specific experimental design to guarantee accuracy of microbial network inference (Remien et al., 2021). GLV models describe the evolution of absolute population, so model parametrization requires time-series of absolute counts (e.g. qPCR or flux cytometry, Section 3.2). Abundance proxies can be used, such as compositional metabarcoding data renormalized in each sample by the dosage of total DNA (Stein *et al.*, 2013). The need for absolute population counts has been relaxed with an alternative GLV formulation for compositional data (Joseph *et al.*, 2020). GLV models are better suited to analyze marked changes of the microbial community, for example after strong perturbations such as pesticide treatment or colonization by exogenous microbes such as pathogens (Remien *et al.*, 2021), although Xiao et al. (2017) does address the steady-state microbiome.

GLV models have intrinsic limitations. First, growth and interspecies interactions are treated phenomenologically without regard to their underlying mechanisms, contrary to other models that supplement pairwise ecological interactions with metabolite-mediated interactions (Momeni *et al.*, 2017). Second, microbial populations are treated as well-mixed without regard to spatial structures caused by nutritional niches (Prosser *et al.*, 2007), which can impair GLV estimates (Armitage & Jones, 2019). Other population dynamics modeling frameworks avoid these drawbacks: GSMN, above, are particularly suitable for describing the metabolism of species subject to trophic interactions such as competition for resources, or cross-feeding in small consortia (Widder *et al.*, 2016); spatially explicit microbial population dynamics models can take into account spatial heterogeneities (Labarthe *et al.*, 2019). These models require, for parameterization, experimental measurements of reduced synthetic communities in controlled environments.

For grapevine, GLV models have not yet been used, but have been to model microbial dynamics in other plant species (Becerra-Lucio *et al.*, 2021). GLV models could be coupled with machine-learning approaches to select pathogen-associated sub-networks before studying their dynamics. They could also be used to study the dynamics of minimal communities identified by discrete modeling.

Culture-dependent approaches to validate microbial interactions and functions

All statistical and computational approaches described above generate hypotheses about the microbiome and its dynamics that must be experimentally validated. Therefore, we ask, how to isolate and culture microorganisms from a microbiome to study their functions and their interactions?

Question #7: How to isolate and culture microorganisms from the grapevine microbiome to study their functions and their interactions?

Culturomics, a high-throughput combination of multiple culture conditions and rapid identification of microorganisms (Fig. 4), has revitalized culture-dependent methods. The landmark studies by Lagier et al. (2018, 2016, 2015) combined high-throughput cultivation with cost-effective rapid identification by Matrix-Assisted Laser Desorption/Ionization Time Of Flight Mass Spectrometry (MALDI-TOF MS), and increased the number of microorganisms identified in the human gut microbiome by more than 50%. Large-scale isolation strategies have since been developed, including new culture media and advanced cultivation technologies. Specific protocols consisting of successive dilutions of a microbial population to the point of no growth, and technologies such as microdroplet and microfluidics, have been proposed to enhance isolation efficiency (Button *et al.*, 1993; Kaminski *et al.*, 2016; Zhang *et al.*, 2021). For the plant microbiome, plant-based media that isolate microorganisms in environmental and nutritional conditions close to their natural habitats have been successfully developed to improve cultivability (Mourad *et al.*, 2018; Sarhan *et al.*, 2018, 2019).

The success of culturomics in improving the catalog of isolated human bacteria and plant endophytic bacterial communities (Bilen *et al.*, 2018; Riva *et al.*, 2022) holds promise for the grapevine microbiome, but the task ahead is huge. Fewer than 3000 plant-associated bacterial genomes are available, out of 70 000 known bacterial genomes (Joint Genome Institute Integrated Microbial Genomes; https://img.jgi.doe.gov/; Trivedi et al., 2021). High-quality sequencing, assembly, and annotation of pure microbial strain genomes is needed to improve gene and protein databases and knowledge of the genome-based mechanisms underlying plant-microbe interactions (Levy et al., 2018; Sarhan et al., 2019; Section 3.3). Genome-resolved metagenomics produces uncurated draft genomes whose gaps, assembly errors and contamination from other genomes limit their usefulness (Chen *et al.*, 2020a); obtaining reference bacterial genome sequences (Trivedi et al., 2021; Section 3.3) will improve quality. Microbial culture collections make it possible to screen for microbial phenotypic traits that foster plant growth (growth promoting bacteria) and plant health (biocontrol agents) and they are imperative for validation of candidate genes. Cultivation and co-cultivation strategies are needed for experimental validation of predictive models of plant-microbiome and pathogen-microbiome interactions, and to provide deeper insight into the functional potential of beneficial plant-associated microbes (Nai & Meyer, 2018; Trivedi *et al.*, 2020).

Conclusion and perspectives

The grapevine microbiome has developed over thousands of years, integrating taxa from Asia, Europe and America, under the pressures of human selection and pathogen invasions. There are many gaps in this history, but the numerous studies of the grapevine microbiome show that it contains beneficial microorganisms (plant growth-promoting bacteria, mycorrhizae, biocontrol agents, microorganisms of oenological interest) whose mode of action is sometimes well documented. These beneficial microorganisms belong to a dynamic microbiome that significantly varies throughout the plant lifetime and throughout the year. The initial

microbiome of grafted plants is determined by the microbiomes of mother plants that produce rootstocks and scions. Those initial microbiomes may contain phytoviruses and fungal pathogens, but also beneficial microorganisms increasing tolerance to biotic and abiotic stressors. Some of the beneficial microorganisms (for instance, the arbuscular mycorrhizal fungi *Rhizophagus irregularis*) can be inoculated at the nursery stage to strenghten the microbiome. Once planted, roots actively release exudates that attract the rhizosphere microbiome from the soil reservoir. Beneficial microorganisms recruited by grapevine roots include plant-growth promoting bacteria (e.g. *Pseudomonas* spp., *Rhizobia* spp.) that make mineral nutrients (phosphorus, nitrogen and phosphate) available to the plant, arbuscular mycorrhizal fungi (e.g. *Glomus* spp.) that help the plant to cope with water stress, and microorganisms whose biocontrol activity (e.g. *Bacillus* spp., *Pythium oligandrum*) relies on various types of microbial interactions including antibiosis, hyperparasitism, spatial and nutritional competition and interference with pathogen signaling. Some beneficial microbes may enter the root and disseminate in the aerial parts, such as the bacterial endophyte *Burkholderia phytofirmans*. The circulating microorganisms, that may also be pathogens like the bacteria *Xylella fastidiosa,* eventually reach leaves and integrate their highly dynamical microbiome, driven by seasonal variations. Throughout the vegetative season, leaves are colonized by major grapevine pathogens, such as the causal agents of mildews (*Plasmopara viticola* and *Erysiphe necator*) which are both introduced pathogens of North-American origin. Leaves also harbor microorganisms with biocontrol activity (e.g. *Bacillus subtilis*, *Aureobasidium pullulans*, *Ampelomyces* spp.) that should be urgently favored to reduce pesticide use in viticulture. In mature grapevines, wood degradation associated with complex sets of microorganisms (e.g. *Phaeomoniella* spp*., Fomitiporia* spp*., Eutypa lata*, *Botryosphaeriaceae* spp.) can appear and lead to plant death. The search for biocontrol agents among mycoviruses, bacteria and fungi present in the wood is an active field of research requiring the inference of microbial interaction networks. Finally, the berry microbiome varies markedly during the development of the berry and contains, at the ripening stage, some fermentative yeasts and bacteria (e.g. *Saccharomyces cerevisiae, Oenococcus oeni)* positively involved in winemaking, but also undesirable microorganisms such as fungi producing off-flavors (e.g. the fungal pathogen *Botrytis cinerea*) and acetic acid bacteria leading to wine defaults.

Omics and associated computational approaches can further improve our understanding of the functioning of the grapevine microbiome, to ultimately design beneficial microbial consortia that could be inoculated to foster grapevine performance (health, growth and berry quality) under conditions of climate change and reduced pesticide use. To reach this objective, we propose to identify beneficial microbial taxa by performing field sampling campaigns informed by grapevine evolutionary history and phenotypic measurements (disease resistance, drought tolerance). Statistical approaches could then be applied to the metabarcoding datasets to identify subsets of microbial taxa whose presence or abundance is significantly related to grapevine phenotypic variations. Shotgun metagenomics could then be used to

uncover microbial genomes and functions in selected samples, while microfluidic qPCR chips could be used to accurately estimate the abundance of selected microbial taxa. These data would then feed mathematical models to decipher metabolic and ecological interactions in small microbial consortia and analyze how these interactions drive microbial community dynamic and variations the plant phenotypic traits. The high-throughput cultivation of environemental samples in parallel with sequencing will be crucial to isolate microbial strains of interest and experimentally validate hypotheses generated by mathematical models.

Based on current knowledge and available methods, we propose the following research avenues to make the grapevine microbiome more functional:

A. Design microbiome studies informed by evolutionary history
- Analyze the microbiome of wild grapevine and ancestral grapevine varieties to discover beneficial microorganisms that may have been lost during domestication and breeding
- Analyze the microbiome of American *Vitis* species to discover potential antagonists of North-American pathogens

B. Consider grapevine as a dynamic system of interactions
- Investigate how rootstock-scion interactions in the graft zone shape the microbiome of the whole plant
- Decipher the microbial interactions that regulate the dynamics of pathogen populations
- Assess the cascading effects of the soil microbiome on the root, trunk, leaf and berry microbiome, and their consequences on plant health
- Analyze the microbial fluxes that govern the seasonal dynamics of the berry microbiome, and their consequences on wine properties
- Identify and monitor the microbiome changes that precede the development of trunk diseases
- Identify the viruses (mycoviruses, phages) that shape the dynamics of the grapevine microbiome

C. Combine metagenomics, culturomics and computational approaches
- Use field experiments and metabarcoding data to highlight small microbial consortia related to variations in grapevine phenotypic traits
- Create and maintain microbial culture collections to perform controlled experiments with the identified consortia
- Develop shotgun metagenomics and metabolic network modeling to understand the functionning of the target microbial consortia
- Monitor target microbial populations with quantitative approaches to model and predict their dynamics in response to environmental changes or management scenarios.

These research avenues are intertwined and not independent of each other: they require the creation of multidisciplinary research consortia with complementary expertise to define the scientific questions, experimental designs and analysis pipelines.

Chapitre 2 : Un nouveau scénario d'interactions pathogène-microbiote pour l'oomycète *Plasmopara viticola*

L'objectif de ce chapitre est d'identifier les propriétés du microbiote spécifiques aux tissus foliaires sains et celles spécifiques aux tissus infectés par le mildiou, dans un contexte d'épidémie de mildiou de la vigne. L'objectif est notamment d'identifier les consortia microbiens qui se maintiennent dans les tissus sains et ceux qui deviennent dominants suite à l'infection par *Plasmopara viticola*.

Pour atteindre ces objectifs, j'ai comparé le microbiote foliaire associé à des tissus sains à celui associé à des tissus présentant des symptômes de mildiou. L'étude couvre l'ensemble du territoire français, avec des échantillons prélevés dans trois grandes régions viticoles : l'Occitanie, la Nouvelle-Aquitaine et la Champagne. L'échantillonnage a eu lieu entre la mi-juin et la mi-juillet de l'année 2018, correspondant au pic de l'épidémie de mildiou. L'analyse du mildiou et du microbiote ont été réalisés à l'échelle du disque foliaire : sur chaque feuille, des disques ont été prélevés dans des tissus asymptomatiques et dans des lésions de mildiou. La quantification du mildiou a été réalisée par deux méthodes : une évaluation visuelle binaire (asymptomatique/symptomatique) et une mesure quantitative de la concentration en *Plasmopara viticola* dans chaque échantillon collecté par PCR quantitative.

Les données de cette étude ont été collectées en juillet 2018 dans le cadre du projet 'BCMicrobiome', financé par le Consortium Biocontrôle (co-dirigé par Corinne Vacher, UMR SAVE et David Bohan, UMR Agroécologie). Les données de séquençage du microbiote et de quantification du mildiou ont fait l'objet d'un 'article de données' (Barroso-Bergadà et al., 2023a). Elles ont également été utilisées pour illustrer une nouvelle méthode d'apprentissage des réseaux d'interaction entre microorganismes, disponible dans le package InfIntE (https://github.com/didacb/InfIntE; Barroso-Bergadà et al. 2023b). En parallèle, les abondances totales des champignons et des bactéries ont été évaluées pour chaque échantillon. Ces données ne font pas partie de l'article de données mais elles font partie de mon chapitre.

Dans ce chapitre, les analyses de données ont été étendues. J'ai ainsi analysé les données de communautés fongiques et bactériennes (tables d'ASV) livrées avec le 'papier de données' de Barroso-Bergadà et al. (2023a). J'ai contribué à la formulation des hypothèses, en collaboration avec Corinne Vacher et Lucile Pellan (UMR SAVE). Puis j'ai réalisé toutes les analyses statistiques et l'interprétation des résultats. J'ai rédigé les sections "analyse statistique" du chapitre « Matériel et méthodes », et les chapitres "résultats" et "discussion", et produit les figures et annexes associées aux résultats. L'introduction et la première partie du matériel et méthodes ont été rédigées par ma collègue Lucile Pellan, en collaboration avec Corinne Vacher. Julie Aubert (MIA Paris-Saclay) a donné des conseils sur les analyses de réseau présentées dans le chapitre.

Tous les auteurs ont contribué aux relectures. Le chapitre sera soumis prochainement à *Frontiers in Microbiology* en tant qu'article de recherche.

Chapitre 2

A new scenario of pathogen-microbiota interactions for the oomycete *Plasmopara viticola*

Paola Fournier, Lucile Pellan, Julie Aubert, Patrice This, Corinne Vacher

In preparation

Abstract

- A key question in microbial ecology is how microbiota regulates the host's invasion by pathogens. Several ecological theories link the diversity, abundance and assembly processes of the microbiota with its resistance to invasion, but there remains a lack of understanding regarding the specific properties of microbial communities that confer protection to the host.
- We addressed this question for the pathogenic oomycete *Plasmopara viticola*, the causal agent of grapevine downy mildew. We compared microbiotas associated with asymptomatic tissues and disease lesions, using state-of-the-art methods in microbial community ecology, to unravel pathogen-microbiota interactions.
- We found that infection triggers only subtle changes in the microbiota despite visible leaf symptoms. These changes included, in particular, an enrichment of the microbiota in basidiomycete yeasts and *Bacillus* species. Tissues that remained asymptomatic during epidemic harbored a more diverse microbiota, but they were not consistently associated with microorganisms known for their biocontrol properties. Instead, asymptomatic tissues were associated with other aerial pathogens of grapevine.
- Taken together, our results suggest that *P. viticola* competes with other pathogens for leaf space, and that infected leaves locally recruit certain microbial taxa with biocontrol activity, such as basidiomycetous yeasts and *Bacillus* species, to counteract disease.

Introduction

The role of the microbiota in the emergence and spread of diseases has long been overlooked. However, the intricate interactions between hosts, pathogens and microbiota are now central to disease research, as host resistance to diseases is, at least in part, driven by the composition of the microbiota and the occupation of the microbial niche (Mendes *et al.*, 2018, 2019; Vannier *et al.*, 2019; Liu *et al.*, 2020; Ping *et al.*, 2024). This growing awareness has spurred the development of new concepts, such as disease ecology and pathobiome (Vayssier-Taussat *et al.*, 2014; Sweet & Bulling, 2017; Brader *et al.*, 2017; Bass *et al.*, 2019; Bernardo-Cravo *et al.*, 2020), and more recently, the concept of a protective microbiota, also known as the resistobiome (Goossens *et al.*, 2023). Central to this field are questions regarding how the microbiota regulates the invasion by pathogens (Teixeira *et al.*, 2019; Li *et al.*, 2021) and how the host maintains microbiota homeostasis (Foster *et al.*, 2017; Hacquard *et al.*, 2017; Karasov *et al.*, 2020; Paasch & He, 2021). Addressing these questions is key to fighting diseases by harnessing the microbiota, whether through preventive or curative inoculation of microorganisms, the use of metabolites that steer microbial ecosystem functioning, or by

modulating host physiology, defense mechanisms, and environmental conditions (Busby *et al.*, 2017; French *et al.*, 2021; Compant *et al.*, 2024).

Over the past decade, numerous studies have compared the microbiotas of "healthy" tissues to those infected by various plant pathogens, aiming to identify the properties of the microbiota that promote or inhibit disease (Jakuschkin *et al.*, 2016; Köberl *et al.*, 2017; Wei *et al.*, 2019; Carrión *et al.*, 2019; López *et al.*, 2020; Zhou *et al.*, 2021; Ahmed *et al.*, 2022; Dastogeer *et al.*, 2022; Gu *et al.*, 2022). Several ecological theories have been tested, including the Anna Karenina Principle (Zaneveld *et al.*, 2017; Arnault *et al.*, 2023) and the diversity-invasibility hypothesis (Jousset *et al.*, 2011; van Elsas *et al.*, 2012; Mallon *et al.*, 2015). According to the Anna Karenina Principle, disease is linked to the loss of the host's capacity to regulate its microbiota, leading to greater stochasticity in microbiota assembly and higher compositional dissimilarity (i.e., β-diversity) among microbiotas associated to infected tissues compared to healthy ones (Arnault *et al.*, 2023). This loss of host control over its microbiota, sometimes termed microbiota "dysbiosis" (Arnault *et al.*, 2023), is also expected to affect microbial load. A recent study demonstrated that microbial load remains under plant control until the pathogen species invades the plant tissues, and that successful colonization by the pathogen is associated with a higher microbial load (Karasov *et al.*, 2020). According to the diversity-invasibility hypothesis, higher microbial diversity limits pathogen invasion (Jousset *et al.*, 2011; van Elsas *et al.*, 2012; Mallon *et al.*, 2015) through at least four mechanisms. Higher microbial community α-diversity increases the likelihood of including beneficial species (sampling effect) and prevents the loss of beneficial functions during stress events (insurance effect). It also increases the occupation of the microbial niche (complementarity effect) and the probability of facilitative interactions between microorganisms that lead to novel protective functions (synergistic effect) (Hooper *et al.*, 2005; Saleem *et al.*, 2019). However, both the Anna Karenina Principle and the diversity-invasibility relationship were recently challenged. A recent study, supported by multiple case studies, argues that neither β-diversity nor α-diversity reliably correlates with host health (Williams *et al.*, 2024). There is therefore a long way to go to fully understand the relationship between microbiota and host health. In this study, we aim to advance the field by investigating the relationship between plant microbiota and a major disease caused by an oomycete pathogen.

Oomycetes cause some of the most devastating crop diseases (Derevnina *et al.*, 2016). Among them are grapevine downy mildew, caused by *Plasmopara viticola*, which devastated European vineyards in the 19th century (Fontaine *et al.*, 2021), and *Phytophthora infestans,* the potato blight responsible for the Great Famine in Ireland (Yoshida *et al.*, 2013). Both continue to cause significant production losses. These eukaryotic microorganisms are characterized by hyphal growth and predominantly asexual reproduction, involving flagellated zoospores capable of moving through the soil or towards their host plant (Grenville-Briggs *et al.*, 2005; Hardham, 2007). Interactions between pathogenic oomycetes and the soil and plant microbiota have been observed at various stages of their life cycle (Conigliaro *et al.*, 2008; Kemen, 2014; Larousse & Galiana, 2017; Eitzen *et al.*, 2021; Gómez-Pérez *et al.*, 2023). The microbiota can

disrupt zoospore mobility, inhibit zoospore attachment to the host plant, or interfere with hyphal growth (Falk, 1995; Kortekamp, 1997; Talontsi *et al.*, 2012; Kasteel *et al.*, 2023). Once infection occurs, the pathogenic oomycete can facilitate the invasion by other pathogen species and restructure the microbiota, becoming a 'hub' species in microbial networks (Agler *et al.*, 2016). A better understanding of the microorganisms and microbial community properties that interfere with the life cycle of pathogenic oomycetes is essential for the development of microbial biocontrol methods for these diseases.

In the case of *Plasmopara viticola*, several microorganisms have been identified as potential biocontrol agents through experiments conducted under controlled conditions. These potential biocontrol agents include several bacteria of the *Bacillus* genus (Zhang *et al.*, 2017; Bruisson *et al.*, 2019), as well as fungi such as *Acremonium byssoides* (Lo Piccolo *et al.*, 2012; Burruano *et al.*, 2016; Zanzotto & Morroni, 2016), Alternaria spp. (Musetti *et al.*, 2006b), *Epicoccum nigrum* (Kortekamp, 1997; Zanzotto & Morroni, 2016; Taguiam *et al.*, 2021), *Fusarium* spp. (Ghule *et al.*, 2018), and *Trichoderma* spp. (Perazzolli *et al.*, 2008; Dagostin *et al.*, 2011; Palmieri *et al.*, 2012; Banani *et al.*, 2014; Lazazzara *et al.*, 2021). A recent study also discovered *Simplicillium lanosoniveum*, a hyperparasite specific to *P. viticola*, through isolations from grapevine lesions (Shen *et al.*, 2022). Despite these promising findings, only one bacterial strain, *Bacillus amyloliquefaciens*, is registered in France for controlling *P. viticola*[8]. Consequently, there is considerable room for improvement in biocontrol strategies targeting grapevine downy mildew. It would be particularly valuable to explore the combination of multiple biocontrol agents (Nicot *et al.*, 2012; Xu & Jeger, 2020), building on ecological theories linking microbiota diversity and composition to disease development (Saleem et al. 2019; Arnault et al. 2023). Such combinations of microorganisms might improve the efficiency and robustness of biocontrol by providing functional redundancy and complementarity in modes of action (Guetsky *et al.*, 2007; Vega *et al.*, 2009; Panebianco *et al.*, 2015).

The goal of this study was to deepen our understanding of the interactions between the grapevine leaf microbiota and the pathogenic oomycete *Plasmopara viticola*, responsible for downy mildew, and to test some debated ecological theories linking microbiota diversity with disease development (Williams *et al.*, 2024). We compared the microbial community composition between asymptomatic and symptomatic tissues on the same leaves, to identify microbial taxa consistently more abundant in asymptomatic leaf tissues. We also inferred microbial interaction networks in asymptomatic and symptomatic leaf tissues, to identify microbial taxa that may regulate the pathogen and be useful for developing future biocontrol strategies. We also tested three hypotheses derived from ecological theories. First, we hypothesized that (H1) leaf tissues that remain asymptomatic during an epidemic harbor a more diverse microbiota than symptomatic tissues, consistent with the diversity-invasibility relationship (Mallon *et al.*, 2015; Saleem *et al.*, 2019). Second, we hypothesized that (H2) the

[8] https://info.agriculture.gouv.fr/boagri/instruction-2022-949

total abundance of the microbiota in asymptomatic tissues is lower than in symptomatic tissues, in line with the dysbiosis concept, which posits that disease is linked to a loss of host's control over its microbiota (Karasov *et al.*, 2020; Arnault *et al.*, 2023). Third, we hypothesized that (H3) microbial communities in symptomatic tissues are more stochastic and more dissimilar to each other, compared to those associated to asymptomatic tissues, in line with the Anna Karenina Principle (Zaneveld *et al.*, 2017; Arnault *et al.*, 2023). Our findings are discussed in the context of developing the microbial biocontrol of downy mildew, by introducing microbial antagonists of *P. viticola* and harnessing the properties of the grapevine microbiota to enhance its resistance to pathogen invasion.

Materials and methods

Experimental design, pathogen quantification and sequencing of fungal and bacterial communities

The experimental design and metabarcoding approaches are described in detail in the data paper authored by Barroso-Bergadà et al. (2023). Briefly, 270 grapevine leaves, each carefully selected to contain both symptomatic sporulating downy mildew lesions (S) and asymptomatic (A) areas, were collected from nine vineyard plots spread over three major French wine-growing regions (Occitanie, Nouvelle-Aquitaine, hereafter referred to as Aquitaine and Champagne) (Fig. 1). The sampling campaign took place during the peak of grapevine downy mildew epidemic in each region, spanning from mid-June to mid-July 2018. Leaves were processed on the day of sampling: on each leaf, four discs of 12 mm diameter each were cut, two from sporulating downy mildew lesions (S) and two from asymptomatic areas (A). These two S discs of each disc were placed together in a collection tube, as well as the two A discs. Leaf samples were dried with silica gel during the sampling campaign and freeze-dried at its end. Total DNA was extracted using the DNeasy Plant Mini kit (Qiagen, France), with a slightly modified version of the protocol as recommended by Kerdraon et al. (2019). The metabarcoding approach targeted the internal transcribed spacer 1 (ITS1) region of the fungal nuclear ribosomal DNA (nrDNA) gene using the primer pair ITS1F-ITS2 (White *et al.*, 1990; Gardes & Bruns, 1993) and the V5-V6 region of the bacterial 16S ribosomal RNA (rRNA) gene using the primer pair 799F-1115R (Chelius & Triplett, 2001a; Redford *et al.*, 2010) (Supplementary Table S1). Sequencing of the amplified ITS and 16S regions was performed on an Illumina MiSeq platform. Sequences were processed using the DADA2 pipeline in R (Callahan *et al.*, 2016). This pipeline involved primer removal, inference of amplicon sequence variants (ASVs), chimera removal, taxonomic assignment, and data filtering to eliminate contaminants, low-abundance ASVs, and sequences not assignable to a bacterial or fungal phylum. The databases used for taxonomic assignment were UNITE All Eukaryotes v8.3 (Abarenkov *et al.*, 2021) and SILVA v138.1 (Quast *et al.*, 2013) for the ITS and 16S sequences, respectively. The ASVs were finally clustered using the LULU algorithm (Frøslev *et al.*, 2017) with default parameters. Moreover, abundance of *P. viticola* was quantified across all samples with quantitative real-time PCR targeting the ITS1 region (Supplementary Table S1).

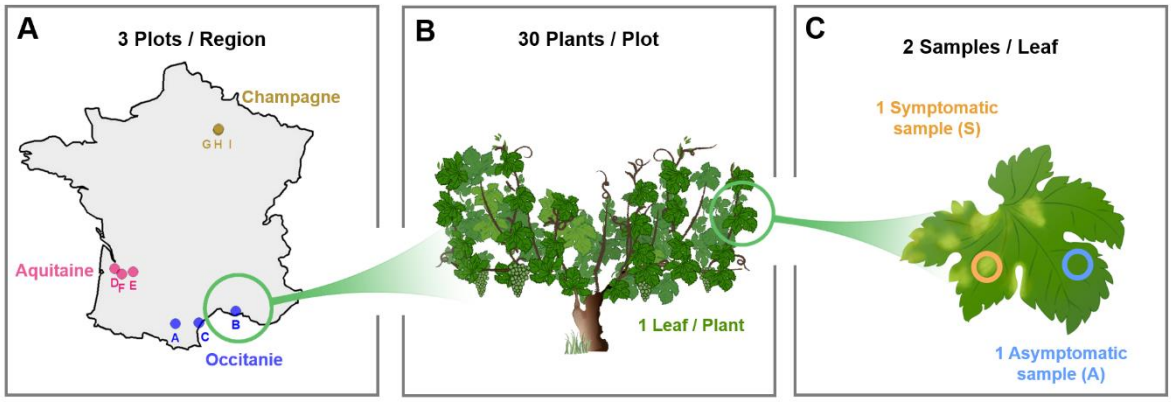


Figure 1: Experimental design to assess the relationship between leaf microbiota and the oomycete *Plasmopara viticola* during a downy mildew epidemic.
(A) In three viticultural regions of France (Occitanie, Aquitaine, and Champagne), three vineyard plots were sampled. (B) From each plot, one leaf showing downy mildew symptoms was collected from 30 grapevine plants at the peak of downy mildew epidemic. (C) On each leaf, two paired samples were taken: one from symptomatic tissue (sporulating, non-necrotic lesions, labeled as S for Symptomatic) and one from asymptomatic tissue (labeled as A for Asymptomatic), resulting in a total of 540 samples (270 paired samples). Each sample consisted of two leaf discs (not shown on the figure for clarity).

Quantification of total abundance of fungal and bacterial communities

In addition, in the present study, we quantified total fungal and bacterial abundance across all samples using digital droplet PCR assays (ddPCR™; Hindson et al., 2011). These ddPCR data were not included in the data paper by Barroso-Bergadà et al. (2023) and provide a new layer of information that allow us to test hypothesis H2. The assays were conducted with the QX200 Droplet Digital PCR System from Bio-Rad at the Genome Transcriptome Facility of Bordeaux (France). Primers and probes were synthesized by Integral DNA Technologies with the probe labeled with 5'6-FAM, an Internal ZENTM and 3'IBFQ quenchers. Fungal DNA was amplified using the universal fungal primer pair ITS86F (5'-GTGAATCATCGAATCTTTGAA-3') and ITS4 (5'-TCCTCCGCTTATTGATATGC-3') as recommended by Beeck et al. (2014). PCR reactions were carried out in a final volume of 22 µl using the ddPCR™ EvaGreen Supermix (Bio-Rad, USA) with 11 µl of 2X EvaGreen Supermix, 1.83 µL of each primer at 1.5 µM and 2 µL of DNA template or ultrapure water in the negative control. DNA extract of *Phaeomoniella chlamydospora,* a pathogenic fungus responsible for the Esca disease in grapevine (González-Domínguez *et al.*, 2020), was used as a positive control. Bacterial DNA was amplified using the universal bacterial primer pair 16S-F (5'-CGGTGAATACGTTCCCGG-3'), 16S-R (5'-TACGGCTACCTTGTTACGACTT-3') and probe 16S-Pr (5'-CTTGTACACACCGCCCGTC-3') as recommended by Furet et al. (2009). PCR reactions were conducted in a final volume of 22 µl using the ddPCR™ Supermix for Probes No dUTP (Bio-Rad, USA), with 11 µl of 2X Supermix, 2.2 µL of each primer at 9 µM, 1.22 µL of probe at 9 µM and 2 µL of DNA template or ultrapure water in the negative control. The positive control was a mock community composed of 14 bacterial strains (*Streptococcus mitis, Streptococcus oralis, Pseudomonas aeruginosa, Stenotrophomonas maltophilia, Staphylococcus epidermidis, Staphylococcus aureus, Acinetobacter baumannii, Klebsiella pneumoniae, Proteus mirabilis, Serratia marcescens, Lactobacillus, Escherichia coli* (ATCC

25922), *Enterobacter cloacae, Enterococcus faecalis* (ATCC 29212)). For both fungi and bacteria, 20 µL of mix containing the sample was partitioned into droplets with the QX200 Droplet Generator and then transferred to 96-well PCR plates. PCRs were performed in a Bio-Rad C1000 (Bio-Rad, USA) instrument, with the following parameters: [95 °C × 5 min; 40 cycles of (95°C × 30 s, 55°C × 1 min, 72°C × 30 s), 4 °C × 5 min, 90°C × 5 min] for fungi and [95 °C × 5 min; 40 cycles of (95°C × 30 s, 60°C × 1 min), 98 °C × 10 min] for bacteria. The QX200 droplet reader analyzed each droplet individually to detect the fluorescence signal. The number of copies of the target sequence per µl of DNA extract was calculated from the number of positive droplets (out of an average of ~20k droplets per sample). The estimated total abundance expressed in ng/µl was obtained by multiplying the estimated concentration (expressed as number of copies/µl) by the volume of sample/buffer mixture (11 µl) and after adjusting for the 1/100 dilution of the DNA extract.

Statistical analysis

All the statistical analyses were performed with R v4.2.3 (R Core Team, 2023). Microbial community analyses were performed using the R packages *phyloseq* v1.48.0 (McMurdie & Holmes, 2013) and *speedyseq* v0.5.3.9018 (McLaren, 2023), and all figures were generated using the *ggplot2* v3 package. 5.1 (Wickham, 2016), *cowplot* v1.1.3 (Wilke, 2024), *ggh4x* v0.2.8 (van den Brand, 2024), ggsignif v0.6.4 (Ahlmann-Eltze & Patil, 2021), *patchwork* v1.2.0 (Pedersen, 2024), *microViz* v0.10.8 (Barnett *et al.*, 2021), and *ggtext* v0.1.2 (Wilke and Wiernik, 2022).

Data preparation

Microbial community analyses were either based on sample × ASV raw count matrices or on matrices transformed to account for compositional effects. The compositional effects were accounted for by transforming raw sequence counts using the centered and log-ratio (CLR) transformation (Gloor *et al.*, 2017). Prior to the CLR transformation, we applied a Bayesian multiplicative treatment of zeros using the *cmultRepl* function of the *zComposition* package v1.5.0.3 (Palarea-Albaladejo & Martín-Fernández, 2015). This function converts zero counts, which would lead to errors in the log ratios, into estimates close to zero, assuming that these zeros are due to undersampling rather than absence. It also drops rows (ASVs) or columns (samples) with more than 80% zeros or missing data.

To build phylogenetic trees of ASVs, we first performed multiple sequence alignment using the *AlignSeqs* function of the package *DECIPHER* v2.26.0 (Wright, 2016). Next, the phylogenetic distance matrix was calculated via maximum likelihood using the *dist.ml* of the package *phangorn* v2.11.1 (Schliep, 2011; Schliep *et al.*, 2016) and the tree was built using the Neighbor-Joining method (*NJ* option of the *phangorn* package). Finally, we evaluated the phylogenetic tree's likelihood in relation to the alignment and chosen model using the *pml* function of the *phangorn* package.

Comparison of *P. viticola* abundance between asymptomatic and symptomatic leaf samples

To begin with, we verified that leaf tissues classified as symptomatic (S) based on visual observations contained a higher abundance of *P. viticola* than tissues defined as asymptomatic (A), according to qPCR data. A pairwise Wilcoxon test was used with the alternative hypothesis that the abundance of *P. viticola* is higher in asymptomatic tissues, by using the alternative argument = "greater" in the *pairwise.wilcox.test* function (package *stats* v4.2.3 (R Core Team, 2023)).

Analysis of factors driving variation in microbial community composition

Principal Component Analysis (PCA) was applied to the sample × ASV CLR-transformed matrix to visualize variation in microbial community composition, using the *microViz* package. We identified key factors influencing community composition using variance partitioning and Redundancy Analysis (RDA) implemented using the *varpart* and *rda* functions of the *vegan* package v2.6.4 (Oksanen *et al.*, 2024), respectively. Nine explanatory factors were used in both analyses. For variance partitioning, we categorized them into three groups: Disease, Geography and Variety. The Disease category represented infection by *P. viticola* and included two variables: *P. viticola* abundance estimated by qPCR (in ng/µl) and visual assessments of downy mildew symptoms (asymptomatic or symptomatic leaf sample). The Variety category comprised a single variable, representing the grapevine variety. This variable had seven modalities, corresponding to the grape varieties (Chasan, Chardonnay, Gamay, Merlot, Cabernet Franc, Meunier, Pinot Noir) included in the experiment (Barroso-Bergadà *et al.*, 2023a). The Geography category represented the sample location and consisted of six variables. The first variable was the vine leaf from which the leaf discs were sampled. This variable captured the pairing of symptomatic (S) and asymptomatic (A) tissue samples taken from the same leaf. The five other variables were the Principal Coordinates of the Neighbourhood Matrix (PCNM; (Borcard & Legendre, 2002)) representing the spatial distribution of the nine vineyard plots included in the experiment (Barroso-Bergadà *et al.*, 2023a).The PCNMs were generated by calculating an Euclidean distance matrix between all samples using their spatial coordinates (longitude and latitude) with the *distance()* function (package *vegan*). The *pcnm()* function (package *vegan*) performed Principal Coordinates Analysis (PCoA) of the truncated matrix and provided us with the eigenvectors associated with positive eigenvalues, the PCNMs, which we used as spatial predictors in the RDA. They captured both the higher proximity of samples collected from the same plot (plot effect) and the higher proximity of samples collected from the same wine-producing region (region effect). For both variance partitioning and RDA, the sample x ASV CLR-transformed matrix was used as the response variable. Nonnumeric explanatory variables were treated as dummy variables, and all variables were standardized using the *scale* function (package *base* v4.2.3 (R Core Team, 2023)). For the RDA, an automatic stepwise selection of explanatory variables, both forward and backward, was performed using the *ordistep* function of the *vegan* package. Finally, an RDA was performed with all selected explanatory variables included as constraints. Permutation tests were performed using the *anova.cca* function of the *vegan* package to

assess the significance of the fitted models and to evaluate the marginal effects of the constraints.

Identification of microbial taxa specific to asymptomatic and symptomatic leaf samples

To determine whether asymptomatic and symptomatic samples exhibited higher abundances of specific microbial taxa, we used a set of four Differential Abundance Analysis (DAA) methods: ANCOM-BC2 (Lin & Peddada, 2024), Maaslin2 (Mallick *et al.*, 2021), LinDA (Zhou *et al.*, 2022) and ZicoSeq (Yang & Chen, 2022). We selected these methods for the following reasons: they were specifically developed for microbiota analysis by explicitly accounting for zero inflation and compositional effects; they allow the specification of random and covariate effects; and they have been recommended in recent methodological studies (Nearing *et al.*, 2022a; Yang & Chen, 2022, 2023; Regueira-Iglesias *et al.*, 2023). This set of four DAA was used to compare ASV abundances between asymptomatic and symptomatic samples, while taking into account microbial community variation among plots. For all four methods, the plot and leaf from which the symptomatic and asymptomatic samples were taken were included as a random factor. The parameters were set to defaults except for the minimum prevalence threshold, which was set to 10%, and the adjusted p-value for an ASV to be considered differentially abundant, which was set to 0.05. All analyses were performed using the sample × ASV raw count matrix. They were performed using the *ANCOMBC* v2.0.3 (Lin & Peddada, 2020; Lin *et al.*, 2022), *Maaslin2* v1.12.0 (Mallick *et al.*, 2021), *GUniFrac* v1.8 (Chen *et al.*, 2023), and *MicrobiomeStat* v1.2 (Zhang *et al.*, 2024) packages. For each ASV identified as differentially abundant by at least one of the four DAA methods, we calculated two scores: (1) the number of methods that identified this ASV as differentially abundant, ranging from 1 to 4, and (2) the average association coefficient across the methods. To calculate the average association coefficient, the coefficients provided by each DAA method were standardized between 0 and 1 when the ASV was more abundant in asymptomatic samples, and between 0 and -1 when the ASV was more abundant in symptomatic samples, before calculating the average coefficient across the methods.

In addition, we identified the microbial taxa whose relative abundance covary with the total abundance of *P. viticola* in leaf samples, as determined by qPCR values, using the Threshold Indicator Taxa ANalysis (TITAN) method of the *TITAN2* package v2.4.3 (Baker *et al.*, 2023a). For this analysis, we used the sample x ASV raw count matrix, keeping only ASVs with more than 100 reads in total and present in at least 3 samples, as required by TITAN. The method identified ASVs whose abundance increased as *P. viticola* DNA concentration decreased, and ASVs whose abundance increased as *P. viticola* DNA concentration increased. These ASVs will hereafter be referred to as indicators of low and high *P. viticola* abundance in leaf. To evaluate the strength of the relationship, we used the standardized Indicator Value (IndVal) score defined by Dufrene and Legendre (Dufrêne & Legendre, 1997) expressed as a z-score.

Inference of microbial interaction networks associated to asymptomatic and symptomatic leaf samples

Ongoing analyses in collaboration with Julie Aubert.

Testing hypothesis H1: is microbiota α-diversity higher in leaf tissues that remain asymptomatic during an epidemic, compared to disease lesions?

To assess whether the α-diversity of leaf microbial communities was higher in asymptomatic leaf tissues than in symptomatic ones, we calculated three diversity indices. These indices are part of the Hill number framework (Chao *et al.*, 2014), which includes a parameter *q* that determines the sensitivity of the indices to the relative abundance of ASVs. This framework gives less weight to rare ASVs as *q* increases. The Hill number corresponding to $q = 0$ represents the richness of ASVs, where each ASV counts for 1 regardless of its relative abundance. The Hill number corresponding to $q = 1$ is the exponential of Shannon's entropy index (Shannon, 1948), where the weight of each ASV is proportional to its relative abundance. The Hill number corresponding to $q = 2$ is the inverse of Simpson's concentration index (Simpson, 1949), which disproportionately favors abundant ASVs and is particularly relevant for metabarcoding data, as rare ASVs often correspond to artifacts, and their inclusion can lead to erroneous ecological conclusions (Taberlet *et al.*, 2018). The three indices were calculated from the sample × ASV raw count matrix using the *ChaoRichness*, *ChaoShannon*, and *ChaoSimpson* functions in the *iNEXT* v3.0.1 package (Chao *et al.*, 2014; Hsieh & Chao, 2024). Microbiota diversity was compared between asymptomatic and symptomatic leaf samples using linear mixed-effects models. We built six models, each corresponding to a combination of microbial kingdom (bacteria or fungi) and α-diversity index (q=1, 2 or 3). These models included visual assessments of downy mildew symptoms (asymptomatic vs symptomatic leaf sample) as a fixed effect and leaf as a random effect, to take into account the pairing of symptomatic and asymptomatic samples taken from the same leaf. Additional fixed effects, such as grapevine variety, plot, and region, were also included to control for potential confounding factors affecting microbial diversity. Graphical checks for homoscedasticity and normality of residuals were performed using the packages *performance* v0.12.0 (Lüdecke *et al.*, 2021) and *DHARMa* v0.4.6 (Hartig & Lohse, 2022). Model construction and evaluation were conducted using the packages *lmerTest* v3.1.3 (Kuznetsova *et al.*, 2017) and *car* v3.1.2 (Fox & Weisberg, 2018). When explanatory factors with more than two levels were significant, post-hoc tests were conducted using the *emmeans* function of the *emmeans* v1.10.1 package (Lenth *et al.*, 2024) to estimate marginal means for each factor level. To adjust for multiple comparisons, we applied the Bonferroni method using the *pairs* function of the *graphics* v4.2.3 package. Finally, means were ranked in descending order, and groupings were identified using the *cld* function of the *lsmeans* v2.30.0 package (Lenth, 2016) to highlight significant differences between factor levels.

Testing hypothesis H2: does fungal and bacterial load increase in disease lesions caused by the oomycete *P. viticola*, suggesting a loss of of plant control over its microbiota?

Linear mixed-effects models were also used to compare microbial load between asymptomatic and symptomatic leaf samples. We built two models, one for each microbial kingdom (bacteria or fungi). The models included visual assessments of downy mildew symptoms (asymptomatic vs symptomatic leaf sample) as a fixed effect and leaf as a random effect, to take into account the pairing of symptomatic and asymptomatic samples taken from the same leaf. Additional fixed effects, such as grapevine variety, plot, and region, were also included to control for potential confounding factors affecting microbial diversity. Model evaluation was performed as described above.

Testing hypothesis H3: are microbiotas in disease lesions more dissimilar to each other and more influenced by stochastic processes, consistent with the Anna Karenina Principle?

To test the Anna Karenina Principle (Zaneveld *et al.*, 2017; Arnault *et al.*, 2023), we used both β-diversity and β-nearest-taxon (βNTI) indices to measure dissimilarity among communities and quantify community assembly processes, respectively. In addition to the βNTI index, we also used the normalized stochasticity ratio (NST) developed by Ning et al. (2019), which is considered relevant for testing the Anna Karenina Principle in plants (Arnault *et al.*, 2023).

To investigate whether microbial communities in disease lesions are more dissimilar to each other than those associated with asymptomatic tissues, we used the weighted UniFrac distance as a β-diversity index. We calculated it by using the *distance* function of the *phyloseq* package. We then calculated the distance of each sample to the group centroid using the *betadisper* function from the *vegan* package (lesions vs. asymptomatic tissues). Finally, we tested whether the differences in dispersion between groups were statistically significant, by using the *permutest* function (*vegan* package).

Then we analyzed community assembly processes. To calculate the βNTI index, we followed the procedure described by Barnett et al. (2020). To calculate the NST index, we followed the procedure described by (Ning *et al.*, 2019). According to Stegen et al. (2013), a β-NTI value comprised between –2 and 2 reveals a dominance of stochastic processes in the assembly, and a |β-NTI| >2 reveals the dominance of deterministic processes. The NST index was developed with 50% as the limit between a more deterministic (<50%) and more stochastic (>50%) assembly. We used a Kruskal-Wallis test to assess whether mean βNTI values differed between symptomatic and asymptomatic leaf samples. We compared NST values between symptomatic and asymptomatic samples using the *nst.boot* function of the *NST* package.

Results

Our results complement and extend previous analyses of the same dataset, which included microbial community profiles (Barroso-Bergadà et al., 2023a) and illustrated a new network learning method using the fungal dataset (Barroso-Bergada et al., 2023b).

qPCR data confirm minimal infection of asymptomatic tissues by *P. viticola*

As expected, the abundance of *P. viticola* was significantly lower in asymptomatic leaf tissues than in symptomatic ones (paired Wilcoxon test, $p < 0.001$, n=512) (Supplementary Fig. S1). In asymptomatic tissues, *P. viticola* abundance was, on average, very close to 0, with minimal variability among samples (mean = 0.0131 +/- sd = 0.0696ng/µL). In disease lesions, the abundance of *P. viticola* was significantly higher, with considerable variability among samples (mean = 2.24 +/- sd = 5.73ng/µL) (Supplementary Fig. S1). These results support the relevance of classifying samples into two categories (asymptomatic vs. symptomatic) based on visual observation of symptoms. They also highlight the presence of a gradient in the abundance of *P. viticola* within symptomatic tissues (Supplementary Fig. S1), which could represent different stages of infection.

Geography, and to a lesser extent grapevine variety, have more influence on microbiota composition than infection by downy mildew

Fungal communities of grapevine leaves were spatially structured, with marked differences in composition between the three wine-producing regions (Fig. 2 and 3 and Supplementary Fig. S2). Fungal community profiles showed a clear gradient from South to North across France (i.e., from Occitanie to Champagne; Fig. 3).

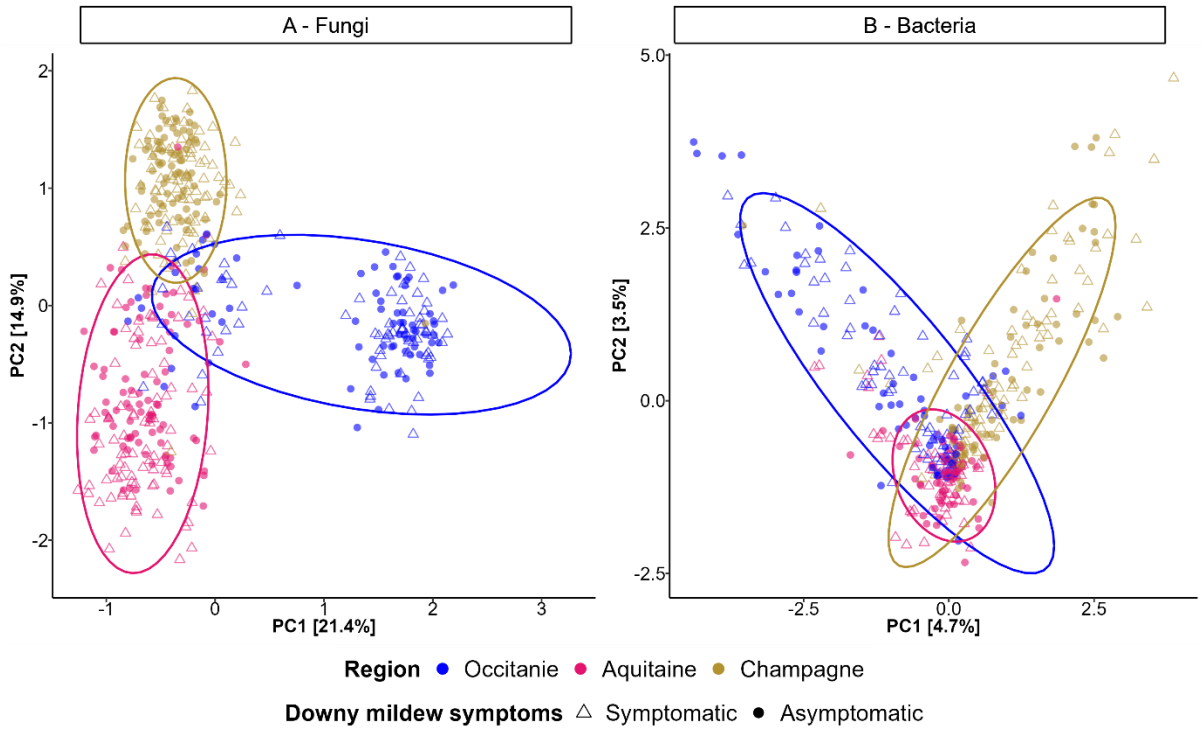


Figure 2: Variation in microbial community composition of grapevine leaves sampled during downy mildew epidemic across three French wine-growing regions. Compositional dissimilarities between (A) fungal and (B) bacterial communities of grapevine leaves, represented by a Principal Component Analysis (PCA). Samples collected from the same wine-growing region are represented with the same color and are surrounded with an ellipse. Symbols indicate the presence or absence of downy mildew symptoms (triangles and circles, respectively).

The proportion of Basidiomycetes, particularly the Tremellomycetes class, decreased from South to North in favor of Ascomycetes, predominantly represented by the class Dothideomycetes (Fig. 3).

The most abundant fungal species were similar across regions (Table 1) but their abundance varied across regions. Among the top 10 most abundant species across regions (Table 1) were the basidiomycete yeasts *Filobasidium chernovii*, *Filobasidium oeirense*, *Vishniacozyma victoriae* and *Sporobolomyces roseus* as well as the ascomycete *Mycosphaerella tassiana*. This latter, which belongs to the Dothideomycetes class, strongly increased in abundance from South to North (7.07% in Occitanie, 12.40% in Aquitaine and 48.10% in Champagne), accounting for the rise in Ascomycete abundance in North of France. Other fungi, such as *Filobasidium wieringae*, *Alternaria metachromatic*, and *Stemphylium solani*, were among the top 10 most abundant species in two of the three regions (Table 1). Variance partitioning confirmed that geography was the most structuring factor. Geography accounted for 36.82% of the variance in fungal communities, followed by grapevine variety, which explained6.16%. Infection by downy mildew had a minimal impact on fungal community composition, accounting for only 0.59% of the variance (Supplementary Fig. S3). According to RDA, all three factors were however significant (Supplementary Table S2).

Bacterial communities were less structured than fungal communities (Fig. 2 and Supplementary Fig. S2) but the hierarchy of driving factors was the same as for fungal communities. Geography accounted for 15.06% of the variance in bacterial communities, followed by grapevine variety which explained 3.31%. Infection by downy mildew had a minimal impact on bacterial community composition, accounting for only 0.51% of the variance (Supplementary Fig. S3). Only Geography had a significant effect on bacterial community composition according to the RDA (Supplementary Table S2). The genera *Sphingomonas*, *Frigobacterium*, *Pantoea*, *Curtobacterium*, and *Methylobacterium* consistently ranked among the top 10 most abundant genera across all three regions but their abundance varied across regions. The genus *Sphingomonas*, in particular, decreased in abundance from South to North (36.95% in Occitanie, 24.20% in Aquitaine and 6.46% in Champagne) (Table 2).

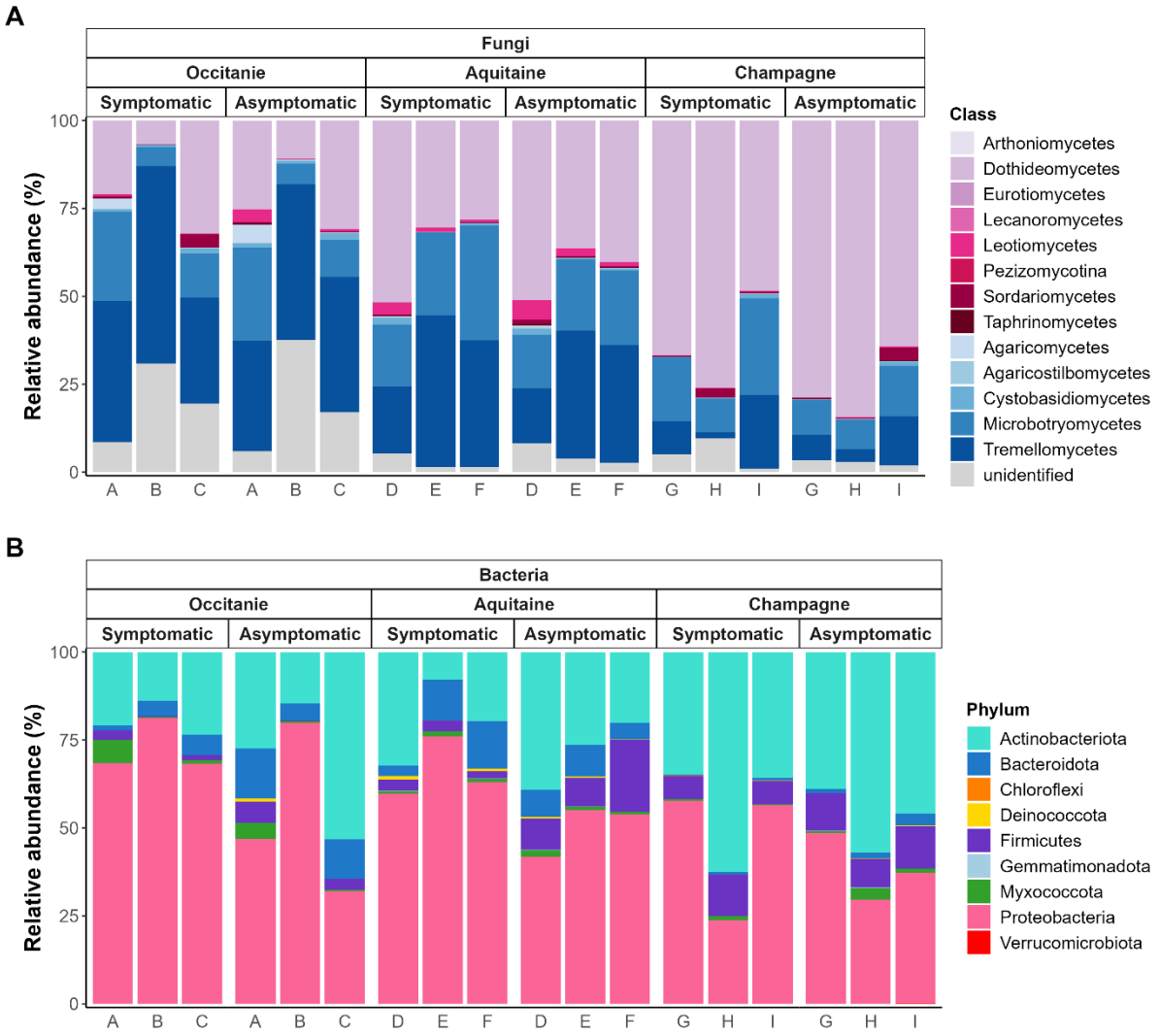


Figure 3: Microbial community profiles of grapevine leaves, depending on the geographic region and infection by downy mildew (*P. viticola*).

(A) Fungal and (B) bacterial community profiles in grapevine leaves collected during the peak of the downy mildew epidemic across nine plots (A–I) in three French wine-growing regions: Aquitaine, Champagne, and Occitanie (Fig. 1). The relative abundance of fungal classes and bacterial phyla are averaged over 30 samples collected for each condition. In fungal community profiles, Ascomycota classes are represented with a gradient of pink, while Basidiomycota classes are represented with a gradient of blue.

Table 1: Most abundant fungal species of grapevine leaves in three French wine-growing regions.

The table shows the top ten most abundant fungal species in Occitanie, Aquitaine and Champagne. Species in bold are among the top ten most abundant species in all three regions, while those in underlined are among the top ten most abundant species in 2 out of 3 regions. Relative abundance (%) indicates the proportion of sequences assigned to the species relative to the total number of sequences in the dataset. Prevalence (%) indicates the percentage of samples where the species is present with at least one sequence.

French region								
Occitanie (Plots A, B, and C)			Aquitaine (Plots D, E, and F)			Champagne (Plots G, H, and I)		
Fungal species	Relative abundance (%)	Prevalence (%)	Fungal species	Relative abundance (%)	Prevalence (%)	Fungal species	Relative abundance (%)	Prevalence (%)
Sporobolomyces roseus (Basidiomycota)	13.37	96.71	***Sporobolomyces roseus*** (Basidiomycota)	19.38	97.13	***Mycosphaerella tassiana*** (Ascomycota)	48.10	100
Mycosphaerella tassiana (Ascomycota)	7.07	95.39	***Filobasidium chernovii*** (Basidiomycota)	12.40	97.13	***Sporobolomyces roseus*** (Basidiomycota)	14.23	100
Cladosporium delicatulum (Ascomycota)	5.40	84.87	***Mycosphaerella tassiana*** (Ascomycota)	9.88	99.43	***Cladosporium delicatulum*** (Ascomycota)	13.63	98.30
Filobasidium chernovii (Basidiomycota)	3.87	88.16	*Filobasidium wieringae* (Basidiomycota)	7.31	87.36	***Vishniacozyma victoriae*** (Basidiomycota)	3.50	97.16
Filobasidium wieringae (Basidiomycota)	3.22	48.03	***Cladosporium delicatulum*** (Ascomycota)	5.34	83.91	*Alternaria metachromatic* (Ascomycota)	3.45	86.36
Vishniacozyma carnescens (Basidiomycota)	2.33	95.39	***Vishniacozyma victoriae*** (Basidiomycota)	1.56	89.66	***Filobasidium chernovii*** (Basidiomycota)	1.59	66.48
Filobasidium oeirense (Basidiomycota)	2.13	82.24	*Itersonilia pannonica* (Basidiomycota)	1.42	71.84	*Stemphylium solani* (Ascomycota)	0.96	91.48
Stemphylium solani (Ascomycota)	1.27	94.08	***Filobasidium oeirense*** (Basidiomycota)	1.15	59.20	***Filobasidium oeirense*** (Basidiomycota)	0.50	76.70
Phlebia rufa (Basidiomycota)	1.10	2.63	*Alternaria metachromatic* (Ascomycota)	1.12	76.44	*Dioszegia hungarica* (Basidiomycota)	0.46	89.77
Vishniacozyma victoriae (Basidiomycota)	1.03	72.37	*Udeniomyces pyricola* (Basidiomycota)	1.02	85.63	*Bulleromyces albus* (Basidiomycota)	0.42	93.75
Total	40.80		Total	60.59		Total	86.85	

Table 2: Most abundant bacterial genera on grapevine leaves in three French wine-growing regions.

The table shows the top ten most abundant fungal species in Occitanie, Aquitaine and Champagne. Genera in bold are among the top ten most abundant genera in all three regions, while those in underlined are among the top ten most abundant genera in 2 out of 3 regions. Relative abundance (%) indicates the proportion of sequences assigned to the genus relative to the total number of sequences in the dataset. Prevalence (%) indicates the percentage of samples where the genus is present with at least one sequence.

French region								
Occitanie (Plots A, B, and C)			Aquitaine (Plots D, E, and F)			Champagne (Plots G, H, and I)		
Bacterial genus	Relative abundance (%)	Prevalence (%)	Bacterial genus	Relative abundance (%)	Prevalence (%)	Bacterial genus	Relative abundance (%)	Prevalence (%)
Sphingomonas (Proteobacteria)	36.95	73.77	***Sphingomonas*** (Proteobacteria)	24.20	24.20	***Sphingomonas*** (Proteobacteria)	11.01	36.62
Frigoribacterium (Actinobacteriota)	10.71	49.18	*Hymenobacter* (Bacteroidota)	6.76	6.76	*Hymenobacter* (Bacteroidota)	9.97	25.35
Massilia (Proteobacteria)	9.56	50.82	***Methylobacterium*** (Proteobacteria)	5.63	5.63	***Methylobacterium*** (Proteobacteria)	7.09	21.83
Pseudomonas (Proteobacteria)	6.65	40.16	***Pantoea*** (Proteobacteria)	4.15	4.15	***Pantoea*** (Proteobacteria)	6.46	67.61
Pantoea (Proteobacteria)	5.90	15.57	*Massilia* (Proteobacteria)	3.66	3.66	*Massilia* (Proteobacteria)	4.37	67.61
Hymenobacter (Bacteroidota)	4.98	53.28	*Pseudomonas* (Proteobacteria)	2.59	2.59	*Pseudomonas* (Proteobacteria)	2.67	51.41
Methylobacterium (Proteobacteria)	4.23	45.90	*Streptococcus* (Firmicutes)	2.34	2.34	*Streptococcus* (Firmicutes)	2.55	33.10
Curtobacterium (Actinobacteriota)	2.14	7.38	*Friedmanniella* (Actinobacteriota)	2.12	2.12	*Friedmanniella* (Actinobacteriota)	2.48	35.92
Kineococcus (Actinobacteriota)	1.11	14.75	***Frigoribacterium*** (Actinobacteriota)	2.02	2.02	***Frigoribacterium*** (Actinobacteriota)	2.28	80.99
Arthrobacter (Actinobacteriota)	0.86	18.85	***Curtobacterium*** (Actinobacteriota)	1.67	1.67	***Curtobacterium*** (Actinobacteriota)	2.09	50.00
Total	83.09		Total	55.14		Total	50.96	

Some fungi, but no bacteria, are consistently more abundant in asymptomatic leaf tissues across wine-producing regions

Differential abundance analyses (DAA) applied to the whole dataset identified 29 fungal ASVs that were significantly more abundant in asymptomatic leaf tissues across the three regions (*Annexe 6*), while TITAN identified 74 fungal ASVs whose relative abundance was negatively correlated with the abundance of *P. viticola* in leaf tissues (*Annexe 7*). Sixteen fungal ASVs were identified by both DAA and TITAN (Fig. 4), all of which belonged to the Ascomycota phylum (Fig 5). DAA analyses applied to the regional level revealed that both Occitanie and Aquitaine had their own set of fungal taxa specific to asymptomatic tissues (Fig. S4 and S5), whereas Champagne had none (Fig. S6). Surprisingly, two fungal ASVS assigned to pathogenic genera, *Erysiphe* (ASV36) and *Botrytis* (ASV208), were significantly more abundant in asymptomatic tissues across all three regions (Fig. 4). Similar results were observed in regional analyses: *Botrytis* (ASV208) was more abundant in asymptomatic tissues in Occitanie and Aquitaine, while *Erysiphe* (ASV36) was more abundant in asymptomatic tissues in Aquitaine (Figs. S5 and S6).

In contrast, DAA applied to the whole dataset did not identify any bacterial ASV that were significantly more abundant in asymptomatic leaf tissues (*Annexe 6* and Supplementary Fig. S7). DAA applied at the regional level identified three bacterial ASVS more abundant in asymptomatic tissues in the Occitanie region, with one ASV assigned to the *Pseudokineococcus* genera and two to the *Methylobacterium* genera (Supplementary Fig. S8). TITAN analysis identified 36 ASVs associated to low concentrations of *P. viticola* DNA in leaves (Fig. 6). Among these ASVs, the most frequently represented bacterial orders included Caulobacterales (*Phenylobacterium*) and Burkholderiales (*Acidovorax, Massilia*) (*Annexe 6 et 7*).

Basidiomycetous yeasts and Bacillales increase in abundance in disease lesions of *P. viticola*

DAA analyses revealed that ten fungal ASVs were significantly more abundant in disease lesions, all of which were basidiomycetous yeasts. They included *Sporobolomyces patagonicus*, *S. roseus* (represented by three different ASVs), *Curvibasidium cygneicollum*, *Cryptococcus laurentii*, *Udeniomyces pyricola*, *Bulleromyces albus*, *Cystofilobasidium macerans*, and an ASV of the genus *Vishniacozyma* (Fig. 4).

Six of these ASVs were also significant in TITAN analysis (Fig. 4 and Fig. 5). This predominance of basidiomycetous yeasts in symptomatic tissues was consistently observed in regional analyses (Supplementary Fig. S4-6), particularly in Aquitaine, where 9 out of 10 differentially abundant ASVs were assigned to basidiomycetous yeasts. Of these, 7 ASVs were also significant in TITAN analysis (Supplementary Fig. S5). Notably, *Sporobolomyces roseus* was consistently found to be significantly more abundant in disease lesions, across all regions and within each region (Fig 4. and Supplementary Fig. S4-6).

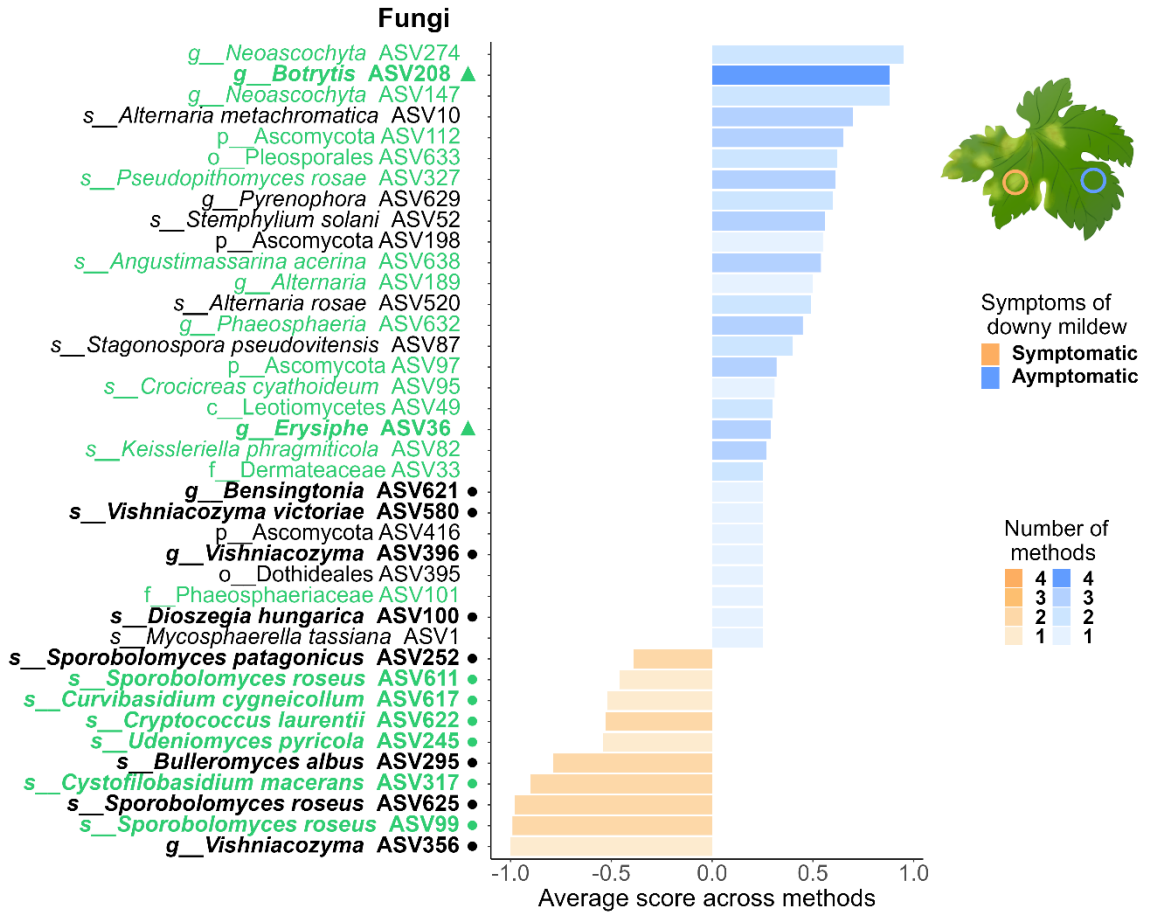


Figure 4: Fungal taxa that vary in abundance between asymptomatic leaf tissues and symptomatic leaf tissues infected by *Plasmopara viticola*.
For each condition (symptomatic vs. asymptomatic), we represented the Amplicon Sequence Variants (ASVs) that were significantly associated with the condition according to at least one method. The four methods used to identify these ASVs are ANCOM-BC2 (Lin & Peddada, 2024), Maaslin2 (Mallick *et al.*, 2021), LinDA (Zhou *et al.*, 2022) and ZicoSeq (Yang & Chen, 2022). Shades of blue and orange indicate the number DAA methods that identified the ASV as differentially abundant. ASVs belonging to Basidiomycete yeasts are highlighted in bold and marked with a dot while those known as foliar pathogens of are marked with a triangle. ASVs that are also significant in the TITAN analysis (Baker *et al.*, 2023b) are highlighted in green but not accounted in the number of methods. The y-axis provides information on the lowest taxonomic level at which the ASV was identified, including its prefix, assignment, and ASV number. The prefix abbreviations are: p for phylum, c for class, o for order, f for family, g for genus, and s for species.

DAA analyses revealed that only a couple bacterial ASVs were significantly more abundant in disease lesions across all regions (2 ASVs assigned to *Sphingomonas* and one to *Frigoribacterium*) (Supplementary Fig. S7). Differentially abundant bacterial ASVs were also found in Occitanie (*Sphingomonas*, *Frigoribacterium*, and *Massilia* (2ASVs)), and in Champagne (*Streptomyces,* and *Bacillus* (2 ASVs)) (Supplementary Fig. S8-S9), but not in Aquitaine. Compared to DAA, TITAN analysis identified more bacterial ASVs with increased relative abundance in disease lesions (Fig. 6). It identified 45 ASVs associated to disease lesions (*Annexe 7*), among which the most frequently represented orders were the Acetobacteriales

(*Acidiphilium* and *Craurococcus-Caldovatus*), Bacillales (*Fictibacillus, Bacillus, Paenisporosarcina* and *Sporosarcina*), Enterobacterales (*Pantoea*), Xanthomonadales (*Xanthomonas*) and Streptomycetales (*Streptomyces*). Four ASVs assigned to *Bacillus*, two assigned to *Sphingomonas* and one assigned to *Streptomyces* were strongly associated to disease lesions according to TITAN analysis (Fig. 6).

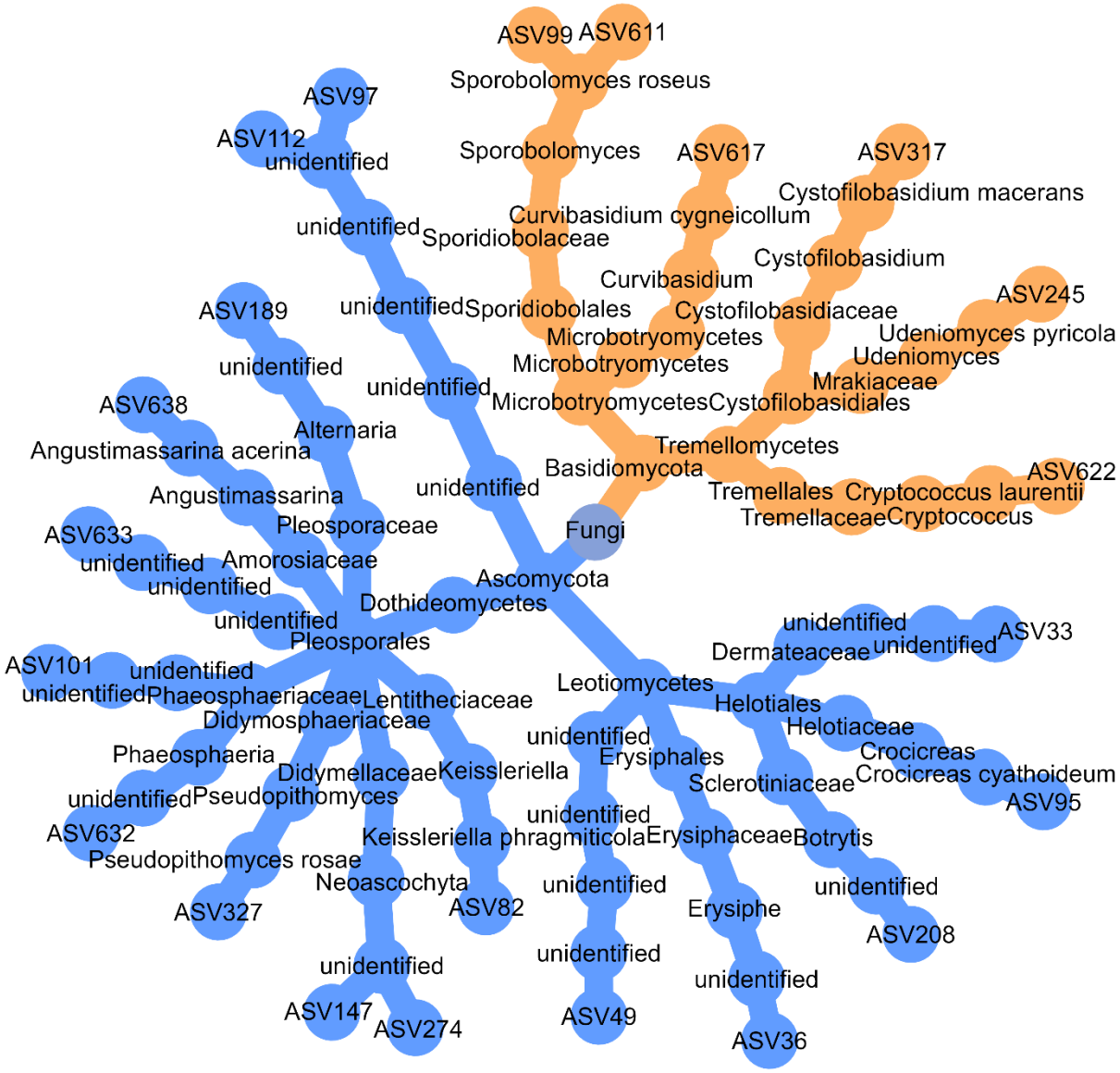


Figure 5: Taxonomic tree of fungal ASVs that vary in abundance between asymptomatic leaf tissues and symptomatic leaf tissues infected by *Plasmopara viticola*.
The figure shows fungal taxa identified as differentially abundant according to at least one method of differential abundance analysis and the TITAN analysis.

Microbial interaction networks differ between asymptomatic tissues and disease lesions

Ongoing analysis in collaboration with Julie Aubert.

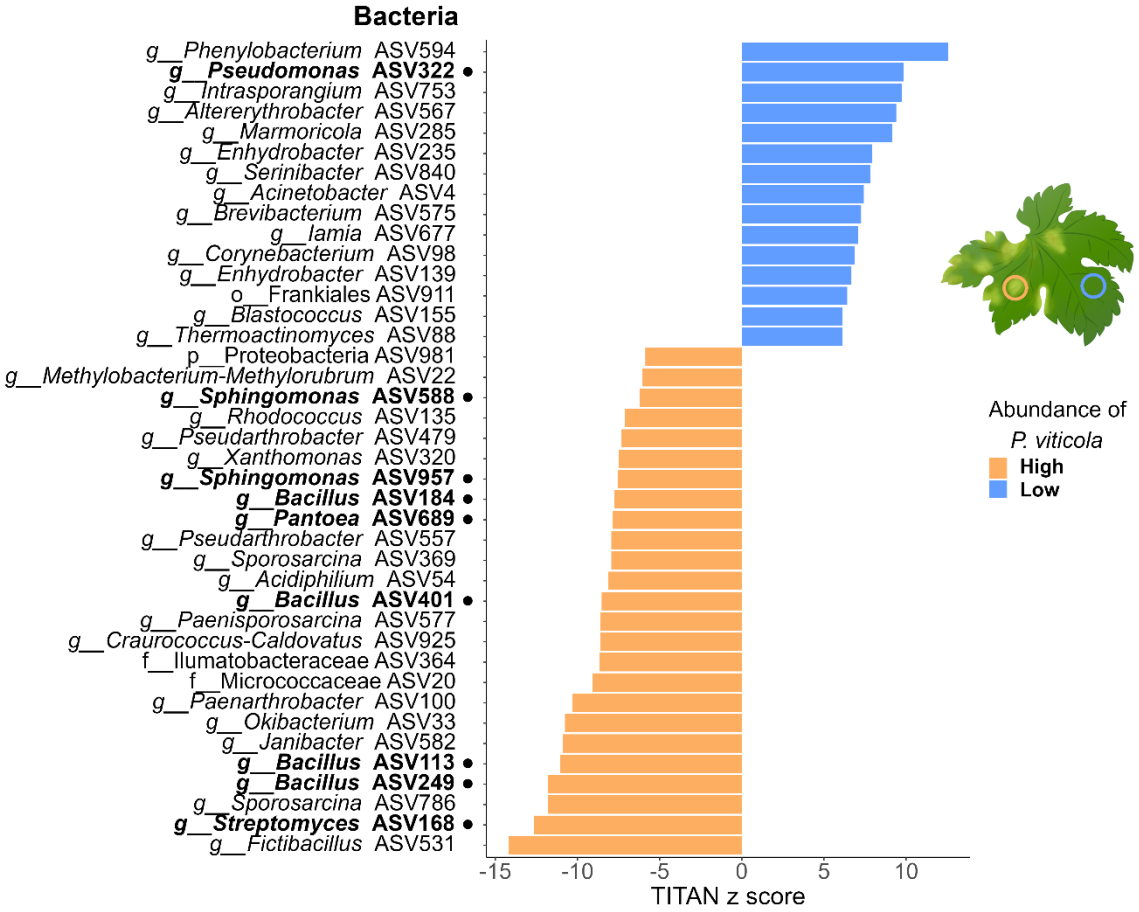


Figure 6: Bacterial taxa whose abundance covaries with *P. viticola* abundance in grapevine leaf tissues. The figure represents the Amplicon Sequence Variants (ASVs) that significantly increase (in orange) or decrease (in blue) in abundance with *P. viticola* DNA concentration in leaf tissues, according to TITAN analysis (Baker et al., 2023). The y-axis provides information on the lowest taxonomic level at which the ASV was identified, including its prefix, assignment, and ASV number. The prefix abbreviations are: p for phylum, c for class, o for order, f for family, g for genus, and s for species. The 40 ASVs with the highest z score are shown in this figure. Members of *Bacillus*, *Streptomyces*, *Pseudomonas* and *Sphingomonas* are shown in bold followed by a circle.

Microbiota α-diversity is higher in asymptomatic tissues compared to disease lesions

Bacterial and fungal community α-diversity were significantly higher in leaf tissues that remained healthy during the downy mildew epidemic (Fig. 7; Table S3) compared to disease lesions. The difference was however not significant when the inverse Simpson's index was applied to fungal communities (Fig. 7), suggesting that variations in diversity between asymptomatic tissues and disease lesions was primarily due to rare fungal ASVs.

Bacterial load, but not fungal load, increases in disease lesions

Bacterial load, but not fungal load, was significantly higher in symptomatic tissues than asymptomatic tissues. Variations in fungal load were poorly explained by both infection and vineyard plot ($R^2c = 0.054$, $R^2m = 0.037$, Table S3).

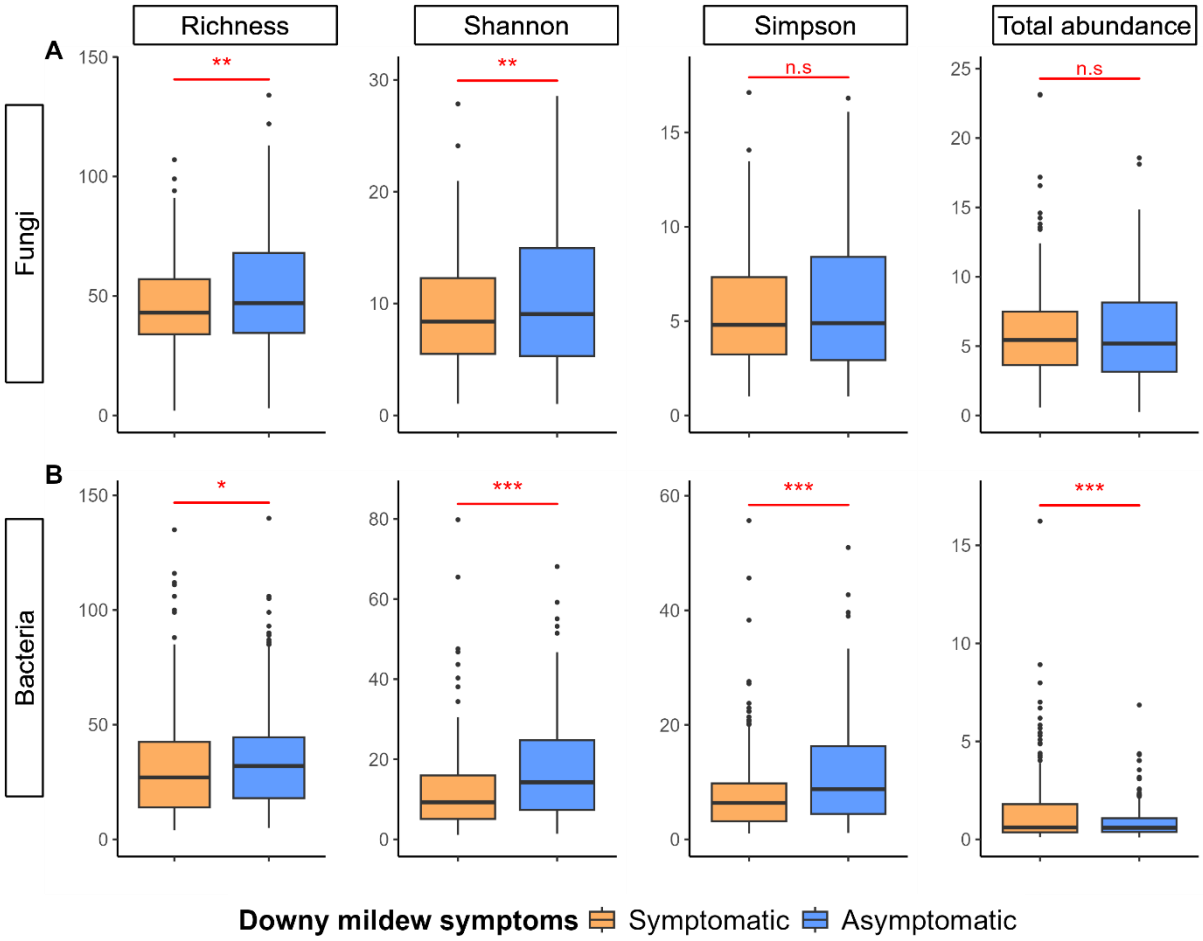


Figure 7: Variation in the α-diversity and total abundance of microbial communities between asymptomatic leaf tissues and symptomatic tissues infected by *Plasmopara viticola*.
The figure shows the diversity and total abundance of (A) fungal and (B) bacterial communities in grapevine leaves collected at the peak of downy mildew epidemic. The diversity indices are, from left to right, the observed total number of ASVs (Hill number q= 0), the exponential of the Shannon entropy index (Hill number q= 1), and the inverse of the Simpson concentration index (Hill number q= 2). Total microbial load was estimated using ddPCR. The statistical significance of the linear mixed effects models is indicated as follows: ns (not significant), . (nonsignificant trend), * (p<0.05), ** (p<0.01), *** (p<0.001).

Stochasticity in microbiota assembly decreases in disease lesions

Bacterial communities associated with disease lesions were significantly more dissimilar from each other (i.e., more dispersed) than those associated with asymptomatic tissues, in accordance with the Anna Karenina Principle. However, this pattern did not hold for fungal communities (Fig. 8).

The assembly of bacterial communities was primarily influenced by stochastic processes, whereas fungal community assembly was more deterministic (Fig. 8). This was consistent with the stronger spatial structuring observed in fungal communities compared to bacterial ones (Fig. 2). Contrary to the Anna Karenina Principle, stochasticity did not increase in disease lesions. Instead, the amount of selection increased in disease lesions for both fungal

communities (as shown by the β-NTI index) and bacterial communities (as shown by the NST index) (Fig. 8).

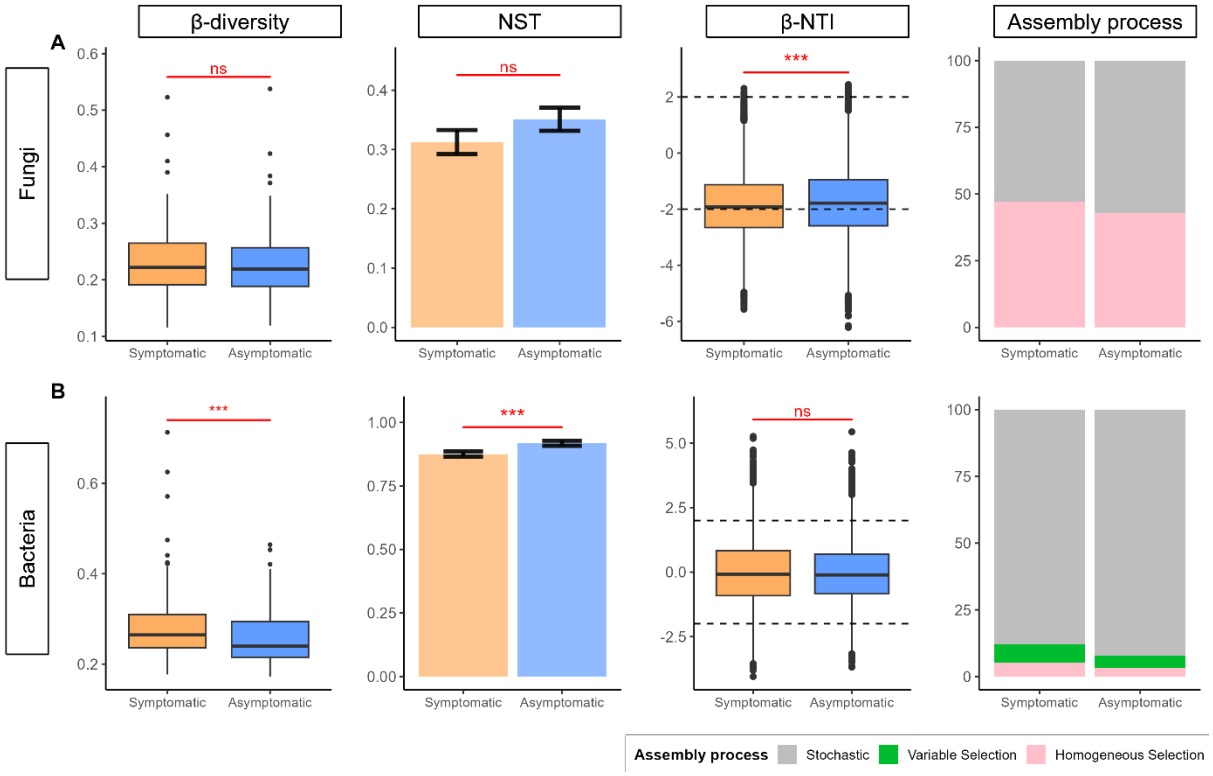


Figure 8: Contributions of deterministic and stochastic processes to the assembly of microbial communities in asymptomatic leaf tissues and in symptomatic tissues infected with *Plasmopara viticola*.

The figure shows the dispersion (β-diversity) and assembly processes (calculated with two indices, NST and βNTI) for (A) fungal and (B) bacterial communities. β-diversity represents the distance to the centroid of each sample based on weighted UniFrac distances. NST quantifies the proportion of stochastic vs. deterministic processes in microbial community assembly. A value of 50% is used as a cutoff, with <50% indicating a more deterministic assembly and >50% indicating a more stochastic assembly. βNTI measures phylogenetic turnover between pairs of samples. βNTI < -2 indicates a significant effect of homogeneous selection, βNTI > 2 indicates a significant effect of variable selection, and |βNTI| < 2 indicates a dominance of stochastic processes. Dashed lines represent the significance thresholds for βNTI. Finally, the assembly process indicates the percentage of sample pairs assigned to each process.

Discussion

In the present study, we compared microbiotas associated with asymptomatic tissues and disease lesions using state-of-the-art methods in microbial community ecology. These analyses allowed us to propose a new scenario of interactions between the microbiota and the pathogenic oomycete *Plasmopara viticola*, responsible for grapevine downy mildew.

A new scenario of pathogen-microbiota interactions

Our analyses revealed that microbial communities associated with asymptomatic tissues and disease lesions were very similar, despite the visible symptoms and the significant increase in

pathogen abundance within symptomatic tissues. Downy mildew infection triggered only subtle changes in the leaf microbiota, which we thoroughly characterized. These changes differed slightly between fungi and bacteria. In the case of fungi, infection consistently selected for several species of basidiomycetous yeasts, such as *Sporobolomyces patagonicus*, *S. roseus*, *Cryptococcus laurentii*, and *Udeniomyces pyricola*. These yeasts increased in abundance upon infection across all wine-growing regions considered in this study. The total fungal load did not increase in disease lesions, suggesting that the yeasts replaced other fungal species. This is consistent with alpha-diversity patterns, which suggest that rare fungal species disappeared from disease lesions. Bacterial communities were primarily influenced by stochastic processes and were much less spatially structured than fungal communities. Our analyses revealed that infection slightly reduced the level of stochasticity in bacterial communities by selecting certain groups of bacteria, such as *Bacillales* and *Streptomycetales*. This shift in composition was accompanied by an increase in bacterial total load and a significant decrease in bacterial diversity, suggesting that the selected bacteria thrived and replaced other members of the bacterial community. However, these changes were not as consistent as those observed for fungi, and there were marked dissimilarities in bacterial community composition among lesions. Surprisingly, tissues that remained asymptomatic during the downy mildew epidemic were not consistently associated with fungi or bacteria known for their biocontrol properties. Instead, they were associated with other aerial pathogens of grapevine. Microbial taxa known for their biocontrol properties, such as basidiomycetous yeasts and *Bacillus* species, were selected in disease lesions. Overall, these results suggest that *P. viticola* competes with other pathogens for leaf space, and that the leaf locally recruits certain microbial taxa with biocontrol activity, particularly basidiomycetous yeasts, upon infection by downy mildew.

Infection has little impact on the leaf microbiota, despite visible symptoms

We were surprised to observe that the infection had such a small effect on the fungal and bacterial communities, according to all the analyses we performed (PCA, RDA, and variance partitioning), despite the significant impact of downy mildew on the leaf structure, physiology and chemistry. The infection manifests as yellow and oily spots on the leaves, which evolve in necrotic tissues (Gessler et al., 2011). In a recent study, the inoculation with *P. viticola* caused a dramatic change in concentration and spatial distribution of several micro- and macronutrients at the leaf level (Cesco *et al.*, 2020). These major changes in microbial habitat conditions are expected to trigger rapid shifts in the composition of the microbiota (Rocca *et al.*, 2019). However, we did not observe such changes by comparing the microbiota between disease lesions and asymptomatic tissues on the same leaf.

Selection of the microbiota increases in disease lesions

Our analyses detected subtle but deterministic shifts in the microbiota of disease lesions, compared to asymptomatic tissues. In contrast to the Anna Karenina principle, which posits that microbiotas associated with disease lesions are predominantly shaped by stochastic processes (Arnault *et al.*, 2023), we observed an increase in deterministic processes in disease lesions. For each microbial domain, bacteria and fungi, the same trend was obtained with two

indices commonly used to analyse community assembly processes, the NST index (Ning *et al.*, 2019) and the β-NTI index (Stegen *et al.*, 2012), namely an increase in determinism in assembly processes in lesions. These indices are considered interchangeable for examining assembly processes (Arnault *et al.*, 2023). According to Arnault et al. (2023), a decrease in β-NTI values, towards values lower than -2, indicates that the same stress applies with the same intensity to all communities. Applied to our study, this suggests that infection altered microbial communities in a similar way among grapevine plants. These deterministic and convergent shifts of the microbiota in the disease lesions could be caused by both environmental filtering of the microbial community by the new conditions in the lesion (Cesco *et al.*, 2020) or by the active selection of specific microorganisms by the plant in response to the stress induced by infection (Teixeira *et al.*, 2019). The two mechanisms are not mutually exclusive and might occur together.

Fungi and bacteria with known biocontrol properties are selected for in disease lesions

According to our analyses, Basidiomycetes yeasts are consistently selected for in disease lesions. We used several methods to identify the fungal taxa that are enriched in disease lesions compared to asymptomatic tissues, or whose abundance is positively correlated with *P. viticola* abundance. All the fungal taxa that met the two criteria were Basidiomycetes yeasts belonging to the classes Microbotryomycetes and Tremellomycetes such as *Sporobolomyces. roseus*, *Cryptococcus laurentii*, and *Udeniomyces pyricola*. These fungi are well known for their biocontrol activity against post-harvest diseases (Liu *et al.*, 2013; Spadaro & Droby, 2016; Freimoser *et al.*, 2019). They reduce the development of pathogens through various mechanisms, including competition for nutrients and space, secretion of toxins, enzymes, and volatile organic compounds, direct parasitism, and indirect mechanisms like resistance induction (Liu *et al.*, 2013; Spadaro & Droby, 2016; Freimoser *et al.*, 2019).

We also identified several bacterial taxa whose abundance increases with that of *P. viticola*. They belonged to the genera *Streptomyces, Bacillus, Pantoea, Pseudomonas*, and *Sphingomonas*, most of which contain strains known for their biocontrol activity against grapevine downy mildew. For instance, Khatmiamycin, produced by a terrestrial Streptomyces species, inhibited and lysed zoospores (Abdalla *et al.*, 2011). Marine Streptomyces extracts also disrupt zoospore motility, leading to lysis (Islam *et al.*, 2016). Antimicrobial substances from *Streptomyces atratus* PY-1 damaged sporangia and sporangiophores (Liang *et al.*, 2016). Finally, *Streptomyces viridosporus* HH1 and *Streptomyces violaceus* HH5 reduced disease severity and also enhanced grapevine growth, yield, and berry quality (El-Sharkawy *et al.*, 2018). *Bacillus* species are also known for their biocontrol activities, including direct antibiosis, competition for niches and nutrients and induction of the host systemic resistance (Compant *et al.*, 2013). They produce various bioactive compounds, such as surfactin, iturin, and fengycin, which display strong suppressive effects on wide range of pathogens (Li *et al.*, 2019). For instance, *Bacillus amyloliquefaciens* is registered in France for *P. viticola* biocontrol and recent studies have shown that *Bacillus pumilus* and *Bacillus subtilis* can also inhibit grapevine downy mildew (Zhang *et al.*, 2017; Li *et al.*, 2019; Biljana *et al.*, 2023). Furthermore, bacterial culture

supernatants from *Bacillus velezensis* and *Bacillus ginsengihumi* decreased the release and motility of *P. viticola* zoospores, while inducing grapevine defenses such as stilbene production (Raveau *et al.*, 2024) under semi-controlled conditions. *Pantoea agglomerans* and *Sphingomonas zeae* are also considered as potential antagonists of *P. viticola* according to *in vitro* confrontation tests (Bruisson *et al.*, 2019).

Therefore, our findings confirm that collections of microorganisms isolated from diseased plants or diseased tissues can be useful for the screening of biocontrol agents (Anees *et al.*, 2010; Tolba & Soliman, 2013; Ait Bahadou *et al.*, 2018). Indeed, disease lesions contain microorganisms that have developed specific survival strategies to compete with pathogens (Huang et al. 2013), in addition to hyperparasites. For instance, Falk (1996) observed *Fusarium proliferatum* growing on *P. viticola* sporangia and sporangiophores, coiling around and invading the sporangiophores after they were isolated them from atypical downy mildew lesions on *Vitis vinifera*. Recently, Shen et al. (2022) isolated *Simplicillium lanosoniveum*, a hyperparasite specific to *P. viticola*, from grapevine lesions. This fungus was seen coiling around *P. viticola* sporangiophores and sporangia, under the microscope, deforming hyphae, reducing pathogen growth, and lowering sporangia numbers.

Asymptomatic tissues are not a source of biocontrol agents in the case of P. viticola

Isolating biocontrol candidate agents from areas where diseases are suppressed is a common practice that stems from common sense. Several studies have shown that effective biocontrol agents can be isolated from the rhizosphere of healthy plants (Nawangsih *et al.*, 2011; Agaras *et al.*, 2015; Sharifazizi *et al.*, 2017; Latz *et al.*, 2020), making disease-suppressive soils valuable sources for naturally occurring BCAs (Adesina *et al.*, 2007). However, in our study, microbiotas associated with asymptomatic tissues were characterized by a higher abundance of the two foliar pathogens of grapevines, *Erysiphe* and *Botrytis*, as well as other plant pathogens such as *Stemphylium solani*, a species of the genus *Alternaria*, and *Blumeria graminis,* probably at the latent state. These findings challenge our initial hypothesis that asymptomatic tissues harbor a distinct set of fungal and bacterial species acting as natural enemies against downy mildew. Our analyses suggest that microbiotas associated with asymptomatic tissues do not contain more protective microorganisms than disease lesions. Actually, many microorganisms with well-known antagonistic properties against plant pathogens, including *Plasmopara viticola*, are found in disease lesions.

Perspectives

One of the most promising findings from our study, which shifts our initial approach, is that symptomatic tissues serve as a valuable reservoir for protective fungal and bacterial microorganisms. The discovery of a significant number of biocontrol agents in downy mildew lesions, from both fungal and bacterial kingdoms, opens exciting new avenues for exploring their complementarity in biological control. With the growing interest in bacterial-fungal interactions, designing SynComs that integrate both fungal and bacterial candidates holds the potential to uncover powerful synergies between these organisms, which could significantly

advance biocontrol strategies. To fully realize this potential, enhancing the assignment of key bacterial ASVs is essential. Multi-omics approaches, combining metagenomics, meta-transcriptomics and metabolomics offers a promising solution, capable of dramatically improving the precision of bacterial identification, and potentially revealing the hidden identity of *Bacillus*, *Streptomyces*, and *Sphingomonas* found in the lesions. In addition, these methods would enable us to elucidate the metabolites produced and exchanged in the lesion (Crandall *et al.*, 2020).

Supplementary figures

Figure S1: Abundance of Plasmopara viticola in grapevine leaf tissue, depending on the presence or absence of downy mildew symptoms.
The abundance of *P. viticola* (in ng/µl) was estimated with qPCR and was log-transformed for improved visualization. The difference in abundance between symptomatic and asymptomatic tissues was assessed using a pairwise Wilcoxon test (*** $p < 0.001$).

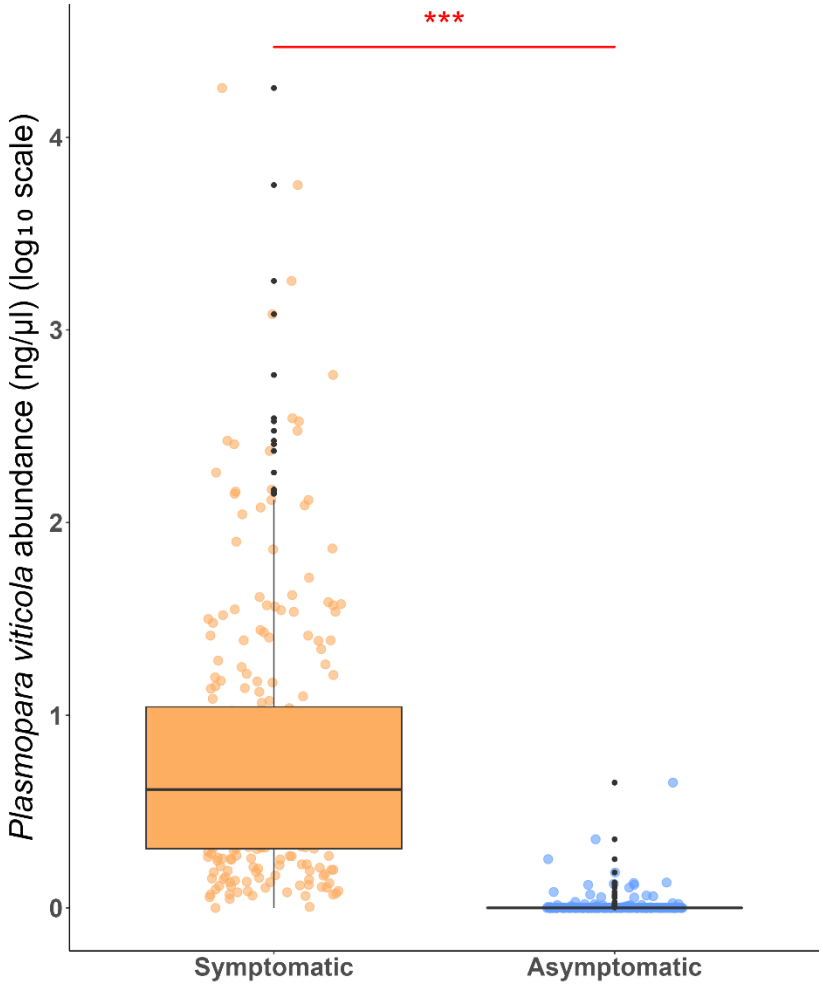


Figure S2: Variation in microbial community composition across vineyard plots.
Compositional dissimilarities between (A) fungal and (B) bacterial communities of grapevine leaves, represented by a Principal Component Analysis (PCA). Samples collected from the same vineyard plot are represented with the same color. Samples belonging to the same region are surrounded by an ellipse (Occitanie in blue, Aquitaine in pink and Champagne in yellow, as in Fig.1). Symbols indicate the presence or absence of downy mildew symptoms (triangles and circles, respectively).

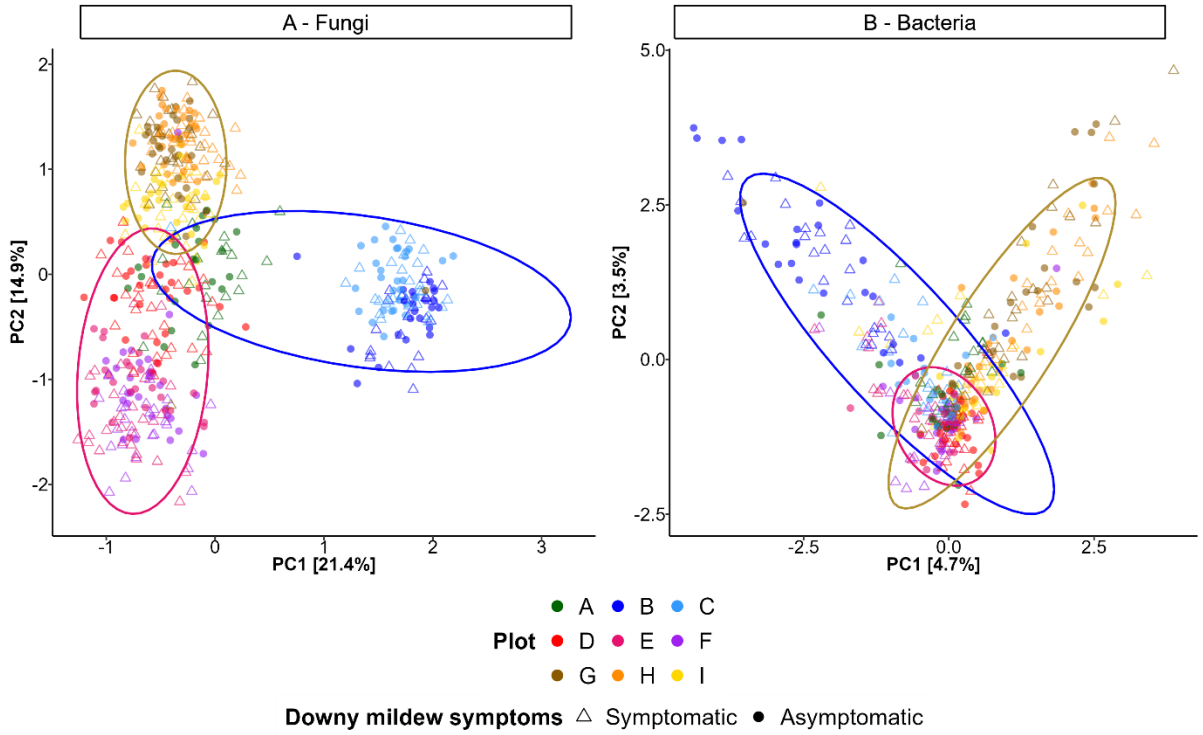


Figure S3: Factors driving variation in microbial community composition according to variance partitioning.

The figure shows the factors influencing the composition of (A) fungal and (B) bacterial communities. The environmental variables were grouped into three categories (Disease, Geography and Vine variety) to perform variance partitioning. The Venn diagrams show the percentage of variance explained by each group of variables, either individually or in combination with other groups.

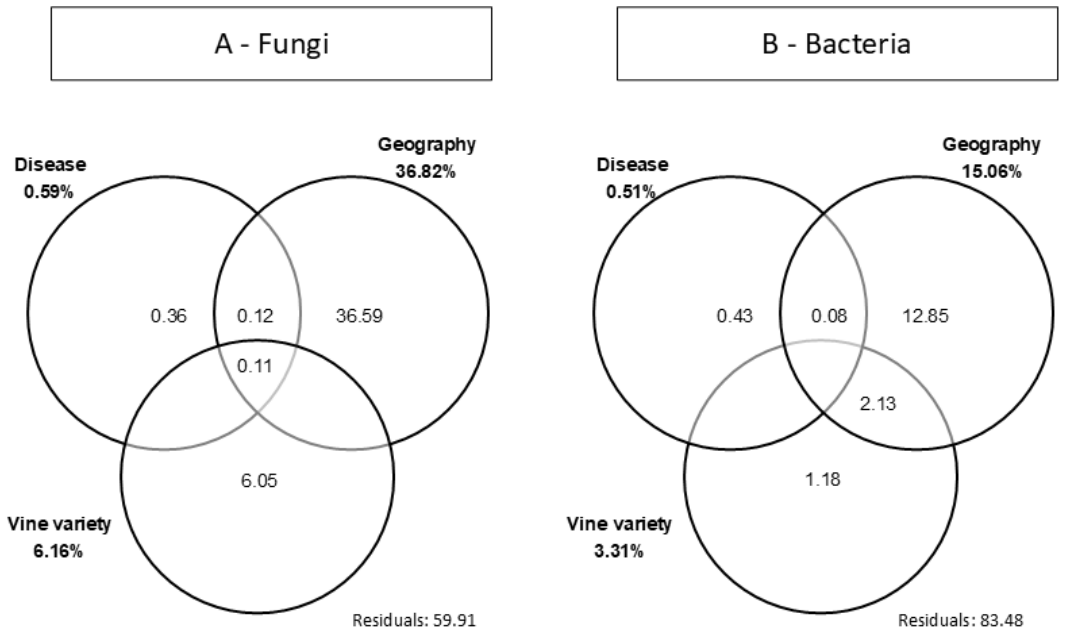


Figure S4: Fungal taxa in Occitanie region that vary in abundance between asymptomatic leaf tissues and symptomatic leaf tissues infected by *Plasmopara viticola*.
For each condition (symptomatic vs. asymptomatic), we represented the Amplicon Sequence Variants (ASVs) that were significantly associated with the condition according to at least one method. The four methods used to identify these ASVs are ANCOM-BC2 (Lin & Peddada, 2024), Maaslin2 (Mallick *et al.*, 2021), LinDA (Zhou *et al.*, 2022) and ZicoSeq (Yang & Chen, 2022). Shades of blue and orange indicate the number DAA methods that identified the ASV as differentially abundant. ASVs belonging to Basidiomycete yeasts are highlighted in bold and marked with a dot while those known as foliar pathogens of are marked with a triangle. ASVs that are also significant in the TITAN analysis (Baker *et al.*, 2023b) are highlighted in green but not accounted in the number of methods. The y-axis provides information on the lowest taxonomic level at which the ASV was identified, including its prefix, assignment, and ASV number. The prefix abbreviations are: p for phylum, c for class, o for order, f for family, g for genus, and s for species.

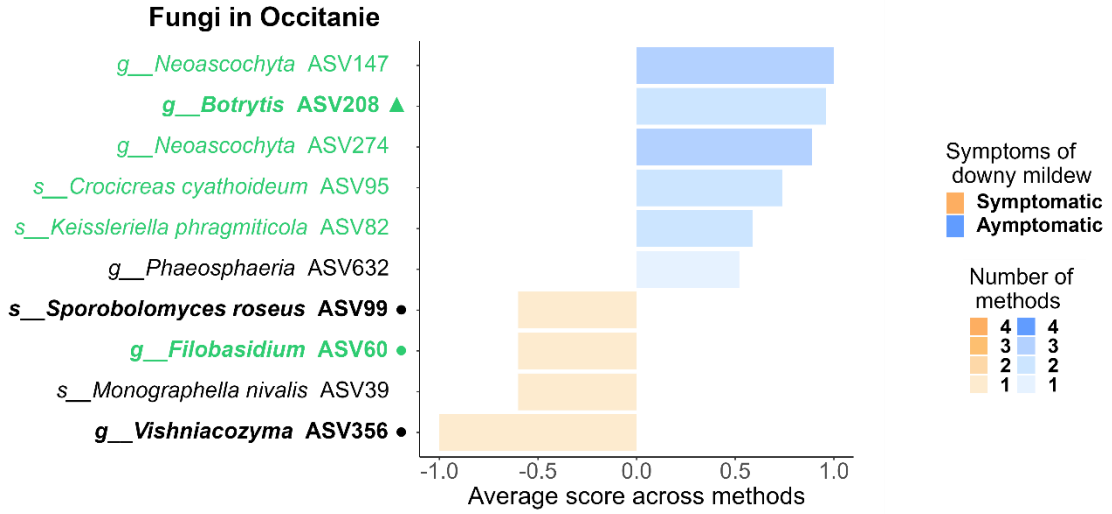


Figure S5: Fungal taxa in Aquitaine region that vary in abundance between asymptomatic leaf tissues and symptomatic leaf tissues infected by *Plasmopara viticola*.
For each condition (symptomatic vs. asymptomatic), we represented the Amplicon Sequence Variants (ASVs) that were significantly associated with the condition according to at least one method. The four methods used to identify these ASVs are ANCOM-BC2 (Lin & Peddada, 2024), Maaslin2 (Mallick *et al.*, 2021), LinDA (Zhou *et al.*, 2022) and ZicoSeq (Yang & Chen, 2022). Shades of blue and orange indicate the number DAA methods that identified the ASV as differentially abundant. ASVs belonging to Basidiomycete yeasts are highlighted in bold and marked with a dot while those known as foliar pathogens of are marked with a triangle. ASVs that are also significant in the TITAN analysis (Baker *et al.*, 2023b) are highlighted in green but not accounted in the number of methods. The y-axis provides information on the lowest taxonomic level at which the ASV was identified, including its prefix, assignment, and ASV number. The prefix abbreviations are: p for phylum, c for class, o for order, f for family, g for genus, and s for species.

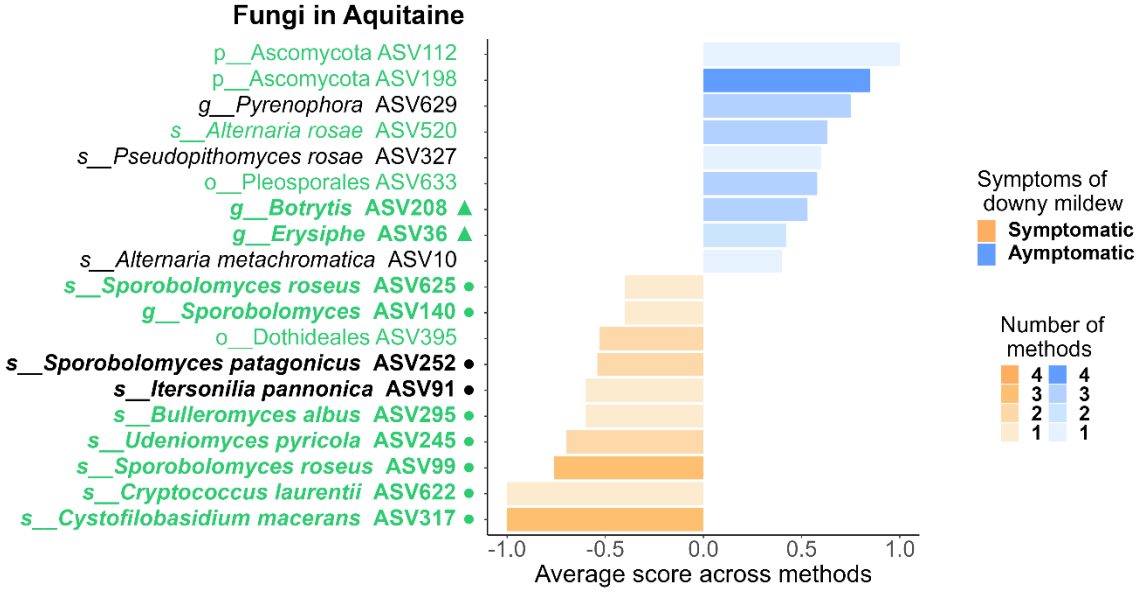


Figure S6: Fungal taxa in Champagne region that vary in abundance between asymptomatic leaf tissues and symptomatic leaf tissues infected by *Plasmopara viticola*.
For each condition (symptomatic vs. asymptomatic), we represented the Amplicon Sequence Variants (ASVs) that were significantly associated with the condition according to at least one method. The four methods used to identify these ASVs are ANCOM-BC2 (Lin & Peddada, 2024), Maaslin2 (Mallick *et al.*, 2021), LinDA (Zhou *et al.*, 2022) and ZicoSeq (Yang & Chen, 2022). Shades of blue and orange indicate the number DAA methods that identified the ASV as differentially abundant. ASVs belonging to Basidiomycete yeasts are highlighted in bold and marked with a dot while those known as foliar pathogens of are marked with a triangle. ASVs that are also significant in the TITAN analysis (Baker *et al.*, 2023b) are highlighted in green but not accounted in the number of methods. The y-axis provides information on the lowest taxonomic level at which the ASV was identified, including its prefix, assignment, and ASV number. The prefix abbreviations are: p for phylum, c for class, o for order, f for family, g for genus, and s for species.

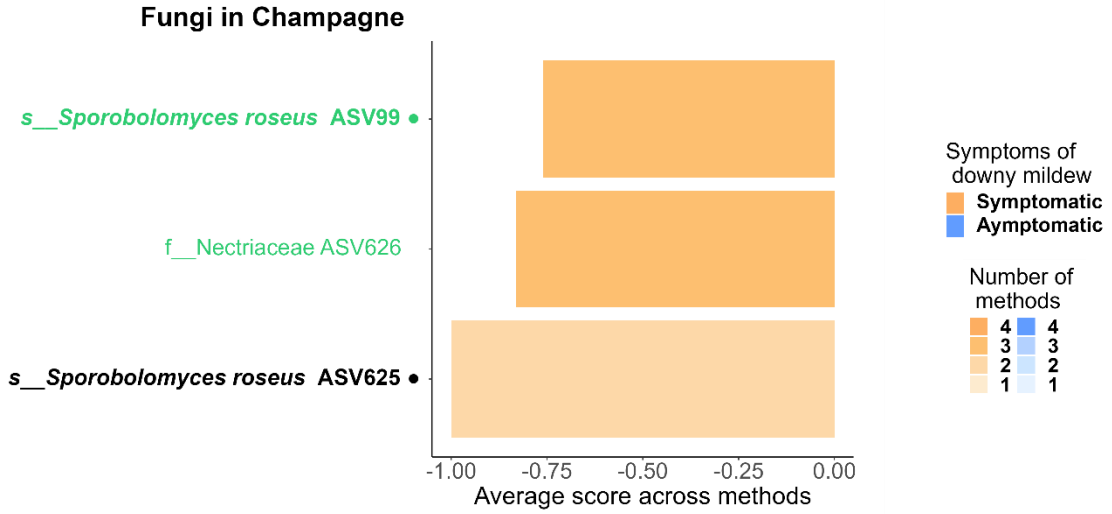


Figure S7: Bacterial taxa that vary in abundance between asymptomatic leaf tissues and symptomatic leaf tissues infected by *Plasmopara viticola*.
For each condition (symptomatic vs. asymptomatic), we represented the Amplicon Sequence Variants (ASVs) that were significantly associated with the condition according to at least one method. The four methods used to identify these ASVs are ANCOM-BC2 (Lin & Peddada, 2024), Maaslin2 (Mallick *et al.*, 2021), LinDA (Zhou *et al.*, 2022) and ZicoSeq (Yang & Chen, 2022). Shades of blue and orange indicate the number DAA methods that identified the ASV as differentially abundant. ASVs that are also significant in the TITAN analysis (Baker *et al.*, 2023b) are highlighted in green but not accounted in the number of methods. The y-axis provides information on the lowest taxonomic level at which the ASV was identified, including its prefix, assignment, and ASV number. The prefix abbreviations are: p for phylum, c for class, o for order, f for family, g for genus, and s for species.

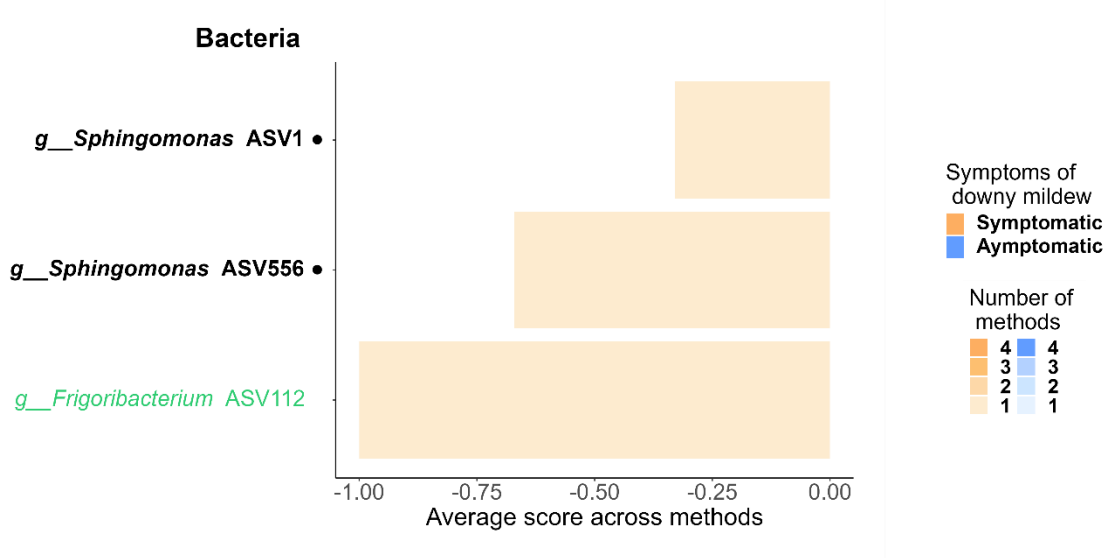


Figure S8: Bacterial taxa in Occitanie region that vary in abundance between asymptomatic leaf tissues and symptomatic leaf tissues infected by *Plasmopara viticola*.
For each condition (symptomatic vs. asymptomatic), we represented the Amplicon Sequence Variants (ASVs) that were significantly associated with the condition according to at least one method. The four methods used to identify these ASVs are ANCOM-BC2 (Lin & Peddada, 2024), Maaslin2 (Mallick *et al.*, 2021), LinDA (Zhou *et al.*, 2022) and ZicoSeq (Yang & Chen, 2022). Shades of blue and orange indicate the number DAA methods that identified the ASV as differentially abundant. ASVs that are also significant in the TITAN analysis (Baker *et al.*, 2023b) are highlighted in green but not accounted in the number of methods. The y-axis provides information on the lowest taxonomic level at which the ASV was identified, including its prefix, assignment, and ASV number. The prefix abbreviations are: p for phylum, c for class, o for order, f for family, g for genus, and s for species.

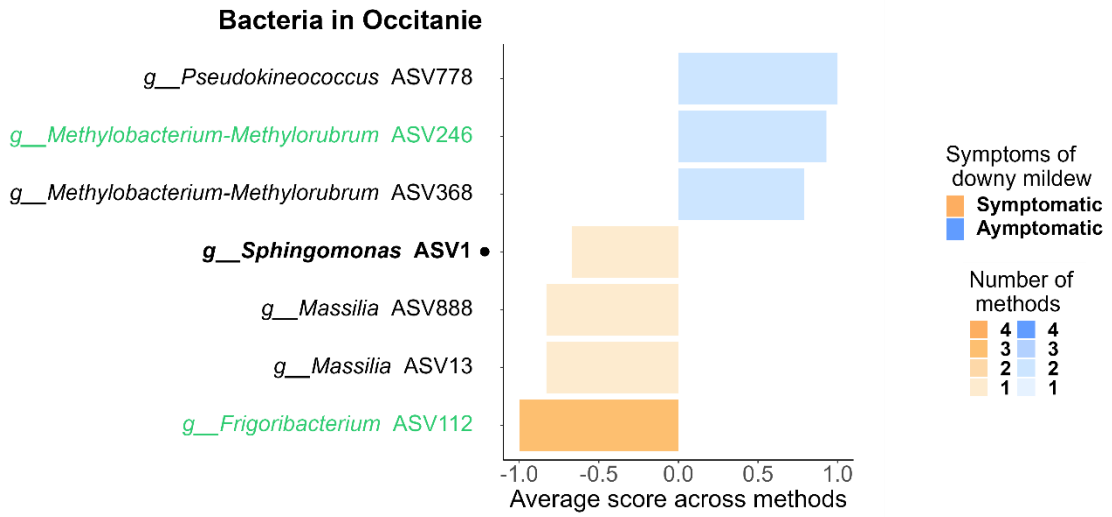
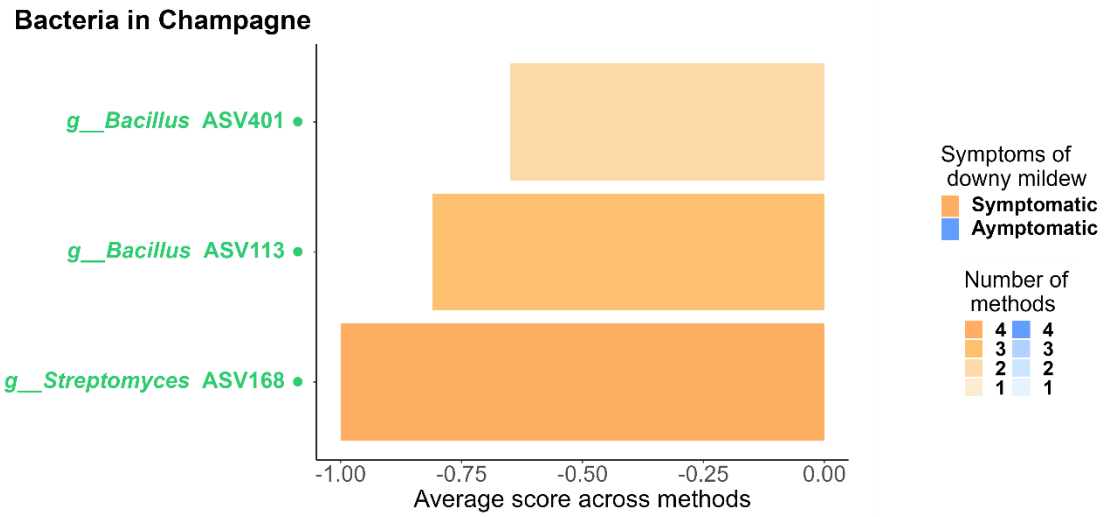


Figure S9: Bacterial taxa in Champagne region that vary in abundance between asymptomatic leaf tissues and symptomatic leaf tissues infected by Plasmopara viticola.
For each condition (symptomatic vs. asymptomatic), we represented the Amplicon Sequence Variants (ASVs) that were significantly associated with the condition according to at least one method. The four methods used to identify these ASVs are ANCOM-BC2 (Lin & Peddada, 2024), Maaslin2 (Mallick *et al.*, 2021), LinDA (Zhou *et al.*, 2022) and ZicoSeq (Yang & Chen, 2022). Shades of blue and orange indicate the number DAA methods that identified the ASV as differentially abundant. ASVs that are also significant in the TITAN analysis (Baker *et al.*, 2023b) are highlighted in green but not accounted in the number of methods. The y-axis provides information on the lowest taxonomic level at which the ASV was identified, including its prefix, assignment, and ASV number. The prefix abbreviations are: p for phylum, c for class, o for order, f for family, g for genus, and s for species.



Supplementary tables

Table S1: Primer and probes along with thermocycler conditions used in this study.

	Targeted region	Primers and probes	PCR mix	PCR conditions	Reference
16S Metabarcoding	V5-V6	799F: 5′-CAAGCAGAAGACGGCATACGAGATGTGACTGGAGTTCAGACGTGTGCTCTTCCGATCTxxxxxxxxxxxxHS-AACMGGATTAGATACCCKG-3′1115R: 5′-AATGATACGGCGACCACCGAGATCTACACTCTTTCCCTACACGACGCTCTTCCGATCTxxxxxxxxxxxxHS-AGGGTTGCGCTCGTTG-3′ where HS represents a 0-7-base-pair heterogeneity spacer and "x" a 12-nucleotide tag	10µL of 2× QIAGEN Multiplex PCR Master Mix (2× final), 2µL each of the 799F-1115R primers (0.1 µM final), 4µL of water, 1µL of 10 mg/mL BSA, 1µL of DNA template. Reaction volume : 20µL.	95 °C × 15 min; 32 cycles of [94°C × 30 s, 53 °C × 90 s, 72°C x 90 s]; 72 °C × 10 min.	(Chelius & Triplett, 2001b; Redford *et al.*, 2010; Barroso-Bergadà *et al.*, 2023a)
ITS Metabarcoding	ITS1	IITS1F: 5′-CAAGCAGAAGACGGCATACGAGATGTGACTGGAGTTCAGACGTGTGCTCTTCCGATCTxxxxxxxxxxxxCTTGGTCATTTAGAGGAAGTAA-3′ ITS2: 5′-AATGATACGGCGACCACCGAGATCTACACTCTTTCCCTACACGACGCTCTTCCGATCTxxxxxxxxxxxxGCTGCGTTCTTCATCGATGC-3′ where "x" is the 12-nucleotide tag	10µL of 2× QIAGEN Multiplex PCR Master Mix (2× final), 2µL each of the ITS1F-ITS2 primers (0.1 µM final), 4µL of water, 1µL of 10 mg/mL BSA, 1µL of DNA template. Reaction volume : 20µL.	95 °C × 15 min; 35 cycles of [94°C × 30 s, 57 °C × 90 s, 72°C x 90 s]; 72 °C × 10 min.	(White *et al.*, 1990; Gardes & Bruns, 1993)
16S ddPCR	SSU rDNA (V3-V9)	16S-F : 5’- CGGTGAATACGTTCCCGG-3’, 16S-R : 5’-TACGGCTACCTTGTTACGACTT-3’ Probe : 16S-Pr : 5’-CTTGTACACACCGCCCGTC-3’	11µL of 2X ddPCR™ Supermix for Probes No dUTP, 2.2µL of 16S-F and 16S-R primer at 9 µM, 1.22µL of probe 16S-Pr at 9 µM, 3.38µL of water, 2µL of DNA template. Reaction volume : 22µL.	95 °C × 5 min; 40 cycles of [95°C × 30 s, 60°C × 1 min, 72°C x 30 s]; 98 °C × 10 min.	(Furet *et al.*, 2009)
ITS ddPCR	ITS2	ITS86F : 5’- GTGAATCATCGAATCTTTGAA-3’ ITS4 : 5’-TCCTCCGCTTATTGATATGC-3’	11µL of 2X ddPCR™ EvaGreen Supermix, 1.83µL of ITS86F and ITS4 primer at 1.5µM, 5.34µL of water, 2µL of DNA template. Reaction volume : 22µL.	95 °C × 5 min; 40 cycles of [95°C × 30 s, 55°C × 1 min, 72°C x 30 s]; 4 °C x 5min; 90°C x 5min	(Beeck *et al.*, 2014)
P. viticola qPCR	ITS1	Giop R: 5’-GGTTGCAGCTAATGGATTCCTA-3’ Giop F: 5’-TCCTGCAATTCGCATTACGT-3’ Probe : Giop P-VIC: 5’-TCGCAGTTCGCAGCGTTCTTCA-3’	1X HOT FIREPol Probe® qPCR Mix Plus no Rox, 900nM of GiopR and GiopF primer, 500 nM of probe Giop P-VIC, XµL of water, 5µL of DNA template. Reaction volume : 20µL.	95 °C × 12 min; 40 cycles of [95°C × 30 s, 60°C × 1 min, 72°C x 30 s]; 72 °C × 10 min.	(Valsesia *et al.*, 2005)

Table S2: Factors driving variation in microbiota composition according to Redundancy Analysis.
The table shows the variables kept by stepwise selection. The box is grey if the variable was not selected. The marginal effects of the variables and the p-value were obtained using the ANOVA permutation test for redundancy analysis (RDA). The significance of the variables is as follows: ns (not significant), . (non-significant trend: 0.1>p>0.05), * (p<0.05), ** (p<0.01), *** (p<0.001).

		Fungi		Bacteria	
Group of variables	Selected variable	Marginal effect	p-value	Marginal effect	p-value
Disease	Abundance of *Plasmopara viticola* (qPCR data)				
	Downy mildew symptoms (symptomatic vs. asymptomatic)	2.093	0.001 ***		
Geography	PCNM1	14.274	0.001 ***	3.815	0.001 ***
	PCNM2	18.282	0.001 ***		
	PCNM3	15.884	0.001 ***	2.079	0.001 **
	PCNM4	16.710	0.001 ***	1.270	0.001 *
	PCNM5	6.315	0.001 ***	2.271	0.001 ***
	Leaf	9.214	0.001 ***	16.188	0.001 ***
Variety	Grapevine variety	23.399	0.001 ***		

Table S3: Factors driving variation in microbiota α-diversity and total abundance.
We analyzed the effects of infection by downy mildew and vineyard plot on microbial community α-diversity and total abundance. R^2m and R^2c represent the marginal and conditional determination coefficients of the model, respectively. N indicates the number of samples included. The significance of the variables is indicated as follows: ns (not significant), nonsignificant trend (0.1>p>0.05), * (p<0.05), ** (p<0.01), *** (p<0.001). To highlight which plots differed in microbial community α-diversity and total abundance, multiple comparisons were conducted and adjusted using the Bonferroni method. Plots (named A to I; Fig. 1) with the same superscript harbor microbiotas with similar diversity or abundance.

Model				Downy mildew disease (Symptomatic vs Asymptomatic)		Plot	
Kingdom	N	R^2c	R^2m	p	Variation direction	p	Variation direction
Diversity index: Richness (Hill number, q = 0)							
Fungi	502	0.530	0.372	**	Asymptomatic > Symptomatic	***	G^1, I^1, H^1, B^1 < E^2, F^2, C^2, D^2, A^2
Bacteria	390	0.293	0.170	*	Asymptomatic > Symptomatic	***	C^1, A^1, B^1< F^{12}, E^{12}< I^{123}< D^{23}, G^{23}< H^3
Diversity index: Shannon (Hill number, q = 1)							
Fungi	502	0.678	0.527	**	Asymptomatic > Symptomatic	***	H^1 < G^{12}, I^{12} < B^2 < E^3, F^3 < A^{34}, C^{34}< D^4
Bacteria	390	0.406	0.259	***	Asymptomatic > Symptomatic	***	B^1< A^{12}, C^{12}< G^{23}< E^{234}, F^{234}< I^{34}, H^{34}< D^4
Diversity index: Simpson (Hill number, q = 2)							
Fungi	502	0.624	0.467	ns	-	***	H^1 < G^{12}, I^{12} < B^2 < E^3, A^3 < F^{34}, C^{34}< D^4
Bacteria	390	0.354	0.234	***	Asymptomatic > Symptomatic	***	B^1 < A^{12}, C^{12} < G^{123} < E^{23}< F^{234}, I^{234}< H^{34}< D^4
Total microbial abundance							
Fungi	502	0.054	0.037	ns	-	***	A^1, D^1, C^1, E^1, F^1, < B^{12}, I^{12}, G^{12} < H^2
Bacteria	390	0.357	0.241	**	Symptomatic > Asymptomatic	***	A^1< I^{12}, H^{12}, C^{12}, G^{12}, D^{12}, F^{12}< E^2 < B^3

Chapitre 3 : Révéler les consortia microbiens qui interfèrent avec le mildiou de la vigne grâce à l'épidémiologie du microbiome

Ce chapitre explore les relations entre les communautés microbiennes naturellement présentes dans les sols et sur les feuilles des vignes, et la sensibilité des parcelles viticoles au mildiou, définie à partir de données épidémiologiques. L'objectif de ce chapitre est d'identifier des consortia microbiens spécifiques aux parcelles moins sensibles au mildiou, susceptibles d'interagir avec les phases asexuées et/ou sexuées du pathogène.

L'étude a été menée dans la région Nouvelle-Aquitaine, avec des échantillons de sol et de feuilles prélevés entre la mi-avril et début mai, au stade phénologique de 2-3 feuilles étalées. L'analyse du microbiote et la quantification de l'inoculum primaire de mildiou a été réalisée à l'échelle de l'individu, tandis que les données épidémiologiques sont disponibles à l'échelle de la parcelle. Les parcelles ont été classées selon leur sensibilité au mildiou (haute ou faible), basée sur des données épidémiologiques longues récoltées par l'Institut Français de la Vigne et du Vin.

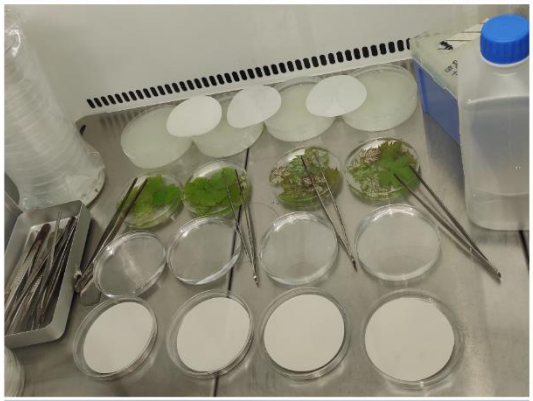
Dans ce chapitre, j'ai d'abord élaboré la stratégie de sélection des parcelles en fonction de leur sensibilité au mildiou. J'ai sélectionné les parcelles en analysant la base de données épidémiologique de l'IFV et en interagissant directement avec les viticulteurs. J'ai organisé et réalisé la campagne d'échantillonnage sur deux ans (printemps 2022 et 2023) pour trois habitats microbiens : le sol de surface, la phyllosphère, et l'endosphère des feuilles. J'ai également développé les protocoles de conservation et de traitement des échantillons, mis au point les protocoles d'extraction d'ADN et d'amplification par PCR, et réalisé moi-même l'ensemble de ces manipulations pour la campagne 2022. Lors de la seconde campagne d'échantillonnage effectuée au printemps 2023, j'ai bénéficié de l'assistance d'Alexandre Chataigner (UMR SAVE) pour la biologie moléculaire. Le séquençage a été réalisé sur la plateforme PGTB à Bordeaux. J'ai collaboré avec Marine Cambon (Univ. Birmingham, UK) pour les analyses prédictives (classification automatique supervisée). J'ai réalisé toutes les autres analyses bioinformatiques et statistiques et j'ai rédigé l'ensemble du chapitre, en lien étroit avec mes encadrants de thèse et les autres co-auteurs, qui a été soumis en tant qu'article de recherche à la revue *Microbiome* le 24 septembre 2024.

En parallèle, les parcelles que j'ai sélectionnées dans ce chapitre ont été utilisées par Jessica Vallance et Aarti Jaswa (UMR SAVE) pour concevoir une collection de microorganismes foliaires. Certaines méthodes d'analyse ont été appliquées à un autre jeu de données, collecté par Lucile Pellan (UMR SAVE) afin d'identifier des bioindicateurs microbiens du rendement de la vigne. Les deux études ont fait l'objet de communications dans des conférences internationales dont les 'proceedings' sont présentés en annexe de cette thèse (Fournier, Jaswa et al. 2023 ; Pellan et al. 2024).

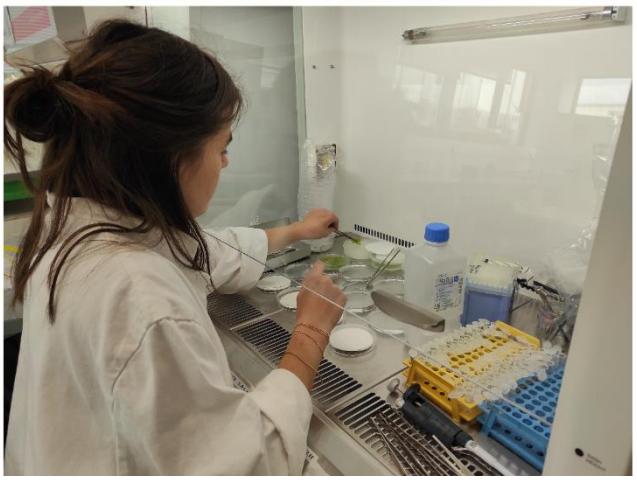












Revealing microbial consortia that interfere with grapevine downy mildew through microbiome epidemiology

Paola Fournier, Lucile Pellan, Aarti Jaswa, Marine Cambon, Alexandre Chataigner, Olivier Bonnard, Marc Raynal, Christian Debord, Charlotte Poeydebat, Simon Labarthe, François Delmotte, Patrice This, Corinne Vacher

Submitted to *Microbiome*

Abstract

Background

Plant and soil microbiomes can interfere with pathogen life cycles, but their influence on disease epidemiology remains understudied. Here, we analyzed the relationships between plant and soil microbiomes and long-term epidemiological records of grapevine downy mildew, a major disease caused by the oomycete *Plasmopara viticola*.

Results

We found that certain microbial taxa were consistently more abundant in plots with lower susceptibility to the disease and that the microbial community composition could predict disease susceptibility. Microbial diversity was not strongly linked to epidemiological records, suggesting that susceptibility is more related to the abundance of specific microbial taxa. These key taxa were identified in the topsoil, where the pathogen's oospores overwinter, and in the phyllosphere, where zoospores infect leaves. By contrast, the leaf endosphere, where the pathogen's mycelium develops, contained few taxa of interest. Surprisingly, the soil microbiota was a better predictor of downy mildew symptoms than the leaf microbiota was, suggesting a significant role of the soil microbiome in this primarily aerial disease.

Conclusion

Our study integrates long-term epidemiological data with microbiome profiles of healthy plants to reveal fungi and bacteria relevant for the biocontrol of grapevine downy mildew. The resulting database provides a valuable resource for designing microbial consortia with potential biocontrol activity. The framework can be applied to other crop systems to guide the development of biocontrol strategies and reduce pesticide use in agriculture.

Keywords

Microbial ecology, disease biocontrol, oomycete, *Vitis vinifera*, *Plasmopara viticola*, soil, phyllosphere, endosphere, metabarcoding, differential abundance analysis.

Background

Chemical pesticides are the most commonly used method for protecting crops against pathogens (Sharma *et al.*, 2019). However, legislation is increasingly restricting their use because of their significant negative impacts on the environment and human health (Hassaan & El Nemr, 2020; Rani *et al.*, 2021; Panis *et al.*, 2022). In addition, the selection of resistance to active molecules in populations of target organisms compromises the efficacy of these chemicals and challenges sustainable plant health management (Massi *et al.*, 2021; Walsh *et al.*, 2022). In response, the European Commission has outlined the "Farm to Fork" strategy, which aims to reduce the use of chemical pesticides by 50% by 2030 as part of the European Green Deal (European Commission, 2020). In the longer term, zero-pesticide agriculture is envisioned (Jacquet *et al.*, 2022). In this context, microbial biocontrol strategies are promising options for enhancing plant protection against pests and diseases while reducing the use of chemical products (Syed Ab Rahman *et al.*, 2018; Legein *et al.*, 2020). These strategies involve the use of microorganisms or their byproducts to control pests and diseases through direct interactions such as antibiosis, predation, parasitism, and competition, or through indirect interactions such as the modulation of plant immunity (Köhl *et al.*, 2019; Legein *et al.*, 2020). Harnessing the diversity of plant microbiota could also be an option, as several studies have established a link between ecosystem functioning and microbial diversity (Bell *et al.*, 2005; Philippot *et al.*, 2013; Delgado-Baquerizo *et al.*, 2016), validating the 'Biodiversity-Ecosystem Functioning' (BEF) theory (Hillebrand & Matthiessen, 2009). These findings suggest that diverse microbial communities can enhance plant protection more effectively than single species can (Berg *et al.*, 2017) through ecological mechanisms such as redundancy, complementarity, and synergy (Saleem *et al.*, 2019). The challenge is to identify those microbial taxa involved in protective functions or interactions among the multitude of microbial taxa that make up the plant microbiota.

The development of microbial biocontrol is crucial for heavily treated diseases, as it can lead to significant reductions in pesticide use. Grapevine downy mildew, caused by the oomycete *Plasmopara viticola* (Gessler *et al.*, 2011; Castrillo-Sequeira *et al.*, 2023), is one such disease (Toffolatti *et al.*, 2018; Castrillo-Sequeira *et al.*, 2023) for which finding pesticide alternatives is essential. Together with powdery mildew (*Erysiphe necator*), it is one of the most damaging diseases of cultivated grapevines (especially *Vitis vinifera*) (Bois *et al.*, 2017). These two diseases account for the majority of fungicide treatments in vineyards in France (Delière *et al.*, 2015). They make the cultivated vine the 4th most treated crop in France, with a fungicide Treatment Frequency Index (TFI) of 10.1 nationally and 12.4 in the Bordeaux region (Agreste, 2019). This level of treatment intensity exceeds that of many other major crops and fruit trees (Agreste, 2019).

Plasmopara viticola (Berk. & M.A. Curtis) Berl. & De Toni is a biotrophic and obligate parasite of grapevine (Göker *et al.*, 2007) originating from North America (Gessler *et al.*, 2011; Fontaine *et al.*, 2021). It was introduced to Europe in the mid-19th century and destroyed a large proportion of French vineyards due to the high susceptibility of *V. vinifera*, which evolved in

the absence of this pathogen (Di Gaspero *et al.*, 2007; Jürges *et al.*, 2009a). This disease is now reported in most wine-producing regions of the world (Bois *et al.*, 2017; Fontaine *et al.*, 2021) and has a significant economic impact (Bois *et al.*, 2017; Taylor & Cook, 2018; Nasehi *et al.*, 2023). The incidence of downy mildew varies from plot to plot and depends, among other things, on the scion and rootstock genotype (Chitarra *et al.*, 2017; Sargolzaei *et al.*, 2020), microclimate (Maddalena *et al.*, 2021; Fernandes de Oliveira *et al.*, 2021), vineyard management practices (de Bem *et al.*, 2016; Fernandes de Oliveira *et al.*, 2021), and *P. viticola* genotype (Li *et al.*, 2016). In temperate climates, *P. viticola* survives the winter through sexual reproduction, producing oospores in grapevine leaves in the fall. The oospores then overwinter in the leaf litter and soil. In the following spring, the oospores germinate to produce zoospores, which are dispersed by wind and rain to infect grapevine leaves and other receptive green tissues. Primary infections occur when zoospores derived from oospores, *i.e.*, primary inoculum, enter leaf tissues through stomata. Secondary infection cycles are initiated by the production of sporangia on the lower surface of infected leaves by asexual reproduction. The sporangia release zoospores, *i.e.*, secondary inoculum, which initiates a new cycle of infection (Gessler *et al.*, 2011; Poeydebat *et al.*, 2022; Castrillo-Sequeira *et al.*, 2023). Without effective disease control measures, favorable weather conditions can trigger multiple cycles of primary and secondary infection within the growing season, potentially resulting in complete crop loss (Gessler *et al.*, 2011). In Western Europe, primary contamination can occur throughout the growing season, highlighting the important role of primary inoculum in grapevine downy mildew epidemics (Gobbin *et al.*, 2005; Boso *et al.*, 2019; Hong *et al.*, 2020; Sargolzaei *et al.*, 2020; Santos *et al.*, 2020a; Maddalena *et al.*, 2021). Biocontrol agents targeting oospores in the soil - the main source of primary contamination - are therefore of major interest since they could contribute to lowering epidemic pressure at the source. This preventive approach could reduce the need for curative chemical control of the asexual stage of *P. viticola*, which is responsible for symptoms. However, preventive methods targeting the primary inoculum of grapevine downy mildew have received little attention so far (Poeydebat *et al.*, 2024).

Grapevines naturally host a diverse microbiota, including leaf epiphytes, which develop on the leaf surface in the microbial habitat known as the phyllosphere (Perazzolli *et al.*, 2014; Singh *et al.*, 2019), and leaf endophytes, which inhabit the internal leaf tissues in the microbial habitat known as the endosphere (Pacifico *et al.*, 2019). Numerous microorganisms isolated from these two habitats have been individually tested for antagonistic activity against downy mildew, both on detached leaves and in field trials. Some have emerged as promising candidates for biocontrol of the asexual stage of *P. viticola* (Gessler *et al.*, 2011; Koledenkova *et al.*, 2022; Nasehi *et al.*, 2023; Castrillo-Sequeira *et al.*, 2023; Peng *et al.*, 2024; Nadalini & Puopolo, 2024). A laboratory experiment has also shown that the entire phyllosphere microbial community can significantly reduce the severity of downy mildew (Perazzolli *et al.*, 2014). In addition to demonstrating the potential of grapevine leaf epiphytes and endophytes to disrupt the asexual stage of the downy mildew life cycle, these studies also revealed the different mechanisms by which these microorganisms act on *P. viticola*. They can act as a primary line of defense by inhibiting zoospore motility, adhesion, and penetration through antibiosis

(Tilcher *et al.*, 1994; Abdalla *et al.*, 2011; Talontsi *et al.*, 2012; Kongue Tatong *et al.*, 2014; Li *et al.*, 2019). They can also reduce sporangia production and sexual reproduction by interacting directly with the pathogen mycelium through hyperparasitism and antibiosis (Kortekamp, 1997; Zang *et al.*, 2020; Ghule *et al.*, 2022). Finally, they can inhibit sporangiophore formation and germination through hyperparasitism and antibiosis (Falk, 1996; Bakshi *et al.*, 2001; Liang *et al.*, 2016; Ghule *et al.*, 2018; Zang *et al.*, 2020; Shen *et al.*, 2022). Despite these promising results, only one bacterial strain, *Bacillus amyloliquefaciens* FZB24, has been formally registered in France for downy mildew biocontrol[9], although it is not yet marketed for this specific application. There is an urgent need to identify new microbial taxa or consortia that disrupt the asexual stage of *P. viticola* and, perhaps more importantly, the sexual stage (oospores).

To date, there has been limited research on the relationship between the soil microbiome and downy mildew oospores. A laboratory study demonstrated the antagonistic activity of *Acremonium byssoides* against *P. viticola* oospores through hyperparasitism and antibiosis (Conigliaro *et al.*, 2008). In another study, bacteria, fungi, and yeasts collected from abandoned vineyards effectively inhibited the germination of oospores overwintering under natural conditions (Dagostin *et al.*, 2006). Additional research on other oomycete species has shown that various bacterial and fungal taxa from natural soils can parasitize oospores of several oomycete species, including *Pythium* sp., *Phytophthora* sp., and *Aphanomyces euteiches* (Sneh *et al.*, 1977; Ayers & Lumsden, 1977; Humble & Lockwood, 1981). Studies of oomycete primary inoculum usually focus on the top 15 cm of soil (Schuh *et al.*, 1988; Kennelly *et al.*, 2007; Van der Heyden *et al.*, 2019; Poeydebat *et al.*, 2024) because it contains oospores capable of infecting host plants (Kennelly *et al.*, 2007; Montes-Borrego *et al.*, 2009). This topsoil harbors the most diverse and active microbial communities, as microbial biomass, diversity, and activity tend to decrease with soil depth (van Leeuwen *et al.*, 2017; Xu *et al.*, 2021). Collectively, these findings suggest that soil microbes in vineyards have the potential to disrupt the sexual stage of the downy mildew life cycle by parasitizing oospores or inhibiting their germination (Conigliaro *et al.*, 2008). They also suggest that the top layer of soil is most likely to harbor microorganisms antagonistic to oospores.

In this study, we integrated microbial community data with long-term epidemiological data, an emerging field known as microbiome epidemiology (VanEvery *et al.*, 2023). We also evaluated the predictive power of microbial data in epidemiology, a currently overlooked aspect (Correa-Garcia *et al.*, 2023). Specifically, we examined the relationships between naturally occurring microbial communities in both vineyard soil and leaves and the susceptibility of vineyard plots to downy mildew, with susceptibility defined by epidemiological data. Our goal was to uncover microbial consortia with the potential to protect vineyards from *P. viticola* and ultimately reduce reliance on chemical fungicides. We tested four hypotheses: (i) the diversity of leaf and

[9] https://www.vignevin.com/wp-content/uploads/2023/04/fiche_biocontrole_vigne_mars_2023v2.pdf

soil microbial communities is higher in plots with low downy mildew susceptibility; (ii) plots with low downy mildew susceptibility harbor a greater abundance of specific microbial taxa that we hypothesize are involved in downy mildew regulation; (iii) downy mildew susceptibility can be predicted from microbiota data; and (iv) the leaf microbiota is a better predictor of downy mildew susceptibility compared to the soil microbiota, as susceptibility levels are defined based on the monitoring of foliar symptoms. To test these hypotheses, we conducted a two-year leaf and soil sampling campaign in 14 vineyard plots in the Bordeaux region (Nouvelle-Aquitaine, France). These plots, selected on the basis of long-term epidemiological records, comprised 7 pairs with contrasting susceptibility to downy mildew. Sampling targeted young emerging leaves (at the phenological stage of 2-3 spread leaves) and topsoil (upper 5 cm). This study was conducted in the spring, early in the growing season, to identify the protective microbiota likely to be present on leaves during colonization by early *P. viticola* zoospores, as well as the microbiota likely to be in contact with germinating oospores in the soil.

Materials and methods

Selection of study sites based on epidemiological records

The study sites were selected based on epidemiological records provided by the *Institut Français de la Vigne et du Vin* (IFV) using a network of 1200 Untreated Controls (hereafter referred to as UCs, Fig. S1) monitored since 2002. Untreated Controls are generally composed of 2*5 vines in staggered rows that do not receive any fungicide treatment. The UC can either remain in the same location over the years or be moved each year, *i.e.*, different vines can be selected as UCs. The UC can be located on the edge or in the center of the plot, depending on the region and the grower's preference. The frequency and intensity of downy mildew attacks on vine leaves and bunches are observed weekly during the growing season. Leaf attack frequency is defined as the number of symptomatic leaves divided by the total number of leaves observed. The intensity of leaf attack is defined as the sum of the percentage of symptomatic leaf area divided by the total number of leaves observed. Similar definitions are used for bunches.

Based on these epidemiological records (downloaded from[10]), we selected pairs of vineyard plots that contrasted in frequency and intensity of downy mildew infection, but were as similar as possible in terms of genetic material, geographic location, and management type. We used 5 criteria to select pairs of plots. To belong to the same pair, plots must be planted with the same grape variety (Criterion 1 - Same Variety), and their geographical distance must not exceed 10 km (Criterion 2 - Proximity). The type of management (organic, conventional or biodynamic) must be the same (Criteria 3 - Same Management). In addition, the UCs within the two plots must have been monitored by IFV for at least 4 common years (Criteria 4 -

[10] https://www.vignevin-epicure.com/

Common Records), including at least one recent year (*i.e.*, 2020 or 2021 for the 2022 sampling campaign and 2021 or 2022 for the 2023 sampling campaign). Finally, the epidemiologic records must be contrasted (Criterion 5 - Contrasted Epidemiology). This means that the area under the disease progress curve of one of the two plots must be higher for the 4 epidemiological variables measured by IFV (intensity of symptoms on leaves, frequency of symptoms on leaves, intensity of symptoms on bunches, frequency of symptoms on bunches) in at least 80% of the years of common epidemiological surveillance.

Within each pair of plots, the plot with the highest disease frequency and intensity was considered a plot with high downy mildew susceptibility, while the plot with the lowest disease frequency and intensity was considered a plot with low downy mildew susceptibility. The plot selection procedure was applied twice. To select plots to be sampled in 2022, we used epidemiological data collected between 2002 and 2021. Then, epidemiological data collected between 2002 and 2022 were used to select plots to be sampled in 2023.

Sampling design

Two sampling campaigns were conducted. The first campaign took place from April 18 to May 2, 2022 and the second campaign took place from April 11 to April 26, 2023. Both campaigns took place at the phenological stage of 2-3 spread leaves, prior to the application of any fungicide treatments.

In the 2022 campaign, samples of young leaves and topsoil were collected from four areas within each plot: the center of the plot (CEN), the edge of the plot (EDG), and the untreated controls (UCs) used by the IFV to monitor disease dynamics in 2021 and 2022 (UC1 and UC2). In the 2023 campaign, samples of young leaves and topsoil were collected only from the center of the plot (CEN). Both the CEN and EDG areas received fungicide treatments the year before sampling. By contrast, UC1 did not receive fungicide treatments the year before sampling. It may or may not be located at the edge of the plot, depending on the grower's choice. The within-plot location and fungicide treatments the year before sampling were variable for UC2. The edge of the plot (EDG) was selected to be as far away from UC1 and UC2 as possible to capture within-plot variability.

Within each sampling area, four adjacent vines from the same row were selected. These vines were representative of the age and general condition of the plot. From each vine, six leaves distributed across the entire plant were collected and pooled into a single composite sample (Supplementary Fig. S2). For soil sampling, three 20 x 20 cm quadrats were defined at a distance of 20 cm from the trunk of each vine (Supplementary Fig. S2). Two quadrats were directly under the row of vines, and one was in the interrow space. The top 5 cm of soil from each quadrat was collected, mixed, and placed into a bag to form a composite sample.

All the samples were collected using surgical gloves and disinfected tools (scissors, shovels, trowels, picks). Before sampling a new plot or a new area within the plot, gloves were changed and tools were disinfected with bleach (3.6% chlorine content) and 70% ethanol. The samples were placed in sterile plastic bags (NASCO™, Whirl-Pak®, USA) and kept on ice in a cooler. The

samples were brought back to the laboratory on the same day. In the laboratory, the samples were stored at 4°C until processing. Leaves were processed the following day, and the soils were processed following week.

Sample processing

The day after sample collection, the leaves were processed to separate the epiphytic microbiota (inhabiting the phyllosphere) from the endophytic microbiota (inhabiting the endosphere) under a Class II Biosafety Cabinet. To isolate epiphytes, each collection plastic bag was supplemented with 50 mL of sterile leaf washing buffer (0.9% NaCl, 0.01% Tween 80) (MilliporeSigma™, Calbiochem™, PBS-TWEEN™ Tablets, USA) and incubated on an orbital shaker at 150 rpm for 1 hour. The buffer was then centrifuged (5525 × g, 4°C) for 20 minutes into 50 mL tubes (Corning Inc., Falcon® Tubes, USA). After the supernatant was removed, the remaining 2 mL, including the pellet, was transferred to a 2 mL tube and centrifuged again (14000 rpm, 4°C) for 20 min. The supernatant was discarded, and the pellet was stored at -80°C.

For endophyte collection, washed leaves were surface sterilized by immersion in 10% calcium hypochlorite solution for 10 min, rinsed in two sterile water baths for 1 min each, dried by placement on sterile filter paper for a few minutes, and transferred to 2 ml tubes with two sterilized 5 mm diameter chromium steel balls. The surface-sterilized leaves were then freeze-dried overnight, ground with TissueLyser II (QIAGEN®, Germany) with 30-second grinding intervals at 30 Hz, separated by 1-minute pauses, and stored at room temperature. In addition, to validate the surface sterilization process, water washes from the final rinse were collected, and microbial DNA was detected by extraction, PCR amplification, and sequencing, following the same procedures as those used for real samples (detailed below).

The soil samples were sieved to 2 mm no later than 10 days after harvest. To avoid cross-contamination, the gloves were changed, and sieves were disinfected between samples from different plots and different areas. The sieves were cleaned by removing the soil with tap water, disinfected with 3.6% bleach, washed with water, sprayed with 70% ethanol, and finally air dried. After sieving, each soil sample was homogenized by hand. Two 50 mL tubes were subsampled from the homogenized soil. One tube was kept at room temperature for physicochemical analysis, whereas the other, intended for metabarcoding analysis, was freeze-dried overnight prior to DNA extraction.

Soil physicochemical analysis

The four soil samples collected from the same sampling area of the same plot were pooled before being sent to the *Laboratoire d'Analyses des Sols d'Arras*, France[11]. The analysis included

[11] https://las.hautsdefrance.hub.inrae.fr/

measurements of the three-fragment particle size, C/N ratio, pH, organic matter content, and content of total limestone, total carbon, total nitrogen and total organic carbon.

DNA extraction

DNA extraction, amplification, library preparation and sequencing were performed at the Genome Transcriptome Facility of Bordeaux (France). Extractions were performed in a confined laboratory dedicated to environmental DNA studies. We used the PowerSoil® Pro Kit (QIAGEN®, Germany) for DNA extraction from the soil and phyllosphere samples and the DNeasy® Mini Plant Kit (QIAGEN®, Germany) for the endosphere samples. These kits were used in individual tubes to limit cross-contamination between samples. For soil DNA extraction, 200 mg of homogenized soil was used, whereas for endosphere DNA extraction, 10 mg of leaf powder was used. Phyllosphere DNA was extracted directly from the frozen pellet. The extractions were performed according to the manufacturer's instructions, with slight modifications. To reduce handling, PowerBeads® from the PowerSoil® Pro Kit were transferred directly into 2 ml collection tubes containing soil and phyllosphere material instead of using PowerBead® Pro Tubes. In addition, to facilitate cell lysis, the tubes were incubated at 65°C for 10 minutes after the addition of CD1 lysis buffer and prior to the homogenization step. The DNA was eluted in 100 µl using the DNeasy® Mini Plant Kit for endosphere samples.

This DNA was then used for bacterial and fungal community profiling by short- and long-read sequencing and for *P. viticola* quantification by digital droplet PCR.

Short-read sequencing of bacterial and fungal communities

To characterize fungal communities, the internal transcribed spacer 1 (ITS1) region of the fungal nuclear ribosomal DNA (nrDNA) ITS gene was amplified using the ITS1F forward primer (Gardes & Bruns, 1993) and the ITS2 reverse primer (White *et al.*, 1990). We also tested the primer set ITS1catta - ITS2ngs (Tedersoo *et al.*, 2018; Tedersoo & Anslan, 2019), which targets the nrDNA ITS gene of both fungi and oomycetes and has been successfully used in grapevine (Behrens & Fischer, 2022b). However, we ultimately did not use this primer set because of its lack of specificity in our samples (Supplementary Methods S1 and Fig. S3 and S4). For bacterial communities, the V5-V6 region of the bacterial 16S ribosomal RNA (rRNA) gene was amplified using the chloroplast-excluding forward primer 799f (Chelius & Triplett, 2001a) and the reverse primer 1115R (Reysenbach & Pace, 1995). PCRs were performed with 5 µL of template DNA, 2 µL of each primer (3 µM concentration), 4 µL of HOT FIREPol® MultiPlex Mix (5X concentration) (Solis BioDyne, Lithuania) and ultrapure water to a total volume of 20 µL. The thermocycling conditions for nrDNA ITS gene amplification were as follows: 95°C/15 min; 95°C/30 s, 56°C/30 s, 72°C/30 s for 35 cycles; and 72°C/5 min. The thermocycling conditions for 16S rRNA gene amplification were as follows: initial denaturation at 95°C for 15 min, followed by 30 cycles at 95°C for 30 s, 49°C for 30 s, and 72°C for 30 s, with a final extension at 72°C for 5 min. Amplification was confirmed by electrophoresis on 2% agarose gels.

We included four types of controls in the PCR plates: negative extraction controls, negative PCR controls, positive PCR controls, and negative sequencing controls. Negative extraction

controls were obtained by performing DNA extractions in empty collection tubes (without samples) to detect and analyze potential contamination during the DNA extraction process. For negative PCR controls, ultrapure water was used instead of a DNA template to detect and analyze potential contamination during the PCR process. Positive PCR controls were used to verify that the PCRs worked well for each plate and to detect cross-contamination. They consisted of pure DNA from two marine bacteria (*Sulfitobacter pontiacus* and *Vibrio splendidus*) and fungi (*Candida ocean*i and *Wallemia sebi*) for PCRs performed on the nrDNA ITS and 16S rRNA genes, respectively. These strains were chosen because they are unlikely to be present in our samples, which helps to detect and evaluate the rate of cross-contamination between wells of the same plate. Negative sequencing controls, consisting of empty wells, were filled with ultrapure water to serve as controls for the second PCR (indexing step). The PCR plate maps were designed according to the guidelines of (Taberlet *et al.*, 2018). Each plate had 2 to 3 extraction negative controls, 2 to 3 PCR negative controls, and 2 to 3 PCR positive controls randomly distributed on the plate. Negative sequencing controls were placed in a diagonal line to estimate tag switch rates for as many index combinations as possible.

The second PCR was used to add Illumina® adapters and tags and was performed by the Genome Transcriptome Facility of Bordeaux (France) following the 16S rRNA gene Metagenomic Sequencing Library Preparation protocol (Illumina®). After this indexing step, the libraries were quantified by fluorescence using the Quant-iT™ dsDNA High Sensitivity Assay Kit (Thermo Fisher Scientific™, USA) and pooled to an equimolar concentration. The final pool was purified using a 300-700 bp size selection on a Pippin Prep® (Sage Science™, USA) to remove large nonspecific fragments and the remaining adapters. Pool size was assessed on a TapeStation 4200 system (Agilent Technologies®, USA), and the concentration was estimated by qPCR on an LC480 II system (Roche®, Switzerland) using the QIAseq® Library Quant Kit (QIAGEN®, Germany). Sequencing was performed on a NextSeq® 2000 system (Illumina®, USA) using P1 reagents and 301:10:10:301 cycles. The samples were split into three sequencing runs. The first run included all 2022 phyllosphere samples and half of the 2022 soil samples. The second run included all 2022 endosphere samples and the remaining soil samples. The third run included all 2023 samples. In each run, nrDNA ITS and 16S rRNA amplicons were mixed a 1:1 ratio. Adapter removal and demultiplexing were performed at the sequencing facility using the Cutadapt tool.

Long-read sequencing of bacterial communities

To improve the taxonomic characterization of the bacterial communities, we also sequenced the entire 16S rRNA gene (V1-V9) using PacBio® HiFi technology. Sequencing was performed at the GeT-IT Genotoul facility (Toulouse, France). We prepared one DNA pool per microbial habitat (soil, leaf endosphere and phyllosphere). Amplification of the full-length 16S rRNA gene was performed with the universal primer set 27F (AGRGTTYGATYMTGGCTCAG) and 1492R (RGYTACCTTGTTACGACTT) (Lane *et al.*, 1985). Amplification was performed at 20 cycles with an annealing temperature of 57°C. SMRTbell® libraries were prepared at the GeT-PlaGe Core Facility (Toulouse, France) from the amplified DNA by blunt-ligation according to the PacBio®

protocol "Preparing SMRTbell® Libraries using PacBio® Barcoded Overhang Adapters for Multiplexing Amplicons" (Pacific Biosciences®). At each step, the DNA was quantified using the Qubit® dsDNA HS Assay Kit (Life Technologies™), and the amplicon size was assessed using the DNF-474-0500_HS NGS Fragment Analysis Kit (Agilent Technologies®). The purification steps were performed using AMPure® PB Beads (PacBio®). Purified SMRTbell® libraries of approximately 1560 bp were then sequenced using Binding Kit 3.1 and Sequencing Kit 2.0 by diffusion loading on a SMARTcell® of the PacBio Sequel® II instrument at 70 pM with a 0.8 hour preextension and a 15 hour run. Circular consensus sequence (CCS) reads were generated from the raw PacBio® sequencing data using the standard software tools provided by the manufacturer (Pacific Biosciences®), with minPasses = 3 and minPredictedAccuracy = 0.999 in SMRT Link software (release_12.0.0.177059).

Quantification of the downy mildew inoculum in the soil samples

The downy mildew inoculum in all soil samples was quantified using droplet digital PCR (ddPCR) at the Transcriptomic-qPCR facility of the Neurocenter Magendie (Bordeaux, France). The primers used for the ddPCRs were Giop F (TCCTGCAATTCGCATTACGT) and Giop R (GGTTGCAGCTAATGGATTCCTA) (Valsesia *et al.*, 2005). PCRs were prepared with the required QX200™ ddPCR™ Supermix for Probes (Bio-Rad®, USA) at a final concentration of 750 nM for each primer and 500 nM for the TaqMan® probe (Giop P-VIC: TCGCAGTTCGCAGCGTTCTTCA) to a final volume of 22 µl. Then, 4 µl of each sample was added. Each reaction was loaded into a sample well of an 8-well disposable cartridge (Bio-Rad®, USA), and 70 µl of droplet generator oil (Bio-Rad®, USA) was added to the oil wells of the cartridge. Droplets were formed in the QX200™ Droplet Generator (Bio-Rad®, USA), transferred to a 96-well PCR plate, heat-sealed with foil in a PX1™ PCR Plate Sealer (Bio-Rad®, USA), and amplified using an Eppendorf™ Mastercycler™ Nexus Gradient (Eppendorf™, Germany) (95°C primary denaturation/activation for 5 min, followed by 40 cycles of 95°C for 30 sec, 60°C for 1 min, and 72°C for 30 sec, followed by 98°C for 10 min). PCRs were analyzed using the QX200™ Droplet Reader (Bio-Rad®, USA), and data analysis was performed using QuantaSoft™ software (version 1.7; Bio-Rad®, USA).

Bioinformatics

Bioinformatic analysis of Illumina and PacBio sequence data was performed using version 4.1 of the FROGS pipeline (Escudié *et al.*, 2018) on the Genotoul remote server (The Galaxy Community, 2024). For Illumina sequence data, separate analyses were performed for each barcode region (nrDNA ITS or 16S rRNA genes). The FROGS pipeline first assembled raw forward and reverse reads for each sample into paired-end reads with a minimum overlap of 10 nucleotides and a maximum mismatch of 0.1 using the VSEARCH algorithm (Rognes *et al.*, 2016). For fungal data, unmerged reads were artificially joined by inserting a 100 N sequence between the forward and reverse reads (Escudié *et al.*, 2018). The primers were removed using Cutadapt (Martin, 2011). Sequences containing ambiguous nucleotides or whose size did not match the expected amplicon size (between 50 and 600 bp for the rDNA ITS gene and 250-400 bp for the 16S rRNA gene) were filtered out. The sequences were then dereplicated and clustered using SWARM (Mahé *et al.*, 2014) with a local clustering threshold parameter set to

1 and the 'fastidious' option enabled (Bernard *et al.*, 2021). These clusters of sequences are very similar in construction to Amplicon Sequence Variants (ASVs) (Hakimzadeh *et al.*, 2024) and are hereafter referred to as ASVs. Chimeras were detected and removed using VSEARCH (Rognes *et al.*, 2016). A stringent filtering step was applied, which consisted of retaining only ASVs representing at least 0.00005% of the sequences in the dataset. For the fungal data, the highly variable part of the ITS1 region was extracted using ITSx (Bengtsson-Palme *et al.*, 2013). PacBio HiFi 16S rRNA raw sequences were processed in a similar manner, specifying that the data were from long-read sequencing and adjusting the expected amplicon size to 500-2000 bp.

Taxonomic assignments of bacterial and fungal ASVs obtained from Illumina sequence data were performed using the SILVA 138.1 (Quast *et al.*, 2013) and UNITE Fungi 8.3 (Nilsson *et al.*, 2019b) reference databases, respectively, using both the RDPClassifier (Wang *et al.*, 2007) and BLASTn+ algorithms (Camacho *et al.*, 2009). In addition, we performed taxonomic assignments using BLASTn+ against a custom reference database. This custom database consisted of Sanger sequences from 462 bacterial strains and 547 fungal strains, all of which were isolated from grapevine leaves collected from two of the plot pairs (Jaswa et al., in preparation). In addition, we aligned the bacterial ASVs obtained from the Illumina sequence data with the bacterial ASVs generated using PacBio technology (Supplementary Methods S2). As a result, we obtained up to three taxonomic assignments for each ASV (Supplementary Methods S3). A decision tree was constructed to select the most reliable assignment (Supplementary Fig. S5).

Finally, we decontaminated the datasets using the *metabaR* R package v1.0.0 (Zinger *et al.*, 2021). Since contamination may vary across experiments, depending on laboratory conditions and reagents, we performed separate decontamination of twelve subsets of the data, each corresponding to a combination of one barcode regions (nrDNA ITS or 16S rRNA genes), one microbial habitat (topsoil, phyllosphere, or endosphere), and one sampling year (2022 or 2023). The *contaslayer* function was used to identify ASVs whose relative abundance in the entire dataset was highest in at least one control compared with true samples (Zinger *et al.*, 2021). These ASVs were considered contaminants and were removed from the dataset. Next, the *tagjumpslayer* function was used to detect artifacts such as tag jumps and reduce the noise they cause by removing an ASV from a given PCR product if its relative abundance across the entire dataset was below a specified threshold. This threshold was determined empirically, as recommended in the metabaR tutorial[12], using the visualization functions of the *metabaR* package created for this purpose. Finally, a histogram of the number of reads per sample was plotted, and samples with low sequencing depth, located in the lower tail of the normal distribution curve, were considered failed PCRs and removed.

[12] https://metabarfactory.github.io/metabaR/articles/metabaRF-vignette.html

Statistical analysis

All the statistical analyses were performed with R v4.2.3 (R Core Team, 2023). Microbial community analyses were performed using the R packages *phyloseq* v1.48.0 (McMurdie & Holmes, 2013) and *speedyseq* v0.5.3.9018 (McLaren, 2023), and all figures were generated using the *ggplot2* v3 package. 5.1 (Wickham, 2016), *cowplot* v1.1.3 (Wilke, 2024), *ggh4x* v0.2.8 (van den Brand, 2024), ggsignif v0.6.4 (Ahlmann-Eltze & Patil, 2021), *patchwork* v1.2.0 (Pedersen, 2024), *microViz* v0.10.8 (Barnett *et al.*, 2021), and *ggtext* v0.1.2 (Wilke & Wiernik, 2022). Microbial community analyses were based on sample × ASV raw count matrices or matrices transformed to account for compositional effects. These effects were accounted for by transforming raw sequence counts using the centered and log-ratio (CLR) transformation (Gloor *et al.*, 2017). Prior to the CLR transformation, we applied a Bayesian multiplicative treatment of zeros in the sample × ASV matrices using the *cmultRepl* function of the *zComposition* package v1.5.0.3 (Palarea-Albaladejo & Martín-Fernández, 2015). This function converts zero counts, which would lead to errors in the log ratios, into estimates close to zero, assuming that these zeros are due to undersampling rather than absence. It also drops rows (ASVs) or columns (samples) with more than 80% zero or missing data. The analyses of beta and alpha diversity and the search for microbial consortia of interest for downy mildew biocontrol presented below were performed separately for each combination of microbial habitat (topsoil, phyllosphere, or leaf endosphere) and PCR marker (nrDNA ITS or 16S rRNA genes).

Analysis of the relationship between downy mildew foliar symptoms and the amount of inoculum in topsoil

We evaluated the relationship between plot susceptibility to downy mildew, which was defined on the basis of several years of foliar symptom monitoring, and the concentration of *P. viticola* DNA in the topsoil at the time of sampling using a linear mixed effects model. The model included the concentration of *P. viticola* DNA in the topsoil as the dependent variable and the susceptibility of the plot to downy mildew (high or low) as a fixed factor. Other variables that may influence the amount of *P. viticola* oospores in the topsoil were also included as fixed factors: the year of sampling (2002 or 2023), whether fungicide treatments were applied to the area sampled the year before sampling (yes or no), and the location of the soil sample within the plot (on the edge of the plot or not). An interaction term between fungicide application and within-plot location was also included, and the plot pair was included as a random effect. Models were built using the *lmer* function from v3.1.3 of the *lmerTest* package (Kuznetsova *et al.*, 2017) and evaluated with Type II ANOVA using v3.1.2 of the *car* package (Fox & Weisberg, 2018). Graphical checks for homoscedasticity and normality of the residuals were performed using the packages *performance* v0.12.0 (Lüdecke *et al.*, 2021) and *DHARMa* v0.4.6 (Hartig & Lohse, 2022). The variance explained by the model was estimated using the conditional coefficient of determination (R^2c) and the marginal coefficient of determination (R^2m) provided by the r2 function of the performance package. The former coefficient

represents the variance explained by the entire model, whereas the latter represents the variance explained by the fixed effects only.

Analysis of the environmental factors driving within-plot and between-plot variation in the microbial composition of topsoil and leaf (endosphere and phyllosphere).

Principal Component Analysis (PCA) was applied to the sample × ASV matrix transformed by CLR to visualize variation in microbial community composition using the *microViz* package. We then identified key factors influencing community composition using variance partitioning and Redundancy Analysis (RDA), implemented using respectively the *varpart* and *rda* functions of the *vegan* package v2.6.4 (Oksanen *et al.*, 2024). The same explanatory factors were used in both analyses (Supplementary Table S1). For variance partitioning, we categorized them into 4 groups: soil physical chemistry (Soil; 9 variables), grape variety and management (Management; 3 variables), weather during the month before sampling (Weather; 30 variables), and sampling location (Space; 4 variables) (Supplementary Table S1). For both variance partitioning and RDA, the sample x ASV matrix transformed by CLR was used as the response. Nonnumeric variables were treated as dummy variables, and all variables were standardized using the scale function. For the RDA, an automatic stepwise selection of explanatory variables, both forward and backward, was performed using the *ordistep* function of the *vegan* package in R. Finally, an RDA was performed with all selected explanatory variables included as constraints. Permutation tests were performed using the *anova.cca* function of the *vegan* package to assess the significance of the fitted models and to evaluate the marginal effects of the constraints.

Testing whether microbial diversity in topsoil and leaves is higher in vineyard plots with lower susceptibility to downy mildew

To investigate whether microbial diversity in topsoil and leaves is higher in vineyard plots with lower susceptibility to downy mildew (hypothesis (i)), we calculated three α diversity indices. These indices are part of the Hill number framework (Chao *et al.*, 2014), which includes a parameter *q* that determines the sensitivity of the indices to the relative abundance of ASVs. This framework gives less weight to rare ASVs as q increases. The Hill number corresponding to $q = 0$ represents the richness of ASVs, where each ASV counts is assigned a value of 1 regardless of its relative abundance. The Hill number corresponding to $q = 1$ is the exponential of Shannon's entropy index (Shannon, 1948), where the weight of each ASV is proportional to its relative abundance. The Hill number corresponding to $q = 2$ is the inverse of Simpson's concentration index (Simpson, 1949), which disproportionately favors abundant ASVs and is particularly relevant for metabarcoding data, as rare ASVs often correspond to artifacts, and their inclusion can lead to erroneous ecological conclusions (Taberlet *et al.*, 2018). The three observed alpha diversity indices, with $q = 0$ to 2, were calculated from the sample × ASV raw count matrix using the *ChaoRichness*, *ChaoShannon*, and *ChaoSimpson* functions in the *iNEXT* v3.0.1 package (Chao *et al.*, 2014; Hsieh & Chao, 2024). The effect of downy mildew susceptibility on microbial community alpha diversity was assessed using linear mixed effects

models. We constructed 18 models, each corresponding to a combination of one microbial habitat (topsoil, phyllosphere or leaf endosphere), one PCR marker (nrDNA ITS or 16S rRNA genes) and one alpha diversity index (q=1, 2 or 3). For the 2022 sampling campaign, the model included three fixed effects: plot susceptibility to downy mildew (high or low), whether fungicides were applied to the sampled area in the year prior to sampling (yes or not), and the location of the sample within the plot (on the edge or not). For the 2023 sampling campaign, the model included only plot susceptibility to downy mildew (high or low) because the samples were collected exclusively from the center of the plots, and all the sampled vines had received fungicide treatment the year before. Both models included pairs of plots as random effects. Graphical checks for homoscedasticity and normality of the residuals were performed using the *performance* and *DHARMa* packages. Model construction and evaluation were performed using the *lmerTest* and *car* packages.

Testing whether plots with low susceptibility to downy mildew harbor a greater abundance of specific microbial taxa in topsoil and leaves

To investigate whether plots with low downy mildew susceptibility harbored a higher abundance of specific microbial taxa (hypothesis (ii)), we used a set of four Differential Abundance Analysis (DAA) methods recommended in the recent literature: ANCOM-BC2 (Lin & Peddada, 2024), Maaslin2 (Mallick *et al.*, 2021), LinDA (Zhou *et al.*, 2022) and ZicoSeq (Yang & Chen, 2022). We selected these methods for the following reasons: they were specifically developed for microbiota analysis by explicitly accounting for zero inflation and compositional effects; they allow the specification of random and covariate effects; and they have been recommended in recent methodological studies (Nearing *et al.*, 2022a; Yang & Chen, 2022, 2023; Regueira-Iglesias *et al.*, 2023). This set at 4 DAA was used to compare ASV abundances between plots with high and low downy mildew susceptibility while accounting for microbial community variation between plot pairs. For all four methods, the plot pair was included as a random factor, and the parameters were set to defaults except for the minimum prevalence threshold, which was set to 10%, and the adjusted p value for an ASV to be considered differentially abundant, which was set to 0.05. All analyses were performed using the sample × ASV raw count matrix. They were performed using the *ANCOMBC* v2.0.3 (Lin & Peddada, 2020; Lin *et al.*, 2022), *Maaslin2* v1.12.0 (Mallick *et al.*, 2021), *GUniFrac* v1.8 (Chen *et al.*, 2023), and *MicrobiomeStat* v1.2 (Zhang *et al.*, 2024) packages.

For each ASV identified as differentially abundant by at least one of the four DAA methods, we calculated two scores: (1) the number of methods that identified that the ASV was differentially abundant, ranging from 1 to 5, and (2) the average association coefficient between the methods. To calculate the average association coefficient, the coefficients provided by each DAA method were standardized between 0 and 1 if the ASV was more abundant in low-susceptibility plots and between 0 and -1 if the ASV was more abundant in high-susceptibility plots before the average coefficient between methods was calculated. Finally, we included the Random Forest (RF) algorithm (see below) as a fifth method and used the Gini index provided by the RF algorithm to calculate the average association coefficient.

Testing whether plots with low amount of downy mildew inoculum harbor a greater abundance of specific microbial taxa in topsoil and leaves

In addition, we investigated whether plots with low amounts of *P. viticola* oospores in the topsoil harbored specific microbial taxa using the Threshold Indicator Taxa ANalysis (TITAN) method of the *TITAN2* package v2.4.3 (Baker *et al.*, 2023a). This method analyzes changes in community composition along ecological gradients. Our goal was to identify microbial taxa that covary with the concentration of *P. viticola* DNA in the topsoil. For this analysis, we used the sample × ASV raw count matrix, retaining only microbial ASVs with more than 100 total reads and present in at least 3 samples, as required by the *titan* function. The method identified ASVs whose abundance increased as the *P. viticola* DNA concentration decreased and ASVs whose abundance increased as the *P. viticola* DNA concentration increased. These ASVs are hereafter referred to as indicators of low and high *P. viticola* DNA concentrations in topsoil. To evaluate the strength of the relationship, we used the standardized Indicator Value (IndVal) score defined by Dufrene and Legendre (Dufrêne & Legendre, 1997) and expressed it as a z score.

Testing whether plot susceptibility to downy mildew is predictable from microbiota composition

We used Random Forest (RF) algorithms to assess the predictive power of microbiota composition. We tested whether plot susceptibility to downy mildew can be predicted from the microbiota composition (hypothesis (iii)) and whether the leaf microbiota is a better predictor of leaf symptoms within the same year, whereas the topsoil microbiota is a better predictor of symptoms in the following year (hypothesis (iv)). For this purpose, we used the *microranger* package v0.0.0.9000 (Cambon *et al.*, 2023; Cambon, 2024), which includes RF classification functions derived from the *ranger* package (Wright & Ziegler, 2017) and was specifically designed to classify microbial communities.

We first analyzed the predictive power of microbiota composition on samples collected within the same year, using data collected in 2022. We used the *rf.opti.mtry.taxo* function to train the RF algorithm on a set of 36 ASV tables for each microbial habitat (phyllosphere, leaf endosphere, and topsoil). Each table was a sample × ASV raw count matrix corresponding to a microbiota subset (fungi only, bacteria only, or both), a filtering threshold (all ASVs or only abundant ASVs), and a level of taxonomic aggregation (ASV, species, genus, family, class, or order). Abundant ASVs were defined as those with a read count greater than the third quartile of the ASV read count distribution. Training of the RF algorithm involved 500 decision trees for each table, with nonrandom k-fold cross-validation. The algorithm used 80% of the pairs of plots as the training dataset and the remaining 20% as the validation dataset. The cross-validation was performed on all possible splits of the entire dataset, with the only condition that the plots belonging to the same pair were both in the training dataset or both in the validation dataset. This condition ensured that the algorithm focused on learning susceptibility to downy mildew rather than the spatial location of the plots. We optimized each algorithm using 20 different values for the mtry parameter, which represents the number of variables

considered at each node division of the decision tree. The best mtry value for each of the 36 ASV tables was selected on the basis of the error rate of the algorithm, as done in Cambon et al. (Cambon *et al.*, 2023). Next, we used the *rf.blind* function to obtain the Gini index and associated p value estimated by permutation using the Altmann method (Altmann *et al.*, 2010), allowing us to identify which ASVs were most important for classification.

Finally, we assessed the predictive power of the microbiome composition on the samples collected the following year. The 2022 dataset was used for training, and the 2023 dataset for validation. To create the validation sets, we randomly grouped pairs of plots sampled in 2023 into groups of two, with each plot assigned to a single validation group. We then used all possible combinations of 80% of the plot pairs sampled in 2022 for training and validated the model on each validation group.

Results

Seven pairs of vineyard plots were selected based on epidemiological records of downy mildew

Seven different pairs of vineyard plots, all located in southwestern France (Fig. 1), were selected for the present study based on the analysis of epidemiological records (Table 1). Both plots within a pair were planted with the same variety, managed in a similar way and located close to each other (Table 1). Each pair of plots consisted of a plot with lower downy mildew susceptibility and a plot with higher downy mildew susceptibility (Fig. 2A and Supplementary Fig. S6). The area under the disease progression curve (AUDPC) was calculated for the years 2019 to 2021 and averaged for each of the 7 pairs and compared with that of the 1200 plots monitored by IFV (Fig. 2B).

The AUDPC values of the 7 plots with low susceptibility to downy mildew were always lower than those of the plots with high susceptibility for the 4 variables of the same pair, as expected by the selection process (Fig. 2B). The differences between low and high values of the same pair varied between pairs and between variables (Fig. 2B). For most pairs except CDB2, all AUDPC values for the low-susceptibility plots are lower than the lowest AUDPC value for the high-susceptibility plots. The values of the selected pairs are among the most frequent values of the 1200 plots but not the extremes (Fig. 2B).

The pairs of plots differed slightly between the 2022 and 2023 sampling campaigns (Table 1). In 2022, 14 vineyard plots, which formed 7 pairs contrasted in terms of epidemiological history, met the 5 selection criteria. However, only 5 pairs (named LIB, ME1, ME2, E2M, and CDB1) could be sampled at the chosen phenological stage and before the first fungicide treatment. In 2023, 12 vineyard plots, which formed 6 pairs contrasted in terms of epidemiological history, met the 5 selection criteria. These pairs included 4 pairs already selected in 2022 (all except CDB1, which started an organic conversion) and two new pairs (ME3, CDB2) (Table 1). All six selected pairs could be sampled at the chosen phenological stage and before the first fungicide treatment. In total, we studied 7 pairs of plots (LIB, ME1, ME2, ME3, E2M, CDB1, and CDB2), and each pair was sampled at least once (Table 1).

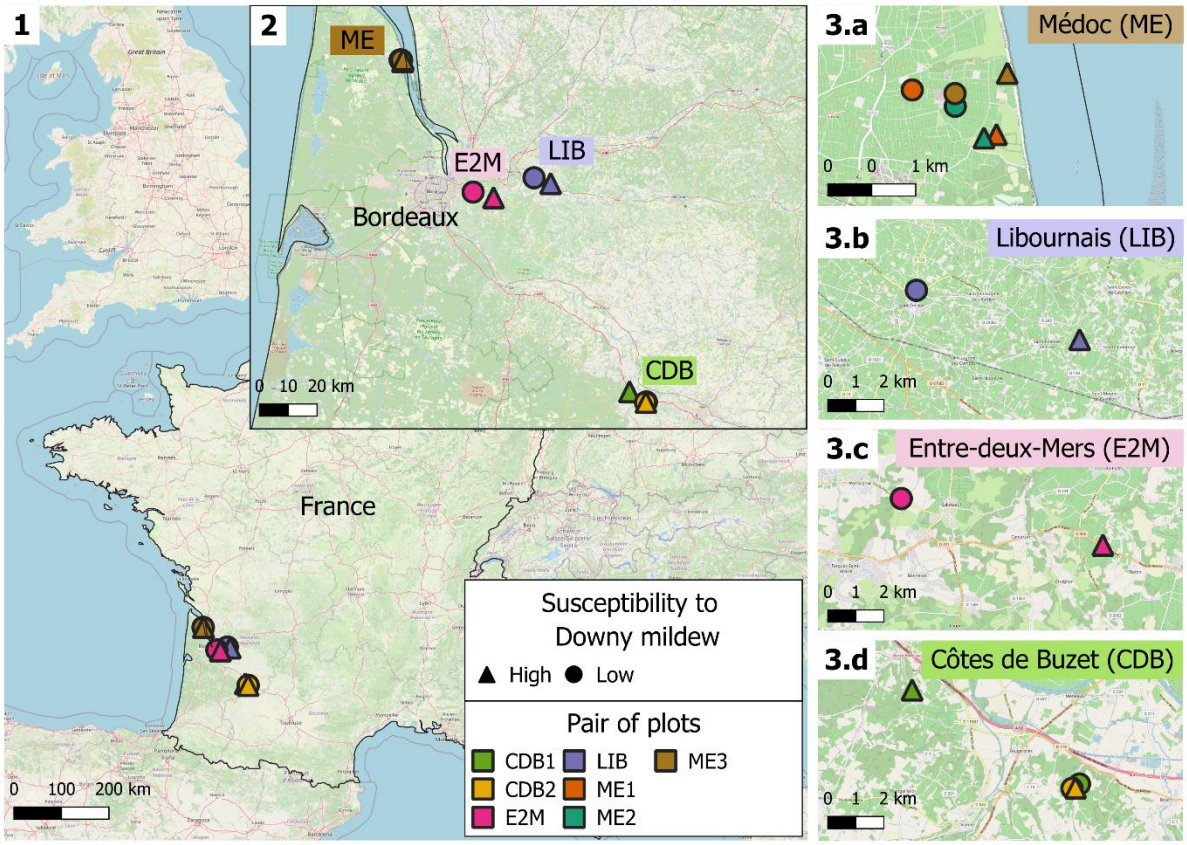


Figure 1: Map of the vineyard plots.

Seven pairs of plots that differed in their susceptibility to downy mildew were selected for the present study. They were all located in France (map 1) in the Nouvelle-Aquitaine region (map 2). They belonged to four wine-growing areas, namely, Médoc (ME), Libournais (LIB), Entre-deux-Mers (E2M) and Côtes de Buzet (CDB) (maps 3a-d). Plots belonging to the same pair are represented with the same color, with symbols indicating high and low susceptibility to downy mildew (triangles and circles, respectively). The distance between plots within a pair ranged from 0 km for pair CDB2 (adjacent plots) to 7.5 km for pair E2M (Table 1).

Table 1: Description of the pairs of vineyard plots.
Each pair consisted of one plot with low susceptibility to downy mildew (labeled _L) and one plot with high susceptibility to downy mildew (labeled _H) according to long-term epidemiological data. Five pairs of plots were sampled in 2022, and six were sampled in 2023.

Plot pair	Plot name	Susceptibility to downy mildew	GPS coordinates	Geographic distance between plots	Grape variety	Management	Sampling year(s)
Libournais (LIB)	LIB_L	Low	44°53'52.4"N 0°09'13.7"W	6 km	Merlot Noir	biodynamic	2022 and 2023
	LIB_H	High	44°52'55.6"N 0°04'48.3"W				
Médoc1 (ME1)	ME1_L	Low	45°14'50.7"N 0°46'00.4"W	1 km	Merlot Noir	organic	2022 and 2023
	ME1_H	High	45°14'35.8"N 0°45'15.4"W				
Médoc2 (ME2)	ME2_L	Low	45°14'45.4"N 0°45'37.6"W	0.5 km	Cabernet Sauvignon	organic	2022 and 2023
	ME2_H	High	45°14'34.3"N 0°45'21.8"W				
Médoc3 (ME3)	ME3_L	Low	45°14'50.1"N 0°45'38.0"W	0.6 km	Merlot Noir	organic	2023
	ME3_H	High	45°14'58.5"N 0°45'11.3"W				
Entre-deux-Mers (E2M)	E2M_L	Low	44°50'43.8"N 0°25'16.3"W	7.5 km	Merlot Noir	conventional	2022 and 2023
	E2M_H	High	44°49'52.1"N 0°19'42.2"W				
Côtes de Buzet1 (CDB1)	CDB1_L	Low	44°12'38.5"N 0°22'21.7"E	6.7 km	Merlot Noir	conventional	2022
	CDB1_H	High	44°14'26.7"N 0°17'53.0"E				
Côtes de Buzet2 (CDB2)	CDB2_L	Low	44°12'33.4"N 0°22'09.7"E	0 km	Merlot Noir	organic	2023
	CDB2_H	High	44°12'33.4"N 0°22'09.7"E				

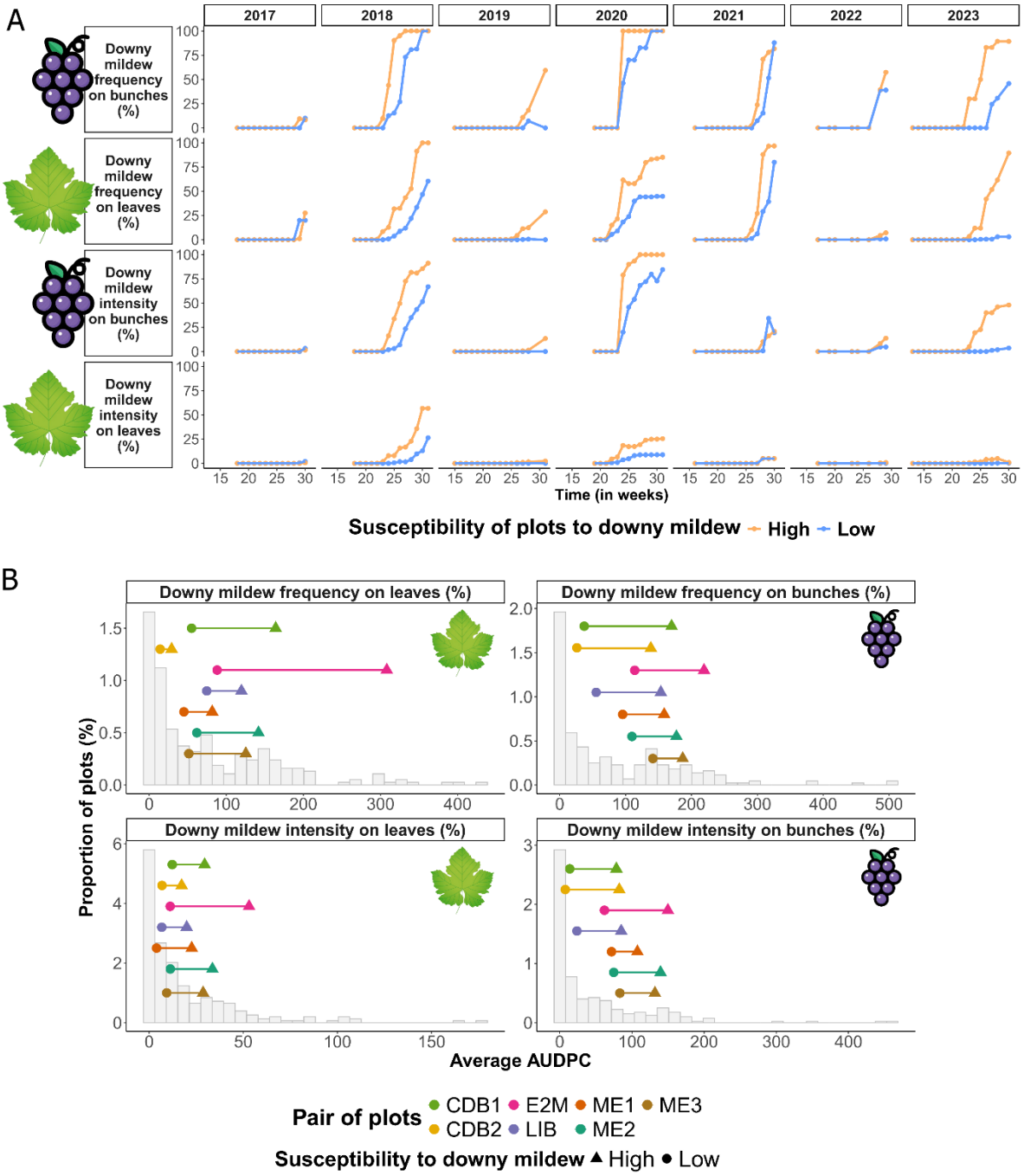


Figure 2: Epidemiological features of vineyard plots.

(A) Downy mildew disease progression curves for the high-susceptibility (in orange) and low-susceptibility (in blue) plots of the ME2 plot pair over seven years of epidemiological monitoring and (B) average areas under the downy mildew progression curves (AUDPC) for the seven pairs of plots selected in the present study. AUDPC values were averaged across the years 2019, 2020, and 2021 (*i.e.*, the common years of epidemiological monitoring for the seven pairs of plots). The Average AUDPC values for plots belonging to the same pair are represented with the same color, with symbols indicating high or low susceptibility to downy mildew (triangles and circles, respectively). The gray histograms represent the distribution of average AUDPC values for the 1200 plots included in the epidemiological database.

The amount of downy mildew in topsoil is lower in plots with a low susceptibility to downy mildew

The topsoil *P. viticola* DNA concentration was significantly lower in plots classified as low susceptibility plots based on symptoms on leaves and bunches (Linear Mixed-Effects Models, $p < 0.05$*; Supplementary Table S2 and Fig. S7). In addition, topsoil samples collected from plots treated with fungicide in the previous year had significantly lower topsoil *P. viticola* DNA concentrations (Linear Mixed-Effects Models, $p < 0.001$***; Supplementary Table S2 and Fig. S7). Within-plot location had a significant effect on the topsoil *P. viticola* DNA concentration, with samples collected along plot edges showing a lower concentration than those collected in the center of the plots (Linear Mixed-Effects Models, $p < 0.001$***; Supplementary Table S2 and Fig. S7). In addition, we detected a higher concentration of *P. viticola* DNA in the soil in 2022 than in 2023 (Linear Mixed-Effects Models, $p < 0.001$***; Supplementary Table S2 and Fig. S7), which was likely due to the more severe downy mildew epidemic in 2021 than in 2022 (Fig. 2A and Supplementary Fig. S6). In addition, we detected a higher concentration of *P. viticola* DNA in the soil in 2022 than in 2023 (Linear Mixed-Effects Models, $p < 0.001$***; Supplementary Table S2 and Fig. S7), which was likely due to the more severe downy mildew epidemic in 2021 than in 2022 (Fig. 2A and Supplementary Fig. S6).

Microbial richness is higher in topsoil than in grapevine leaves

After filtering, the final fungal dataset contained 136,681,217 reads grouped into 795 ASVs, while the final bacterial dataset contained 32,678,727 reads grouped into 1,561 ASVs (Supplementary Table S3). Using PacBio sequencing, we obtained 35,934 reads representing 524 bacterial ASVs, allowing us to improve the taxonomic assignment of 154 bacterial ASVs (out of 1,561). Using Sanger sequencing of our collection of grapevine foliar microorganisms, we were able to improve the taxonomic assignment of 88 fungal ASVs (out of 795).

On average, topsoil samples contained 299 ± 41 fungal ASVs and 920 ± 177 bacterial ASVs. The phyllosphere samples contained 232 ± 78 fungal ASVs and 356 ± 189 bacterial ASVs. The leaf endosphere samples contained 54 ± 33 fungal ASVs and 19 ± 11 bacterial ASVs. Thus, topsoil was the habitat with the highest microbial community richness in terms of ASVs.

Topsoil, phyllosphere and leaf endosphere microbial communities have different compositions

The microbial community composition differed between the topsoil, phyllosphere and leaf endosphere. The topsoil and leaf endosphere fungal communities were dominated by Ascomycota (representing 75% and 91% of the fungal reads in the 2022 dataset, respectively), followed by Basidiomycota (20% and 6%, respectively). By contrast, the phyllosphere had a higher proportion of Basidiomycota (47%) than both the topsoil and the leaf endosphere (Fig. 3; Table 2). Actinobacteria were predominant (50%) in the topsoil while Proteobacteria were dominant in both the phyllosphere and leaf endosphere (61% and 51%, respectively) (Fig. 3; Table 3). Similar values were obtained in 2023 (Supplementary Fig. S8; Supplementary Tables S4 and S5).

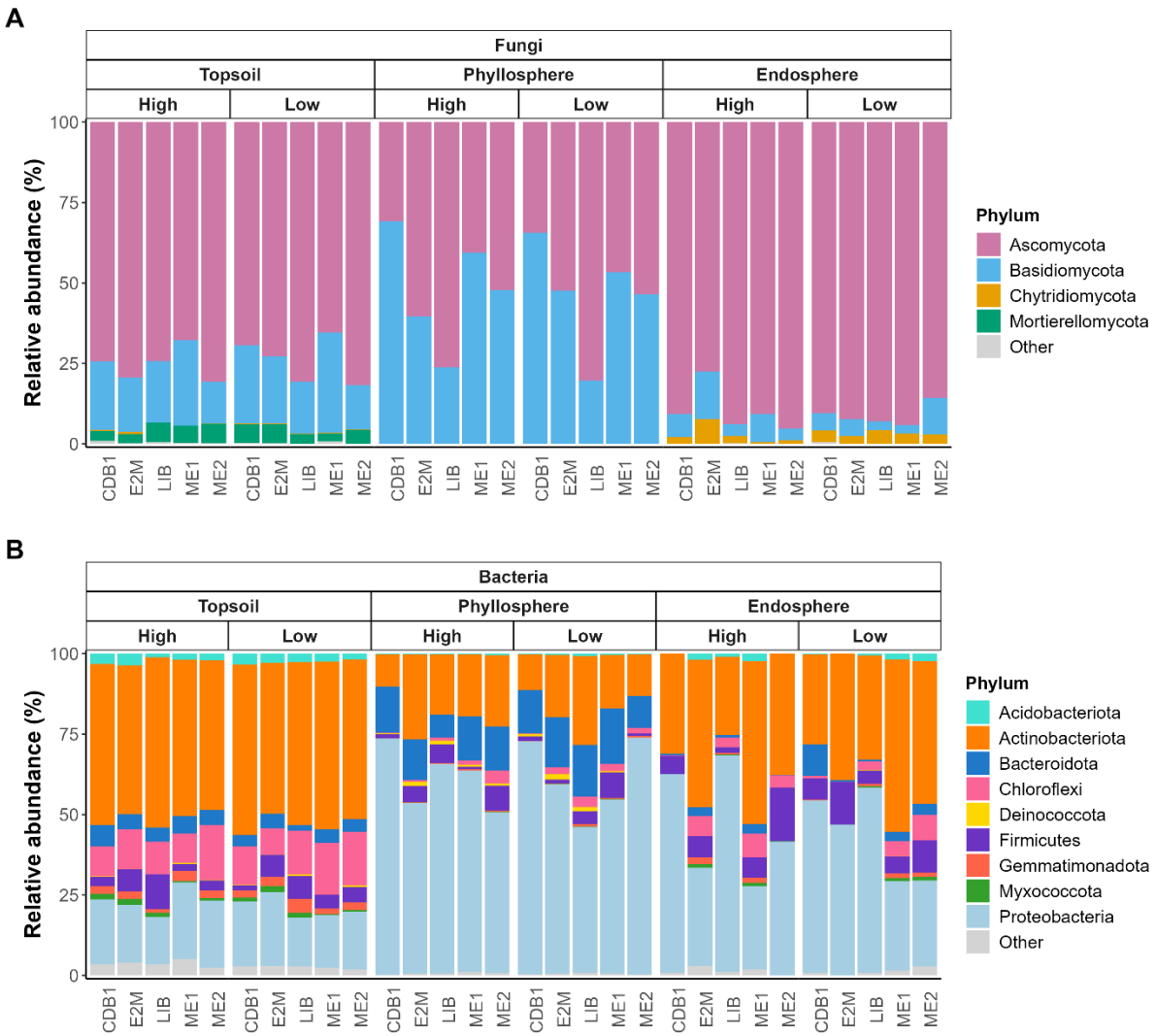


Figure 3: Microbial community profiles depending on vineyard plot susceptibility to downy mildew. (A) Fungal and (B) bacterial community profiles of the topsoil, phyllosphere and leaf endosphere, representing the relative abundance of the different phyla averaged over the sixteen samples collected in each plot and each microbial habitat during the 2022 sampling campaign. Phyla representing less than 1% of the sequences were grouped into the "Other" category.

The most abundant fungal species and bacterial genera differed between the topsoil, phyllosphere, and leaf endosphere but remained consistent across years. Among the 10 most abundant fungal species and 10 most abundant bacterial genera in each microbial habitat in 2022, approximately half were also among the 10 most abundant in 2023 (Tables 2 and 3; Supplementary Tables S4 and S5). For example, *Gibberela intricans* was consistently the most abundant fungal species in the topsoil. *Aureobasidium pullulans* and *Vishniacozyma carnescens* were consistently among the top three fungal species in the grapevine phyllosphere, while *Epiccoccum nigrum* and *Alternaria alternata* were consistently among the top three fungal species in the leaf endosphere (Table 2; Supplementary Table S4). The topsoil was consistently dominated by bacteria of the genera *Nocardioides*, *Rubrobacter*, and *Bacillus*. The phyllosphere was dominated by bacteria belonging to the genera *Sphingomonas*, *Hymenobacter* and

Methylobacterium, whereas the genera *Nocardioides*, *Bacillus* and *Wolbachia* were consistently among the top 10 bacterial genera in the leaf endosphere (Table 3; Supplementary Table S5). This difference in microbial community composition between the phyllosphere and the leaf endosphere indicates that we successfully separated the epiphytic and endophytic fractions of the leaf microbial communities. This finding is consistent with the sequencing of water washes collected after leaf surface sterilization. The water washes had microbial profiles very similar to those of the negative extraction and PCR controls, indicating that leaf surface sterilization was effective.

Soil physico-chemistry and weather have a stronger influence on microbiota composition than does grape variety and management practices

Topsoil microbial communities (both fungi and bacteria) and phyllosphere fungal communities were spatially structured, with marked differences in composition between plots and plot pairs. This spatial structuring was consistent across years (Fig. 4 for 2022 and Supplementary Fig. S9 for 2023). Each plot pair had its own microbial community composition, and the plot pairs that were geographically close (for example, ME1 and ME2 in 2022, both located in the Medoc region; Fig. 1) had more similar communities (Fig. 4 and Supplementary Fig. S9). In contrast, the phyllosphere bacterial communities and leaf endosphere communities (both fungi and bacteria) showed little spatial structuring (Fig. 4 for 2022 and Supplementary Fig. S9 for 2023).

The composition of the topsoil fungal and bacterial communities, as well as the phyllosphere fungal communities, was mainly structured by two factors: the weather of the past month (*Weather*) and the physicochemical properties of the soil (*Soil*) (Supplementary Table S1). In 2022, *Weather* explained 43.01% of the variance in topsoil fungal community composition, 53.56% of the variance in topsoil bacterial community composition, and 33.75% of the variance in phyllosphere fungal communities (Supplementary Fig. S10). *Soil* was nearly as influential, accounting for 42.08% of the variance in topsoil fungal community composition, 54.76% of the variance in topsoil bacterial community composition, and 29.77% of the variance in phyllosphere fungal communities (Supplementary Fig. S10). In 2023, the ranking of environmental drivers remained similar, with *Weather* and *Soil* being the primary drivers of topsoil fungal and bacterial communities and phyllosphere fungal communities (Supplementary Fig. S11 and *Annexe 8*).

Management factors, including grape variety, management type (organic, biodynamic, conventional), and whether fungicide treatments were applied the year before sampling, had less influence on the microbiota composition than did *Weather* and *Soil* (Supplementary Fig. S10) but were still retained as significant variables (*Annexe 8*)). For example, management type, grape variety and fungicide treatment applied the year before sampling significantly influenced the composition of phyllosphere fungal communities (*Annexe 8*).

Table 2: Most abundant fungal species in the topsoil, phyllosphere and leaf endosphere of vineyard plots.

The table represents the top ten most abundant fungal species in the 2022 dataset. Species in bold are also among the top ten most abundant species in 2023. Relative abundance (%) indicates the proportion of sequences assigned to the species relative to the total number of sequences in the dataset. Prevalence (%) indicates the percentage of samples where the species is present with at least one sequence.

Topsoil			Leaf phyllosphere			Leaf endosphere		
Fungal species	Relative abundance (%)	Prevalence (%)	Fungal species	Relative abundance (%)	Prevalence (%)	Fungal species	Relative abundance (%)	Prevalence (%)
Gibberella intricans (Ascomycota)	12.08	99.37	***Aureobasidium pullulans*** (Ascomycota)	11.24	94.3	***Epicoccum nigrum*** (Ascomycota)	15.67	61.88
Cladosporium cladosporioides (Ascomycota)	4.56	97.48	***Cladosporium cladosporioides*** (Ascomycota)	9.61	99.37	***Alternaria alternata*** (Ascomycota)	7.44	44.38
Saitozyma podzolica (Basidiomycota)	4.34	75.47	***Vishniacozyma carnescens*** (Basidiomycota)	7.21	92.41	*Botrytis cinerea* (Ascomycota)	4.93	45
Vishniacozyma victoriae (Basidiomycota)	3.27	93.71	*Itersonilia pannonica* (Basidiomycota)	6.9	79.11	***Didymella negriana*** (Ascomycota)	4.8	10
Fusarium avenaceum (Ascomycota)	2.25	96.86	***Cladosporium allicinum*** (Ascomycota)	6.8	95.57	*Hirsutella lecaniicola* (Ascomycota)	3.19	6.25
Plectosphaerella cucumerina (Ascomycota)	2.06	91.19	***Vishniacozyma victoriae*** (Basidiomycota)	6.17	99.37	***Blumeria graminis*** (Ascomycota)	2.94	33.12
Mortierella elongata (Mortierellomycota)	1.74	84.91	*Filobasidium stepposum* (Basidiomycota)	5.31	99.37	***Alternaria infectoria*** (Ascomycota)	2.47	38.12
Boeremia exigua (Ascomycota)	1.47	79.87	*Udeniomyces pyricola* (Basidiomycota)	4.41	73.42	***Itersonilia perplexans*** (Basidiomycota)	2.29	19.38
Didymella pomorum (Ascomycota)	1.46	88.68	***Cladosporium ramotenellum*** (Ascomycota)	3.83	84.81	*Cladosporium cycadicola* (Ascomycota)	2.17	30
Clonostachys rosea (Ascomycota)	1.43	94.97	*Botrytis cinerea* (Ascomycota)	2.42	92.41	*Cladosporium allicinum* (Ascomycota)	2.12	27.5
Total	34.66		Total	63.9		Total	48.02	

Table 3: Most abundant bacterial genera in the topsoil, phyllosphere and leaf endosphere of vineyard plots.

The table represents the top ten most abundant bacterial genera in the 2022 dataset. Genera in bold are also among the top ten most abundant genera in 2023. Relative abundance (%) indicates the proportion of sequences assigned to the genera relative to the total number of sequences in the dataset. Prevalence (%) indicates the percentage of samples where the genera is present with at least one sequence.

Topsoil			Leaf phyllosphere			Leaf endosphere		
Bacterial genus	Relative abundance (%)	Prevalence (%)	Bacterial genus	Relative abundance (%)	Prevalence (%)	Bacterial genus	Relative abundance (%)	Prevalence (%)
Nocardioides (Actinobacteriota)	5.85	100	***Sphingomonas*** (Proteobacteria)	18.13	99.38	*Cutibacterium* (Actinobacteriota)	17.17	82.5
Bacillus (Firmicutes)	3.91	100	***Pseudomonas*** (Proteobacteria)	13.03	93.75	*Rickettsiella* (Proteobacteria)	10.46	3.75
Rubrobacter (Actinobacteriota)	3.28	81.25	***Hymenobacter*** (Bacteroidota)	9.74	98.12	*Chryseolinea* (Bacteroidota)	2.26	0.62
Gaiella (Actinobacteriota)	2.82	100	*Massilia* (Proteobacteria)	7.11	99.38	*Variovorax* (Proteobacteria)	1.85	46.88
Pseudarthrobacter (Actinobacteriota)	2.52	98.12	***Methylobacterium-Methylorubrum*** (Proteobacteria)	6.27	98.75	***Wolbachia*** (Proteobacteria)	1.48	21.88
Sphingomonas (Proteobacteria)	2.44	100	***Nocardioides*** (Actinobacteriota)	1.75	99.38	*Thermoanaerobacterium* (Firmicutes)	1.47	41.25
Arthrobacter (Actinobacteriota)	2.31	100	*Pseudarthrobacter* (Actinobacteriota)	1.62	83.12	*Caulobacter* (Proteobacteria)	1.33	25
Blastococcus (Actinobacteriota)	1.96	99.38	*Friedmanniella* (Actinobacteriota)	1.4	85.62	*Nocardioides* (Actinobacteriota)	1.29	50.62
Streptomyces (Actinobacteriota)	1.58	100	***Variovorax*** (Proteobacteria)	1.32	91.88	***Bacillus*** (Firmicutes)	1.23	43.75
Massilia (Proteobacteria)	1.41	100	*Spirosoma* (Bacteroidota)	1.03	87.5	*Rhizobacter* (Proteobacteria)	1.17	20
Total	**28.08**		Total	**61.4**		Total	**39.71**	

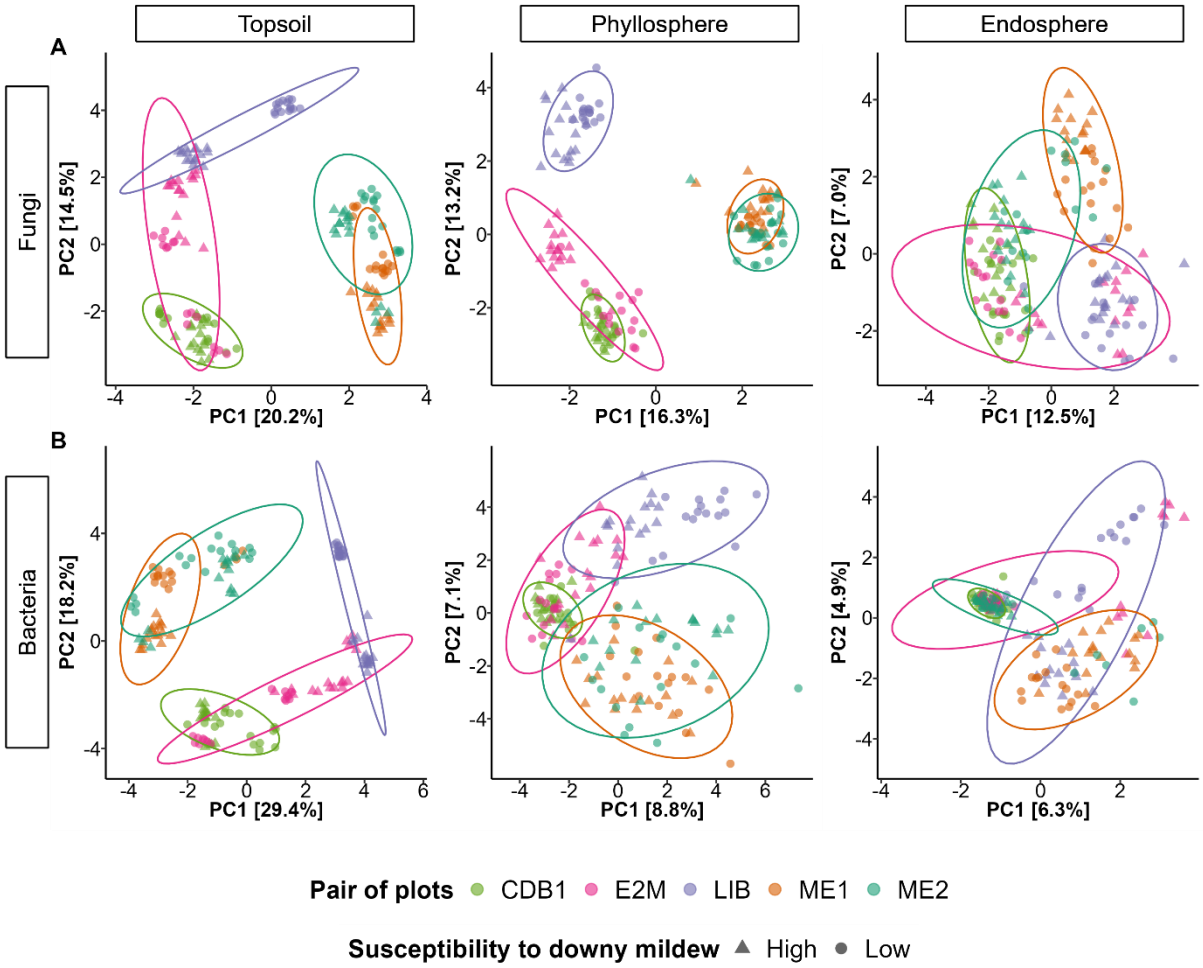


Figure 4: Variation in microbial community composition across vineyard plots.
Dissimilarities among (A) fungal and (B) bacterial communities of the topsoil, phyllosphere and leaf endosphere for the five pairs of plots sampled in 2022, represented with a Principal Component Analysis (PCA). Samples collected from the same pair of plots are represented with the same color, with symbols indicating high and low susceptibility to downy mildew (triangles and circles, respectively).

Fungicide treatments decrease microbiota diversity in both topsoil and grapevine leaves, whereas edge effects increase it

Fungicide treatments altered not only the composition of phyllosphere fungal communities (*Annexe 8*)) but also their diversity (Supplementary Tables S6 and S7). Using the 2022 dataset, we showed that fungicide treatments applied the year before sampling decreased the diversity of fungal communities in both the phyllosphere and topsoil (Supplementary Table S6). In contrast, edge effects increased microbiota diversity. Topsoil fungal and bacterial communities, as well as endosphere fungal communities, were more diverse at the edge of the plot than at the center (Supplementary Table S6). These analyses could not be applied to the 2023 data because samples were collected exclusively from the center of the plots in that year, and all of these samples came from grapes that had received fungicide treatment the year before.

Microbial diversity is not consistently higher in plots with lower susceptibility to downy mildew

According to hypothesis (i), phyllosphere and endosphere fungal communities sampled in 2022 were more diverse in plots with low downy mildew susceptibility than in plots with high downy mildew susceptibility (Supplementary Table S6 and Fig. S12). Differences were significant when diversity was measured by Shannon's index but not Simpson's index or observed richness (Supplementary Table S6 and Fig. S12). However, these results were not consistent across years. In 2023, there was no difference in phyllosphere fungal diversity between the low- and high-susceptibility plots (Supplementary Table S7 and Fig. S13). In addition, the diversity of endophytic fungi showed the opposite pattern from that in 2022 (Supplementary Tables S6 and S7 and Fig. S12 and S13). Similarly, the difference in topsoil microbiota diversity between plots with low and high downy mildew susceptibility was not consistent across years. In 2022, both topsoil fungal and bacterial communities were more diverse in plots with high downy mildew susceptibility, contrary to hypothesis (i), while these differences were not significant in 2023 (Supplementary Tables S6 and S7 and Fig. S12 and S13).

Plots with low susceptibility to downy mildew harbor a greater abundance of specific microbial taxa

Consistent with hypothesis (ii), our analyses of the 2022 dataset revealed 241 fungal and 462 bacterial ASVs that were significantly more abundant in plots with low downy mildew susceptibility (*Annexe 9*). Differentially abundant ASVs were mainly found in the topsoil (141 fungal and 453 bacterial ASVs) and, to a lesser extent, in the phyllosphere (128 fungal and 70 bacterial ASVs). Only 11 differentially abundant taxa, all of which were fungi, were detected in the leaf endosphere (Supplementary Fig. S14). In the topsoil, fungal species such as *Coniochaeta fasciculata*, *Fusarium brachygibbosum*, *Didymella pomorum*, *Volutella ciliata*, *Robillarda sessilis*, *Paraphoma pye*, and the *Trichoderma* species (*T. virens* and *T. lixii*) scored the highest (Supplementary Fig. S15). Additionally, the genus *Mortierella* (including *M. exigua*, *M. alpina*, and *M. elongata*) and basidiomycetous yeasts, such as *Papiliotrema* (including *P. laurentii*, *P. terrestris*, and *P. flavescens*), *Rhodotorula* (including *Rhodotorula babjevae* and *Rhodotorula nothofagi*), *Leucosporidium* (*L. scottii* and *L. fragarium*), *Cystofilobasidium infirmominiatum*, *Erythrobasidium yunnanense*, *Filobasidium magnum*, *F. oeirense*, and *Dioszegia hungarica* were also well-represented (Supplementary Fig. S15 and *Annexe 9*). In the phyllosphere, a large proportion of the taxa that were significantly more abundant in plots with low downy mildew susceptibility were basidiomycete yeasts, such as *Erythrobasidium yunnanense*, *Tausonia pullulans*, *Cystofilobasidium infirmominiatum*, *C. capitatum*, *Rhodotorula nothofagi*, *Vishniacozyma tephrensis*, *Buckleyzyma aurantiaca*, *Itersonilia perplexans*, *Filobasidium magnum*, *F. wieringae*, and *F. oeirense* (Fig. 5). *Buckleyzyma aurantiaca* and *Sphaerulina amelanchier* were consistently associated with low downy mildew susceptibility across all five DAA methods (Fig. 5). Conversely, some fungal ASVs were significantly more abundant in high-susceptibility plots, such as the grapevine foliar pathogen *Botrytis cinerea*, which was more abundant in both the topsoil and phyllosphere (*Annexe 9*).

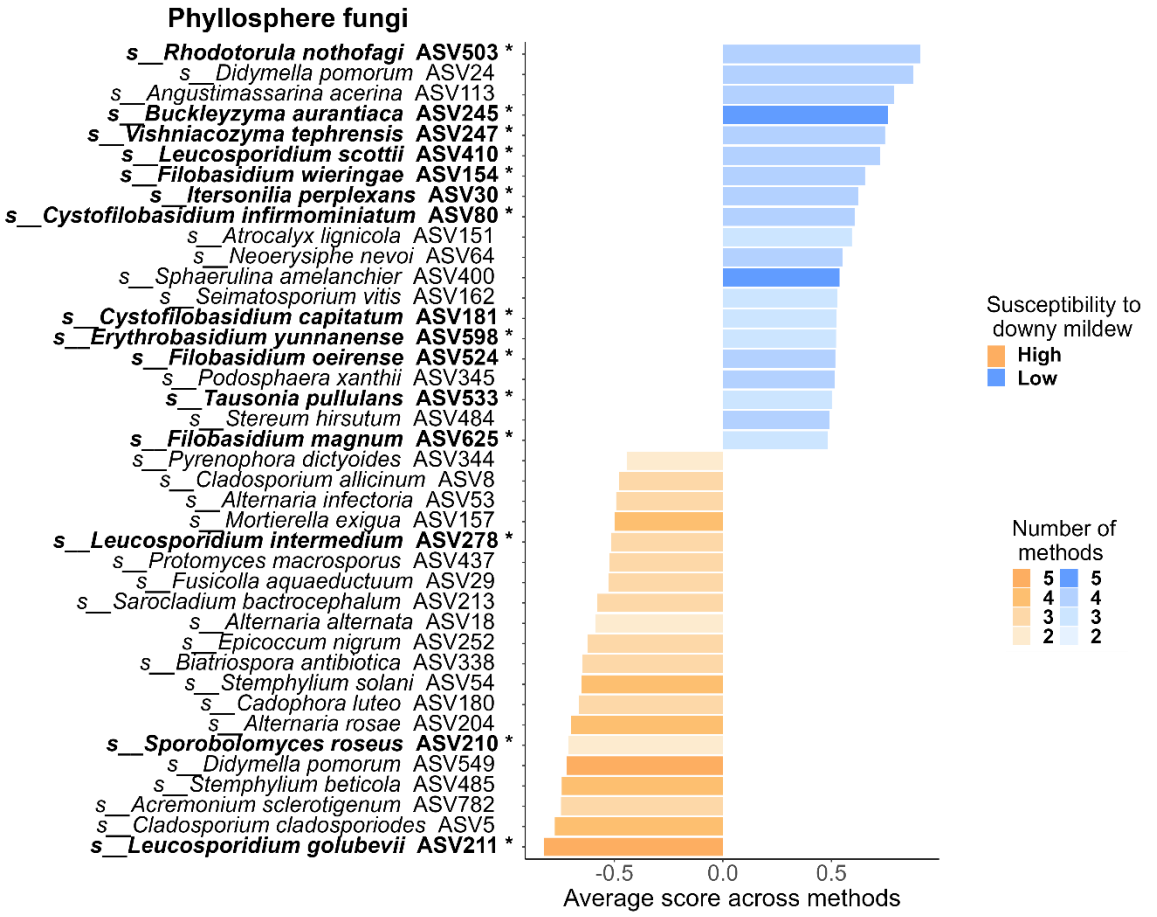


Figure 5: Phyllosphere fungal taxa that vary in abundance with susceptibility to downy mildew.
For each condition (high vs. low susceptibility), we represented the 20 Amplicon Sequence Variants (ASVs) that were significantly associated with the condition according to at least two methods and that had the highest average association scores. The five methods used to identify these ASVs were ANCOM-BC2 (Lin & Peddada, 2024), Maaslin2 (Mallick *et al.*, 2021), LinDA (Zhou *et al.*, 2022), ZicoSeq (Yang & Chen, 2022) and Random Forest Classification (Cambon *et al.*, 2023). The results are based on data collected in 2022. ASVs belonging to Basidiomycete yeasts are highlighted in bold and marked with an asterisk (*).

The most represented bacterial genera among the ASVs that could be assigned to species level were *Pseudarthrobacter*, including *P. equi* (represented by 2 different *ASVs*), *P. oxydans*, and *P. sulfonivorans*; *Pseudomonas*, such as *P. graminis* and *P. viridiflava*; *Streptomyces*, which includes *S. albidoflavus*, *S. ambofaciens*, *S. hygroscopicus*, and *S. xinghaiensis*; *Massilia*, encompassing *M. violaceinigra*, *M. putida*, and *M. aurea*; *Bacillus*, comprising *B. nealsonii*, *B. litoralis*, *B. megaterium*, and *B. thermolactis*; and *Sphingomonas*, featuring *S. astaxanthinifaciens*, *S. aurantiaca*, and *S. sediminicola* (represented by 2 different *ASVs*) (Fig. 6 and *Annexe 9*). In addition, five ASVs of *Arthrobacter globiformis* were also found to be significant (Fig. 6 and *Annexe 9*). In the phyllosphere, two bacterial ASVs were more abundant in low-susceptibility plots by at least two methods and could be assigned to species level: *Arthrobacter pascens* and *Corynebacterium stationis* (Supplementary Fig. S16).

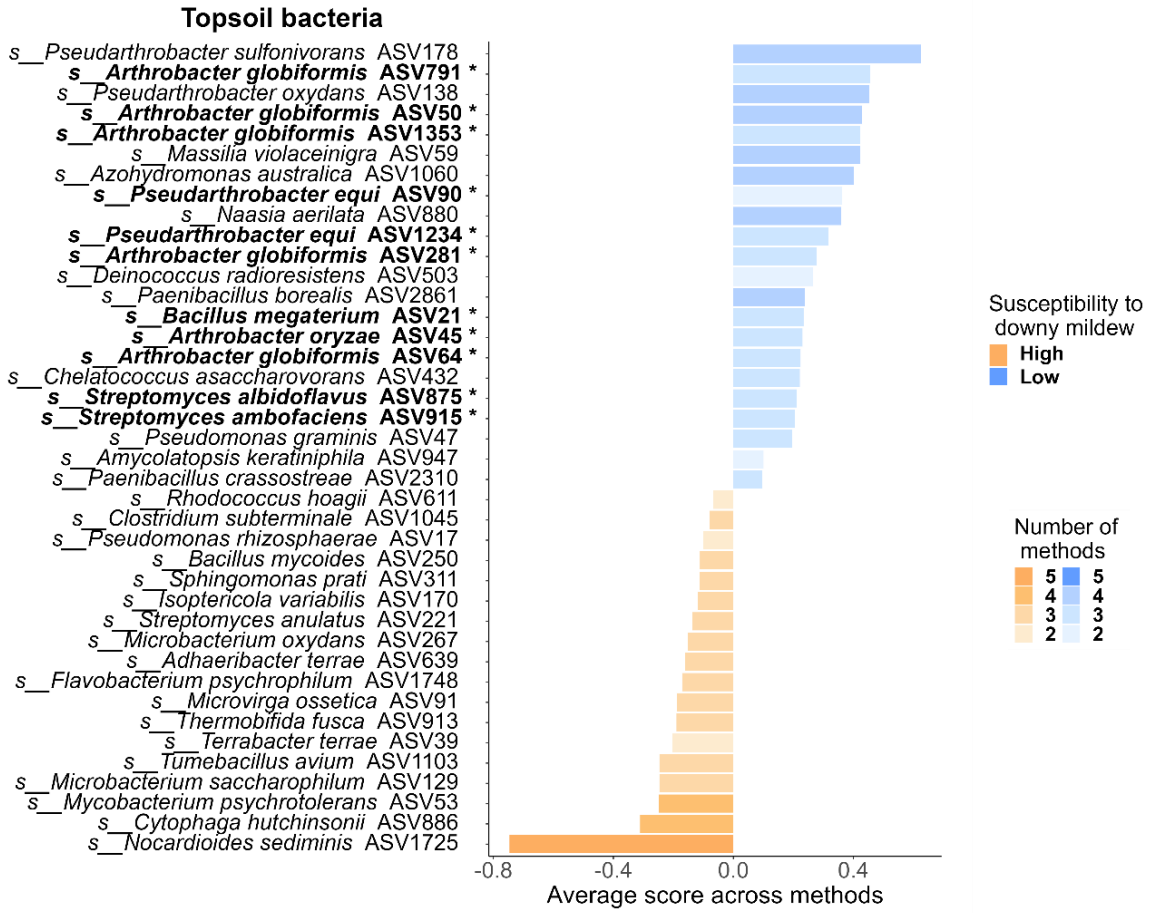


Figure 6: Topsoil bacterial taxa that vary in abundance with susceptibility to downy mildew.
For each condition (high vs. low susceptibility), we represented the 20 Amplicon Sequence Variants (ASVs) that were significantly associated with the condition according to at least two methods and that had the highest average association scores. The five methods used to identify these ASVs were ANCOM-BC2 (Lin & Peddada, 2024), Maaslin2 (Mallick *et al.*, 2021), LinDA (Zhou *et al.*, 2022), ZicoSeq (Yang & Chen, 2022) and Random Forest Classification (Cambon *et al.*, 2023). The results are based on data collected in 2022. ASVs highlighted in bold and marked with an asterisk (*) also scored highest in the TITAN (Baker *et al.*, 2023a) analysis.

Similar analyses were performed with the 2023 dataset, which was smaller than the 2022 dataset because 4 samples per plot were collected in 2023, whereas 16 samples per plot were collected in 2022. Using this smaller dataset, we identified 75 fungal and 374 bacterial ASVs that were significantly more abundant in plots with low downy mildew susceptibility (*Annexe 9*). Most of the differentially abundant ASVs were found in the topsoil (73 fungal ASVs and 373 bacterial ASVs). More than half of these ASVs (40 fungal ASVs and 227 bacterial ASVs) were also found to be differentially abundant in the 2022 dataset, indicating some reproducibility of the results across years. In addition, four differentially abundant ASVs (2 fungal ASVs and 2 bacterial ASVs) were detected in the phyllosphere in the 2023 dataset, one of which (*Pseudopeziza medicaginis* ASV720) had already been identified as differentially abundant in the 2022 dataset (*Annexe 9*).

Areas with low amounts of downy mildew primary inoculum in the topsoil harbor a greater abundance of specific microbial taxa

Consistent with hypothesis (ii), our analyses of the 2022 data identified 205 fungal ASVs and 518 bacterial ASVs whose relative abundances changed significantly with *P. viticola* DNA concentration in the topsoil (*Annexe 10*). Among them, 94 fungal ASVs (57 in the topsoil, 37 in the phyllosphere, and 7 in the endosphere) and 387 bacterial ASVs (196 in the topsoil, 272 in the phyllosphere, and none in the endosphere) were indicators of low DNA concentrations of *P. viticola* (*Annexe 10*). More than half of these indicators of low amounts of *P. viticola* primary inoculum in the topsoil were identified as more abundant in plots classified as low downy mildew susceptible based on symptoms observed on leaves and bunches (*Annexe 9 - 10*). Among the fungal ASVs most strongly associated with low levels of *P. viticola* primary inoculum, we detected *Trichoderma hamatum, Rhodotorula babjevae* in the topsoil, *Bullera alba, Aureobasidium pullulans, Cystofilobasidium infirmominiatum, Cystofilobasidium macerans* in the phyllosphere, and *Vishniacozyma dimennae* in the endosphere (Supplementary Tab. S8 and *Annexe 10*). The most represented bacterial genera among the ASVs that could be assigned to the species level were *Bacillus*, *Sphingomonas*, *Pseudarthrobacter*, *Pseudomonas*, *Methylobacterium*, and *Streptomyces* (*Annexe 10*). *Streptomyces albidoflavus*, *S. ambofaciens*, *S. oralis*, *Bacillus megaterium*, *Arthrobacter globiformis* and *Pseudarthrobacter equi* were the most abundant in topsoil and phyllosphere (Tab. 4).

Table 4: Bacterial taxa indicators of low downy mildew primary inoculum in topsoil.
These ten bacterial ASVs increase significantly in abundance as the concentration of *P. viticola* DNA in the topsoil decreases, according to the Threshold Indicator Taxa Analysis (TITAN) method (Baker *et al.*, 2023a), and they have the highest z scores. These results are based on the 2022 topsoil data. Relative abundance (%) indicates the proportion of sequences assigned to the taxa relative to the total number of sequences in the dataset. Prevalence (%) indicates the percentage of samples where the taxa are present with at least one sequence. ASVs highlighted in bold also scored highest in the Differential Abundance Analysis.

Bacterial ASV	TITAN z score	Relative abundance (%)	Prevalence (%)
Exiguobacterium sibiricum ASV169	7.08	0.01	26.88
***Streptomyces ambofaciens* ASV915**	6.73	0.02	69.38
***Bacillus megaterium* ASV21**	6.72	1.23	92.50
***Streptomyces albidoflavus* ASV875**	6.05	0.02	66.25
***Arthrobacter globiformis* ASV281**	5.69	0.16	80.63
***Arthrobacter globiformis* ASV64**	5.57	0.62	81.88
***Pseudarthrobacter equi* ASV1234**	5.29	0.02	50.63
***Arthrobacter globiformis* ASV791**	5.19	0.07	10.00
***Arthrobacter globiformis* ASV1353**	5.11	0.03	10.00
***Arthrobacter oryzae* ASV45**	4.97	0.89	91.88

Vineyard susceptibility to downy mildew can be predicted from microbiota composition, with soil fungal communities being the best predictor

According to hypothesis (iii), downy mildew susceptibility could be predicted from microbiota data. The RF algorithm trained with topsoil samples collected in 2022 successfully predicted downy mildew susceptibility for other topsoil samples collected in the same year. The lowest error rate was 15% ± 0.10%. This was achieved using a data subset that included abundant fungal taxa aggregated to the species level (Fig. 7). The optimal mean mtry value was 35, indicating that a set of 35 topsoil fungal species best predicted downy mildew susceptibility. The lowest error rates for the phyllosphere and leaf endosphere samples were much higher (34% ± 0.12 and 52% ± 19, respectively) than those for the topsoil samples (Supplementary Fig. S17). Therefore, contrary to hypothesis (iv), the topsoil microbiota was a better predictor of leaf symptoms than the leaf microbiota was.

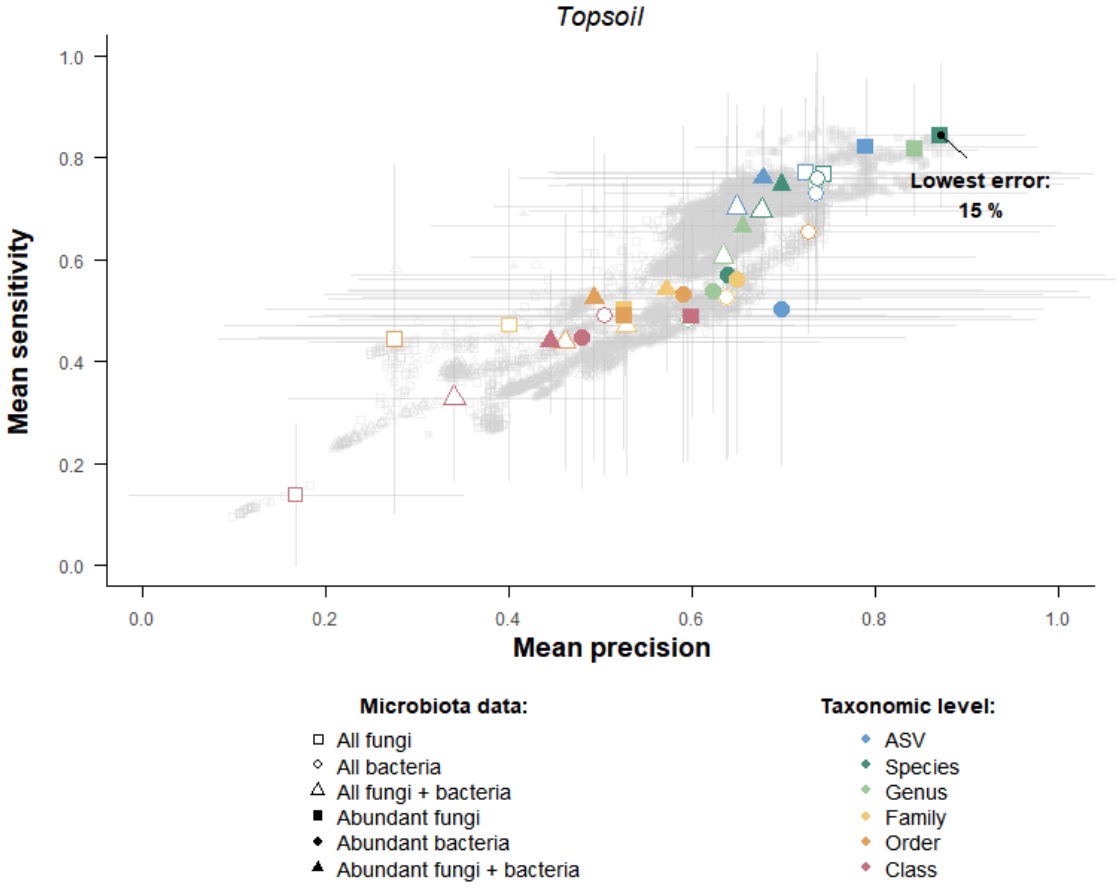


Figure 7: Random Forest algorithm performance in predicting grapevine susceptibility to downy mildew using topsoil microbiota composition.
Each dot represents the mean sensitivity and precision obtained for a given subset of the topsoil microbiota data collected in 2022. The subsets differ in their composition (all fungi, all bacteria, all taxa or only abundant ones) and their level of taxonomic aggregation (from no aggregation of the ASVs to aggregation to the class level). The colored dots are those obtained with the optimal mtry value (i.e., the value that predicts low susceptibility to downy mildew with the lowest error rate). The bars represent the standard deviation over the various iterations of the cross-validation step. The lowest error rate is indicated as a percentage. The analysis and figure use the scripts developed by Cambon et al. (Cambon *et al.*, 2023).

In addition, our analyses revealed that the topsoil fungal community can predict symptoms in the following year. The RF algorithm trained on topsoil samples from 2022 successfully predicted the susceptibility for topsoil samples collected in 2023. The lowest error rate was 6% +/- 12, achieved using abundant fungal taxa aggregated to the genus level, and the mean mtry value was 12 (Supplementary Fig. S18). In comparison, phyllosphere and leaf endosphere microbial communities were poorer predictors, with the lowest error rates of 0.35% +/- 15 and 41% +/- 0.17, respectively. (Supplementary Fig. S19).

Similarly, analysis of the smaller dataset collected in 2023 revealed 27 fungal ASVs (22 in the topsoil, 5 in the phyllosphere and none in the endosphere) and 68 bacterial ASVs (57 in the topsoil, 12 in the phyllosphere and none in the endosphere) that were indicators of low *P. viticola* DNA concentrations in the topsoil (*Annexe 10*). Among these, 9 fungal ASVs and 26 bacterial ASVs were also identified as indicators using the data from 2022 (*Annexe 10*).

Discussion

To our knowledge, this study is the first to demonstrate a relationship between disease epidemiology and the host microbiome in a plant pathosystem. To elucidate the interactions between plant diseases and the microbiome, studies typically compare the microbiomes of symptomatic and asymptomatic tissue samples (Faist *et al.*, 2016; Kovalchuk *et al.*, 2018; Mina *et al.*, 2020; Huang *et al.*, 2022; Barroso-Bergadà *et al.*, 2023b). The originality of our study lies in the fact that we analyzed the microbiome of healthy plants only. These plants were selected from plots with contrasting susceptibility to the disease, according to long-term epidemiological data. We analyzed the microbiome of young, asymptomatic leaves to test the hypothesis that the microbiome that develops before the pathogen spreads to the leaves can influence or indicate the likelihood of disease development.

Our experimental design was specifically designed to avoid potential confounding effects that may obscure the relationships between disease epidemiology and the plant microbiome (Fournier *et al.*, 2022b). To achieve this goal, we selected pairs of plots with contrasting disease susceptibility over the years but otherwise as similar as possible (planted with the same variety, managed with the same practices, and geographically close to each other). We also repeated the sampling over two consecutive years to ensure robust results. Finally, we improved the taxonomic assignment of microbial taxa by sequencing a subset of the samples using long-read technology and by sequencing a collection of cultivable microorganisms isolated from the biological material of the study (Taberlet *et al.*, 2018). Using this approach, we were able to improve the taxonomic assignments for 11% of the fungal ASVs and 10% of the bacterial ASVs. Obtaining the most accurate taxonomic assignments was critical because the interpretation of our analyses, which aim to identify candidates for disease biocontrol, largely depends on our ability to assign DNA sequences to specific species.

Using microbiome data as a predictor of disease susceptibility

Recent research in human health indicates that microbiome data can improve the accuracy of disease risk screening and predict dietary and lifestyle changes that are likely to slow disease progression in individuals (Ferreiro *et al.*, 2023; Ratiner *et al.*, 2024). Such predictive approaches, which are based on microbiome data collected at the individual level, are still in their infancy in terms of plant health. Our study explored the potential of the plant microbiome for precision agriculture (French *et al.*, 2021) by attempting to predict plot susceptibility to a major disease (grapevine downy mildew caused by *P. viticola*) based on topsoil and leaf microbiomes. Advances in human health and our promising results highlight the potential of using microorganisms to predict health, whether in humans or plants.

In the present study, we showed that the topsoil microbiome in vineyards is an accurate predictor of downy mildew susceptibility, with an error rate of 15% for within-year predictions and 6% for between-year predictions. Surprisingly, the best predictions of downy mildew susceptibility, defined based on symptoms observed on aerial organs (leaves and grapes), were obtained using topsoil fungal abundance as a predictor. Foliar communities (in the endosphere and phyllosphere) were poorer predictors of downy mildew susceptibility, with error rates exceeding 30%. These results may be explained by the fact that the soil is the reservoir of microorganisms that colonize the aerial organs of grapevines (Zarraonaindia *et al.*, 2015a; Swift *et al.*, 2021). In this study, we sampled the vineyard microbiota early in the growing season. At this time of year, the topsoil contained both the microorganisms that can inhibit the germination of downy mildew oospores and the microorganisms that can subsequently spread to grapevine leaves and inhibit infection by zoospores. With another sampling strategy, the leaf microbiota might have been a better predictor. For instance, collecting leaf microbiota samples at different times throughout the season could have enhanced the predictive power of leaf microbiota data, since the microbiota has a strong dynamics over the season (Fan *et al.*, 2020; Liu & Howell, 2021; Wicaksono *et al.*, 2023). Performing predictions at the individual plant level might also increase the predictive power of the leaf microbiota. Indeed, a dysbiotic state of the microbiota, characterized at the individual level by a temporary loss of the plant's ability to regulate its microbiota (Bettenfeld *et al.*, 2021; Arnault *et al.*, 2023), is considered as the proximate cause of disease.

The greater richness of the soil microbiota than that of the leaf microbiota may also account for its higher predictive power. This greater richness increases the number of variables (*i.e.*, ASVs) that can be used as predictors. The greater richness of the soil microbiota than the leaf microbiota is a biological reality that has been demonstrated in many other studies of plant microbiota (Zarraonaindia *et al.*, 2015a; Dong *et al.*, 2019; Sun *et al.*, 2021a; Liu & Howell, 2021; Bettenfeld *et al.*, 2021). Moreover, this difference in microbiota richness between soil and leaves could be exacerbated by molecular biology protocols. In our study, obtaining high-quality DNA in sufficient amounts was more challenging for leaves than for soil. We had less biological material from the phyllosphere, from which we extracted microbial DNA from microbial pellets, than from soil (100 mg lyophilized soil). Moreover, grapevine leaves have a

high content of secondary metabolites, such as polysaccharides, polyphenols and tannins, which not only bind to nucleic acids during extraction, leading to their loss but also act as PCR inhibitors, making it a challenging microbial habitat for characterization (Lodhi *et al.*, 1994; Hanania *et al.*, 2004; Lo Piccolo *et al.*, 2012). In the case of the leaf endosphere, the DNA extracts likely contain more grapevine DNA than microbial DNA does, making amplification of target microbial DNA less effective and leaving room for amplification of nontarget, contaminating sequences. This problem is particularly true for bacteria because we used degenerate primers to avoid chloroplast amplification of the 16S rRNA gene, which results in less effective amplification (Cambon *et al.*, 2023). These methodological issues may explain why the topsoil microbiota was a better predictor than the leaf microbiota was and why fungi were better predictors than bacteria were. These results parallel those of Cambon et al. (Cambon *et al.*, 2023), who used the same random forest algorithms (*microranger* R package) to assess the predictive power of the microbiota of several tree species. These authors reported that prediction error rates were inversely correlated with sequencing depth and emphasized that high-quality sequencing data are crucial for accurate microbiota-based predictions (Cambon *et al.*, 2023).

Relationship between microbiome diversity and disease susceptibility

Increasing microbial diversity is generally considered beneficial for the health of organisms and ecosystems (Berg *et al.*, 2017; Saleem *et al.*, 2019). Loss of microbial diversity is typically considered a marker of deteriorating health, as it may lead to loss of microbial functions and disruption of microbial interaction networks (Berg *et al.*, 2017). However, contrary to these expectations, we did not find a strong relationship between microbial diversity and susceptibility of grapevines to downy mildew. Only the leaf fungal communities sampled in 2022 had higher diversity in plots with low downy mildew susceptibility, which is consistent with the Biodiversity-Ecosystem Functioning (BEF) theory (Hillebrand & Matthiessen, 2009). However, these results did not extend to the leaf bacterial communities, nor to the soil fungal and bacterial communities. Furthermore, they could not be replicated in 2023, suggesting that microbiome diversity alone may not be a critical factor in susceptibility.

Microbial consortia that may interfere with the pathogen asexual stage

Plant pathogens often have complex life cycles that span multiple microbial habitats (Agrios, 2005). In the case of grapevine downy mildew, the asexual stage of the life cycle occurs in green organs during the growing season (Gessler *et al.*, 2011; Castrillo-Sequeira *et al.*, 2023). During this period, *P. viticola* can interact with microorganisms inhabiting both the phyllosphere and the leaf endosphere. In the present study, we show that interactions with phyllosphere microorganisms, especially basidiomycete yeasts, are more likely than interactions with endophytes. Twenty species of epiphytic basidiomycete yeasts were associated with low susceptibility to downy mildew or low levels of primary pathogen inoculum. They belong to several genera, including *Buckleyzyma*, *Bullera*, *Cystofilobasidium*, *Dioszegia*, *Erythrobasidium*, *Filobasidium*, *Itersonilia*, *Leucosporidum*, *Naganishia*, *Papiliotrema*, *Rhodotorula*, *Tausonia*, and *Vishniacozyma*. The biocontrol activity of

basidiomycete yeasts is well documented, as several species are already used as biocontrol agents (BCAs) against postharvest diseases (Liu *et al.*, 2013; Spadaro & Droby, 2016; Freimoser *et al.*, 2019). These yeasts regulate plant pathogens through various mechanisms, including competition for nutrients and space, secretion of toxins, enzymes, and volatile organic compounds (VOCs), parasitism, and indirect mechanisms, such as resistance induction (Liu *et al.*, 2013; Spadaro & Droby, 2016; Freimoser *et al.*, 2019). These mechanisms could be effective in controlling foliar diseases, including downy mildew.

The yeast species *Buckleyzyma aurantiaca* (previously classified as *Rhodotorula aurantiaca*) is particularly promising, as its higher abundance in low-susceptibility than in high-susceptibility plots was confirmed by all the methods used. Moreover, this yeast species is known to reduce the incidence of blue mold in pears (Chand-Goyal & Spotts, 1996) and the severity of soft rot in peppers (Silva *et al.*, 2014). It has also shown promising results in the control of bacterial fruit blotch in melons (Conceição *et al.*, 2014; de Melo *et al.*, 2015). In addition, regarding grape pathogens *B. aurantiaca,* liquid culture reduced the growth of *Erysiphe necator* by approximately 30% and significantly increased the number of collapsed conidia (Pauvert *et al.*, 2020). However, it had no effect on Botrytis cinerea (Raspor *et al.*, 2010b).

According to our results, other yeast species that may act as a primary line of defense against *P. viticola* in young leaves include *Leucosporidium scottii*, *Filobasidium oeirense*, *Vishniacozyma carnescens*, and *Bullera alba*. The yeast *Leucosporidium scottii* has been identified as a good BCA against apple blue and gray mold caused by *Penicillium expansum* and *B. cinerea*, respectively (Vero *et al.*, 2013). *Filobasidium oeirense* and *Vishniacozyma carnescens* are known to inhibit *B. cinerea* development through VOC production (Tejero *et al.*, 2021). *Bullera alba* has been shown to produce a lethal toxin that inhibits many yeast-like ascomycete and basidiomycete fungi and to have an excellent biocontrol effect on apple gray mold (Golubev *et al.*, 1997; Yu *et al.*, 2024).

Finally, we found that the ubiquitous ascomycete yeast *Aureobasidium pullulans* is more abundant in vineyard plots with low susceptibility to downy mildew. The biocontrol activity of this yeast species is well known. In France, it is commercialized in products such as BOTECTOR®, CINERKIL, AUREO SHIELD, and Blossom Protect™. The presence of yeast consortia early in the season in the phyllosphere of low-susceptibility plots seems to be a good indicator of plot downy mildew susceptibility.

Microbial consortia that may interfere with the pathogen sexual stage

In contrast to the asexual stage, the sexual stage of the downy mildew life cycle occurs primarily in the soil during fall and winter (Gessler *et al.*, 2011; Castrillo-Sequeira *et al.*, 2023). *P. viticola* overwinters as oospores in the topsoil, where it can interact with the multitude of microorganisms present in this biodiversity reservoir. These belowground interactions have been largely overlooked, but our results suggest that they exist, as we found several hundred fungal and bacterial ASVs that varied in abundance between plots with high and low downy mildew susceptibility. Among these numerous ASVs, some may directly affect oospore survival

and germination, while others are likely merely indicators of soil conditions unfavorable to oospores (Poeydebat *et al.*, 2024).

In addition, we showed that the amount of *P. viticola* DNA in the topsoil is significantly lower in plots classified as having low downy mildew susceptibility, based on epidemiological records of symptoms on leaves and bunches. This correlation between the amount of oospores in the topsoil and disease symptoms in aerial organs suggests that reducing the amount of primary pathogen inoculum in the soil through prophylaxis or soil microbial management (Carisse, 2016; Poeydebat *et al.*, 2022) may be an effective strategy for controlling disease epidemics. However, soil microbial management needs clear targets to be effective. Our analyses provide some insight into the soil microbial taxa that may be relevant targets.

Our analyses revealed several fungal species that were significantly more abundant in the topsoil of vineyard plots with low susceptibility to downy mildew than in the topsoil of plots with high susceptibility to downy mildew. Among them, five species are known for their biocontrol activity against the asexual stage of downy mildew: *Albifimbria verrucaria* (Vidhate *et al.*, 2015), *Alternaria alternata* (Musetti *et al.*, 2006b, 2007), *Fusarium brachygibbosum* (Ghule & Sawant, 2018; Ghule *et al.*, 2018), and *Epicoccum nigrum* (Kortekamp, 1997). Our analyses do not allow us to determine whether these fungal species detected in topsoil samples interact with downy mildew oospores (sexual stage) in the topsoil or if they first colonize young leaves and then interact with downy mildew zoospores (asexual stage).

In addition, our results revealed that several basidiomycetous yeasts were more abundant in the topsoil of plots with low downy mildew susceptibility. Among them, four species were also more abundant in the phyllosphere of vineyard plots with low downy mildew susceptibility. All four are known for their biocontrol properties against plant pathogens: *Bullera alba* (Golubev *et al.*, 1997; Yu *et al.*, 2024), *Filobasidium oeirense* (Ruiz-Moyano *et al.*, 2020), *Papiliotrema laurentii* (de Almeida *et al.*, 2022; Das *et al.*, 2023), and *Papiliotrema terrestris* (previously classified as *Cryptococcus laurentii*) (Lima *et al.*, 1998; Castoria *et al.*, 2021a). These congruent results between topsoil and young leaves indicate that both microbial habitats are connected by microorganism dispersal at the beginning of the growing season, suggesting that management of the topsoil microbiota may influence the phyllosphere microbiota composition.

Filamentous fungi with known biocontrol properties were also found in higher abundance in the topsoil of vineyard plots with low susceptibility to downy mildew. These included *Bjerkandera adusta* (Chen *et al.*, 2021b), *Issatchenkia orientalis* (Bleve *et al.*, 2006; Chanchaichaovivat *et al.*, 2007; Korres *et al.*, 2011), *Mortierella alpina* (Wani *et al.*, 2016), and two species of *Trichoderma* (*Trichoderma lixii* and *Trichoderma virens*). While the biocontrol properties of *T. lixii* have not been studied, *T. virens* is a well-established biocontrol agent with the ability to produce antibiotics, parasitize pathogenic fungi, and induce systemic resistance in plants (Howell, 2006; Ghazanfar *et al.*, 2018). Strains of *Trichoderma* are widely distributed in soil environments and can parasitize a wide range of plant pathogens, including the downy and powdery mildews of grapevines (Perazzolli *et al.*, 2008, 2011; Sawant, 2014; Ahmed, 2018).

The higher abundance of these bacteria in low-susceptibility than in high-susceptibility plots supports our comparative approach.

Soil bacteria of the genus *Streptomyces* (including *S. albidoflavus*, *S. ambofaciens*, *S. hygroscopicus*, and *S. xinghaiensis*) were also associated with low susceptibility to downy mildew. They stand out as promising candidates for the biocontrol of downy mildew because of their well-documented properties. Streptomyces species have previously been identified as effective biocontrol agents against oomycete pathogens, including grapevine downy mildew, owing to their potent antimicrobial properties (Chen *et al.*, 2016; Liang *et al.*, 2016; Volynchikova & Kim, 2022; Nadalini & Puopolo, 2024). For example, Abdalla et al. (Abdalla *et al.*, 2011) demonstrated that khatmiamycin, a compound isolated from a terrestrial *Streptomyces* species, exhibited inhibitory and lytic activities against the zoospores of *P. viticola*. Similarly, Islam et al. (Islam *et al.*, 2016) reported that extracts from several marine *Streptomyces* strains impaired zoospore motility and caused their lysis. Antimicrobial substances in the fermentation broth of the strain *Streptomyces atratus* PY-1 were also shown to be effective against downy mildew by damaging sporangia and sporangiophores (Liang *et al.*, 2016). Finally, El-Sharkawy et al. (El-Sharkawy *et al.*, 2018) reported that *Streptomyces viridosporus* HH1 and *Streptomyces violaceus* HH5 can reduce the severity of downy mildew in the field. These results suggest that soil-borne microorganisms could prevent the infection of aerial parts by *P. viticola*. During the winter season, the soil could act as a reservoir for protective strains that would colonize the aerial parts of the vines later in the growing season.

Environmental and anthropogenic drivers of microbiota composition

According to our results, the microbial taxa that varied in abundance between the low- and high-susceptibility plots were both rare and abundant. Their relative abundance ranged from approximately 0.00006% to 14% of the total number of sequences. Increasing the abundance of the rare taxa of interest by inoculation of microbial strains or consortia seems possible, but increasing the abundance of taxa that are already quite abundant may be more challenging. In the latter case, microbiota management could rely on changes in vineyard management practices. Our analysis provides some insight into the practices that may have an impact on the resident microbiota.

Our analyses revealed that grape variety had small but significant effects on the microbiota composition. The significant influence of grape variety on the leaf and soil microbiota is consistent with the findings of other studies (Casieri *et al.*, 2009; Mezzasalma *et al.*, 2018; Singh *et al.*, 2018; Zhang *et al.*, 2020; Bettenfeld *et al.*, 2021; Bao *et al.*, 2022; Cui *et al.*, 2024). This result is interesting because genotype can influence resistance to downy mildew (Sargolzaei *et al.*, 2020) and may also affect the recruitment of microorganisms with biocontrol properties that could protect the plant from pathogens.

In addition, our results suggest that reducing the frequency of fungicide treatments and favoring the proximity of the vines to the plot edges could alter the composition of the microbiota and increase microbial diversity. The absence of fungicide application increased

microbial diversity in the soil, as documented in other studies (Setati *et al.*, 2015; Hendgen *et al.*, 2018; Hernandez & Menéndez, 2019). It also increased microbial diversity in the phyllosphere the following spring, probably due to the dispersal of microorganisms from the soil to the leaves. Meanwhile, proximity to the plot edge increased microbial diversity in the topsoil, phyllosphere, and endosphere. These results parallel those of Ricono et al. (Ricono *et al.*, 2022), who reported a decrease in diversity with increasing distance from the edge in the endosphere of wheat roots. These findings suggest that vegetation along plot edges may serve as a microbial reservoir in addition to the soil.

Conclusion and perspectives

We identified bacterial and fungal taxa naturally occurring in vineyard environments that may be promising candidates for the biocontrol of downy mildew. These microorganisms may play a role in disrupting either the sexual or asexual stages of the pathogen, offering potential alternatives to conventional control methods. The results of this study open the door to further research aimed at assessing the efficacy and sustainability of these biocontrol agents under different climatic conditions, soil types and vineyard management practices. A deeper understanding of their mode of action and interactions with the pathogen will be essential for the development of more robust and environmentally friendly integrated management strategies to protect vineyards from downy mildew. Our study also provides insights into vineyard management practices that could help harness vineyard microbiota. In particular, grape variety had a small but significant effect on the microbiota composition. To build on this, we recommend analyzing the microbiota of a wide range of grapevine genotypes and species, including those that are naturally resistant to downy mildew, such as American Vitis species (Fournier *et al.*, 2022a). These studies could help identify additional microbial taxa with biocontrol properties against downy mildew that complement our findings (Brum *et al.*, 2012; Felber *et al.*, 2016; Kernaghan *et al.*, 2017). To date, few studies have focused on the microbiota of American cultivars that are naturally resistant to downy mildew (Brum *et al.*, 2012; Felber *et al.*, 2016; Kernaghan *et al.*, 2017; Fan *et al.*, 2020; Cureau *et al.*, 2021; Wicaksono *et al.*, 2023). More comparisons are needed to identify new biocontrol agents for downy mildew.

Supplementary methods

Methods S1: Amplification trial with the primer pair ITS1catta - ITS2ngs.

To characterize fungal communities interacting with the oomycete *Plasmopara viticola*, we tested the primer pair ITS1catta - ITS2ngs (Tedersoo *et al.*, 2018, 2021) because it targets the internal transcribed spacer 1 (ITS1) region of the nuclear ribosomal DNA (nrDNA) ITS gene of both fungi and oomycetes and was used successfully on grapevine (Behrens & Fischer, 2022a). We confirmed that these primers indeed amplified the nrDNA ITS gene of both fungi and oomycete by performing PCR on the DNA of two fungal strains (*Debaromyces hansenii* and *Wallemia sebi*) and a strain of *P. viticola*. However, when applied to endosphere samples, the primer pair lacked specificity. We observed variable PCR profiles between endosphere samples on agarose gels, with the number of bands ranging from 1 to 4 and the intensity of the bands varying among samples. Sequencing of a few PCR products obtained using the ITS1catta - ITS2ngs primer pair confirmed the amplification of nontarget sequences (Fig. S3). Although the ITS1catta - ITS2ngs primer pair successfully amplified both fungi and oomycetes (represented by 5 ASVs; Fig. S4), a significant portion of the sequences was also attributed to other groups, including Alveolata, Metazoa, Rhizaria, and Viridiplantae (Fig. S3). In contrast, the ITS1F-ITS2 primer pair was highly specific to the fungal nrDNA ITS gene, with 100% of the sequences belonging to fungi (Fig. S3). These findings parallel those obtained by Savian et al. (Savian *et al.*, 2022). Using the ITS1catta - ITS4ngs primer pair, they reported that some samples presented a large band (750 bp) on agarose gels, probably due to amplification of plant-derived DNA. Therefore, we chose the ITS1F–ITS2 primer pair for our study. This primer pair allowed us to explore a greater range of fungal diversity than the ITS1catta-ITS2ngs primer. In our trial, the ITS1F-ITS2 dataset consisted of 110 fungal ASVs, while the ITS1catta-ITS2ngs dataset included only 74 ASVs.

Methods S2: Custom reference database built from a microbial culture collection.

Building a custom reference database is recommended for assigning metabarcoding sequence data since including species from the regional species pool increases the reliability of taxonomic assignments (Taberlet *et al.*, 2018). Therefore, we isolated cultivable fungal and bacterial strains from grapevine leaves collected from two pairs of plots (ME1 and ME2; Table 1) using four culture media. Leaves were collected from the center (CEN) of each plot on the same day as the leaves collected for the present study. We obtained 1008 isolates (462 bacteria, 547 fungi), which were identified by Sanger sequencing of the 16S region for bacteria using the 8f (Schütte *et al.*, 2008) and 1115r (Reysenbach & Pace, 1995) primer pair, and the nrDNA ITS gene for fungi using the ITS1F–ITS4 primer pair (White, 1990; Gardes & Bruns, 1993). Taxonomic assignments of the Sanger sequences were made using the BLASTn+ algorithm (Camacho *et al.*, 2009), with the NCBI standard database used as a reference. In the case of fungi, our final custom reference database consisted of the Sanger sequences of cultivable microorganisms. For bacteria, we extended the Sanger database by adding the 16S longreads obtained using PacBio technology and assigned using BLASTn+ and RDPClassifier against SILVA 138.1 (Quast *et al.*, 2013).

Methods S3: Taxonomic assignments using both public and custom reference databases.

We used three methods to assign the metabarcoding sequence data. For bacteria, we used (1) the BLASTn+ algorithm (Camacho *et al.*, 2009) with SILVA 138.1 (Quast *et al.*, 2013) as the reference database; (2) the BLASTn+ algorithm with our custom reference database; and (3) the RDPClassifier algorithm (Wang *et al.*, 2007) with SILVA 138.1 as the reference database. The same approach was used for fungi, except that UNITE Fungi 8.3 (Nilsson *et al.*, 2019b) was used as the public reference database.

To choose between the different taxonomic assignments available for a given ASV, we built decision trees (Fig. S5). We considered that assignments obtained using BLASTn+ were more reliable than those obtained using RDPClassifier (Escudié *et al.*, 2018). If an ASV was successfully assigned to the species level using BLASTn+ (*i.e.,* e-value <= e-20, percentage identity >=97% for fungi and >=99% for bacteria, query coverage >=90%) (Tedersoo *et al.*, 2014; Sabat *et al.*, 2017; Nilsson *et al.*, 2019b; F. Escapa *et al.*, 2020), with both the public database and our custom database, we compared the e-values obtained with both databases. The ASV was assigned according to which database provided the best score (lowest e value). If an ASV was successfully assigned to the species level using BLASTn+ with only one database, it was assigned using this database. If an ASV could not be assigned using BLASTn+, the RDPClassifier assignment was considered. The ASV was assigned to the lowest taxonomic level with a confidence score >= 0.8 (Sommermann *et al.*, 2018; Anslan *et al.*, 2018). ASVs with a confidence score < 0.8 at the phylum level were discarded (Brandt *et al.*, 2021). Finally, we discarded the ASVs assigned to the archaea, cyanobacteria, chloroplast and mitochondria.

Supplementary figures

Figure S1: Map of vineyard plots monitored for downy mildew symptoms.
Each blue dot represents a vineyard plot including a set of untreated control vines (UCs). Symptoms of downy mildew are monitored in each UC by the *Institut Français de la Vigne et du Vin* (IFV). These epidemiological records were used to select pairs of vineyard plots for the present study.

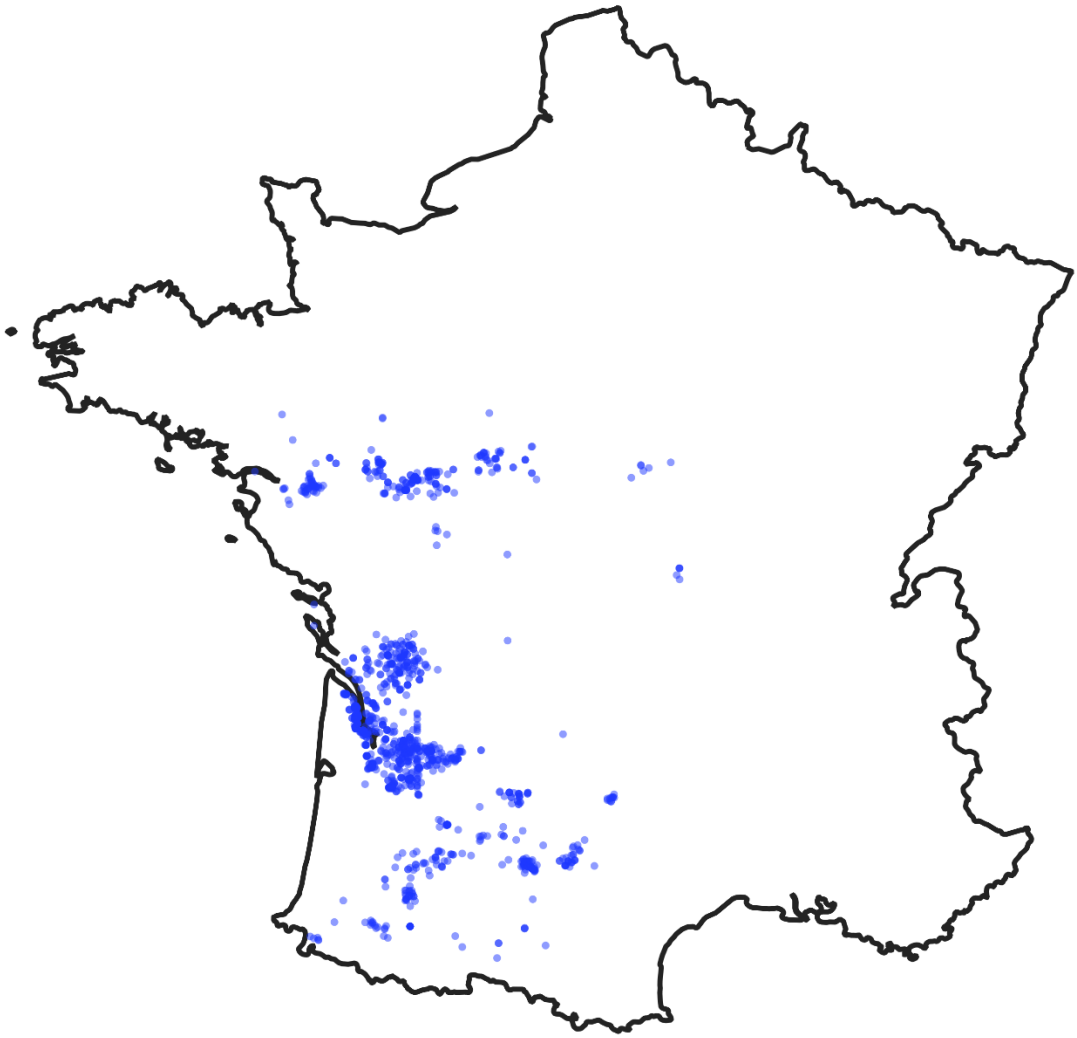


Figure S2: Sampling design.

In each sampling area, we selected four adjacent vines in the same row, typically between two stakes and representative of the age and condition of the plot. Six leaves distributed across the entire plant were collected and pooled into a single composite sample. For the soil, three 20 × 20 cm quadrats were defined at a distance of 20 cm from the trunk of each vine. Two quadrats were directly under the row of vines, and one was in the interrow space. The top 5 cm of soil from each quadrat was collected, mixed and placed into a bag to form a composite sample.

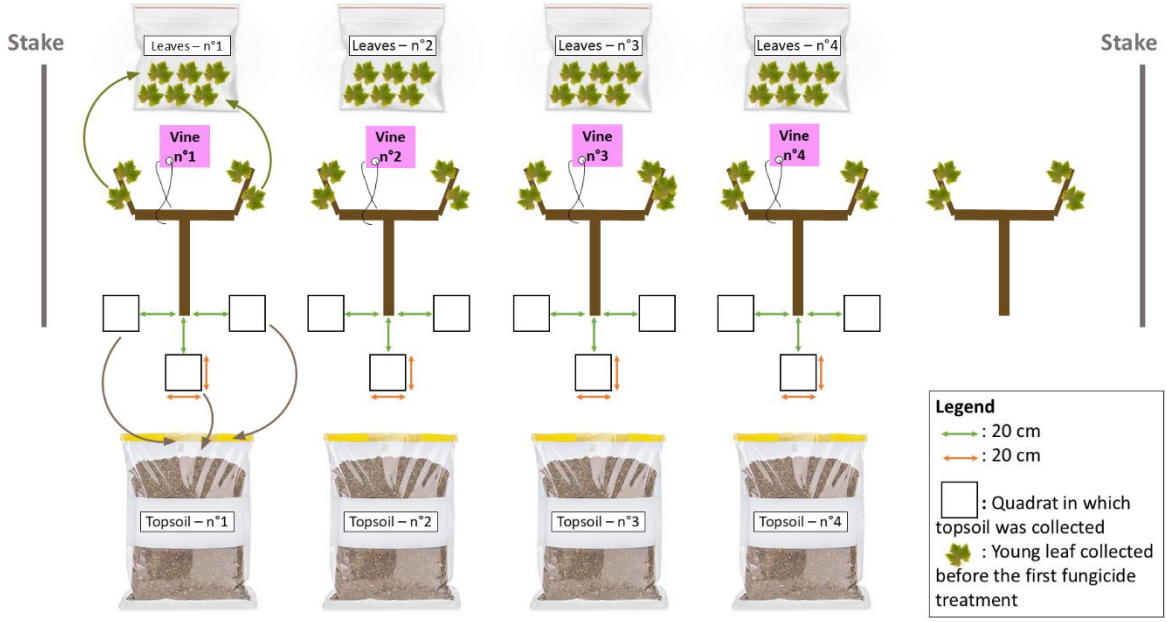


Figure S3: Comparison of microbial community profiles for the leaf endosphere depending on the primer pair.

Six endosphere samples amplified with both the ITS1catta-ITS2ngs primer pair and the ITS1F-ITS2 primer pair were sequenced. These six samples were selected because they had different amplification profiles on agarose gels with the ITS1catta-ITS2ngs primer pair (number of bands ranging from 1 to 4, contrasting intensity of bands among samples). The bar plot represents the proportion of sequences assigned to each domain (A) and phylum (B) in each sample. For fungi, phyla representing less than 1% of sequences were grouped into the 'other' category. To ensure a fair comparison between the two primer pairs, some modifications were made to the bioinformatic pipeline described in the main text. Specifically, the ITSx step, which extracts the highly variable ITS1 and ITS2 subregions, was omitted, and taxonomic assignments were performed using UNITE Eukaryote 8.3 as the public reference database.

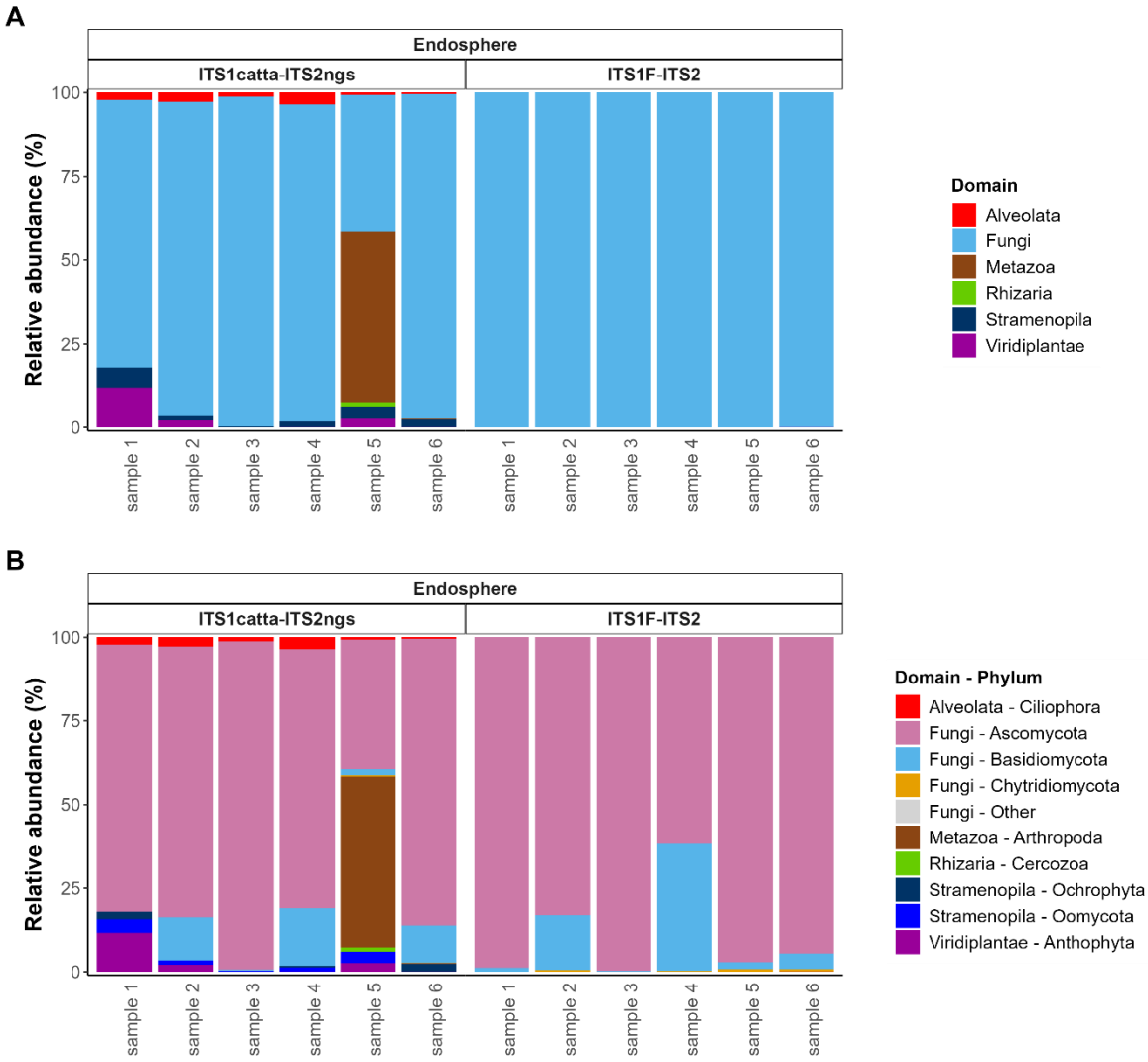


Figure S4: Oomycetes detected in the leaf endosphere using the ITS1catta-ITS2ngs primer pair.
The figure shows the relative abundance of oomycetes among the six endosphere samples that were sequenced with the ITS1catta-ITS2ngs primer pair. Five ASVs assigned to the OOmycota phylum were detected. The bar plot represents their relative abundance. Note that the ASV (ASV28) assigned to Saprolegnia maragheica was also found in sample 3, with a relative abundance of 0.0007%, which is not visible in the figure.

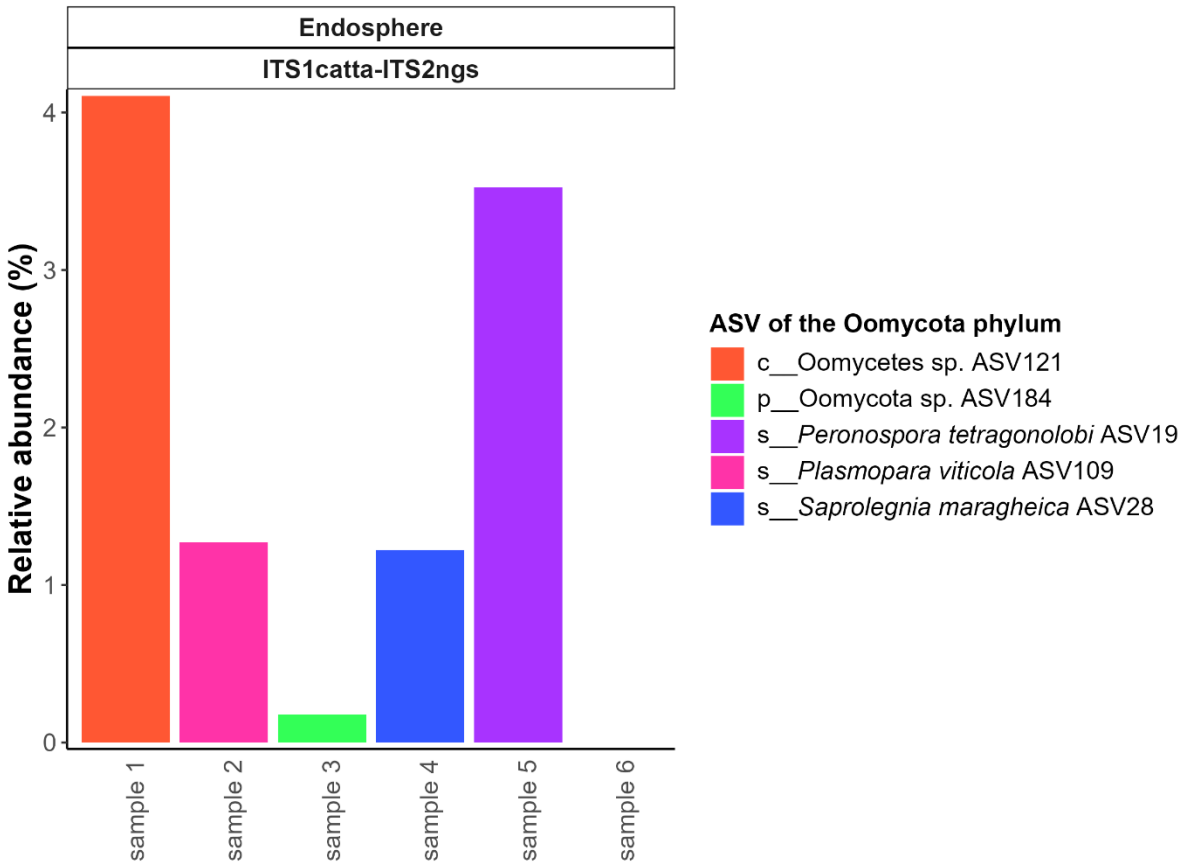
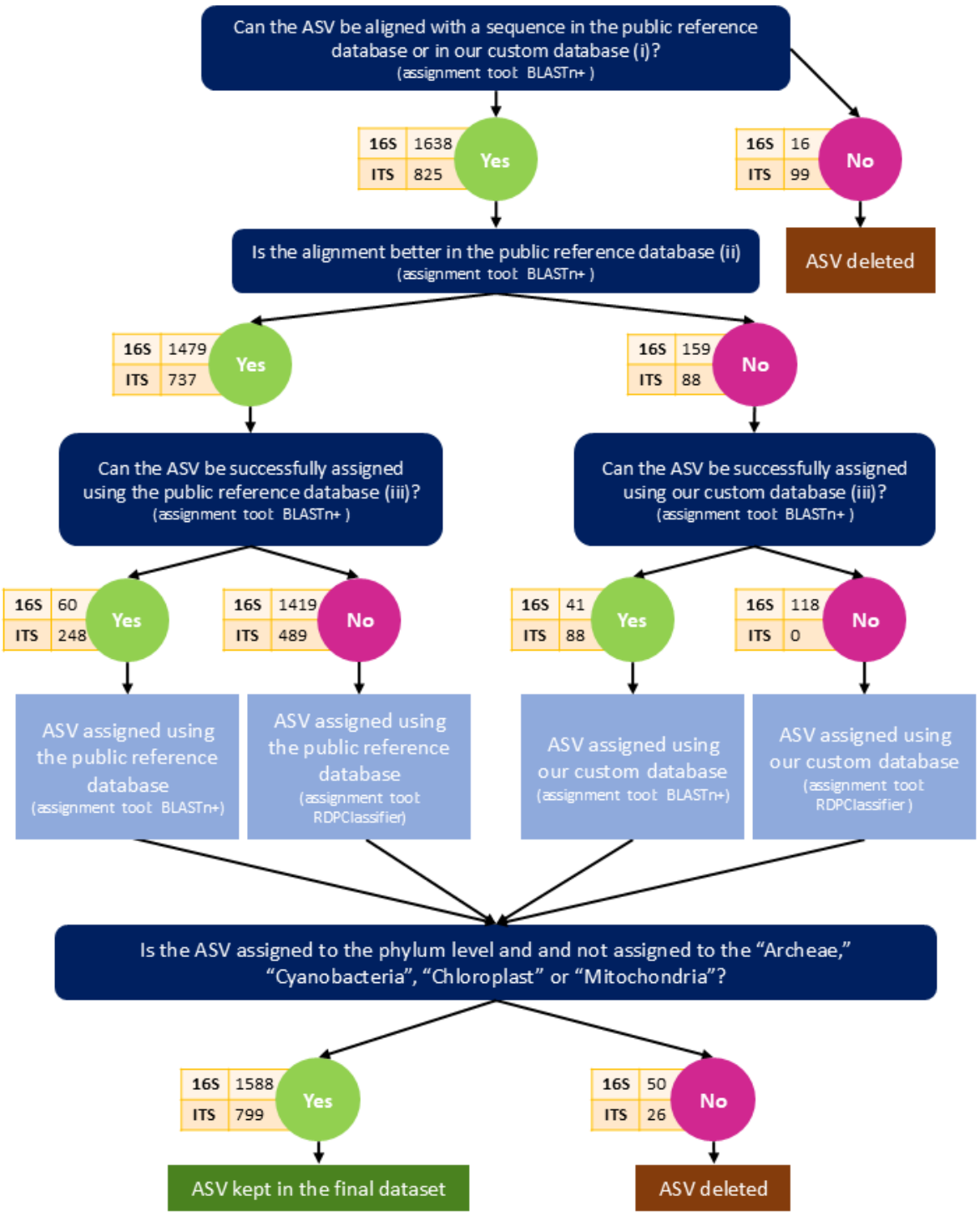


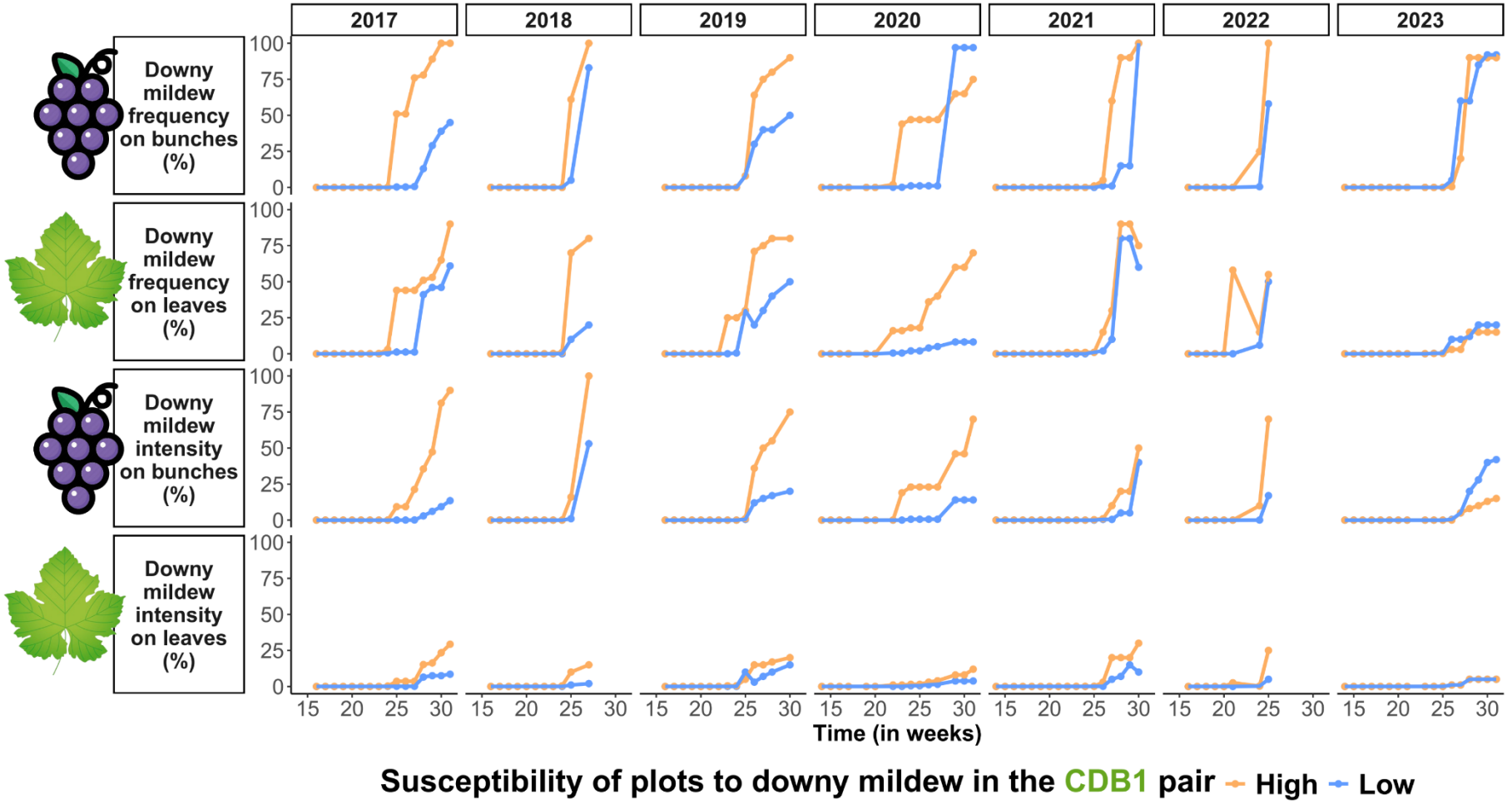
Figure S5: Decision tree for assigning fungal (nrDNA ITS gene) and bacterial (16S rRNA gene) sequences. Each ASV was assigned using a combination of two tools (BLASTn+ and the RDPClassifier algorithm) and two databases (a public reference database and a custom database) (Supplementary Methods S2 and S3). The decision tree describes the questions that allowed us to choose the most reliable taxonomic assignment. The tables indicate the number of ASVs corresponding to each response (yes or no). The final dataset is the whole dataset, corresponding to the microbial habitats (topsoil, phyllosphere and leaf endosphere) and the two sampling campaigns (2022 and 2023).

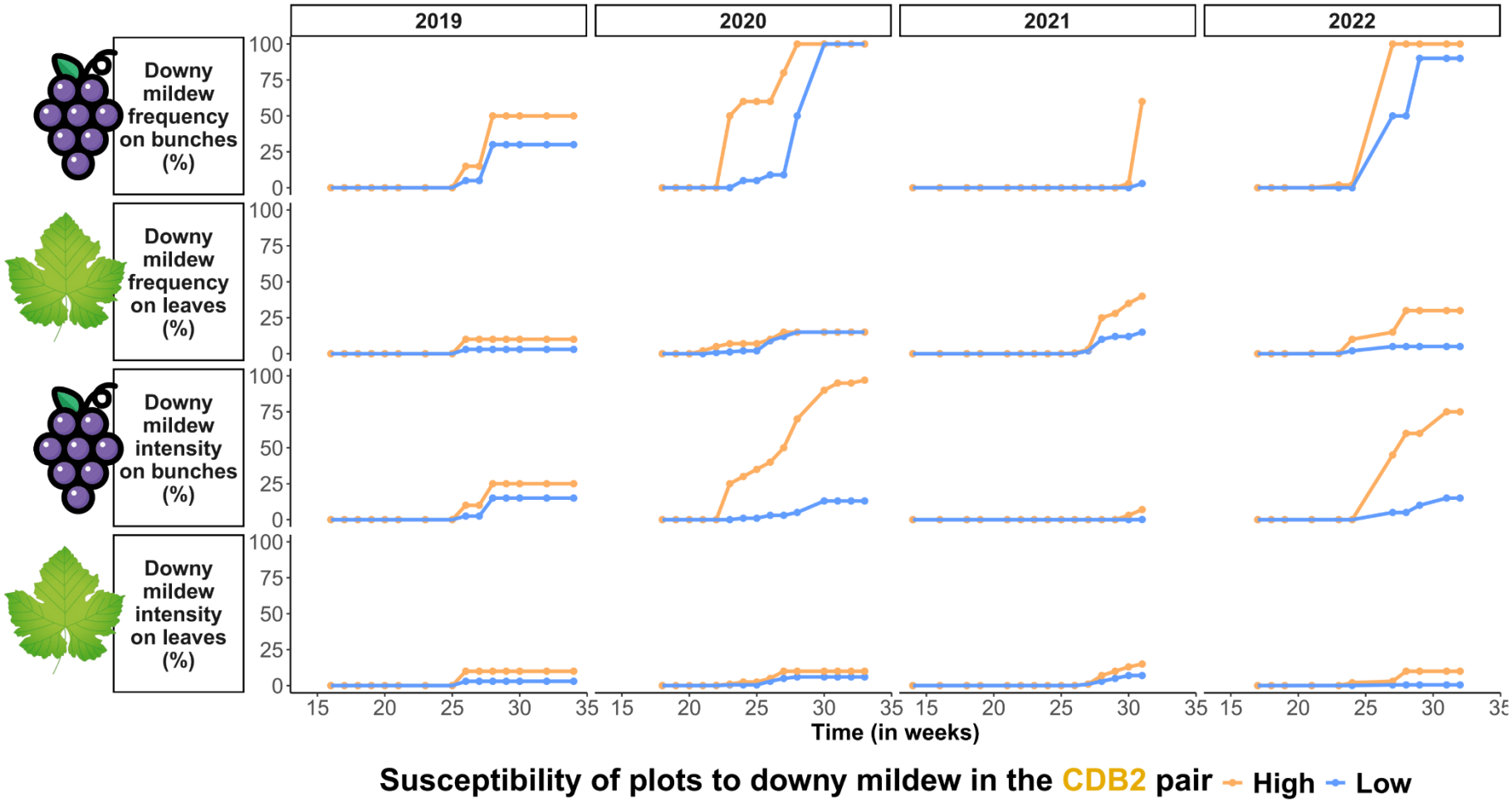


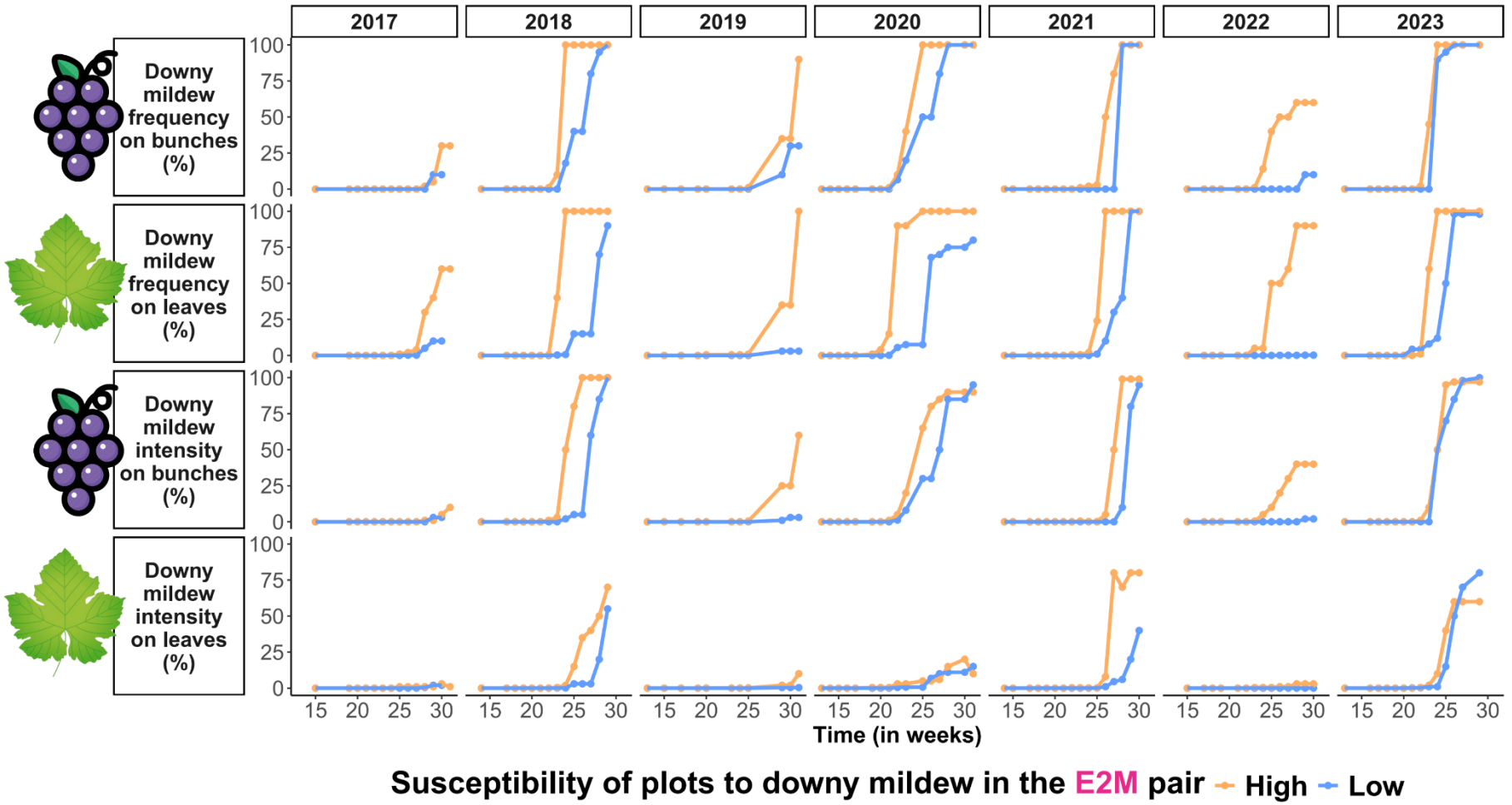
(i) Condition for Yes: the BLAST result is not equal to "no data"
(ii) Condition for Yes: the e-value of the BLAST in the public reference database is lower than the e-value for the custom database
(iii) Condition for Yes: e-value ≤ e-20, percentage identity ≥ 97% for ITS and ≥ 99% for bacteria, query coverage ≥ 90%

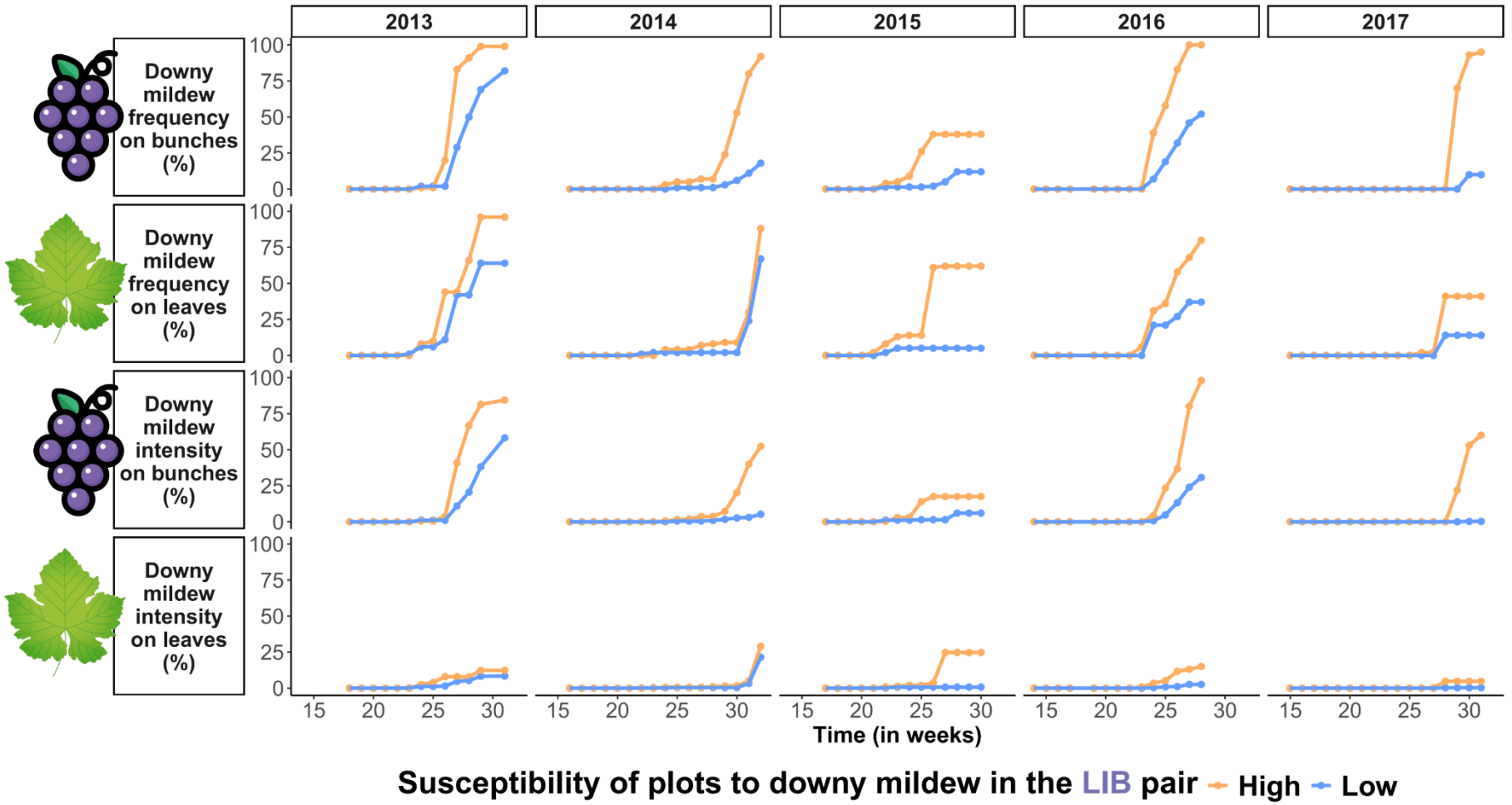
Figure S6: Disease progression curves for the 7 plot pairs.

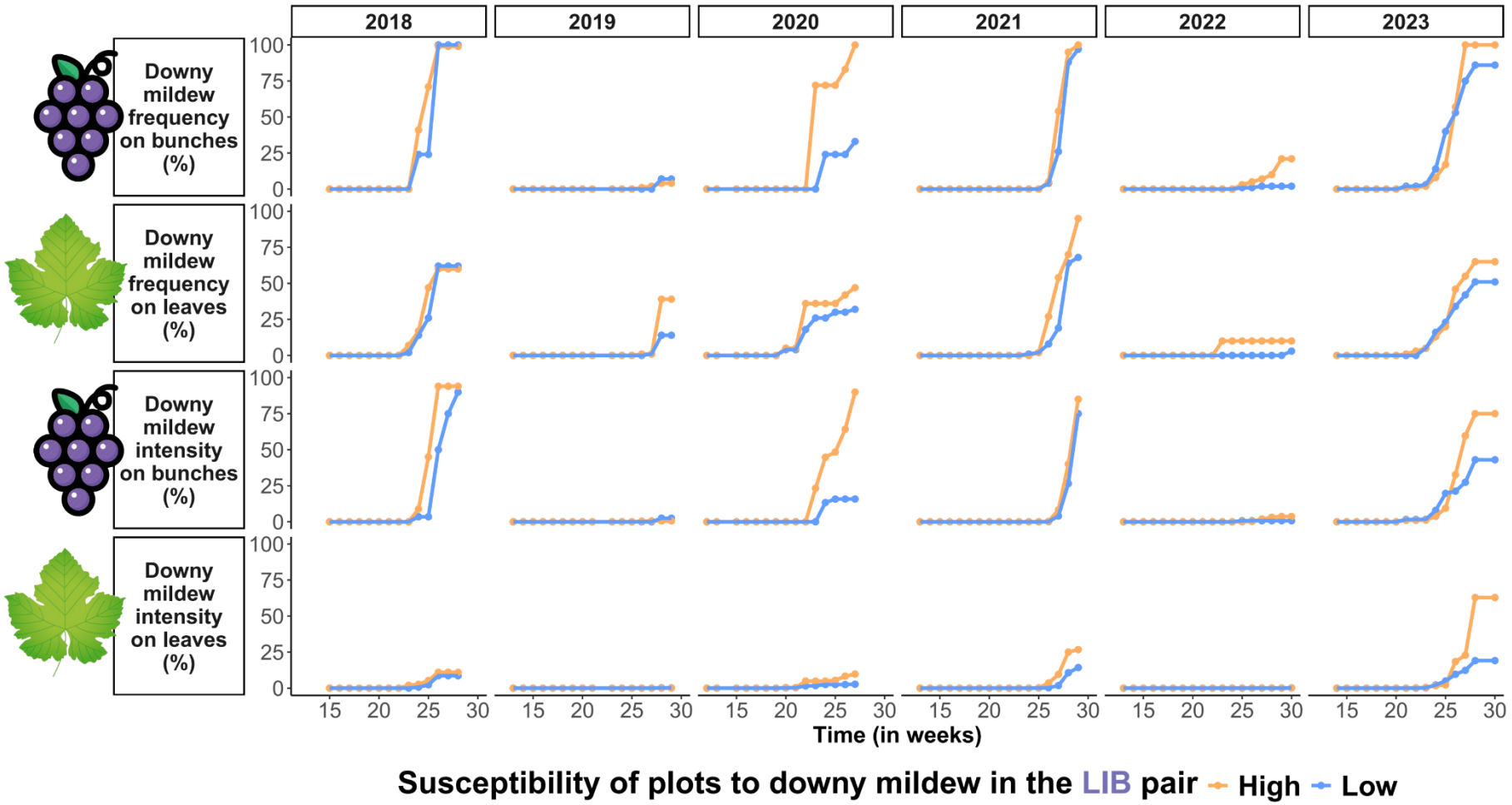
Disease curves for the 4 epidemiological variables measured by IFV (intensity of symptoms on leaves, frequency of symptoms on leaves, intensity of symptoms on bunches, frequency of symptoms on bunches) for the pairs CDB1, CDB2, E2M, LIB, ME1 and ME3 for all the years of joint monitoring of the two plots forming the pair. For the pair LIB, the curves are split into two figures due to 11 years of joint monitoring. For better readability, the first figure shows 2013–2017, and the second covers 2018–2023.

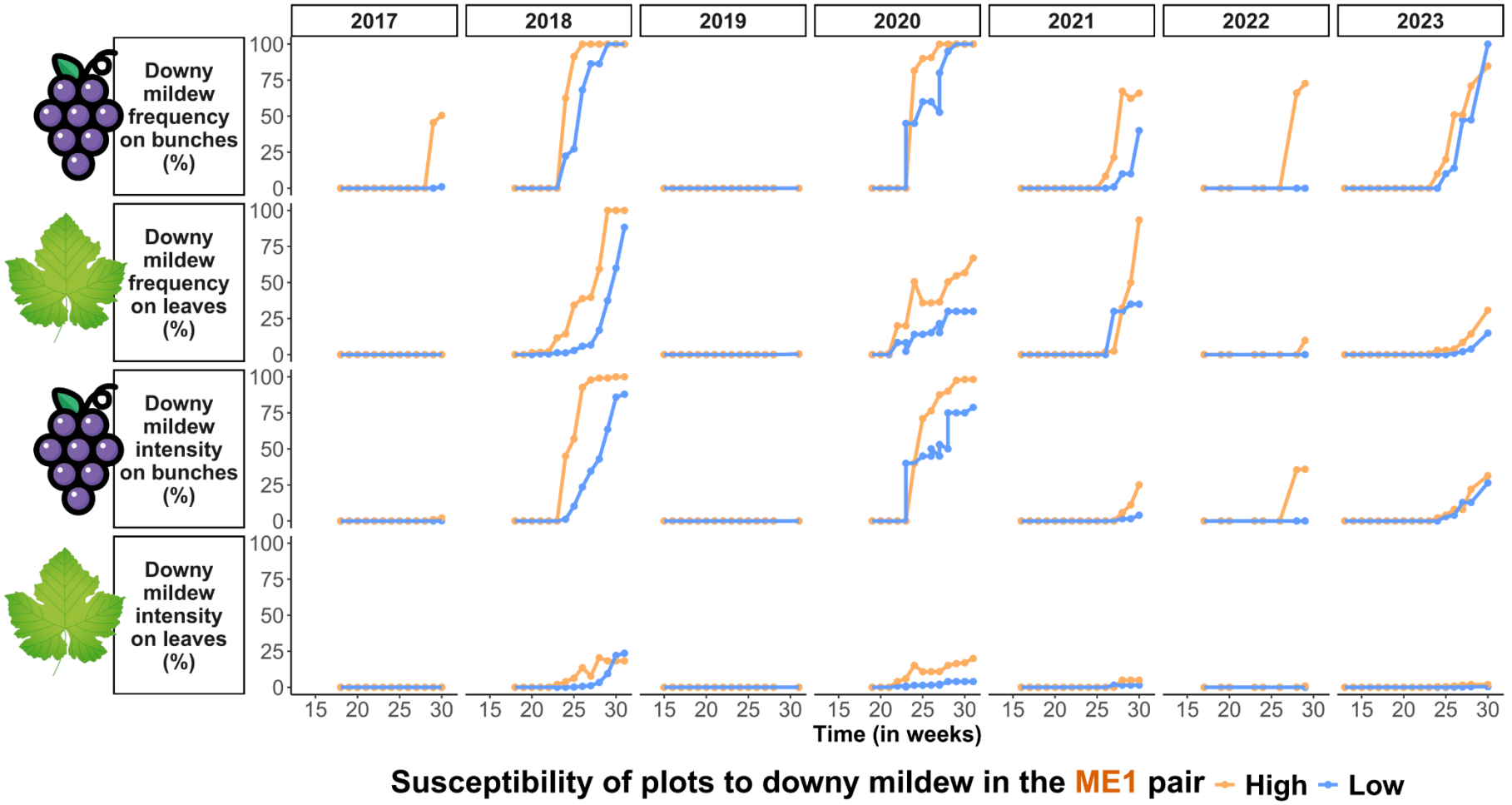



2019
2020
2021
2022
Downy mildew frequency on bunches (%)
Downy mildew frequency on leaves (%)
Downy mildew intensity on bunches (%)
Downy mildew intensity on leaves (%)
100
75
50
25
0
15
20
25
30
35
Time (in weeks)
Susceptibility of plots to downy mildew in the CDB2 pair
High
Low


2017
2018
2019
2020
2021
2022
2023
Downy mildew frequency on bunches (%)
Downy mildew frequency on leaves (%)
Downy mildew intensity on bunches (%)
Downy mildew intensity on leaves (%)
0
25
50
75
100
15
20
25
30
Time (in weeks)
Susceptibility of plots to downy mildew in the E2M pair
High
Low


2013
2014
2015
2016
2017
Downy mildew frequency on bunches (%)
Downy mildew frequency on leaves (%)
Downy mildew intensity on bunches (%)
Downy mildew intensity on leaves (%)
100
75
50
25
0
15
20
25
30
Time (in weeks)
Susceptibility of plots to downy mildew in the LIB pair
High
Low


2018
2019
2020
2021
2022
2023
Downy mildew frequency on bunches (%)
Downy mildew frequency on leaves (%)
Downy mildew intensity on bunches (%)
Downy mildew intensity on leaves (%)
0
25
50
75
100
15
20
25
30
Time (in weeks)
Susceptibility of plots to downy mildew in the LIB pair
High
Low


2017
2018
2019
2020
2021
2022
2023
Downy mildew frequency on bunches (%)
Downy mildew frequency on leaves (%)
Downy mildew intensity on bunches (%)
Downy mildew intensity on leaves (%)
100
75
50
25
0
15
20
25
30
Time (in weeks)
Susceptibility of plots to downy mildew in the ME1 pair
High
Low

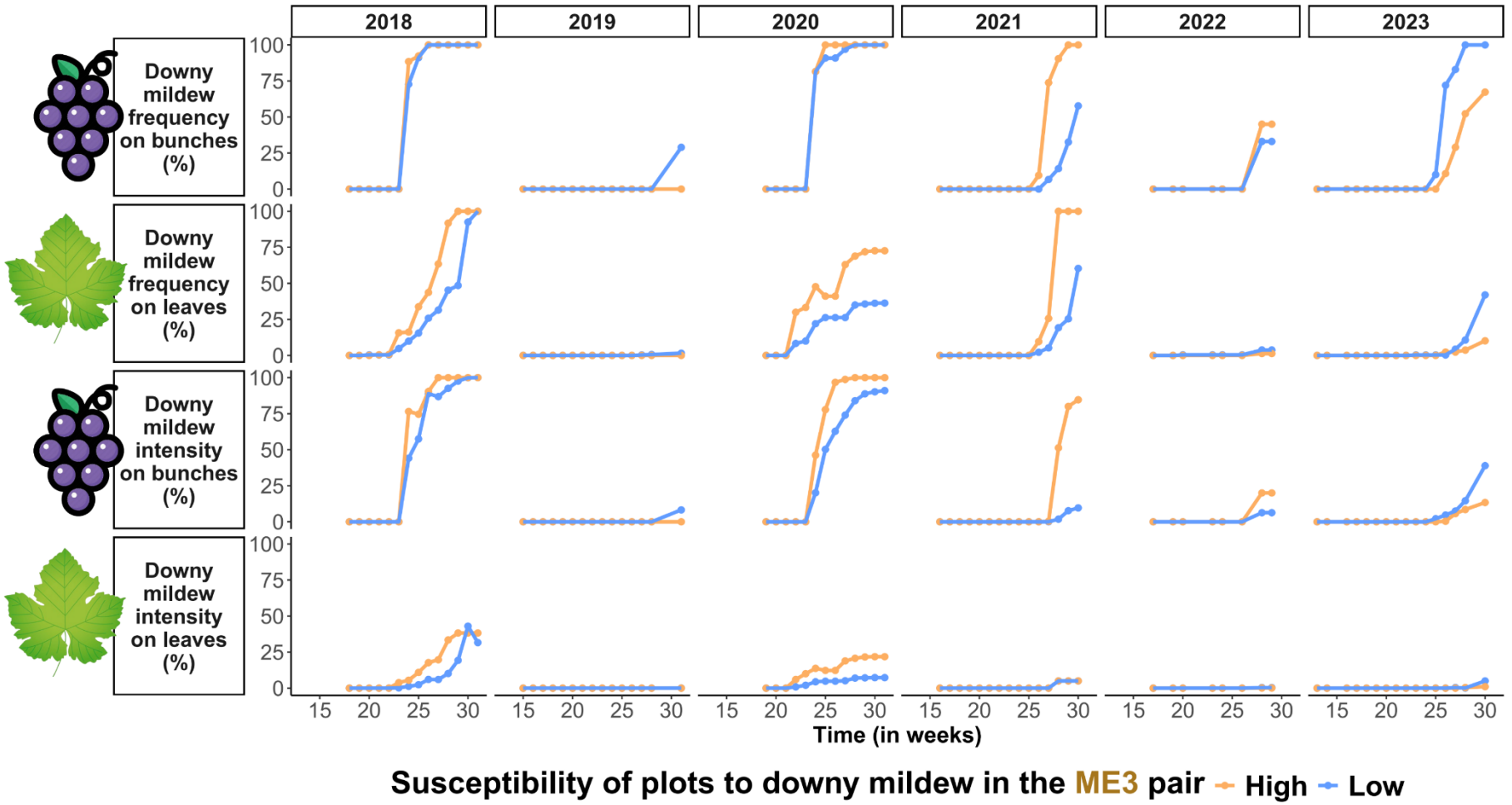

2018
2019
2020
2021
2022
2023
Downy mildew frequency on bunches (%)
Downy mildew frequency on leaves (%)
Downy mildew intensity on bunches (%)
Downy mildew intensity on leaves (%)
0
25
50
75
100
15
20
25
30
Time (in weeks)
Susceptibility of plots to downy mildew in the ME3 pair
High
Low

Figure S7: Variation in downy mildew primary inoculum in topsoil.
The figure shows the concentration of *P. viticola* DNA in topsoil as a function of the susceptibility of the plot to downy mildew, the year of sampling, whether the topsoil sample was collected at the edge of the plot, and whether fungicides were applied to the sampled area in the year before sampling. The statistical significance of the linear mixed effects models is indicated as follows: ns (not significant). (nonsignificant trend), *, (p<0.05), ** (p<0.01), *** (p<0.001).

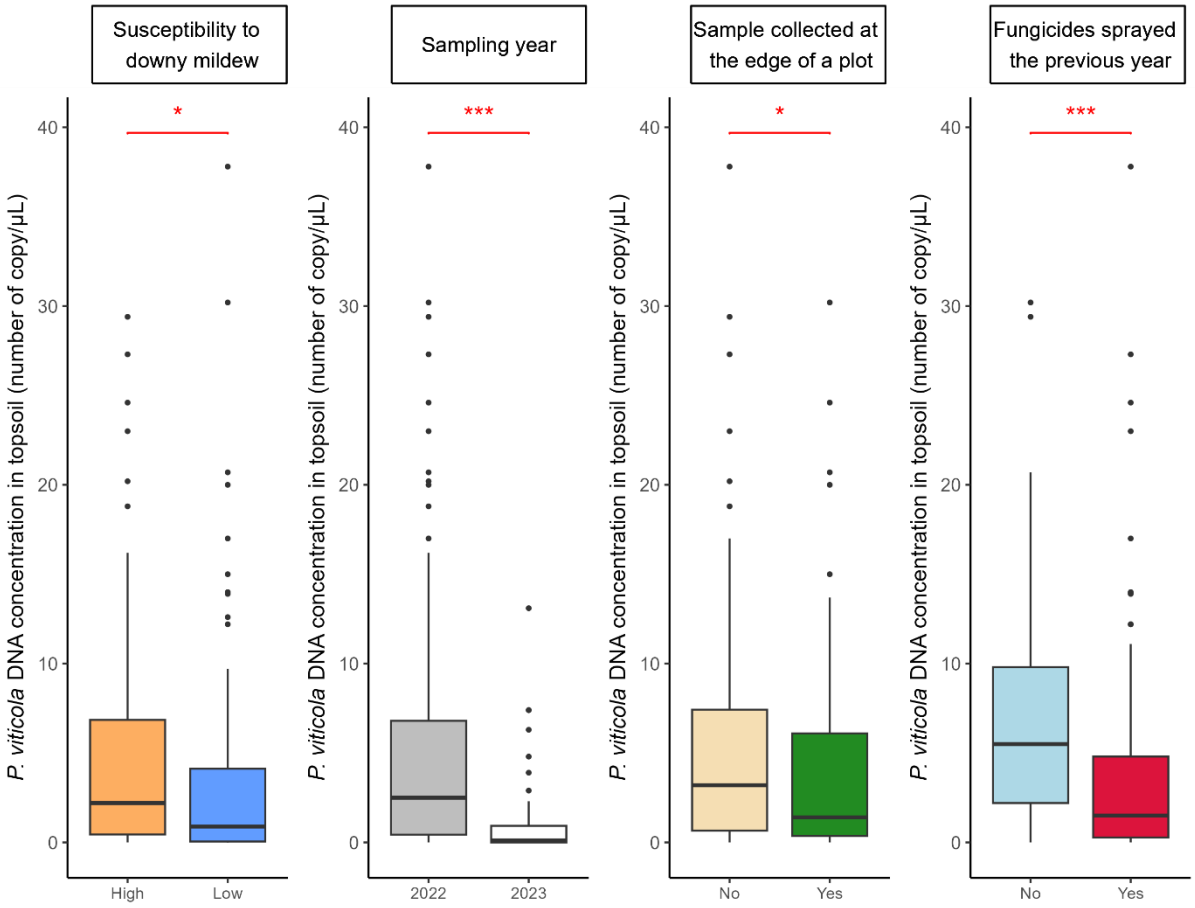


Figure S8: Microbial community profiles depending on vineyard plot susceptibility to downy mildew. (A) Fungal and (B) bacterial community profiles of the topsoil, phyllosphere and leaf endosphere, representing the relative abundance of the different phyla averaged over the four samples collected in each plot and each microbial habitat during the 2023 sampling campaign. Phyla representing less than 1% of the sequences were grouped into the "Other" category.

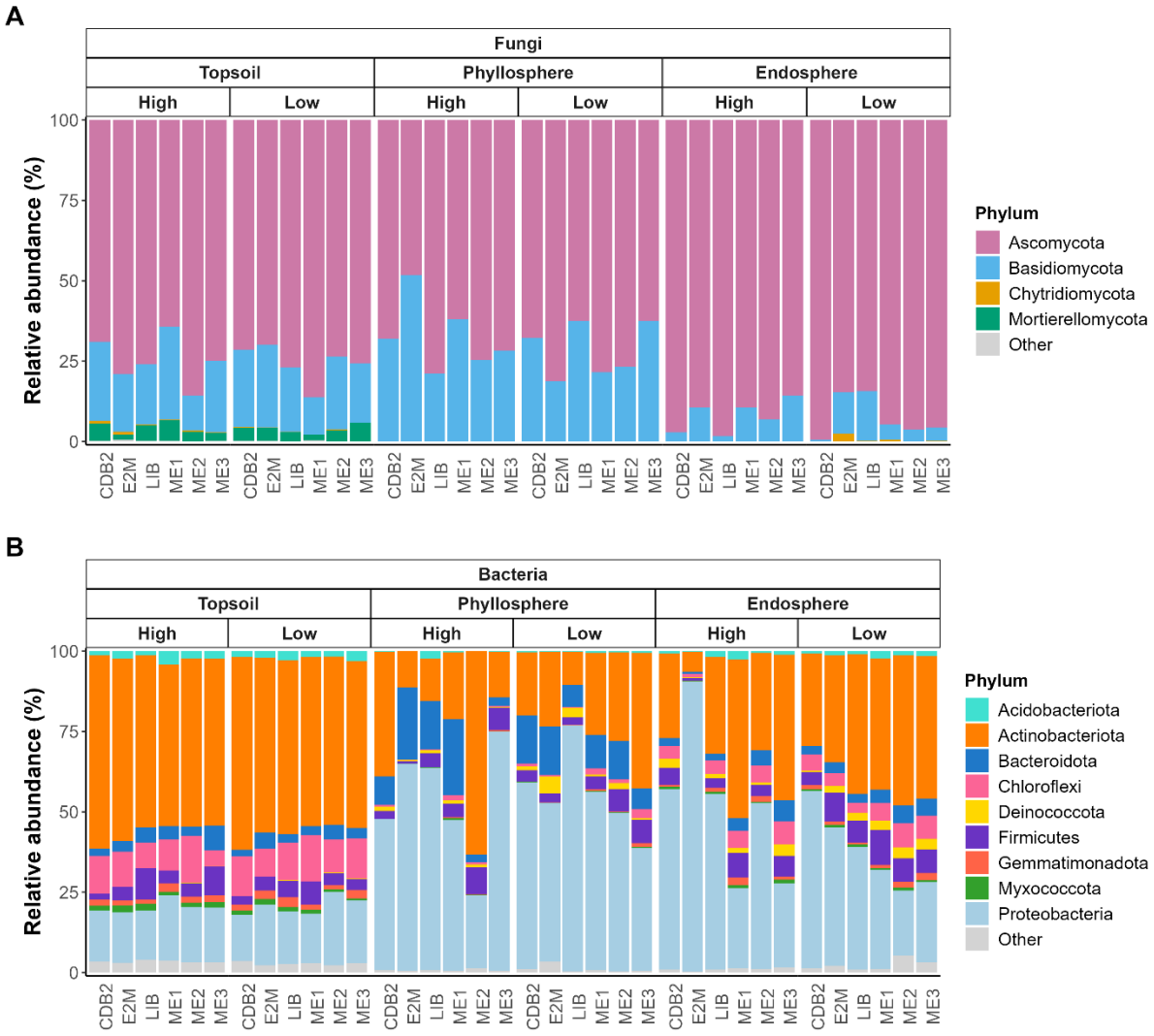


Figure S9: Variation in microbial community composition across vineyard plots.
Dissimilarities among (A) fungal and (B) bacterial communities of the topsoil, phyllosphere and leaf endosphere for the five pairs of plots sampled in 2023, represented with a Principal Component Analysis (PCA). Samples collected from the same pair of plots are represented with the same color, with symbols indicating high and low susceptibility to downy mildew (triangles and circles, respectively).

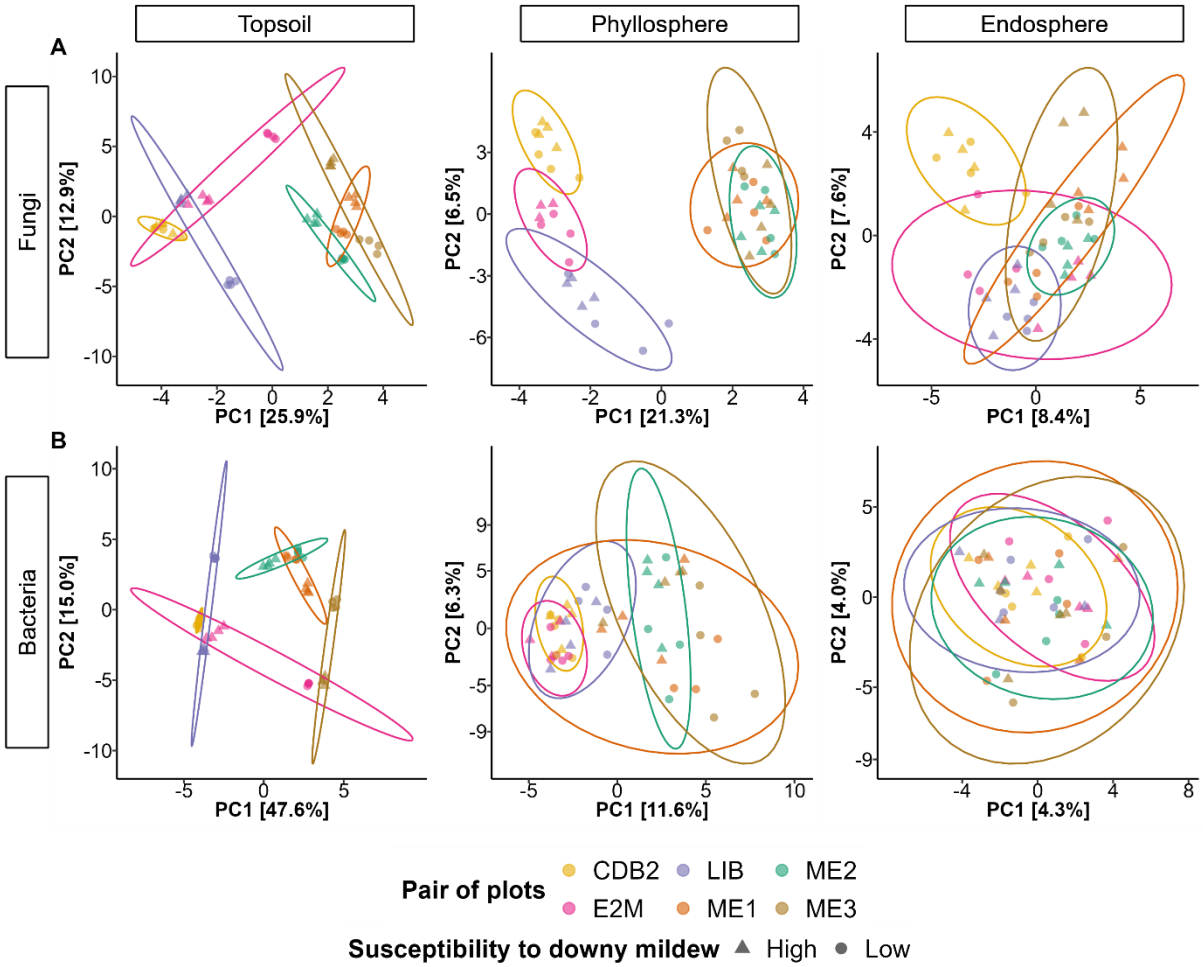


Figure S10: Environmental factors driving variation in microbial community composition in 2022.
The figure shows the factors influencing the composition of the (A) fungal and (B) bacterial communities. The environmental variables were grouped into four categories (Soil, Management, Space, and Weather; Table S1) for variance partitioning. The Venn diagrams show the percentage of variance explained by each group of variables, either individually or in combination with other groups.

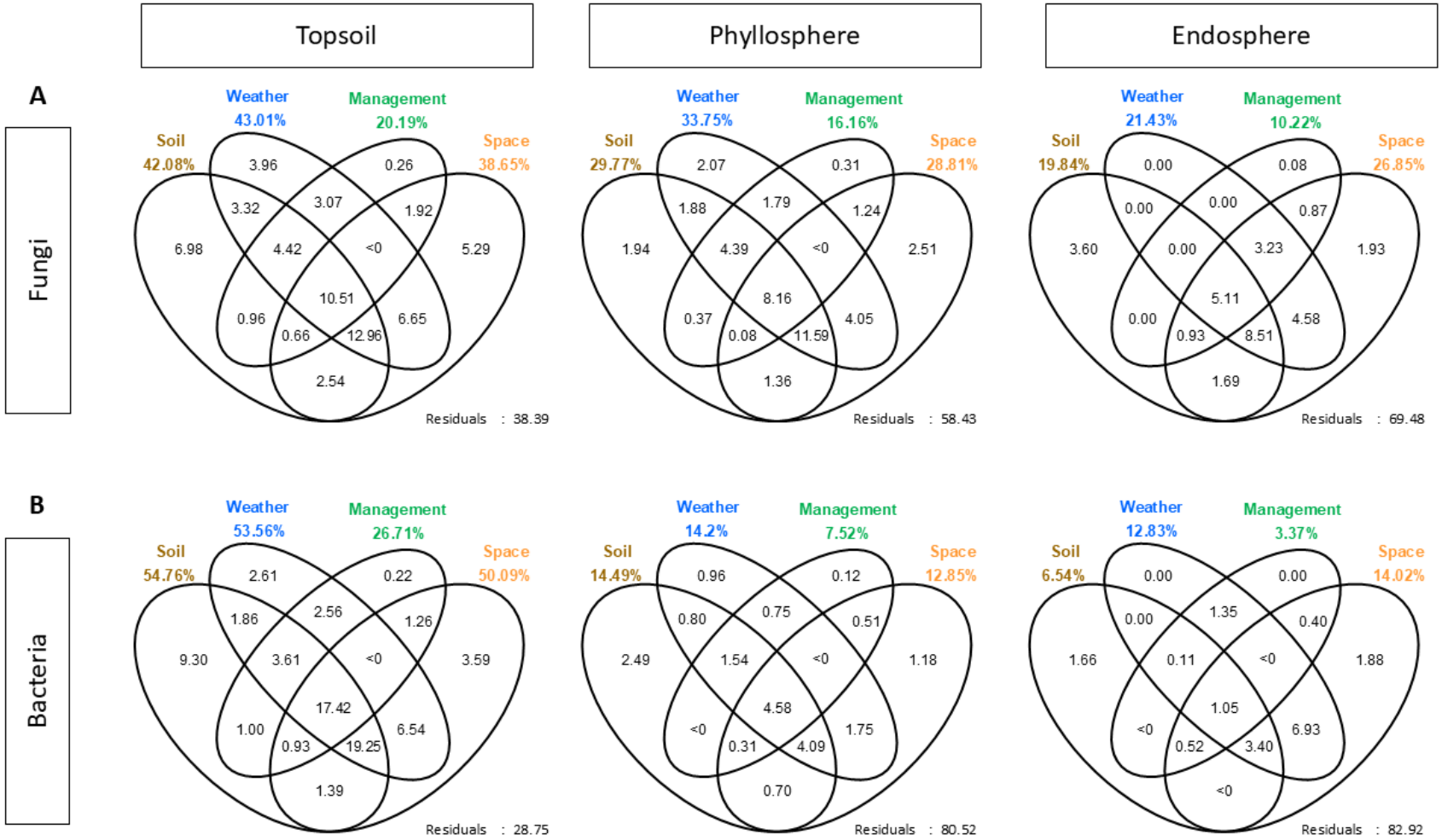


Figure S11: Environmental factors driving variation in microbial community composition in 2023.
The figure shows the factors influencing the composition of the (A) fungal and (B) bacterial communities. The environmental variables were grouped into four categories (Soil, Management, Space, and Weather; Table S1) for variance partitioning. The Venn diagrams show the percentage of variance explained by each group of variables, either individually or in combination with other groups.

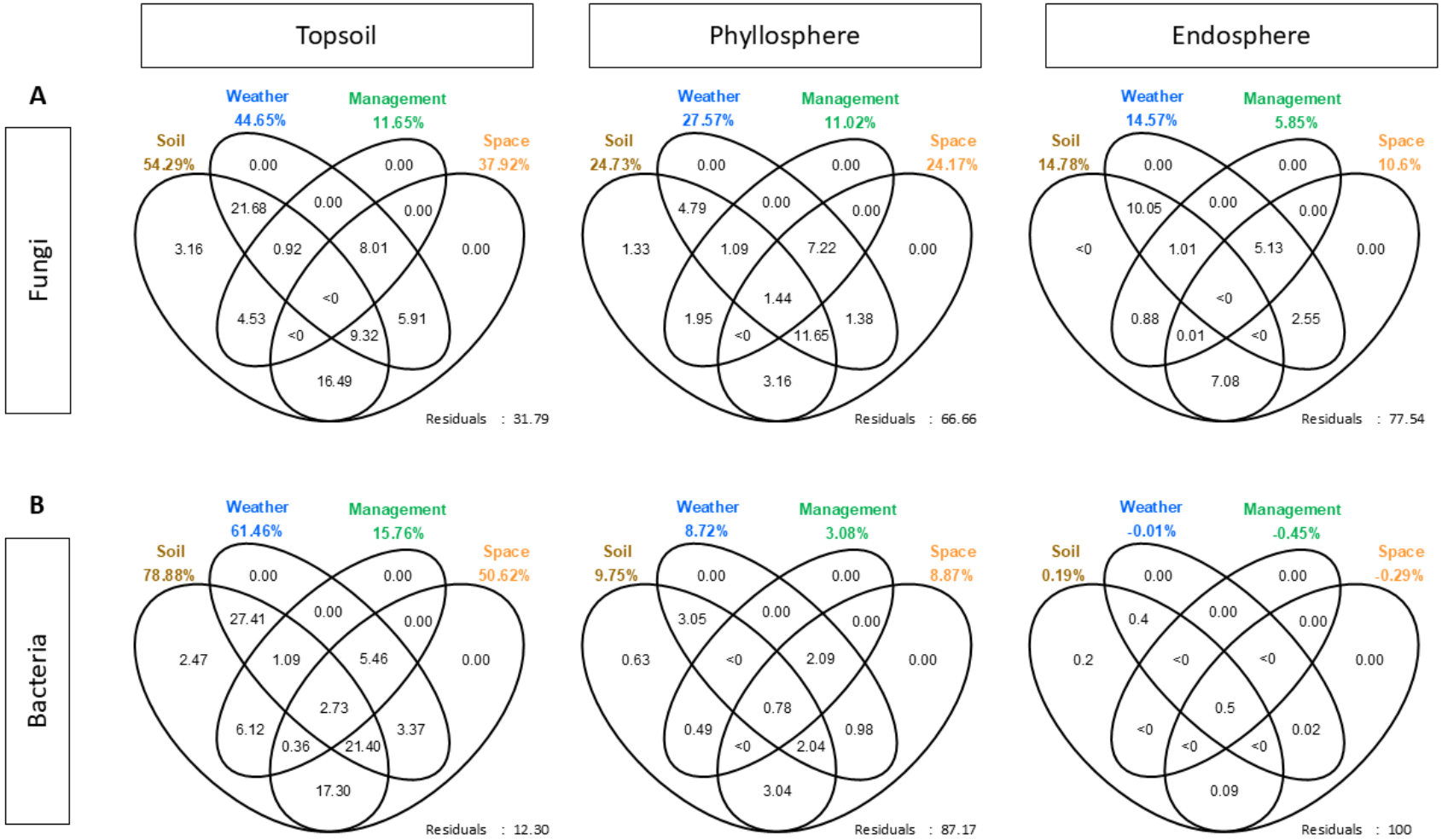


Figure S12: Variations in the diversity of microbial communities depending on vineyard plot susceptibility to downy mildew (2022 data).

The figure shows the diversity of (A) fungal and (B) bacterial communities in the topsoil, phyllosphere and endosphere of young grapevine leaves collected before the first phytosanitary treatment. The diversity indices are, from left to right, the observed total number of ASVs (Hill number q= 0), the exponential of the Shannon entropy index (Hill number q= 1), and the inverse of the Simpson concentration index (Hill number q= 2). The indices were calculated for each sample collected in 2022. The statistical significance of the linear mixed effects models is indicated as follows: ns (not significant). (nonsignificant trend), *, (p<0.05), ** (p<0.01), *** (p<0.001).

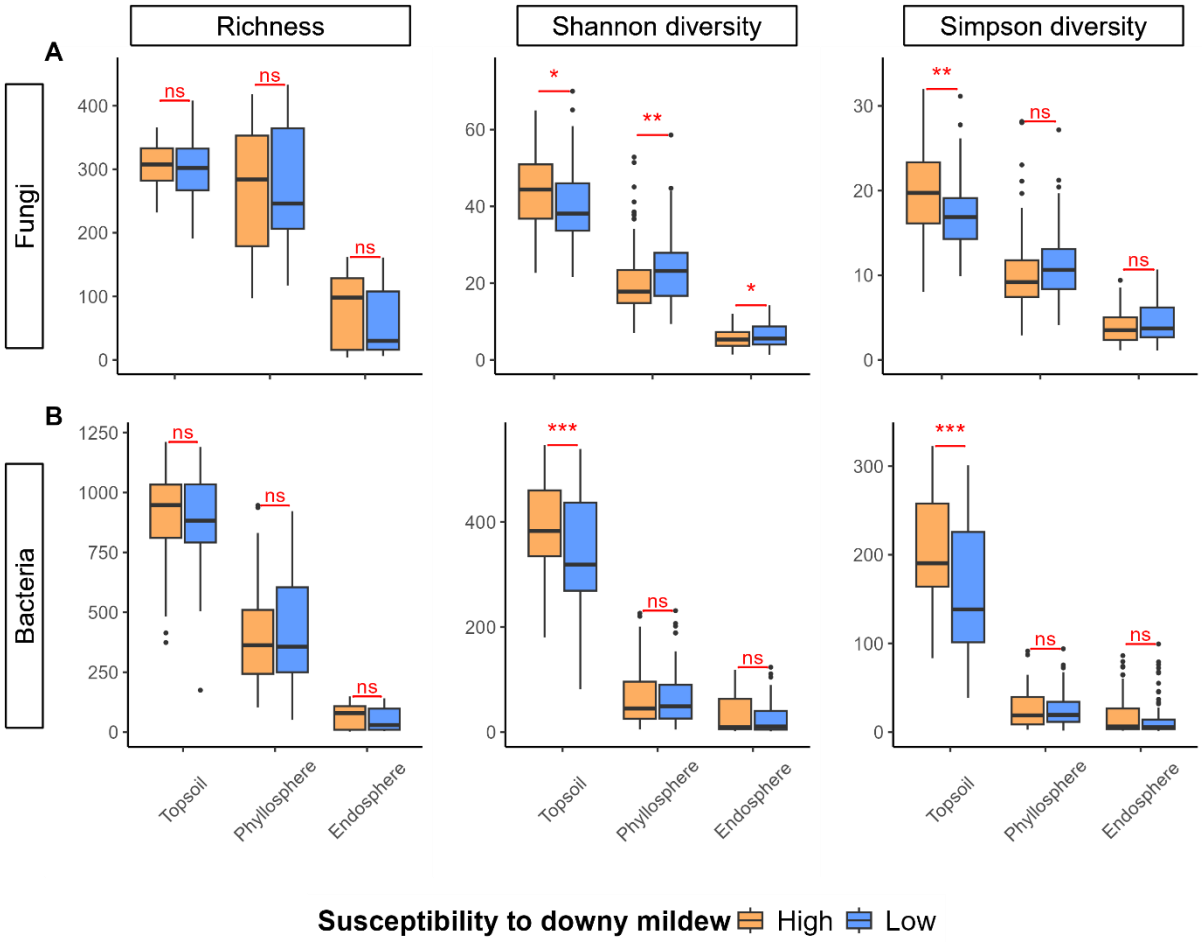


Figure S13: Variations in the diversity of microbial communities depending on vineyard plot susceptibility to downy mildew (2023 data).

The figure shows the diversity of (A) fungal and (B) bacterial communities in the topsoil, phyllosphere and endosphere of young grapevine leaves collected before the first phytosanitary treatment. The diversity indices are, from left to right, the observed total number of ASVs (Hill number q= 0), the exponential of the Shannon entropy index (Hill number q= 1), and the inverse of the Simpson concentration index (Hill number q= 2). The indices were calculated for each sample collected in 2022. The statistical significance of the linear mixed effects models is indicated as follows: ns (not significant). (nonsignificant trend), *, (p<0.05), ** (p<0.01), *** (p<0.001).

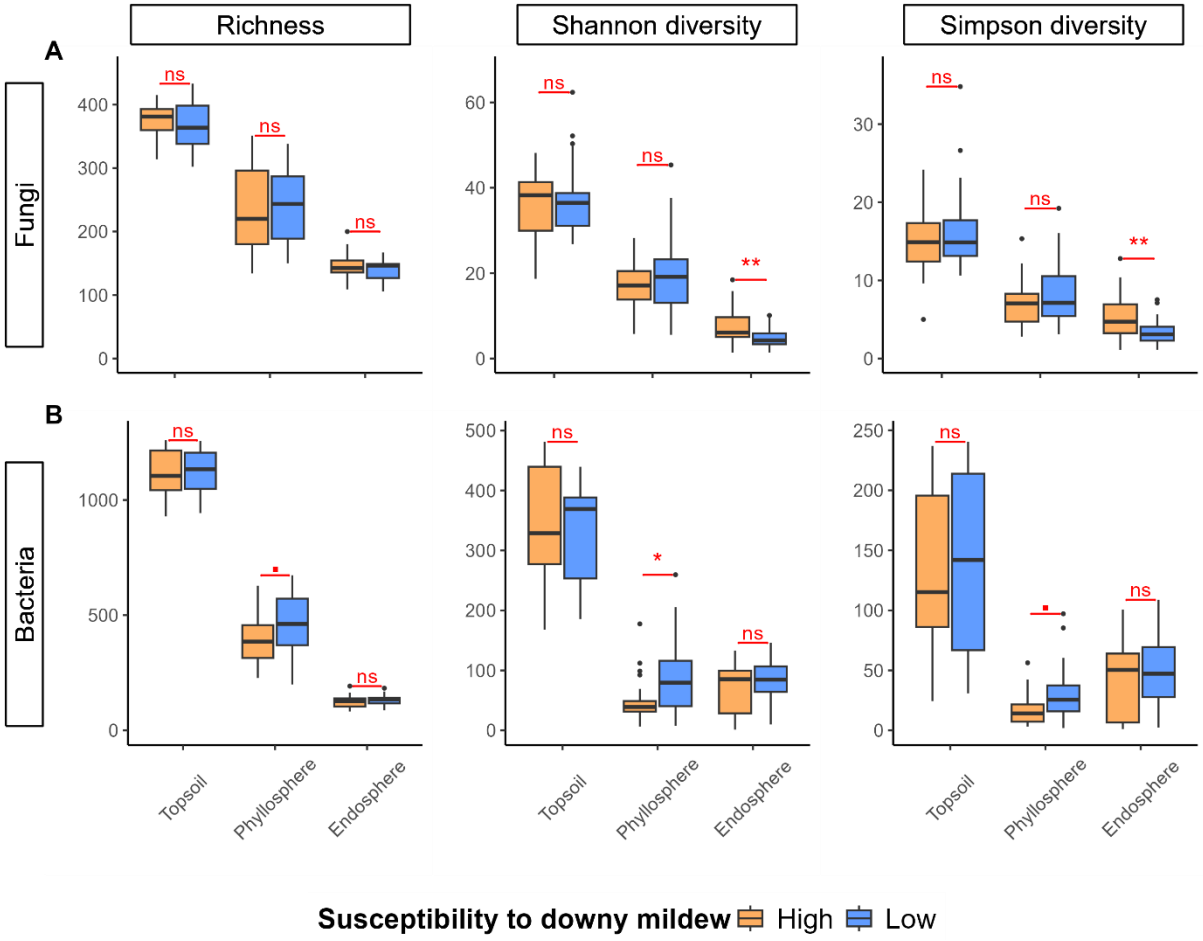


Figure S14: Endosphere fungal taxa that vary in abundance with susceptibility to downy mildew.

For each condition (high *vs.* low susceptibility), we represented the 20 Amplicon Sequence Variants (ASVs) that were significantly associated with the condition according to at least two methods and that had the highest average association scores. The five methods used to identify these ASVs were ANCOM-BC2 (Lin & Peddada, 2024), Maaslin2 (Mallick *et al.*, 2021), LinDA (Zhou *et al.*, 2022), ZicoSeq (Yang & Chen, 2022) and Random Forest Classification (Cambon *et al.*, 2023). The results are based on data collected in 2022.

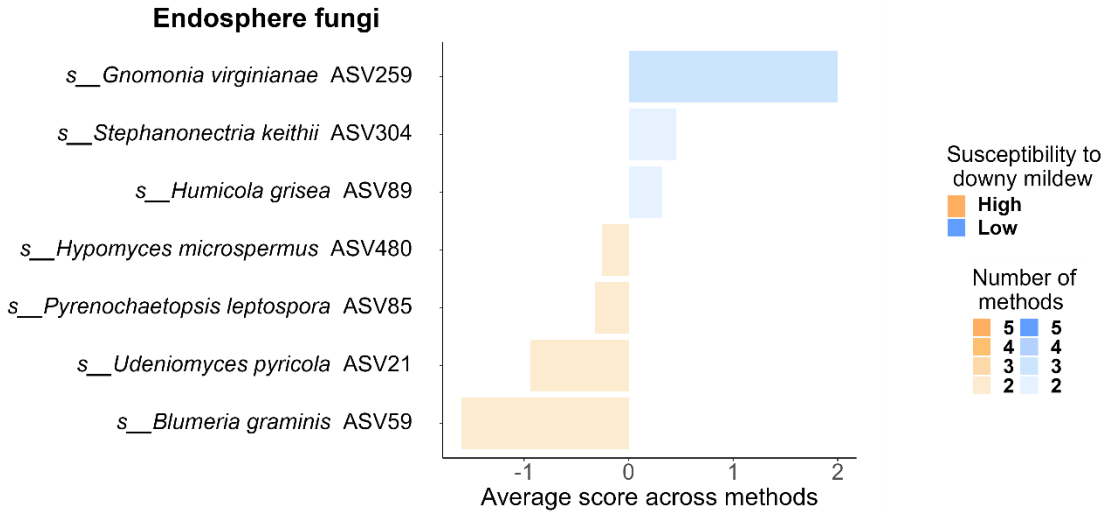


Figure S15: Topsoil fungal taxa that vary in abundance with susceptibility to downy mildew.

For each condition (high vs. low susceptibility), we represented the 20 Amplicon Sequence Variants (ASVs) that were significantly associated with the condition according to at least two methods and that had the highest average association scores. The five methods used to identify these ASVs are ANCOM-BC2 (Lin & Peddada, 2024), Maaslin2 (Mallick *et al.*, 2021), LinDA (Zhou *et al.*, 2022), ZicoSeq (Yang & Chen, 2022) and Random Forest Classification (Cambon *et al.*, 2023). The results are based on data collected in 2022.

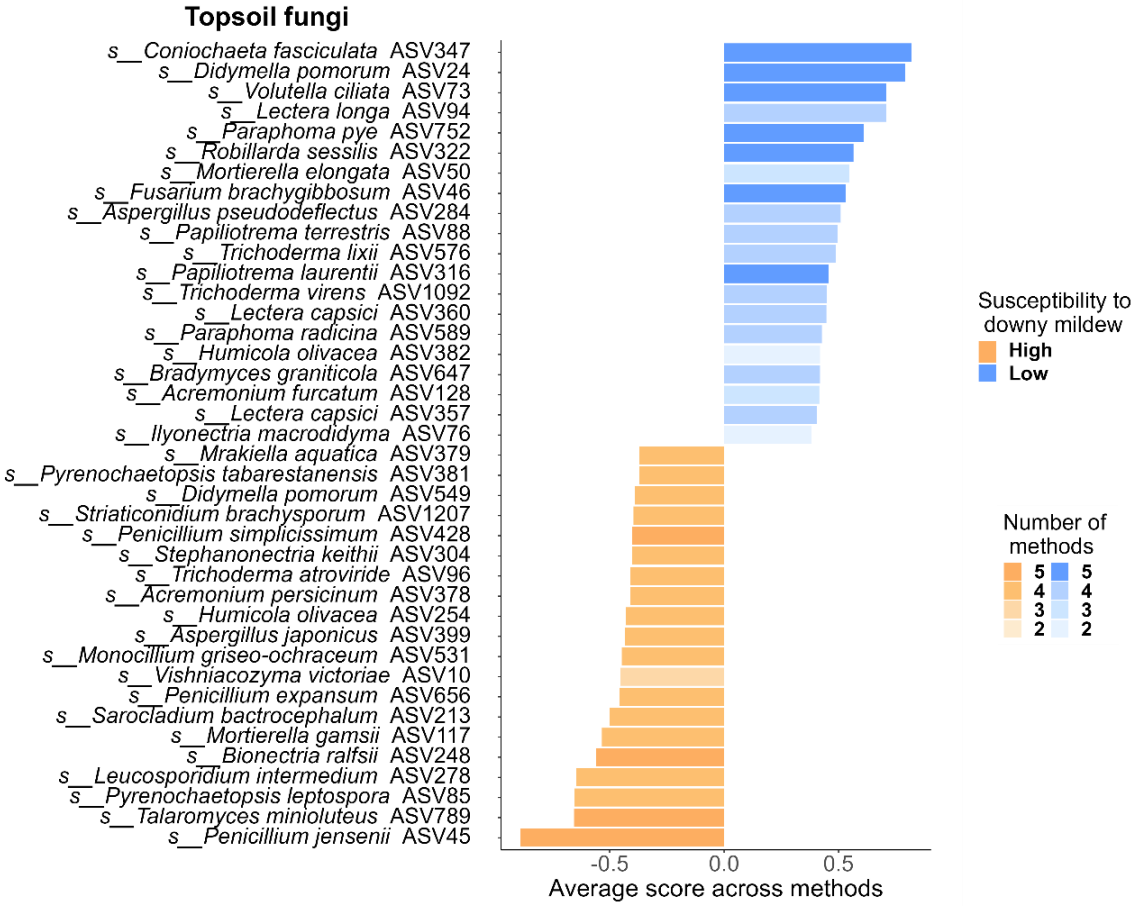


Figure S16: Phyllosphere bacterial taxa that vary in abundance with susceptibility to downy mildew. For each condition (high vs. low susceptibility), we represented the 20 Amplicon Sequence Variants (ASVs) that were significantly associated with the condition according to at least two methods and that had the highest average association scores. The five methods used to identify these ASVs are ANCOM-BC2 (Lin & Peddada, 2024), Maaslin2 (Mallick *et al.*, 2021), LinDA (Zhou *et al.*, 2022), ZicoSeq (Yang & Chen, 2022) and Random Forest Classification (Cambon *et al.*, 2023). The results are based on data collected in 2022.

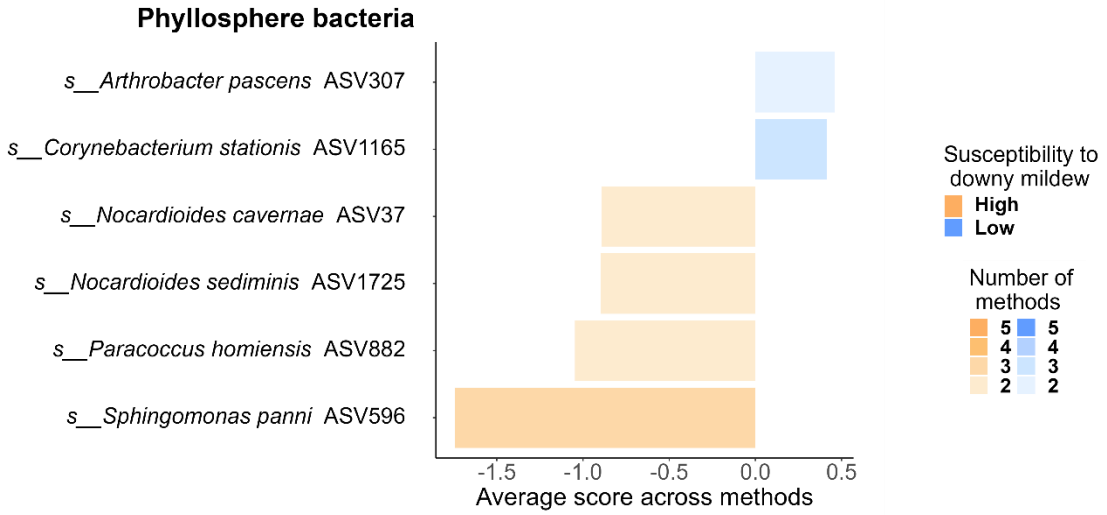


Figure S17: Random Forest algorithm performance in predicting grapevine susceptibility to downy mildew using leaf microbiota composition.

Each dot represents the mean sensitivity and precision obtained for a given subset of the phyllosphere or endosphere microbiota data collected in 2022. The subsets differ in their composition (all fungi, all bacteria, all taxa or only abundant ones) and their level of taxonomic aggregation (from no aggregation of the ASVs to aggregation to the class level). The colored dots are those obtained with the optimal *mtry* value (*i.e.*, the value that predicts low susceptibility to downy mildew with the lowest error rate). The bars represent the standard deviation over the various iterations of the cross-validation step. The lowest error rate is indicated as a percentage. The analysis and figure use the scripts developed by (Cambon *et al.*, 2023).

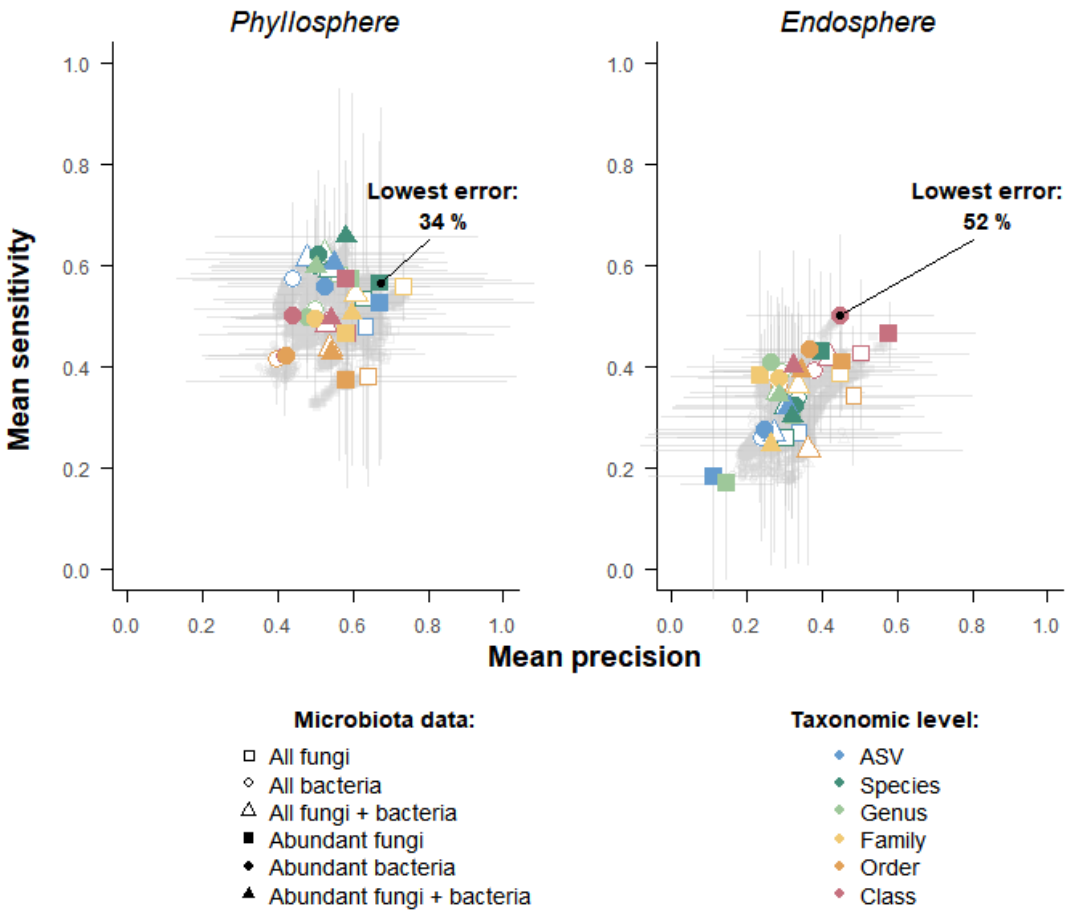


Figure S18: Random Forest algorithm performance in predicting grapevine susceptibility to downy mildew using topsoil microbiota data year-to-year.

Each point represents the average sensitivity and accuracy obtained for a given subset of soil microbiota data collected in 2022 (training dataset) and 2023 (validation dataset). The subsets differ in their composition (all fungi, all bacteria, all taxa or only abundant ones) and their level of taxonomic aggregation (from no aggregation of the ASVs to aggregation to the class level). The colored dots are those obtained with the optimal mtry value (*i.e.*, the value that predicts low susceptibility to downy mildew with the lowest error rate). The bars represent the standard deviation over the various iterations of the cross-validation step. The lowest error rate is indicated as a percentage. The analysis and figure use the scripts developed by (Cambon *et al.*, 2023).

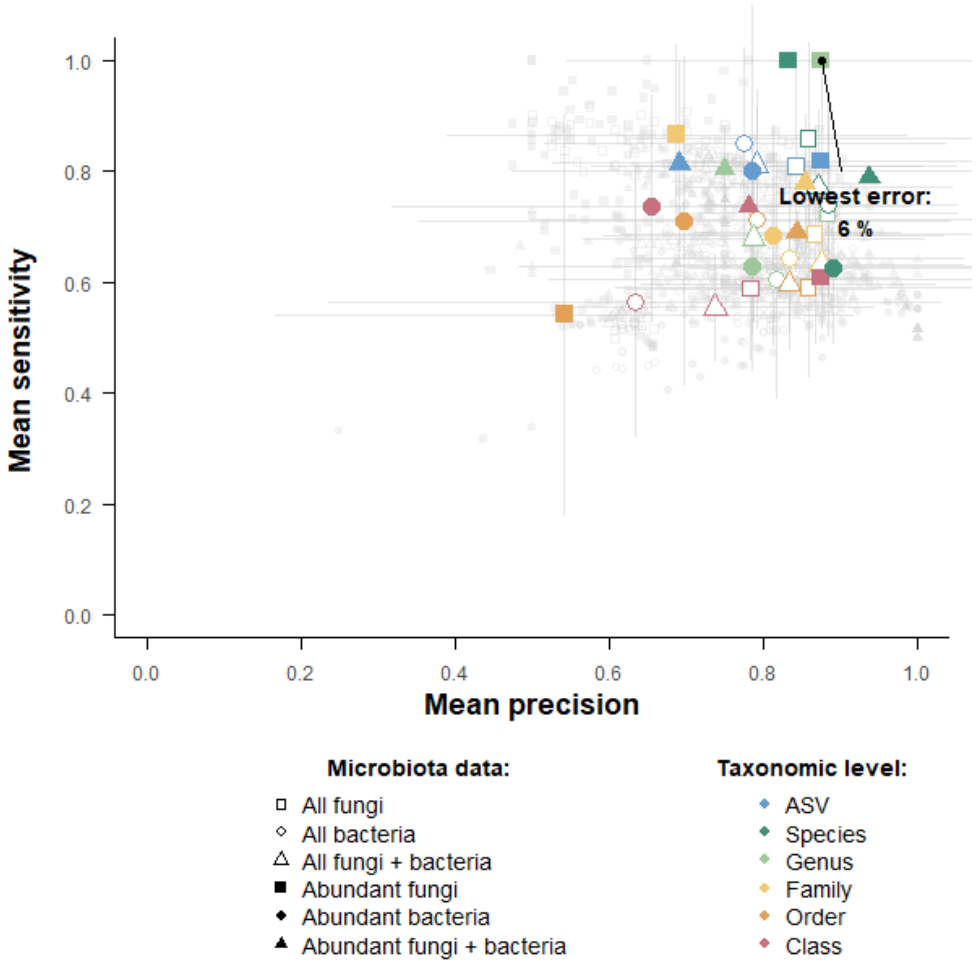
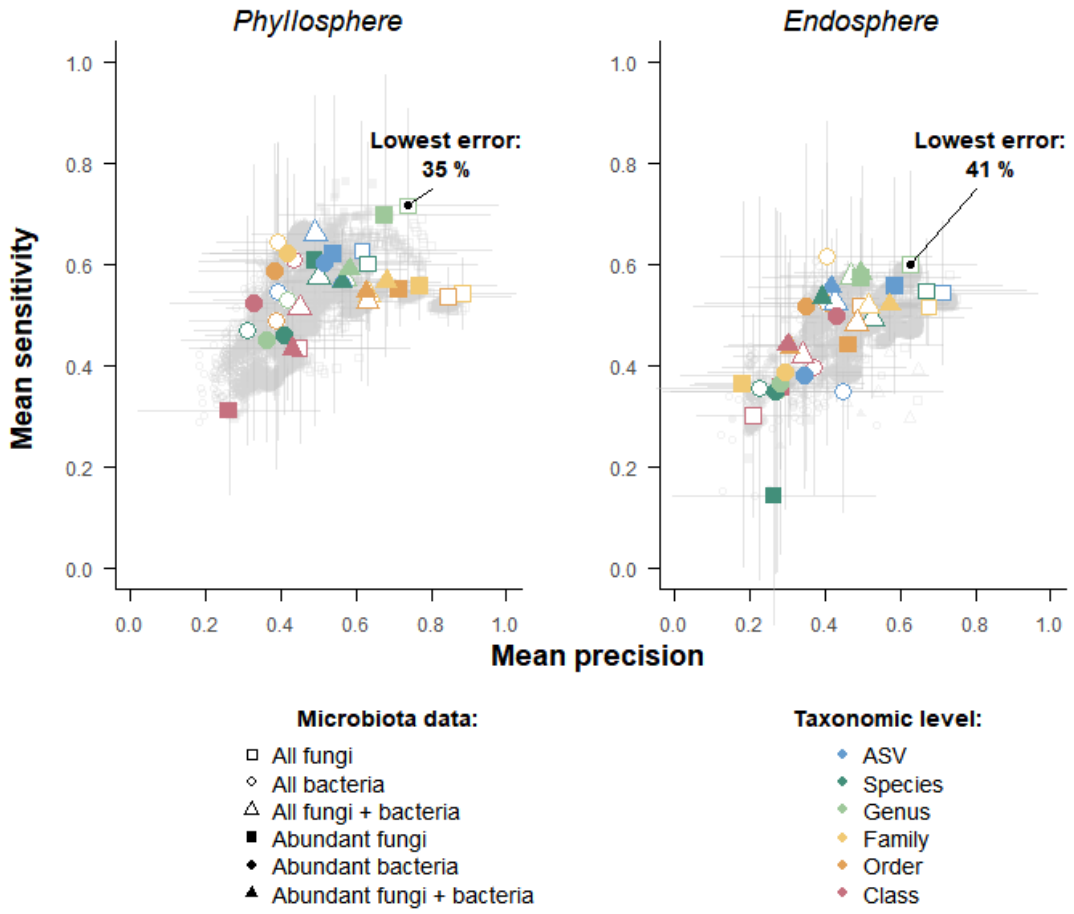


Figure S19: Random Forest algorithm performance in predicting grapevine susceptibility to downy mildew using leaf microbiota data year-to-year.

Each point represents the average sensitivity and accuracy obtained for a given subset of the phyllosphere or endosphere microbiota data collected in 2022 (training dataset) and 2023 (validation dataset). The subsets differ in their composition (all fungi, all bacteria, all taxa or only abundant ones) and their level of taxonomic aggregation (from no aggregation of the ASVs to aggregation to the class level). The colored dots are those obtained with the optimal *mtry* value (*i.e.*, the value that predicts low susceptibility to downy mildew with the lowest error rate). The bars represent the standard deviation over the various iterations of the cross-validation step. The lowest error rate is indicated as a percentage. The analysis and figure use the scripts developed by (Cambon *et al.*, 2023).



Supplementary tables

Table S1: Environmental variables used to explain the variation in microbiota composition.
The variables were grouped into four categories (Soil, Management, Space and Weather) to perform variance partitioning. The variables included in the analyses of the 2022 and 2023 datasets were the same, except for the variables 'vine individual located near the plot edge (Yes/No)' and 'phytosanitary treatments applied the year before sampling (Yes/No)'. These variables were excluded from the 2023 analysis because we collected samples only from the center of each plot, which had been treated the year before.

Group	Explanatory variables
Soil physical chemistry (*Soil*)	Clays (g/kg), sands (g/kg), silts (g/kg), C/N ratio, pH, organic matter (g/kg), total carbon (g/kg), total limestone (g/kg), total nitrogen (g/kg), total organic carbon (g/kg)
Vine variety and management (*Management*)	Vine variety (Cabernet-Sauvignon vs. Merlot Noir), management (Organic, Biodynamic, Conventional), whether fungicides were applied or not to the sampled area the year before sampling (Yes or No)
Position of the plot and position of the vine within the plot (*Space*)	Principal Coordinates of Neighborhood Matrix representing plot location (PCNM1 to PCNM5), within-plot location of the sample (edge vs. nonedge)
Weather during the month before sampling (*Weather*)	Total humidity (%), rainfall (mm) and temperature (°C) at 5 a.m., 10 a.m., 3 p.m. and 10 p.m. on the day before sampling, and at 5 a.m. and 10 a.m. on the day of sampling. Maximum humidity (%), maximum insolation (hours), maximum temperature (°C) and total rainfall (mm) on the day of sampling, as well as averages of these measures for the 24 hours, 15 days and 30 days before sampling.

Table S2: Factors driving variation in downy mildew inoculum in topsoil.

We analyzed the effects of plot susceptibility to downy mildew, sampling year, sample location (whether on the plot edge or not), and application of fungicide treatment the year before sampling on the *Plasmopara viticola* DNA concentration in topsoil samples. R^2m and R^2c correspond to the marginal and conditional coefficients of determination of the model, respectively. N corresponds to the number of topsoil samples included in the model. The significance of the variables is as follows: ns (not significant). (nonsignificant trend: 0.1>p>0.05), * (p<0.05), ** (p<0.01), *** (p<0.001).

Model			**Susceptibility to downy mildew (High or Low)**		**Sampling year (2022 or 2023)**		**Vine located to the edge plot (Yes or No)**		**Vine treated with fungicides the previous year (Yes or No)**		**Interaction between location and fungicide treatment**	
N	R^2c	R^2m	p	Variation direction	p	Variation direction	p	Variation direction	p	Variation direction	p	Variation direction
208	0.234	0.227	*	High> Low	***	2022>2023	*	No > Yes	***	No > Yes	ns	-

Table S3: Summary of read and ASV loss during data processing.

The table shows the number of sequences and ASVs at different stages of the bioinformatic pipeline, including data decontamination using the metabaR R package v1.0.0 [1]. The "Input fasta file" refers to the raw, unmerged fasta file provided by the sequencing facility. "Reads processed" indicates the number of reads successfully assembled, trimmed and dereplicated to form ASVs. "Chimera removed" indicates the number of ASVs that are not chimeras. "Rare ASVs filtered out" includes ASVs that represent at least 0.00005% of the sequences. "ITS1 subregion extracted" denotes ASVs containing the ITS1 region in their DNA sequence. "Taxonomically assigned" refers to ASVs with reliable affiliations corresponding to fungi or bacteria. "Dataset decontaminated" indicates ASVs not considered contaminants.

	barcode region: fungal nrDNA ITS genes		barcode region: bacterial 16S rRNA	
	Sequences	ASVs	Sequences	ASVs
Input fasta file	201,915,252	x	99,358,259	x
Reads processed	200,734,858	11,834,604	93,942,170	3,498,571
Chimera removed	200,199,438	11,704,682	87,655,868	495,519
Rare ASVs filtered out	175,672,262	929	72,005,795	1,654
ITS1 subregion extracted	175,217,886	924	x	x
Taxonomically assigned	160,840,561	799	47,536,337	1,588
Dataset decontaminated	136,681,217	795	32,678,727	1,561

Table S4: Most abundant fungal species in the topsoil, phyllosphere and leaf endosphere of vineyard plots.

The table represents the top ten most abundant fungal species in the 2023 dataset. Species in bold are also among the top ten most abundant species in 2023. *Relative abundance (%)* indicates the proportion of sequences assigned to the species relative to the total number of sequences in the dataset. *Prevalence (%)* indicates the percentage of samples where the species is present with at least one sequence.

Topsoil			Leaf phyllosphere			Leaf endosphere		
Fungal species	Relative abundance (%)	Prevalence (%)	Fungal species	Relative abundance (%)	Prevalence (%)	Fungal species	Relative abundance (%)	Prevalence (%)
Gibberella intricans (Ascomycota)	11.57	100	***Aureobasidium pullulans*** (Ascomycota)	23.63	97.87	***Didymella negriana*** (Ascomycota)	10.6	31.25
Saitozyma podzolica (Basidiomycota)	3.72	93.75	*Cryptovalsa ampelina* (Ascomycota)	11.15	74.47	***Epicoccum nigrum*** (Ascomycota)	7.92	56.25
Humicola sardiniae (Ascomycota)	3.37	100	***Vishniacozyma carnescens*** (Basidiomycota)	7.01	95.74	***Alternaria alternata*** (Ascomycota)	4.98	52.08
Solicoccozyma phenolica (Basidiomycota)	2.06	85.42	*Diplodia seriata* (Ascomycota)	5.36	82.98	*Golovinomyces artemisiae* (Ascomycota)	4.29	22.92
Truncatella angustata (Ascomycota)	1.67	100	***Cladosporium cladosporioides*** (Ascomycota)	3.18	91.49	*Aureobasidium pullulans* (Ascomycota)	4.27	87.5
Penicillium jensenii (Ascomycota)	1.52	93.75	***Cladosporium ramotenellum*** (Ascomycota)	3.13	91.49	***Alternaria infectoria*** (Ascomycota)	3.8	68.75
Neocosmospora rubicola (Ascomycota)	1.46	100	***Cladosporium allicinum*** (Ascomycota)	2.11	76.6	*Diplodia seriata* (Ascomycota)	3.35	64.58
Vishniacozyma victoriae (Basidiomycota)	1.45	100	***Vishniacozyma victoriae*** (Basidiomycota)	1.72	100	***Itersonilia perplexans*** (Basidiomycota)	3	50
Fusarium avenaceum (Ascomycota)	1.32	100	*Peniophora versicolor* (Basidiomycota)	1.51	95.74	***Blumeria graminis*** (Ascomycota)	2.92	58.33
Mortierella elongata (Mortierellomycota)	1.31	100	*Itersonilia perplexans* (Basidiomycota)	1.45	80.85	*Cryptovalsa ampelina* (Ascomycota)	2.28	75
Total	**29.45**		Total	**60.25**		Total	**47.41**	

Table S5: Most abundant bacterial genera in the topsoil, phyllosphere and leaf endosphere of vineyard plots.

The table represents the top ten most abundant bacterial genera in the 2023 dataset. Genera in bold are also among the top ten most abundant genera in 2023. Relative abundance (%) indicates the proportion of sequences assigned to the genera relative to the total number of sequences in the dataset. Prevalence (%) indicates the percentage of samples where the genera is present with at least one sequence.

Topsoil			Leaf phyllosphere			Leaf endosphere		
Bacterial genus	Relative abundance	Prevalence	Bacterial genus	Relative abundance	Prevalence	Bacterial genus	Relative abundance	Prevalence
Rubrobacter (Actinobacteriota)	7.24	100	***Sphingomonas*** (Proteobacteria)	11.22	100	***Wolbachia*** (Proteobacteria)	32.26	47.92
Nocardioides (Actinobacteriota)	4.32	100	***Hymenobacter*** (Bacteroidota)	9.56	97.87	*Rubrobacter* (Actinobacteriota)	2.6	97.92
Bacillus (Firmicutes)	3.65	100	***Methylobacterium-Methylorubrum*** (Proteobacteria)	8.88	100	***Nocardioides*** (Actinobacteriota)	2.24	97.92
Gaiella (Actinobacteriota)	2.84	100	*Tepidiphilus* (Proteobacteria)	8.62	95.74	***Bacillus*** (Firmicutes)	1.73	95.83
Pseudarthrobacter (Actinobacteriota)	2.67	100	***Pseudomonas*** (Proteobacteria)	4.14	100	*Sphingomonas* (Proteobacteria)	1.71	93.75
Sphingomonas (Proteobacteria)	2.43	100	*Bifidobacterium* (Actinobacteriota)	2.55	19.15	*Pseudomonas* (Proteobacteria)	1.62	43.75
Arthrobacter (Actinobacteriota)	2.41	100	*Mycobacterium* (Actinobacteriota)	2.48	97.87	*Deinococcus* (Deinococcota)	1.5	47.92
Streptomyces (Actinobacteriota)	2.4	100	***Nocardioides*** (Actinobacteriota)	1.75	100	*Pseudarthrobacter* (Actinobacteriota)	1.45	93.75
Blastococcus (Actinobacteriota)	1.77	100	*Erwinia* (Proteobacteria)	1.72	63.83	*Bifidobacterium* (Actinobacteriota)	1.27	10.42
Mycobacterium (Actinobacteriota)	1.69	100	***Variovorax*** (Proteobacteria)	1.52	95.74	*Enhydrobacter* (Proteobacteria)	1.26	37.5
Total	**31.42**		Total	**52.44**		Total	**47.64**	

Table S6: Factors driving variation in microbiota alpha diversity. We analyzed the effects of plot susceptibility to downy mildew, application of fungicide treatment the year before sampling, and sample location (whether on the plot edge or not) and their interactions on the microbial diversity in the 2022 data. R^2m and R^2c correspond reciprocally to the marginal and conditional determination coefficient of the model. N represents the number of samples included in the model. The significance of the variables is as follows: ns (not significant). (nonsignificant trend: 0.1>p>0.05), *, (p<0.05), ** (p<0.01), *** (p<0.001).

Model				Susceptibility to downy mildew		Vine located to the edge plot		Vine treated with fungicides the previous year		Edge : Fungicides	
	N	R^2c	R^2m	p	Variation direction	p	Variation direction	p	Variation direction	p	Variation direction
Diversity index: Richness (Hill number, q = 0)											
Fungi in Topsoil	159	0.222	0.055	ns	-	ns	-	**	No > Yes	ns	-
Fungi in Phyllosphere	158	0.836	0.015	ns	-	**	No > Yes	ns	-	ns	-
Fungi in Endosphere	160	0.810	0.047	ns	-	***	Yes > No	ns	-	ns	
Bacteria in Topsoil	160	0.577	0.011	ns	-	ns	-	.	No > Yes	ns	-
Bacteria in Phyllosphere	160	0.344	0.036	ns	-	ns	-	.	No > Yes	.	-
Bacteria in Endosphere	160	0.788	0.067	ns	-	**	Yes > No	*	No > Yes	ns	-
Diversity index: Shannon (Hill number, q = 1)											
Fungi in Topsoil	159	0.321	0.225	*	High > Low	*	Yes > No	***	No > Yes	**	
Fungi in Phyllosphere	158	0.441	0.077	**	Low > High	ns	-	**	No > Yes	.	
Fungi in Endosphere	160	0.147	0.090	*	Low > High	**	Yes > No	ns	-	ns	-
Bacteria in Topsoil	160	0.471	0.341	***	High > Low	***	Yes > No	ns	-	*	
Bacteria in Phyllosphere	160	0.059	0.030	ns	-	ns	-	ns	-	.	
Bacteria in Endosphere	160	0.487	0.038	ns	-	*	Yes > No	ns	-	ns	-
Diversity index: Simpson (Hill number, q = 2)											
Fungi in Topsoil	159	0.353	0.312	**	High > Low	**	Yes > No	***	No > Yes	***	
Fungi in Phyllosphere	158	0.233	0.054	ns	-	ns	-	.	No > Yes	*	
Fungi in Endosphere	160	0.109	0.053	ns	-	*	Yes > No	ns	-	ns	-
Bacteria in Topsoil	160	0.512	0.392	***	High > Low	***	Yes > No	ns	-	*	
Bacteria in Phyllosphere	160	0.024	0.018	ns	-	ns	-	ns	-	ns	-
Bacteria in Endosphere	160	0.383	0.048	ns	-	*	Yes > No	ns	-	ns	-

Table S7: Factors driving variation in microbiota alpha diversity.

We analyzed the effects of plot susceptibility to downy mildew on the microbial diversity in 2023. R^2m and R^2c correspond reciprocally to the marginal and conditional determination coefficient of the model. N represents the number of samples included in the model. The significance of the variables is as follows: ns (not significant). (nonsignificant trend: 0.1>p>0.05), *, (p<0.05), ** (p<0.01), *** (p<0.001).

Model				Susceptibility to downy mildew	
	N	R^2c	R^2m	p	Variation direction
Diversity index: Richness (Hill number, q = 0)					
Fungi in Topsoil	48	0.398	0.017	ns	-
Fungi in Phyllosphere	47	0.744	0.00	ns	-
Fungi in Endosphere	48	0.154	0.024	ns	-
Bacteria in Topsoil	48	0.865	0.001	ns	-
Bacteria in Phyllosphere	47	0.169	0.053	.	Low > High
Bacteria in Endosphere	48	0.102	0.017	ns	-
Diversity index: Shannon (Hill number, q = 1)					
Fungi in Topsoil	48	0.328	0.010	ns	-
Fungi in Phyllosphere	47	0.029	0.014	ns	-
Fungi in Endosphere	48	0.291	0.123	**	High > Low
Bacteria in Topsoil	48	0.954	0.002	ns	-
Bacteria in Phyllosphere	47	0.214	0.103	*	Low > High
Bacteria in Endosphere	48	0.183	0.028	ns	-
Diversity index: Simpson (Hill number, q = 2)					
Fungi in Topsoil	48	0.281	0.018	ns	-
Fungi in Phyllosphere	47	0.418	0.024	ns	-
Fungi in Endosphere	48	0.210	0.112	**	High > Low
Bacteria in Topsoil	48	0.632	0.004	ns	-
Bacteria in Phyllosphere	47	0.196	0.090	.	Low > High
Bacteria in Endosphere	48	0.229	0.023	ns	-

Table S8: Fungal taxa indicators of low downy mildew primary inoculum in topsoil.
Fungal ASVs which increase significantly in abundance as the concentration of P. viticola DNA in the topsoil decreases, according to the Threshold Indicator Taxa Analysis (TITAN) method (Baker *et al.*, 2023b), and they have the highest z scores. These results are based on the 2022 topsoil data. Relative abundance (%) indicates the proportion of sequences assigned to the taxa relative to the total number of sequences in the dataset. Prevalence (%) indicates the percentage of samples where the taxa are present with at least one sequence.

Microbial habitat	Fungal ASV	TITAN z score	Relative abundance (%)	Prevalence (%)
Topsoil	*Neocosmospora rubicola* ASV37	5.96	1.21	93.71
	Penicillium decumbens ASV66	5.8	0.56	75.47
	Bradymyces graniticola ASV647	5.45	0.02	11.95
	Emericellopsis minima ASV351	5.3	0.13	25.79
	Volutella ciliata ASV73	4.8	0.37	68.55
	Paraphoma pye ASV752	4.8	0.02	47.80
	Pseudeurotium bakeri ASV159	4.68	0.13	69.18
	Ascochyta medicaginicola ASV350	4.63	0.05	20.75
	Trichoderma hamatum ASV299	4.56	0.09	43.40
	Paraphoma radicina ASV589	4.46	0.01	64.78
Phyllosphere	*Plagiostoma pulchellum* ASV784	5.96	0.00	27.85
	Plectosphaerella cucumerina ASV645	5.87	0.00	32.28
	Curvularia hawaiiensis ASV326	5.73	0.00	25.32
	Cytospora prunicola ASV575	5.34	0.01	26.58
	Hormonema macrosporum ASV596	5.32	0.00	68.35
	Tremella phaeophysciae ASV523	5.27	0.03	49.37
	Bullera alba ASV242	4.04	0.17	83.54
	Plectosphaerella cucumerina ASV31	4.02	0.04	71.52
	Penicillium dierckxii ASV861	4.02	0.00	6.96
	Torula acaciae ASV805	3.83	0.01	53.16
Endosphere	*Fusarium brachygibbosum* ASV46	4.59	0.00	16.88
	Malassezia restricta ASV932	3.91	0.03	18.75
	Vishniacozyma dimennae ASV79	3.19	0.00	13.75

Table S9: Bacterial taxa indicators of low downy mildew primary inoculum in topsoil.
Bacterial ASVs which increase significantly in abundance as the concentration of P. viticola DNA in the topsoil decreases, according to the Threshold Indicator Taxa Analysis (TITAN) method (Baker *et al.*, 2023a), and they have the highest z scores. These results are based on the 2022 topsoil data. Relative abundance (%) indicates the proportion of sequences assigned to the taxa relative to the total number of sequences in the dataset. Prevalence (%) indicates the percentage of samples where the taxa are present with at least one sequence.

Microbial habitat	Bacterial ASV	TITAN z score	Relative abundance (%)	Prevalence (%)
Topsoil	*Exiguobacterium sibiricum* ASV169	7.08	0.01	26.88
	Streptomyces ambofaciens ASV915	6.73	0.02	69.38
	Bacillus megaterium ASV21	6.72	1.23	92.50
	Streptomyces albidoflavus ASV875	6.05	0.02	66.25
	Arthrobacter globiformis ASV281	5.69	0.16	80.63
	Arthrobacter globiformis ASV64	5.57	0.62	81.88
	Pseudarthrobacter equi ASV1234	5.29	0.02	50.63
	Arthrobacter globiformis ASV791	5.19	0.07	10.00
	Arthrobacter globiformis ASV1353	5.11	0.03	10.00
	Arthrobacter oryzae ASV45	4.97	0.89	91.88
Phyllosphere	*Clostridium magnum* ASV2013	8.73	0.00	8.13
	Terribacillus goriensis ASV1216	7.48	0.01	7.50
	Arthrobacter globiformis ASV281	7.45	0.03	38.75
	Methylobacterium isbiliense ASV1222	6.61	0.01	26.25
	Arthrobacter globiformis ASV791	6.59	0.01	10.00
	Arthrobacter globiformis ASV1353	6.38	0.00	8.75
	Caulobacter vibrioides ASV1261	5.93	0.01	13.75
	Arthrobacter pascens ASV307	5.3	0.04	43.75
	Streptomyces albidoflavus ASV875	5.15	0.01	26.25
	Streptococcus oralis ASV1602	5	0.07	31.25

Chapitre 4 : Le microbiome des espèces américaines de *Vitis* est-il impliqué dans leur résistance au mildiou de la vigne ?

Ce chapitre étudie comment le microbiote foliaire de deux espèces sauvages de *Vitis, Vitis aestivalis* et *Vitis labrusca*, présentes en Amérique du Nord et considérées comme les hôtes d'origine du mildiou qui infecte les vignes cultivées en Europe, pourrait contribuer à la résistance des vignes américaines à cette maladie. L'objectif de ce chapitre est d'identifier des consortia microbiens associés aux vignes résistantes au mildiou et de déterminer si ces consortia sont présents sur le territoire français.

L'échantillonnage s'est déroulé simultanément en Amérique du Nord et en Europe, avec des échantillons collectés dans plusieurs États du Nord-Est des États-Unis et dans trois collections ampélographiques en France. L'échantillonnage, effectué sur trois mois, de début juin à mi-août 2023, a consisté à collecter des feuilles de vignes sauvages, domestiquées, et de leurs hybrides dans des environnements naturels et cultivés (collections ampélographiques). L'analyse du microbiote foliaire et de la résistance au mildiou a été réalisée à l'échelle de l'individu. Le robot d'imagerie Blackbird été utilisé pour quantifier le développement du mildiou après 6 jours d'inoculation sur des disques foliaires.

Ce chapitre de ma thèse a été réalisé en collaboration avec Lance Cadle-Davidson (USDA) et les membres de son équipe basés à l'Université de Cornell. J'ai effectué un séjour de quatre mois dans l'État de New York, de juin à septembre 2023, durant lequel j'ai participé à la collecte de tous les échantillons américains, avec l'aide des collègues américains et avec l'aide de Patrice This (AGAP Institut) pour les deux premières semaines de mon séjour. En parallèle, j'ai coordonné à distance la collecte d'échantillons dans les trois collections ampélographiques françaises, menée sur le terrain par Corinne Vacher (UMR SAVE), Patrice This (AGAP Institut) et Père Mestre (UMR SVQV). J'ai également participé aux expériences de phénotypage de la résistance au mildiou sous la responsabilité d'Anna Underhill (USDA). Les extractions d'ADN des échantillons américains ont été réalisées par moi-même avec l'aide d'Amy Szewc-McFadden (USDA), tandis que les échantillons français ont été traités par Alexandre Chataigner (UMR SAVE). Le génotypage de la vigne a été réalisé par l'équipe de Lance Cadle-Davidson (USDA).

Le séquençage du microbiote est en cours sur la plateforme de séquençage adossée à AGAP Institut à Montpellier. Les données devraient être disponibles en octobre ou novembre 2024. Pour l'instant, j'ai donc rédigé l'introduction du chapitre et une partie des matériels et méthodes. Des analyses préliminaires des données de phénotypage et de génotypage de la vigne sont présentées.



Is the microbiome of American *Vitis* species involved in their resistance to grapevine downy mildew?

Paola Fournier, Corinne Vacher, Erin Galarneau, Anna Underhill, Alexandre Chataigner, Pere Mestre, Elsa Petit, Lance Cadle-Davidson, Patrice This.

In preparation

Introduction

North America shares a long history with both grapevines and their pathogens. North America is home to approximately 30 wild *Vitis* species (Zecca *et al.*, 2012), and recent studies suggest it is the center of origin of the genus (Zecca *et al.*, 2012; Wan *et al.*, 2013), though an alternative hypothesis suggests an Asian origin (Péros *et al.*, 2011). Many pathogen species, which are highly detrimental to European cultivated grapevine (*Vitis vinifera* L.), also originate from North America (Vorwerk & Forneck, 2006; Brewer & Milgroom, 2010). These pathogen species, which include the causal agents of phylloxera and mildews, were inadvertently introduced to Europe during the 19th century and are now widespread in most wine-growing regions worldwide (Bois *et al.*, 2017; Pirrello *et al.*, 2019). The wild *Vitis* species native to North America harbor accessions with varying degrees of resistance to these diseases (Cadle-Davidson, 2008; Péros et al., 2021). As a consequence, American *Vitis* species have played crucial roles in viticulture, initially as sources of phylloxera-resistant rootstocks and later as parents of interspecific rootstocks or grape producing interspecific hybrids cultivated on their own roots. More recently, they have emerged as valuable reservoirs of disease resistance genes in grapevine breeding programs (This *et al.*, 2006; Merdinoglu *et al.*, 2018; Schneider *et al.*, 2019). Whether or not they are also valuable reservoirs of beneficial microorganisms is still an open question that we explore in the present study.

The oomycete *Plasmopara viticola* (Berk. & M.A. Curtis) Berl. & De Toni, the causal agent of downy mildew, is one of the pathogen species of North-American origin that causes significant worldwide economic losses to viticulture (Taylor & Cook, 2018). *P. viticola* has been described on numerous genera within the American *Vitaceae* family (Rouxel *et al.*, 2013, 2014; Fontaine *et al.*, 2021). Five cryptic species have recently been identified within the *P. viticola* species complex, each exhibiting varying degrees of specialization within the *Vitaceae* family (Rouxel *et al.*, 2013, 2014). Recent research has shed light on the global invasion history of *P. viticola*: a specific cluster of *P. viticola* clade *aestivalis* served as the source for the invasion of cultivated grapevines in Europe in the mid-19th century. All invasive populations of grapevine downy mildew worldwide (outside the United States) belong to the small clade *P. viticola* f. sp. *aestivalis*, to which cultivated grapevine (*Vitis vinifera* L.) is highly sensitive. *P. viticola* f. sp. *aestivalis* parasitizes two grapevine species native to North America, *V. aestivalis* and *V. labrusca* within the northeastern United States. These two *Vitis* species are therefore considered the original hosts of the *P. viticola* populations that have invaded the world (Rouxel *et al.*, 2013, 2014; Fontaine *et al.*, 2021).

V. aestivalis and *V. labrusca* are widely distributed in the wild forests of eastern North America, primarily concentrated in the eastern regions of the United States and southern Canada. Natural interspecific hybrids between *V. labrusca* and *V. aestivalis*, as well as hybrids with other wild vines such as *V. riparia*, *V. rupestris*, and *V. cinerea*, have occasionally been observed and described. These crosses are made possible by the fact that these *Vitis* species are inter-fertile and their ranges overlap (Heinitz *et al.*, 2019).)For this reason, and because their display resistance to mildews (Cadle-Davidson, 2008; Péros et al., 2020), numerous interspecific hybrids between *V. vinifera* and *V. aestivalis*, and between *V. vinifera* and *V. labrusca* and between the 3 species, were created in the 19th century to combine desirable traits of each parent, such as disease resistance, grape flavor, vigor, and cold-hardiness. These crosses resulted in well-known varieties like 'Isabella', 'Concord', 'Niagara', and 'Catawba', which are cultivated in North America for wine production but also for sweet juice and jelly production. In Europe, these interspecific hybrid varieties and their wild parents are hardly cultivated but some individuals are present in grape collections.

The genetic basis of resistance to *P. viticola* has been studied through quantitative trait locus (QTL) analysis in various *Vitis* species from North America and Asia, resulting in the identification of 35 resistance (R) loci (Ricciardi *et al.*, 2024). These loci, referred to as Rpv (resistance to *P. viticola*), confer different levels of resistance, ranging from partial to complete (Dry *et al.*, 2019). Recent research suggests that interactions with the microbiome may also play an important role in protecting grapevines from pathogens (Koledenkova et al., 2022; Wicaksono et al., 2023, Fournier et al., submitted). Studies of the microbiome of wild American grapevines have found a high richness of endophytes (Kernaghan *et al.*, 2017; Fan *et al.*, 2020) and isolated strains with biocontrol properties against North American-origin pathogens (Brum *et al.*, 2012; Felber *et al.*, 2016; Kernaghan *et al.*, 2017). To date, there is little understanding of the relative contribution of disease resistance genes and of microorganisms on the resistance of American *Vitis* species to downy mildew.

The goal of the present study is to investigate the microbial drivers of disease resistance in grapevine. We specifically investigated whether the leaf microbiota of wild American *Vitis* species contributes to their resistance to downy mildew. First, we tested the hypothesis that (i) the removal of the phyllosphere microbiota, through surface-sterilization, decreases the resistance of *V. labrusca* and *V. aestivalis* to downy mildew. Then, we investigated whether (ii) the composition of the leaf microbiota correlates with the level of resistance to downy mildew, using various species and accessions of *Vitis* growing in North America to create a gradient in disease resistance. By using plants growing the same North-American collection, we also tested whether (iii) certain microbial taxa are more abundant in the leaves of *V. labrusca* and *V. aestivalis* compared to *V. vinifera*, potentially contributing to mildew resistance of *V. labrusca* and *V. aestivalis*. Finally, we extended the sampling to grape collections in France to investigate whether some of these potentially protective species are present in Europe on disease-resistant species or varieties.

Material and methods

Sampling of wild grapevines in North America

Between May 31 and June 8, 2023, leaves were collected from wild *V. aestivalis* and *V. labrusca* grapevines across various states in the northeastern USA, encompassing Maine, New Hampshire, Rhode Island, and Virginia. Additionally, on August 16 and 17, leaves from wild *V. aestivalis* were collected in the state of Massachusetts (Supplementary Table S1). On each plant, we collected eight leaves that were free from symptoms of downy mildew, using surgical gloves and disinfected scissors. The leaves were collected from different shoots of the same plant, by choosing the fifth leaf from the growing tip (Divilov et al., 2017) due to its consistent and predictable susceptibility to mildew.

Four leaves per plant (out of eight) were stored in a plastic bag for subsequent phenotyping of their resistance to downy mildew. Two leaves, sampled from 2 shoots growing close together, were stored in sterile plastic bags (NASCO™, Whirl-Pak®, USA) to analyze the total leaf microbiota, including both epiphytes and endophytes. Two leaves, also sampled from 2 shoots growing close together, were processed directly in the field to sample epiphytes (i.e. phyllosphere microbes *sensu stricto*). Each leaf was placed on autoclaved filter paper and microorganisms on the leaf surface were sampled by a complete swabbing of both sides of the leaf, using sterile cotton swabs (SARSTEDT, European Union) moistened with autoclaved PBS-tween buffer.

Leaves and swabs were shipped from field sampling locations to the lab in Geneva, NY overnight on ice. In the laboratory, samples dedicated to microbiota analyses were stored at -20◦ C, and samples intended for phenotyping were maintained at 4 °C until processed, the following day.

Sampling of grapevines growing in American and European collections

In addition, we collected grapevine leaves in four ampelographic repositories: the USDA Cold-Hardy Grape (Vitis) Collection (July 7, 2023) located in New York, USA; The Vine Biological Resource Centre (CRB-Vigne) located in Marseillan, France (July 18, 2023); the grape collection of Inrae Bordeaux at La Grande Ferrade in Villenave d'Ornon, France (July 7, 2023); and the grape collection of Inrae Colmar at Bergheim, France (July 20 and 21, 2023).

In each collection, we sampled vines identified as pure species (*V. vinifera*, *V. labrusca*, *V. aestivalis*) and interspecific hybrids derived exclusively from two or three of these species, based on family trees from the Vitis International Variety Catalogue (https://www.vivc.de/). Using unpublished phenotyping data, we selected *V. vinifera*, *V. labrusca*, and *V. aestivalis* accessions from the USDA Cold-Hardy Grape Collection to capture a range of susceptibility to downy mildew within each species. We included all interspecific hybrids that met our criteria. For *V. vinifera*, interspecific hybrids, and *V. aestivalis*, the number of sampled accessions was limited by the availability in the collection, while for *V. labrusca*, we restricted our sampling to 10 different accessions.

In the French collections, we selected *V. vinifera* cultivars and interspecific hybrids that overlapped with those in the USDA collection, along with some *V. labrusca* and *V. aestivalis* plants, though the latter two species were limited due to their low availability.

For each selected accession, we sampled two or three plants, depending on availability. Leaves were collected from different shoots, selecting the fifth leaf from the growing tip, free from downy mildew symptoms, using sterile gloves and disinfected scissors (as described above). In the USDA collection, we sampled eight leaves per plant (as described above), while in the three French collections, we took two leaves per plant: one leaf was used to analyse the total leaf microbiota (including both epiphytes and endophytes), while the other was swabbed in the laboratory to specifically sample epiphytes (i.e. phyllosphere microbes *sensu stricto*).

Effect of removal of phyllosphere microbiota with bleach on disease symptoms

Leaves collected in America (from wild and domesticated plants) for disease resistance phenotyping were used in a controlled experiment to assess the effect of epiphyte removal on downy mildew resistance. Each leaf was cut in half with a razor and placed in perforated plastic sleeves. One half of the leaf was treated with bleach to remove epiphytes. The other half was left untreated (control treatment). The bleached leaf halves were washed in an 8% sodium hypochlorite solution for 2 minutes and then rinsed in deionised water for 6 minutes. Leaves from both treatments were then stored at 4°C until leaf discs could be prepared for disease resistance phenotyping on the same day.

Phenotyping for downy mildew (DM) resistance

Phenotyping for downy mildew resistance was performed at the phenotyping center in Geneva, NY, following a protocol outlined in previous studies (Qiu et al., 2022; Sapkota et al., 2023). Discs were punched out of each leaf using a 1cm leather punch, then were placed the abaxial side up on a 0.7% (w/v) agar in water. Blackbird imaging tray. Due to logistical constraints related to the number of samples processed daily, we cut 2 or 4 discs per leaf (1 or 2 on each side of the main vein). A sporangia suspension was prepared by collecting sporangia from the surface of a grapevine leaf with water. The concentration was estimated under a microscope using a Malassez cell, and water was added until it reached approximately 1.0 x 10^5sporangia/mL. The disks were inoculated by evenly spraying the sporangia suspension onto the leaf disks using a 15 mL tube (Corning Inc., Falcon® Tubes, USA) with a spray screwed on instead of the cap. Trays were then placed in the dark for about 14 hrs after inoculation, after which droplets were blotted from samples. Samples were incubated at 20° C with a 12hr day/night cycle. We added multiple discs from Thompson Seedless or Chardonnay grape variety, known to be susceptible to DM, to each tray as a negative control.

Sample trays were removed from incubators and imaged at 3, 4, 5, and 6 dpi (post-infection days) using the Blackbird imaging system (Printersys, Algayón, Spain). The downy mildew resistance phenotype of the vines was measured as the percentage of the surface of each disc covered by downy mildew symptoms. This measurement was carried out using ImageJ software (Schneider *et al.*, 2012).

DNA extraction of leaf samples collected in North America

DNA extractions were performed at the USDA Grape Genetics Research Unit in Geneva, New York, USA. We used the PowerSoil® Pro Kit (QIAGEN®, Germany) to extract DNA from the swabs used to sample phyllosphere microorganisms. The heads of the two cotton swabs used to swab each two leaves forming a sample were placed together into one PowerBead® Pro Tube (QIAGEN®, Germany). To enhance the cell lysis step, the tubes were incubated at 65°C for 10 minutes after the addition of CD1 lysis buffer and before the homogenization step. The DNeasy 96 Plant Kits (QIAGEN®, Germany) was used to extract DNA from the total leaf microbiota. We cut a 0.8 mm diameter disc on each of the two leaves collected from the same plant. The two discs were placed together in a tube of a 96-well extraction plate. Following a protocol previously described in the literature (Hyma et al., 2015), two stainless steel beads were added to each tube, and the entire plate was frozen at -80°C. Once completely frozen, the plates were agitated using a Geno/Grinder 2000 (OPS Diagnostics LLC, Lebanon NJ, USA). The plates were then stored at -80°C until DNA extraction. To enhance DNA quality and quantity, we added PVP-40 (2% w/v) to the AP1 lysis buffer before heating. We otherwise followed to protocol of the manufacturer. At the end of the extraction process, DNA solutions were lyophilized and then sent to France, where they were rehydrated in the elution buffer used for extraction.

DNA extraction of leaf samples collected in France

DNA extraction protocols for leaf samples collected in France were identical to those used for American samples, except for three differences. Only one swab head was used to extract DNA from phyllosphere samples, the two 0.8 mm diameter discs were collected from the same leaf, and the plates were agitated using a TissueLyser II (QIAGEN®, Germany).

Metabarcoding of fungal and bacterial communities

To characterize bacterial communities, we amplified the V5-V6 region of the bacterial 16S ribosomal RNA (rRNA) gene using the chloroplast-excluding forward primer 799f (Chelius and Triplett 2001) and the reverse primer 1115R (Reysenbach and Pace 1995) (primers forward TACGGRAGGCAGCAG, reverse AGGGTTGCGCTCGTTG). For fungi, we targeted the internal transcribed spacer 1 (ITS1) region of the fungal ITS ribosomal DNA gene using the forward primer ITS1F (Gardes and Bruns 1993) and the reverse primer ITS2 (White et al. 1990) (primers forward, CTTGGTCATTTAGAGGAAGTAA, reverse GCTGCGTTCTTCATCGATGC). Primers targeting these regions were designed with an Illumina tail. In order to reduce interference during Illumina sequencing, we also added frame-shifts of 1 to 6 random nucleotides for the forward primers and 2 to 7 nucleotides for the reverse primers, between the target sequence and the Illumina tail. All the primers used are listed in (Supplementary Table S2). For each forward or reverse primer, an equal mix of the three primers containing the different frame-shifts was added to the PCR mix.

PCRs were performed with 2 µl of template DNA, 0.75µl of each equimolar mix of primers concentrated to 10µM, 0.2 µl of KAPA3G Plant DNA Polymerase concentrated to 2.5U/µL, 13.5 µl of KAPA Plant PCR Buffer (2X) containing MgCl2 and dNTPs, and ultrapure water to 23 µl.

We utilized the KAPA3G Plant kit (Kapa Biosystems, Wilmington, MA, USA) due to the resilience of the KAPA3G Plant DNA Polymerase against the presence of grape polyphenol residues in the reaction mix (Kapa Biosystems, Technical Data Sheet, Wilmington, MA, USA). The thermocycling conditions for 16S amplification were as follows: initial denaturation at 95°C for 15 min, followed by 30 cycles at 95°C for 30 s, 49°C for 30 s, 72°C for 30 s, with a final extension of 72°C for 5 min. Thermocycling conditions for ITS amplification were: 95°C/15 min; 95°C/30 s, 56°C/30 s, 72°C/30 s for 35 cycles; and 72°C/5 min. Amplifications were confirmed by electrophoresis on a 2% agarose gel.

Each PCR plate had three types of controls. Negative DNA extraction controls involved PCR amplification of an extraction performed in an initially empty tube, without any sample. Negative PCR controls replaced the DNA template with ultrapure water during PCR amplification. Positive PCR controls comprised PCR amplifications utilizing the DNA of specific known species. These included two marine bacteria, *Sulfitobacter pontiacus* and *Vibrio splendidus*, and two fungi, *Candida oceani* and *Yamadazyma barbieri*, selected because they are unlikely to be found in our samples.

The second PCR was used for the incorporation of Illumina Nextera dual-indexed adapters (with 12 cycles). Bead purifications were carried out after each PCR step. Quantification, normalization and pooling were carried out before sequencing on an Illumina NovaSeq 6000 SP flowcell with the 2 x 250 bases paire-end protocol.

Grapevine genotyping

Genotyping was used to validate the correct visual assignment of grapevines collected in the wild and in the USDA Cold-Hardy Grape (*Vitis*) Collection. Leaf samples collected in America were all genotyped using rhAmpSeq markers as initially described (Zou *et al.*, 2020).

Bioinformatics

Bioinformatic analysis of Illumina sequence data was performed using version 4.1 of the FROGS pipeline (Escudié *et al.*, 2018) on the Genotoul remote server (The Galaxy Community, 2024). Separate analyses were performed for each barcode region (nrDNA ITS or 16S rRNA genes). The FROGS pipeline first assembled raw forward and reverse reads for each sample into paired-end reads with a minimum overlap of 10 nucleotides and a maximum mismatch of 0.1 using the VSEARCH algorithm (Rognes *et al.*, 2016). For fungal data, unmerged reads were artificially joined by inserting a 100 N sequence between the forward and reverse reads (Escudié *et al.*, 2018). The primers were removed using Cutadapt (Martin, 2011). Sequences containing ambiguous nucleotides or whose size did not match the expected amplicon size (between 50 and 600 bp for the rDNA ITS gene and 250-400 bp for the 16S rRNA gene) were filtered out. The sequences were then dereplicated and clustered using SWARM (Mahé *et al.*, 2014) with a local clustering threshold parameter set to 1 and the 'fastidious' option enabled (Bernard *et al.*, 2021). These clusters of sequences are very similar in construction to Amplicon Sequence Variants (ASVs) (Hakimzadeh *et al.*, 2024) and are hereafter referred to as ASVs. Chimeras were detected and removed using VSEARCH (Rognes *et al.*, 2016). A stringent filtering step was

applied, which consisted of retaining only ASVs representing at least 0.00005% of the sequences in the dataset. For the fungal data, the highly variable part of the ITS1 region was extracted using ITSx (Bengtsson-Palme *et al.*, 2013).

Taxonomic assignments of bacterial and fungal ASVs obtained from Illumina sequence data were performed using the SILVA 138.1 (Quast *et al.*, 2013) and UNITE Fungi 8.3 (Nilsson *et al.*, 2019b) reference databases, respectively, using both the RDPClassifier (Wang *et al.*, 2007) and BLASTn+ algorithms (Camacho *et al.*, 2009).

Finally, we decontaminated the datasets using the *metabaR* R package v1.0.0 (Zinger *et al.*, 2021). The *contaslayer* function was used to identify ASVs whose relative abundance in the entire dataset was highest in at least one control compared with true samples (Zinger *et al.*, 2021). These ASVs were considered contaminants and were removed from the dataset. Next, the *tagjumpslayer* function was used to detect artifacts such as tag jumps and reduce the noise they cause by removing an ASV from a given PCR product if its relative abundance across the entire dataset was below a specified threshold. This threshold was determined empirically, as recommended in the metabaR tutorial ("Let's metabaR! • metabaR"), using the visualization functions of the *metabaR* package created for this purpose. Finally, a histogram of the number of reads per sample was plotted, and samples with low sequencing depth, located in the lower tail of the normal distribution curve, were considered failed PCRs and removed.

Statistical analysis

All the statistical analyses were performed with R v4.2.3 (R Core Team, 2023). Microbial community analyses were performed using the R packages *phyloseq* v1.48.0 (McMurdie & Holmes, 2013) and *speedyseq* v0.5.3.9018 (McLaren, 2023), and all figures were generated using the *ggplot2* v3 package. 5.1 (Wickham, 2016), *cowplot* v1.1.3 (Wilke, 2024), *ggh4x* v0.2.8 (van den Brand, 2024), ggsignif v0.6.4 (Ahlmann-Eltze & Patil, 2021), *patchwork* v1.2.0 (Pedersen, 2024), *microViz* v0.10.8 (Barnett *et al.*, 2021), and *ggtext* v0.1.2 (Wilke and Wiernik, 2022).

Multidimensional Scaling (MDS) analysis was performed on rhAmpSeq data to verify whether wild-collected vines were genetically pure *Vitis aestivalis* or *Vitis labrusca*. Vines were grouped into three categories: those from the USDA Cold Hardy Grape (Vitis) Collection as either (1) expected pure species (*V. vinifera*, *V. aestivalis*, and *V. labrusca*) or (2) expected hybrids (interspecific hybrid vines), and those collected from the wild whose status was "to be determined". We drew ellipses around the samples expected to be pure species or interspecific hybrids, generating four distinct clusters: interspecific hybrids, *V. vinifera*, *V. aestivalis*, and *V. labrusca*. The goal was to see if the wild vines clustered within the *V. aestivalis* or *V. labrusca* ellipses, validating their visual identification for use in further analyses that require genotype as an explanatory variable (such as differential abundance analyses). Otherwise, these wild vines were excluded from future genotype-related analyses.

Analysis of the impact of phyllosphere microbiota presence on the susceptibility phenotype of *Vitis* plants to downy mildew

We evaluated the relationship between the presence or absence of phyllosphere microbiota on the leaf, experimentally removed or not through surface sterilization, and the susceptibility phenotype of *Vitis* plants to downy mildew (hypothesis i) using a linear mixed-effects model. The model included susceptibility phenotype to downy mildew, measured as the percentage of disc leaf covered by downy mildew symptoms as the dependent variable and the presence of phyllosphere microbiota (yes or no) as a fixed factor. Additional fixed factors that could influence phenotype were also considered: plant species or variety, life context (wild or cultivated), and geography. The replicate number of each disc belonging to the same sample (between 8 and 16 depending on the experiment) and the number of the tray containing the disc during the phenotyping stage were included as random effects. Models were built using the *lmer* function from v3.1.3 of the *lmerTest* package (Kuznetsova *et al.*, 2017) and evaluated with Type II ANOVA using v3.1.2 of the *car* package (Fox & Weisberg, 2018). Graphical checks for homoscedasticity and normality of the residuals were performed using the packages *performance* v0.12.0 (Lüdecke *et al.*, 2021) and *DHARMa* v0.4.6 (Hartig & Lohse, 2022). The variance explained by the model was estimated using the conditional coefficient of determination (R^2c) and the marginal coefficient of determination (R^2m) provided by the r2 function of the *performance* package. The former coefficient represents the variance explained by the entire model, whereas the latter represents the variance explained by the fixed effects only.

Testing whether the composition of the leaf microbiota correlates with the resistance phenotype of *Vitis* plants to downy mildew

In addition, we investigated whether the composition of the leaf microbiota correlates with theresistance phenotype of *Vitis* plants to downy mildew (hypothesis ii), and specifically if samples with high values of susceptibility phenotype harbored in their microbiota, a specific set of microbial taxa, using the Threshold Indicator Taxa ANalysis (TITAN) method of the *TITAN2* package v2.4.3 (Baker *et al.*, 2023a).

Testing whether certain microbial taxa are more abundant in the leaves of *V. labrusca* and *V. aestivalis* compared to *V. vinifera*

To investigate whether certain microbial taxa are more abundant in the leaves of *V. labrusca* and *V. aestivalis* compared to *V. vinifera* (hypothesis iii), we used a set of four Differential Abundance Analysis (DAA) methods recommended in the recent literature: ANCOM-BC2 (Lin & Peddada, 2024), Maaslin2 (Mallick *et al.*, 2021), LinDA (Zhou *et al.*, 2022) and ZicoSeq (Yang & Chen, 2022). For all four methods, the life context (wild or cultivated) was included Leaf disc replicates and trays were included as random effects, and the parameters were set to defaults except for the minimum prevalence threshold, which was set to 10%, and the adjusted p value for an ASV to be considered differentially abundant, which was set to 0.05. All analyses were performed using the *ANCOMBC* v2.0.3 (Lin & Peddada, 2020; Lin *et al.*, 2022), *Maaslin2* v1.12.0 (Mallick *et al.*, 2021), *GUniFrac* v1.8 (Chen *et al.*, 2023), and *MicrobiomeStat* v1.2 (Zhang *et al.*, 2024) packages.

Results

In total, we collected 330 leaf samples, 117 of *Vitis labrusca*, 57 of *Vitis aestivalis*, 106 of *Vitis vinifera*, and 50 interspecific hybrids of these (Table 1). A total of 122 individuals were sampled in the wild and 208 in cultivated conditions (Table 1 and Fig. 1). Additional data from these individuals are presented in Supplementary Table S2. Vines collected in the wild were visually identified and classified as either *V. labrusca* or *V. aestivalis* by expert opinion.

Table 1: Summary of the numbers of collected samples.
We collected the non-domesticated grapevines *V. labrusca* and *V. aestivalis*, both in wild and cultivated conditions and *V. vinifera* only in grape collections.

	Northeastern United States		France			Total
	Wild	Collection (NY states)	Collection (Bordeaux)	Collection (Bergheim)	Collection (Marseillan)	
V. labrusca	87*	19 (9)**	3 (1)**	4 (2)**	4 (2)**	117
V. aestivalis	35*	11 (5)**	3 (2)**	4 (2)**	4 (2)**	57
Interspecific hybrid	0	32 (17)**	2 (unknown)	8 (2)**	8 (5)**	50
V. vinifera	0	18 (13)**	30 (unknown)	31 (10)**	27 (13)**	106
Total	122	80	38	47	43	330

*The grapevines collected in the wild were visually identified and classified either as *V. labrusca* or *V. aestivalis*
**: in parenthesis, number of accessions sampled

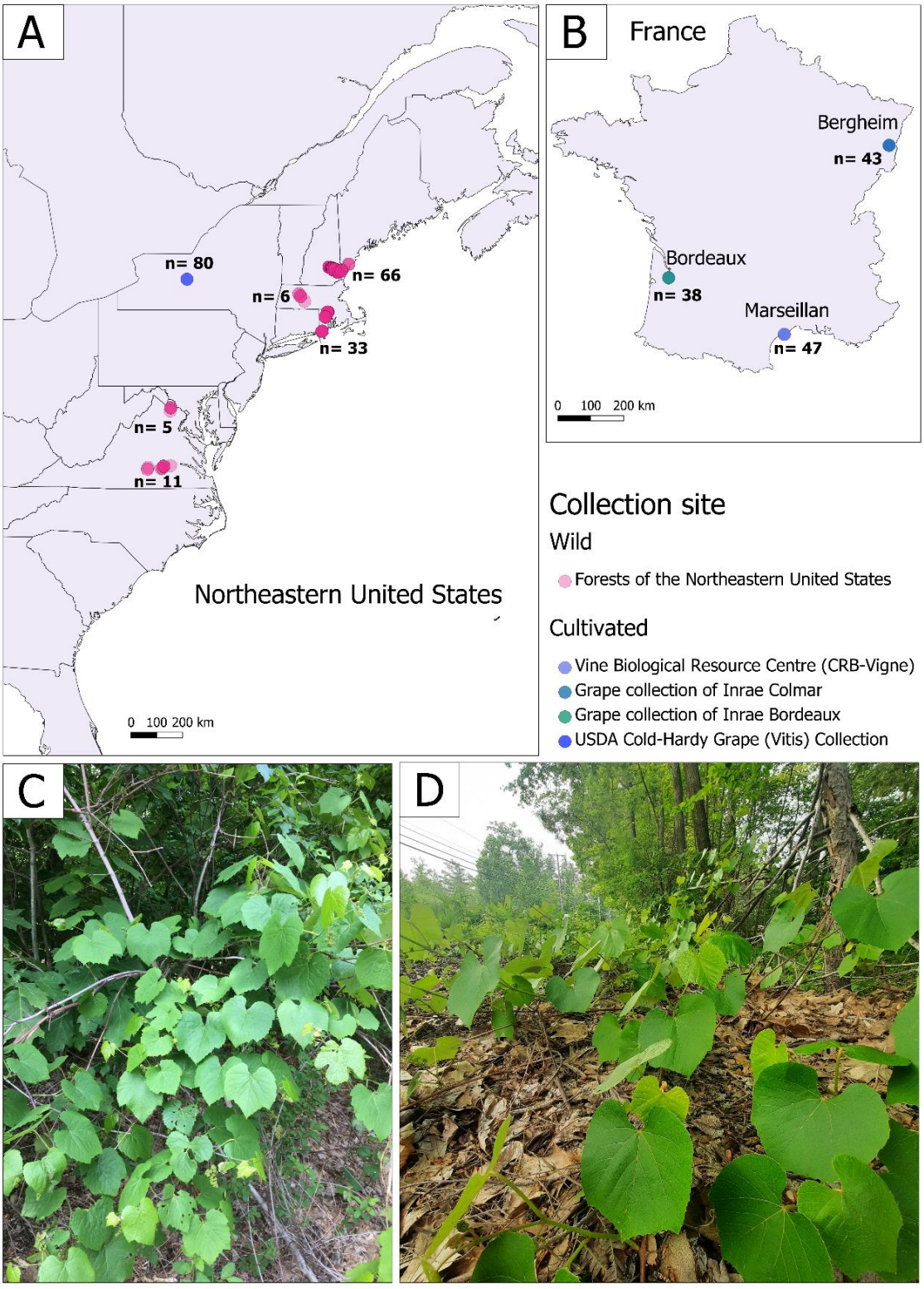


Figure 1: Location of collected samples.
Leaves of *V. aestivalis* and *V. Labrusca* were collected under wild conditions in various states of the north-eastern United States as indicated on the map of NE USA (A). (Other samples of *V. aestivalis, V. labrusca, V. vinifera* and hybrids were collected under cultivated conditions in a collection located in the USDA Cold-Hardy Grape (Vitis) Collection in Geneva, NY (A) and in three collections in France (B). The number of samples corresponding to each point or group of points is indicated on the maps by 'n'. *Vitis aestivalis* (C) and *Vitis labrusca* (D) growing in their natural conditions at the roadside, spreading over various supports such as soil, hedges and trees. Source : P. Fournier (UMR SAVE, INRAE) et P. THIS (UMR AGAP, INRAE).

Grapevine genotyping

We confirmed the visual identification of samples collected in the wild by carrying out a complete analysis of the dataset using rhAmpSeq markers, specifically designed to distinguish *Vitis* species (Zou *et al.*, 2020). Most of the visual identifications were successful. Indeed, wild grapevines, visually assigned to *V. labrusca* and *V. aestivalis* species, clustered closely with samples of these same species from the USDA Cold-Hardy Grape (*Vitis*) collection, for which assignments are assumed to be reliable (Fig. 2). Samples within the *V. aestivalis* (light-blue) and *V. labrusca* (dark-blue) ellipses of the PCA are most likely pure *V. aestivalis* and *V. labrusca,* representing 23 and 82 samples, respectively. In addition, the five light blue stars in the bottom right of the *V. aestivalis* ellipse (light-blue) are probably pure *V. aestivalis* (5 samples), compiling 28 samples of pure *V. aestivalis* in total. The mixture of light and dark blue stars along the path between the two blue ellipses are probably interspecific hybrids between *V. aestivalis* and *V. labrusca* (9 samples).

Finally, it is likely that some plants in the collection, notably 5 *V. labrusca*, 1 *V. aestivalis* and 7 *V. vinifera*, are interspecific hybrids incorrectly identified as pure species, or that errors were made during sampling.

Grapevine phenotyping for downy mildew resistance

Overall, we observed a gradient of susceptibility to downy mildew, ranging from 0 to 49% of the leaf surface covered by downy mildew symptoms in cultivated conditions (Fig. 3A) and from 0 to 55% in wild conditions (Fig. 3B). As expected, the grapevines showing the highest susceptibility phenotypes were *V. vinifera* in cultivated conditions, in particular the variety named Zengoe, Karmrajut, Zefir, Feteasca Neagra, Agriay, Ehrenfelser and Norakert (Fig. 3A). In general, *V. aestivalis* and *V. labrusca* occupied the lowest values of the gradient, except for two accessions, *V. aestivalis* 3303 and *V. labrusca* Rem NE 20, while interspecific hybrids occupied the center of the gradient (Fig. 3A). These hierarchy in susceptibility are in line with our expectations. However, we note the total resistance of two *V. vinifera* cultivars in this experiment, namely Feteasca alba and Lampheare.

Sequencing data from the samples have been obtained only on October 17th, too late to be analyzed in time to include the results in the present document. They will be analyzed as soon as possible and will be included in the final version of the manuscript.

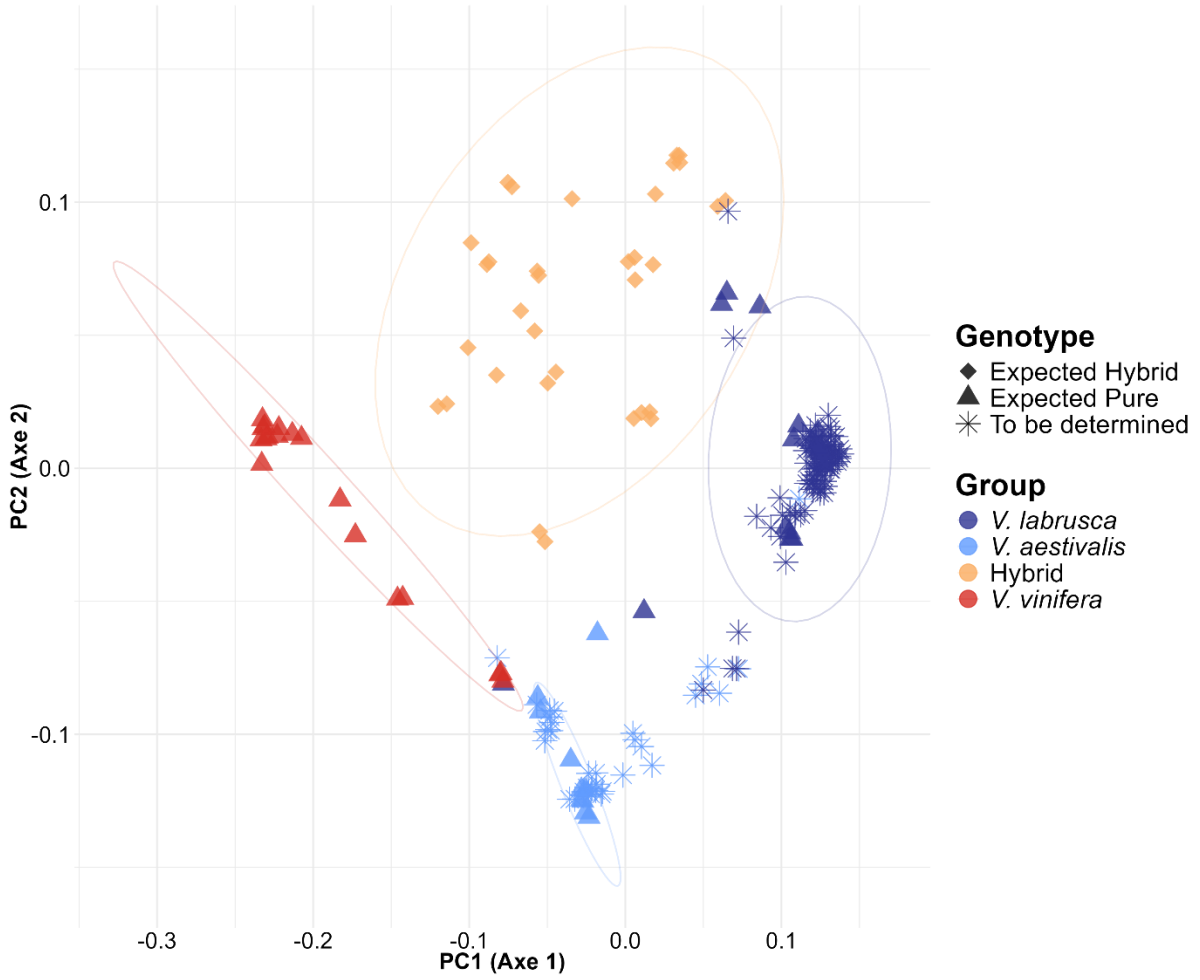


Figure 2: Multidimensional Scaling (MDS) analysis based on rhAmpSeq markers for American samples.

Each point represents a sample. Samples from the USDA Cold-Hardy Grape (Vitis) collection are those for which identification is assumed to be reliable; interspecific hybrids are represented by a diamond symbol, while pure species such as *V. vinifera*, *V. labrusca*, and *V. aestivalis* are indicated by a triangle symbol. Samples collected from the wild have only a visual identification, represented by a star ("to be determined"), and their assignment by the group variable requires confirmation. Depending on the position of the point for a specific sample, it can be considered either as a pure species if it is grouped with other pure species samples, or as a interspecific hybrid if it is grouped with interspecific hybrids or between pure species points.

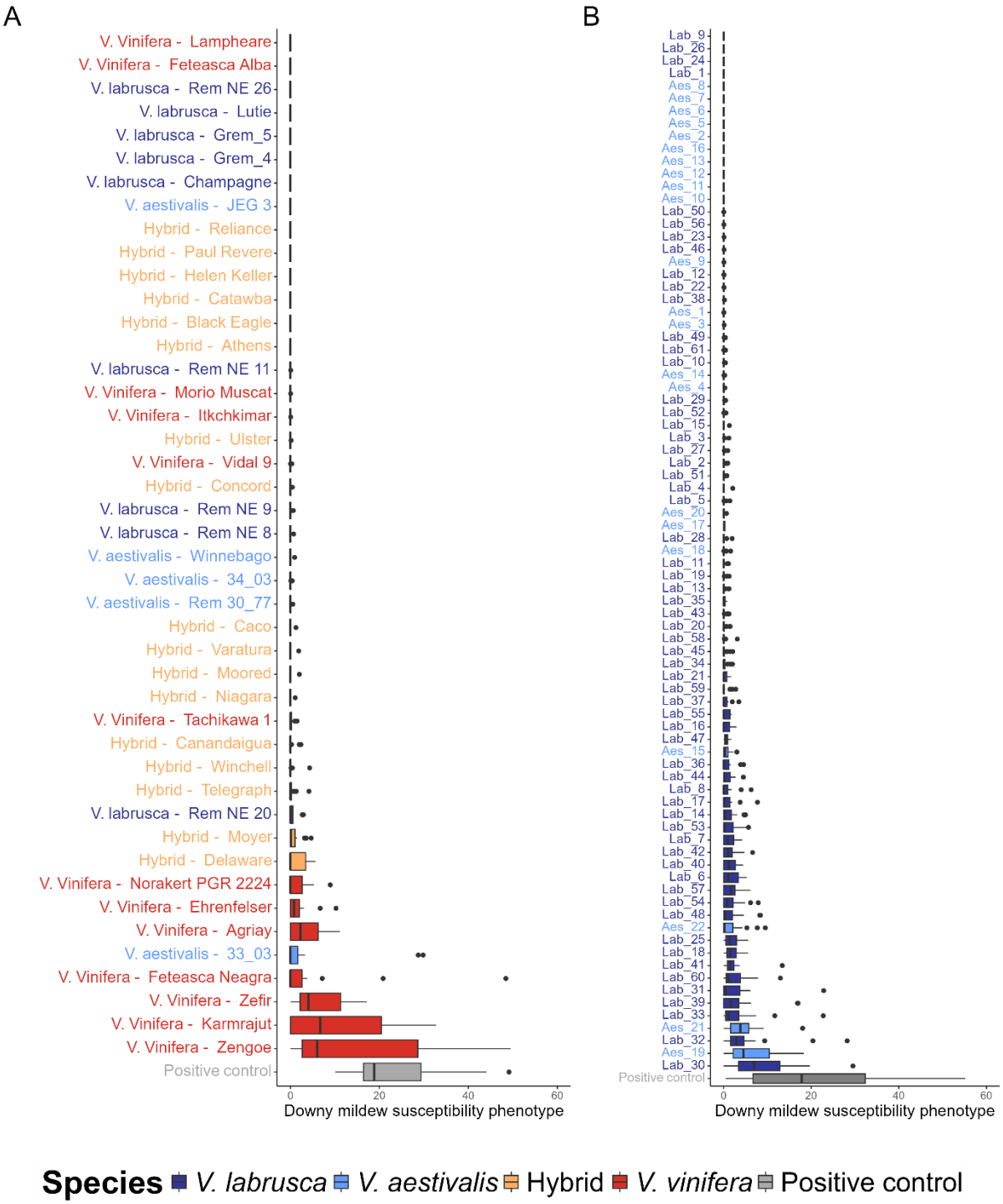
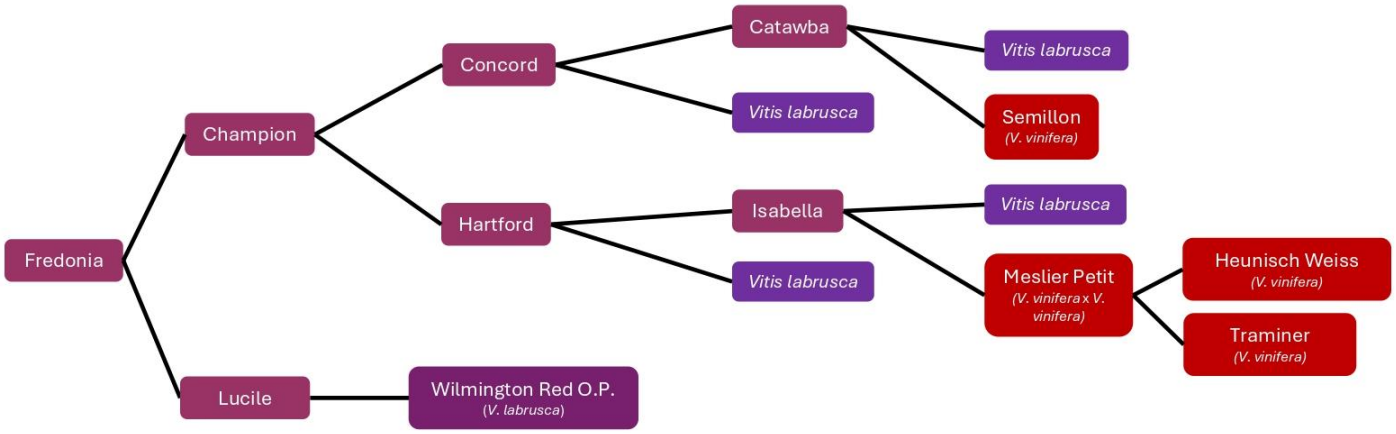
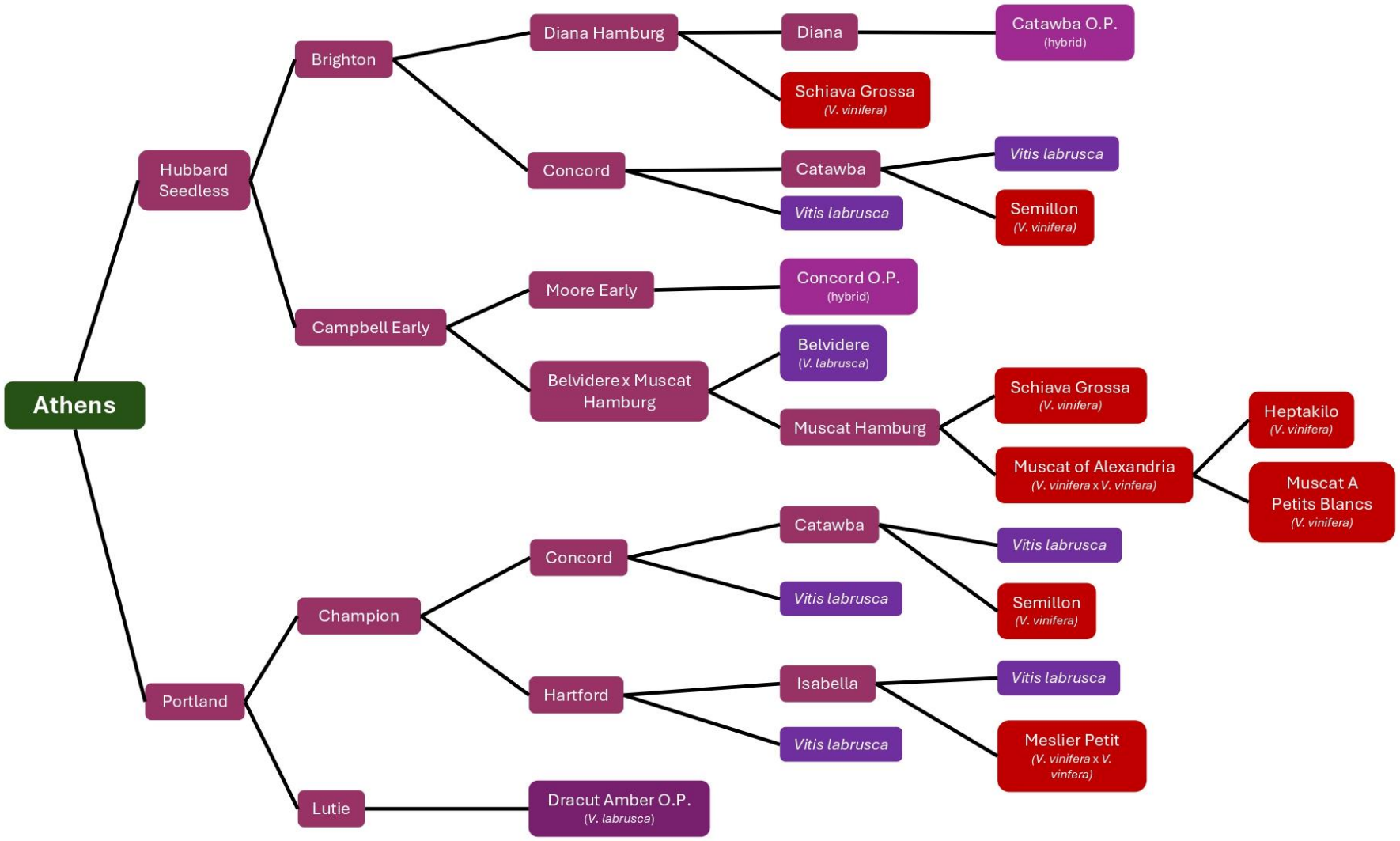


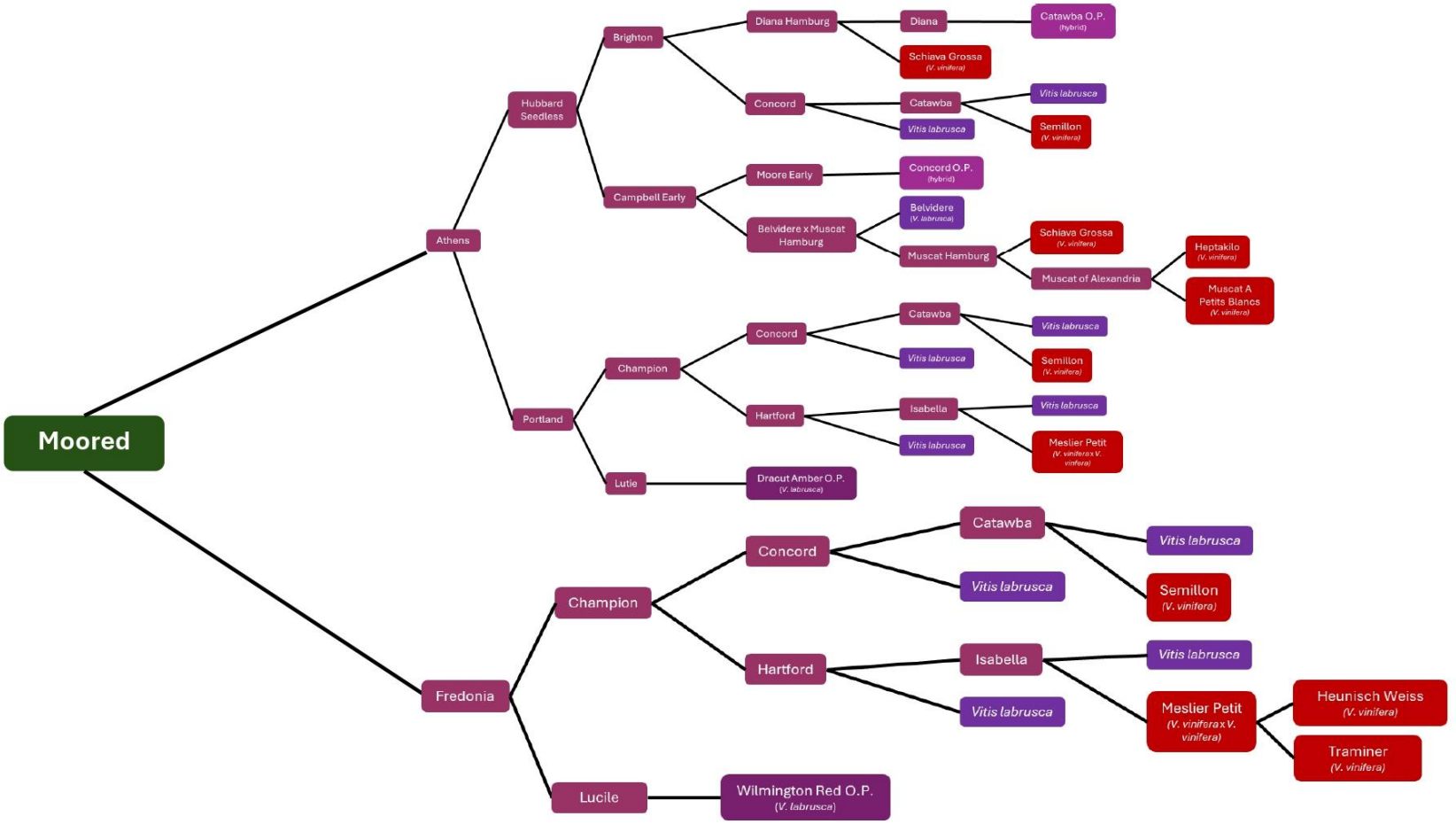
Figure 3: Susceptibility phenotype of samples to downy mildew.
Percentage of leaf disc area covered by downy mildew in samples collected from (A) cultivated (USDA Cold-Hardy Vitis Collection) with expected reliable genotype and (B) wild conditions. Each boxplot represents data from one or two plants of the same accession, with (A) 8 discs/plant and (B) 6 discs/plant. (A), y-axis labels indicate species followed by the variety or accession name for *V. aestivalis* and *V. labrusca*. (B) sample names are shown, with names starting with 'Aes' and 'Lab' visually assigned to *V. aestivalis* and *V. labrusca*, respectively. Samples are sorted by the mean across replicates.

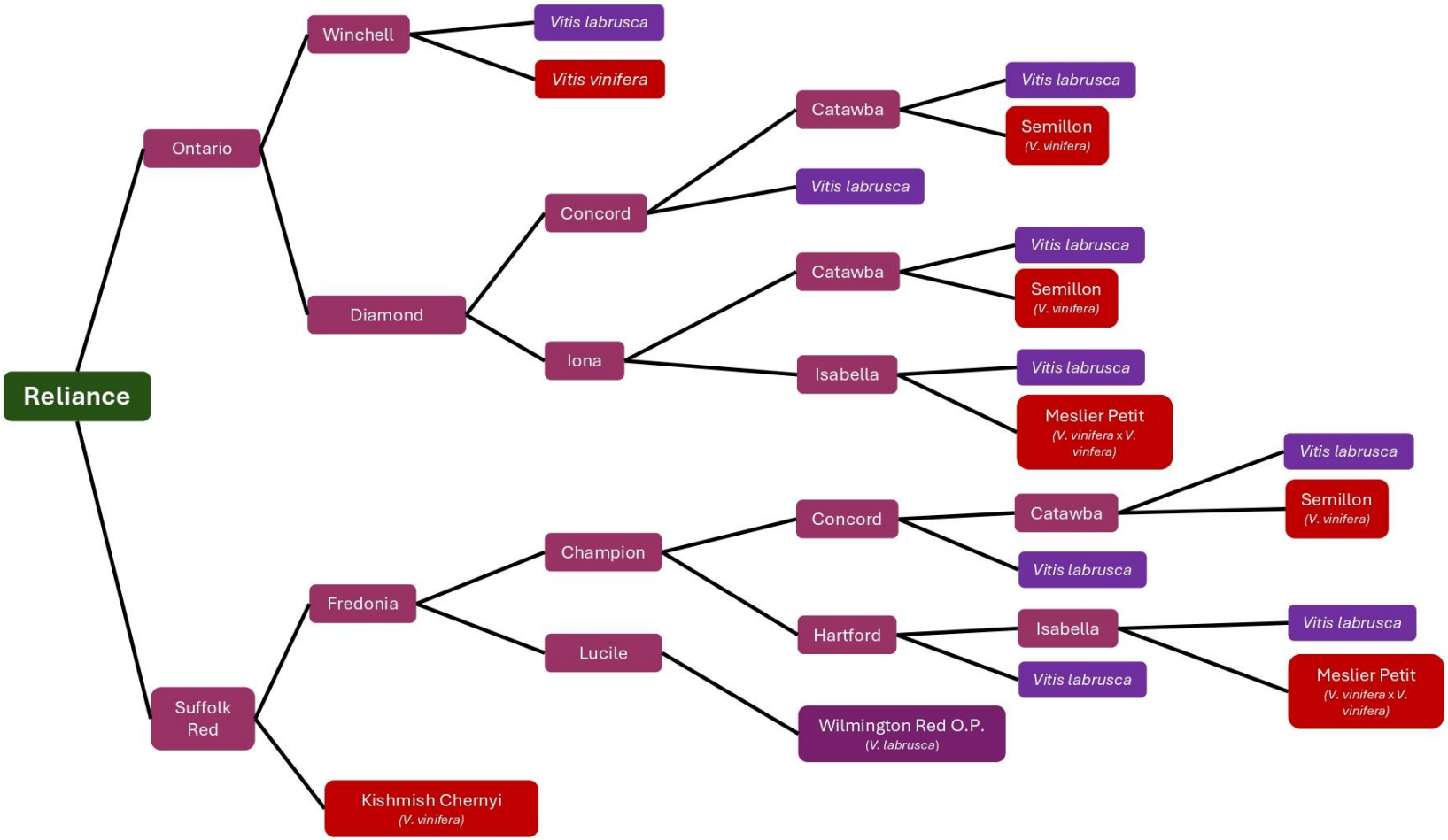
Supplementary figures

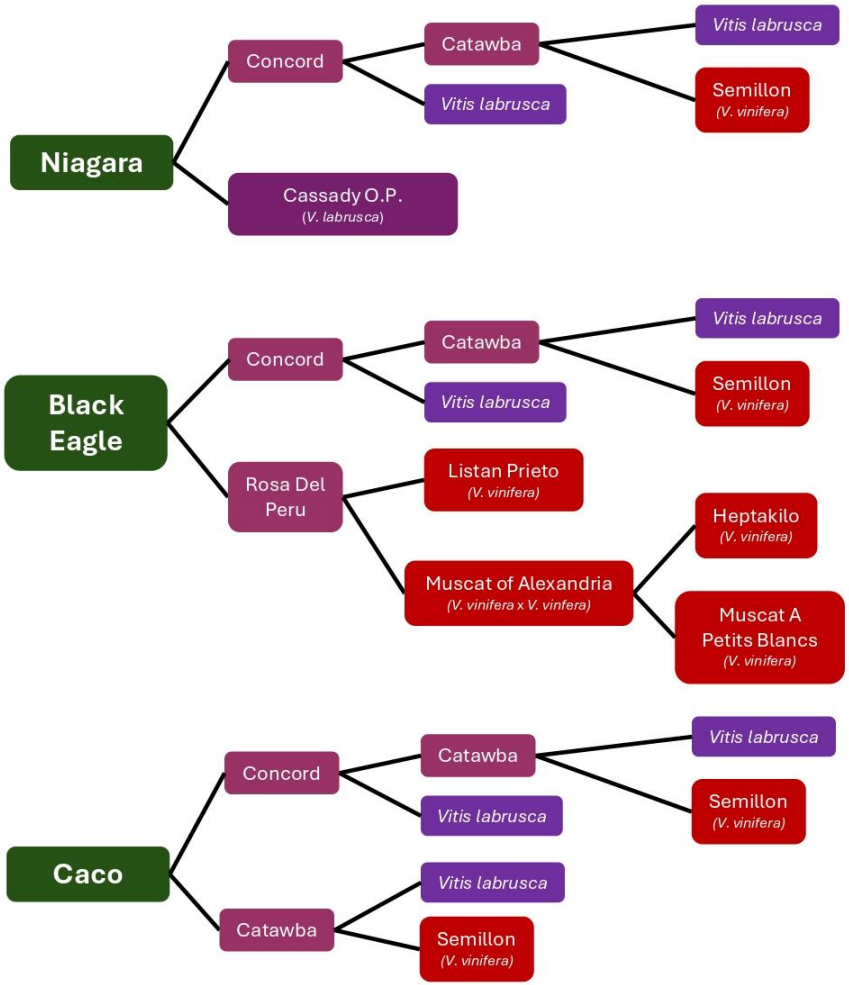
Supplementary Figure 1: Pedigree of interspecific hybrid grape varieties in the USDA Cold-Hardy Grape (Vitis) Collection. Varieties in red indicate a pure *Vitis vinifera*, in purple a pure *Vitis labrusca*, and in pink a interspecific hybrid between *Vitis aestivalis* and *Vitis labrusca*. These pedigrees illustrate the lineage of the different variety of interspecific hybrids sampled in the repository, showing the parentage and the crosses that contributed to their development. Source: Erin Galarneau (USDA-ARS).

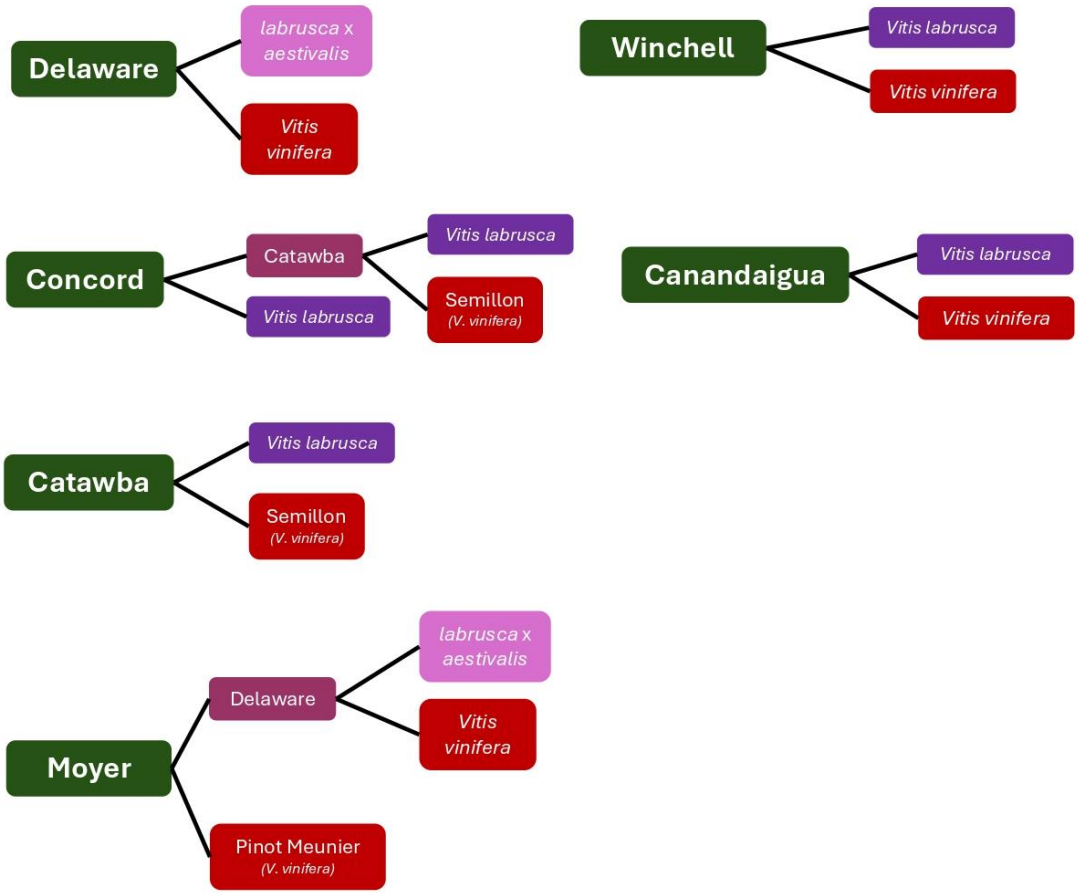



Athens
Hubbard Seedless
Brighton
Diana Hamburg
Diana
Catawba O.P. (hybrid)
Schiava Grossa (V. vinifera)
Concord
Catawba
Vitis labrusca
Semillon (V. vinifera)
Vitis labrusca
Campbell Early
Moore Early
Concord O.P. (hybrid)
Belvidere x Muscat Hamburg
Belvidere (V. labrusca)
Muscat Hamburg
Schiava Grossa (V. vinifera)
Muscat of Alexandria (V. vinifera x V. vinfera)
Heptakilo (V. vinifera)
Muscat A Petits Blancs (V. vinifera)
Portland
Champion
Concord
Catawba
Vitis labrusca
Semillon (V. vinifera)
Vitis labrusca
Hartford
Isabella
Vitis labrusca
Meslier Petit (V. vinifera x V. vinfera)
Vitis labrusca
Lutie
Dracut Amber O.P. (V. labrusca)


Moored
Athens
Hubbard Seedless
Brighton
Diana Hamburg
Diana
Catawba O.P. (hybrid)
Schiava Grossa (V. vinifera)
Concord
Catawba
Vitis labrusca
Semillon (V. vinifera)
Vitis labrusca
Campbell Early
Moore Early
Concord O.P. (hybrid)
Belvidere x Muscat Hamburg
Belvidere (V. labrusca)
Muscat Hamburg
Schiava Grossa (V. vinifera)
Muscat of Alexandria
Heptakilo (V. vinifera)
Muscat A Petits Blancs (V. vinifera)
Portland
Champion
Concord
Catawba
Vitis labrusca
Semillon (V. vinifera)
Vitis labrusca
Hartford
Isabella
Vitis labrusca
Meslier Petit (V. vinifera x V. vinifera)
Vitis labrusca
Lutie
Dracut Amber O.P. (V. labrusca)
Fredonia
Champion
Concord
Catawba
Vitis labrusca
Semillon (V. vinifera)
Vitis labrusca
Hartford
Isabella
Vitis labrusca
Meslier Petit (V. vinifera x V. vinifera)
Heunisch Weiss (V. vinifera)
Traminer (V. vinifera)
Vitis labrusca
Lucile
Wilmington Red O.P. (V. labrusca)


Reliance
Ontario
Winchell
Vitis labrusca
Vitis vinifera
Diamond
Concord
Catawba
Vitis labrusca
Semillon
(V. vinifera)
Vitis labrusca
Iona
Catawba
Vitis labrusca
Semillon
(V. vinifera)
Isabella
Vitis labrusca
Meslier Petit
(V. vinifera x V. vinfera)
Suffolk Red
Fredonia
Champion
Concord
Catawba
Vitis labrusca
Semillon
(V. vinifera)
Vitis labrusca
Hartford
Isabella
Vitis labrusca
Meslier Petit
(V. vinifera x V. vinifera)
Vitis labrusca
Lucile
Wilmington Red O.P.
(V. labrusca)
Kishmish Chernyi
(V. vinifera)


Niagara
Concord
Catawba
Vitis labrusca
Semillon
(V. vinifera)
Vitis labrusca
Cassady O.P.
(V. labrusca)
Black Eagle
Concord
Catawba
Vitis labrusca
Semillon
(V. vinifera)
Vitis labrusca
Rosa Del Peru
Listan Prieto
(V. vinifera)
Muscat of Alexandria
(V. vinifera x V. vinfera)
Heptakilo
(V. vinifera)
Muscat A Petits Blancs
(V. vinifera)
Caco
Concord
Catawba
Vitis labrusca
Semillon
(V. vinifera)
Vitis labrusca
Catawba
Vitis labrusca
Semillon
(V. vinifera)


Delaware
labrusca x aestivalis
Vitis vinifera
Winchell
Vitis labrusca
Vitis vinifera
Concord
Catawba
Vitis labrusca
Vitis labrusca
Semillon (V. vinifera)
Canandaigua
Vitis labrusca
Vitis vinifera
Catawba
Vitis labrusca
Semillon (V. vinifera)
Moyer
Delaware
labrusca x aestivalis
Vitis vinifera
Pinot Meunier (V. vinifera)

Supplementary tables

Table S1: Detailed list of the primers used for the metabarcoding analysis.
Illumina tails are showed in bold and frame-shift spacers are underlined.

Genomic region	Primer name	Primer sequence
16S V5-V6	Illu2 16SV799F	**CGTCGGCAGCGTCAGATGTGTATAAGAGACAG**NNAACMGGATTAGATACCCKG
	Illu4 16SV799F	**CGTCGGCAGCGTCAGATGTGTATAAGAGACAG**NNBBAACMGGATTAGATACCCKG
	Illu6 16SV799F	**CGTCGGCAGCGTCAGATGTGTATAAGAGACAG**NNNNKKAACMGGATTAGATACCCKG
	Illu2 16S115R	**CTCGTGGGCTCGGAGATGTGTATAAGAGACAG**NNAGGGTTGCGCTCGTTG
	Illu5 16S115R	**CTCGTGGGCTCGGAGATGTGTATAAGAGACAG**NNBHHAGGGTTGCGCTCGTTG
	Illu6 16S115R	**CTCGTGGGCTCGGAGATGTGTATAAGAGACAG**NNNNNYMAGGGTTGCGCTCGTTG
ITS2	Illu1 ITS1F	**CGTCGGCAGCGTCAGATGTGTATAAGAGACAG**NCTTGGTCATTTAGAGGAAGTAA
	Illu3 ITS1F	**CGTCGGCAGCGTCAGATGTGTATAAGAGACAG**NDVCTTGGTCATTTAGAGGAAGTAA
	Illu5 ITS1F	**CGTCGGCAGCGTCAGATGTGTATAAGAGACAG**NNNRMCTTGGTCATTTAGAGGAAGTAA
	Illu2 ITS2	**CTCGTGGGCTCGGAGATGTGTATAAGAGACAG**NNGCTGCGTTCTTCATCGATGC
	Illu3 ITS2	**CTCGTGGGCTCGGAGATGTGTATAAGAGACAG**NNHGCTGCGTTCTTCATCGATGC
	Illu4 ITS2	**CTCGTGGGCTCGGAGATGTGTATAAGAGACAG**NNNWGCTGCGTTCTTCATCGATGC

Table S2: List of accessions analysed in this study.

The rhAmpSeq result column indicates the new assignment that we gave after studying the rhAMPSeq data (fig. 2).

Sample	Sampling place	Latitude	Longitude	Group	Environment	Accession	Variety	Genotype	rhAmpSeq results
aes1	wild	39.06454	-77.64636	*V. aestivalis*	wild	NA	NA	To be determined	*V. aestivalis*
aes10	wild	37.18195	-77.99425	*V. aestivalis*	wild	NA	NA	To be determined	*V. aestivalis*
aes11	wild	37.19274	-77.97359	*V. aestivalis*	wild	NA	NA	To be determined	*V. aestivalis*
aes12	wild	37.17546	-78.03151	*V. aestivalis*	wild	NA	NA	To be determined	*V. aestivalis*
aes13	wild	37.2169	-78.53978	*V. aestivalis*	wild	NA	NA	To be determined	*V. aestivalis*
aes14	wild	37.15892	-78.5682	*V. aestivalis*	wild	NA	NA	To be determined	Hybrid
aes15	wild	37.160788	-78.570283	*V. aestivalis*	wild	NA	NA	To be determined	*V. aestivalis*
aes16	wild	43.182344	-71.172566	*V. aestivalis*	wild	NA	NA	To be determined	*V. aestivalis*
aes17	wild	43.18232	-71.1732	*V. aestivalis*	wild	NA	NA	To be determined	*V. aestivalis*
aes18	wild	NA	NA	*V. aestivalis*	wild	NA	NA	To be determined	*V. aestivalis*
aes19	wild	43.181597	-71.177939	*V. aestivalis*	wild	NA	NA	To be determined	Hybrid
aes2	wild	39.06432	-77.6468	*V. aestivalis*	wild	NA	NA	To be determined	V. *aestivalis*
aes20	wild	43.181597	-71.177939	*V. aestivalis*	wild	NA	NA	To be determined	Hybrid
aes21	wild	43.181597	-71.177939	*V. aestivalis*	wild	NA	NA	To be determined	Hybrid
aes22	wild	43.181232	-71.179702	*V. aestivalis*	wild	NA	NA	To be determined	*V. aestivalis*
aes23	wild	41.93671	-71.44153	*V. aestivalis*	wild	NA	NA	To be determined	*V. aestivalis*
aes24	wild	41.93772	-71.439436	*V. aestivalis*	wild	NA	NA	To be determined	Hybrid
aes25	wild	41.93818	-71.43949	*V. aestivalis*	wild	NA	NA	To be determined	V. *aestivalis*
aes26	wild	41.9356	-71.44572	*V. aestivalis*	wild	NA	NA	To be determined	Hybrid
aes27	wild	41.9356	-71.44572	*V. aestivalis*	wild	NA	NA	To be determined	*V. labrusca*
aes28	wild	41.9356	-71.44572	*V. aestivalis*	wild	NA	NA	To be determined	*V. aestivalis*
aes29	wild	41.9356	-71.44572	*V. aestivalis*	wild	NA	NA	To be determined	*V. aestivalis*
aes3	wild	39.06393	-77.6469	*V. aestivalis*	wild	NA	NA	To be determined	*V. aestivalis*
aes30	USDA Cold-Hardy Grape (Vitis) Collection	42.893985	-77.008515	*V. aestivalis*	cultivated	GVIT 1664	33/03	Expected Pure	*V. aestivalis*
aes31	USDA Cold-Hardy Grape (Vitis) Collection	42.893985	-77.008515	*V. aestivalis*	cultivated	GVIT 1664	33/03	Expected Pure	*V. aestivalis*
aes32	USDA Cold-Hardy Grape (Vitis) Collection	42.893985	-77.008515	*V. aestivalis*	cultivated	GVIT 1665	34/03	Expected Pure	*V. aestivalis*

aes33	USDA Cold-Hardy Grape (Vitis) Collection	42.893985	-77.008515	*V. aestivalis*	cultivated	GVIT 1665	34/03	Expected Pure	Hybrid
aes34	USDA Cold-Hardy Grape (Vitis) Collection	42.893985	-77.008515	*V. aestivalis*	cultivated	GVIT 1665	34/03	Expected Pure	*V. aestivalis*
aes35	USDA Cold-Hardy Grape (Vitis) Collection	42.893985	-77.008515	*V. aestivalis*	cultivated	GVIT 1675	Winnebago	Expected Pure	*V. aestivalis*
aes36	USDA Cold-Hardy Grape (Vitis) Collection	42.893985	-77.008515	*V. aestivalis*	cultivated	GVIT 1675	Winnebago	Expected Pure	*V. aestivalis*
aes37	USDA Cold-Hardy Grape (Vitis) Collection	42.893985	-77.008515	*V. aestivalis*	cultivated	PI 483185	Rem 30-77	Expected Pure	*V. aestivalis*
aes38	USDA Cold-Hardy Grape (Vitis) Collection	42.893985	-77.008515	*V. aestivalis*	cultivated	PI 483185	Rem 30-77	Expected Pure	*V. aestivalis*
aes4	wild	38.96715	-77.67172	*V. aestivalis*	wild	NA	NA	To be determined	*V. aestivalis*
aes41	USDA Cold-Hardy Grape (Vitis) Collection	42.893985	-77.008515	*V. aestivalis*	cultivated	PI 588677	JEG 3	Expected Pure	*V. aestivalis*
aes42	USDA Cold-Hardy Grape (Vitis) Collection	42.893985	-77.008515	*V. aestivalis*	cultivated	PI 588677	JEG 3	Expected Pure	*V. aestivalis*
aes43	wild	42.40086	-72.51568	*V. aestivalis*	wild	NA	NA	To be determined	*V. aestivalis*
aes44	wild	42.46789	-72.59137	*V. aestivalis*	wild	NA	NA	To be determined	*V. aestivalis*
aes45	wild	42.46981	-72.59235	*V. aestivalis*	wild	NA	NA	To be determined	*V. aestivalis*
aes46	wild	42.25129	-72.36097	*V. aestivalis*	wild	NA	NA	To be determined	*V. aestivalis*
aes47	Grape collection of Inrae Bordeaux	44.791334	-0.577185	*V. aestivalis*	cultivated	11051	11051	Expected Pure	*V. aestivalis*
aes47	wild	42.39465	-72.52153	*V. aestivalis*	wild	NA	NA	To be determined	*V. aestivalis*
aes48	Grape collection of Inrae Bordeaux	44.791334	-0.577185	*V. aestivalis*	cultivated	11053	11053	Expected Pure	*V. aestivalis*
aes48	wild	42.39593	-72.52099	*V. aestivalis*	wild	NA	NA	To be determined	*V. aestivalis*
aes49	Grape collection of Inrae Bordeaux	44.791334	-0.577185	*V. aestivalis*	cultivated	11053	11053	Expected Pure	*V. aestivalis*
aes5	wild	37.26654	-77.65126	*V. aestivalis*	wild	NA	NA	To be determined	*V. aestivalis*
aes51	Vine Biological Resource Centre (CRB-Vigne)	43.332984	3.568644	*V. aestivalis*	cultivated	8337MTP89	8337MTP89	Expected Pure	*V. aestivalis*
aes52	Vine Biological Resource Centre (CRB-Vigne)	43.332984	3.568644	*V. aestivalis*	cultivated	8337MTP89	8337MTP89	Expected Pure	*V. aestivalis*
aes53	Vine Biological Resource Centre (CRB-Vigne)	43.332984	3.568644	*V. aestivalis*	cultivated	8337MTP91	8337MTP91	Expected Pure	*V. aestivalis*
aes54	Vine Biological Resource Centre (CRB-Vigne)	43.332984	3.568644	*V. aestivalis*	cultivated	8337MTP91	8337MTP91	Expected Pure	*V. aestivalis*
aes55	Grape collection of Inrae Colmar	48.060223	7.326799	*V. aestivalis*	cultivated	1	1	Expected Pure	*V. aestivalis*
aes56	Grape collection of Inrae Colmar	48.060223	7.326799	*V. aestivalis*	cultivated	1	1	Expected Pure	*V. aestivalis*
aes59	Grape collection of Inrae Colmar	48.060223	7.326799	*V. aestivalis*	cultivated	4	4	Expected Pure	*V. aestivalis*
aes6	wild	37.24323	-77.91621	*V. aestivalis*	wild	NA	NA	To be determined	*V. aestivalis*
aes60	Grape collection of Inrae Colmar	48.060223	7.326799	*V. aestivalis*	cultivated	4	4	Expected Pure	*V. aestivalis*
aes7	wild	37.24763	-77.93507	*V. aestivalis*	wild	NA	NA	To be determined	*V. aestivalis*
aes8	wild	37.2473	-77.93468	*V. aestivalis*	wild	NA	NA	To be determined	*V. aestivalis*

aes9	wild	37.2473	-77.93468	*V. aestivalis*	wild	NA	NA	To be determined	*V. aestivalis*
hyb1	USDA Cold-Hardy Grape (Vitis) Collection	42.893985	-77.008515	Hybrid	cultivated	PI 588158	Athens	Expected Hybrid	Hybrid
hyb10	USDA Cold-Hardy Grape (Vitis) Collection	42.893985	-77.008515	Hybrid	cultivated	PI 588070	Catawba	Expected Hybrid	Hybrid
hyb11	USDA Cold-Hardy Grape (Vitis) Collection	42.893985	-77.008515	Hybrid	cultivated	PI 588077	Concord	Expected Hybrid	Hybrid
hyb12	USDA Cold-Hardy Grape (Vitis) Collection	42.893985	-77.008515	Hybrid	cultivated	PI 588077	Concord	Expected Hybrid	Hybrid
hyb13	USDA Cold-Hardy Grape (Vitis) Collection	42.893985	-77.008515	Hybrid	cultivated	PI 588078	Delaware	Expected Hybrid	Hybrid
hyb14	USDA Cold-Hardy Grape (Vitis) Collection	42.893985	-77.008515	Hybrid	cultivated	PI 588078	Delaware	Expected Hybrid	Hybrid
hyb15	USDA Cold-Hardy Grape (Vitis) Collection	42.893985	-77.008515	Hybrid	cultivated	PI 597246	Helen Keller	Expected Hybrid	Hybrid
hyb16	USDA Cold-Hardy Grape (Vitis) Collection	42.893985	-77.008515	Hybrid	cultivated	PI 597246	Helen Keller	Expected Hybrid	Hybrid
hyb17	USDA Cold-Hardy Grape (Vitis) Collection	42.893985	-77.008515	Hybrid	cultivated	PI 588067	Moored	Expected Hybrid	Hybrid
hyb18	USDA Cold-Hardy Grape (Vitis) Collection	42.893985	-77.008515	Hybrid	cultivated	PI 588067	Moored	Expected Hybrid	Hybrid
hyb19	USDA Cold-Hardy Grape (Vitis) Collection	42.893985	-77.008515	Hybrid	cultivated	PI 597103	Moyer	Expected Hybrid	Hybrid
hyb2	USDA Cold-Hardy Grape (Vitis) Collection	42.893985	-77.008515	Hybrid	cultivated	PI 588158	Athens	Expected Hybrid	Hybrid
hyb20	USDA Cold-Hardy Grape (Vitis) Collection	42.893985	-77.008515	Hybrid	cultivated	PI 597103	Moyer	Expected Hybrid	Hybrid
hyb22	USDA Cold-Hardy Grape (Vitis) Collection	42.893985	-77.008515	Hybrid	cultivated	PI 588106	Niagara	Expected Hybrid	Hybrid
hyb24	USDA Cold-Hardy Grape (Vitis) Collection	42.893985	-77.008515	Hybrid	cultivated	PI 597270	Paul Revere	Expected Hybrid	Hybrid
hyb25	USDA Cold-Hardy Grape (Vitis) Collection	42.893985	-77.008515	Hybrid	cultivated	PI 597233	Reliance	Expected Hybrid	Hybrid
hyb26	USDA Cold-Hardy Grape (Vitis) Collection	42.893985	-77.008515	Hybrid	cultivated	PI 597233	Reliance	Expected Hybrid	Hybrid
hyb27	USDA Cold-Hardy Grape (Vitis) Collection	42.893985	-77.008515	Hybrid	cultivated	PI 597099	Telegraph	Expected Hybrid	Hybrid
hyb28	USDA Cold-Hardy Grape (Vitis) Collection	42.893985	-77.008515	Hybrid	cultivated	PI 597099	Telegraph	Expected Hybrid	Hybrid
hyb29	USDA Cold-Hardy Grape (Vitis) Collection	42.893985	-77.008515	Hybrid	cultivated	PI 597271	Ulster	Expected Hybrid	Hybrid
hyb3	USDA Cold-Hardy Grape (Vitis) Collection	42.893985	-77.008515	Hybrid	cultivated	PI 597206	Black Eagle	Expected Hybrid	Hybrid
hyb30	USDA Cold-Hardy Grape (Vitis) Collection	42.893985	-77.008515	Hybrid	cultivated	PI 597271	Ulster	Expected Hybrid	Hybrid
hyb31	USDA Cold-Hardy Grape (Vitis) Collection	42.893985	-77.008515	Hybrid	cultivated	PI 597254	Varatura	Expected Hybrid	Hybrid
hyb32	USDA Cold-Hardy Grape (Vitis) Collection	42.893985	-77.008515	Hybrid	cultivated	PI 597254	Varatura	Expected Hybrid	Hybrid
hyb33	USDA Cold-Hardy Grape (Vitis) Collection	42.893985	-77.008515	Hybrid	cultivated	PI 588130	Winchell	Expected Hybrid	Hybrid
hyb34	USDA Cold-Hardy Grape (Vitis) Collection	42.893985	-77.008515	Hybrid	cultivated	PI 588130	Winchell	Expected Hybrid	Hybrid
hyb4	USDA Cold-Hardy Grape (Vitis) Collection	42.893985	-77.008515	Hybrid	cultivated	PI 597206	Black Eagle	Expected Hybrid	Hybrid
hyb5	USDA Cold-Hardy Grape (Vitis) Collection	42.893985	-77.008515	Hybrid	cultivated	PI 588301	Caco	Expected Hybrid	Hybrid
hyb6	USDA Cold-Hardy Grape (Vitis) Collection	42.893985	-77.008515	Hybrid	cultivated	PI 588301	Caco	Expected Hybrid	Hybrid

hyb7	USDA Cold-Hardy Grape (Vitis) Collection	42.893985	-77.008515	Hybrid	cultivated	PI 597225	Canandaigua	Expected Hybrid	Hybrid
hyb72	Grape collection of Inrae Bordeaux	44.791334	-0.577185	Hybrid	cultivated	NA	Isabelle	Expected Hybrid	Hybrid
hyb73	Grape collection of Inrae Bordeaux	44.791334	-0.577185	Hybrid	cultivated	NA	Isabelle	Expected Hybrid	Hybrid
hyb74	Vine Biological Resource Centre (CRB-Vigne)	43.332984	3.568644	Hybrid	cultivated	6605Mtp3	Niagara	Expected Hybrid	Hybrid
hyb75	Vine Biological Resource Centre (CRB-Vigne)	43.332984	3.568644	Hybrid	cultivated	6605Mtp3	Niagara	Expected Hybrid	Hybrid
hyb76	Vine Biological Resource Centre (CRB-Vigne)	43.332984	3.568644	Hybrid	cultivated	5000Mtp97	Reliance	Expected Hybrid	Hybrid
hyb77	Vine Biological Resource Centre (CRB-Vigne)	43.332984	3.568644	Hybrid	cultivated	5000Mtp97	Reliance	Expected Hybrid	Hybrid
hyb78	Vine Biological Resource Centre (CRB-Vigne)	43.332984	3.568644	Hybrid	cultivated	5000Mtp392	Catawba	Expected Hybrid	Hybrid
hyb79	Vine Biological Resource Centre (CRB-Vigne)	43.332984	3.568644	Hybrid	cultivated	5000Mtp392	Catawba	Expected Hybrid	Hybrid
hyb8	USDA Cold-Hardy Grape (Vitis) Collection	42.893985	-77.008515	Hybrid	cultivated	PI 597225	Canandaigua	Expected Hybrid	Hybrid
hyb80	Vine Biological Resource Centre (CRB-Vigne)	43.332984	3.568644	Hybrid	cultivated	6542MTP3	Concord	Expected Hybrid	Hybrid
hyb81	Vine Biological Resource Centre (CRB-Vigne)	43.332984	3.568644	Hybrid	cultivated	6542MTP3	Concord	Expected Hybrid	Hybrid
hyb82	Vine Biological Resource Centre (CRB-Vigne)	43.332984	3.568644	Hybrid	cultivated	6604Mtp3	Delaware	Expected Hybrid	Hybrid
hyb83	Vine Biological Resource Centre (CRB-Vigne)	43.332984	3.568644	Hybrid	cultivated	6604Mtp3	Delaware	Expected Hybrid	Hybrid
hyb84	Grape collection of Inrae Colmar	48.060223	7.326799	Hybrid	cultivated	1	Isabelle	Expected Hybrid	Hybrid
hyb85	Grape collection of Inrae Colmar	48.060223	7.326799	Hybrid	cultivated	1	Isabelle	Expected Hybrid	Hybrid
hyb86	Grape collection of Inrae Colmar	48.060223	7.326799	Hybrid	cultivated	1	Isabelle	Expected Hybrid	Hybrid
hyb87	Grape collection of Inrae Colmar	48.060223	7.326799	Hybrid	cultivated	1	Isabelle	Expected Hybrid	Hybrid
hyb9	USDA Cold-Hardy Grape (Vitis) Collection	42.893985	-77.008515	Hybrid	cultivated	PI 588070	Catawba	Expected Hybrid	Hybrid
lab1	wild	39.0657	-77.64556	*V. labrusca*	wild	NA	NA	To be determined	*V. labrusca*
lab10	wild	43.091633	-71.00918	*V. labrusca*	wild	NA	NA	To be determined	*V. labrusca*
lab100	USDA Cold-Hardy Grape (Vitis) Collection	42.893985	-77.008515	*V. labrusca*	cultivated	PI 588584	Grem-5	Expected Pure	*V. labrusca*
lab101	USDA Cold-Hardy Grape (Vitis) Collection	42.893985	-77.008515	*V. labrusca*	cultivated	PI 483151	Rem NE 9	Expected Pure	*V. labrusca*
lab102	USDA Cold-Hardy Grape (Vitis) Collection	42.893985	-77.008515	*V. labrusca*	cultivated	PI 483151	Rem NE 9	Expected Pure	*V. labrusca*
lab103	USDA Cold-Hardy Grape (Vitis) Collection	42.893985	-77.008515	*V. labrusca*	cultivated	PI 588658	Lutie	Expected Pure	Hybrid
lab105	USDA Cold-Hardy Grape (Vitis) Collection	42.893985	-77.008515	*V. labrusca*	cultivated	PI 588583	Grem-4	Expected Pure	*V. labrusca*
lab106	USDA Cold-Hardy Grape (Vitis) Collection	42.893985	-77.008515	*V. labrusca*	cultivated	PI 588583	Grem-4	Expected Pure	*V. labrusca*
lab107	Grape collection of Inrae Bordeaux	44.791334	-0.577185	*V. labrusca*	cultivated	11056	11056	Expected Pure	*V. labrusca*
lab107	USDA Cold-Hardy Grape (Vitis) Collection	42.893985	-77.008515	*V. labrusca*	cultivated	PI 483151	Rem NE 9	Expected Pure	*V. labrusca*
lab108	Grape collection of Inrae Bordeaux	44.791334	-0.577185	*V. labrusca*	cultivated	11056	11056	Expected Pure	*V. labrusca*

lab108	USDA Cold-Hardy Grape (Vitis) Collection	42.893985	-77.008515	*V. labrusca*	cultivated	PI 483151	Rem NE 9	Expected Pure	*V. labrusca*
lab109	Grape collection of Inrae Bordeaux	44.791334	-0.577185	*V. labrusca*	cultivated	11056	11056	Expected Pure	*V. labrusca*
lab11	wild	43.091633	-71.00918	*V. labrusca*	wild	NA	NA	To be determined	*V. labrusca*
lab111	Vine Biological Resource Centre (CRB-Vigne)	43.332984	3.568644	*V. labrusca*	cultivated	8337MTP109	8337MTP109	Expected Pure	*V. labrusca*
lab112	Vine Biological Resource Centre (CRB-Vigne)	43.332984	3.568644	*V. labrusca*	cultivated	8337MTP109	8337MTP109	Expected Pure	*V. labrusca*
lab113	Vine Biological Resource Centre (CRB-Vigne)	43.332984	3.568644	*V. labrusca*	cultivated	8337MTP110	8337MTP110	Expected Pure	*V. labrusca*
lab114	Vine Biological Resource Centre (CRB-Vigne)	43.332984	3.568644	*V. labrusca*	cultivated	8337MTP110	8337MTP110	Expected Pure	*V. labrusca*
lab115	Grape collection of Inrae Colmar	48.060223	7.326799	*V. labrusca*	cultivated	10307	10307	Expected Pure	*V. labrusca*
lab116	Grape collection of Inrae Colmar	48.060223	7.326799	*V. labrusca*	cultivated	10307	10307	Expected Pure	*V. labrusca*
lab117	Grape collection of Inrae Colmar	48.060223	7.326799	*V. labrusca*	cultivated	10308	10308	Expected Pure	*V. labrusca*
lab118	Grape collection of Inrae Colmar	48.060223	7.326799	*V. labrusca*	cultivated	10308	10308	Expected Pure	*V. labrusca*
lab12	wild	43.0979	-71.06001	*V. labrusca*	wild	NA	NA	To be determined	*V. labrusca*
lab13	wild	43.10231	-71.0763	*V. labrusca*	wild	NA	NA	To be determined	*V. labrusca*
lab14	wild	43.10314	-71.07697	*V. labrusca*	wild	NA	NA	To be determined	*V. labrusca*
lab15	wild	43.1029	-71.07699	*V. labrusca*	wild	NA	NA	To be determined	*V. labrusca*
lab16	wild	43.11291	-71.09646	*V. labrusca*	wild	NA	NA	To be determined	*V. labrusca*
lab17	wild	43.11276	-71.09683	*V. labrusca*	wild	NA	NA	To be determined	*V. labrusca*
lab18	wild	43.11276	-71.09683	*V. labrusca*	wild	NA	NA	To be determined	*V. labrusca*
lab19	wild	43.11276	-71.09683	*V. labrusca*	wild	NA	NA	To be determined	*V. labrusca*
lab2	wild	43.32785	-70.62259	*V. labrusca*	wild	NA	NA	To be determined	*V. labrusca*
lab20	wild	43.11246	-71.0964	*V. labrusca*	wild	NA	NA	To be determined	*V. labrusca*
lab21	wild	43.11246	-71.0964	*V. labrusca*	wild	NA	NA	To be determined	*V. labrusca*
lab22	wild	43.243854	-71.405354	*V. labrusca*	wild	NA	NA	To be determined	*V. labrusca*
lab23	wild	43.243916	-71.405445	*V. labrusca*	wild	NA	NA	To be determined	*V. labrusca*
lab24	wild	43.243908	-71.405536	*V. labrusca*	wild	NA	NA	To be determined	*V. labrusca*
lab25	wild	43.243946	-71.405633	*V. labrusca*	wild	NA	NA	To be determined	*V. labrusca*
lab26	wild	43.243985	-71.405738	*V. labrusca*	wild	NA	NA	To be determined	*V. labrusca*
lab27	wild	43.223169	-71.334553	*V. labrusca*	wild	NA	NA	To be determined	*V. labrusca*
lab28	wild	43.222939	-71.33441	*V. labrusca*	wild	NA	NA	To be determined	*V. labrusca*
lab29	wild	43.22297	-71.334654	*V. labrusca*	wild	NA	NA	To be determined	*V. labrusca*

lab3	wild	43.32778	-70.62281	*V. labrusca*	wild	NA	NA	To be determined	*V. labrusca*
lab30	wild	43.22287	-71.33341	*V. labrusca*	wild	NA	NA	To be determined	*V. labrusca*
lab31	wild	43.22287	-71.33341	*V. labrusca*	wild	NA	NA	To be determined	*V. labrusca*
lab32	wild	43.221413	-71.293755	*V. labrusca*	wild	NA	NA	To be determined	*V. labrusca*
lab33	wild	43.219697	-71.291235	*V. labrusca*	wild	NA	NA	To be determined	*V. labrusca*
lab34	wild	43.20898	-71.28108	*V. labrusca*	wild	NA	NA	To be determined	*V. labrusca*
lab35	wild	43.20898	-71.28108	*V. labrusca*	wild	NA	NA	To be determined	*V. labrusca*
lab36	wild	43.20898	-71.28108	*V. labrusca*	wild	NA	NA	To be determined	*V. labrusca*
lab37	wild	43.20898	-71.28108	*V. labrusca*	wild	NA	NA	To be determined	*V. labrusca*
lab38	wild	43.20898	-71.28108	*V. labrusca*	wild	NA	NA	To be determined	*V. labrusca*
lab39	wild	43.20898	-71.28108	*V. labrusca*	wild	NA	NA	To be determined	*V. labrusca*
lab4	wild	43.32785	-70.62287	*V. labrusca*	wild	NA	NA	To be determined	*V. labrusca*
lab40	wild	43.19716	-71.27216	*V. labrusca*	wild	NA	NA	To be determined	*V. labrusca*
lab41	wild	43.1958	-71.27188	*V. labrusca*	wild	NA	NA	To be determined	*V. labrusca*
lab42	wild	43.19475	-71.27109	*V. labrusca*	wild	NA	NA	To be determined	*V. labrusca*
lab43	wild	43.19437	-71.27106	*V. labrusca*	wild	NA	NA	To be determined	*V. labrusca*
lab44	wild	43.19437	-71.27106	*V. labrusca*	wild	NA	NA	To be determined	*V. labrusca*
lab45	wild	43.19437	-71.27106	*V. labrusca*	wild	NA	NA	To be determined	*V. labrusca*
lab46	wild	43.19437	-71.27106	*V. labrusca*	wild	NA	NA	To be determined	*V. labrusca*
lab47	wild	43.19437	-71.27106	*V. labrusca*	wild	NA	NA	To be determined	*V. labrusca*
lab48	wild	43.19173	-71.26963	*V. labrusca*	wild	NA	NA	To be determined	*V. labrusca*
lab49	wild	43.16381	-71.24469	*V. labrusca*	wild	NA	NA	To be determined	*V. labrusca*
lab5	wild	43.172746	-70.885986	*V. labrusca*	wild	NA	NA	To be determined	*V. labrusca*
lab50	wild	43.16381	-71.24469	*V. labrusca*	wild	NA	NA	To be determined	*V. labrusca*
lab51	wild	43.16381	-71.24469	*V. labrusca*	wild	NA	NA	To be determined	*V. labrusca*
lab52	wild	43.16381	-71.24469	*V. labrusca*	wild	NA	NA	To be determined	*V. labrusca*
lab53	wild	43.16381	-71.24469	*V. labrusca*	wild	NA	NA	To be determined	*V. labrusca*
lab54	wild	43.16381	-71.24469	*V. labrusca*	wild	NA	NA	To be determined	*V. labrusca*
lab55	wild	43.16297	-71.24367	*V. labrusca*	wild	NA	NA	To be determined	*V. labrusca*
lab56	wild	43.187456	-71.15672	*V. labrusca*	wild	NA	NA	To be determined	*V. labrusca*

lab57	wild	43.186611	-71.160123	*V. labrusca*	wild	NA	NA	To be determined	*V. labrusca*
lab58	wild	43.18658	-71.16079	*V. labrusca*	wild	NA	NA	To be determined	Hybrid
lab59	wild	43.18658	-71.16079	*V. labrusca*	wild	NA	NA	To be determined	Hybrid
lab6	wild	43.16355	-70.89359	*V. labrusca*	wild	NA	NA	To be determined	Hybrid
lab60	wild	43.181502	-71.17826	*V. labrusca*	wild	NA	NA	To be determined	*V. labrusca*
lab61	wild	43.181502	-71.17826	*V. labrusca*	wild	NA	NA	To be determined	*V. labrusca*
lab62	wild	41.93845	-71.43991	*V. labrusca*	wild	NA	NA	To be determined	*V. labrusca*
lab63	wild	41.93473	-71.44554	*V. labrusca*	wild	NA	NA	To be determined	*V. labrusca*
lab64	wild	41.93486	-71.44668	*V. labrusca*	wild	NA	NA	To be determined	Hybrid
lab65	wild	41.93486	-71.44668	*V. labrusca*	wild	NA	NA	To be determined	Hybrid
lab66	wild	41.9356	-71.44572	*V. labrusca*	wild	NA	NA	To be determined	*V. labrusca*
lab67	wild	41.934924	-71.45593	*V. labrusca*	wild	NA	NA	To be determined	*V. labrusca*
lab68	wild	41.934924	-71.45593	*V. labrusca*	wild	NA	NA	To be determined	*V. labrusca*
lab7	wild	43.145563	-70.907796	*V. labrusca*	wild	NA	NA	To be determined	*V. labrusca*
lab70	wild	41.93492	-71.45552	*V. labrusca*	wild	NA	NA	To be determined	*V. labrusca*
lab71	wild	41.93503	-71.45633	*V. labrusca*	wild	NA	NA	To be determined	*V. labrusca*
lab72	wild	41.792624	-71.540872	*V. labrusca*	wild	NA	NA	To be determined	*V. labrusca*
lab73	wild	41.792905	-71.540452	*V. labrusca*	wild	NA	NA	To be determined	*V. labrusca*
lab74	wild	41.791823	-71.540378	*V. labrusca*	wild	NA	NA	To be determined	*V. labrusca*
lab75	wild	41.79263	-71.553	*V. labrusca*	wild	NA	NA	To be determined	Hybrid
lab76	wild	41.79437	-71.55398	*V. labrusca*	wild	NA	NA	To be determined	*V. labrusca*
lab77	wild	41.79437	-71.55398	*V. labrusca*	wild	NA	NA	To be determined	*V. labrusca*
lab78	wild	41.79479	-71.553	*V. labrusca*	wild	NA	NA	To be determined	*V. labrusca*
lab79	wild	41.79479	-71.553	*V. labrusca*	wild	NA	NA	To be determined	*V. labrusca*
lab8	wild	43.124632	-70.920723	*V. labrusca*	wild	NA	NA	To be determined	*V. labrusca*
lab80	wild	41.363084	-71.684597	*V. labrusca*	wild	NA	NA	To be determined	*V. labrusca*
lab81	wild	41.363378	-71.685322	*V. labrusca*	wild	NA	NA	To be determined	*V. labrusca*
lab82	wild	41.37225	-71.66906	*V. labrusca*	wild	NA	NA	To be determined	*V. labrusca*
lab83	wild	41.37225	-71.66906	*V. labrusca*	wild	NA	NA	To be determined	*V. labrusca*
lab84	wild	41.37225	-71.66906	*V. labrusca*	wild	NA	NA	To be determined	*V. labrusca*

lab85	wild	41.37225	-71.66906	*V. labrusca*	wild	NA	NA	To be determined	*V. labrusca*
lab86	wild	41.37225	-71.66906	*V. labrusca*	wild	NA	NA	To be determined	*V. labrusca*
lab87	wild	41.37225	-71.66906	*V. labrusca*	wild	NA	NA	To be determined	*V. labrusca*
lab88	wild	41.37225	-71.66906	*V. labrusca*	wild	NA	NA	To be determined	*V. labrusca*
lab89	USDA Cold-Hardy Grape (Vitis) Collection	42.893985	-77.008515	*V. labrusca*	cultivated	PI 588307	Champagne	Expected Pure	Hybrid
lab9	wild	43.091675	-71.007452	*V. labrusca*	wild	NA	NA	To be determined	*V. labrusca*
lab90	USDA Cold-Hardy Grape (Vitis) Collection	42.893985	-77.008515	*V. labrusca*	cultivated	PI 588307	Champagne	Expected Pure	Hybrid
lab91	USDA Cold-Hardy Grape (Vitis) Collection	42.893985	-77.008515	*V. labrusca*	cultivated	PI 483161	Rem NE 26	Expected Pure	*V. labrusca*
lab92	USDA Cold-Hardy Grape (Vitis) Collection	42.893985	-77.008515	*V. labrusca*	cultivated	PI 483161	Rem NE 26	Expected Pure	*V. labrusca*
lab93	USDA Cold-Hardy Grape (Vitis) Collection	42.893985	-77.008515	*V. labrusca*	cultivated	PI 483150	Rem NE 8	Expected Pure	*V. labrusca*
lab94	USDA Cold-Hardy Grape (Vitis) Collection	42.893985	-77.008515	*V. labrusca*	cultivated	PI 483150	Rem NE 8	Expected Pure	*V. labrusca*
lab95	USDA Cold-Hardy Grape (Vitis) Collection	42.893985	-77.008515	*V. labrusca*	cultivated	PI 483152	Rem NE 11	Expected Pure	*V. labrusca*
lab96	USDA Cold-Hardy Grape (Vitis) Collection	42.893985	-77.008515	*V. labrusca*	cultivated	PI 483152	Rem NE 11	Expected Pure	Hybrid
lab97	USDA Cold-Hardy Grape (Vitis) Collection	42.893985	-77.008515	*V. labrusca*	cultivated	PI 483157	Rem NE 20	Expected Pure	Hybrid
lab98	USDA Cold-Hardy Grape (Vitis) Collection	42.893985	-77.008515	*V. labrusca*	cultivated	PI 483157	Rem NE 20	Expected Pure	*V. labrusca*
lab99	USDA Cold-Hardy Grape (Vitis) Collection	42.893985	-77.008515	*V. labrusca*	cultivated	PI 588584	Grem-5	Expected Pure	*V. labrusca*
vin1	USDA Cold-Hardy Grape (Vitis) Collection	42.893985	-77.008515	*V. vinifera*	cultivated	PI 340969	Vidal 9	Expected Pure	Hybrid
vin10	USDA Cold-Hardy Grape (Vitis) Collection	42.893985	-77.008515	*V. vinifera*	cultivated	PI 348889	Feteasca Neagra	Expected Pure	*V. vinifera*
vin100	Vine Biological Resource Centre (CRB-Vigne)	43.332984	3.568644	*V. vinifera*	cultivated	336Mtp2	Merlot	Expected Pure	*V. vinifera*
vin101	Vine Biological Resource Centre (CRB-Vigne)	43.332984	3.568644	*V. vinifera*	cultivated	2728Mtp1	Morio Muscat	Expected Pure	*V. vinifera*
vin102	Vine Biological Resource Centre (CRB-Vigne)	43.332984	3.568644	*V. vinifera*	cultivated	2728Mtp1	Morio Muscat	Expected Pure	*V. vinifera*
vin103	Vine Biological Resource Centre (CRB-Vigne)	43.332984	3.568644	*V. vinifera*	cultivated	584Mtp1	Muscat de Hambourg	Expected Pure	*V. vinifera*
vin104	Vine Biological Resource Centre (CRB-Vigne)	43.332984	3.568644	*V. vinifera*	cultivated	584Mtp1	Muscat de Hambourg	Expected Pure	*V. vinifera*
vin105	Vine Biological Resource Centre (CRB-Vigne)	43.332984	3.568644	*V. vinifera*	cultivated	150Mtp7	Syrah	Expected Pure	*V. vinifera*
vin106	Vine Biological Resource Centre (CRB-Vigne)	43.332984	3.568644	*V. vinifera*	cultivated	150Mtp7	Syrah	Expected Pure	*V. vinifera*
vin107	Vine Biological Resource Centre (CRB-Vigne)	43.332984	3.568644	*V. vinifera*	cultivated	74Mtp31	Ugni blanc	Expected Pure	*V. vinifera*
vin108	Vine Biological Resource Centre (CRB-Vigne)	43.332984	3.568644	*V. vinifera*	cultivated	74Mtp31	Ugni blanc	Expected Pure	*V. vinifera*
vin11	USDA Cold-Hardy Grape (Vitis) Collection	42.893985	-77.008515	*V. vinifera*	cultivated	PI 348888	Feteasca Alba	Expected Pure	Hybrid

vin111	Grape collection of Inrae Colmar	48.060223	7.326799	*V. vinifera*	cultivated	1	Concord	Expected Pure	*V. vinifera*
vin112	Grape collection of Inrae Colmar	48.060223	7.326799	*V. vinifera*	cultivated	1	Concord	Expected Pure	*V. vinifera*
vin113	Grape collection of Inrae Colmar	48.060223	7.326799	*V. vinifera*	cultivated	1	Concord	Expected Pure	*V. vinifera*
vin114	Grape collection of Inrae Colmar	48.060223	7.326799	*V. vinifera*	cultivated	1	Concord	Expected Pure	*V. vinifera*
vin115	Grape collection of Inrae Colmar	48.060223	7.326799	*V. vinifera*	cultivated	1	Grenache	Expected Pure	*V. vinifera*
vin116	Grape collection of Inrae Colmar	48.060223	7.326799	*V. vinifera*	cultivated	1	Grenache	Expected Pure	*V. vinifera*
vin117	Grape collection of Inrae Colmar	48.060223	7.326799	*V. vinifera*	cultivated	1	Grenache	Expected Pure	*V. vinifera*
vin118	Grape collection of Inrae Colmar	48.060223	7.326799	*V. vinifera*	cultivated	1	Grenache	Expected Pure	*V. vinifera*
vin119	Grape collection of Inrae Colmar	48.060223	7.326799	*V. vinifera*	cultivated	1	Merlot	Expected Pure	*V. vinifera*
vin12	USDA Cold-Hardy Grape (Vitis) Collection	42.893985	-77.008515	*V. vinifera*	cultivated	PI 588670	AgriaÂ =Turan	Expected Pure	*V. vinifera*
vin120	Grape collection of Inrae Colmar	48.060223	7.326799	*V. vinifera*	cultivated	1	Merlot	Expected Pure	*V. vinifera*
vin121	Grape collection of Inrae Colmar	48.060223	7.326799	*V. vinifera*	cultivated	1	Merlot	Expected Pure	*V. vinifera*
vin122	Grape collection of Inrae Colmar	48.060223	7.326799	*V. vinifera*	cultivated	1	Merlot	Expected Pure	*V. vinifera*
vin123	Grape collection of Inrae Colmar	48.060223	7.326799	*V. vinifera*	cultivated	1	Morio Muskat	Expected Pure	*V. vinifera*
vin124	Grape collection of Inrae Colmar	48.060223	7.326799	*V. vinifera*	cultivated	1	Morio Muskat	Expected Pure	*V. vinifera*
vin125	Grape collection of Inrae Colmar	48.060223	7.326799	*V. vinifera*	cultivated	1	Morio Muskat	Expected Pure	*V. vinifera*
vin126	Grape collection of Inrae Colmar	48.060223	7.326799	*V. vinifera*	cultivated	1	Morio Muskat	Expected Pure	*V. vinifera*
vin127	Grape collection of Inrae Colmar	48.060223	7.326799	*V. vinifera*	cultivated	1	Muscat de Hambourg	Expected Pure	*V. vinifera*
vin128	Grape collection of Inrae Colmar	48.060223	7.326799	*V. vinifera*	cultivated	1	Muscat de Hambourg	Expected Pure	*V. vinifera*
vin129	Grape collection of Inrae Colmar	48.060223	7.326799	*V. vinifera*	cultivated	1	Muscat de Hambourg	Expected Pure	*V. vinifera*
vin13	USDA Cold-Hardy Grape (Vitis) Collection	42.893985	-77.008515	*V. vinifera*	cultivated	PI 588676	Norakert PGR 2224	Expected Pure	*V. vinifera*
vin130	Grape collection of Inrae Colmar	48.060223	7.326799	*V. vinifera*	cultivated	1	Muscat de Hambourg	Expected Pure	*V. vinifera*
vin131	Grape collection of Inrae Colmar	48.060223	7.326799	*V. vinifera*	cultivated	1	Syrah	Expected Pure	*V. vinifera*
vin132	Grape collection of Inrae Colmar	48.060223	7.326799	*V. vinifera*	cultivated	1	Syrah	Expected Pure	*V. vinifera*
vin133	Grape collection of Inrae Colmar	48.060223	7.326799	*V. vinifera*	cultivated	73	Syrah	Expected Pure	*V. vinifera*
vin134	Grape collection of Inrae Colmar	48.060223	7.326799	*V. vinifera*	cultivated	73	Syrah	Expected Pure	*V. vinifera*

vin135	Grape collection of Inrae Colmar	48.060223	7.326799	*V. vinifera*	cultivated	76	Chardonnay	Expected Pure	*V. vinifera*
vin136	Grape collection of Inrae Colmar	48.060223	7.326799	*V. vinifera*	cultivated	76	Chardonnay	Expected Pure	*V. vinifera*
vin137	Grape collection of Inrae Colmar	48.060223	7.326799	*V. vinifera*	cultivated	169	Cabernet sauvignon	Expected Pure	*V. vinifera*
vin138	Grape collection of Inrae Colmar	48.060223	7.326799	*V. vinifera*	cultivated	169	Cabernet sauvignon	Expected Pure	*V. vinifera*
vin139	Grape collection of Inrae Colmar	48.060223	7.326799	*V. vinifera*	cultivated	169	Cabernet sauvignon	Expected Pure	*V. vinifera*
vin14	USDA Cold-Hardy Grape (Vitis) Collection	42.893985	-77.008515	*V. vinifera*	cultivated	PI 588676	Norakert PGR 2224	Expected Pure	*V. vinifera*
vin140	Grape collection of Inrae Colmar	48.060223	7.326799	*V. vinifera*	cultivated	169	Cabernet sauvignon	Expected Pure	*V. vinifera*
vin141	Grape collection of Inrae Colmar	48.060223	7.326799	*V. vinifera*	cultivated	638	Ugni Blanc	Expected Pure	*V. vinifera*
vin142	Grape collection of Inrae Colmar	48.060223	7.326799	*V. vinifera*	cultivated	638	Ugni Blanc	Expected Pure	*V. vinifera*
vin143	Grape collection of Inrae Colmar	48.060223	7.326799	*V. vinifera*	cultivated	638	Ugni Blanc	Expected Pure	*V. vinifera*
vin144	Grape collection of Inrae Colmar	48.060223	7.326799	*V. vinifera*	cultivated	809	Chardonnay	Expected Pure	*V. vinifera*
vin145	Grape collection of Inrae Colmar	48.060223	7.326799	*V. vinifera*	cultivated	809	Chardonnay	Expected Pure	*V. vinifera*
vin15	USDA Cold-Hardy Grape (Vitis) Collection	42.893985	-77.008515	*V. vinifera*	cultivated	PI 588668	Zengoe	Expected Pure	*V. vinifera*
vin16	USDA Cold-Hardy Grape (Vitis) Collection	42.893985	-77.008515	*V. vinifera*	cultivated	PI 588709	Ehrenfelser	Expected Pure	Hybrid
vin17	USDA Cold-Hardy Grape (Vitis) Collection	42.893985	-77.008515	*V. vinifera*	cultivated	PI 588709	Ehrenfelser	Expected Pure	*V. vinifera*
vin18	USDA Cold-Hardy Grape (Vitis) Collection	42.893985	-77.008515	*V. vinifera*	cultivated	PI 588720	Itkchkimar	Expected Pure	Hybrid
vin19	USDA Cold-Hardy Grape (Vitis) Collection	42.893985	-77.008515	*V. vinifera*	cultivated	PI 594346	Karmrajut	Expected Pure	*V. vinifera*
vin2	USDA Cold-Hardy Grape (Vitis) Collection	42.893985	-77.008515	*V. vinifera*	cultivated	PI 340969	Vidal 9	Expected Pure	Hybrid
vin20	USDA Cold-Hardy Grape (Vitis) Collection	42.893985	-77.008515	*V. vinifera*	cultivated	GVIT 1614	Zefir	Expected Pure	*V. vinifera*
vin43	Grape collection of Inrae Bordeaux	44.791334	-0.577185	*V. vinifera*	cultivated	347	Merlot_Noir	Expected Pure	*V. vinifera*
vin44	Grape collection of Inrae Bordeaux	44.791334	-0.577185	*V. vinifera*	cultivated	347	Merlot_Noir	Expected Pure	*V. vinifera*
vin45	Grape collection of Inrae Bordeaux	44.791334	-0.577185	*V. vinifera*	cultivated	181	Merlot_Noir	Expected Pure	*V. vinifera*
vin46	Grape collection of Inrae Bordeaux	44.791334	-0.577185	*V. vinifera*	cultivated	337	Cabernet Sauvignon	Expected Pure	*V. vinifera*
vin47	Grape collection of Inrae Bordeaux	44.791334	-0.577185	*V. vinifera*	cultivated	337	Cabernet Sauvignon	Expected Pure	*V. vinifera*

vin48	Grape collection of Inrae Bordeaux	44.791334	-0.577185	*V. vinifera*	cultivated	341	Cabernet Sauvignon	Expected Pure	*V. vinifera*
vin49	Grape collection of Inrae Bordeaux	44.791334	-0.577185	*V. vinifera*	cultivated	877	Syrah	Expected Pure	*V. vinifera*
vin5	USDA Cold-Hardy Grape (Vitis) Collection	42.893985	-77.008515	*V. vinifera*	cultivated	PI 318883	Tachikawa 1	Expected Pure	Hybrid
vin50	Grape collection of Inrae Bordeaux	44.791334	-0.577185	*V. vinifera*	cultivated	877	Syrah	Expected Pure	*V. vinifera*
vin51	Grape collection of Inrae Bordeaux	44.791334	-0.577185	*V. vinifera*	cultivated	877	Syrah	Expected Pure	*V. vinifera*
vin52	Grape collection of Inrae Bordeaux	44.791334	-0.577185	*V. vinifera*	cultivated	NA	Grenache_Noir	Expected Pure	*V. vinifera*
vin53	Grape collection of Inrae Bordeaux	44.791334	-0.577185	*V. vinifera*	cultivated	NA	Grenache_Noir	Expected Pure	*V. vinifera*
vin54	Grape collection of Inrae Bordeaux	44.791334	-0.577185	*V. vinifera*	cultivated	NA	Grenache_Noir	Expected Pure	*V. vinifera*
vin55	Grape collection of Inrae Bordeaux	44.791334	-0.577185	*V. vinifera*	cultivated	384	Ugni_Blanc	Expected Pure	*V. vinifera*
vin56	Grape collection of Inrae Bordeaux	44.791334	-0.577185	*V. vinifera*	cultivated	384	Ugni_Blanc	Expected Pure	*V. vinifera*
vin57	Grape collection of Inrae Bordeaux	44.791334	-0.577185	*V. vinifera*	cultivated	384	Ugni_Blanc	Expected Pure	*V. vinifera*
vin58	Grape collection of Inrae Bordeaux	44.791334	-0.577185	*V. vinifera*	cultivated	95	Chardonnay	Expected Pure	*V. vinifera*
vin59	Grape collection of Inrae Bordeaux	44.791334	-0.577185	*V. vinifera*	cultivated	95	Chardonnay	Expected Pure	*V. vinifera*
vin6	USDA Cold-Hardy Grape (Vitis) Collection	42.893985	-77.008515	*V. vinifera*	cultivated	PI 318883	Tachikawa 1	Expected Pure	Hybrid
vin60	Grape collection of Inrae Bordeaux	44.791334	-0.577185	*V. vinifera*	cultivated	124	Chardonnay	Expected Pure	*V. vinifera*
vin61	Grape collection of Inrae Bordeaux	44.791334	-0.577185	*V. vinifera*	cultivated	NA	Feteasca_Alba	Expected Pure	*V. vinifera*
vin62	Grape collection of Inrae Bordeaux	44.791334	-0.577185	*V. vinifera*	cultivated	NA	Feteasca_Alba	Expected Pure	*V. vinifera*
vin63	Grape collection of Inrae Bordeaux	44.791334	-0.577185	*V. vinifera*	cultivated	NA	Feteasca_Alba	Expected Pure	*V. vinifera*
vin64	Grape collection of Inrae Bordeaux	44.791334	-0.577185	*V. vinifera*	cultivated	NA	Karmrajut	Expected Pure	*V. vinifera*
vin65	Grape collection of Inrae Bordeaux	44.791334	-0.577185	*V. vinifera*	cultivated	NA	Karmrajut	Expected Pure	*V. vinifera*
vin66	Grape collection of Inrae Bordeaux	44.791334	-0.577185	*V. vinifera*	cultivated	NA	Karmrajut	Expected Pure	*V. vinifera*
vin67	Grape collection of Inrae Bordeaux	44.791334	-0.577185	*V. vinifera*	cultivated	NA	Feteasca_Neagra	Expected Pure	*V. vinifera*
vin68	Grape collection of Inrae Bordeaux	44.791334	-0.577185	*V. vinifera*	cultivated	NA	Feteasca_Neagra	Expected Pure	*V. vinifera*
vin69	Grape collection of Inrae Bordeaux	44.791334	-0.577185	*V. vinifera*	cultivated	NA	Feteasca_Neagra	Expected Pure	*V. vinifera*
vin7	USDA Cold-Hardy Grape (Vitis) Collection	42.893985	-77.008515	*V. vinifera*	cultivated	PI 588429	Lampheare	Expected Pure	*V. vinifera*
vin70	Grape collection of Inrae Bordeaux	44.791334	-0.577185	*V. vinifera*	cultivated	NA	Lampheare	Expected Pure	*V. vinifera*
vin71	Grape collection of Inrae Bordeaux	44.791334	-0.577185	*V. vinifera*	cultivated	NA	Lampheare	Expected Pure	*V. vinifera*
vin72	Grape collection of Inrae Bordeaux	44.791334	-0.577185	*V. vinifera*	cultivated	NA	Lampheare	Expected Pure	*V. vinifera*
vin8	USDA Cold-Hardy Grape (Vitis) Collection	42.893985	-77.008515	*V. vinifera*	cultivated	PI 588425	Morio Muscat	Expected Pure	*V. vinifera*

vin83	Vine Biological Resource Centre (CRB-Vigne)	43.332984	3.568644	*V. vinifera*	cultivated	322Mtp25	Cabernet Sauvignon	Expected Pure	*V. vinifera*
vin84	Vine Biological Resource Centre (CRB-Vigne)	43.332984	3.568644	*V. vinifera*	cultivated	322Mtp25	Cabernet Sauvignon	Expected Pure	*V. vinifera*
vin85	Vine Biological Resource Centre (CRB-Vigne)	43.332984	3.568644	*V. vinifera*	cultivated	199Mtp4	Chardonnay	Expected Pure	*V. vinifera*
vin86	Vine Biological Resource Centre (CRB-Vigne)	43.332984	3.568644	*V. vinifera*	cultivated	199Mtp4	Chardonnay	Expected Pure	*V. vinifera*
vin87	Vine Biological Resource Centre (CRB-Vigne)	43.332984	3.568644	*V. vinifera*	cultivated	2703Mtp1	Ehrenfelser	Expected Pure	*V. vinifera*
vin88	Vine Biological Resource Centre (CRB-Vigne)	43.332984	3.568644	*V. vinifera*	cultivated	2703Mtp1	Ehrenfelser	Expected Pure	*V. vinifera*
vin89	Vine Biological Resource Centre (CRB-Vigne)	43.332984	3.568644	*V. vinifera*	cultivated	1661MTP3	Feteasca Alba	Expected Pure	*V. vinifera*
vin9	USDA Cold-Hardy Grape (Vitis) Collection	42.893985	-77.008515	*V. vinifera*	cultivated	PI 348889	Feteasca Neagra	Expected Pure	*V. vinifera*
vin91	Vine Biological Resource Centre (CRB-Vigne)	43.332984	3.568644	*V. vinifera*	cultivated	1672Mtp3	Feteasca Neagra	Expected Pure	*V. vinifera*
vin92	Vine Biological Resource Centre (CRB-Vigne)	43.332984	3.568644	*V. vinifera*	cultivated	1672Mtp3	Feteasca Neagra	Expected Pure	*V. vinifera*
vin93	Vine Biological Resource Centre (CRB-Vigne)	43.332984	3.568644	*V. vinifera*	cultivated	34Mtp6	Grenache	Expected Pure	*V. vinifera*
vin94	Vine Biological Resource Centre (CRB-Vigne)	43.332984	3.568644	*V. vinifera*	cultivated	34Mtp6	Grenache	Expected Pure	*V. vinifera*
vin95	Vine Biological Resource Centre (CRB-Vigne)	43.332984	3.568644	*V. vinifera*	cultivated	2845Mtp1	Itchkimar biely	Expected Pure	*V. vinifera*
vin96	Vine Biological Resource Centre (CRB-Vigne)	43.332984	3.568644	*V. vinifera*	cultivated	2845Mtp1	Itchkimar biely	Expected Pure	*V. vinifera*
vin97	Vine Biological Resource Centre (CRB-Vigne)	43.332984	3.568644	*V. vinifera*	cultivated	3648 (0MTP573)	Karmraiute	Expected Pure	*V. vinifera*
vin98	Vine Biological Resource Centre (CRB-Vigne)	43.332984	3.568644	*V. vinifera*	cultivated	3648 (0MTP573)	Karmraiute	Expected Pure	*V. vinifera*
vin99	Vine Biological Resource Centre (CRB-Vigne)	43.332984	3.568644	*V. vinifera*	cultivated	336Mtp2	Merlot	Expected Pure	*V. vinifera*

Discussion générale

De nouveaux micro-organismes potentiellement antagonistes du mildiou ont été mis en évidence, afin de guider les futures expérimentations

L'objectif principal de cette thèse était de caractériser les interactions potentielles entre *Plasmopara viticola* (l'oomycète pathogène responsable du mildiou de la vigne) et les microbiotes de la vigne et des sols viticoles, dans le but d'identifier des bactéries et des champignons susceptibles d'interférer avec les cycles sexués et asexués du mildiou et de contribuer au développement du biocontrôle microbien du mildiou.

La thèse était basée sur des hypothèses fortes. Le chapitre 3, en particulier, faisait l'hypothèse que des parcelles relativement homogènes en terme de variété, pratique culturale et microclimat, mais qui ont des réponses différentes face au mildiou, ont un microbiote différent. Nos résultats ont validé cette hypothèse, en mettant en évidence des taxons systématiquement plus abondants dans les parcelles peu sensibles au mildiou au travers de toutes les paires de parcelles considérées (Fournier et al. soumis à *Microbiome*). Le chapitre 2, qui teste quant à lui plusieurs théories écologiques liant les propriétés du microbiote avec sa résistance à l'invasion par un pathogène, comme la relation diversité-invasibilité (Mallon *et al.*, 2015; Saleem *et al.*, 2019) ou le principe d'Anna Karénine (Zaneveld *et al.*, 2017; Arnault *et al.*, 2023), a permis d'identifier d'autres taxons d'intérêt.

Les taxons qui ont été identifiés dans les chapitres 2 et 3 de la thèse comme des antagonistes potentiels du mildiou de la vigne sont listés en annexe de la thèse (Annexes 6, 7, 9 et 10). Ceux qui sont les plus prometteurs sont répertoriés dans les tableaux ci-dessous. Certains taxons avaient déjà été identifiés comme des antagonistes du mildiou ou d'autres agents pathogènes dans la littérature. Dans ce cas, les connaissances à leur sujet (écologie, mode d'action) sont indiquées. Les taxons connus pour être des pathogènes de plantes ou des pathogène humains ne sont pas reportés dans les tableaux ci-dessous car ils ne pourront pas être exploitées pour le développement du biocontrôle.

Tableau 1 : Principaux taxons fongiques susceptibles d'interférer avec le cycle asexué du mildiou selon les résultats de cette thèse.

Seuls les taxons d'intérêt identifiés avec au moins 4 méthodes statistiques dans le chapitre 2 ou le chapitre 3 sont reportés ici. La liste complète est en annexe.

Taxon identifié dans la thèse comme un antagoniste potentiel du mildiou	Ecologie et mode d'action décrits dans la littérature	Sources
Sporolobomyces roseus	Espèce de levure basidiomycète abondante dans la phyllosphère de nombreuses plantes ; activité de biocontrôle contre plusieurs champignons pathogènes, par compétition pour les nutriments.	Chapitre 2 (Gouka *et al.*, 2022; Barroso-Bergada *et al.*, 2023; Kot *et al.*, 2024)
Rhodotorula nothofagi	Espèce de levure basidiomycète colonisant les parties aériennes de la vigne ; pas d'activité de biocontrôle connue pour cette espèce mais le genre *Rhodotorula* contient des agents de biocontrôle contre des maladies post-récolte.	Chapitre 3 ((Zhang *et al.*, 2009; Čadež *et al.*, 2010; Li *et al.*, 2011; Lederer *et al.*, 2013; Milanović *et al.*, 2013; Cordero-Bueso *et al.*, 2017; Lorenzini & Zapparoli, 2019; Esteves *et al.*, 2023)
Buckleyzyma aurantiaca (synonyme : *Rhodotorula aurantiaca*)	Espèce de levure basidiomycète colonisant les feuilles de nombreuses plantes ; activité de biocontrôle contre des maladies post-récolte. Les mécanismes d'action ne sont pas connus.	Chapitre 1 et Chapitre 3 (Chand-Goyal & Spotts, 1996; Conceição *et al.*, 2014; Silva *et al.*, 2014; de Melo *et al.*, 2015; Satianpakiranakorn *et al.*, 2020; Kwaśna *et al.*, 2021; Wang *et al.*, 2021; Macaya-Sanz *et al.*, 2023; Ettinger *et al.*, 2023)
Papiliotrema laurentii (synonyme : *Cryptococcus laurentii*)	Espèce de levure basidiomycète distribuée dans de nombreux habitats tels que les sols, les plantes et les débris végétaux ; activité de biocontrôle contre des maladies post-récolte, par la compétition pour les nutriments, et la production d'enzymes antioxydantes	Chapitre 2 et 3 (Meng *et al.*, 2010; Wei *et al.*, 2014; Lai *et al.*, 2018; Castoria *et al.*, 2021a; de Almeida *et al.*, 2022)
Bullera alba (synonyme : *Bulleromyces albus*)	Espèce de levure basidiomycète qui colonise divers compartiments de la plante (parties aériennes, rhizosphère, sol, graines) ; activité de biocontrôle contre des maladies post-récolte par la production de toxines létales.	Chapitre 2 et 3 (Golubev *et al.*, 1997; Paul *et al.*, 2012; Kosel *et al.*, 2019; Barnett *et al.*, 2020a; Ņečajeva *et al.*, 2023; Yu *et al.*, 2024)
Aureobasidium pullulans	Espèce de levure ascomycète dominante dans la phyllosphère de la vigne, connue pour son activité de biocontrôle contre différents pathogènes, notamment *Botrytis cinerea*, par compétition pour l'espace et les nutriments, et production d'enzymes hydrolytiques et d composés volatils organiques	Chapitre 1 et Chapitre 3 (Pertot *et al.*, 2017b; Bozoudi & Tsaltas, 2018)
Leucosporidium scottii	Espèce de levure basidiomycète isolée des régions polaires ou des régions tempérées pendant les saisons froides, à partir d'eau de mer, de sols, de mousses et de lacs salés ; activité	Chapitre 3 (Vero *et al.*, 2013; Moguel *et al.*, 2020)

	de biocontrôle contre des maladies post-récolte, par la production de substances antifongiques.	

Tableau 2 : Principaux taxons fongiques susceptibles d'interférer avec le cycle sexué du mildiou selon les résultats de cette thèse.
Seuls les taxons d'intérêt identifiés avec au moins 4 méthodes statistiques dans le chapitre 2 ou le chapitre 3 sont reportés ici. La liste complète est en annexe.

Taxon identifié dans la thèse comme un antagoniste potentiel du mildiou	Ecologie et mode d'action décrits dans la littérature	Sources
Papiliotrema laurentii (synonyme : *Cryptococcus laurentii*)	Espèce de levure basidiomycète distribuée dans de nombreux habitats tels que les sols, les plantes et les débris végétaux ; activité de biocontrôle contre des maladies post-récolte, par la compétition pour les nutriments, et la production d'enzymes antioxydantes	Chapitre 2 et 3 (Meng *et al.*, 2010; Wei *et al.*, 2014; Lai *et al.*, 2018; Castoria *et al.*, 2021a; de Almeida *et al.*, 2022)
Papiliotrema terrestris	Espèce de levure basidiomycète ubiquitaire dans les sols ; activité de biocontrôle contre des maladies post-récolte, par compétition pour les nutriments et antibiose.	Chapitre 3 (Castoria *et al.*, 2021b; Palmieri *et al.*, 2022)
Bjerkandera adusta	Espèce de champignon filamenteux basidiomycète qui colonise le bois mort ; activité de biocontrôle contre divers agents pathogènes fongiques par la compétition pour les nutriments et l'espace, le parasitisme et l'antibiose.	Chapitre 3 (Burnevica *et al.*, 2022; Chen *et al.*, 2022; Li *et al.*, 2022a; Yazid *et al.*, 2023)
Trichoderma virens	Espèce de champignon filamenteux ascomycète largement présent dans les sols, en particulier dans la rhizosphère ; activité de biocontrôle contre divers agent pathogènes fongiques par parasitisme, antibiose, compétition pour les nutriments et l'espace et induction de la résistance systémique des plantes.	Chapitre 3 (Howell, 2006; Ghazanfar *et al.*, 2018; Ghasemi *et al.*, 2020)
Trichoderma lixii	Espèce de champignon filamenteux ascomycète largement présent dans les sols et débris végétaux ; activité de biocontrôle contre des maladies telluriques.	Chapitre 3 (Pehlivan *et al.*, 2017; Kumar & Dwivedi, 2021; Omara & El-maghraby, 2023)
Bullera alba (synonyme : *Bulleromyces albus*)	Espèce de levure basidiomycète qui colonise divers compartiments de la plante (parties aériennes, rhizosphère, sol, graines) ; activité de biocontrôle contre des maladies post-récolte par la production de toxines létales.	Chapitre 2 et 3 (Golubev *et al.*, 1997; Paul *et al.*, 2012; Kosel *et al.*, 2019; Barnett *et al.*, 2020a; Ņečajeva *et al.*, 2023; Yu *et al.*, 2024)

Tableau 3 : Principaux taxons bactériens susceptibles d'interférer avec le cycle asexué du mildiou selon les résultats de cette thèse.

Seuls les taxons d'intérêt identifiés avec au moins 4 méthodes statistiques dans le chapitre 2 ou le chapitre 3 sont reportés ici. La liste complète est en annexe.

Taxon identifié dans la thèse comme un antagoniste potentiel du mildiou	Ecologie et mode d'action décrits dans la littérature	Sources
Genre *Bacillus*	Bactéries Gram-positives omniprésentes, dans le sol, l'eau et l'air, ainsi que sur les surfaces et la rhizosphère des plantes ; activité de biocontrôle par la production de composés antimicrobiens, l'induction d'une résistance systémique chez les plantes et la compétition pour les niches écologiques avec les agents pathogènes des plantes. *B .amyloliquefaciens*, *B. pumilus* et *B. subtilis* ont montré de l'antagonisme contre le mildiou.	Chapitre 1 et 2 (Zhang *et al.*, 2017; Fira *et al.*, 2018; Li *et al.*, 2019; Biljana *et al.*, 2023)
Genre *Streptomyces*	Bactéries Gram-positives omniprésentes dans le sol ; activité de biocontrôle contre divers agents pathogènes fongiques par la production de métabolites secondaires et la compétition pour des ressources comme le carbone et le fer et la stimulation du système immunitaire des plantes. Les espèces *Streptomyces atratus*, *S. viridosporus* et *S. violaceus* ont montré de l'antagonisme contre le mildiou.	Chapitre 1 et 2 (Abdalla *et al.*, 2011; Liang *et al.*, 2016; Islam *et al.*, 2016; El-Sharkawy *et al.*, 2018; LeBlanc, 2022)

Tableau 4 : Principaux taxons bactériens susceptibles d'interférer avec le cycle sexué du mildiou selon les résultats de cette thèse.
Seuls les taxons d'intérêt identifiés avec au moins 4 méthodes statistiques dans le chapitre 2 ou le chapitre 3 sont reportés ici. La liste complète est en annexe.

Taxon identifié dans la thèse comme un antagoniste potentiel du mildiou	Ecologie et mode d'action décrits dans la littérature	Sources
Arthrobacter globiformis	Espèce bactérienne communément isolées à partir des sols et capables de vivre dans des conditions extrêmes pendant de longues périodes ; activité de biocontrôle par la production d'antibiotiques, antifongiques et anti-oomycètes.	Chapitre 3 (Casida & Liu, 1974; Mongodin *et al.*, 2006; Santos *et al.*, 2020b)
Streptomyces *albidoflavus* *Streptomyces ambofaciens*	Bactéries Gram-positives omniprésentes, dans le sol, l'eau et l'air, ainsi que sur les surfaces et la rhizosphère des plantes ; activité de biocontrôle contre les champignons pathogènes de plantes, par la production de composés antifongiques et la stimulation du système immunitaire des plantes.	Chapitre 3 (Mahadevan & Crawford, 1997; Lim Seng Heng, 2015; Abbasi *et al.*, 2019; Carlucci *et al.*, 2022; Du *et al.*, 2022)
Bacillus megaterium	Bactéries Gram-positives omniprésentes, dans le sol, l'eau et l'air, ainsi que sur les surfaces et la rhizosphère des plantes ; activité de biocontrôle contre les champignons pathogènes de plantes par des mécanismes non élucidés.	Chapitre 3 (Akgül & Mirik, 2008; Kildea *et al.*, 2008; Kong *et al.*, 2010; Acurio Vásconez *et al.*, 2020; Saleh *et al.*, 2021)

Des expérimentations, si possible réalisées avec des souches des taxons d'intérêt isolées dans les mêmes parcelles que celles étudiées dans les chapitres 2 et 3, seront nécessaires pour valider ces interactions.

Des corrélations entre la quantité d'oospores dans le sol et le microbiote du sol superficiel ont été démontrées, ce qui ouvre la voie au biocontrôle microbien de l'inoculum hivernant

Pendant plusieurs années, la littérature scientifique sur le mildiou de la vigne a convenu que la maladie n'était initiée que par quelques infections primaires survenant sur une courte période au printemps, et que la progression de la maladie et les réductions de rendement qui en découlaient étaient principalement dues à des infections secondaires (Gessler et al. 2011). Cependant, des travaux ont ensuite mis en évidence l'importance des infections primaires par les oospores dans la progression de l'épidémie de mildiou tout au long de la saison (Gobbin *et al.*, 2005; Boso *et al.*, 2019; Hong *et al.*, 2020; Sargolzaei *et al.*, 2020; Santos *et al.*, 2020a;

Maddalena *et al.*, 2021). La réduction de l'inoculum hivernant a donc été proposée en tant que méthode préventive des épidémies de mildiou (Vecchione *et al.*, 2007; Carisse, 2016; Poeydebat *et al.*, 2022).

Il a été montré qu'un grand nombre de feuilles infectées à l'automne augmente la sévérité de la maladie au printemps suivant et peut avancer le démarrage de l'épidémie de plusieurs jours (Fig. 1 d'après (Carisse, 2016)). Ceci pourrait être expliqué par la plus grande quantité d'oospores dans le sol, qui favoriserait la synchronisation entre la germination des oospores et la période de sensibilité des organes vers de la vigne, notamment les inflorescences. Les résultats obtenus dans le chapitre 3 de la thèse confirment ces résultats. Nous avons observé que les parcelles présentant une forte sensibilité au mildiou se distinguaient par l'apparition plus précoce des premiers symptômes et par une intensité plus marquée de l'épidémie dès le début de celle-ci (Fig. 2). De plus, ces parcelles présentaient une quantité plus importante d'oospores dans le sol (Fig. 2), confirmant ainsi l'importance de réduire la quantité d'inoculum hivernant.

En outre, dans le chapitre 3, nous avons identifié des micro-organismes du sol dont l'abondance est négativement corrélée à celle des oospores dans le sol, ce qui ouvre la voie à un biocontrôle microbien de l'inoculum hivernant. Les microorganismes qui pourraient être antagonistes des oospores dans le sol sont listés en Annexe 2.

L'effet de ces microorganismes sur la germination des oospores pourra être validée expérimentalement, en utilisant le protocole de biotest récemment développé à l'UMR SAVE (Poeydebat *et al.*, 2024). Les micro-organismes les plus efficaces pourraient ensuite intégrer un programme de gestion de l'inoculum hivernant du mildiou, dans lequel le biocontrôle microbien des oospores viendrait compléter les mesures prophylactiques visant à réduire leur abondance, comme l'exportation des feuilles en fin de saison (Poeydebat *et al.*, 2024). Il s'agit d'une piste de recherche originale que très peu d'études ont jusqu'à présent explorée. A notre connaissance, seules deux études du groupe d'Ilaria Pertot en Italie (Dagostin *et al.*, 2006; Vecchione *et al.*, 2007) ont évoqué cette possibilité. Ces études ont montré que la germination des oospores de mildiou pouvait être inhibée en conditions naturelles par des consortia microbiens. La composition des consortia n'est pas indiquée dans les études et il semble que les travaux n'ont pas été poursuivis.

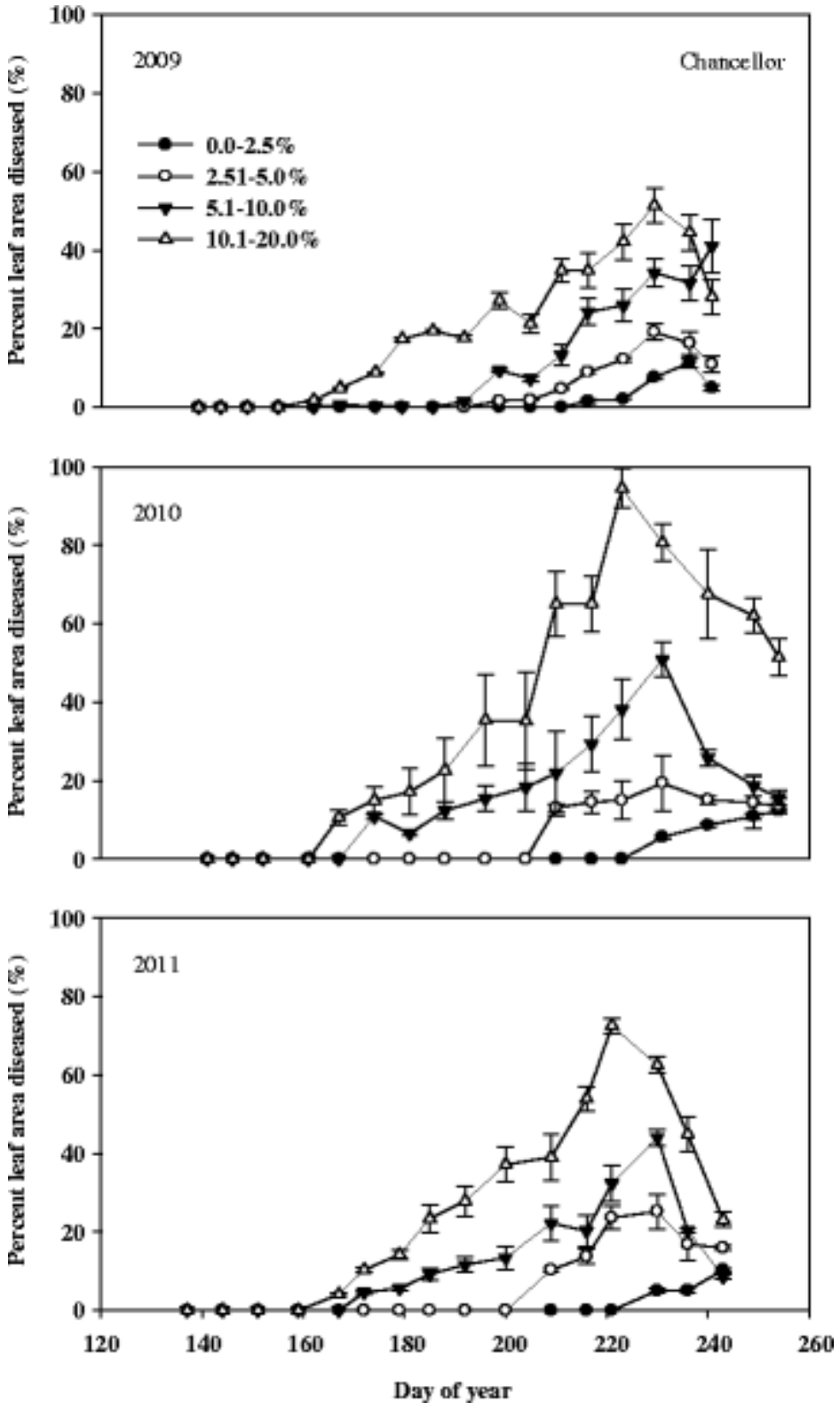


Fig. 1 : Sévérité de l'épidémie de mildiou en fonction du pourcentage de feuilles symptomatiques à l'automne précédent, sur trois années consécutives (d'après Carisse 2016).
Plus le pourcentage de feuilles symptomatiques à l'automne est élevé, plus le démarrage de l'épidémie au printemps suivant est précoce.

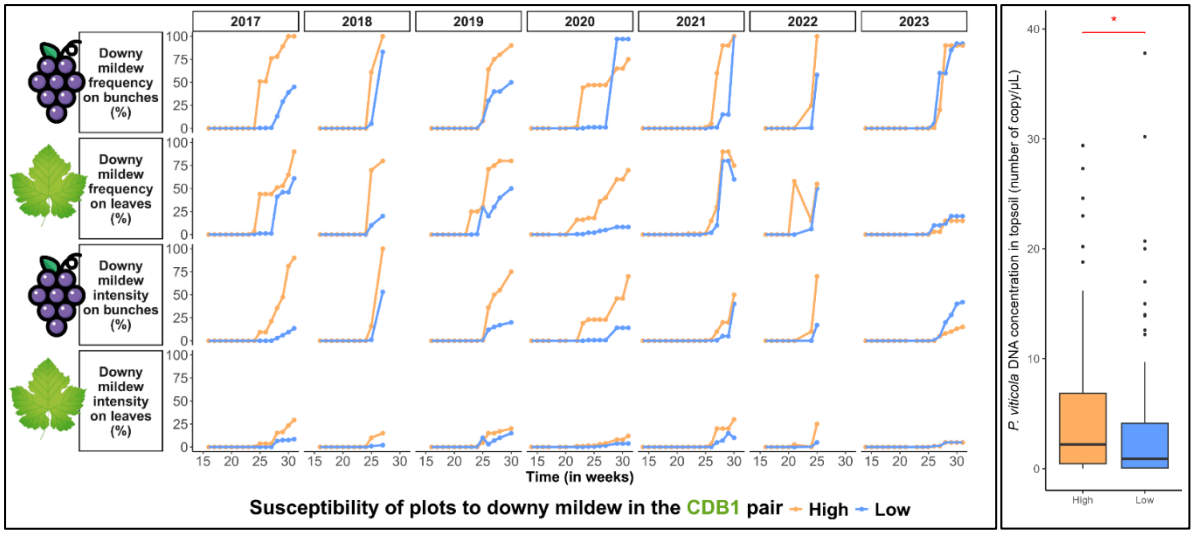


Fig. 2 : Sévérité et intensité de l'épidémie de mildiou, sur sept années consécutives, dans une parcelle sensible au mildiou (en orange) et dans une parcelle moins sensible (en bleu).
La parcelle plus sensible au mildiou contient plus d'oospores dans le sol et l'épidémie de mildiou y démarre plus tôt dans la saison (d'après Fournier et al. soumis à *Microbiome*).

Plusieurs microorganismes de la phyllosphère pourraient avoir une double action, préventive et curative, contre le mildiou

Un résultat intéressant de cette thèse est la correspondance observée entre les taxons microbiens plus abondants dans les parcelles peu sensibles au mildiou, en particulier dans la phyllosphère en début de saison (chapitre 3), et ceux retrouvés dans les lésions foliaires de mildiou au pic de l'épidémie (chapitre 2). Bien que ce constat puisse sembler contre-intuitif au premier abord, il suggère que ces taxons microbiens pourraient jouer un rôle dans la prévention des épidémies en amont des premières infections, puis avoir une action directe sur le pathogène, au sein des lésions, pendant l'épidémie.

Pour mieux comprendre à quel moment de la saison ces microorganismes de la phyllosphère pourraient interférer avec le cycle de vie du mildiou, il serait intéressant de suivre leur dynamique tout au long de la saison dans les tissus asymptomatiques et dans les lésions, à l'aide d'outils de diagnostic moléculaire (qPCR, ddPCR). Il serait également intéressant d'évaluer leur abondance dans les infrastructures agro-écologiques non-permanentes (couverts végétaux dans la parcelle) et permanentes (haies arbustives ou arbres isolés dans la parcelle, habitats semi-naturels aux alentours de l'exploitation), afin de développer un biocontrôle microbien par conservation. Cette piste de recherche est originale dans le cas du mildiou de la vigne mais elle a été étudiée pour d'autres bioagresseurs. Les réservoirs environnementaux de deux champignons entomopathogènes, *Beauveria bassiana* et *Metarhizium anosipliae*, ont par exemple été recherchés pour lutter contre les insectes ravageurs des cultures (Meyling & Eilenberg, 2007; Pell *et al.*, 2010). Ces études insistent sur le fait qu'une bonne connaissance de l'écologie des microorganismes à favoriser est nécessaire pour la mise en place d'un biocontrôle microbien par conservation.

Une originalité de la thèse est l'étude du microbiote des hôtes d'origine de *Plasmopara viticola* dans l'aire d'origine de l'agent pathogène

Les études du microbiote dans des populations naturelles de vigne se sont pour l'instant limitées à la sous-espèce sauvage de *Vitis vinifera* subsp. *sylvestris* (Ocete *et al.*, 2015; Campisano *et al.*, 2015b; Puig-Pujol *et al.*, 2016; Radić *et al.*, 2021; Fournier *et al.*, 2022a), ainsi qu'à l'espèce *Vitis amurensis* dans l'extrême-orient russe (Aleynova *et al.*, 2022b,a). D'autres études ont dévoilé le microbiote des *Vitis* américains et asiatiques naturellement résistants au mildiou, mais ces plantes étaient cultivées (Brum *et al.*, 2012; Felber *et al.*, 2016; Wicaksono *et al.*, 2023). Dans cette thèse, nous nous sommes intéressés au microbiote des vignes sauvages américaines qui poussent dans leur environnement naturel et qui sont naturellement résistantes au mildiou. Contrairement à leur homologue européen cultivé (*V. vinifera*), qui n'a été en contact avec le mildiou que depuis la fin du XIXe siècle, la résistance au mildiou observée dans certaines accessions américaines de *Vitis* (Cadle-Davidson, 2008; Péros *et al.*, 2021) est attribuée à une plus longue histoire de coévolution avec ce pathogène (Jürges *et al.*, 2009b). Selon la théorie de l'hologénome, les pressions de sélection agissent non seulement sur le génome de l'hôte, mais aussi sur les génomes des micro-organismes associés (Rosenberg & Zilber-Rosenberg, 2018). Dans ce cadre, la coévolution plante-pathogène peut conduire à la sélection de traits de résistance à la fois dans le génome de l'hôte et dans le microbiome associé. C'est l'hypothèse que nous faisons dans le chapitre 4 en cherchant des micro-organismes d'intérêt dans le microbiote des hôtes d'origine du mildiou (*V. labrusca* et *V. aestivalis*) et dans leur région d'origine (le Nord-Est des États-Unis). Cependant, une limite de notre étude est que nous n'avons pas accès aux génomes microbiens, et donc aux gènes potentiellement impliquées dans la résistance à la colonisation par le mildiou, car nous avons utilisé des approches de *métabarcoding* pour caractériser le microbiote de la phyllosphère des vignes américaines. Un séquençage complet du microbiome, par des approches de métagénomique *shotgun*, serait intéressant à mettre en place.

Malgré cette limite, ce chapitre de ma thèse est innovant car il n'y a, à notre connaissance, aucune étude à ce jour sur le microbiote des hôtes d'origine d'un agent pathogène dans l'aire d'origine de cet agent pathogène. Il existe en revanche quelques études sur le microbiote des plantes cultivées dans leur centre d'origine afin d'identifier des microorganismes bénéfiques (Pérez-Jaramillo *et al.*, 2018). Le microbiote a par exemple été analysé sur le sorgho en Ethiopie, le haricot en Colombie, la tomate au Pérou et le téosinte au Mexique (Pérez-Jaramillo *et al.*, 2017; Abera *et al.*, 2022; Runge *et al.*, 2023; Barnes *et al.*, 2024). L'étude sur le sorgo, par exemple, montre des différences entre les microbiotes rhizospheriques des génotypes sauvages et cultivés et tente de mettre en relation les génotypes de sorgho, leur phénotypes et certains groupes microbiens. C'est dans cette direction que nous pourrons aller dès lors que nous aurons reçu les données de séquençage du chapitre 4.

La suite de la discussion porte sur les méthodes utilisées dans la thèse, depuis le choix des sites d'étude jusqu'aux analyses statistiques.

Le choix des parcelles d'étude est une étape cruciale pour mettre en relation le microbiote avec les données épidémiologiques

Le plan initial pour le chapitre 3, tel qu'il avait été envisagé lors de la conception du projet VITAE, prévoyait d'étudier 20 paires de parcelles réparties dans plusieurs régions viticoles. Finalement, cela n'a pas pu être mis en œuvre pour deux raisons : (i) l'IFV ne disposait pas de suivi épidémiologique sur des vignes non traitées dans les parties est et sud de la France, notamment parce que le mildiou est moins présent en région méditerranéenne, et (ii) il a été difficile de trouver des paires de parcelles répondant à nos cinq critères (même cépage, même mode de gestion, proximité géographique, suivi épidémiologique commun pendant au moins 4 années et relevés épidémiologiques contrastés). Cette difficulté résidait principalement dans le fait que, dans la majorité des cas, chaque domaine viticole suivait uniquement une parcelle, à l'exception du Château Montrose, qui possède trois des sept paires de parcelles que nous avons finalement étudiées. En conséquence, les parcelles suivies étaient souvent situées à plus de 10 km les unes des autres, ce qui ne permettait pas de respecter le critère de distance maximale de 10 km.

En effet, notre dispositif expérimental a été spécifiquement conçu pour étudier l'effet de la sensibilité des parcelles au mildiou, tout en minimisant les facteurs de confusion potentiels. Pour cela, nous avons constitué des paires de parcelles présentant une sensibilité variable au mildiou, en standardisant le cépage et les pratiques de gestion, et en minimisant la distance intra-parcelle pour homogénéiser les autres variables de l'environnement. Durant ma thèse, la question d'une conception alternative m'a souvent été posée : pourquoi ne pas avoir caractérisé le microbiote dans de nombreuses parcelles représentant un gradient de sensibilité au mildiou, au lieu de se limiter à quelques paires de parcelles contrastées ?

La réponse n'est pas simple. Un dispositif expérimental de type « gradient » aurait permis de corréler directement les microbiotes avec la sensibilité des parcelles au mildiou, plutôt que d'utiliser un facteur binaire de sensibilité. Elle aurait aussi offert la possibilité d'explorer une plus grande diversité de variables environnementales et de gestion, avec le risque cependant, que le gradient de sensibilité au mildiou reflète principalement les conditions climatiques. Les parcelles situées aux extrêmes du gradient de sensibilité au mildiou auraient pu être caractérisées pour leur microbiote, mais aussi pour leurs conditions environnementales et agronomiques. Ceci aurait fourni des informations précieuses sur les conditions agro-écologiques favorisant la présence de certains micro-organismes, ce qui aurait été particulièrement pertinent dans le cadre de la lutte biologique par conservation (Bartoli et al., 2020). Le gradient aurait pu être divisé, *a posteriori*, en sous-ensembles correspondant aux mêmes conditions environnementales, pratiques de gestion, et niveaux de sensibilité au mildiou. Cela aurait ensuite permis d'identifier les taxons dont l'abondance varie de manière significative entre ces groupes. L'étude d'un très grand nombre de parcelles aurait cependant été nécessaire pour former ces groupes, ce qui aurait été très complexe à mettre en œuvre en raison des exigences logistiques. Travailler avec sept paires de parcelles a déjà demandé des efforts considérables pour collecter les feuilles et le sols sur toutes les parcelles avant les

premiers traitements fongicides. L'échantillonnage a été effectué au stade phénologique de 2-3 feuilles étalées, soit au début de la période de réceptivité de la vigne aux attaques de *P. viticola*, et juste avant que les premiers traitement fongiques soient appliqués. Ce créneau était très court et difficile à anticiper, car dépendant de la météo et des décisions des viticulteurs. Une solution à ce problème aurait été de demander aux viticulteurs de collecter et stocker eux-mêmes les échantillons, ou encore de réduire le nombre d'échantillons prélevés par parcelle, mais cela aurait introduit d'autres problèmes en termes de qualité et de standardisation des données.

Améliorations du protocole pour analyser le microbiote de la phyllosphère de la vigne

De nos jours, une multitude de protocoles pour analyser le microbiote des plantes sont disponibles dans la littérature, et chaque laboratoire semble avoir développé son propre protocole. Bien que des comparaisons de méthodes d'extraction d'ADN (Giangacomo *et al.*, 2021) ou des amorces PCR soient disponibles dans la littérature (Thijs *et al.*, 2017; Wasimuddin *et al.*, 2020), il reste difficile de choisir une méthode de la littérature sans la tester et l'adapter, en raison de la spécificité des échantillons, des objectifs de recherche et de la faisabilité des protocoles sur le terrain et au laboratoire.

Dans le cas de la vigne, l'extraction d'ADN et l'amplification des marqueurs ITS et 16S depuis les tissus foliaires reste un défi important en raison de la forte teneur des feuilles en métabolites secondaires, tels que les polysaccharides, les polyphénols et les tanins, qui non seulement se lient aux acides nucléiques lors de l'extraction, entraînant leur perte, mais agissent également comme des inhibiteurs de la PCR (Lodhi *et al.*, 1994; Hanania *et al.*, 2004; Lo Piccolo *et al.*, 2012). C'est pourquoi je souhaite ici partager mon expérience sur les deux méthodes d'analyse du microbiote foliaire que j'ai utilisées dans les chapitres 3 et 4 de cette thèse et conseiller une méthode à utiliser à l'avenir.

Pour l'étape d'isolement des épiphytes foliaires, nous avons utilisé deux approches : la collecte par agitation des feuilles dans un tampon PBS (*Phosphate Buffered Saline*) , inspirée de Behrens et Fischer (2022) (chapitre 3), et la collecte par écouvillonnage des feuilles (chapitre 4). La méthode des écouvillons s'est révélée plus pratique, nécessitant seulement deux minutes par échantillon et pouvant être réalisée directement sur le terrain, ce qui permettait d'économiser des manipulations de retour au laboratoire. Pour extraire l'ADN, la tête cotonnée des écouvillons a été introduite dans le tube d'extraction et coupée à sa limite avec des ciseaux, de manière très simple et facilitant un travail à haut débit. La méthode d'extraction à partir du tampon était plus longue, nécessitant davantage de manipulations : ajouter du PBS (*Phosphate Buffered Saline*) dans le sac d'échantillonnage, incuber 1 heure, retirer le PBS du sac et le transférer dans un tube de 50 mL, centrifuger et récupérer le culot.

Pour l'extraction d'ADN à partir de tissus foliaires (et non pas de la phyllosphère), nous avons utilisé deux kits d'extraction d'ADN: le kit DNeasy Plant Mini (Qiagen, France) dans le chapitre 3 et le kit DNeasy 96 Plant (QIAGEN®, Allemagne) dans le chapitre 4. Le premier kit permet d'extraire l'ADN dans des tubes individuels, tandis que le second utilise des plaques. Ce dernier

protocole a été légèrement modifié par l'ajout de PVP-40 (2% p/v) au tampon de lyse AP1, conformément à la méthode (Hyma *et al.*, 2015) développée et utilisée dans le laboratoire de Lance Cadle-Davidson (Grape Genetics Research Unit, USDA, ARS, Geneva, NY, USA*).* Cette modification vise à améliorer l'extraction d'ADN à partir de tissus riches en composés phénoliques, tels que ceux de la vigne. Nous avons observé un signal PCR1 plus intense sur gel avec ce second protocole.

Un des défis inhérents au *metabarcoding* des tissus végétaux est la gestion de l'homologie entre les gènes d'ARNr 16S bactériens et 16S chloroplastiques qui restreint les paires d'amorces possibles (Hanshew *et al.*, 2013). Pour les communautés bactériennes, la région V5-V6 du gène 16S a été amplifiée à l'aide de la paire 799f-1115r (Reysenbach & Pace, 1995; Chelius & Triplett, 2001a) qui exclut les chloroplastes. Ces amorces minimisent la contamination des amplicons par les chloroplastes (Hanshew *et al.*, 2013), bien qu'elles présentent l'inconvénient de capter une diversité réduite par rapport à des amorces dites universelles (Thijs *et al.*, 2017). Elles se sont avérées très efficaces dans nos études. Lorsque des amorces classiques ont été utilisées au cours de la thèse, comme par exemple dans l'amplification et le séquençage de la région 16S complète sur un séquenceur PacBio (chapitres 2 et 3), les jeu de données obtenus ne contenaient que des séquences chloroplastiques ou mitochondriales et n'étaient pas exploitables dès lors que l'échantillon contenait des tissus foliaires.

Pour caractériser les communautés fongiques, la région de l'espaceur transcrit interne 1 (ITS1) de l'ADN ribosomique nucléaire fongique (ADNr) a été amplifiée à l'aide de la paire d'amorces ITS1F-ITS2 (White *et al.*, 1990; Gardes & Bruns, 1993) qui cible le gène ITS de champignons uniquement (Tedersoo & Anslan, 2019; Nilsson *et al.*, 2019a). Nous avons également testé le jeu d'amorces ITS1catta - ITS2ngs (Tedersoo *et al.*, 2018; Tedersoo & Anslan, 2019), qui cible le gène ITS des champignons et des oomycètes, et qui a été utilisé avec succès sur des plants de vigne (Behrens & Fischer, 2022b). Malheureusement, dans les tissus foliaires (endosphère foliaire), en plus d'amplifier des séquences de champignons et d'oomycètes, elles ont amplifié de l'ADN de plantes (chapitre 3).

Il faut enfin noter que le choix de l'enzyme polymérase est crucial pour les approches de *metabarcoding* (Nagai *et al.*, 2022). Trois types d'enzyme polymérase ont été utilisés au cours de cette thèse : la KAPA3G (Kapa Biosystems, Wilmington, MA, USA) qui a été employée dans le chapitre 4 est résiliente contre la présence de résidus de polyphénols de raisin dans le mélange réactionnel (Kapa Biosystems, fiche technique, Wilmington, MA, USA). Cette dernière enzyme est celle qui a donné les meilleurs résultats.

In fine, mes recommandations pour la caractérisation du microbiote de la phyllosphère ou de l'endosphère foliaire sont les suivantes. Pour la collecte des épiphytes, je préconise l'utilisation d'écouvillons plutôt que le lavage des tissus. Concernant l'extraction de l'ADN l'endosphère foliaire ou de la feuille entière, je recommande d'utiliser le kit DNeasy 96 Plant (QIAGEN®, Allemagne), selon (Hyma *et al.*, 2015), avec l'ajout de PVP-40 (2% p/v) au tampon de lyse AP1. La version en tube de ce kit peut également être envisagée. Pour l'amplification et le

séquençage court-brin des communautés bactériennes, les amorces 799f-1115r (Reysenbach & Pace, 1995; Chelius & Triplett, 2001a) donnent de bons résultats. Les assignations taxonomiques peuvent être améliorées en séquençant la région 16S complète par séquençage long-brin. Pour les communautés fongiques, je recommande les amorces ITS1F-ITS2 (White *et al.*, 1990; Gardes & Bruns, 1993) plutôt que les amorces ITS1catta - ITS2ngs (Tedersoo *et al.*, 2018; Tedersoo & Anslan, 2019), qui amplifient la vigne. L'enzyme polymérase KAPA3G (Kapa Biosystems, Wilmington, MA, USA) donne de bons résultats.

La caractérisation du microbiote de l'endosphère foliaire, ainsi que de la feuille entière (surface et intérieur des tissus) reste plus problématique, conduisant à l'observation surprenante selon laquelle la phyllosphère serait plus riche en diversité microbienne que la feuille entière (Behrens & Fischer, 2022a). Il me semble donc essentiel que des efforts soient consacrés à l'optimisation de l'extraction de l'ADN et des amplifications PCR dans les tissus foliaires de vigne afin de pouvoir étudier ce compartiment de manière plus approfondie.

Un pipeline d'analyse combinant plusieurs méthodes a été mis en place pour identifier des taxons d'intérêt dans des jeux de données de métabarcoding

Dans cette thèse, j'ai mis en place un pipeline permettant d'identifier des taxons microbiens d'intérêt dans des jeux de données de métabarcoding. Ce pipeline repose sur une combinaison de méthodes d'analyse d'abondance différentielle récentes et recommandées dans la littérature (Nearing *et al.*, 2022a; Yang & Chen, 2022, 2023; Regueira-Iglesias *et al.*, 2023), spécialement conçues pour l'étude du microbiote, prenant explicitement en compte l'inflation des zéros dans les données d'abondance microbiennes et la compositionalité des données. Ces méthodes sont ANCOM-BC2 (Lin & Peddada, 2024), Maaslin2 (Mallick *et al.*, 2021), LinDA (Zhou *et al.*, 2022) and ZicoSeq (Yang & Chen, 2022). Ces résultats ont été complétés par une méthode de détection de taxons indicateurs de seuil, appliquée en parallèle (Threshold Indicator Taxa ANalysis (TITAN) (Baker *et al.*, 2023a)). Ces différents types de méthodes – certaines nécessitant une variable explicative qualitative, d'autres une variable quantitative – ont permis d'exploiter toutes nos mesures d'abondance du pathogène. Nous disposions en effet de mesures qualitatives (tissu symptomatique versus asymptomatique, parcelle sensible versus peu sensible) et de mesures quantitatives (abondance absolue du pathogène mesurée par qPCR ou ddPCR, phénotype de sensibilité au mildiou, exprimé par le pourcentage de surface foliaire couvert par des symptômes de la maladie, et mesuré à l'aide du robot de phénotypage "Blackbird").

Dans les chapitres 2 et 3, je me suis posée la question d'utiliser une seule méthode, qui aurait été celle la plus largement recommandée dans la littérature, ou bien combiner différentes méthodes. J'ai finalement choisi de combiner plusieurs méthodes d'analyse d'abondance différentielle, car je ne souhaitais pas me limiter à une seule des approches recommandées. (Nearing *et al.*, 2022b) ont recommandé l'usage de méthodes plutôt conservatrices, telles qu'ANCOM-II, mais ont également avancé que MaAsLin2 pourrait être un choix raisonnable pour ceux cherchant une plus grande puissance statistique. Nous avons pris en compte le fait que les méthodes trop puissantes peuvent générer trop de faux positifs, tandis que les

méthodes conservatrices risquent d'aboutir à trop de faux négatifs. En combinant plusieurs méthodes et en appliquant un score pour chaque taxon, nous pouvons interpréter les résultats en connaissance de cause, en distinguant les taxons rarement identifiés comme différentiellement abondants de ceux souvent identifiés. Le code R que j'ai développé pour combiner les différentes méthodes a été déposé dans une archive libre (https://doi.org/10.57745/XNEH5O), ce qui permettra sa réutilisation dans d'autres études.

Conclusion et perspectives

Dans cette thèse, j'ai produit des données de métabarcoding et combiné de nombreuses méthodes d'analyses statistiques afin de générer des hypothèses sur les interactions entre *Plasmopara viticola* et le microbiote de la vigne et des sols viticoles. La limite principale de cette approche est qu'elle ne permet d'établir que des liens corrélatifs, et non causaux, entre l'abondance du pathogène et la composition du microbiote. En effet, ma thèse n'inclut ni observation directe des interactions par microscopie, ni validation expérimentale des interactions par des tests de confrontation en conditions contrôlées ou par des inoculations sur plante entière en serre ou au champ. Ma thèse se situe en amont de ces recherches expérimentales : elle fournit des bases de données de micro-organismes d'intérêt, qui pourront guider les futures expérimentations visant à développer le biocontrôle microbien du mildiou.

Les expérimentations pour valider les interactions générées par ma thèse ont déjà débuté dans le projet VITAE. Une collection microbienne (bactéries, levures et champignons filamenteux) a été créée à partir des échantillons foliaires que j'ai collectés dans le chapitre 3. Les isolements ont été réalisés en utilisant des milieux de culture classiques ainsi qu'un milieu à base de feuilles de vigne (Annexes 2A et 2B ; Jaswa *et al.*, *in prep*). Ce travail fait partie de la thèse d'Aarti Jaswa, également réalisée au sein de l'UMR SAVE. Aarti Jaswa a conçu des communautés microbiennes synthétiques (SynCom), qui intègrent une partie des taxons microbiens d'intérêt que j'ai identifiés. Ces communautés, qui mélangent jusqu'à une quarantaine de souches, ont été confrontées au mildiou en conditions contrôlées. Les souches seules ont également été confrontées au mildiou. Les résultats sont en cours d'analyse. Ces expérimentations permettront de valider expérimentalement une partie des hypothèses d'interaction générées dans ma thèse et de commencer à élucider les modes d'action des micro-organismes. En outre, une puce microfluidique de qPCR a été développée pour quantifier l'abondance des taxons d'intérêt. Elle sera utilisée pour suivre la dynamique de colonisation des taxons microbiens sur les feuilles, en présence ou non de *Plasmopara viticola*, et permettra à terme d'identifier les réservoirs environnementaux des taxons d'intérêt afin d'envisager une lutte biologique par conservation.

Pour aller plus loin dans la compréhension des interactions entre le mildiou et le microbiote de la vigne, des approches expérimentales et fonctionnelles seront nécessaires. Les approches de métabarcoding que j'ai utilisées dans ma thèse ne donnent accès qu'à la composition taxonomique des communautés microbiennes. Les assignations taxonomiques sont peu précises, notamment pour les bactéries, ceci malgré le couplage d'approches de séquençage court-brin avec des approches long-brin (chapitre 3). Une inférence de la fonction des microorganismes à partir de la taxonomie a été tentée, en utilisant différentes méthodes telles que FungalTraits (Põlme *et al.*, 2020) and FunGuild (Nguyen *et al.*, 2016), mais les résultats ne semblaient pas pertinents. La collection microbienne créée dans le projet VITAE va nous permettre d'aller plus loin, en donnant accès aux souches potentiellement responsables des

effets observés dans mon travail de thèse. Pour un même taxon d'intérêt, identifié avec des analyses de métabarcoding, plusieurs souches pourront être étudiées car il est bien établi que l'antagonisme est souvent spécifique à la souche, particulièrement chez les bactéries (Wang *et al.*, 2020). Des approches multi-omiques, combinant métagénomqiue, méta-transcriptomique et métabolomique (Crandall *et al.*, 2020), pourront ensuite être utilisées pour élucider les mécanismes des interactions entre la plante, le microbiote et le mildiou.

En plus de ces approches expérimentales fonctionnelles, ma thèse ouvre des perspectives dans le domaine de la modélisation du fonctionnement des communautés microbiennes. Les analyses d'abondance différentielle que j'ai utilisées tout au long de ma thèse comparent les abondances de chaque ASV, prise individuellement, entre deux conditions (typiquement, les parcelles peu versus très sensibles au mildiou). Ces méthodes sont puissantes pour détecter des changements d'abondance et sont bien adaptées à mon objectif principal : générer une liste de taxons différentiellement abondants. Toutefois, ces méthodes ne tiennent pas compte des interactions entre les taxons au sein de la communauté microbienne. La factorisation positive de matrice (NMF, pour *non-negative factorisation*) est une technique de réduction de dimension permettant d'identifier des invariants dans des matrices de comptages ou de fréquences (Raguideau *et al.*, 2016). Dans cette méthode, la matrice de comptage est interprétée comme le mélange pondéré d'un petit nombre de guildes (typiquement 4 ou 5), définies comme des ensembles d'entités taxonomiques ou fonctionnelles qui co-varient à travers les échantillons, un aspect crucial dans les communautés microbiennes où les espèces interagissent. Cela permet de capturer des structures complexes dans les données, telles que des groupes d'espèces qui se comportent de manière similaire dans certaines conditions. Ce type de méthode pourrait être pertinent à utiliser sur les données de ma thèse pour inférer des hypothèses sur le fonctionnement des communautés microbiennes, et pourrait aider à concevoir des communautés synthétiques pour le biocontrôle du mildiou par inoculation.

Enfin, ma thèse ouvre une autre voie pour le biocontrôle du mildiou : le biocontrôle microbien par conservation. Il était clair, dès le démarrage du programme prioritaire de recherche « Cultiver et protéger autrement », que le zéro-pesticide en agriculture ne pourra être atteint qu'en associant différents leviers. Ma thèse propose un nouveau levier, même s'il reste encore du travail à faire pour identifier les pratiques et les infrastructures agroécologiques qui favorisent, naturellement et en l'absence de toute inoculation, les microorganismes qui interfèrent avec le cycle sexué et asexué de *Plasmopara viticola*. Ma thèse a permis de faire un petit pas en avant, en identifiant quelques espèces microbiennes, naturellement présentes dans les vignobles et liées à une faible sensibilité des parcelles au mildiou, dont il serait intéressant de mieux connaitre l'écologie.

Références

Abarenkov K, Zirk A, Piirman T *et al.*, 2021. UNITE general FASTA release for Eukaryotes. Version 8.3.

Abbasi S, Safaie N, Sadeghi A, Shamsbakhsh M, 2019. Streptomyces Strains Induce Resistance to Fusarium oxysporum f. sp. lycopersici Race 3 in Tomato Through Different Molecular Mechanisms. *Frontiers in Microbiology* 10.

Abdalla MA, Win HY, Islam MT, von Tiedemann A, Schüffler A, Laatsch H, 2011. Khatmiamycin, a motility inhibitor and zoosporicide against the grapevine downy mildew pathogen *Plasmopara viticola* from Streptomyces sp. ANK313. *The Journal of Antibiotics* 64, 655–659.

Abdallah M, Ameye M, Saeger S, Audenaert K, Haesaert G, 2018. Biological Control of Mycotoxigenic Fungi and Their Toxins: An Update for the Pre-Harvest Approach

Abdelfattah A, Sanzani SM, Wisniewski M, Berg G, Cacciola SO, Schena L, 2019. Revealing Cues for Fungal Interplay in the Plant–Air Interface in Vineyards. *Frontiers in Plant Science* 10.

Abera S, Shimels M, Tessema T, Raaijmakers J, Dini-Andreote F, 2022. Back to the roots: defining the core microbiome of Sorghum bicolor in agricultural field soils from the centre of origin. *FEMS microbiology ecology* 98.

Abrego N, Roslin T, Huotari T *et al.*, 2020. Accounting for environmental variation in co-occurrence modelling reveals the importance of positive interactions in root-associated fungal communities. *Molecular Ecology* 29, 2736–2746.

Acurio Vásconez RD, Tenorio Moya EM, Collaguazo Yépez LA, Chiluisa-Utreras VP, Vaca Suquillo I de los Á, 2020. Evaluation of *Bacillus megaterium* strain AB4 as a potential biocontrol agent of *Alternaria japonica*, a mycopathogen of *Brassica oleracea* var. *italica. Biotechnology Reports* 26, e00454.

Adesina MF, Lembke A, Costa R, Speksnijder A, Smalla K, 2007. Screening of bacterial isolates from various European soils for *in vitro* antagonistic activity towards *Rhizoctonia solani* and *Fusarium oxysporum*: Site-dependent composition and diversity revealed. *Soil Biology and Biochemistry* 39, 2818–2828.

Agaras BC, Scandiani M, Luque A *et al.*, 2015. Quantification of the potential biocontrol and direct plant growth promotion abilities based on multiple biological traits distinguish different groups of *Pseudomonas* spp. isolates. *Biological Control* 90, 173–186.

Agler MT, Ruhe J, Kroll S *et al.*, 2016. Microbial Hub Taxa Link Host and Abiotic Factors to Plant Microbiome Variation. *PLOS Biology* 14, e1002352.

Agreste, 2019. Enquête Pratiques culturales en viticulture en 2019 - IFT et nombre de traitements|.

Agreste, 2023. Enquête Pratiques culturales en viticulture en 2019 - IFT et nombre de traitements. Données révisées Mars 2023, n° 4

Agrios GN. 2005. *Plant Pathology*. 5th Ed. Academic Press. New York, USA. 922p.

Ahlmann-Eltze C, Patil I, 2021. *ggsignif: R Package for Displaying Significance Brackets for "ggplot2."*

Ahmed MFA, 2018. Evaluation of some biocontrol agents to control Thompson seedless grapevine powdery mildew disease. *Egyptian Journal of Biological Pest Control* **28**, 93.

Ahmed W, Dai Z, Liu Q *et al.*, 2022. Microbial Cross-Talk: Dissecting the Core Microbiota Associated With Flue-Cured Tobacco (Nicotiana tabacum) Plants Under Healthy and Diseased State. *Frontiers in Microbiology* **13**.

Ait Bahadou S, Ouijja A, Karfach A, Tahiri A, Lahlali R, 2018. New potential bacterial antagonists for the biocontrol of fire blight disease (*Erwinia amylovora*) in Morocco. *Microbial Pathogenesis* **117**, 7–15.

Akgül DS, Mirik M, 2008. Biocontrol of Phytophthora Capsici on Pepper Plants by Bacillus Megaterium Strains. *Journal of Plant Pathology* **90**, 29–34.

Aleklett K, Hart M, Shade A, 2014. The microbial ecology of flowers: an emerging frontier in phyllosphere research. *Botany* **92**, 253–266.

Aleynova OA, Nityagovsky NN, Dubrovina AS, Kiselev KV, 2022a. The Biodiversity of Grapevine Bacterial Endophytes of *Vitis amurensis* Rupr. *Plants* **11**, 1128.

Aleynova OA, Nityagovsky NN, Suprun AR, Ananev AA, Dubrovina AS, Kiselev KV, 2022b. The Diversity of Fungal Endophytes from Wild Grape Vitis amurensis Rupr. *Plants* **11**, 2897.

Alkowni R, Zhang Y-P, Rowhani A, Uyemoto JK, Minafra A, 2011. Biological, molecular, and serological studies of a novel strain of grapevine leafroll-associated virus 2. *Virus Genes* **43**, 102–110.

Alleweldt G, Possingham JV, 1988. Progress in grapevine breeding. *Theoretical and Applied Genetics* **75**, 669–673.

de Almeida ELM, Ventorim RZ, de Moura Ferreira MA, da Silveira WB, 2022. *Papiliotrema laurentii*: general features and biotechnological applications. *Applied Microbiology and Biotechnology* **106**, 6963–6976.

Altmann A, Toloşi L, Sander O, Lengauer T, 2010. Permutation importance: a corrected feature importance measure. *Bioinformatics* **26**, 1340–1347.

Anderson K, Aryal NR, 2013. *Which Winegrape Varieties are Grown Where? A global empirical picture*. University of Adelaide Press.

Andrews JH, Harris RF, 2000. The Ecology and Biogeography of Microorganisms on Plant Surfaces. *Annual Review of Phytopathology* **38**, 145–180.

Anees M, Tronsmo A, Edel-Hermann V, Hjeljord LG, Héraud C, Steinberg C, 2010. Characterization of field isolates of *Trichoderma* antagonistic against *Rhizoctonia solani*. *Fungal Biology* **114**, 691–701.

Angelotti F, Hamada E, Magalhães EE, Ghini R, Garrido L da R, Pedro MJ, 2017. Climate change and the occurrence of downy mildew in Brazilian grapevines. *Pesquisa Agropecuária Brasileira* **52**, 426–434.

Anslan S, Nilsson RH, Wurzbacher C, Baldrian P, Leho Tedersoo, Bahram M, 2018. Great differences in performance and outcome of high-throughput sequencing data analysis platforms for fungal metabarcoding. *MycoKeys*, 29–40.

Arkin AP, Cottingham RW, Henry CS *et al.*, 2018. KBase: The United States Department of Energy Systems Biology Knowledgebase. *Nature Biotechnology* **36**, 566–569.

Armijo G, Schlechter R, Agurto M, Muñoz D, Nuñez C, Arce-Johnson P, 2016. Grapevine Pathogenic Microorganisms: Understanding Infection Strategies and Host Response Scenarios. *Frontiers in Plant Science* **7**.

Armitage DW, Jones SE, 2019. How sample heterogeneity can obscure the signal of microbial interactions. *The ISME Journal* **13**, 2639–2646.

Arnault G, Mony C, Vandenkoornhuyse P, 2023. Plant microbiota dysbiosis and the Anna Karenina Principle. *Trends in Plant Science* **28**, 18–30.

Arnold C, Schnitzler A, Douard A, Peter R, Gillet F, 2005. Is there a future for wild grapevine (*Vitis vinifera* subsp. *silvestris*) in the Rhine Valley? *Biodiversity and Conservation* **14**, 1507–1523.

Arroyo-García R, Ruiz-García L, Bolling L *et al.*, 2006. Multiple origins of cultivated grapevine (*Vitis vinifera* L. ssp. *sativa*) based on chloroplast DNA polymorphisms. *Molecular Ecology* **15**, 3707–3714.

Asad NI, Tremblay J, Dozois J *et al.*, 2022. Predictive microbial-based modelling of wheat yields and grain baking quality across a 500 km transect in Québec. *FEMS Microbiology Ecology* **97**, fiab160.

Asghari S, Harighi B, Ashengroph M *et al.*, 2020. Induction of systemic resistance to *Agrobacterium tumefaciens* by endophytic bacteria in grapevine. *Plant Pathology* **69**, 827–837.

Asghari S, Harighi B, Mozafari AA, Esmaeel Q, Ait Barka E, 2019. Screening of endophytic bacteria isolated from domesticated and wild growing grapevines as potential biological control agents against crown gall disease. *BioControl* **64**, 723–735.

Ayers WA, Lumsden RD, 1977. Mycoparasitism of oospores of *Pythium* and *Aphanomyces* species by *Hyphochytrium catenoides*. *Canadian Journal of Microbiology* **23**, 38–44.

Azevedo-Silva D, Rasmussen JA, Carneiro M, Gilbert MTP, Azevedo H, 2021. Feasibility of applying shotgun metagenomic analyses to grapevine leaf, rhizosphere and soil microbiome characterisation. *Australian Journal of Grape and Wine Research* **27**, 519–526.

Aziz A, Perazzolli M, Gramaje D, Zyprian EM, Cantu D, 2020. Editorial: Recent Advances on Grapevine-Microbe Interactions: From Signal Perception to Resistance Response. *Frontiers in Plant Science* **11**, 1164.

Aziz A, Verhagen B, Magnin-Robert M *et al.*, 2016. Effectiveness of beneficial bacteria to promote systemic resistance of grapevine to gray mold as related to phytoalexin production in vineyards. *Plant and Soil* **405**, 141–153.

Badri DV, Vivanco JM, 2009. Regulation and function of root exudates. *Plant, Cell & Environment* **32**, 666–681.

Bais HP, Weir TL, Perry LG, Gilroy S, Vivanco JM, 2006. The role of root exudates in rhizosphere interactions with plants and other organisms. *Annual Review of Plant Biology* **57**, 233–266.

Baker ME, King RS, Kahle D, 2015. TITAN2: Threshold indicator taxa analysis. R package version 2.1.

Baker ME, King RS, Kahle D, 2023a. TITAN2: Threshold Indicator Taxa Analysis.

Baker ME, King RS, Kahle [aut D, cph, cre, 2023b. TITAN2: Threshold Indicator Taxa Analysis.

Bakker MG, Manter DK, Sheflin AM, Weir TL, Vivanco JM, 2012. Harnessing the rhizosphere microbiome through plant breeding and agricultural management. *Plant and Soil* **360**, 1–13.

Bakshi S, Sztejnberg A, Yarden O, 2001. Isolation and Characterization of a Cold-Tolerant Strain of *Fusarium proliferatum* , a Biocontrol Agent of Grape Downy Mildew. *Phytopathology®* **91**, 1062–1068.

Baldan E, Nigris S, Romualdi C *et al.*, 2015. Beneficial Bacteria Isolated from Grapevine Inner Tissues Shape *Arabidopsis thaliana* Roots (P Mergaert, Ed,). *PLOS ONE* **10**, e0140252.

Balestrini R, Magurno F, Walker C, Lumini E, Bianciotto V, 2010. Cohorts of arbuscular mycorrhizal fungi (AMF) in *Vitis vinifera*, a typical Mediterranean fruit crop: Cohorts of AM fungi in vineyards. *Environmental Microbiology Reports* **2**, 594–604.

Balint-Kurti P, Simmons SJ, Blum JE, Ballaré CL, Stapleton AE, 2010. Maize Leaf Epiphytic Bacteria Diversity Patterns Are Genetically Correlated with Resistance to Fungal Pathogen Infection. *Molecular Plant-Microbe Interactions®* **23**, 473–484.

Banani H, Roatti B, Ezzahi B *et al.*, 2014. Characterization of resistance mechanisms activated by *Trichoderma harzianum* T39 and benzothiadiazole to downy mildew in different grapevine cultivars. *Plant Pathology* **63**, 334–343.

Bao L, Sun B, Wei Y *et al.*, 2022. Grape Cultivar Features Differentiate the Grape Rhizosphere Microbiota. *Plants* **11**, 1111.

Barata A, Malfeito-Ferreira M, Loureiro V, 2012. The microbial ecology of wine grape berries. *International Journal of Food Microbiology* **153**, 243–259.

Barnes CJ, Bünner MS, Ramírez-Flores MR *et al.*, 2024. The ancestral environment of teosinte populations shapes their root microbiome. *Environmental Microbiome* **19**, 64.

Barnett D, Arts I, Penders J, 2021. microViz: an R package for microbiome data visualization and statistics. *Journal of Open Source Software* **6**, 3201.

Barnett SE, Cala AR, Hansen JL *et al.*, 2020a. Evaluating the Microbiome of Hemp. *Phytobiomes Journal*.

Barnett SE, Youngblut ND, Buckley DH, 2020b. Soil characteristics and land-use drive bacterial community assembly patterns. *FEMS Microbiology Ecology* **96**, fiz194.

Barret M, Briand M, Bonneau S *et al.*, 2015. Emergence Shapes the Structure of the Seed Microbiota. *Applied and Environmental Microbiology* **81**, 1257–1266.

Barroso-Bergadà D, Delmotte F, Faivre d'Arcier J *et al.*, 2023a. Leaf Microbiome Data for European Cultivated Grapevine (*Vitis vinifera*) During Downy Mildew (*Plasmopara*

viticola) Epidemics in Three Wine-Producing Regions in France. *PhytoFrontiers*^{TM}, PHYTOFR-11-22-0138-A.

Barroso-Bergadà D, Delmotte F, Faivre d'Arcier J *et al.*, 2023b. Leaf Microbiome Data for European Cultivated Grapevine (*Vitis vinifera*) During Downy Mildew (*Plasmopara viticola*) Epidemics in Three Wine-Producing Regions in France. *PhytoFrontiers*^{TM} **3**, 477–483.

Barroso-Bergadà D, Pauvert C, Vallance J *et al.*, 2021. Microbial networks inferred from environmental DNA data for biomonitoring ecosystem change: Strengths and pitfalls. *Molecular Ecology Resources* **21**, 762–780.

Barroso-Bergada D, Tamaddoni-Nezhad A, Muggleton SH, Vacher C, Galic N, Bohan DA, 2022. Machine Learning of Microbial Interactions Using Abductive ILP and Hypothesis Frequency/Compression Estimation. In: Katzouris N,, Artikis A, eds. *Inductive Logic Programming*. Lecture Notes in Computer Science. Cham: Springer International Publishing, 26–40.

Barroso-Bergada D, Tamaddoni-Nezhad A, Varghese D *et al.*, 2023. Unravelling the web of dark interactions: Explainable inference of the diversity of microbial interactions. In: *Advances in Ecological Research*. Elsevier, 155–183.

Bartoli C, Aubertot J-N, Litrico-Chiarelli I, Mougel C, 2020. Protection agroécologique pour le maintien de la santé des plantes. In: *Biocontrôle. Éléments pour une protection agroécologique des cultures*. 376.

Bass D, Stentiford GD, Wang H-C, Koskella B, Tyler CR, 2019. The Pathobiome in Animal and Plant Diseases. *Trends in Ecology & Evolution* **34**, 996–1008.

Becerra-Lucio AA, Labrín-Sotomayor NY, Becerra-Lucio PA *et al.*, 2021. Diversity and Interactomics of Bacterial Communities Associated with Dominant Trees During Tropical Forest Recovery. *Current Microbiology* **78**, 3417–3429.

Beeck MOD, Lievens B, Busschaert P, Declerck S, Vangronsveld J, Colpaert JV, 2014. Comparison and Validation of Some ITS Primer Pairs Useful for Fungal Metabarcoding Studies. *PLOS ONE* **9**, e97629.

Beghini F, McIver LJ, Blanco-Míguez A *et al.*, 2021. Integrating taxonomic, functional, and strain-level profiling of diverse microbial communities with bioBakery 3. *eLife* **10**, e65088.

Behrens FH, Fischer M, 2022a. Evaluation of Different Phyllosphere Sample Types for Parallel Metabarcoding of Fungi and Oomycetes in *Vitis vinifera*. *Phytobiomes Journal*, PBIOMES-11-21-0072-SC.

Behrens FH, Fischer M, 2022b. Evaluation of Different Phyllosphere Sample Types for Parallel Metabarcoding of Fungi and Oomycetes in *Vitis vinifera*. *Phytobiomes Journal* **6**, 207–213.

Bekris F, Vasileiadis S, Papadopoulou E *et al.*, 2021. Grapevine wood microbiome analysis identifies key fungal pathogens and potential interactions with the bacterial community implicated in grapevine trunk disease appearance. *Environmental Microbiome* **16**, 23.

Belcour A, Frioux C, Aite M, Bretaudeau A, Hildebrand F, Siegel A, 2020. Metage2Metabo, microbiota-scale metabolic complementarity for the identification of key species. *eLife* **9**, e61968.

Belcour A, Ruiz B, Frioux C, Blanquart S, Siegel A, 2022. EsMeCaTa: Estimating metabolic capabilities from taxonomic affiliations. *bioRxiv*, 2022.03.16.484574.

Belessi C, Chalvantzi I, Marmaras I, Nisiotou A, 2022. The effect of vine variety and vintage on wine yeast community structure of grapes and ferments. *Journal of Applied Microbiology* **132**, 3672–3684.

Bell T, Newman JA, Silverman BW, Turner SL, Lilley AK, 2005. The contribution of species richness and composition to bacterial services. *Nature* **436**, 1157–1160.

Bellin D, Peressotti E, Merdinoglu D *et al.*, 2009. Resistance to Plasmopara viticola in grapevine 'Bianca' is controlled by a major dominant gene causing localised necrosis at the infection site. *Theoretical and Applied Genetics* **120**, 163–176.

de Bem BP, Bogo A, Everhart SE *et al.*, 2016. Effect of four training systems on the temporal dynamics of downy mildew in two grapevine cultivars in southern Brazil. *Tropical Plant Pathology* **41**, 370–379.

Bengtsson-Palme J, Ryberg M, Hartmann M *et al.*, 2013. Improved software detection and extraction of ITS1 and ITS2 from ribosomal ITS sequences of fungi and other eukaryotes for analysis of environmental sequencing data. *Methods in Ecology and Evolution* **4**, 914–919.

Berendsen RL, Pieterse CMJ, Bakker PAHM, 2012. The rhizosphere microbiome and plant health. *Trends in Plant Science* **17**, 478–486.

Berendsen RL, Vismans G, Yu K *et al.*, 2018. Disease-induced assemblage of a plant-beneficial bacterial consortium. *The ISME Journal* **12**, 1496–1507.

Berg G, Köberl M, Rybakova D, Müller H, Grosch R, Smalla K, 2017. Plant microbial diversity is suggested as the key to future biocontrol and health trends. *FEMS Microbiology Ecology* **93**, fix050.

Berlanas C, Berbegal M, Elena G *et al.*, 2019. The Fungal and Bacterial Rhizosphere Microbiome Associated With Grapevine Rootstock Genotypes in Mature and Young Vineyards. *Frontiers in Microbiology* **10**, 1142.

Bernard M, Rué O, Mariadassou M, Pascal G, 2021. FROGS: a powerful tool to analyse the diversity of fungi with special management of internal transcribed spacers. *Briefings in Bioinformatics* **22**, bbab318.

Bernardo-Cravo AP, Schmeller DS, Chatzinotas A, Vredenburg VT, Loyau A, 2020. Environmental Factors and Host Microbiomes Shape Host–Pathogen Dynamics. *Trends in Parasitology* **36**, 616–633.

Bertsch C, Ramírez-Suero M, Magnin-Robert M *et al.*, 2013. Grapevine trunk diseases: complex and still poorly understood: *Grapevine trunk diseases*. *Plant Pathology* **62**, 243–265.

Bettenfeld P, Cadena i Canals J, Jacquens L *et al.*, 2021. The microbiota of the grapevine holobiont: A key component of plant health. *Journal of Advanced Research*, S2090123221002617.

Bhowmick TS, Das M, Heinz KM, Krauter PC, Gonzalez CF, 2016. Transmission of phage by glassy-winged sharpshooters, a vector of *Xylella fastidiosa*. *Bacteriophage* **6**, e1218411.

Bickhart DM, Kolmogorov M, Tseng E *et al.*, 2022. Generating lineage-resolved, complete metagenome-assembled genomes from complex microbial communities. *Nature Biotechnology*, 1–9.

Biget M, Wang T, Mony C *et al.*, submitted. Evaluating the Hologenome Concept by the Analysis of the Root-Endosphere Microbiota of Chimeric Plants.

Biggs MB, Medlock GL, Kolling GL, Papin JA, 2015. Metabolic network modeling of microbial communities. *Wiley Interdisciplinary Reviews: Systems Biology and Medicine* **7**, 317–334.

Bilen M, Dufour J-C, Lagier J-C *et al.*, 2018. The contribution of culturomics to the repertoire of isolated human bacterial and archaeal species. *Microbiome* **6**, 94.

Biljana K, Rade R, Katerina BO, Mirjana J, 2023. BACILLUS SPP. – A POTENT BIOLOGICAL CONTROL AGENTS AGAINST DOWNY MILDEW OF GRAPEVINE. *Journal of Agricultural, Food and Environmental Sciences, JAFES* **77**, 26–32.

Bitsadze N, Chipashvili R, Tskhvedadze L *et al.*, 2014. Screening of the Georgian Grape Germplasm to Susceptibility of Downy Mildew: Preliminary Results. *Acta horticulturae* **Volume 1**, 191–196.

Blasi P, Blanc S, Wiedemann-Merdinoglu S *et al.*, 2011. Construction of a reference linkage map of Vitis amurensis and genetic mapping of Rpv8, a locus conferring resistance to grapevine downy mildew. *Theoretical and Applied Genetics* **123**, 43–53.

Bleach C, Ridgway HJ, Jaspers MV, Jones EE, 2021. The relative susceptibility of grapevine rootstocks to black foot disease is dependent on inoculum pressure. *New Zealand Plant Protection* **74**, 62–69.

Bleve G, Grieco F, Cozzi G, Logrieco A, Visconti A, 2006. Isolation of epiphytic yeasts with potential for biocontrol of *Aspergillus carbonarius* and *A. niger* on grape. *International Journal of Food Microbiology* **108**, 204–209.

Bodenhausen N, Bortfeld-Miller M, Ackermann M, Vorholt JA, 2014. A Synthetic Community Approach Reveals Plant Genotypes Affecting the Phyllosphere Microbiota. *PLOS Genetics* **10**, e1004283.

Bodin E, Bellée A, Dufour M-C, André O, Corio-Costet M-F, 2020. Grapevine Stimulation: A Multidisciplinary Approach to Investigate the Effects of Biostimulants and a Plant Defense Stimulator. *Journal of Agricultural and Food Chemistry* **68**, 15085–15096.

Bois B, Zito S, Calonnec A, 2017. Climate vs grapevine pests and diseases worldwide: the first results of a global survey. *OENO One* **51**, 133–139.

Bokulich NA, Thorngate JH, Richardson PM, Mills DA, 2014. Microbial biogeography of wine grapes is conditioned by cultivar, vintage, and climate. *Proceedings of the National Academy of Sciences* **111**.

Bona E, Massa N, Novello G *et al.*, 2018. Metaproteomic characterization of *Vitis vinifera* rhizosphere. *FEMS Microbiology Ecology*.

Borcard D, Legendre P, 2002. All-scale spatial analysis of ecological data by means of principal coordinates of neighbour matrices. *Ecological Modelling* **153**, 51–68.

Borderes M, Gasc C, Prestat E *et al.*, 2021. A comprehensive evaluation of binning methods to recover human gut microbial species from a non-redundant reference gene catalog. *NAR Genomics and Bioinformatics* **3**, lqab009-.

Boso S, Gago P, Santiago J-L, de la Fuente M, Martínez M-C, 2019. Factors Affecting the Vineyard Populational Diversity of *Plasmopara viticola*. *The Plant Pathology Journal* **35**, 125–136.

Botstein D, Fink GR, 2011. Yeast: An Experimental Organism for 21st Century Biology. *Genetics* **189**, 695–704.

Bowers J, Boursiquot J-M, This P, Chu K, Johansson H, Meredith C, 1999. Historical Genetics: The Parentage of Chardonnay, Gamay, and Other Wine Grapes of Northeastern France. *Science* **285**, 1562–1565.

Bozoudi D, Tsaltas D, 2018. The Multiple and Versatile Roles of *Aureobasidium pullulans* in the Vitivinicultural Sector. *Fermentation* **4**, 85.

Brader G, Compant S, Vescio K *et al.*, 2017. Ecology and Genomic Insights into Plant-Pathogenic and Plant-Nonpathogenic Endophytes. *Annual Review of Phytopathology* **55**, 61–83.

van den Brand T, 2024. ggh4x: Hacks for "ggplot2."

Brandt MI, Trouche B, Quintric L *et al.*, 2021. Bioinformatic pipelines combining denoising and clustering tools allow for more comprehensive prokaryotic and eukaryotic metabarcoding. *Molecular Ecology Resources* **21**, 1904–1921.

Brewer MT, Milgroom MG, 2010. Phylogeography and population structure of the grape powdery mildew fungus, *Erysiphe necator*, from diverse *Vitis* species. *BMC Evolutionary Biology* **10**, 268.

Brito LM de, Zanette F, Biasi LA, Costa MD, Passos JFM dos, 2019. Morphological identification of *Ilyonectria liriodendri* and its interaction with plant growth-promoting bacteria in grapevine rootstocks. *Revista Brasileira de Fruticultura* **41**, e-140.

Bruez E, Baumgartner K, Bastien S, Travadon R, Guérin-Dubrana L, Rey P, 2016. Various fungal communities colonise the functional wood tissues of old grapevines externally free from grapevine trunk disease symptoms: Fungal microflora of GTD-free old vines. *Australian Journal of Grape and Wine Research* **22**, 288–295.

Bruez E, Haidar R, Alou MT *et al.*, 2015. Bacteria in a wood fungal disease: characterization of bacterial communities in wood tissues of esca-foliar symptomatic and asymptomatic grapevines. *Frontiers in Microbiology* **6**, 1137.

Bruez E, Lecomte P, Grosman J *et al.*, 2013. Overview of grapevine trunk diseases in France in the 2000s. *Phytopathologia Mediterranea* **52**, 262−275.

Bruez E, Vallance J, Gautier A *et al.*, 2020. Major changes in grapevine wood microbiota are associated with the onset of esca, a devastating trunk disease. *Environmental Microbiology* **22**, 5189–5206.

Bruez E, Vallance J, Gerbore J *et al.*, 2014. Analyses of the Temporal Dynamics of Fungal Communities Colonizing the Healthy Wood Tissues of Esca Leaf-Symptomatic and Asymptomatic Vines (BA Vinatzer, Ed,). *PLoS ONE* **9**, e95928.

Bruisson S, Zufferey M, L'Haridon F *et al.*, 2019. Endophytes and Epiphytes From the Grapevine Leaf Microbiome as Potential Biocontrol Agents Against Phytopathogens. *Frontiers in Microbiology* **10**, 2726.

Brum MCP, Araújo WL, Maki CS, Azevedo JL, 2012. Endophytic fungi from *Vitis labrusca* L. 'Niagara Rosada') and its potential for the biological control of *Fusarium oxysporum*. *Genetics and Molecular Research* **11**, 4187–4197.

Bucci V, Tzen B, Li N *et al.*, 2016. MDSINE: Microbial Dynamical Systems INference Engine for microbiome time-series analyses. *Genome Biology* **17**, 121.

Bulgarelli D, Garrido-Oter R, Münch PC *et al.*, 2015. Structure and Function of the Bacterial Root Microbiota in Wild and Domesticated Barley. *Cell Host & Microbe* **17**, 392–403.

Bulgarelli D, Schlaeppi K, Spaepen S, Themaat EVL van, Schulze-Lefert P, 2013. Structure and Functions of the Bacterial Microbiota of Plants. *Annual Review of Plant Biology* **64**, 807–838.

Buonassisi D, Colombo M, Migliaro D *et al.*, 2017. Breeding for grapevine downy mildew resistance: a review of "omics" approaches. *Euphytica* **213**, 103.

Burnevica N, Klavina D, Lione G *et al.*, 2022. In vitro screening of Latvian isolates of Bjerkandera adusta and Sistotrema brinkmannii as potential biocontrol agents against Heterobasidion root and butt rots.

Burruano S, 2000. The life-cycle of *Plasmopara viticola*, cause of downy mildew of vine. *Mycologist* **14**, 179–182.

Burruano S, Alfonzo A, Lo Piccolo S *et al.*, 2008. Interaction between *Acremonium byssoides* and *Plasmopara viticola* in *Vitis vinifera*. *Phytopathologia Mediterranea* **47**, 122–131.

Burruano S, Mondello V, Conigliaro G, 2016. Endophytic fungi in asymptomatic *Vitis vinifera* L. and their effects on *Plasmopara viticola*. In: Compant S,, Mathieu F, eds. *Biocontrol of major grapevine diseases: leading research*. Wallingford: CABI, 98–112.

Busby PE, Soman C, Wagner MR *et al.*, 2017. Research priorities for harnessing plant microbiomes in sustainable agriculture. *PLOS Biology* **15**, e2001793.

Button DK, Schut F, Quang P, Martin R, Robertson BR, 1993. Viability and Isolation of Marine Bacteria by Dilution Culture: Theory, Procedures, and Initial Results. *Applied and Environmental Microbiology* **59**, 881–891.

Čadež N, Zupan J, Raspor P, 2010. The effect of fungicides on yeast communities associated with grape berries. *FEMS Yeast Research* **10**, 619–630.

Cadle-Davidson L, 2008. Variation Within and Between Vitis spp. for Foliar Resistance to the Downy Mildew Pathogen Plasmopara viticola. *Plant Disease* **92**, 1577–1584.

Cadle-Davidson L, Chicoine DR, Consolie NH, 2011. Variation Within and Among *Vitis* spp. for Foliar Resistance to the Powdery Mildew Pathogen *Erysiphe necator*. *Plant Disease* **95**, 202–211.

Caffi T, Gilardi G, Monchiero M, Rossi V, 2013. Production and Release of Asexual Sporangia in Plasmopara viticola. *Phytopathology®* **103**, 64–73.

Callahan BJ, McMurdie PJ, Holmes SP, 2017. Exact sequence variants should replace operational taxonomic units in marker-gene data analysis. *The ISME Journal* **11**, 2639–2643.

Callahan BJ, McMurdie PJ, Rosen MJ, Han AW, Johnson AJA, Holmes SP, 2016. DADA2: High-resolution sample inference from Illumina amplicon data. *Nature Methods* **13**, 581–583.

Calonnec A, Cartolaro P, Naulin J-M, Bailey D, Langlais M, 2008. A host-pathogen simulation model: powdery mildew of grapevine. *Plant Pathology* **57**, 493–508.

Calonnec A, Jolivet J, Vivin P, Schnee S, 2018. Pathogenicity Traits Correlate With the Susceptible *Vitis vinifera* Leaf Physiology Transition in the Biotroph Fungus *Erysiphe necator*: An Adaptation to Plant Ontogenic Resistance. *Frontiers in Plant Science* **9**, 1808.

Camacho C, Coulouris G, Avagyan V *et al.*, 2009. BLAST+: architecture and applications. *BMC Bioinformatics* **10**, 421.

Cambon MC, 2024. marccamb/microranger.

Cambon MC, Cartry D, Chancerel E *et al.*, 2022. Drought tolerance traits in Neotropical trees correlate with the composition of phyllosphere fungal communities. *Phytobiomes Journal*, PBIOMES-04-22-0023-R.

Cambon MC, Trillat M, Lesur-Kupin I *et al.*, 2023. Microbial biomarkers of tree water status for next-generation biomonitoring of forest ecosystems. *Molecular Ecology* **32**, 5944–5958.

Campisano A, Antonielli L, Pancher M, Yousaf S, Pindo M, Pertot I, 2014. Bacterial Endophytic Communities in the Grapevine Depend on Pest Management (LS van Overbeek, Ed,). *PLoS ONE* **9**, e112763.

Campisano A, Pancher M, Puopolo G *et al.*, 2015a. Diversity in Endophyte Populations Reveals Functional and Taxonomic Diversity between Wild and Domesticated Grapevines. *American Journal of Enology and Viticulture* **66**, 12–21.

Campisano A, Pancher M, Puopolo G *et al.*, 2015b. Diversity in Endophyte Populations Reveals Functional and Taxonomic Diversity between Wild and Domesticated Grapevines. *American Journal of Enology and Viticulture* **66**, 12–21.

Canfora L, Vendramin E, Felici B, Tarricone L, Florio A, Benedetti A, 2018. Vineyard microbiome variations during different fertilisation practices revealed by 16s rRNA gene sequencing. *Applied Soil Ecology* **125**, 71–80.

Cantalapiedra CP, Hernández-Plaza A, Letunic I, Bork P, Huerta-Cepas J, 2021. eggNOG-mapper v2: Functional Annotation, Orthology Assignments, and Domain Prediction at the Metagenomic Scale. *Molecular Biology and Evolution* **38**, msab293-.

Carbone MJ, Alaniz S, Mondino P *et al.*, 2021. Drought Influences Fungal Community Dynamics in the Grapevine Rhizosphere and Root Microbiome. *Journal of Fungi* **7**, 686.

Carisse O, 2016. Development of grape downy mildew (*Plasmopara viticola*) under northern viticulture conditions: influence of fall disease incidence. *European Journal of Plant Pathology* **144**, 773–783.

Carlucci A, Raimondo ML, Colucci D, Lops F, 2022. Streptomyces albidoflavus Strain CARA17 as a Biocontrol Agent against Fungal Soil-Borne Pathogens of Fennel Plants. *Plants* **11**, 1420.

Carmichael PC, Siyoum N, Chidamba L, Korsten L, 2019. Exploring the microbial communities associated with *Botrytis cinerea* during berry development in table grape with emphasis on potential biocontrol yeasts. *European Journal of Plant Pathology* **154**, 919–930.

Carr A, Diener C, Baliga NS, Gibbons SM, 2019. Use and abuse of correlation analyses in microbial ecology. *The ISME Journal* **13**, 2647–2655.

Carrere C, Spilmont A-S, Loupit G *et al.*, 2022. Evaluation of criteria to assist the selection of good quality grafted grapevines prior to their commercialisation. *OENO One* **56**, 15–27.

Carrión VJ, Perez-Jaramillo J, Cordovez V *et al.*, 2019. Pathogen-induced activation of disease-suppressive functions in the endophytic root microbiome. *Science* **366**, 606–612.

Casida LE, Liu K-C, 1974. Arthrobacter globiformis and Its Bacteriophage in Soil. *Applied Microbiology* **28**, 951–959.

Casieri L, Hofstetter V, Viret O, Gindro K, 2009. Fungal communities living in the wood of different cultivars of young *Vitis vinifera* plants. *Phytopathologia Mediterranea* **48**, 73–83.

Castañeda LE, Barbosa O, 2017. Metagenomic analysis exploring taxonomic and functional diversity of soil microbial communities in Chilean vineyards and surrounding native forests. *PeerJ* **5**, e3098.

Castañeda LE, Miura T, Sánchez R, Barbosa O, 2018. Effects of agricultural management on phyllosphere fungal diversity in vineyards and the association with adjacent native forests. *PeerJ* **6**, e5715.

Castoria R, Miccoli C, Barone G *et al.*, 2021a. Molecular Tools for the Yeast *Papiliotrema terrestris* LS28 and Identification of Yap1 as a Transcription Factor Involved in Biocontrol Activity. *Applied and Environmental Microbiology* **87**, e02910-20.

Castoria R, Miccoli C, Barone G *et al.*, 2021b. Molecular Tools for the Yeast Papiliotrema terrestris LS28 and Identification of Yap1 as a Transcription Factor Involved in Biocontrol Activity. *Applied and Environmental Microbiology* **87**, e02910-20.

Castrillo-Sequeira D, Jiménez-Robles R, Granados-Montero MD, 2023. Current situation of viticulture in Costa Rica and management strategies for downy mildew (*Plasmopara viticola*). *Mexican Journal of Phytopathology* **42**.

Cavalieri D, McGovern PE, Hartl DL, Mortimer R, Polsinelli M, 2003. Evidence for S. cerevisiae Fermentation in Ancient Wine. *Journal of Molecular Evolution* **57**, S226–S232.

Cesco S, Tolotti A, Nadalini S *et al.*, 2020. Plasmopara viticola infection affects mineral elements allocation and distribution in Vitis vinifera leaves. *Scientific Reports* **10**, 18759.

Chanchaichaovivat A, Ruenwongsa P, Panijpan B, 2007. Screening and identification of yeast strains from fruits and vegetables: Potential for biological control of postharvest chilli anthracnose (*Colletotrichum capsici*). *Biological Control* **42**, 326–335.

Chand-Goyal T, Spotts RA, 1996. Control of postharvest pear diseases using natural saprophytic yeast colonists and their combination with a low dosage of thiabendazole. *Postharvest Biology and Technology* **7**, 51–64.

Chandra M, Mota M, Silva AC, Malfeito-Ferreira M, 2020. Forest Oak Woodlands and Fruit Tree Soils Are Reservoirs of Wine-Related Yeast Species. *American Journal of Enology and Viticulture* **71**, 191–197.

Chao A, Gotelli NJ, Hsieh TC *et al.*, 2014. Rarefaction and extrapolation with Hill numbers: a framework for sampling and estimation in species diversity studies. *Ecological Monographs* **84**, 45–67.

Chaparro JM, Badri DV, Vivanco JM, 2014. Rhizosphere microbiome assemblage is affected by plant development. *The ISME Journal* **8**, 790–803.

Chaudhry V, Runge P, Sengupta P, Doehlemann G, Parker JE, Kemen E, 2021. Shaping the leaf microbiota: plant–microbe–microbe interactions (S Kopriva, Ed,). *Journal of Experimental Botany* **72**, 36–56.

Chelius MK, Triplett EW, 2001a. The Diversity of Archaea and Bacteria in Association with the Roots of *Zea mays* L. *Microbial Ecology* **41**, 252–263.

Chelius MK, Triplett EW, 2001b. The Diversity of Archaea and Bacteria in Association with the Roots of *Zea mays* L. *Microbial ecology*, 252–263.

Chen L-X, Anantharaman K, Shaiber A, Eren AM, Banfield JF, 2020a. Accurate and complete genomes from metagenomes. *Genome Research* **30**, 315–333.

Chen M, Brun F, Raynal M, Makowski D, 2019. Timing of Grape Downy Mildew Onset in Bordeaux Vineyards. *Phytopathology®* **109**, 787–795.

Chen Y-Y, Chen P-C, Tsay T-T, 2016. The biocontrol efficacy and antibiotic activity of *Streptomyces plicatus* on the oomycete *Phytophthora capsici*. *Biological Control* **98**, 34–42.

Chen Y-H, Chiang P-W, Rogozin DY, Degermendzhy AG, Chiu H-H, Tang S-L, 2021a. Salvaging high-quality genomes of microbial species from a meromictic lake using a hybrid sequencing approach. *Communications Biology* **4**, 996.

Chen Y-H, Chiang P-W, Rogozin DY, Degermendzhy AG, Chiu H-H, Tang S-L, 2021b. Salvaging high-quality genomes of microbial species from a meromictic lake using a hybrid sequencing approach. *Communications Biology* **4**, 996.

Chen F, Guo YB, Wang JH, Li JY, Wang HM, 2007. Biological Control of Grape Crown Gall by *Rahnella aquatilis* HX2. *Plant Disease* **91**, 957–963.

Chen T, Nomura K, Wang X *et al.*, 2020b. A plant genetic network for preventing dysbiosis in the phyllosphere. *Nature* **580**, 653–657.

Chen Y, Wan Y, Jiang X, Liu Q, Wei T, Wang M, 2022. A novel fungal strain, Bjerkandera adusta BK-1, as a promising broad-spectrum biological control agent against plant fungal diseases. *Biocontrol Science and Technology* **32**, 515–519.

Chen X, Wicaksono WA, Berg G, Cernava T, 2021c. Bacterial communities in the plant phyllosphere harbour distinct responders to a broad-spectrum pesticide. *Science of The Total Environment* **751**, 141799.

Chen J, Zhang X, Yang L, Zhang L, 2023. GUniFrac: Generalized UniFrac Distances, Distance-Based Multivariate Methods and Feature-Based Univariate Methods for Microbiome Data Analysis.

Chiapello M, Rodríguez-Romero J, Ayllón MA, Turina M, 2020. Analysis of the virome associated to grapevine downy mildew lesions reveals new mycovirus lineages. *Virus Evolution* **6**, veaa058.

Chiquet J, Robin S, Mariadassou M, 2019. Variational Inference for sparse network reconstruction from count data. In: *Proceedings of the 36th International Conference on Machine Learning*. PMLR, 1162–1171.

Chitarra W, Perrone I, Avanzato CG *et al.*, 2017. Grapevine grafting: scion transcript profiling and defense-related metabolites induced by rootstocks. *Frontiers in Plant Science* **8**.

Chitwood DH, Klein LL, O'Hanlon R *et al.*, 2016. Latent developmental and evolutionary shapes embedded within the grapevine leaf. *New Phytologist* **210**, 343–355.

Claisse O, Chaïb A, Jaomanjaka F *et al.*, 2021. Distribution of Prophages in the *Oenococcus oeni* Species. *Microorganisms* **9**, 856.

Clavijo-Coppens F, Ginet N, Cesbron S, Briand M, Jacques M-A, Ansaldi M, 2021. Novel Virulent Bacteriophages Infecting Mediterranean Isolates of the Plant Pest *Xylella fastidiosa* and *Xanthomonas albilineans*. *Viruses* **13**, 725.

Cobo-Díaz JF, Legrand F, Le Floch G, Picot A, 2022. Influence of maize residues in shaping soil microbiota and *Fusarium* spp. communities. *Microbial Ecology* **83**, 702–713.

Cobos R, Ibañez A, Diez-Galán A, Calvo-Peña C, Ghoreshizadeh S, Coque JJR, 2022. The Grapevine Microbiome to the Rescue: Implications for the Biocontrol of Trunk Diseases. *Plants* **11**, 840.

Compant S, Brader G, Muzammil S, Sessitsch A, Lebrihi A, Mathieu F, 2013. Use of beneficial bacteria and their secondary metabolites to control grapevine pathogen diseases. *BioControl* **58**, 435–455.

Compant S, Cambon MC, Vacher C, Mitter B, Samad A, Sessitsch A, 2021. The plant endosphere world – bacterial life within plants. *Environmental Microbiology* **23**, 1812–1829.

Compant S, Cassan F, Kostić T *et al.*, 2024. Harnessing the plant microbiome for sustainable crop production. *Nature Reviews Microbiology*, 1–15.

Compant S, Samad A, Faist H, Sessitsch A, 2019. A review on the plant microbiome: Ecology, functions, and emerging trends in microbial application. *Journal of Advanced Research* **19**, 29–37.

Compant, Stéphane S, Kaplan H, Sessitsch A, Nowak J, Ait Barka E, Clément C, 2008. Endophytic colonization of *Vitis vinifera* L. by *Burkholderia phytofirmans* strain PsJN: from the rhizosphere to inflorescence tissues. *FEMS Microbiology Ecology* **63**, 84–93.

Conceição CS, Felix KCS, Mariano RLR, Medeiros EV, Souza EB, 2014. Combined effect of yeast and silicon on the control of bacterial fruit blotch in melon. *Scientia Horticulturae* 174, 164–170.

Conigliaro G, Ferraro V, Martorana A, Burruano S, 2008. In vivo antagonism of *Acremonium byssoides* endophyte in *Vitis vinifera*, towards *Plasmopara viticola*.

Cookson SJ, Clemente Moreno MJ, Hevin C *et al.*, 2013. Graft union formation in grapevine induces transcriptional changes related to cell wall modification, wounding, hormone signalling, and secondary metabolism. *Journal of Experimental Botany* 64, 2997–3008.

Cordero-Bueso G, Mangieri N, Maghradze D *et al.*, 2017. Wild Grape-Associated Yeasts as Promising Biocontrol Agents against *Vitis vinifera* Fungal Pathogens. *Frontiers in Microbiology* 8, 2025.

Cordero-Bueso G, Vigentini I, Foschino R *et al.*, 2022. Culturable Yeast Diversity of Grape Berries from *Vitis vinifera* ssp. *sylvestris* (Gmelin) Hegi. *Journal of Fungi* 8, 410.

Correa-Garcia S, Constant P, Yergeau E, 2023. The forecasting power of the microbiome. *Trends in Microbiology* 31, 444–452.

Crandall SG, Gold KM, Jiménez-Gasco M del M, Filgueiras CC, Willett DS, 2020. A multi-omics approach to solving problems in plant disease ecology. *PLOS ONE* 15, e0237975.

Crane SL, van Dorst J, Hose GC, King CK, Ferrari BC, 2018. Microfluidic qPCR Enables High Throughput Quantification of Microbial Functional Genes but Requires Strict Curation of Primers. *Frontiers in Environmental Science* 6.

Crisp P, Wicks TJ, Bruer D, Scott ES, 2006. An evaluation of biological and abiotic controls for grapevine powdery mildew. 2. Vineyard trials. *Australian Journal of Grape and Wine Research* 12, 203–211.

Cruz-Silva A, Figueiredo A, Sebastiana M, 2021. First Insights into the Effect of Mycorrhizae on the Expression of Pathogen Effectors during the Infection of Grapevine with *Plasmopara viticola*. *Sustainability* 13, 1226.

Cui S, Zhou L, Fang Q, Xiao H, Jin D, Liu Y, 2024. Growth period and variety together drive the succession of phyllosphere microbial communities of grapevine. *Science of The Total Environment* 950, 175334.

Cureau N, Threlfall R, Marasini D, Lavefve L, Carbonero F, 2021. Year, Location, and Variety Impact on Grape-Associated Mycobiota of Arkansas-Grown Wine Grapes for Wine Production. *Microbial Ecology* 82, 845–858.

Dagostin S, Schärer H-J, Pertot I, Tamm L, 2011. Are there alternatives to copper for controlling grapevine downy mildew in organic viticulture? *Crop Protection* 30, 776–788.

Dagostin S, Vecchione A, Zulini L, Ferrari A, Gobbin D, Pertot I, 2006. Potential use of biocontrol agents to prevent *Plasmopara viticola* oospore germination.

Damme RV, Hölzer M, Viehweger A, Müller B, Bongcam-Rudloff E, Brandt C, 2021. Metagenomics workflow for hybrid assembly, differential coverage binning, metatranscriptomics and pathway analysis (MUFFIN). *PLOS Computational Biology* 17, e1008716.

Darriaut R, Lailheugue V, Masneuf-Pomarède I *et al.*, 2022. Grapevine rootstock and soil microbiome interactions: Keys for a resilient viticulture. *Horticulture Research* **9**, uhac019.

Darriaut R, Martins G, Dewasme C *et al.*, 2021. Grapevine decline is associated with difference in soil microbial composition and activity. *OENO One* **55**.

Das M, Bhowmick TS, Ahern SJ, Young R, Gonzalez CF, 2015. Control of Pierce's Disease by Phage (A Rashed, Ed,). *PLOS ONE* **10**, e0128902.

Das S, Rabha J, Narzary D, 2023. Assessment of soil yeasts *Papiliotrema laurentii* S-08 and *Saitozyma podzolica* S-77 for plant growth promotion and biocontrol of *Fusarium* wilt of brinjal. *Journal of Applied Microbiology* **134**, lxad252.

Dastogeer KMG, Yasuda M, Okazaki S, 2022. Microbiome and pathobiome analyses reveal changes in community structure by foliar pathogen infection in rice. *Frontiers in Microbiology* **13**.

Del Frari G, Gobbi A, Aggerbeck MR, Oliveira H, Hansen LH, Ferreira RB, 2019. Characterization of the Wood Mycobiome of Vitis vinifera in a Vineyard Affected by Esca. Spatial Distribution of Fungal Communities and Their Putative Relation With Leaf Symptoms. *Frontiers in Plant Science* **10**, 910.

Delgado-Baquerizo M, Giaramida L, Reich PB *et al.*, 2016. Lack of functional redundancy in the relationship between microbial diversity and ecosystem functioning. *Journal of Ecology* **104**, 936–946.

Delière L, Cartolaro P, Léger B, Naud O, 2015. Field evaluation of an expertise-based formal decision system for fungicide management of grapevine downy and powdery mildews. *Pest Management Science* **71**, 1247–1257.

Derevnina L, Petre B, Kellner R *et al.*, 2016. Emerging oomycete threats to plants and animals. *Philosophical Transactions of the Royal Society B: Biological Sciences* **371**, 20150459.

Derocles SAP, Bohan DA, Dumbrell AJ *et al.*, 2018. Biomonitoring for the 21st Century: Integrating Next-Generation Sequencing Into Ecological Network Analysis. In: *Advances in Ecological Research*. Elsevier, 1–62.

Deyett E, Rolshausen PE, 2019. Temporal Dynamics of the Sap Microbiome of Grapevine Under High Pierce's Disease Pressure. *Frontiers in Plant Science* **10**, 1246.

Deyett E, Rolshausen PE, 2020. Endophytic microbial assemblage in grapevine. *FEMS Microbiology Ecology* **96**, fiaa053.

DGAL/SAS/2022-949

Di Gaspero G, Cipriani G, Adam-Blondon A-F, Testolin R, 2007. Linkage maps of grapevine displaying the chromosomal locations of 420 microsatellite markers and 82 markers for R-gene candidates. *Theoretical and Applied Genetics* **114**, 1249–1263.

Di Gaspero G, Copetti D, Coleman C *et al.*, 2012. Selective sweep at the Rpv3 locus during grapevine breeding for downy mildew resistance. *Theoretical and Applied Genetics* **124**, 277–286.

Di Vecchi-Staraz M, Laucou V, Bruno G *et al.*, 2009. Low Level of Pollen-Mediated Gene Flow from Cultivated to Wild Grapevine: Consequences for the Evolution of the Endangered Subspecies *Vitis vinifera* L. subsp. *silvestris*. *Journal of Heredity* **100**, 66–75.

Ding Y, Wei R, Wang L, Yang C, Li H, Wang H, 2021. Diversity and dynamics of microbial ecosystem on berry surface during the ripening of Ecolly (*Vitis vinifera* L.) grape in Wuhai, China. *World Journal of Microbiology and Biotechnology* **37**, 214.

Dohlman AB, Shen X, 2019. Mapping the microbial interactome: Statistical and experimental approaches for microbiome network inference. *Experimental Biology and Medicine* **244**, 445–458.

Dong C-J, Wang L-L, Li Q, Shang Q-M, 2019. Bacterial communities in the rhizosphere, phyllosphere and endosphere of tomato plants. *PLOS ONE* **14**, e0223847.

Douglas GM, Maffei VJ, Zaneveld JR *et al.*, 2020. PICRUSt2 for prediction of metagenome functions. *Nature Biotechnology* **38**, 685–688.

Dreier M, Berthoud H, Shani N, Wechsler D, Junier P, 2021. Development of a High-Throughput Microfluidic qPCR System for the Quantitative Determination of Quality-Relevant Bacteria in Cheese. *Frontiers in Microbiology* **11**.

Dries L, Bussotti S, Pozzi C *et al.*, 2021. Rootstocks Shape Their Microbiome—Bacterial Communities in the Rhizosphere of Different Grapevine Rootstocks. *Microorganisms* **9**, 822.

Dry I, Riaz S, Fuchs M, Sosnowski M, Thomas M, 2019. Scion Breeding for Resistance to Biotic Stresses. In: Cantu D,, Walker MA, eds. *The Grape Genome*. Cham: Springer International Publishing, 319–347.

Du Y, Wang T, Jiang J *et al.*, 2022. Biological control and plant growth promotion properties of Streptomyces albidoflavus St-220 isolated from Salvia miltiorrhiza rhizosphere. *Frontiers in Plant Science* **13**.

Dufour M-C, Magnin N, Dumas B, Vergnes S, Corio-Costet M-F, 2016. High-throughput gene-expression quantification of grapevine defense responses in the field using microfluidic dynamic arrays. *BMC Genomics* **17**, 957.

Dufrêne M, Legendre P, 1997. Species assemblages and indicator species: the need for a flexible asymmetrical approach. *Ecological Monographs* **67**, 345–366.

Ebenhöh O, Handorf T, Heinrich R, 2004. Structural analysis of expanding metabolic networks. *Genome informatics. International Conference on Genome Informatics* **15**, 35–45.

Eder M, Nidelet T, Sanchez I, Camarasa C, Legras J-L, Dequin S, 2020. QTL mapping of modelled metabolic fluxes reveals gene variants impacting yeast central carbon metabolism. *Scientific Reports* **10**, 2162.

Eichmeier A, Pečenka J, Peňázová E *et al.*, 2018. High-throughput amplicon sequencing-based analysis of active fungal communities inhabiting grapevine after hot-water treatments reveals unexpectedly high fungal diversity. *Fungal Ecology* **36**, 26–38.

Eitzen K, Sengupta P, Kroll S, Kemen E, Doehlemann G, 2021. A fungal member of the Arabidopsis thaliana phyllosphere antagonizes Albugo laibachii via a GH25 lysozyme (C Gutjahr, CS Hardtke, C Gutjahr, Eds,). *eLife* **10**, e65306.

Elena G, Bruez E, Rey P, Luque J, 2018. Microbiota of grapevine woody tissues with or without esca-foliar symptoms in northeast Spain. *Phytopathologia Mediterranea* **57**, 425–438.

van Elsas JD, Chiurazzi M, Mallon CA, Elhottovā D, Krištůfek V, Salles JF, 2012. Microbial diversity determines the invasion of soil by a bacterial pathogen. *Proceedings of the National Academy of Sciences* **109**, 1159–1164.

El-Sayed ASA, Ali GS, 2020. *Aspergillus flavipes* is a novel efficient biocontrol agent of *Phytophthora parasitica*. *Biological Control* **140**, 104072.

El-Sharkawy HHA, Abo-El-Wafa TSA, Ibrahim SA-A, 2018. Biological control agents improve the productivity and induce the resistance against downy mildew of grapevine. *Journal of Plant Pathology* **100**, 33–42.

Escudié F, Auer L, Bernard M *et al.*, 2018. FROGS: Find, Rapidly, OTUs with Galaxy Solution. *Bioinformatics* **34**, 1287–1294.

Esmaeel Q, Jacquard C, Sanchez L, Clément C, Ait Barka E, 2020. The mode of action of plant associated Burkholderia against grey mould disease in grapevine revealed through traits and genomic analyses. *Scientific Reports* **10**, 19393.

Estaki M, Jiang L, Bokulich NA *et al.*, 2020. QIIME 2 Enables Comprehensive End-to-End Analysis of Diverse Microbiome Data and Comparative Studies with Publicly Available Data. *Current Protocols in Bioinformatics* **70**.

Esteves M, Lage P, Sousa J *et al.*, 2023. Biocontrol potential of wine yeasts against four grape phytopathogenic fungi disclosed by time-course monitoring of inhibitory activities. *Frontiers in Microbiology* **14**.

Ettinger CL, Wu-Woods J, Kurbessoian T *et al.*, 2023. Geographical survey of the mycobiome and microbiome of Southern California glassy-winged sharpshooters. *mSphere* **8**, e00267-23.

European Commission, 2020. *A Farm to Fork Strategy for a Fair, Healthy and Environmentally-Friendly Food System.*

F. Escapa I, Huang Y, Chen T *et al.*, 2020. Construction of habitat-specific training sets to achieve species-level assignment in 16S rRNA gene datasets. *Microbiome* **8**, 65.

Faist H, Keller A, Hentschel U, Deeken R, 2016. Grapevine (*Vitis vinifera*) Crown Galls Host Distinct Microbiota. *Applied and Environmental Microbiology* **82**, 5542–5552.

Falk SP, 1995. Parasitism of *Uncinula necator* Cleistothecia by the Mycoparasite *Ampelomyces quisqualis*. *Phytopathology* **85**, 794.

Falk S, 1996. *Fusarium proliferatum* as a Biocontrol Agent Against Grape Downy Mildew. *Phytopathology* **86**, 1010.

Fan Y, Gao L, Chang P, Li Z, 2020. Endophytic fungal community in grape is correlated to foliar age and domestication. *Annals of Microbiology* **70**, 30.

Fang H, Huang C, Zhao H, Deng M, 2015. CCLasso: correlation inference for compositional data through Lasso. *Bioinformatics* **31**, 3172–3180.

Faust K, Bauchinger F, Laroche B *et al.*, 2018. Signatures of ecological processes in microbial community time series. *Microbiome* **6**, 120.

Fay JC, Benavides JA, 2005. Evidence for Domesticated and Wild Populations of *Saccharomyces cerevisiae* (JE Haber, Ed,). *PLoS Genetics* **1**, e5.

Fay JC, McCullough HL, Sniegowski PD, Eisen MB, 2004. Population genetic variation in gene expression is associated with phenotypic variation in *Saccharomyces cerevisiae*. *Genome Biology* **5**, R26.

Feechan A, Anderson C, Torregrosa L *et al.*, 2013. Genetic dissection of a TIR-NB-LRR locus from the wild North American grapevine species *Muscadinia rotundifolia* identifies paralogous genes conferring resistance to major fungal and oomycete pathogens in cultivated grapevine. *The Plant Journal* **76**, 661–674.

Feechan A, Kocsis M, Riaz S *et al.*, 2015. Strategies for *RUN1* Deployment Using *RUN2* and *REN2* to Manage Grapevine Powdery Mildew Informed by Studies of Race Specificity. *Phytopathology®* **105**, 1104–1113.

Felber AC, Orlandelli RC, Rhoden SA *et al.*, 2016. Bioprospecting foliar endophytic fungi of *Vitis labrusca* Linnaeus, Bordô and Concord cv. *Annals of Microbiology* **66**, 765–775.

Fernandes de Oliveira A, Serra S, Ligios V, Satta D, Nieddu G, 2021. Assessing the Effects of Vineyard Soil Management on Downy and Powdery Mildew Development. *Horticulturae* **7**, 209.

Ferreiro AL, Choi J, Ryou J *et al.*, 2023. Gut microbiome composition may be an indicator of preclinical Alzheimer's disease. *Science Translational Medicine* **15**, eabo2984.

Fira D, Dimkić I, Berić T, Lozo J, Stanković S, 2018. Lutte biologique contre les agents pathogènes des plantes par les espèces *de Bacillus*. *Journal of Biotechnology* **285**, 44–55.

Fleet GH, 1993. *Wine Microbiology and Biotechnology*. Switzerland.

Fontaine MC, Austerlitz F, Giraud T *et al.*, 2013. Genetic signature of a range expansion and leap-frog event after the recent invasion of Europe by the grapevine downy mildew pathogen *Plasmopara viticola*. *Molecular Ecology* **22**, 2771–2786.

Fontaine MC, Labbé F, Dussert Y *et al.*, 2021. Europe as a bridgehead in the worldwide invasion history of grapevine downy mildew, *Plasmopara viticola*. *Current Biology* **31**, 2155-2166.e4.

Fort T, Pauvert C, Zanne AE *et al.*, 2021. Maternal effects shape the seed mycobiome in *Quercus petraea*. *New Phytologist* **230**, 1594–1608.

Fort T, Robin C, Capdevielle X, Delière L, Vacher C, 2016. Foliar fungal communities strongly differ between habitat patches in a landscape mosaic. *PeerJ* **4**, e2656.

Foster KR, Schluter J, Coyte KZ, Rakoff-Nahoum S, 2017. The evolution of the host microbiome as an ecosystem on a leash. *Nature* **548**, 43–51.

Fournier P, Pellan L, Barroso-Bergadà D *et al.*, 2022a. The functional microbiome of grapevine throughout plant evolutionary history and lifetime. *Advances in Ecological Research* **67**, 27.

Fournier P, Pellan L, Barroso-Bergadà D *et al.*, 2022b. Chapter Two - The functional microbiome of grapevine throughout plant evolutionary history and lifetime. In: Bohan DA,,

Dumbrell A, eds. *Advances in Ecological Research*. Functional Microbiomes. Academic Press, 27–99.

Fox J, Weisberg S, 2018. *An R Companion to Applied Regression*. SAGE Publications.

FranceAgrimer (2024) LES PERFORMANCES À L'EXPORT DES FILIÈRES AGRICOLES ET AGROALIMENTAIRES FRANÇAISES SITUATION EN 2023, 69pp

Francesca S, Simona G, Francesco Nicola T *et al.*, 2006. Downy mildew (Plasmopara viticola) epidemics on grapevine under climate change. *Global Change Biology* **12**, 1299–1307.

Freiberg E, 1998. Microclimatic parameters influencing nitrogen fixation in the phyllosphere in a Costa Rican premontane rain forest. *Oecologia* **117**, 9–18.

Freimoser FM, Rueda-Mejia MP, Tilocca B, Migheli Q, 2019. Biocontrol yeasts: mechanisms and applications. *World Journal of Microbiology and Biotechnology* **35**, 154.

French E, Kaplan I, Iyer-Pascuzzi A, Nakatsu CH, Enders L, 2021. Emerging strategies for precision microbiome management in diverse agroecosystems. *Nature Plants* **7**, 256–267.

Friedman J, Alm EJ, 2012. Inferring Correlation Networks from Genomic Survey Data. *PLOS Computational Biology* **8**, e1002687.

Friedman J, Higgins LM, Gore J, 2017. Community structure follows simple assembly rules in microbial microcosms. *Nature Ecology & Evolution* **1**, 1–7.

Frioux C, Fremy E, Trottier C, Siegel A, 2018. Scalable and exhaustive screening of metabolic functions carried out by microbial consortia. *Bioinformatics* **34**, i934–i943.

Frioux C, Singh D, Korcsmaros T, Hildebrand F, 2020. From bag-of-genes to bag-of-genomes: metabolic modelling of communities in the era of metagenome-assembled genomes. *Computational and Structural Biotechnology Journal* **18**, 1722–1734.

Fröbel S, Zyprian E, 2019. Colonization of Different Grapevine Tissues by Plasmopara viticola—A Histological Study. *Frontiers in Plant Science* **10**.

Frøslev TG, Kjøller R, Bruun HH *et al.*, 2017. Algorithm for post-clustering curation of DNA amplicon data yields reliable biodiversity estimates. *Nature Communications* **8**, 1188.

Furet J-P, Firmesse O, Gourmelon M *et al.*, 2009. Comparative assessment of human and farm animal faecal microbiota using real-time quantitative PCR. *FEMS Microbiology Ecology* **68**, 351–362.

Gadoury DM, Cadle-Davidson L, Wilcox WF, Dry IB, Seem RC, Milgroom MG, 2012. Grapevine powdery mildew (*Erysiphe necator*): a fascinating system for the study of the biology, ecology and epidemiology of an obligate biotroph: Grapevine powdery mildew. *Molecular Plant Pathology* **13**, 1–16.

Gambetta GA, Herrera JC, Dayer S, Feng Q, Hochberg U, Castellarin SD, 2020. The physiology of drought stress in grapevine: towards an integrative definition of drought tolerance (J Zhang, Ed,). *Journal of Experimental Botany* **71**, 4658–4676.

Gan HM, Szegedi E, Fersi R *et al.*, 2019. Insight Into the Microbial Co-occurrence and Diversity of 73 Grapevine (*Vitis vinifera*) Crown Galls Collected Across the Northern Hemisphere. *Frontiers in Microbiology* **10**, 1896.

Garbaye J, 1994. Tansley Review No. 76 Helper bacteria: a new dimension to the mycorrhizal symbiosis. *New Phytologist* **128**, 197–210.

Gardes M, Bruns TD, 1993. ITS primers with enhanced specificity for basidiomycetes - application to the identification of mycorrhizae and rusts. *Molecular Ecology* **2**, 113–118.

Gessler C, Pertot I, Perazzolli M, 2011. *Plasmopara viticola*: a review of knowledge on downy mildew of grapevine and effective disease management. *Phytopathologia Mediterranea* **50**, 3–44.

Ghasemi S, Safaie N, Shahbazi S, Shams-Bakhsh M, Askari H, 2020. The Role of Cell Wall Degrading Enzymes in Antagonistic Traits of Trichoderma virens Against Rhizoctonia solani. *Iranian Journal of Biotechnology* **18**, e2333.

Ghazanfar MU, Raza M, Raza W, Qamar MI, 2018. *Trichoderma* as potential biocontrol agent, its exploitation in agriculture: A review. *Plant Protection* **2**.

Ghorbanpour M, Omidvari M, Abbaszadeh-Dahaji P, Omidvar R, Kariman K, 2018. Mechanisms underlying the protective effects of beneficial fungi against plant diseases. *Biological Control* **117**, 147–157.

Ghule M, Sawant I, 2018. Potential of *Fusarium* spp. for biocontrol of downy mildew of grapes. **23**.

Ghule MR, Sawant IS, Oulkar D, Hingmire S, Shabeer A, Holkar S, 2022. Identification of secondary metabolites in mycoparasites *Fusarium* strains and antifungal activity of fusaric acid against *Plasmopara viticola*. *Archives of Phytopathology and Plant Protection* **55**, 1283–1297.

Ghule SB, Sawant IS, Sawant SD, Saha S, Devarumath RM, 2019. Isolation and identification of three new mycoparasites of *Erysiphe necator* for biological control of grapevine powdery mildew. *Australasian Plant Pathology* **48**, 351–367.

Ghule MR, Sawant IS, Sawant SD, Sharma R, Shouche YS, 2018. Identification of *Fusarium* species as putative mycoparasites of *Plasmopara viticola* causing downy mildew in grapevines. *Australasian Plant Disease Notes* **13**, 16.

Giangacomo C, Mohseni M, Kovar L, Wallace JG, 2021. Comparing DNA Extraction and 16S rRNA Gene Amplification Methods for Plant-Associated Bacterial Communities. *Phytobiomes Journal* **5**, 190–201.

Glawe DA, 2008. The Powdery Mildews: A Review of the World's Most Familiar (Yet Poorly Known) Plant Pathogens. *Annual Review of Phytopathology* **46**, 27–51.

Gloor GB, Macklaim JM, Pawlowsky-Glahn V, Egozcue JJ, 2017. Microbiome Datasets Are Compositional: And This Is Not Optional. *Frontiers in Microbiology* **8**, 2224.

Gobbi A, Kyrkou I, Filippi E, Ellegaard-Jensen L, Hansen LH, 2020. Seasonal epiphytic microbial dynamics on grapevine leaves under biocontrol and copper fungicide treatments. *Scientific Reports* **10**, 681.

Gobbin D, Jermini M, Loskill B, Pertot I, Raynal M, Gessler C, 2005. Importance of secondary inoculum of Plasmopara viticola to epidemics of grapevine *Plasmopara viticola*. *Plant Pathology* **54**, 522–534.

Gobbin D, Rumbou A, Linde CC, Gessler C, 2006. Population genetic structure of *Plasmopara viticola* after 125 years of colonization in European vineyards: Population genetics of *P. viticola* in Europe. *Molecular Plant Pathology* **7**, 519–531.

Göker M, Voglmayr H, Riethmüller A, Oberwinkler F, 2007. How do obligate parasites evolve? A multi-gene phylogenetic analysis of downy mildews. *Fungal Genetics and Biology* **44**, 105–122.

Golubev W, Ikeda R, Shinoda T, Nakase T, 1997. Antifungal activity of *Bullera alba* (Hanna) Derx. *Mycoscience* **38**, 25–29.

Gómez-Pérez D, Schmid M, Chaudhry V *et al.*, 2023. Proteins released into the plant apoplast by the obligate parasitic protist Albugo selectively repress phyllosphere-associated bacteria. *New Phytologist* **239**, 2320–2334.

González-Domínguez E, Berlanas C, Gramaje D, Armengol J, Rossi V, Berbegal M, 2020. Temporal Dispersal Patterns of Phaeomoniella chlamydospora, Causal Agent of Petri Disease and Esca, in Vineyards. *Phytopathology®* **110**, 1216–1225.

González-García S, Álvarez-Pérez JM, Sáenz de Miera LE *et al.*, 2019. Developing tools for evaluating inoculation methods of biocontrol *Streptomyces* sp. strains into grapevine plants (Z Abdo, Ed,). *PLOS ONE* **14**, e0211225.

Gonze D, Coyte KZ, Lahti L, Faust K, 2018. Microbial communities as dynamical systems. *Current Opinion in Microbiology* **44**, 41–49.

Goossens P, Spooren J, Baremans KCM *et al.*, 2023. Obligate biotroph downy mildew consistently induces near-identical protective microbiomes in Arabidopsis thaliana. *Nature Microbiology* **8**, 2349–2364.

Gopal M, Gupta A, 2016. Microbiome Selection Could Spur Next-Generation Plant Breeding Strategies. *Frontiers in Microbiology* **7**.

Gouka L, Raaijmakers JM, Cordovez V, 2022. Ecology and functional potential of phyllosphere yeasts. *Trends in Plant Science* **27**, 1109–1123.

Gramaje D, Armengol J, 2011. Fungal Trunk Pathogens in the Grapevine Propagation Process: Potential Inoculum Sources, Detection, Identification, and Management Strategies. *Plant Disease* **95**, 1040–1055.

Gramaje D, Eichmeier A, Spetik M *et al.*, 2022. Exploring the Temporal Dynamics of the Fungal Microbiome in Rootstocks, the Lesser-Known Half of the Grapevine Crop. *Journal of Fungi* **8**, 421.

Gramaje D, Úrbez-Torres JR, Sosnowski MR, 2018. Managing Grapevine Trunk Diseases With Respect to Etiology and Epidemiology: Current Strategies and Future Prospects. *Plant Disease* **102**, 12–39.

Grassi F, De Lorenzis G, 2021. Back to the Origins: Background and Perspectives of Grapevine Domestication. *International Journal of Molecular Sciences* **22**, 4518.

Grenville-Briggs LJ, Avrova AO, Bruce CR *et al.*, 2005. Elevated amino acid biosynthesis in *Phytophthora infestans* during appressorium formation and potato infection. *Fungal Genetics and Biology* **42**, 244–256.

Griggs RG, Steenwerth KL, Mills DA, Cantu D, Bokulich NA, 2021. Sources and Assembly of Microbial Communities in Vineyards as a Functional Component of Winegrowing. *Frontiers in Microbiology* **12**, 673810.

Grube M, Schmid F, Berg G, 2011. Black fungi and associated bacterial communities in the phyllosphere of grapevine. *Fungal Biology* **115**, 978–986.

Gu Y, Banerjee S, Dini-Andreote F *et al.*, 2022. Small changes in rhizosphere microbiome composition predict disease outcomes earlier than pathogen density variations. *The ISME Journal* **16**, 2448–2456.

Gu C, Kim GB, Kim WJ, Kim HU, Lee SY, 2019. Current status and applications of genome-scale metabolic models. *Genome Biology* **20**, 121.

Guarnaccia V, Groenewald JZ, Woodhall J *et al.*, 2018. *Diaporthe* diversity and pathogenicity revealed from a broad survey of grapevine diseases in Europe. *Persoonia - Molecular Phylogeny and Evolution of Fungi* **40**, 135–153.

Guetsky R, Shtienberg D, Elad Y, Dinoor A, 2007. Combining Biocontrol Agents to Reduce the Variability of Biological Control. *Phytopathology®* **91**, 621–627.

Gur L, Reuveni M, Cohen Y *et al.*, 2021. Population structure of *Erysiphe necator* on domesticated and wild vines in the Middle East raises questions on the origin of the grapevine powdery mildew pathogen. *Environmental Microbiology* **23**, 6019–6037.

Habbadi K, Duplay Q, Chapulliot D *et al.*, 2020. Characterization and phylogenetic diversity of *Allorhizobium vitis* isolated from grapevine in Morocco. *Journal of Applied Microbiology* **128**, 828–839.

Hacquard S, Spaepen S, Garrido-Oter R, Schulze-Lefert P, 2017. Interplay Between Innate Immunity and the Plant Microbiota. *Annual Review of Phytopathology* **55**, 565–589.

Haidar R, Compant S, Antonelli J *et al.* Bacteria associated with wood tissues of Esca-diseased grapevines: functional diversity and synergy with Fomitiporia mediterranea to degrade wood components. , (submitted).

Haidar R, Yacoub A, Vallance J *et al.*, 2021. Bacteria associated with wood tissues of Esca-diseased grapevines: functional diversity and synergy with *Fomitiporia mediterranea* to degrade wood components. *Environmental Microbiology* **23**, 6104–6121.

Hakimzadeh A, Abdala Asbun A, Albanese D *et al.*, 2024. A pile of pipelines: An overview of the bioinformatics software for metabarcoding data analyses. *Molecular Ecology Resources* **24**, e13847.

Hanania U, Velcheva M, Sahar N, Perl A, 2004. An improved method for isolating high-quality DNA from *Vitis vinifera* nuclei. *Plant Molecular Biology Reporter* **22**, 173–177.

Haney CH, Samuel BS, Bush J, Ausubel FM, 2015. Associations with rhizosphere bacteria can confer an adaptive advantage to plants. *Nature Plants* **1**, 1–9.

Hanshew AS, Mason CJ, Raffa KF, Currie CR, 2013. Minimization of chloroplast contamination in 16S rRNA gene pyrosequencing of insect herbivore bacterial communities. *Journal of Microbiological Methods* **95**, 149–155.

Hao Z, van Tuinen D, Fayolle L *et al.*, 2018. Arbuscular mycorrhiza affects grapevine fanleaf virus transmission by the nematode vector *Xiphinema index*. *Applied Soil Ecology* **129**, 107–111.

Hardham AR, 2007. Cell biology of plant–oomycete interactions. *Cellular Microbiology* **9**, 31–39.

Hardoim PR, van Overbeek LS, Berg G *et al.*, 2015. The Hidden World within Plants: Ecological and Evolutionary Considerations for Defining Functioning of Microbial Endophytes. *Microbiology and Molecular Biology Reviews* **79**, 293–320.

Hartig F, Lohse L, 2022. DHARMa: Residual Diagnostics for Hierarchical (Multi-Level / Mixed) Regression Models.

Hassaan MA, El Nemr A, 2020. Pesticides pollution: Classifications, human health impact, extraction and treatment techniques. *Egyptian Journal of Aquatic Research* **46**, 207–220.

Hassani MA, Durán P, Hacquard S, 2018. Microbial interactions within the plant holobiont. *Microbiome* **6**, 58.

Heid CA, Stevens J, Livak KJ, Williams PM, 1996. Real time quantitative PCR. *Genome Research* **6**, 986–994.

van der Heijden MGA, de Bruin S, Luckerhoff L, van Logtestijn RSP, Schlaeppi K, 2016. A widespread plant-fungal-bacterial symbiosis promotes plant biodiversity, plant nutrition and seedling recruitment. *The ISME Journal* **10**, 389–399.

Heinitz CC, Uretsky J, Dodson Peterson JC, Huerta-Acosta KG, Walker MA, 2019. Crop Wild Relatives of Grape (Vitis vinifera L.) Throughout North America. In: Greene SL,, Williams KA,, Khoury CK,, Kantar MB,, Marek LF, eds. *North American Crop Wild Relatives, Volume 2: Important Species*. Cham: Springer International Publishing, 329–351.

Héloir M-C, Adrian M, Brulé D *et al.*, 2019. Recognition of Elicitors in Grapevine: From MAMP and DAMP Perception to Induced Resistance. *Frontiers in Plant Science* **10**, 1117.

Hendgen M, Hoppe B, Döring J *et al.*, 2018. Effects of different management regimes on microbial biodiversity in vineyard soils. *Scientific Reports* **8**, 9393.

Hernandez MM, Menéndez CM, 2019. Influence of seasonality and management practices on diversity and composition of fungal communities in vineyard soils. *Applied Soil Ecology* **135**, 113–119.

Hildebrand F, Tadeo R, Voigt AY, Bork P, Raes J, 2014. LotuS: an efficient and user-friendly OTU processing pipeline. *Microbiome* **2**, 30.

Hillebrand H, Matthiessen B, 2009. Biodiversity in a complex world: consolidation and progress in functional biodiversity research. *Ecology Letters* **12**, 1405–1419.

Hindson BJ, Ness KD, Masquelier DA *et al.*, 2011. High-Throughput Droplet Digital PCR System for Absolute Quantitation of DNA Copy Number. *Analytical Chemistry* **83**, 8604–8610.

Hiruma K, Gerlach N, Sacristán S *et al.*, 2016. Root Endophyte Colletotrichum tofieldiae Confers Plant Fitness Benefits that Are Phosphate Status Dependent. *Cell* **165**, 464–474.

Hladnik M, Unković N, Janakiev T *et al.*, 2023. An Insight into an Olive Scab on the "Istrska Belica" Variety: Host-Pathogen Interactions and Phyllosphere Mycobiome. *Microbial Ecology* **86**, 1343–1363.

Hocking AD, Leong SL, Kazi BA, Emmett RW, Scott ES, 2007. Fungi and mycotoxins in vineyards and grape products. *International Journal of Food Microbiology* **119**, 84–88.

Hofstetter V, Buyck B, Croll D, Viret O, Couloux A, Gindro K, 2012. What if esca disease of grapevine were not a fungal disease? *Fungal Diversity* **54**, 51–67.

Hong C-F, Brewer MT, Brannen PM, Scherm H, 2020. Temporal disease dynamics and relative importance of sexual and asexual reproduction of grape downy mildew (*Plasmopara viticola*) in an isolated vineyard in the North Georgia Mountains, USA. *Plant Pathology* **69**, 1721–1730.

Hooper DU, Chapin III FS, Ewel JJ *et al.*, 2005. Effects of Biodiversity on Ecosystem Functioning: A Consensus of Current Knowledge. *Ecological Monographs* **75**, 3–35.

Horton MW, Bodenhausen N, Beilsmith K *et al.*, 2014. Genome-wide association study of Arabidopsis thaliana leaf microbial community. *Nature Communications* **5**, 5320.

Howell CR, 2006. Understanding the Mechanisms Employed by *Trichoderma virens* to Effect Biological Control of Cotton Diseases. *Phytopathology®* **96**, 178–180.

Hsieh TC, Chao KHM and A, 2024. iNEXT: Interpolation and Extrapolation for Species Diversity.

Huang K, Sun X, Zou Y *et al.*, 2022. Comparison of the Endophytic Bacterial Microbiota of Asymptomatic and Symptomatic Ginger Rhizomes During the Activation of Adventitious Bud Development. *Plant Disease* **106**, 2470–2479.

Huang J, Wei Z, Tan S *et al.*, 2013. The rhizosphere soil of diseased tomato plants as a source for novel microorganisms to control bacterial wilt. *Applied Soil Ecology* **72**, 79–84.

Humble SJ, Lockwood JL, 1981. Hyperparasitism of oospores of *Phytophthora megasperma* var. *sojae*. *Soil Biology and Biochemistry* **13**, 355–360.

Hunter PJ, Hand P, Pink D, Whipps JM, Bending GD, 2010. Both Leaf Properties and Microbe-Microbe Interactions Influence Within-Species Variation in Bacterial Population Diversity and Structure in the Lettuce (Lactuca Species) Phyllosphere. *Applied and Environmental Microbiology* **76**, 8117–8125.

Hyma KE, Barba P, Wang M *et al.*, 2015. Heterozygous Mapping Strategy (HetMappS) for High Resolution Genotyping-By-Sequencing Markers: A Case Study in Grapevine. *PLOS ONE* **10**, e0134880.

INSEE (2018) Insee Première, n° 1714

Islam MT, Laatsch H, von Tiedemann A, 2016. Inhibitory Effects of Macrotetrolides from *Streptomyces* spp. On Zoosporogenesis and Motility of Peronosporomycete Zoospores Are Likely Linked with Enhanced ATPase Activity in Mitochondria. *Frontiers in Microbiology* **7**.

Jaarsveld WJ, Halleen F, Bester MC, Pierron RJ, Stempien E, Mostert L, 2021. Investigation of *Trichoderma* species colonization of nursery grapevines for improved management of black foot disease. *Pest Management Science* **77**, 397–405.

Jacoby R, Peukert M, Succurro A, Koprivova A, Kopriva S, 2017. The Role of Soil Microorganisms in Plant Mineral Nutrition—Current Knowledge and Future Directions. *Frontiers in Plant Science* **8**.

Jacquet F, Jeuffroy M-H, Jouan J *et al.*, 2022. Pesticide-free agriculture as a new paradigm for research. *Agronomy for Sustainable Development* **42**, 8.

Jakuschkin B, Fievet V, Schwaller L, Fort T, Robin C, Vacher C, 2016. Deciphering the pathobiome: intra- and interkingdom interactions involving the pathogen *Erysiphe alphitoides*. *Microbial Ecology* **72**, 870–880.

Jara C, Laurie VF, Mas A, Romero J, 2016. Microbial Terroir in Chilean Valleys: Diversity of Non-conventional Yeast. *Frontiers in Microbiology* **7**.

Jassey VEJ, Reczuga MK, Zielińska M *et al.*, 2018. Tipping point in plant–fungal interactions under severe drought causes abrupt rise in peatland ecosystem respiration. *Global Change Biology* **24**, 972–986.

JONES K, 1970. Nitrogen Fixation in the Phyllosphere of the Douglas Fir, Pseudotsuga douglasii. *Annals of Botany* **34**, 239–244.

Jones JDG, Dangl JL, 2006. The plant immune system. *Nature* **444**, 323–329.

Joseph TA, Shenhav L, Xavier JB, Halperin E, Pe'er I, 2020. Compositional Lotka-Volterra describes microbial dynamics in the simplex. *PLOS Computational Biology* **16**, e1007917.

Jousset A, Schulz W, Scheu S, Eisenhauer N, 2011. Intraspecific genotypic richness and relatedness predict the invasibility of microbial communities. *The ISME Journal* **5**, 1108–1114.

Judelson HS, Blanco FA, 2005. The spores of Phytophthora: weapons of the plant destroyer. *Nature Reviews Microbiology* **3**, 47–58.

Jürges G, Kassemeyer H-H, Dürrenberger M, Düggelin M, Nick P, 2009a. The mode of interaction between *Vitis* and *Plasmopara viticola* Berk. & Curt. Ex de Bary depends on the host species. *Plant Biology* **11**, 886–898.

Jürges G, Kassemeyer H-H, Dürrenberger M, Düggelin M, Nick P, 2009b. The mode of interaction between *Vitis* and *Plasmopara viticola* Berk. & Curt. Ex de Bary depends on the host species. *Plant Biology* **11**, 886–898.

Kaminski TS, Scheler O, Garstecki P, 2016. Droplet microfluidics for microbiology: techniques, applications and challenges. *Lab on a Chip* **16**, 2168–2187.

Kamoun S, Furzer O, Jones JDG *et al.*, 2015. The Top 10 oomycete pathogens in molecular plant pathology. *Molecular Plant Pathology* **16**, 413–434.

Kang DD, Li F, Kirton E *et al.*, 2019. MetaBAT 2: an adaptive binning algorithm for robust and efficient genome reconstruction from metagenome assemblies. *PeerJ* **7**, e7359.

Karasov TL, Neumann M, Duque-Jaramillo A *et al.*, 2020. The relationship between microbial population size and disease in the Arabidopsis thaliana phyllosphere. , 828814.

Karp PD, Midford PE, Billington R *et al.*, 2019. Pathway Tools version 23.0 update: software for pathway/genome informatics and systems biology. *Briefings in Bioinformatics*.

Karp PD, Weaver D, Latendresse M, 2018. How accurate is automated gap filling of metabolic models? *BMC Systems Biology* **12**, 73.

Kasteel M, Ketelaar T, Govers F, 2023. Fatal attraction: How *Phytophthora* zoospores find their host. *Seminars in Cell & Developmental Biology* **148–149**, 13–21.

Kemen E, 2014. Microbe–microbe interactions determine oomycete and fungal host colonization. *Current Opinion in Plant Biology* **20**, 75–81.

Kennelly MM, Gadoury DM, Wilcox WF, Magarey PA, Seem RC, 2007. Primary Infection, Lesion Productivity, and Survival of Sporangia in the Grapevine Downy Mildew Pathogen *Plasmopara viticola*. *Phytopathology®* **97**, 512–522.

Kerdraon L, Barret M, Laval V, Suffert F, 2019. Differential dynamics of microbial community networks help identify microorganisms interacting with residue-borne pathogens: the case of *Zymoseptoria tritici* in wheat. *Microbiome* **7**, 125.

Kernaghan G, Mayerhofer M, Griffin A, 2017. Fungal endophytes of wild and hybrid *Vitis* leaves and their potential for vineyard biocontrol. *Canadian Journal of Microbiology* **63**, 583–595.

Khalifa ME, MacDiarmid RM, 2021. A Mechanically Transmitted DNA Mycovirus Is Targeted by the Defence Machinery of Its Host, *Botrytis cinerea*. *Viruses* **13**, 1315.

Khodayari A, Zomorrodi AR, Liao JC, Maranas CD, 2014. A kinetic model of Escherichia coli core metabolism satisfying multiple sets of mutant flux data. *Metabolic Engineering* **25**, 50–62.

Kiers ET, Duhamel M, Beesetty Y *et al.*, 2011. Reciprocal Rewards Stabilize Cooperation in the Mycorrhizal Symbiosis. *Science* **333**, 880–882.

Kildea S, Ransbotyn V, Khan MR *et al.*, 2008. *Bacillus megaterium* shows potential for the biocontrol of septoria tritici blotch of wheat. *Biological Control* **47**, 37–45.

Kiss L, 2003. A review of fungal antagonists of powdery mildews and their potential as biocontrol agents. *Pest Management Science* **59**, 475–483.

Kleyer H, Tecon R, Or D, 2017. Resolving Species Level Changes in a Representative Soil Bacterial Community Using Microfluidic Quantitative PCR. *Frontiers in Microbiology* **8**.

Knapp DG, Lázár A, Molnár A *et al.*, 2021. Above-ground parts of white grapevine *Vitis vinifera* cv. Furmint share core members of the fungal microbiome. *Environmental Microbiology Reports* **13**, 509–520.

Köberl M, Dita M, Martinuz A, Staver C, Berg G, 2017. Members of Gammaproteobacteria as indicator species of healthy banana plants on Fusarium wilt-infested fields in Central America. *Scientific Reports* **7**, 45318.

Köhl J, Kolnaar R, Ravensberg WJ, 2019. Mode of Action of Microbial Biological Control Agents Against Plant Diseases: Relevance Beyond Efficacy. *Frontiers in Plant Science* **10**.

Koledenkova K, Esmaeel Q, Jacquard C, Nowak J, Clément C, Ait Barka E, 2022. *Plasmopara viticola* the Causal Agent of Downy Mildew of Grapevine: From Its Taxonomy to Disease Management. *Frontiers in Microbiology* **13**, 889472.

Kong Q, Shan S, Liu Q, Wang X, Yu F, 2010. Biocontrol of *Aspergillus flavus* on peanut kernels by use of a strain of marine *Bacillus megaterium*. *International Journal of Food Microbiology* **139**, 31–35.

Kongue Tatong MD, Talontsi FM, Abdel Rahim HMD, Islam MdT, Oswald RB, Laatsch H, 2014. Banchromene and other secondary metabolites from the endophytic fungus *Fusarium* sp. obtained from *Piper guineense* inhibit the motility of phytopathogenic *Plasmopara viticola* zoospores. *Tetrahedron Letters* **55**, 4057–4061.

Korres AMN, Buss DS, Ventura JA, Fernandes PMB, 2011. *Candida krusei* and *Kloeckera apis* inhibit the causal agent of pineapple fusariosis, *Fusarium guttiforme*. *Fungal Biology* **115**, 1251–1258.

Kortekamp A, 1997. *Epicoccum nigrum* Link: A biological control agent of *Plasmopara viticola* (Berk et Curt.) Berl. et De Toni? *Vitis* **36**, 215–216.

Kortekamp A, 2005. Growth, occurrence and development of septa in Plasmopara viticola and other members of the Peronosporaceae using light- and epifluorescence-microscopy. *Mycological Research* **109**, 640–648.

Kosel J, Raspor P, Čadež N, 2019. Maximum residue limit of fungicides inhibits the viability and growth of desirable non-Saccharomyces wine yeasts. *Australian Journal of Grape and Wine Research* **25**, 43–52.

Kot AM, Laszek P, Kieliszek M, Pobiega K, Błażejak S, 2024. Biotechnological potential of red yeast isolated from birch forests in Poland. *Biotechnology Letters* **46**, 641–669.

Kovalchuk A, Mukrimin M, Zeng Z *et al.*, 2018. Mycobiome analysis of asymptomatic and symptomatic Norway spruce trees naturally infected by the conifer pathogens *Heterobasidion* spp. *Environmental Microbiology Reports* **10**, 532–541.

Kraus C, Voegele RT, Fischer M, 2019. Temporal Development of the Culturable, Endophytic Fungal Community in Healthy Grapevine Branches and Occurrence of GTD-Associated Fungi. *Microbial Ecology* **77**, 866–876.

Kumar V, Dwivedi SK, 2021. Mécanisme de bioremédiation et potentiel du cuivre par le champignon en croissance active *Trichoderma lixii* CR700 isolé des eaux usées de galvanoplastie. *Journal of Environmental Management* **277**, 111370.

Kuntal BK, Gadgil C, Mande SS, 2019. Web-gLV: A Web Based Platform for Lotka-Volterra Based Modeling and Simulation of Microbial Populations. *Frontiers in Microbiology* **10**.

Kurtz ZD, Müller CL, Miraldi ER, Littman DR, Blaser MJ, Bonneau RA, 2015. Sparse and Compositionally Robust Inference of Microbial Ecological Networks (C von Mering, Ed,). *PLOS Computational Biology* **11**, e1004226.

Kusstatscher P, Wicaksono WA, Bergna A *et al.*, 2020. Trichomes form genotype-specific microbial hotspots in the phyllosphere of tomato. *Environmental Microbiome* **15**, 17.

Kuznetsova A, Brockhoff PB, Christensen RHB, 2017. lmerTest Package: Tests in Linear Mixed Effects Models. *Journal of Statistical Software* **82**.

Kwaśna H, Szewczyk W, Baranowska M, Gallas E, Wiśniewska M, Behnke-Borowczyk J, 2021. Mycobiota Associated with the Vascular Wilt of Poplar. *Plants* **10**, 892.

La Guerche S, Chamont S, Blancard D, Dubourdieu D, Darriet P, 2005. Origin of (−)-Geosmin on Grapes: On the Complementary Action of Two Fungi, *Botrytis cinerea* and *Penicillium Expansum*. *Antonie van Leeuwenhoek* **88**, 131–139.

La Guerche S, De Senneville L, Blancard D, Darriet P, 2007. Impact of the *Botrytis cinerea* strain and metabolism on (−)-geosmin production by *Penicillium expansum* in grape juice. *Antonie van Leeuwenhoek* **92**, 331–341.

Labarthe S, Polizzi B, Phan T, Goudon T, Ribot M, Laroche B, 2019. A mathematical model to investigate the key drivers of the biogeography of the colon microbiota. *Journal of Theoretical Biology* **462**, 552–581.

Lacombe T, 2023. Vitis genetic resources: current challenges, achievements and perspectives. *Vitis* **62**, 1.

Lacombe T, Boursiquot J-M, Laucou V, Di Vecchi-Staraz M, Péros J-P, This P, 2013. Large-scale parentage analysis in an extended set of grapevine cultivars (*Vitis vinifera* L.). *Theoretical and Applied Genetics* **126**, 401–414.

Lade SB, Štraus D, Oliva J, 2022. Variation in Fungal Community in Grapevine (*Vitis vinifera*) Nursery Stock Depends on Nursery, Variety and Rootstock. *Journal of Fungi* **8**, 47.

Laforest-Lapointe I, Paquette A, Messier C, Kembel SW, 2017. Leaf bacterial diversity mediates plant diversity and ecosystem function relationships. *Nature* **546**, 145–147.

Lagier J-C, Dubourg G, Million M *et al.*, 2018. Culturing the human microbiota and culturomics. *Nature Reviews Microbiology* **16**, 540–550.

Lagier J-C, Hugon P, Khelaifia S, Fournier P-E, La Scola B, Raoult D, 2015. The Rebirth of Culture in Microbiology through the Example of Culturomics To Study Human Gut Microbiota. *Clinical Microbiology Reviews* **28**, 237–264.

Lagier J-C, Khelaifia S, Alou MT *et al.*, 2016. Culture of previously uncultured members of the human gut microbiota by culturomics. *Nature Microbiology* **1**, 1–8.

Lai J, Cao X, Yu T *et al.*, 2018. Effect of *Cryptococcus laurentii* on inducing disease resistance in cherry tomato fruit with focus on the expression of defense-related genes. *Food Chemistry* **254**, 208–216.

Laimer M, Lemaire O, Herrbach E *et al.*, 2009. Resistance to viruses, phytoplasmas and their vectors in the grapevine in Europe: a review. *Journal of Plant Pathology* **91**, 7–23.

Lane DJ, Pace B, Olsen GJ, Stahl DA, Sogin ML, Pace NR, 1985. Rapid determination of 16S ribosomal RNA sequences for phylogenetic analyses. *Proceedings of the National Academy of Sciences* **82**, 6955–6959.

Larousse M, Galiana E, 2017. Microbial Partnerships of Pathogenic Oomycetes. *PLOS Pathogens* **13**, e1006028.

Latz MAC, Jensen B, Collinge DB, Lyngs Jørgensen HJ, 2020. Identification of two endophytic fungi that control Septoria tritici blotch in the field, using a structured screening approach. *Biological Control* **141**, 104128.

Lazazzara V, Vicelli B, Bueschl C *et al.*, 2021. Trichoderma spp. volatile organic compounds protect grapevine plants by activating defense-related processes against downy mildew. *Physiologia Plantarum* **172**, 1950–1965.

Leach JE, Triplett LR, Argueso CT, Trivedi P, 2017. Communication in the Phytobiome. *Cell* **169**, 587–596.

LeBlanc N, 2022. Bacteria in the genus Streptomyces are effective biological control agents for management of fungal plant pathogens: a meta-analysis. *BioControl* **67**, 111–121.

Lederer MA, Nielsen DS, Toldam-Andersen TB, Herrmann JV, Arneborg N, 2013. Yeast species associated with different wine grape varieties in Denmark. *Acta Agriculturae Scandinavica, Section B – Soil & Plant Science*.

van Leeuwen JP, Djukic I, Bloem J *et al.*, 2017. Effects of land use on soil microbial biomass, activity and community structure at different soil depths in the Danube floodplain. *European Journal of Soil Biology* **79**, 14–20.

van Leeuwen C, Sgubin G, Bois B *et al.*, 2024. Climate change impacts and adaptations of wine production. *Nature Reviews Earth & Environment* **5**, 258–275.

Legein M, Smets W, Vandenheuvel D *et al.*, 2020. Modes of Action of Microbial Biocontrol in the Phyllosphere. *Frontiers in Microbiology* **11**.

Legras J-L, Merdinoglu D, Cornuet J-M, Karst F, 2007. Bread, beer and wine: *Saccharomyces cerevisiae* diversity reflects human history. *Molecular Ecology* **16**, 2091–2102.

Lemanceau P, Barret M, Mazurier S *et al.*, 2017. Chapter Five - Plant Communication With Associated Microbiota in the Spermosphere, Rhizosphere and Phyllosphere. In: Becard G, ed. *Advances in Botanical Research*. How Plants Communicate with their Biotic Environment. Academic Press, 101–133.

Lemos LN, Mendes LW, Baldrian P, Pylro VS, 2021. Genome-Resolved Metagenomics Is Essential for Unlocking the Microbial Black Box of the Soil. *Trends in Microbiology* **29**, 279–282.

van Lenteren JC, Bolckmans K, Köhl J, Ravensberg WJ, Urbaneja A, 2018. Biological control using invertebrates and microorganisms: plenty of new opportunities. *BioControl* **63**, 39–59.

Lenth RV, 2016. Least-Squares Means: The R Package lsmeans. *Journal of Statistical Software* **69**, 1–33.

Lenth RV, Bolker B, Buerkner P *et al.*, 2024. emmeans: Estimated Marginal Means, aka Least-Squares Means.

Let's metabaR! • metabaR

Levy A, Salas Gonzalez I, Mittelviefhaus M *et al.*, 2018. Genomic features of bacterial adaptation to plants. *Nature Genetics* **50**, 138–150.

Li Y, Héloir M-C, Zhang X *et al.*, 2019. Surfactin and fengycin contribute to the protection of a *Bacillus subtilis* strain against grape downy mildew by both direct effect and defence stimulation. *Molecular Plant Pathology* **20**, 1037–1050.

Li S, Li Y, Feng X, Zhang J, He X, 2022a. A Bjerkandera adust new strain as a potential biocontrol agent against wheat scab. *International Microbiology* **25**, 831–838.

Li D, Liu C-M, Luo R, Sadakane K, Lam T-W, 2015. MEGAHIT: an ultra-fast single-node solution for large and complex metagenomics assembly via succinct de Bruijn graph. *Bioinformatics* **31**, 1674–1676.

Li J, Wang C, Liang W, Liu S, 2021. Rhizosphere Microbiome: The Emerging Barrier in Plant-Pathogen Interactions. *Frontiers in Microbiology* **12**.

Li R, Yang S, Lin M *et al.*, 2022b. The Biogeography of Fungal Communities Across Different Chinese Wine-Producing Regions Associated With Environmental Factors and Spontaneous Fermentation Performance. *Frontiers in Microbiology* **12**, 636639.

Li X, Yin L, Ma L, Zhang Y, An Y, Lu J, 2016. Pathogenicity Variation and Population Genetic Structure of *Plasmopara viticola* in China. *Journal of Phytopathology* **164**, 863–873.

Li R, Zhang H, Liu W, Zheng X, 2011. Biocontrol of postharvest gray and blue mold decay of apples with *Rhodotorula mucilaginosa* and possible mechanisms of action. *International Journal of Food Microbiology* **146**, 151–156.

Liang C, Zang C, McDermott MI, Zhao K, Yu S, Huang Y, 2016. Two imide substances from a soil-isolated *Streptomyces atratus* strain provide effective biocontrol activity against grapevine downy mildew. *Biocontrol Science and Technology* **26**, 1337–1351.

Likar M, Stres B, Rusjan D, Potisek M, Regvar M, 2017. Ecological and conventional viticulture gives rise to distinct fungal and bacterial microbial communities in vineyard soils. *Applied Soil Ecology* **113**, 86–95.

Lim Seng Heng J, 2015. Streptomyces ambofaciens S2 - A Potential Biological Control Agent for Colletotrichum gleosporioides the Causal Agent for Anthracnose in Red Chilli Fruits. *Journal of Plant Pathology & Microbiology* **s1**.

Lima G, De Curtis F, Castoria R, De Cicco V, 1998. Activity of the Yeasts *Cryptococcus laurentii* and *Rhodotorula glutinis* Against Post-harvest Rots on Different Fruits. *Biocontrol Science and Technology* **8**, 257–267.

Lin H, Eggesbø M, Peddada SD, 2022. Linear and nonlinear correlation estimators unveil undescribed taxa interactions in microbiome data. *Nature Communications* **13**, 4946.

Lin H, Peddada SD, 2020. Analysis of compositions of microbiomes with bias correction. *Nature Communications* **11**, 3514.

Lin H, Peddada SD, 2024. Multigroup analysis of compositions of microbiomes with covariate adjustments and repeated measures. *Nature Methods* **21**, 83–91.

Lindow SE, Brandl MT, 2003. Microbiology of the Phyllosphere. *Applied and Environmental Microbiology* **69**, 1875–1883.

Liu H, Brettell LE, Qiu Z, Singh BK, 2020. Microbiome-Mediated Stress Resistance in Plants. *Trends in Plant Science* **25**, 733–743.

Liu D, Howell K, 2021. Community succession of the grapevine fungal microbiome in the annual growth cycle. *Environmental Microbiology* **23**, 1842–1857.

Liu J, Sui Y, Wisniewski M, Droby S, Liu Y, 2013. Review: Utilization of antagonistic yeasts to manage postharvest fungal diseases of fruit. *International Journal of Food Microbiology* **167**, 153–160.

Liu D, Zhang P, Chen D, Howell K, 2019. From the Vineyard to the Winery: How Microbial Ecology Drives Regional Distinctiveness of Wine. *Frontiers in Microbiology* **10**, 2679.

Lo C, Marculescu R, 2017. MPLasso: Inferring microbial association networks using prior microbial knowledge (N Segata, Ed,). *PLOS Computational Biology* **13**, e1005915.

Lo Piccolo S, Alfonzo A, Conigliaro G, Moschetti G, Burruano S, Barone A, 2012. A simple and rapid DNA extraction method from leaves of grapevine suitable for polymerase chain reaction analysis. *AFRICAN JOURNAL OF BIOTECHNOLOGY* **11**.

Lodhi MA, Ye G-N, Weeden NF, Reisch BI, 1994. A simple and efficient method for DNA extraction from grapevine cultivars andVitis species. *Plant Molecular Biology Reporter* **12**, 6–13.

López SMY, Pastorino GN, Fernández-González AJ, Franco MEE, Fernández-López M, Balatti PA, 2020. The endosphere bacteriome of diseased and healthy tomato plants. *Archives of Microbiology* **202**, 2629–2642.

Lorenzini M, Zapparoli G, 2019. Yeast-like fungi and yeasts in withered grape carposphere: Characterization of *Aureobasidium pullulans* population and species diversity. *International Journal of Food Microbiology* **289**, 223–230.

Lou J, Yang L, Wang H, Wu L, Xu J, 2018. Assessing soil bacterial community and dynamics by integrated high-throughput absolute abundance quantification. *PeerJ* **6**, e4514.

Louca S, Parfrey LW, Doebeli M, 2016. Decoupling function and taxonomy in the global ocean microbiome. *Science* **353**, 1272–1277.

Lüdecke D, Ben-Shachar M, Patil I, Waggoner P, Makowski D, 2021. performance: An R Package for Assessment, Comparison and Testing of Statistical Models. *Journal of Open Source Software* **6**, 3139.

Lyu D, Msimbira LA, Nazari M *et al.*, 2021. The Coevolution of Plants and Microbes Underpins Sustainable Agriculture. *Microorganisms* **9**, 1036.

Macaya-Sanz D, Witzell J, Collada C, Gil L, Martín JA, 2023. Core endophytic mycobiome in Ulmus minor and its relation to Dutch elm disease resistance. *Frontiers in Plant Science* **14**.

Maddalena G, Russo G, Toffolatti SL, 2021. The Study of the Germination Dynamics of *Plasmopara viticola* Oospores Highlights the Presence of Phenotypic Synchrony With the Host. *Frontiers in Microbiology* **12**.

Magnin-Robert M, Trotel-Aziz P, Quantinet D, Biagianti S, Aziz A, 2007. Biological control of *Botrytis cinerea* by selected grapevine-associated bacteria and stimulation of chitinase and β-1,3 glucanase activities under field conditions. *European Journal of Plant Pathology* **118**, 43–57.

Mahadevan B, Crawford DL, 1997. Properties of the chitinase of the antifungal biocontrol agent Streptomyces lidicus WYEC108. *Enzyme Microbiology and Technology* **20**, 293–489.

Mahadevan R, Edwards JS, Doyle FJ, 2002. Dynamic Flux Balance Analysis of Diauxic Growth in *Escherichia coli*. *Biophysical Journal* **83**, 1331–1340.

Mahé F, Rognes T, Quince C, Vargas C de, Dunthorn M, 2014. Swarm: robust and fast clustering method for amplicon-based studies. *PeerJ* **2**, e593.

Maher N, Piot J, Bastien S, Vallance J, Rey P, Guérin-Dubrana L, 2012. Wood necrosis in ESCA-affected vines: Types, relationships and possible links with foliar symptom expression. *Journal International des Sciences de la Vigne et du Vin* **46**, 15–27.

Majer P, Hideg É, 2012. Developmental stage is an important factor that determines the antioxidant responses of young and old grapevine leaves under UV irradiation in a green-house. *Plant Physiology and Biochemistry* **50**, 15–23.

Maliogka VI, Martelli GP, Fuchs M, Katis NI, 2015. Control of Viruses Infecting Grapevine. In: *Advances in Virus Research*. Elsevier, 175–227.

Mallick H, Rahnavard A, McIver LJ *et al.*, 2021. Multivariable association discovery in population-scale meta-omics studies. *PLOS Computational Biology* **17**, e1009442.

Mallon CA, Elsas JD van, Salles JF, 2015. Microbial Invasions: The Process, Patterns, and Mechanisms. *Trends in Microbiology* **23**, 719–729.

Manching HC, Balint-Kurti PJ, Stapleton AE, 2014. Southern leaf blight disease severity is correlated with decreased maize leaf epiphytic bacterial species richness and the phyllosphere bacterial diversity decline is enhanced by nitrogen fertilization. *Frontiers in Plant Science* **5**.

Marais A, Faure C, Comont G, Candresse T, Stempien E, Corio-Costet M-F, 2021. Characterization of the Mycovirome of the Phytopathogenic Fungus, *Neofusicoccum parvum*. *Viruses* **13**, 375.

Marasco R, Alturkey H, Fusi M *et al.*, 2022. Rootstock–scion combination contributes to shape diversity and composition of microbial communities associated with grapevine root system. *Environmental Microbiology*, 1462-2920.16042.

Marasco R, Rolli E, Fusi M, Michoud G, Daffonchio D, 2018. Grapevine rootstocks shape underground bacterial microbiome and networking but not potential functionality. *Microbiome* **6**, 3.

Marchesi JR, Ravel J, 2015. The vocabulary of microbiome research: a proposal. *Microbiome* **3**, 31.

Mardanov AV, Chizhevskaya EP, Lazarev AM *et al.*, 2019. Complete Genome Sequences of Endophytic Bacilli Isolated from Grapevine Plants (JJ Dennehy, Ed,). *Microbiology Resource Announcements* **8**, e01265-19.

Marín O, González B, Poupin MJ, 2021. From Microbial Dynamics to Functionality in the Rhizosphere: A Systematic Review of the Opportunities With Synthetic Microbial Communities. *Frontiers in Plant Science* **12**, 650609.

Marino S, Baxter NT, Huffnagle GB, Petrosino JF, Schloss PD, 2014. Mathematical modeling of primary succession of murine intestinal microbiota. *Proceedings of the National Academy of Sciences* **111**, 439–444.

Marsit S, Dequin S, 2015. Diversity and adaptive evolution of *Saccharomyces* wine yeast: a review (J Nielsen, Ed,). *FEMS Yeast Research* **15**, fov067.

Martelli GP, 1999. *Proceedings of the Mediterranean Network on Grapevine Closteroviruses 1992-1997 and the Viroses and Virus-Like Diseases of the Grapevine*. Centre international de hautes études agronomiques méditerranéennes.

Martin M, 2011. Cutadapt removes adapter sequences from high-throughput sequencing reads. *EMBnet.journal* **17**, 10–12.

Martínez-Diz M del P, Andrés-Sodupe M, Bujanda R, Díaz-Losada E, Eichmeier A, Gramaje D, 2019. Soil-plant compartments affect fungal microbiome diversity and composition in grapevine. *Fungal Ecology* **41**, 234–244.

Martini M, Musetti R, Grisan S *et al.*, 2009. DNA-Dependent Detection of the Grapevine Fungal Endophytes *Aureobasidium pullulans* and *Epicoccum nigrum*. *Plant Disease* **93**, 993–998.

Martins GE, Casini C, Da Costa J-P, Geny L, Lonvaud A, Masneuf-Pomarède I, 2020. Correlation between water activity (aw) and microbial epiphytic communities associated with grapes berries. *OENO One* **54**, 49–61.

Martins G, Miot-Sertier C, Lauga B *et al.*, 2012. Grape berry bacterial microbiota: Impact of the ripening process and the farming system. *International Journal of Food Microbiology* **158**, 93–100.

Martins G, Vallance J, Mercier A *et al.*, 2014. Influence of the farming system on the epiphytic yeasts and yeast-like fungi colonizing grape berries during the ripening process. *International Journal of Food Microbiology* **177**, 21–28.

Massi F, Torriani SFF, Borghi L, Toffolatti SL, 2021. Fungicide Resistance Evolution and Detection in Plant Pathogens: *Plasmopara viticola* as a Case Study. *Microorganisms* **9**, 119.

Matsumoto H, Fan X, Wang Y *et al.*, 2021. Bacterial seed endophyte shapes disease resistance in rice. *Nature Plants* **7**, 60–72.

McLaren M, 2023. speedyseq: Faster implementations of phyloseq functions.

McMurdie PJ, Holmes S, 2013. phyloseq: An R Package for Reproducible Interactive Analysis and Graphics of Microbiome Census Data. *PLOS ONE* **8**, e61217.

Mechan Llontop ME, Tian L, Sharma P *et al.*, 2021. Experimental Evidence Pointing to Rain as a Reservoir of Tomato Phyllosphere Microbiota. *Phytobiomes Journal* **5**, 382–399.

de Melo EA, de Lima R. Mariano R, Laranjeira D, dos Santos LA, de Omena Gusmão L, Barbosa de Souza E, 2015. Efficacy of Yeast in the Biocontrol of Bacterial Fruit Blotch in Melon Plants. *Tropical Plant Pathology* **40**, 56–64.

Mendes LW, de Chaves MG, Fonseca M de C, Mendes R, Raaijmakers JM, Tsai SM, 2019. Resistance Breeding of Common Bean Shapes the Physiology of the Rhizosphere Microbiome. *Frontiers in Microbiology* **10**, 2252.

Mendes R, Garbeva P, Raaijmakers JM, 2013. The rhizosphere microbiome: significance of plant beneficial, plant pathogenic, and human pathogenic microorganisms. *FEMS Microbiology Reviews* **37**, 634–663.

Mendes LW, Raaijmakers JM, de Hollander M, Mendes R, Tsai SM, 2018. Influence of resistance breeding in common bean on rhizosphere microbiome composition and function. *The ISME Journal* **12**, 212–224.

Mendoza SN, Cañón PM, Contreras Á, Ribbeck M, Agosín E, 2017. Genome-Scale Reconstruction of the Metabolic Network in *Oenococcus oeni* to Assess Wine Malolactic Fermentation. *Frontiers in Microbiology* **8**.

Meng X-H, Qin G-Z, Tian S-P, 2010. Influences of preharvest spraying *Cryptococcus laurentii* combined with postharvest chitosan coating on postharvest diseases and quality of table grapes in storage. *LWT - Food Science and Technology* **43**, 596–601.

Merdinoglu D, Schneider C, Prado E, Wiedemann-Merdinoglu S, Mestre P, 2018. Breeding for durable resistance to downy and powdery mildew in grapevine. *OENO One* **52**, 203–209.

Merdinoglu D, Wiedeman-Merdinoglu S, Coste P *et al.*, 2003. GENETIC ANALYSIS OF DOWNY MILDEW RESISTANCE DERIVED FROM MUSCADINIA ROTUNDIFOLIA. *Acta Horticulturae*, 451–456.

Meyling NV, Eilenberg J, 2007. Ecology of the entomopathogenic fungi *Beauveria bassiana* and *Metarhizium anisopliae* in temperate agroecosystems: Potential for conservation biological control. *Biological Control* **43**, 145–155.

Mezzasalma V, Sandionigi A, Guzzetti L *et al.*, 2018. Geographical and Cultivar Features Differentiate Grape Microbiota in Northern Italy and Spain Vineyards. *Frontiers in Microbiology* **9**.

Milanović V, Comitini F, Ciani M, 2013. Grape berry yeast communities: Influence of fungicide treatments. *International Journal of Food Microbiology* **161**, 240–246.

Mina D, Pereira JA, Lino-Neto T, Baptista P, 2020. Impact of plant genotype and plant habitat in shaping bacterial pathobiome: a comparative study in olive tree. *Scientific Reports* **10**, 3475.

Miotto-Vilanova L, Jacquard C, Courteaux B *et al.*, 2016. *Burkholderia phytofirmans* PsJN Confers Grapevine Resistance against *Botrytis cinerea* via a Direct Antimicrobial Effect Combined with a Better Resource Mobilization. *Frontiers in Plant Science* **7**.

Miura T, Sánchez R, Castañeda LE, Godoy K, Barbosa O, 2017. Is microbial terroir related to geographic distance between vineyards?: Microbial terroir related to geographic distance. *Environmental Microbiology Reports* **9**, 742–749.

Miura T, Sánchez R, Castañeda LE, Godoy K, Barbosa O, 2019. Shared and unique features of bacterial communities in native forest and vineyard phyllosphere. *Ecology and Evolution* **9**, 3295–3305.

Moguel IS, Yamakawa CK, Pessoa A, Mussatto SI, 2020. L-asparaginase Production by Leucosporidium scottii in a Bench-Scale Bioreactor With Co-production of Lipids. *Frontiers in Bioengineering and Biotechnology* **8**.

Molitor D, Beyer M, 2014. Epidemiology, identification and disease management of grape black rot and potentially useful metabolites of black rot pathogens for industrial applications - a review. *Annals of Applied Biology* **165**, 305–317.

Momeni B, Xie L, Shou W, 2017. Lotka-Volterra pairwise modeling fails to capture diverse pairwise microbial interactions (B Levin, Ed,). *eLife* **6**, e25051.

Mondello V, Songy A, Battiston E *et al.*, 2018. Grapevine Trunk Diseases: A Review of Fifteen Years of Trials for Their Control with Chemicals and Biocontrol Agents. *Plant Disease* **102**, 1189–1217.

Mongodin EF, Shapir N, Daugherty SC *et al.*, 2006. Secrets of Soil Survival Revealed by the Genome Sequence of Arthrobacter aurescens TC1. *PLOS Genetics* **2**, e214.

Montes-Borrego M, Ledesma FJM, Jiménez-Díaz RM, Landa BB, 2009. A Nested-Polymerase Chain Reaction Protocol for Detection and Population Biology Studies of *Peronospora arborescens*, the Downy Mildew Pathogen of *Opium Poppy*, Using *Herbarium* Specimens and Asymptomatic, Fresh Plant Tissues. *Phytopathology®* **99**, 73–81.

Morales-Cedeño LR, Orozco-Mosqueda Ma del C, Loeza-Lara PD, Parra-Cota FI, de los Santos-Villalobos S, Santoyo G, 2021. Plant growth-promoting bacterial endophytes as biocontrol agents of pre- and post-harvest diseases: Fundamentals, methods of application and future perspectives. *Microbiological Research* **242**, 126612.

Morgan HH, du Toit M, Setati ME, 2017. The Grapevine and Wine Microbiome: Insights from High-Throughput Amplicon Sequencing. *Frontiers in Microbiology* **8**, 820.

Mourad EF, Sarhan MS, Daanaa H-SA *et al.*, 2018. Plant Materials are Sustainable Substrates Supporting New Technologies of Plant-Only-Based Culture Media for *in vitro* Culturing of the Plant Microbiota. *Microbes and Environments* **advpub**, ME17135.

Mugnai L, Graniti A, Surico G, 1999. Esca (Black Measles) and Brown Wood-Streaking: Two Old and Elusive Diseases of Grapevines. *Plant Disease* **83**, 404–418.

Müller DB, Vogel C, Bai Y, Vorholt JA, 2016. The Plant Microbiota: Systems-Level Insights and Perspectives. *Annual Review of Genetics* **50**, 211–234.

Musetti R, Polizzotto R, Vecchione A *et al.*, 2007. Antifungal activity of diketopiperazines extracted from *Alternaria alternata* against *Plasmopara viticola*: An ultrastructural study. *Micron* **38**, 643–650.

Musetti R, Vecchione A, Stringher L *et al.*, 2006a. Inhibition of Sporulation and Ultrastructural Alterations of Grapevine Downy Mildew by the Endophytic Fungus *Alternaria alternata*. *Phytopathology®* **96**, 689–698.

Musetti R, Vecchione A, Stringher L *et al.*, 2006b. Inhibition of Sporulation and Ultrastructural Alterations of Grapevine Downy Mildew by the Endophytic Fungus *Alternaria alternata*. *Phytopathology®* **96**, 689–698.

Myles S, Boyko AR, Owens CL *et al.*, 2011. Genetic structure and domestication history of the grape. *Proceedings of the National Academy of Sciences* **108**, 3530–3535.

Nadalini S, Puopolo G, 2024. Biological control of *Plasmopara viticola*: where are we now? In: Kumar A,, Santoyo G,, Singh J, eds. *Biocontrol Agents for Improved Agriculture*. Plant and Soil Microbiome. Academic Press, 67–100.

Nagai S, Sildever S, Nishi N *et al.*, 2022. Comparing PCR-generated artifacts of different polymerases for improved accuracy of DNA metabarcoding. *Metabarcoding and Metagenomics* **6**, e77704.

Nai C, Meyer V, 2018. From Axenic to Mixed Cultures: Technological Advances Accelerating a Paradigm Shift in Microbiology. *Trends in Microbiology* **26**, 538–554.

Narduzzi-Wicht B, Jermini M, Gessler C, Broggini GAL, 2014. Microsatellite markers for population studies of the ascomycete *Phyllosticta ampelicida*, the pathogen causing grape black rot. *Phytopathologia Mediterranea* **53**.

Nasehi A, Nasr Esfahani M, Nasr Esfahani A, Mohammadbagheri L, Yazdi MJ, Mohammadi M, 2023. Endophytic fungi as potential inhibitory agents of downy mildews: A review and future prospects. *Ecological Genetics and Genomics* 29, 100211.

Naveed M, Mitter B, Reichenauer TG, Wieczorek K, Sessitsch A, 2014. Increased drought stress resilience of maize through endophytic colonization by *Burkholderia phytofirmans* PsJN and *Enterobacter* sp. FD17. *Environmental and Experimental Botany* 97, 30–39.

Nawangsih AA, Damayanti I, Wiyono S, Kartika JG, 2011. Selection and Characterization of Endophytic Bacteria as Biocontrol Agents of Tomato Bacterial Wilt Disease. *HAYATI Journal of Biosciences* 18, 66–70.

Nayfach S, Roux S, Seshadri R *et al.*, 2020. A genomic catalog of Earth's microbiomes. *Nature Biotechnology*, 1–11.

Nearing JT, Douglas GM, Hayes MG *et al.*, 2022a. Microbiome differential abundance methods produce different results across 38 datasets. *Nature Communications* 13, 342.

Nearing JT, Douglas GM, Hayes MG *et al.*, 2022b. Microbiome differential abundance methods produce different results across 38 datasets. *Nature Communications* 13, 342.

Ņečajeva J, Borodušķe A, Nikolajeva V *et al.*, 2023. Epiphytic and Endophytic Fungi Colonizing Seeds of Two Poaceae Weed Species and Fusarium spp. Seed Degradation Potential In Vitro. *Microorganisms* 11, 184.

Nelson EB, 2004. MICROBIAL DYNAMICS AND INTERACTIONS IN THE SPERMOSPHERE. *Annual Review of Phytopathology* 42, 271–309.

Nemergut DR, Schmidt SK, Fukami T *et al.*, 2013. Patterns and Processes of Microbial Community Assembly. *Microbiology and Molecular Biology Reviews* 77, 342–356.

Nerva L, Garcia JF, Favaretto F *et al.*, 2022. The hidden world within plants: metatranscriptomics unveils the complexity of wood microbiomes (M Gifford, Ed,). *Journal of Experimental Botany* 73, 2682–2697.

Nerva L, Turina M, Zanzotto A *et al.*, 2019. Isolation, molecular characterization and virome analysis of culturable wood fungal endophytes in esca symptomatic and asymptomatic grapevine plants. *Environmental Microbiology* 21, 2886–2904.

Nguyen NH, Song Z, Bates ST *et al.*, 2016. FUNGuild: An open annotation tool for parsing fungal community datasets by ecological guild. *Fungal Ecology* 20, 241–248.

Nicot P, Alabouvette C, Bardin M, Blum B, Köhl J, Ruocco M, 2012. Review of factors influencing the success or failure of biocontrol: technical, industrial and socio-economic perspectives. *IOBC/WPRS Bulletin* 78, 95–98.

Nidelet T, Brial P, Camarasa C, Dequin S, 2016. Diversity of flux distribution in central carbon metabolism of *S. cerevisiae* strains from diverse environments. *Microbial Cell Factories* 15, 58.

Nilsson RH, Anslan S, Bahram M, Wurzbacher C, Baldrian P, Tedersoo L, 2019a. Mycobiome diversity: high-throughput sequencing and identification of fungi. *Nature Reviews Microbiology* 17, 95–109.

Nilsson RH, Larsson K-H, Taylor AFS *et al.*, 2019b. The UNITE database for molecular identification of fungi: handling dark taxa and parallel taxonomic classifications. *Nucleic Acids Research* **47**, D259–D264.

Ning D, Deng Y, Tiedje JM, Zhou J, 2019. A general framework for quantitatively assessing ecological stochasticity. *Proceedings of the National Academy of Sciences* **116**, 16892–16898.

Nishad R, Ahmed T, Rahman VJ, Kareem A, 2020. Modulation of Plant Defense System in Response to Microbial Interactions. *Frontiers in Microbiology* **11**.

Noman M, Ahmed T, Ijaz U *et al.*, 2021. Plant–Microbiome Crosstalk: Dawning from Composition and Assembly of Microbial Community to Improvement of Disease Resilience in Plants. *International Journal of Molecular Sciences* **22**, 6852.

Novello G, Gamalero E, Bona E *et al.*, 2017. The Rhizosphere Bacterial Microbiota of *Vitis vinifera* cv. Pinot Noir in an Integrated Pest Management Vineyard. *Frontiers in Microbiology* **8**, 1528.

Nurk S, Meleshko D, Korobeynikov A, Pevzner PA, 2017. metaSPAdes: a new versatile metagenomic assembler. *Genome Research* **27**, 824–834.

Ocete R, Armendariz I, Cantos M, Álvarez D, Azcón R, 2015. Ecological characterization of wild grapevine habitats focused on arbuscular mycorrhizal symbiosis. *Vitis* **54**, 207–211.

Ofek-Lalzar M, Gur Y, Ben-Moshe S *et al.*, 2016. Diversity of fungal endophytes in recent and ancient wheat ancestors *Triticum dicoccoides* and *Aegilops sharonensis* (L Johnson, Ed,). *FEMS Microbiology Ecology* **92**, fiw152.

Oksanen J, Simpson GL, Blanchet FG *et al.*, 2024. vegan: Community Ecology Package.

Olien WC, 1990. The Muscadine Grape: Botany, Viticulture, History, and Current Industry.

Oliveira M, Arenas M, Lage O, Cunha M, Amorim MI, 2018. Epiphytic fungal community in *Vitis vinifera* of the Portuguese wine regions. *Letters in Applied Microbiology* **66**, 93–102.

Oliver JE, Fuchs MF, 2011. Fanleaf degeneration/decline disease of grapevines.

Omara AE-D, El-maghraby FM, 2023. Novel Bioformulations with Trichoderma lixii to Improve the Growth Dynamics and Biocontrol of the Cowpea Damping-Off Disease. *Microbiology Research* **14**, 2041–2066.

Orth JD, Thiele I, Palsson BØ, 2010. What is flux balance analysis? *Nature Biotechnology* **28**, 245–248.

Osono T, 2014. Diversity and Ecology of Endophytic and Epiphytic Fungi of Tree Leaves in Japan: A Review. In: Verma VC,, Gange AC, eds. *Advances in Endophytic Research*. New Delhi: Springer India, 3–26.

Ouadi L, Bruez E, Bastien S *et al.*, 2019. Ecophysiological impacts of Esca, a devastating grapevine trunk disease, on *Vitis vinifera* L. (H Gerós, Ed,). *PLOS ONE* **14**, e0222586.

Ouadi L, Bruez E, Bastien S *et al.*, 2021. Sap Flow Disruption in Grapevine Is the Early Signal Predicting the Structural, Functional, and Genetic Responses to Esca Disease. *Frontiers in Plant Science* **12**, 695846.

Ovaskainen O, Tikhonov G, Norberg A *et al.*, 2017. How to make more out of community data? A conceptual framework and its implementation as models and software. *Ecology Letters* **20**, 561–576.

Paasch BC, He SY, 2021. Toward understanding microbiota homeostasis in the plant kingdom. *PLOS Pathogens* **17**, e1009472.

Pacifico D, Squartini A, Crucitti D *et al.*, 2019. The Role of the Endophytic Microbiome in the Grapevine Response to Environmental Triggers. *Frontiers in Plant Science* **10**, 1256.

Palarea-Albaladejo J, Martín-Fernández JA, 2015. zCompositions — R package for multivariate imputation of left-censored data under a compositional approach. *Chemometrics and Intelligent Laboratory Systems* **143**, 85–96.

Palmero D, Rodríguez JM, de Cara M, Camacho F, Iglesias C, Tello JC, 2011. Fungal microbiota from rain water and pathogenicity of Fusarium species isolated from atmospheric dust and rainfall dust. *Journal of Industrial Microbiology and Biotechnology* **38**, 13–20.

Palmieri D, Miccoli C, Notardonato I *et al.*, 2022. Modulation of extracellular Penicillium expansum-driven acidification by Papiliotrema terrestris affects biosynthesis of patulin and has a possible role in biocontrol activity. *Frontiers in Microbiology* **13**.

Palmieri MC, Perazzolli M, Matafora V, Moretto M, Bachi A, Pertot I, 2012. Proteomic analysis of grapevine resistance induced by Trichoderma harzianum T39 reveals specific defence pathways activated against downy mildew. *Journal of Experimental Botany* **63**, 6237–6251.

Pandey B, Naidu RA, Grove GG, 2018. Detection and analysis of mycovirus-related RNA viruses from grape powdery mildew fungus *Erysiphe necator*. *Archives of Virology* **163**, 1019–1030.

Panebianco S, Vitale A, Polizzi G, Scala F, Cirvilleri G, 2015. Enhanced control of postharvest citrus fruit decay by means of the combined use of compatible biocontrol agents. *Biological Control* **84**, 19–27.

Panis C, Kawassaki ACB, Crestani APJ *et al.*, 2022. Evidence on Human Exposure to Pesticides and the Occurrence of Health Hazards in the Brazilian Population: A Systematic Review. *Frontiers in Public Health* **9**.

Panstruga R, Kuhn H, 2019. Mutual interplay between phytopathogenic powdery mildew fungi and other microorganisms. *Molecular Plant Pathology* **20**, 463–470.

Paolinelli M, Escoriaza G, Cesari C, Garcia-Lampasona S, Hernandez-Martinez R, 2022. Characterization of Grapevine Wood Microbiome Through a Metatranscriptomic Approach. *Microbial Ecology* **83**, 658–668.

Paul ND, Moore JP, McPherson M *et al.*, 2012. Ecological responses to UV radiation: interactions between the biological effects of UV on plants and on associated organisms. *Physiologia Plantarum* **145**, 565–581.

Pauvert C, Buée M, Laval V *et al.*, 2019. Bioinformatics matters: The accuracy of plant and soil fungal community data is highly dependent on the metabarcoding pipeline. *Fungal Ecology* **41**, 23–33.

Pauvert C, Fort T, Calonnec A *et al.*, 2020. Microbial association networks give relevant insights into plant pathobiomes. , 2020.02.21.958033.

Pearson MN, Bailey AM, 2013. Viruses of *Botrytis*. In: *Advances in Virus Research*. Elsevier, 249–272.

Pedersen TL, 2024. patchwork: The Composer of Plots.

Pehlivan N, Yesilyurt AM, Durmus N, Karaoglu SA, 2017. Trichoderma lixii ID11D seed biopriming mitigates dose dependent salt toxicity in maize. *Acta Physiologiae Plantarum* **39**, 79.

Pell JK, Hannam JJ, Steinkraus DC, 2010. Conservation biological control using fungal entomopathogens. *BioControl* **55**, 187–198.

Peng J, Wang X, Wang H *et al.*, 2024. Advances in understanding grapevine downy mildew: From pathogen infection to disease management. *Molecular Plant Pathology* **25**, e13401.

Perazzolli M, Antonielli L, Storari M *et al.*, 2014. Resilience of the Natural Phyllosphere Microbiota of the Grapevine to Chemical and Biological Pesticides (HL Drake, Ed,). *Applied and Environmental Microbiology* **80**, 3585–3596.

Perazzolli M, Dagostin S, Ferrari A, Elad Y, Pertot I, 2008. Induction of systemic resistance against *Plasmopara viticola* in grapevine by *Trichoderma harzianum* T39 and benzothiadiazole. *Biological Control* **47**, 228–234.

Perazzolli M, Roatti B, Bozza E, Pertot I, 2011. *Trichoderma harzianum* T39 induces resistance against downy mildew by priming for defense without costs for grapevine. *Biological Control* **58**, 74–82.

Perera D, Savocchia S, Prenzler PD, Thomson PC, Steel CC, 2021. Occurrence of fumonisin-producing black aspergilli in Australian wine grapes: effects of temperature and water activity on fumonisin production by *A. niger* and *A. welwitschiae*. *Mycotoxin Research* **37**, 327–339.

Peressotti E, Wiedemann-Merdinoglu S, Delmotte F *et al.*, 2010. Breakdown of resistance to grapevine downy mildew upon limited deployment of a resistant variety. *BMC Plant Biology* **10**, 147.

Pérez-Jaramillo JE, Carrión VJ, Bosse M *et al.*, 2017. Linking rhizosphere microbiome composition of wild and domesticated Phaseolus vulgaris to genotypic and root phenotypic traits. *The ISME Journal* **11**, 2244–2257.

Pérez-Jaramillo JE, Carrión VJ, de Hollander M, Raaijmakers JM, 2018. The wild side of plant microbiomes. *Microbiome* **6**, 143.

Péros J-P, Berger G, Portemont A, Boursiquot J-M, Lacombe T, 2011. Genetic variation and biogeography of the disjunct Vitis subg. Vitis (Vitaceae). *Journal of Biogeography* **38**, 471–486.

Péros J-P, Cousins P, Launay A *et al.*, 2021. Genetic diversity and population structure in Vitis species illustrate phylogeographic patterns in eastern North America. *Molecular Ecology* **30**, 2333–2348.

Pertot I, Caffi T, Rossi V *et al.*, 2017a. A critical review of plant protection tools for reducing pesticide use on grapevine and new perspectives for the implementation of IPM in viticulture. *Crop Protection* 97, 70–84.

Pertot I, Giovannini O, Benanchi M, Caffi T, Rossi V, Mugnai L, 2017b. Combining biocontrol agents with different mechanisms of action in a strategy to control *Botrytis cinerea* on grapevine. *Crop Protection* 97, 85–93.

Philippe C, Krupovic M, Jaomanjaka F, Claisse O, Petrel M, le Marrec C, 2018. Bacteriophage GC1, a Novel Tectivirus Infecting *Gluconobacter Cerinus*, an Acetic Acid Bacterium Associated with Wine-Making. *Viruses* 10, 39.

Philippot L, Spor A, Hénault C *et al.*, 2013. Loss in microbial diversity affects nitrogen cycling in soil. *The ISME Journal* 7, 1609–1619.

Pieterse CMJ, Zamioudis C, Berendsen RL, Weller DM, Wees SCMV, Bakker PAHM, 2014. Induced Systemic Resistance by Beneficial Microbes. *Annual Review of Phytopathology* 52, 347–375.

Pilar Martínez-Diz M, Díaz-Losada E, Andrés-Sodupe M *et al.*, 2021. Field evaluation of biocontrol agents against black-foot and Petri diseases of grapevine. *Pest Management Science* 77, 697–708.

Ping X, Khan RAA, Chen S *et al.*, 2024. Deciphering the role of rhizosphere microbiota in modulating disease resistance in cabbage varieties. *Microbiome* 12, 160.

Pinto C, Pinho D, Sousa S, Pinheiro M, Egas C, C. Gomes A, 2014. Unravelling the Diversity of Grapevine Microbiome (A Driks, Ed,). *PLoS ONE* 9, e85622.

Pirrello C, Mizzotti C, Tomazetti TC *et al.*, 2019. Emergent Ascomycetes in Viticulture: An Interdisciplinary Overview. *Frontiers in Plant Science* 10, 1394.

Poeydebat C, Courchinoux E, Delière L, Raynal M, Delmotte F, 2022. Quantification and management of *Plasmopara viticola* primary inoculum in soil – Towards prophylactic control of grapevine downy mildew (T Caffi, V Rossi, G Fedele, Eds,). *BIO Web of Conferences* 50, 03011.

Poeydebat C, Courchinoux E, Demeaux I *et al.*, 2024. Quantitative assessment and spatial distribution of *Plasmopara viticola* oospores in vineyard soil.

Põlme S, Abarenkov K, Henrik Nilsson R *et al.*, 2020. FungalTraits: a user-friendly traits database of fungi and fungus-like stramenopiles. *Fungal Diversity* 105, 1–16.

Poudel R, Jumpponen A, Schlatter DC *et al.*, 2016. Microbiome Networks: A Systems Framework for Identifying Candidate Microbial Assemblages for Disease Management. *Phytopathology®* 106, 1083–1096.

Prodhomme D, Valls Fonayet J, Hévin C *et al.*, 2019. Metabolite profiling during graft union formation reveals the reprogramming of primary metabolism and the induction of stilbene synthesis at the graft interface in grapevine. *BMC Plant Biology* 19, 599.

Props R, Kerckhof F-M, Rubbens P *et al.*, 2017. Absolute quantification of microbial taxon abundances. *The ISME Journal* 11, 584–587.

Prosser JI, Bohannan BJM, Curtis TP *et al.*, 2007. The role of ecological theory in microbial ecology. *Nature Reviews Microbiology* 5, 384–392.

Puig-Pujol A, Ferrando N, Capdevila F, Ocete R, Revilla E, 2016. Yeast biodiversity from *Vitis vinifera* L., subsp. sylvestris (Gmelin) Hegi to face up the oenological consequences of climate change (J-M Aurand, Ed,). *BIO Web of Conferences* **7**, 02026.

Qiu W, Feechan A, Dry I, 2015. Current understanding of grapevine defense mechanisms against the biotrophic fungus (*Erysiphe necator*), the causal agent of powdery mildew disease. *Horticulture Research* **2**, 15020.

Quast C, Pruesse E, Yilmaz P *et al.*, 2013. The SILVA ribosomal RNA gene database project: improved data processing and web-based tools. *Nucleic Acids Research* **41**, D590–D596.

Quince C, Walker AW, Simpson JT, Loman NJ, Segata N, 2017. Shotgun metagenomics, from sampling to analysis. *Nature Biotechnology* **35**, 833–844.

R Core Team, 2023. R: A language and environment for statistical computing. *R Foundation for Statistical Computing, Vienna, Austria.*

Raaijmakers JM, Mazzola M, 2012. Diversity and Natural Functions of Antibiotics Produced by Beneficial and Plant Pathogenic Bacteria. *Annual Review of Phytopathology* **50**, 403–424.

Radić T, Likar M, Hančević K, Regvar M, Čarija M, Zdunić G, 2021. Root-associated community composition and co-occurrence patterns of fungi in wild grapevine. *Fungal Ecology* **50**, 101034.

Raguideau S, Plancade S, Pons N, Leclerc M, Laroche B, 2016. Inferring Aggregated Functional Traits from Metagenomic Data Using Constrained Non-negative Matrix Factorization: Application to Fiber Degradation in the Human Gut Microbiota. *PLOS Computational Biology* **12**, e1005252.

Rani L, Thapa K, Kanojia N *et al.*, 2021. An extensive review on the consequences of chemical pesticides on human health and environment. *Journal of Cleaner Production* **283**, 124657.

Raspor P, Miklič-Milek D, Avbelj M, Čadež N, 2010a. *Food Technology & Biotechnology* **48**, 336–343.

Raspor P, Miklič-Milek D, Avbelj M, Čadež N, 2010b. Biocontrol of Grey Mould Disease on Grape Caused by *Botrytis cinerea* with Autochthonous Wine Yeasts. *Food Technology & Biotechnology* **48**, 336–343.

Rastogi G, Sbodio A, Tech JJ, Suslow TV, Coaker GL, Leveau JHJ, 2012. Leaf microbiota in an agroecosystem: spatiotemporal variation in bacterial community composition on field-grown lettuce. *The ISME Journal* **6**, 1812–1822.

Rathnayake RMSP, Savocchia S, Schmidtke LM, Steel CC, 2018. Characterisation of *Aureobasidium pullulans* isolates from *Vitis vinifera* and potential biocontrol activity for the management of bitter rot of grapes. *European Journal of Plant Pathology* **151**, 593–611.

Ratiner K, Ciocan D, Abdeen SK, Elinav E, 2024. Utilization of the microbiome in personalized medicine. *Nature Reviews Microbiology* **22**, 291–308.

Raveau R, Ilbert C, Héloir M-C *et al.*, 2024. Broad-Spectrum Efficacy and Modes of Action of Two Bacillus Strains against Grapevine Black Rot and Downy Mildew. *Journal of Fungi* **10**, 471.

Raymaekers K, Ponet L, Holtappels D, Berckmans B, Cammue BPA, 2020. Screening for novel biocontrol agents applicable in plant disease management – A review. *Biological Control* **144**, 104240.

Redford AJ, Bowers RM, Knight R, Linhart Y, Fierer N, 2010. The ecology of the phyllosphere: geographic and phylogenetic variability in the distribution of bacteria on tree leaves. *Environmental Microbiology* **12**, 2885–2893.

Regueira-Iglesias A, Balsa-Castro C, Blanco-Pintos T, Tomás I, 2023. Critical review of 16S rRNA gene sequencing workflow in microbiome studies: From primer selection to advanced data analysis. *Molecular Oral Microbiology* **38**, 347–399.

Remien CH, Eckwright MJ, Ridenhour BJ, 2021. Structural identifiability of the generalized Lotka–Volterra model for microbiome studies. *Royal Society Open Science* **8**, 201378.

Reysenbach A-L, Pace NR, 1995. Reliable amplification of hyperthermophilic archaeal 16S rRNA genes by the polymerase chain reaction. *Archaea: a laboratory manual*, 101–107.

Rezgui A, Ben Ghnaya-Chakroun A, Vallance J *et al.*, 2016. Endophytic bacteria with antagonistic traits inhabit the wood tissues of grapevines from Tunisian vineyards. *Biological Control* **99**, 28–37.

Ricciardi V, Crespan M, Maddalena G *et al.*, 2024. Novel loci associated with resistance to downy and powdery mildew in grapevine. *Frontiers in Plant Science* **15**.

Ricono C, Vandenkoornhuyse P, Aviron S *et al.*, 2022. Organic agriculture and field edges uphold endospheric wheat microbiota at field and landscape scale. *FEMS Microbiology Ecology* **98**, fiac027.

Ridout ME, Schroeder KL, Hunter SS, Styer J, Newcombe G, 2019. Priority effects of wheat seed endophytes on a rhizosphere symbiosis. *Symbiosis* **78**, 19–31.

Rijavec T, Lapanje A, 2016. Hydrogen Cyanide in the Rhizosphere: Not Suppressing Plant Pathogens, but Rather Regulating Availability of Phosphate. *Frontiers in Microbiology* **7**.

Rillig MC, Antonovics J, Caruso T *et al.*, 2015. Interchange of entire communities: microbial community coalescence. *Trends in Ecology & Evolution* **30**, 470–476.

Rinaldi PA, Paffetti D, Comparini C, Broggini GAL, Gessler C, Mugnai L, 2017. Genetic Variability of *Phyllosticta ampelicida*, the Agent of Black Rot Disease of Grapevine. *Phytopathology®* **107**, 1406–1416.

Ritpitakphong U, Falquet L, Vimoltust A, Berger A, Métraux J-P, L'Haridon F, 2016. The microbiome of the leaf surface of Arabidopsis protects against a fungal pathogen. *New Phytologist* **210**, 1033–1043.

Riva V, Mapelli F, Bagnasco A, Mengoni A, Borin S, 2022. A Meta-Analysis Approach to Defining the Culturable Core of Plant Endophytic Bacterial Communities. *Applied and Environmental Microbiology* **88**, e02537-21.

Rivas GA, Semorile L, Delfederico L, 2022. Microbial diversity of the soil, rhizosphere and wine from an emerging wine-producing region of Argentina. *LWT* **153**, 112429.

Rizaludin MS, Stopnisek N, Raaijmakers JM, Garbeva P, 2021. The Chemistry of Stress: Understanding the 'Cry for Help' of Plant Roots. *Metabolites* **11**, 357.

Rocca JD, Simonin M, Blaszczak JR *et al.*, 2019. The Microbiome Stress Project: Toward a Global Meta-Analysis of Environmental Stressors and Their Effects on Microbial Communities. *Frontiers in Microbiology* **9**.

Rochefort A, Simonin M, Marais C, Guillerm-Erckelboudt A-Y, Barret M, Sarniguet A, 2021. Transmission of Seed and Soil Microbiota to Seedling. *mSystems* **6**, 10.1128/msystems.00446-21.

Rodríguez CE, Antonielli L, Mitter B, Trognitz F, Sessitsch A, 2020. Heritability and Functional Importance of the Setaria viridis Bacterial Seed Microbiome. *Phytobiomes Journal* **4**, 40–52.

Rognes T, Flouri T, Nichols B, Quince C, Mahé F, 2016. VSEARCH: a versatile open source tool for metagenomics. *PeerJ* **4**, e2584.

Rolli E, Marasco R, Vigani G *et al.*, 2015. Improved plant resistance to drought is promoted by the root-associated microbiome as a water stress-dependent trait. *Environmental Microbiology* **17**, 316–331.

Rondot Y, Reineke A, 2019. Endophytic *Beauveria bassiana* activates expression of defence genes in grapevine and prevents infections by grapevine downy mildew *Plasmopara viticola*. *Plant Pathology* **68**, 1719–1731.

Roossinck MJ, 2010. Lifestyles of plant viruses. *Philosophical Transactions of the Royal Society B: Biological Sciences* **365**, 1899–1905.

Rosenberg E, Sharon G, Atad I, Zilber-Rosenberg I, 2010. The evolution of animals and plants via symbiosis with microorganisms: Evolution via symbiosis. *Environmental Microbiology Reports* **2**, 500–506.

Rosenberg E, Zilber-Rosenberg I, 2018. The hologenome concept of evolution after 10 years. *Microbiome* **6**, 78.

Ross T, McMeekin TA, 1994. Predictive microbiology. *International Journal of Food Microbiology* **23**, 241–264.

Röttjers L, Faust K, 2018. From hairballs to hypotheses–biological insights from microbial networks. *FEMS Microbiology Reviews* **42**, 761–780.

Rouxel M, Mestre P, Baudoin A *et al.*, 2014. Geographic Distribution of Cryptic Species of *Plasmopara viticola* Causing Downy Mildew on Wild and Cultivated Grape in Eastern North America. *Phytopathology®* **104**, 692–701.

Rouxel M, Mestre P, Comont G, Lehman BL, Schilder A, Delmotte F, 2013. Phylogenetic and experimental evidence for host-specialized cryptic species in a biotrophic oomycete. *New Phytologist* **197**, 251–263.

Rovenich H, Thomma BPHJ, 2023. Battle of the bugs: how an oomycete pathogen shapes the microbiota of its host. *New Phytologist* **239**, 2064–2066.

Rowhani A, Uyemoto JK, Golino DA, Daubert SD, Al Rwahnih M, 2017. Viruses Involved in Graft Incompatibility and Decline. In: Meng B,, Martelli GP,, Golino DA,, Fuchs M, eds.

Grapevine Viruses: Molecular Biology, Diagnostics and Management. Cham: Springer International Publishing, 289–302.

Ruiz-Moyano S, Hernández A, Galvan AI *et al.*, 2020. Selection and application of antifungal VOCs-producing yeasts as biocontrol agents of grey mould in fruits. *Food Microbiology* 92, 103556.

Ruiz-Padilla A, Rodríguez-Romero J, Gómez-Cid I, Pacifico D, Ayllón MA, 2021. Novel mycoviruses discovered in the mycovirome of a necrotrophic fungus (RB Wickner, Ed,). *mBio* 12, e03705-20.

Runge P, Ventura F, Kemen E, Stam R, 2023. Distinct Phyllosphere Microbiome of Wild Tomato Species in Central Peru upon Dysbiosis. *Microbial Ecology* 85, 168–183.

Sabat AJ, van Zanten E, Akkerboom V *et al.*, 2017. Targeted next-generation sequencing of the 16S-23S rRNA region for culture-independent bacterial identification - increased discrimination of closely related species. *Scientific Reports* 7, 3434.

Saijo Y, Loo EP, Yasuda S, 2018. Pattern recognition receptors and signaling in plant–microbe interactions. *The Plant Journal* 93, 592–613.

Saikkonen K, Nissinen R, Helander M, 2020. Toward Comprehensive Plant Microbiome Research. *Frontiers in Ecology and Evolution* 8, 61.

Saleem M, Hu J, Jousset A, 2019. More Than the Sum of Its Parts: Microbiome Biodiversity as a Driver of Plant Growth and Soil Health. *Annual Review of Ecology, Evolution, and Systematics* 50, 145–168.

Saleh AE, Ul-Hassan Z, Zeidan R *et al.*, 2021. Biocontrol Activity of Bacillus megaterium BM344-1 against Toxigenic Fungi. *ACS Omega* 6, 10984–10990.

Salinari F, Giosuè S, Rossi V, Tubiello FN, Rosenzweig C, Gullino ML, 2007. Downy mildew outbreaks on grapevine under climate change: elaboration and application of an empirical-statistical model. *EPPO Bulletin* 37, 317–326.

Salvetti E, Campanaro S, Campedelli I *et al.*, 2016. Whole-Metagenome-Sequencing-Based Community Profiles of Vitis vinifera L. cv. Corvina Berries Withered in Two Post-harvest Conditions. *Frontiers in Microbiology* 7, 937.

Santos RF, Ciampi-Guillardi M, Fraaije BA, de Oliveira AA, Amorim L, 2020a. The Climate-Driven Genetic Diversity Has a Higher Impact on the Population Structure of *Plasmopara viticola* Than the Production System or QoI Fungicide Sensitivity in Subtropical Brazil. *Frontiers in Microbiology* 11.

Santos A, Marquina DY 2004, 2004. Killer toxin of *Pichia membranifaciens* and its possible use as a biocontrol agent against grey mould disease of grapevine. *Microbiology* 150, 2527–2534.

Santos A, Núñez-Montero K, Lamilla C *et al.*, 2020b. ANTIFUNGAL ACTIVITY SCREENING OF ANTARCTIC ACTINOBACTERIA AGAINST PHYTOPATHOGENIC FUNGI. *Acta Biológica Colombiana* 25, 353–358.

Saraf M, Jha CK, Patel D, 2010. The Role of ACC Deaminase Producing PGPR in Sustainable Agriculture. In: Plant Growth and Health Promoting Bacteria. In: Maheshwari DK, ed.

Plant Growth and Health Promoting Bacteria. Microbiology Monographs. Berlin, Heidelberg: Springer Berlin Heidelberg, 251–272.

Sargolzaei M, Maddalena G, Bitsadze N *et al.*, 2020. Rpv29, Rpv30 and Rpv31: three novel genomic loci associated with resistance to *Plasmopara viticola* in *Vitis vinifera*. *Frontiers in Plant Science* **11**, 698586.

Sargolzaei M, Rustioni L, Cola G *et al.*, 2021. Georgian Grapevine Cultivars: Ancient Biodiversity for Future Viticulture. *Frontiers in Plant Science* **12**, 630122.

Sarhan MS, Hamza MA, Youssef HH *et al.*, 2019. Culturomics of the plant prokaryotic microbiome and the dawn of plant-based culture media – A review. *Journal of Advanced Research* **19**, 15–27.

Sarhan MS, Patz S, Hamza MA *et al.*, 2018. G3 PhyloChip Analysis Confirms the Promise of Plant-Based Culture Media for Unlocking the Composition and Diversity of the Maize Root Microbiome and for Recovering Unculturable Candidate Divisions/Phyla. *Microbes and Environments* **advpub**, ME18023.

Satianpakiranakorn P, Khunnamwong P, Limtong S, 2020. Yeast communities of secondary peat swamp forests in Thailand and their antagonistic activities against fungal pathogens cause of plant and postharvest fruit diseases. *PLOS ONE* **15**, e0230269.

Savian F, Marroni F, Ermacora P, Firrao G, Martini M, 2022. A Metabarcoding Approach to Investigate Fungal and Oomycete Communities Associated with Kiwifruit Vine Decline Syndrome in Italy. *Phytobiomes Journal* **6**, 290–304.

Sawant IS, 2014. *Trichoderma*- Foliar Pathogen Interactions. *The Open Mycology Journal* **8**, 58–70.

Schacherer J, Shapiro JA, Ruderfer DM, Kruglyak L, 2009. Comprehensive polymorphism survey elucidates population structure of *Saccharomyces cerevisiae*. *Nature* **458**, 342–345.

Schliep KP, 2011. phangorn: phylogenetic analysis in R. *Bioinformatics* **27**, 592–593.

Schliep K, Potts AA, Morrison DA, Grimm GW, 2016. *Intertwining phylogenetic trees and networks*. PeerJ Inc.

Schloss PD, Westcott SL, Ryabin T *et al.*, 2009. Introducing mothur: Open-Source, Platform-Independent, Community-Supported Software for Describing and Comparing Microbial Communities ▿ . *Applied and Environmental Microbiology* **75**, 7537–7541.

Schneider C, Onimus C, Prado E *et al.*, 2019. INRA-ResDur: the French grapevine breeding programme for durable resistance to downy and powdery mildew. *Acta Horticulturae*, 207–214.

Schneider CA, Rasband WS, Eliceiri KW, 2012. NIH Image to ImageJ: 25 years of Image Analysis. *Nature methods* **9**, 671–675.

Schuh W, Jeger MJ, Frederiksen RA, 1988. Comparisons of spatial patterns of oospores of *Peronosclerospora sorghi* in the soil and of sorghum plants with systemic downy mildew. *Phytopathology* **78**, 432–434.

Schütte UME, Abdo Z, Bent SJ *et al.*, 2008. Advances in the use of terminal restriction fragment length polymorphism (T-RFLP) analysis of 16S rRNA genes to characterize microbial communities. *Applied Microbiology and Biotechnology* **80**, 365–380.

Seaver SMD, Liu F, Zhang Q *et al.*, 2020. The ModelSEED Biochemistry Database for the integration of metabolic annotations and the reconstruction, comparison and analysis of metabolic models for plants, fungi and microbes. *Nucleic Acids Research*, gkaa746-.

Seemann T, 2014. Prokka: rapid prokaryotic genome annotation. *Bioinformatics* **30**, 2068–2069.

Sereika M, Kirkegaard RH, Karst SM *et al.*, 2022. Oxford Nanopore R10.4 long-read sequencing enables the generation of near-finished bacterial genomes from pure cultures and metagenomes without short-read or reference polishing. *Nature Methods* **19**, 823–826.

Sessitsch A, Pfaffenbichler N, Mitter B, 2019. Microbiome Applications from Lab to Field: Facing Complexity. *Trends in Plant Science* **24**, 194–198.

Setati ME, Jacobson D, Bauer FF, 2015. Sequence-based Analysis of the *Vitis vinifera* L. cv Cabernet Sauvignon Grape Must Mycobiome in Three South African Vineyards Employing Distinct Agronomic Systems. *Frontiers in Microbiology* **6**.

Shahzad R, Khan AL, Bilal S, Asaf S, Lee I-J, 2018. What Is There in Seeds? Vertically Transmitted Endophytic Resources for Sustainable Improvement in Plant Growth. *Frontiers in Plant Science* **9**.

Shakir S, Zaidi SS-A, de Vries FT, Mansoor S, 2021. Plant Genetic Networks Shaping Phyllosphere Microbial Community. *Trends in Genetics* **37**, 306–316.

Shannon CE, 1948. A Mathematical Theory of Communication. *The Bell system technical journal* **27**, 379–423.

Sharifazizi M, Harighi B, Sadeghi A, 2017. Evaluation of biological control of *Erwinia amylovora*, causal agent of fire blight disease of pear by antagonistic bacteria. *Biological Control* **104**, 28–34.

Sharma A, Kumar V, Shahzad B *et al.*, 2019. Worldwide pesticide usage and its impacts on ecosystem. *SN Applied Sciences* **1**, 1446.

Sharma S, Sundaresha S, Bhardwaj V, 2021. Biotechnological approaches in management of oomycetes diseases. *3 Biotech* **11**, 274.

Shen H, Shi X, Ran L, 2022. Hyperparasitism on *Plasmopara viticola* by *Simplicillium lanosoniveum*. *PhytoFrontiers™* **2**, 101–104.

Shvets D, Porotikova E, Sandomirsky K, Vinogradova S, 2022. Virome of Grapevine Germplasm from the Anapa Ampelographic Collection (Russia). *Viruses* **14**, 1314.

Silva MS e, Carvalho FCQ, Silva JR da, Lins SR de O, Oliveira SMA de, 2014. Use of antagonists and alternative products to manage post-harvest soft rot in pepper. *Revista Ciência Agronômica* **45**, 718–725.

Simonin M, Briand M, Chesneau G *et al.*, 2022. Seed microbiota revealed by a large-scale meta-analysis including 50 plant species. *New Phytologist* **234**, 1448–1463.

Simpson EH, 1949. Measurement of Diversity. *Nature* **163**, 688–688.

Singh P, Santoni S, This P, Péros J-P, 2018. Genotype-Environment Interaction Shapes the Microbial Assemblage in Grapevine's Phyllosphere and Carposphere: An NGS Approach. *Microorganisms* **6**, 96.

Singh P, Santoni S, Weber A, This P, Péros J-P, 2019. Understanding the phyllosphere microbiome assemblage in grape species (Vitaceae) with amplicon sequence data structures. *Scientific Reports* **9**, 14294.

Sivan A, Rahimi O, Lavi B *et al.*, 2021. Genomic evidence supports an independent history of Levantine and Eurasian grapevines. *Plants, People, Planet* **3**, 414–427.

Smith NA, Eamens AL, Wang M-B, 2011. Viral Small Interfering RNAs Target Host Genes to Mediate Disease Symptoms in Plants (S-W Ding, Ed,). *PLoS Pathogens* **7**, e1002022.

Smith SE, Read DJ, 2010. *Mycorrhizal Symbiosis*. Academic Press.

Sneh B, Humble SJ, Lockwood JL, 1977. Parasitism of oospores of *Phytophthora megasperma* var. *sojae*, *P. cactorum*, *Pythium* sp., and *Aphanomyces euteiches* in soil by Oomycetes, Chytridiomycetes, Hyphomycetes, Actinomycetes, and Bacteria. *Phytopathology* **67**, 622–628.

Sommermann L, Geistlinger J, Wibberg D *et al.*, 2018. Fungal community profiles in agricultural soils of a long-term field trial under different tillage, fertilization and crop rotation conditions analyzed by high-throughput ITS-amplicon sequencing. *PLOS ONE* **13**, e0195345.

Spadaro D, Droby S, 2016. Development of biocontrol products for postharvest diseases of fruit: The importance of elucidating the mechanisms of action of yeast antagonists. *Trends in Food Science & Technology* **47**, 39–49.

Staudt G, Kassemeyer HH, 1995. Evaluation of downy mildew resistance in various accessions of wild *Vitis* species. *Vitis* **34**, 225–228.

Stefanini I, Cavalieri D, 2018. Metagenomic Approaches to Investigate the Contribution of the Vineyard Environment to the Quality of Wine Fermentation: Potentials and Difficulties. *Frontiers in Microbiology* **9**, 991.

Stegen JC, Lin X, Fredrickson JK *et al.*, 2013. Quantifying community assembly processes and identifying features that impose them. *The ISME Journal* **7**, 2069–2079.

Stegen JC, Lin X, Konopka AE, Fredrickson JK, 2012. Stochastic and deterministic assembly processes in subsurface microbial communities. *The ISME Journal* **6**, 1653–1664.

Steimetz E, Trouvelot S, Gindro K *et al.*, 2012. Influence of leaf age on induced resistance in grapevine against *Plasmopara viticola*. *Physiological and Molecular Plant Pathology* **79**, 89–96.

Stein RR, Bucci V, Toussaint NC *et al.*, 2013. Ecological Modeling from Time-Series Inference: Insight into Dynamics and Stability of Intestinal Microbiota. *PLOS Computational Biology* **9**, e1003388.

Stempien E, Pierron RJ, Adendorff I, van Jaarsveld WJ, Halleen F, Mostert L, 2020. Host defence activation and root colonization of grapevine rootstocks by the biological control fungus *Trichoderma atroviride*. *Phytopathologia Mediterranea* **59**, 615–626.

Stranska M, Dzuman Z, Prusova N *et al.*, 2022. Fungal Endophytes of *Vitis vinifera*—Plant Growth Promoters or Potentially Toxinogenic Agents? *Toxins* **14**, 66.

Sun A, Jiao X-Y, Chen Q *et al.*, 2021a. Microbial communities in crop phyllosphere and root endosphere are more resistant than soil microbiota to fertilization. *Soil Biology and Biochemistry* **153**, 108113.

Sun X, Kosman E, Sharon A, 2020. Stem Endophytic Mycobiota in Wild and Domesticated Wheat: Structural Differences and Hidden Resources for Wheat Improvement. *Journal of Fungi* **6**, 180.

Sun D, Qu J, Huang Y, Lu J, Yin L, 2021b. Analysis of microbial community diversity of muscadine grape skins. *Food Research International* **145**, 110417.

Sweet MJ, Bulling MT, 2017. On the Importance of the Microbiome and Pathobiome in Coral Health and Disease. *Frontiers in Marine Science* **4**.

Swift JF, Hall ME, Harris ZN, Kwasniewski MT, Miller AJ, 2021. Grapevine Microbiota Reflect Diversity among Compartments and Complex Interactions within and among Root and Shoot Systems. *Microorganisms* **9**, 92.

Syed Ab Rahman SF, Singh E, Pieterse CMJ, Schenk PM, 2018. Emerging microbial biocontrol strategies for plant pathogens. *Plant Science* **267**, 102–111.

Taberlet P, Bonin A, Zinger L, Coissac E, 2018. *Environmental DNA: For Biodiversity Research and Monitoring*. Oxford University Press.

Taguiam JD, Evallo E, Balendres MA, 2021. Epicoccum species: ubiquitous plant pathogens and effective biological control agents. *European Journal of Plant Pathology* **159**, 713–725.

Talontsi FM, Islam MdT, Facey P, Douanla-Meli C, von Tiedemann A, Laatsch H, 2012. Depsidones and other constituents from *Phomopsis* sp. CAFT69 and its host plant *Endodesmia calophylloides* with potent inhibitory effect on motility of zoospores of grapevine pathogen *Plasmopara viticola*. *Phytochemistry Letters* **5**, 657–664.

Tamaddoni-Nezhad A, Bohan D, Milani GA, Raybould A, Muggleton S, 2021. Human–Machine Scientific Discovery. In: *Human-Like Machine Intelligence*. Oxford University Press, 297–315.

Taylor AS, Cook DC, 2018. An economic assessment of the impact on the Western Australian viticulture industry from the incursion of grapevine downy mildew. *Journal of Plant Diseases and Protection* **125**, 397–403.

Tedersoo L, Anslan S, 2019. Towards PacBio-based pan-eukaryote metabarcoding using full-length ITS sequences. *Environmental Microbiology Reports* **11**, 659–668.

Tedersoo L, Bahram M, Põlme S *et al.*, 2014. Global diversity and geography of soil fungi. *Science* **346**, 1256688.

Tedersoo L, Bahram M, Zinger L *et al.*, 2021. *Best practices in metabarcoding of fungi: from experimental design to results*. Preprints.

Tedersoo L, Tooming-Klunderud A, Anslan S, 2018. PacBio metabarcoding of Fungi and other eukaryotes: errors, biases and perspectives. *New Phytologist* **217**, 1370–1385.

Tedesco S, Fevereiro P, Kragler F, Pina A, 2022. Plant grafting and graft incompatibility: A review from the grapevine perspective. *Scientia Horticulturae* **299**, 111019.

Teixeira PJP, Colaianni NR, Fitzpatrick CR, Dangl JL, 2019. Beyond pathogens: microbiota interactions with the plant immune system. *Current Opinion in Microbiology* **49**, 7–17.

Tejero P, Martín A, Rodríguez A, Galván AI, Ruiz-Moyano S, Hernández A, 2021. In Vitro Biological Control of *Aspergillus flavus* by *Hanseniaspora opuntiae* L479 and *Hanseniaspora uvarum* L793, Producers of Antifungal Volatile Organic Compounds. *Toxins* **13**, 663.

Terral J-F, Tabard E, Bouby L *et al.*, 2010. Evolution and history of grapevine (*Vitis vinifera*) under domestication: new morphometric perspectives to understand seed domestication syndrome and reveal origins of ancient European cultivars. *Annals of Botany* **105**, 443–455.

The Galaxy Community, 2024. The Galaxy platform for accessible, reproducible, and collaborative data analyses: 2024 update. *Nucleic Acids Research* **52**, W83–W94.

Thibon C, Cluzet S, Mérillon JM, Darriet P, Dubourdieu D, 2011. 3-Sulfanylhexanol Precursor Biogenesis in Grapevine Cells: The Stimulating Effect of *Botrytis cinerea*. *Journal of Agricultural and Food Chemistry* **59**, 1344–1351.

Thibon C, Shinkaruk S, Jourdes M, Bennetau B, Dubourdieu D, Tominaga T, 2010. Aromatic potential of botrytized white wine grapes: Identification and quantification of new cysteine-S-conjugate flavor precursors. *Analytica Chimica Acta* **660**, 190–196.

Thijs S, Op De Beeck M, Beckers B *et al.*, 2017. Comparative Evaluation of Four Bacteria-Specific Primer Pairs for 16S rRNA Gene Surveys. *Frontiers in Microbiology* **8**.

This P, Lacombe T, Thomas M, 2006. Historical origins and genetic diversity of wine grapes. *Trends in Genetics* **22**, 511–519.

Thrall PH, Hochberg ME, Burdon JJ, Bever JD, 2007. Coevolution of symbiotic mutualists and parasites in a community context. *Trends in Ecology & Evolution* **22**, 120–126.

Tikhonov G, Opedal ØH, Abrego N *et al.*, 2020. Joint species distribution modelling with the r-package Hmsc. *Methods in Ecology and Evolution* **11**, 442–447.

Tilcher R, Wolf GAI fuer P und P, Brendel G, 1994. Effects of microbial antagonists on leaf infestation, sporangia germination and zoospore behaviour of *Plasmopara viticola* (Berk. and Curtis) Berl. and de Toni. *Mededelingen - Faculteit Landbouwkundige en Toegepaste Biologische Wetenschappen Universiteit Gent (Belgium)* **59**.

Toffolatti SL, De Lorenzis G, Costa A *et al.*, 2018. Unique resistance traits against downy mildew from the center of origin of grapevine (*Vitis vinifera*). *Scientific Reports* **8**, 12523.

Toju H, Peay KG, Yamamichi M *et al.*, 2018. Core microbiomes for sustainable agroecosystems. *Nature Plants* **4**, 247–257.

Tolba IH, Soliman MA, 2013. Efficacy of native antagonistic bacterial isolates in biological control of crown gall disease in Egypt. *Annals of Agricultural Sciences* **58**, 43–49.

Trivedi P, Leach JE, Tringe SG, Sa T, Singh BK, 2020. Plant–microbiome interactions: from community assembly to plant health. *Nature Reviews Microbiology* **18**, 607–621.

Trivedi P, Mattupalli C, Eversole K, Leach JE, 2021. Enabling sustainable agriculture through understanding and enhancement of microbiomes. *New Phytologist* **230**, 2129–2147.

Trouvelot S, Bonneau L, Redecker D, van Tuinen D, Adrian M, Wipf D, 2015. Arbuscular mycorrhiza symbiosis in viticulture: a review. *Agronomy for Sustainable Development* **35**, 1449–1467.

Tshikantwa TS, Ullah MW, He F, Yang G, 2018. Current Trends and Potential Applications of Microbial Interactions for Human Welfare. *Frontiers in Microbiology* **9**, 1156.

Uyemoto JK, Rowhani A, Ludivisi D, 2000. An association of rootstock stem lesions in *Vitis* species and different graft-transmissible agents. *Proceedings of the 13th ICVG Meetings. Adelaide, Australia* **83**.

Uyemoto JK, Rowhani A, Luvisi D, Krag CR, 2001. New closterovirus in 'Redglobe' grape causes decline of grafted plants. *California Agriculture* **55**, 28–31.

Vacher C, Francioni C, Michel M *et al.*, in press. Fungal metabarcoding data for two grapevine varieties (Regent and *Vitis vinifera* L. cv. Cabernet–Sauvignon) inoculated with powdery mildew (*Erysiphe necator*) under drought conditions. *Phytobiomes Journal, in press*.

Vacher C, Hampe A, Porté AJ, Sauer U, Compant S, Morris CE, 2016a. The Phyllosphere: Microbial Jungle at the Plant–Climate Interface. *Annual Review of Ecology, Evolution, and Systematics* **47**, 1–24.

Vacher C, Tamaddoni-Nezhad A, Kamenova S *et al.*, 2016b. Chapter One - Learning Ecological Networks from Next-Generation Sequencing Data. In: Woodward G,, Bohan DA, eds. *Advances in Ecological Research*. Ecosystem Services: From Biodiversity to Society, Part 2. Academic Press, 1–39.

Valsesia G, Gobbin D, Patocchi A, Vecchione A, Pertot I, Gessler C, 2005. Development of a High-Throughput Method for Quantification of *Plasmopara viticola* DNA in Grapevine Leaves by Means of Quantitative Real-Time Polymerase Chain Reaction. *Phytopathology®* **95**, 672–678.

Van der Ent S, Van Hulten M, Pozo MJ *et al.*, 2009. Priming of plant innate immunity by rhizobacteria and β-aminobutyric acid: differences and similarities in regulation. *New Phytologist* **183**, 419–431.

Van der Heyden H, Wallon T, Lévesque CA, Carisse O, 2019. Detection and Quantification of *Pythium tracheiphilum* in Soil by Multiplex Real-Time qPCR. *Plant Disease* **103**, 475–483.

Vandenkoornhuyse P, Quaiser A, Duhamel M, Le Van A, Dufresne A, 2015. The importance of the microbiome of the plant holobiont. *New Phytologist* **206**, 1196–1206.

VanEvery H, Franzosa EA, Nguyen LH, Huttenhower C, 2023. Microbiome epidemiology and association studies in human health. *Nature Reviews Genetics* **24**, 109–124.

Vannier N, Agler M, Hacquard S, 2019. Microbiota-mediated disease resistance in plants (C Zipfel, Ed,). *PLOS Pathogens* **15**, e1007740.

Vannier N, Mony C, Bittebière A-K, Vandenkoornhuyse P, 2015. Epigenetic Mechanisms and Microbiota as a Toolbox for Plant Phenotypic Adjustment to Environment. *Frontiers in Plant Science* **6**.

Vass M, Székely AJ, Lindström ES, Langenheder S, 2020. Using null models to compare bacterial and microeukaryotic metacommunity assembly under shifting environmental conditions. *Scientific Reports* **10**, 2455.

Vayssier-Taussat M, Albina E, Citti C *et al.*, 2014. Shifting the paradigm from pathogens to pathobiome: new concepts in the light of meta-omics. *Frontiers in Cellular and Infection Microbiology* **4**.

Vecchione A, Zulini L, Pertot I, Musetti R, 2007. BIOLOGICAL CONTROL OF PLASMOPARA VITICOLA: A MULTISITE APPROACH. *Acta Horticulturae*, 361–366.

Vega FE, Goettel MS, Blackwell M *et al.*, 2009. Fungal entomopathogens: new insights on their ecology. *Fungal Ecology* **2**, 149–159.

Velasquez-Camacho L, Otero M, Basile B, Pijuan J, Corrado G, 2023. Current Trends and Perspectives on Predictive Models for Mildew Diseases in Vineyards. *Microorganisms* **11**, 73.

Vellend M, 2010. Conceptual Synthesis in Community Ecology. *The Quarterly Review of Biology* **85**, 183–206.

Venuti S, Copetti D, Foria S *et al.*, 2013. Historical Introgression of the Downy Mildew Resistance Gene Rpv12 from the Asian Species Vitis amurensis into Grapevine Varieties. *PLOS ONE* **8**, e61228.

Vero S, Garmendia G, González MB, Bentancur O, Wisniewski M, 2013. Evaluation of yeasts obtained from Antarctic soil samples as biocontrol agents for the management of postharvest diseases of apple (*Malus* × *domestica*). *FEMS Yeast Research* **13**, 189–199.

Vidhate R, Singh J, Ghormade V, Chavan S, Patil A, Deshpande M, 2015. Use of Hydrolytic Enzymes of *Myrothecium verrucaria* and Conidia of *Metarhizium anisopliae*, Singly and Sequentially to Control Pest and Pathogens in Grapes and their Compatibility with Pesticides Used in the Field. *Biopesticides International* **11**, 48–60.

Villano C, Aversano R, 2020. Towards grapevine (*Vitis vinifera* L.) mildews resistance: Molecular defence mechanisms and New Breeding Technologies. *Italus Hortus* **27**, 1.

Vitulo N, Lemos WJF, Calgaro M *et al.*, 2019. Bark and Grape Microbiome of *Vitis vinifera*: Influence of Geographic Patterns and Agronomic Management on Bacterial Diversity. *Frontiers in Microbiology* **9**, 3203.

Vlasselaer L, Crauwels S, Lievens B, De Coninck B, 2024. Unveiling the microbiome of hydroponically cultivated lettuce: impact of Phytophthora cryptogea infection on plant-associated microorganisms. *FEMS Microbiology Ecology* **100**, fiae010.

Volynchikova E, Kim KD, 2022. Biological Control of Oomycete Soilborne Diseases Caused by *Phytophthora capsici*, *Phytophthora infestans*, and *Phytophthora nicotianae* in Solanaceous Crops. *Mycobiology* **50**, 269–293.

Vorholt JA, 2012. Microbial life in the phyllosphere. *Nature Reviews Microbiology* **10**, 828–840.

Vorholt JA, Vogel C, Carlström CI, Müller DB, 2017. Establishing Causality: Opportunities of Synthetic Communities for Plant Microbiome Research. *Cell Host & Microbe* **22**, 142–155.

Vorwerk S, Forneck A, 2006. Reproductive mode of grape phylloxera (Daktulosphaira vitifoliae, Homoptera: Phylloxeridae) in Europe: molecular evidence for predominantly asexual populations and a lack of gene flow between them. *Genome* **49**, 678–687.

Vukicevich E, Thomas Lowery D, Úrbez-Torres JR, Bowen P, Hart M, 2018. Groundcover management changes grapevine root fungal communities and plant-soil feedback. *Plant and Soil* **424**, 419–433.

Wagner MR, Busby PE, Balint-Kurti P, 2020. Analysis of leaf microbiome composition of near-isogenic maize lines differing in broad-spectrum disease resistance. *New Phytologist* **225**, 2152–2165.

Waite H, Whitelaw-Weckert M, Torley P, 2015. Grapevine propagation: principles and methods for the production of high-quality grapevine planting material. *New Zealand Journal of Crop and Horticultural Science* **43**, 144–161.

Wallace JG, Kremling KA, Kovar LL, Buckler ES, 2018. Quantitative Genetics of the Maize Leaf Microbiome. *Phytobiomes Journal* **2**, 208–224.

Walsh TK, Heckel DG, Wu Y, Downes S, Gordon KHJ, Oakeshott JG, 2022. Determinants of Insecticide Resistance Evolution: Comparative Analysis Among Heliothines. *Annual Review of Entomology* **67**, 387–406.

Wan Y, Schwaninger HR, Baldo AM, Labate JA, Zhong G-Y, Simon CJ, 2013. A phylogenetic analysis of the grape genus (*Vitis* L.) reveals broad reticulation and concurrent diversification during neogene and quaternary climate change. *BMC Evolutionary Biology* **13**, 141.

Wang Q, Garrity GM, Tiedje JM, Cole JR, 2007. Naïve Bayesian Classifier for Rapid Assignment of rRNA Sequences into the New Bacterial Taxonomy. *Applied and Environmental Microbiology* **73**, 5261–5267.

Wang M, Geng L, Sun X, Shu C, Song F, Zhang J, 2020. Screening of *Bacillus thuringiensis* strains to identify new potential biocontrol agents against *Sclerotinia sclerotiorum* and *Plutella xylostella* in *Brassica campestris* L. *Biological Control* **145**, 104262.

Wang X, Schlatter DC, Glawe DA *et al.*, 2021. Native yeast and non-yeast fungal communities of Cabernet Sauvignon berries from two Washington State vineyards, and persistence in spontaneous fermentation. *International Journal of Food Microbiology* **350**, 109225.

Wang Z, Wang Y, Zheng L, Yang X, Liu H, Guo J, 2014. Isolation and characterization of an antifungal protein from *Bacillus licheniformis* HS10. *Biochemical and Biophysical Research Communications* **454**, 48–52.

Wang W, Zhai Y, Cao L, Tan H, Zhang R, 2016. Endophytic bacterial and fungal microbiota in sprouts, roots and stems of rice (*Oryza sativa* L.). *Microbiological Research* **188–189**, 1–8.

Wani ZA, Mirza DN, Arora P, Riyaz-Ul-Hassan S, 2016. Molecular phylogeny, diversity, community structure, and plant growth promoting properties of fungal endophytes associated with the corms of saffron plant: An insight into the microbiome of *Crocus sativus* Linn. *Fungal Biology* **120**, 1509–1524.

Warringer J, Zörgö E, Cubillos FA *et al.*, 2011. Trait Variation in Yeast Is Defined by Population History (L Kruglyak, Ed,). *PLoS Genetics* **7**, e1002111.

Wasimuddin, Schlaeppi K, Ronchi F, Leib SL, Erb M, Ramette A, 2020. Evaluation of primer pairs for microbiome profiling from soils to humans within the One Health framework. *Molecular Ecology Resources* **20**, 1558–1571.

Wei Z, Gu Y, Friman V-P *et al.*, 2019. Initial soil microbiome composition and functioning predetermine future plant health. *Science Advances* **5**, eaaw0759.

Wei Y, Mao S, Tu K, 2014. Effect of preharvest spraying *Cryptococcus laurentii* on postharvest decay and quality of strawberry. *Biological Control* **73**, 68–74.

Weiss S, Van Treuren W, Lozupone C *et al.*, 2016. Correlation detection strategies in microbial data sets vary widely in sensitivity and precision. *The ISME Journal* **10**, 1669–1681.

Weiss S, Xu ZZ, Peddada S *et al.*, 2017. Normalization and microbial differential abundance strategies depend upon data characteristics. *Microbiome* **5**, 27.

Welter L, Tisch C, Kortekamp A, Topfer R, Zyprian E, 2017. Powdery mildew responsive genes of resistant grapevine cultivar "regent." *Vitis - Journal of Grapevine Research* **56**, 181–188.

Wemheuer F, Taylor JA, Daniel R *et al.*, 2020. Tax4Fun2: prediction of habitat-specific functional profiles and functional redundancy based on 16S rRNA gene sequences. *Environmental Microbiome* **15**, 11.

White TJ, 1990. PCR protocols: a guide to methods and applications | CiNii Research.

White TJ, Bruns T, Lee S *et al.*, 1990. PCR Protocols: A Guide to Methods and Applications. , 315–322.

Wicaksono WA, Morauf C, Müller H, Abdelfattah A, Donat C, Berg G, 2023. The mature phyllosphere microbiome of grapevine is associated with resistance against *Plasmopara viticola*. *Frontiers in Microbiology* **14**.

Wickham H, 2016. *ggplot2: Elegant Graphics for Data Analysis*. Cham: Springer International Publishing.

Widder S, Allen RJ, Pfeiffer T *et al.*, 2016. Challenges in microbial ecology: building predictive understanding of community function and dynamics. *The ISME Journal* **10**, 2557–2568.

Wilke CO, 2024. cowplot: Streamlined Plot Theme and Plot Annotations for "ggplot2."

Wilke CO, Wiernik BM, 2022. ggtext: Improved Text Rendering Support for "ggplot2."

Williams CE, Hammer TJ, Williams CL, 2024. Diversity alone does not reliably indicate the healthiness of an animal microbiome. *The ISME Journal* **18**, wrae133.

Wright E S, 2016. Using DECIPHER v2.0 to Analyze Big Biological Sequence Data in R. *The R Journal* **8**, 352.

Wright MN, Ziegler A, 2017. ranger: A Fast Implementation of Random Forests for High Dimensional Data in C++ and R. *Journal of Statistical Software* **77**, 1–17.

Wu X, Cui Z, Peng J, Zhang F, Liesack W, 2022a. Genome-resolved metagenomics identifies the particular genetic traits of phosphate-solubilizing bacteria in agricultural soil. *ISME Communications* **2**, 17.

Wu X, Rensing C, Han D *et al.*, 2022b. Genome-Resolved Metagenomics Reveals Distinct Phosphorus Acquisition Strategies between Soil Microbiomes. *mSystems* **7**, e01107-21.

Wu Y-W, Simmons BA, Singer SW, 2016. MaxBin 2.0: an automated binning algorithm to recover genomes from multiple metagenomic datasets. *Bioinformatics* **32**, 605–607.

Wu M, Zhang L, Li G, Jiang D, Ghabrial SA, 2010. Genome characterization of a debilitation-associated mitovirus infecting the phytopathogenic fungus *Botrytis cinerea*. *Virology* **406**, 117–126.

Xiao Y, Angulo MT, Friedman J, Waldor MK, Weiss ST, Liu Y-Y, 2017. Mapping the ecological networks of microbial communities. *Nature Communications* **8**, 2042.

Xie M, Jia J, Luan D, Li R, Zhang J, Zhang J, 2024. Processes of assembly of endophytic prokaryotic and rhizosphere fungal communities in table grape are preponderantly deterministic. *Applied Soil Ecology* **203**, 105660.

Xin X-F, He SY, 2013. Pseudomonas syringae pv. tomato DC3000: A Model Pathogen for Probing Disease Susceptibility and Hormone Signaling in Plants. *Annual Review of Phytopathology* **51**, 473–498.

Xu T, Chen X, Hou Y, Zhu B, 2021. Changes in microbial biomass, community composition and diversity, and functioning with soil depth in two alpine ecosystems on the Tibetan plateau. *Plant and Soil* **459**, 137–153.

Xu X, Jeger M, 2020. More Ecological Research Needed for Effective Biocontrol of Plant Pathogens. In: De Cal A,, Melgarejo P,, Magan N, eds. *How Research Can Stimulate the Development of Commercial Biological Control Against Plant Diseases*. Cham: Springer International Publishing, 15–30.

Xu N, Zhang Z, Shen Y *et al.*, 2022. Compare the performance of multiple binary classification models in microbial high-throughput sequencing datasets. *Science of The Total Environment* **837**, 155807.

Yacoub A, Gerbore J, Magnin N *et al.*, 2016. Ability of *Pythium oligandrum* strains to protect *Vitis vinifera* L., by inducing plant resistance against *Phaeomoniella chlamydospora*, a pathogen involved in Esca, a grapevine trunk disease. *Biological Control* **92**, 7–16.

Yang L, Chen J, 2022. A comprehensive evaluation of microbial differential abundance analysis methods: current status and potential solutions. *Microbiome* **10**, 130.

Yang L, Chen J, 2023. Benchmarking differential abundance analysis methods for correlated microbiome sequencing data. *Briefings in Bioinformatics* **24**, bbac607.

Yazid SNE, Tajudin NI, Razman NAA *et al.*, 2023. Mycotoxigenic fungal growth inhibition and multi-mycotoxin reduction of potential biological control agents indigenous to grain maize. *Mycotoxin Research* **39**, 177–192.

Yergeau É, Quiza L, Tremblay J, 2020. Microbial indicators are better predictors of wheat yield and quality than N fertilization. *FEMS Microbiology Ecology* **96**, fiz205.

Yin L, An Y, Qu J *et al.*, 2017. Genome sequence of Plasmopara viticola and insight into the pathogenic mechanism. *Scientific Reports* **7**, 46553.

Yoshida K, Schuenemann VJ, Cano LM *et al.*, 2013. The rise and fall of the Phytophthora infestans lineage that triggered the Irish potato famine (D Baulcombe, Ed,). *eLife* **2**, e00731.

Yousaf S, Bulgari D, Bergna A *et al.*, 2014. Pyrosequencing detects human and animal pathogenic taxa in the grapevine endosphere. *Frontiers in Microbiology* **5**.

Yu L, Sang W, Wu M-D *et al.*, 2015. Novel Hypovirulence-Associated RNA Mycovirus in the Plant-Pathogenic Fungus *Botrytis cinerea*: Molecular and Biological Characterization (D Cullen, Ed,). *Applied and Environmental Microbiology* **81**, 2299–2310.

Yu X, Zhang K, Liu J *et al.*, 2024. Identification and evaluation of an endophytic antagonistic yeast for the control of gray mold (*Botrytis cinerea*) in apple and mechanisms of action. *Food Microbiology* **123**, 104583.

Yue Y, Huang H, Qi Z *et al.*, 2020. Evaluating metagenomics tools for genome binning with real metagenomic datasets and CAMI datasets. *BMC Bioinformatics* **21**, 334.

Zaller JG, Cantelmo C, Santos GD *et al.*, 2018. Herbicides in vineyards reduce grapevine root mycorrhization and alter soil microorganisms and the nutrient composition in grapevine roots, leaves, xylem sap and grape juice. *Environmental Science and Pollution Research* **25**, 23215–23226.

Zamioudis C, Korteland J, Van Pelt JA *et al.*, 2015. Rhizobacterial volatiles and photosynthesis-related signals coordinate 72 expression in Arabidopsis roots during onset of induced systemic resistance and iron-deficiency responses. *The Plant Journal* **84**, 309–322.

Zaneveld JR, McMinds R, Vega Thurber R, 2017. Stress and stability: applying the Anna Karenina principle to animal microbiomes. *Nature Microbiology* **2**, 1–8.

Zang C, Lin Q, Xie J, Lin Y, Zhao K, Liang C, 2020. The biological control of the grapevine downy mildew disease using *Ochrobactrum* sp. *Plant Protection Science* **56**, 52–61.

Zanne AE, Abarenkov K, Afkhami ME *et al.*, 2020. Fungal functional ecology: bringing a trait-based approach to plant-associated fungi. *Biological Reviews* **95**, 409–433.

Zanzotto A, Morroni M, 2016. Major biocontrol studies and measures against fungal and oomycete pathogens of grapevine. In: Compant S,, Mathieu F, eds. *Biocontrol of major grapevine diseases: leading research*. Wallingford: CABI, 1–34.

Zarraonaindia I, Owens SM, Weisenhorn P *et al.*, 2015a. The Soil Microbiome Influences Grapevine-Associated Microbiota (JK Jansson, Ed,). *mBio* **6**, e02527-14.

Zarraonaindia I, Owens SM, Weisenhorn P *et al.*, 2015b. The Soil Microbiome Influences Grapevine-Associated Microbiota (JK Jansson, Ed,). *mBio* **6**, e02527-14.

Zecca G, Abbott JR, Sun W-B, Spada A, Sala F, Grassi F, 2012. The timing and the mode of evolution of wild grapes (*Vitis*). *Molecular Phylogenetics and Evolution* **62**, 736–747.

Zhang X, Chen J, Zhou H, 2024. MicrobiomeStat: Statistical Methods for Microbiome Compositional Data.

Zhang J, Liu Y-X, Guo X *et al.*, 2021. High-throughput cultivation and identification of bacteria from the plant root microbiota. *Nature Protocols* **16**, 988–1012.

Zhang S, Wang Y, Chen X, Cui B, Bai Z, Zhuang G, 2020. Variety features differentiate microbiota in the grape leaves. *Canadian Journal of Microbiology* **66**, 653–663.

Zhang H, Wang L, Ma L *et al.*, 2009. Biocontrol of major postharvest pathogens on apple using *Rhodotorula glutinis* and its effects on postharvest quality parameters. *Biological Control* **48**, 79–83.

Zhang X, Zhou Y, Li Y, Fu X, Wang Q, 2017. Screening and characterization of endophytic *Bacillus* for biocontrol of grapevine downy mildew. *Crop Protection* **96**, 173–179.

Zherdev A, Vinogradova S, Byzova N, Porotikova E, Kamionskaya A, Dzantiev B, 2018. Methods for the Diagnosis of Grapevine Viral Infections: A Review. *Agriculture* **8**, 195.

Zhou H, He K, Chen J, Zhang X, 2022. LinDA: linear models for differential abundance analysis of microbiome compositional data. *Genome Biology* **23**, 95.

Zhou J, Ning D, 2017. Stochastic Community Assembly: Does It Matter in Microbial Ecology? *Microbiology and Molecular Biology Reviews* **81**, e00002-17.

Zhou X, Wang J-T, Wang W-H, Tsui CK, Cai L, 2021. Changes in Bacterial and Fungal Microbiomes Associated with Tomatoes of Healthy and Infected by Fusarium oxysporum f. sp. lycopersici. *Microbial Ecology* **81**, 1004–1017.

Zilber-Rosenberg I, Rosenberg E, 2008. Role of microorganisms in the evolution of animals and plants: the hologenome theory of evolution. *FEMS Microbiology Reviews* **32**, 723–735.

Zinger L, Lionnet C, Benoiston A-S, Donald J, Mercier C, Boyer F, 2021. metabaR: An r package for the evaluation and improvement of DNA metabarcoding data quality. *Methods in Ecology and Evolution* **12**, 586–592.

Zito S, Caffarra A, Richard Y, Castel T, Bois B, 2018. Climate change and vine protection : the case of mildews management in Burgundy. *E3S Web of Conferences* **50**, 01006.

Zohary D, Hopf M, 1993. Domestication of plants in the old world. In: Zohary D,, Hopf, eds. *The origin and spread of cultivated plants on West Asia, Europe and the Nile valley.* Oxford, England, pp 143–150: Clarendon Press,.

Zolti A, Green SJ, Sela N, Hadar Y, Minz D, 2020. The microbiome as a biosensor: functional profiles elucidate hidden stress in hosts. *Microbiome* **8**, 71.

Zorrilla F, Buric F, Patil KR, Zelezniak A, 2021. metaGEM: reconstruction of genome scale metabolic models directly from metagenomes. *Nucleic Acids Research* **49**, e126–e126.

Zou C, Karn A, Reisch B *et al.*, 2020. Haplotyping the Vitis collinear core genome with rhAmpSeq improves marker transferability in a diverse genus. *Nature Communications* **11**, 413.

Annexes

Annexe n°1

Plan d'expérience pour identifier des antagonistes microbiens de *Plasmopara viticola*, un agent pathogène foliaire majeur de la vigne cultivée (*Vitis vinifera* L.).



P. Fournier[1,3,4] , M. Raynal[2] , C. Debord[2], F. Delmotte[1], L. Deliere[1], P. This*[3], C. Vacher*[4]

[1]INRAE, Bordeaux Sciences Agro, ISVV, SAVE, 33140 Villenave-d'Ornon, France. [2]IFV, 33290 Blanquefort, France. [3]INRAE, CIRAD, Univ Montpellier, Institut AGRO, AGAP, 34398 Montpellier, France. [4]INRAE, Univ, Bordeaux, BioGeCo, 33615 Pessac, France. (*co-directeurs de thèse)

1. Contexte et hypothèse

La vigne cultivée, *Vitis vinifera*, est très sensible aux attaques de l'agent pathogène *Plasmopara viticola*, responsable du mildiou[1] ; et des différences de sensibilité entre les sites viticoles ont été observées[2]. La sensibilité d'un site peut être appréciée par des mesures d'intensité et de fréquence de symptômes[3] et peut être expliquée par différents facteurs[3-10] (Fig. 1). Cependant la seule prise en compte de ces facteurs n'est pas suffisante pour prévoir précisément les risques de dégâts causés par *P. viticola* à l'échelle de la parcelle.



Mildiou
Plasmopara viticola
Oomycète

La différence de fréquence et d'intensité des symptômes de mildiou observée entre les parcelles de *Vitis vinifera* peut-elle être mise en relation avec l'abondance de taxons bactériens ou fongiques particuliers dans le microbiote de la vigne ?

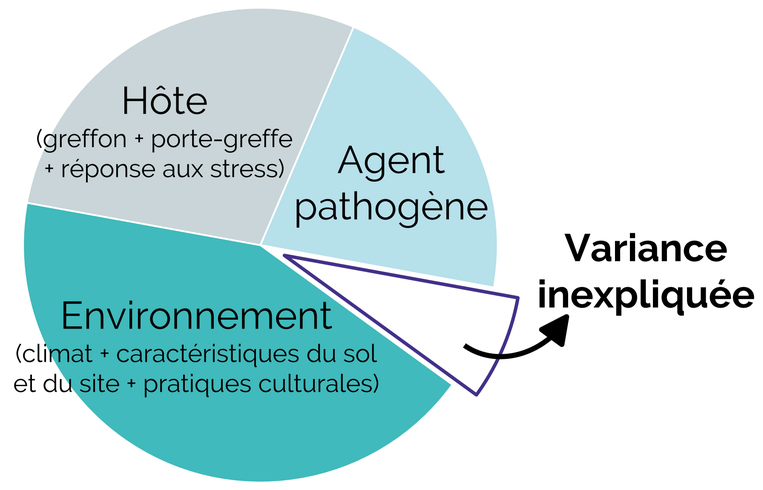


Figure 1 : Facteurs expliquant la sensibilité d'une parcelle au mildiou. La hiérarchie entre les facteurs est schématisée par la différence de taille entre les secteurs

Nous présentons ici une méthode de sélection de parcelles de vignes adaptée pour étudier le lien entre le microbiote de la vigne et des relevés épidémiologiques de symptômes de mildiou. Nous sélectionnons des paires de parcelles différant significativement par la fréquence et l'intensité des symptômes de mildiou, toutes choses étant par ailleurs aussi similaires que possible.

2. Données & Méthodes

a) Système d'information Epicure4

Evaluations visuelles hebdomadaires de la **fréquence** et de l'**intensité** de symptômes de mildiou sur les **grappes** et les **feuilles** de **Témoins Non Traités** (portion de parcelle ne recevant aucun traitement fongicide) de *Vitis vinifera*.

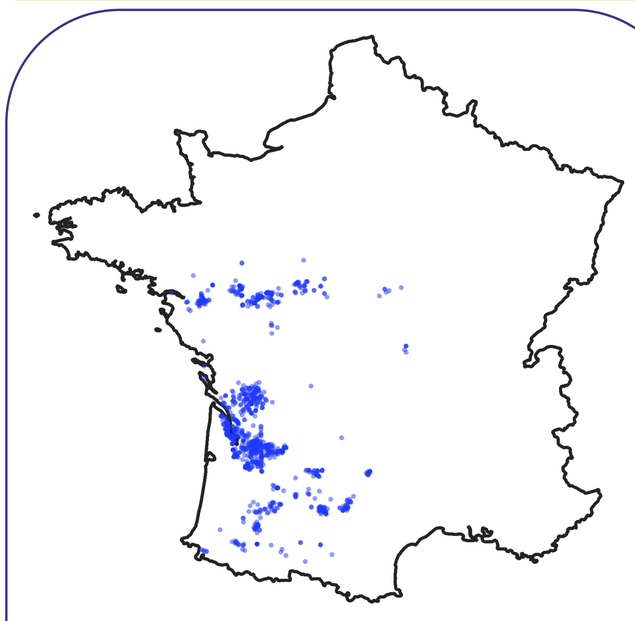


Figure 2 : Répartition des 1235 TNT suivis entre 2002 et 2022

Suivis réalisés **depuis 2002** dans 4 régions françaises (Fig. 2) :
- Nouvelle-Aquitaine
- Occitanie
- Pays de la Loire
- Centre - Val de Loire

b) Sélection des paires de parcelles

Nous avons utilisé 5 critères pour identifier des paires de parcelles **différant** par la **fréquence et l'intensité** des symptômes mais **comparables** en termes de matériel génétique, de localisation et de pratique culturale.

1) **Aire sous la courbe** d'évolution de la maladie d'une parcelle plus élevée pour les **4 variables**, **au moins 80%** des années de suivi épidémiologique commun (exemple Fig. 4).
2) *A minima* **4 ans de suivi commun** dont **2020 et/ou 2021**
3) **Cépage identique**
4) Distance géographique <= **10 km**
5) **Mode de conduite similaire**

3. Résultats

Sept paires ont été identifiées par la méthode mise en place. Elles sont réparties dans la région Nouvelle-Aquitaine (Fig. 3).

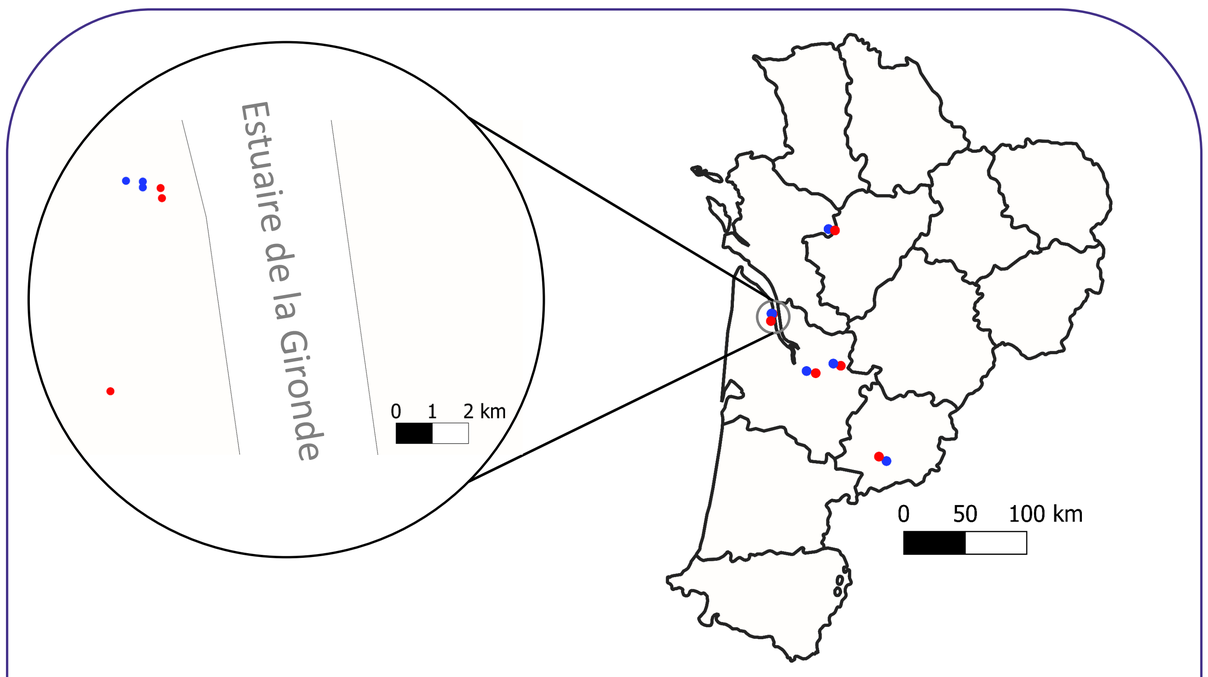


Figure 3 : Localisation des 7 paires de parcelles en Gironde, Lot-et Garonne et Charente-Maritime.
Le grossissement permet une meilleure visualisation de 3 paires situées au niveau de l'estuaire de la gironde

Légende Figures
Sensibilité de la parcelle au mildiou :
: Elevée
: Faible

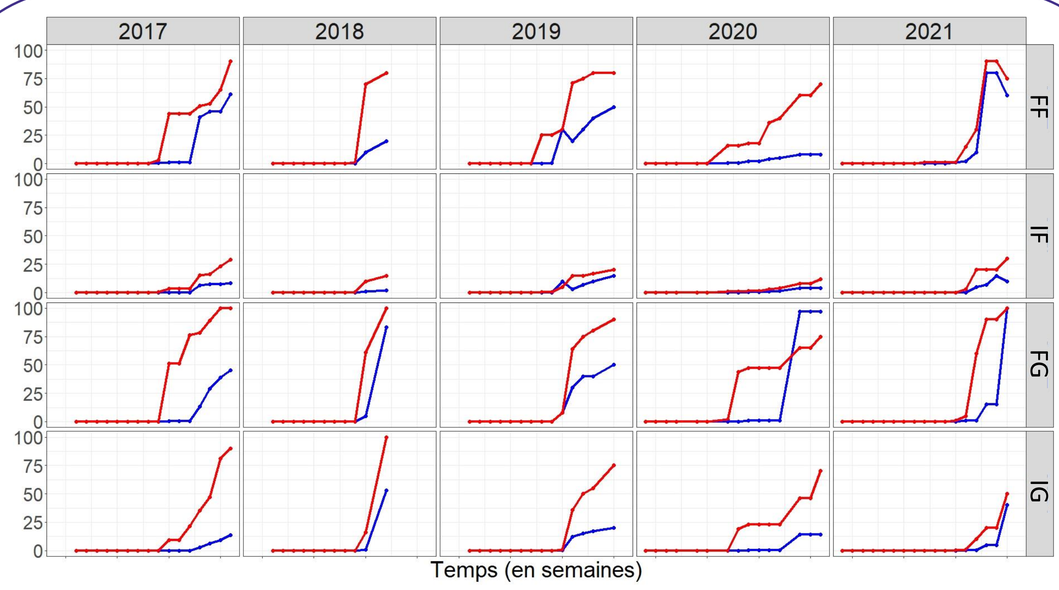


Figure 4 : Courbe d'évolution du mildiou d'une paire sélectionnée (illustration du critère 1 validé)

FF = Fréquence des symptômes sur Feuilles
IF = Intensité des symptômes sur Feuilles
FG = Fréquence des symptômes sur Grappes
IG = Intensité des symptômes sur Grappes

4. Conclusion

La méthode présentée a permis d'identifier 7 paires de parcelles différant par la fréquence et l'intensité des symptômes de mildiou mais comparables en termes de cépage, de localisation et de pratique culturale. Au printemps 2022, du sol et des feuilles ont été échantillonnés dans ces parcelles afin d'étudier le lien entre le microbiote de la vigne et sa sensibilité au mildiou, ainsi qu'identifier des taxons microbiens associés positivement à la santé des vignes.

Bibliographie

1. Boso, S. *et al., 2008. Vitis.*
2. Thuerig, B. *et al.*, 2011. *Eur. J. Plant Pathol.*
3. de Bem, B.P. *et al.*, 2015. *Sci. Hortic.*
4. Chitarra, W., et al, 2017. Front. Plant Sci.
5. Boso, S. *et al., 2004. Plant Disease*
6. Heyman, L. *et al.*, 2021. *Plants.*
7. Li, X. *et al.*, 2016. *J. Phytopathol.*
8. Fernandes de Oliveira, A. *et al.*, 2021. *Hortic.*
9. Rossi, V. *et al.*, 2012. *Phytopathology.*
10. Caffi, T. *et al.*, 2013. *Phytopathology.*

Financement
Ce projet s'inscrit dans VITAE, lauréat à l'appel à projet du Programme Prioritaire de Recherche « Cultiver et protéger autrement » financé par le gouvernement français.

Centre
Bordeaux Nouvelle-Aquitaine

paola.fournier@inrae.fr

Annexe n°2A

Towards microbiota-based disease management: analysis of grapevine microbiota in plots with contrasted levels of downy mildew infection

P. Fournier[1,2,3] and A. Jaswa[1,4], L. Pellan[1], J. Vallance[1], E. Chancerel[2], O. Bonnard[2], I. Masneuf-Pomarede[4], G. Martins[4], M. Raynal[5], C. Debord[5], S. Labarthe[2], L. Deliere[1], F. Delmotte[1], P. This[3], C. Vacher[2]

[1]INRAE, Bordeaux Sciences Agro, ISVV, SAVE, 33140 Villenave-d'Ornon, France. [2]INRAE, Univ Bordeaux, BioGeCo, 33610 Cestas, France. [3]INRAE, CIRAD, Univ Montpellier, Institut AGRO, AGAP institut, 34398 Montpellier, France. [4]Univ Bordeaux, UMR oenologie, INRAE, Bx INP, Bordeaux Sciences Agro, ISVV, 33882 Villenave d'Ornon, France. [5]IFV, 33290 Blanquefort, France.





Contact: paola.fournier@inrae.fr
aarti.jaswa@inrae.fr

1. Context and hypotheses

Vineyards are colonized by a myriad of microorganisms that interact with each other and with grapevine plants[1,2]. Some microorganisms are plant pathogens, such as the oomycete *Plasmopara viticola* that causes grapevine downy mildew. Others have a positive influence on vine health, such as plant growth promoting bacteria and disease biocontrol agents. These beneficial interactions have gained more attention in recent years because they could represent an alternative to the use of fungicides in viticulture[3].



Downy mildew
Plasmopara viticola
Oomycete

To develop microbiota-based disease management, we aim to cultivate the myriad of microorganisms that colonize grapevine leaves and then assemble multi-strain microbial consortia that could protect vines against *P. viticola*. To increase the probability of isolating microorganisms of interest, we developed a plant-based culture medium. We tested the hypothesis that it increases the cultivable microbial diversity in comparison to standard culture media.

2. Materials and methods

We combined metabarcoding (Fig.1(2.a)) and culture-dependent (Fig.1(2.b)) approaches to analyze the microbiota of soil and leaf samples collected in plots with contrasted levels of downy mildew infection.

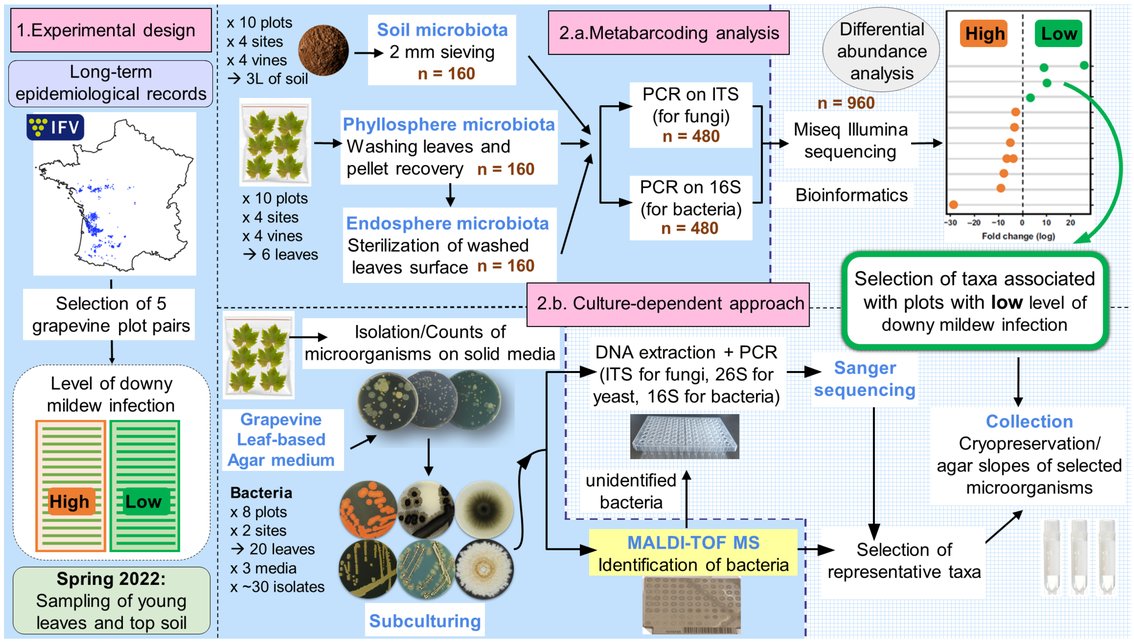


Fig.1: Workflow to characterize and isolate bacterial and fungal communities naturally colonizing vineyard soil and leaves in plots with contrasted levels of downy mildew infection. Media used for bacteria: Tryptic Soy Agar (TSA), Luria Bertani Broth Agar (LBA) and a Grapevine Leaf-based Agar medium (GLA).

Color legend
- The task has been completed
- The task is in progress
- The results of this task are presented here

Bibliography
1. Bettenfeld *et al.*, 2021. *J. Adv. Res.*
2. Fournier, Pellan *et al.*, 2022. *Adv. Ecol. Res.*
3. Busby *et al.*, 2017. *PLOS Biol.*

Funding
This work is part of the VITAE project ('Cultivating grapevine without pesticide') funded by the French National Research Agency (ANR, 20-PCPA-0010).

3. Results and discussion

MALDI-TOF MS
Identification of bacteria

- A total of 1262 bacterial isolates were analyzed by MALDI-TOF, of which 60% could be identified at least to genus level (Fig.2).
- Strains isolated from GLA and LBA were less well assigned than those isolated from TSA (higher % of non-identification and lower % of assignment to the species level) (Fig.2).
- A total of 32 bacterial genera were identified on the three culture media. Eight genera were isolated on all three media (Fig.3).
- The genera *Gordonia* and *Rahnella* were isolated only on GLA (Fig.3).

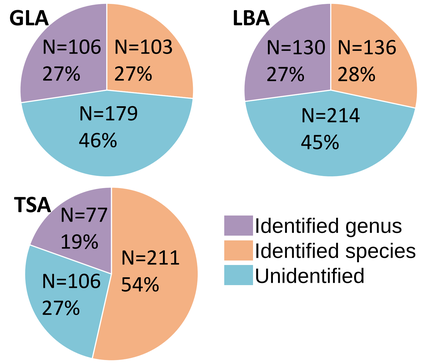


Fig.2: Number of bacterial strains isolated on each culture media and percentage of taxonomic assignments by MALDI-TOF MS.

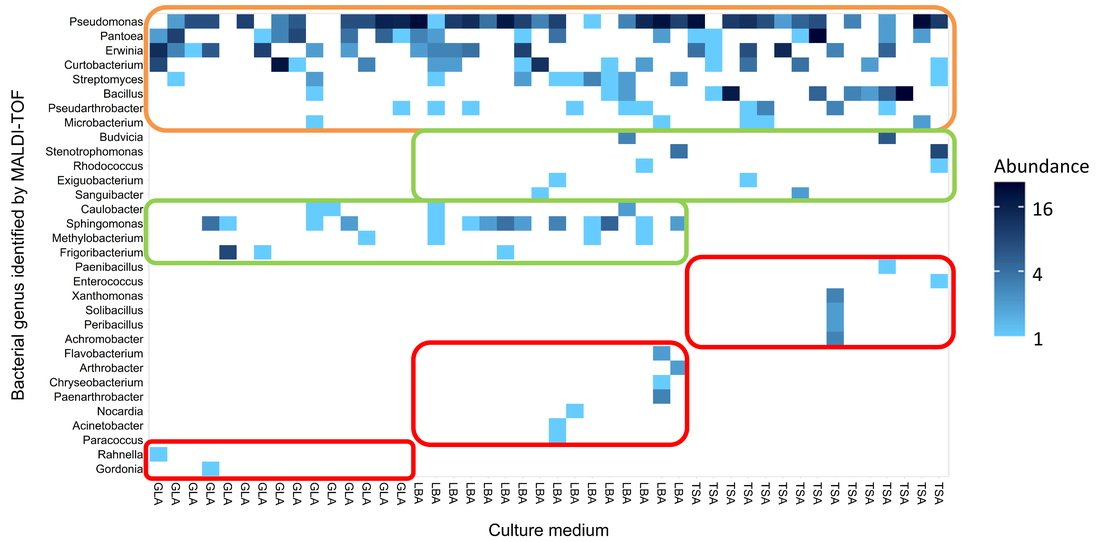


Fig.3: Bacterial genera identified using MALDI-TOF MS in grapevine leaf samples, depending on the culture media (GLA, LBA and TSA). Abundance is the number of bacterial isolates belonging to each genus. Bacterial genera identified in only one, two or three culture media are circled in red, green and orange, respectively.

4. Conclusion and perspectives

We were able to cultivate and isolate >1000 bacterial strains from grapevine leaves. Diversifying the culture media allowed us to isolate more strains. After completing the Sanger sequencing of all microbial isolates (including yeasts and filamentous fungi; Fig. 1 (2.b)), we will analyze the complementarities between the grapevine leaf-based culture medium and standard culture media. We will test the hypothesis that the vine-based medium selects for microbial taxa that are different from those selected on standard media and/or poorly referenced in the current version of the MALDI-TOF MS database. Statistical analysis of metabarcoding data (Fig. 1 (2.a)) will provide an estimate of the % of cultivable taxa and will allow us to identify microbial taxa that are significantly more abundant in vineyard plots with low levels of downy mildew infection. Those microorganisms will be retrieved from our microbial collection. Their effect on *P. viticola* will be tested in vitro and in planta, as single strains and as consortia. Modes of action will be elucidated for the most promising microbial consortia (those that thrive on grapevine leaves, are resilient to disturbances and have a biocontrol activity against *P. viticola*).

Annexe n°2B

TOWARDS MICROBIOTA-BASED DISEASE MANAGEMENT: ANALYSIS OF GRAPEVINE MICROBIOTA IN PLOTS WITH CONTRASTED LEVELS OF DOWNY MILDEW INFECTION

Authors: Paola FOURNIER[1,2,3,†] and Aarti JASWA[1,4,†], Lucile PELLAN[1], Jessica VALLANCE[1], Emilie CHANCEREL[2], Olivier BONNARD[2], Isabelle MASNEUF-POMAREDE[4], Guilherme MARTINS[4], Marc RAYNAL[5], Christian DEBORD[5], Simon LABARTHE[2], Laurent DELIERE[1], François DELMOTTE[1], Patrice THIS[3], Corinne VACHER[2*]

[1]*INRAE, Bordeaux Sciences Agro, ISVV, SAVE, 33140 Villenave-d'Ornon, France*
[2]*INRAE, Univ Bordeaux, BioGeCo, 33610 Cestas, France*
[3]*INRAE, CIRAD, Univ Montpellier, Institut AGRO, AGAP institut, 34398 Montpellier, France*
[4]*Univ Bordeaux, UMR oenologie, INRAE, Bx INP, Bordeaux Sciences Agro, ISVV, 33882 Villenave d'Ornon, France*
[5]*IFV, 33290 Blanquefort, France*

† Co-first authors
*Corresponding author: corinne.vacher@inrae.fr

Abstract:

Context and purpose of the study

Vineyards harbor a myriad of microorganisms that interact with each other and with the grapevines. Some microorganisms are plant pathogens, such as the oomycete *Plasmopara viticola* that causes grapevine downy mildew. Others, such as plant growth promoting bacteria and disease biocontrol agents, have a positive influence on vine health. The present study aims to (1) investigate whether vine-based culture media increase the cultivability of the grapevine microbiota, in comparison to standard culture media and (2) identify and isolate bacterial taxa naturally present in grapevine leaves and significantly more abundant in plots showing low susceptibility to downy mildew.

Material and methods

Seven pairs of vineyard plots differing significantly in downy mildew symptoms frequency and intensity were selected based on a long-term epidemiological survey conducted in France by the *Institut Français de la Vigne et du Vin* (IFV). In each plot, we sampled young leaves before the first fungicide treatments. Leaves were shredded and washed in a buffer to isolate and cultivate foliar bacteria, yeasts and filamentous fungi. We assessed the abundance (CFU/ml) of cultivable bacterial and fungal cells for several culture media, including a vine-based culture medium. Bacterial isolates were identified using MALDI-TOF MS.

Results

Yeasts, filamentous fungi, and bacteria were significantly less abundant on the vine-based culture medium than on the other media. Out of 965 total bacterial isolates analyzed, 597 were identified at least to the genus level by MALDI-TOF MS, and of these, 23% to the species level. Two bacterial genera, *Gordonia* and *Rahnella,* were isolated exclusively on the vine-based culture medium. On the other hand, 10 genera, *Rahnella*, *Paracoccus*, *Acinetobacter*, *Nocardia*, *Achromobacter*, *Peribacillus*, *Solibacillu*, *Xanthomona*, *Budvicia* and *Paenibacillus* were isolated exclusively from samples collected from plots with low infection levels.

Keywords: Grapevine, downy mildew, microbial biodiversity, culturomics, phyllosphere, biocontrol

1. Introduction

The oomycete *Plasmopara viticola* (Berk. & M.A. Curtis) Berl. & De Toni is a biotrophic and obligate parasite causing downy mildew, a major disease of cultivated grapevines reported in most wine-growing regions of the world (Bois et al., 2017; Fontaine et al., 2021; Koledenkova et al., 2022). *P. viticola* is a polycyclic pathogen that causes both primary and secondary infection cycles through the release of sexual and asexual spores, respectively (Gessler et al., 2011). The sexual spores differentiate in the fall on infected tissues and overwinter as oospores in soil (Rossi et al., 2009). The epidemic stage consists of a succession of asexual generations on green and young tissues during grapevine vegetative period. Due to the high susceptibility of *Vitis vinifera* L. to *P. viticola*, chemical fungicides are, to date, the major means of disease control (Gessler et al., 2011; Koledenkova et al., 2022). Research on alternative means of control, including microbiota management, represents a priority because of the proven negative consequences of fungicides on environmental and human health (Busby et al., 2017; Jacquet et al., 2022).

In the present study, we attempted to cultivate the myriad of microorganisms that colonize grapevine leaves (Bettenfeld et al., 2021; Fournier et al., 2022) to assemble microbial consortia that could protect vines against the asexual stage of *P. viticola*. To increase the probability of isolating microorganisms of interest for future biocontrol solutions, we developed a new plant-based culture medium and investigated whether it increases the cultivable microbial diversity in comparison to standard culture media.

2. Material and methods

Selection of study sites based on epidemiological records

Vineyard plots were selected based on the epidemiological data provided by the *Institut Français de la Vigne et du Vin* (IFV). The IFV performs weekly visual assessments of the intensity of downy mildew symptoms on leaves, the frequency of symptoms on leaves, the intensity of symptoms on bunches and the frequency of symptoms on bunches. The symptoms are visually assessed on vine rows that do not receive any fungicide treatment. These Untreated Controls (UC) are located within cultivated plots. Since 2002, the IFV has monitored 1200 UC, representing 4 major wine-producing regions in France. Based on these epidemiological records, we identified pairs of plots that differed in the frequency and intensity of downy mildew attacks (Fig. 1), while being geographically close (< 10 km), planted with the same grape variety and managed with the same farming practices. We considered that plots were contrasted in terms of downy mildew attacks if the area under the disease progression curve (AUDPC) of one of the two plots was higher for the 4 variables, for at least 80% of the years of common monitoring. We only kept plot pairs that had been monitored jointly for at least 4 years, including 2020 and/or 2021.

Sampling design

The sampling campaign occurred from April 18 to May 2 2022, corresponding to the phenological stage of 2-3 spread leaves. In each plot, we sampled leaves in 2 areas: the untreated controls used by IFV to monitor disease in 2021 (UC1) and the center of the plot (CEN). In each area, leaves were collected from four adjacent vines representative of the age and general condition of the plot. About 20 leaves were collected in the UC1 and CEN areas for analysis of the cultivable diversity (Fig. 1).

Isolation of cultivable microorganisms from leaf samples

Isolation and enumeration – On the day of sampling, leaves were shredded and then washed in a sterile buffer composed of 9g/L NaCl and 100µL/L Tween 20 in deionised water to recover and cultivate epiphytic and endophytic microorganisms indiscriminately. Three types of media were used for bacteria: Tryptic Soy Agar (TSA), Luria Bertani Broth diluted 1:10 and supplemented with 20g/L agar (LBA), and a solid medium consisting of 50mL/L grapevine (Cabernet-Sauvignon) leaf extract and 20g/L agar (GLA). All three media had their pH adjusted to 7 and were supplemented with 150mg/L biphenyl and 100mg/L pimaricin. Two types of solid media were used for yeasts and filamentous fungi: malt extract agar (MEA) and the GLA medium described above supplemented with 100mg/L chloramphenicol. Cell suspensions were serially diluted and plated in triplicate on

the solid media. Bacterial plates were incubated at 30°C for 2-5 days while fungal and yeast plates were incubated at 25°C for 5-12 days. We assessed the abundance of cultivable microorganisms (CFU/ml) at the end of the incubation period.

Taxonomic identification - For each sample, a single plate containing between 30 and 300 colonies was selected among the replicates of dilution and approximately 30 colonies were subcultured for identification and collection. The bacteria were identified by MALDI-TOF MS (Fig. 1).

Statistics

We used linear mixed-effects models to explain variation in CFU/ml for bacteria and fungi. The models had culture media type as fixed effect, and plot pair and susceptibility to downy mildew as random effects.

3. Results and discussion

3.1. *Seven pairs of vineyard plots (with low vs high susceptibility to downy mildew) were selected according to epidemiological records*

Fourteen vineyard plots, forming 7 pairs contrasted in terms of frequency and intensity of downy mildew attacks on leaves and bunches, passed the criteria of selection. We managed to sample ten plots, forming 5 pairs, at the chosen phenological stage and before the first fungicide treatments. The experimental design was therefore composed of 5 pairs of plots.

3.2. *Vine-based medium isolated a lower abundance of bacteria, yeasts and filamentous fungi compared to standard culture media*

At the end of the incubation period, the abundance (CFU/mL) of cultivable yeast and filamentous fungi was significantly lower on GLA compared to MEA ($n = 118$; $p < 0.05$). Similarly, the abundance of cultivable bacteria was significantly lower on GLA compared to LBA and TSA ($n = 168$; $p < 0.05$). These results are likely a consequence of the GLA medium not being as nutrient rich as the other media.

3.3. *62% of bacterial isolates were identified at the genus or species level using MALDI-TOF MS*

A total of 965 bacterial isolates were analyzed with MALDI-TOF MS. Of these, 597 (62%) were identified at the genus level, including 23% identified at the species level. Among the 30 bacterial genera identified across the three culture media, 22 were found on LBA, 18 on TSA and 13 on GLA. Eight genera - *Bacillus, Curtobacterium, Erwinia, Microbacterium, Pantoea, Pseudarthrobacter, Pseudomonas,* and *Streptomyces* - were found on all three media (Fig. 2), with *Pseudomonas* being most abundant on LBA and GLA, and *Bacillus* on TSA.

3.4. *Plot susceptibility to downy mildew may influence community composition of cultivable bacteria*

Of the bacterial genera identified at the genus level, 10 were exclusively isolated from samples collected from plots with lower infection levels. These genera were *Rahnella, Paracoccus, Acinetobacter, Nocardia, Achromobacter, Peribacillus, Solibacillu, Xanthomona* and *Budvicia*.

4. Perspectives

We will use metabarcoding approaches to analyze bacterial and fungal communities in leaves and soil in the same plots (Fig. 1). Statistical analysis of metabarcoding data will allow us to identify microbial taxa that are significantly more abundant in the vineyard plots that have a low susceptibility to downy mildew. Those microorganisms will be retrieved from our microbial collection (Fig. 1), or from international microbial repositories if they are not present in our collection. Their effect on *P. viticola* will be tested *in vitro* and *in planta*, as single strains and as consortia. Modes of action will be elucidated for the most promising consortia. Moreover, after completing the sequencing of the microbial isolates, we will analyze thoroughly the complementarities between the vine-based culture medium (GLA) and other culture media (Fig. 2). We will test

the hypothesis that the vine-based medium selects for microbial assemblages that are different from those selected on standard media and/or poorly referenced in the current version of the MALDI-TOF MS database. These analyses will allow us to provide recommendations for future studies requiring culturomics of grapevine microbiota.

5. Acknowledgments

This study was supported by the French National Research Agency (ANR) under the grants 20-PCPA-0010 (PPR VITAE) and ANR-17-CE32-0011 (NGB). AJ and LP received funding *Bordeaux Sciences Agro* and *Fondation Bordeaux Université*, respectively.

6. Literature cited

Bettenfeld, P., Cadena i Canals, J., Jacquens, L., Fernandez, O., Fontaine, F., van Schaik, E., Courty, P.-E., Trouvelot, S., 2021. The microbiota of the grapevine holobiont: A key component of plant health. J. Adv. Res. 40, 1-15.

Bois, B., Zito, S., Calonnec, A., 2017. Climate vs grapevine pests and diseases worldwide: the first results of a global survey. OENO One 51, 133–139.

Busby, P.E., Soman, C., Wagner, M.R., Friesen, M.L., Kremer, J., Bennett, A., Morsy, M., Eisen, J.A., Leach, J.E., Dangl, J.L., 2017. Research priorities for harnessing plant microbiomes in sustainable agriculture. PLOS Biol. 15, e2001793.

Fontaine, M.C., Labbé, F., Dussert, Y., Delière, L., Richart-Cervera, S., Giraud, T., Delmotte, F., 2021. Europe as a bridgehead in the worldwide invasion history of grapevine downy mildew, *Plasmopara viticola*. Curr. Biol. 31, 2155-2166.e4.

Fournier, P., Pellan, L., Barroso-Bergadà, D., Bohan, D., Candresse, T., Delmotte, F., Dufour, M.-C., Lauvergeat, V., Marrec, C.L., Marais, A., Martins, G., Masneuf-Pomarède, I., Rey, P., Sherman, D.J., This, P., Frioux, C., Labarthe, S., Vacher, C., 2022. The functional microbiome of grapevine throughout plant evolutionary history and lifetime. Adv. Ecol. Res. 67, 27.

Gessler, C., Pertot, I., Perazzolli, M., 2011. *Plasmopara viticola*: a review of knowledge on downy mildew of grapevine and effective disease management. Phytopathol. Mediterr. 50, 3–44.

Jacquet, F., Jeuffroy, M.-H., Jouan, J., Le Cadre, E., Litrico, I., Malausa, T., Reboud, X., Huyghe, C., 2022. Pesticide-free agriculture as a new paradigm for research. Agron. Sustain. Dev. 42, 8.

Koledenkova, K., Esmaeel, Q., Jacquard, C., Nowak, J., Clément, C., Ait Barka, E., 2022. *Plasmopara viticola* the Causal Agent of Downy Mildew of Grapevine: From Its Taxonomy to Disease Management. Front. Microbiol. 13, 889472.

Maddalena, G., Russo, G., Toffolatti, S.L., 2021. The Study of the Germination Dynamics of *Plasmopara viticola* Oospores Highlights the Presence of Phenotypic Synchrony With the Host. Front. Microbiol. 12.

Rossi, V., Giosuè, S., Caffi, T., 2009. Modelling the Dynamics of Infections Caused by Sexual and Asexual Spores During *Plasmopara Viticola* Epidemics. J. Plant Pathol. 91, 615–627.

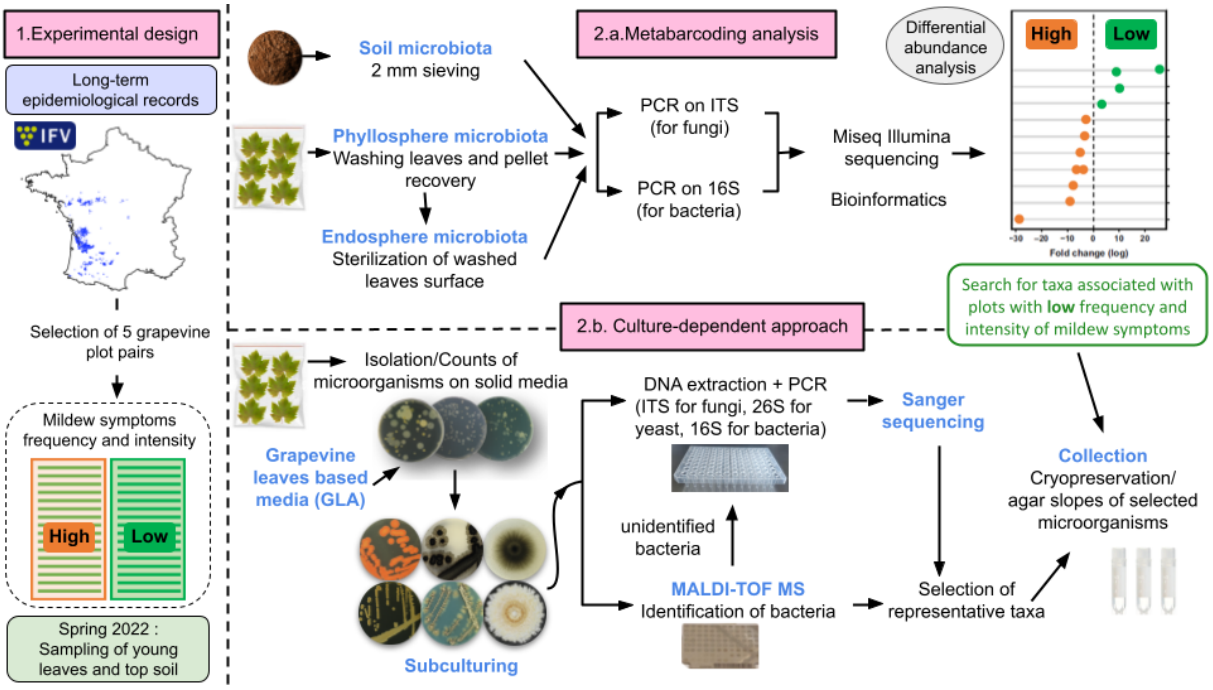


Figure 1: General workflow used in the present study to characterize and isolate bacterial and fungal communities naturally colonizing vineyard soil and leaves in plots with low vs high susceptibility to downy mildew. Results presented here belong to work packages 1 and 2.b.

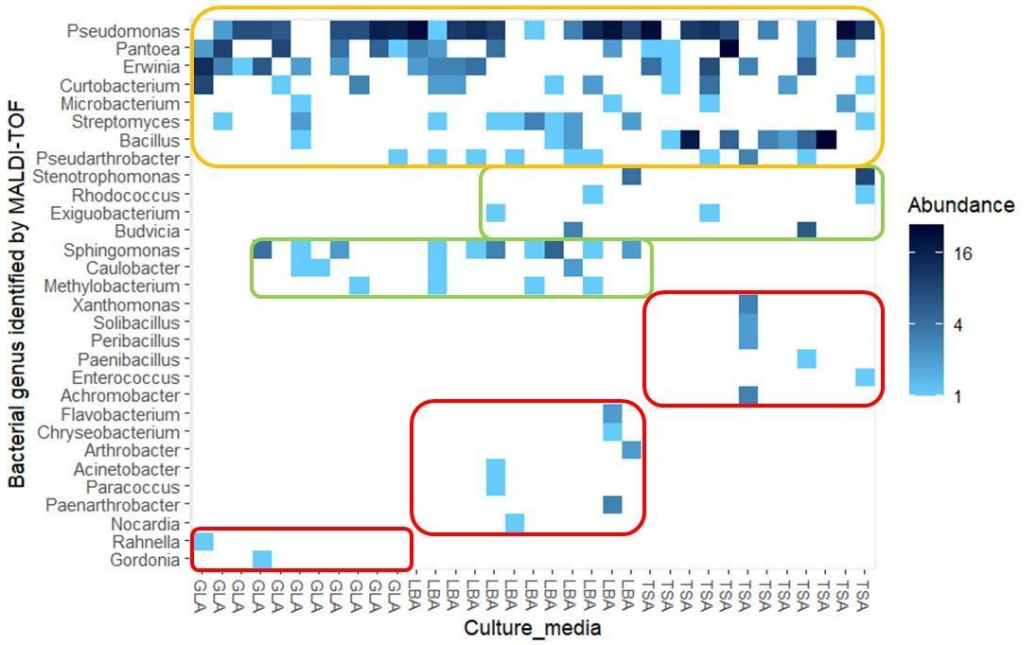


Figure 2: Bacterial genera identified using MALDI-TOF MS in grapevine leaf samples, depending on the culture media (GLA, LB and TSA). Abundance is the number of bacterial isolates belonging to each genera. Bacterial genera identified in only one, two or three culture media are circled in red, green and orange, respectively.

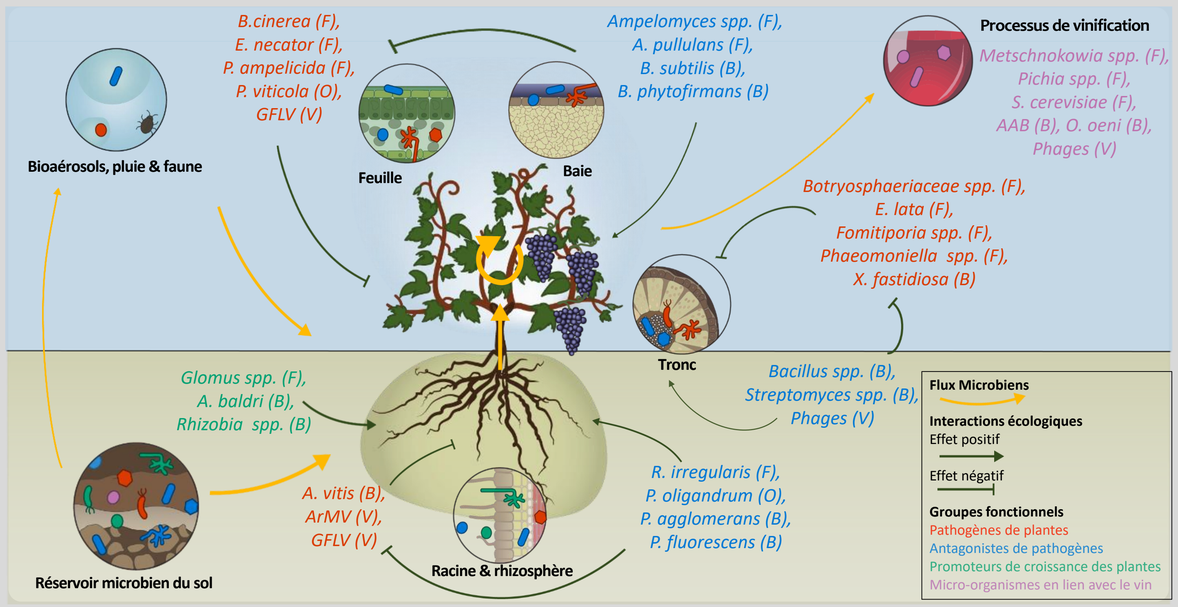
Annexe n°3

Recherche de Bioindicateurs Microbiens de la Résilience de la Vigne en Champagne

L. Pellan[(1)], L. Mercier[(3)], P. Fournier[(1)], E. Chancerel[(2)], J. Vallance[(1)], F. Delmotte[(1)], C. Vacher[(1)]

Contact: lucile.pellan@inrae.fr

(1) INRAE, Bordeaux Sciences Agro, ISVV, SAVE, Villenave-d'Ornon, France
(2) INRAE, Univ Bordeaux, BioGeCo, 33610 Cestas, France
(3) Centre de Recherche Robert-Jean de Vogüé, Moët-Henessy, Oiry, France



La vigne est colonisée par des communautés microbiennes diversifiées. Ces micro-organismes contribuent à la santé de la plante et répondent rapidement aux changements environnementaux (changement climatiques, transition agroécologique, etc.) du fait des temps de génération courts des micro-organismes. En outre, certains micro-organismes sont connus pour contribuer à la santé du sol et de la plante, de manière positive (protection contre les pathogènes, résistance aux stress abiotiques, amélioration de la nutrition) ou négative (déclenchement de maladies) (Fournier & Pellan et al. 2022). Les microbiotes du sol et de la plante pourraient donc constituer de bons bioindicateurs de l'état de santé général de l'écosystème viticole (Djemiel et al. 2022).

L'objectif de l'étude est de définir des bioindicateurs microbiens de la santé de l'écosystème viticole, définie ici à l'échelle de la parcelle comme la stabilité (résilience) des rendements au cours du temps. A partir de l'analyse des communautés fongiques et bactériennes de parcelles à forte versus faible résilience, nous souhaitons répondre aux questions suivantes:

(i) Quelles espèces ou consortia de micro-organismes sont positivement associés à la résilience de l'écosystème viticole ?

(ii) Quels compartiments (sol, racines, feuilles) abritent ces micro-organismes ?

(iii) La résilience de l'écosystème viticole est-elle spécifiquement corrélée à la présence des champignons mycorhiziens à arbuscules ?

(iv) Peut-on prédire la résilience d'une parcelle de vigne à partir des mesures de son microbiote ?

Ces bioindicateurs permettront de diagnostiquer la santé de parcelles viticoles et d'identifier les pratiques culturales qui favorisent les micro-organismes clés.

1. Sélection de parcelles à faible vs forte résilience

Base de données parcelles en production en Champagne

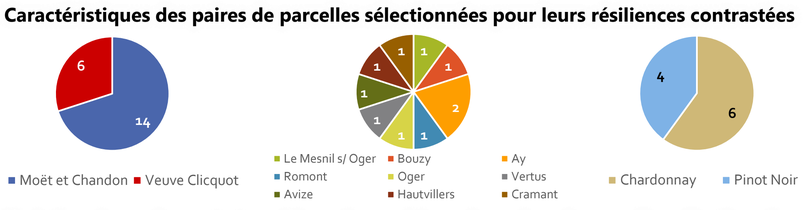
Caractéristiques de la vigne et de sa gestion, position géographique et topographie des parcelles et historique de production 2009-2019.

↓

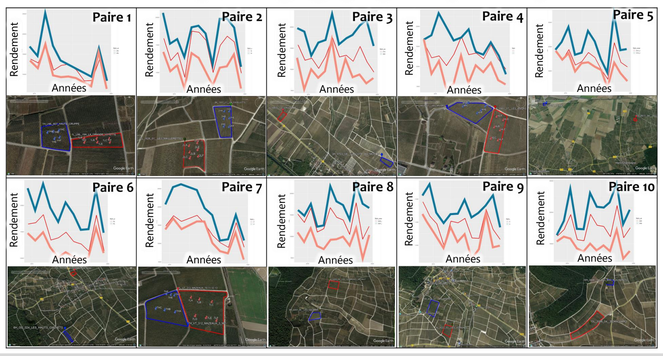
Sélection des parcelles à faible vs forte résilience

Création de groupe géographique homogène (Parcelles avec même Maison, Cépage et méthode de taille associée, Porte – Greffe, Age de la plantation) puis sélection dans ces groupes de paires de parcelles associant une parcelle avec un rendement inferieur et une avec un rendement supérieur à la moyenne du groupe pour 80% des années et la plus courte distance géographique possible (max 5 km).

Caractéristiques des paires de parcelles sélectionnées pour leurs résiliences contrastées

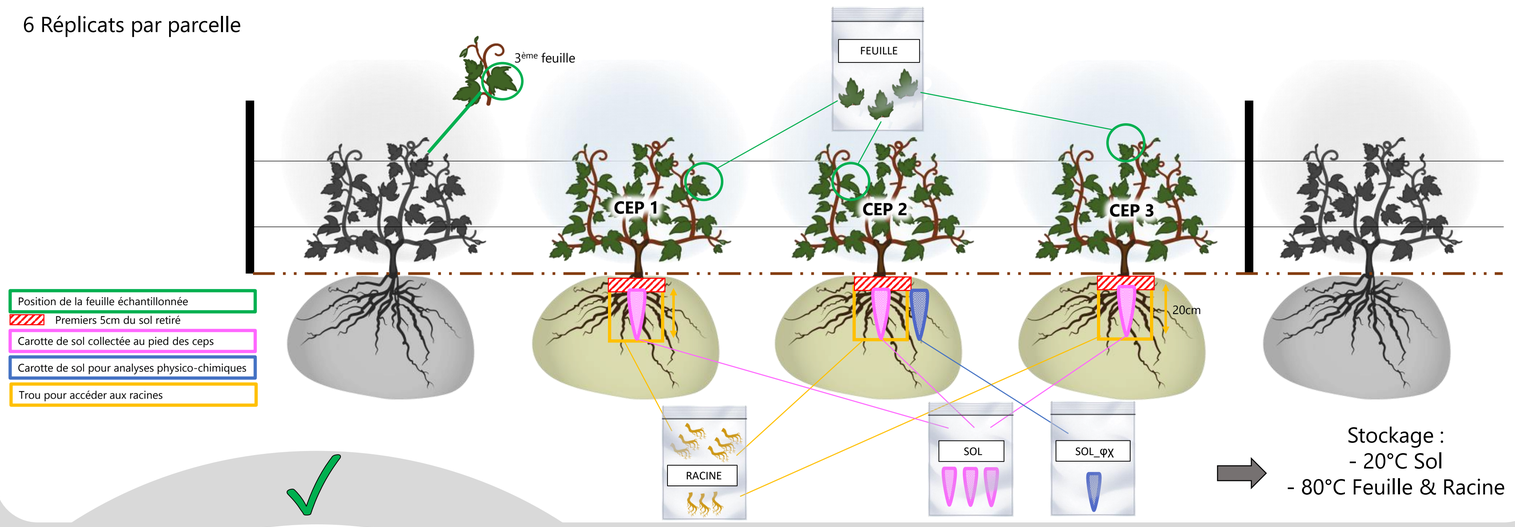


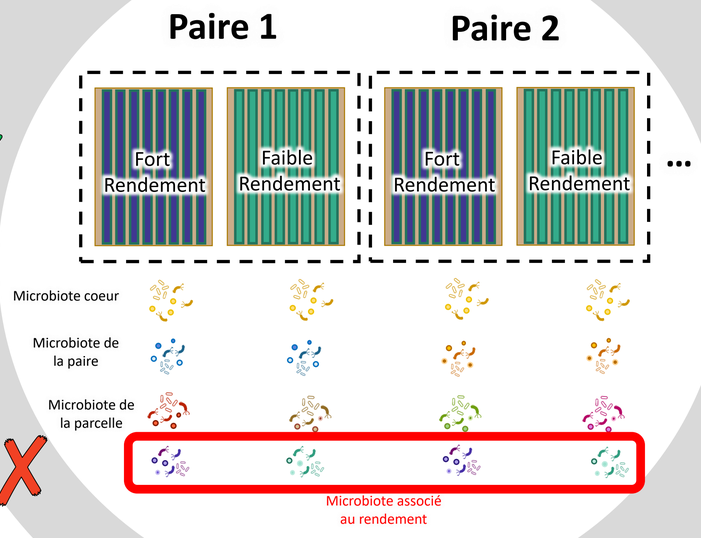
Variation de rendement et position géographique des paires de parcelles sélectionnées



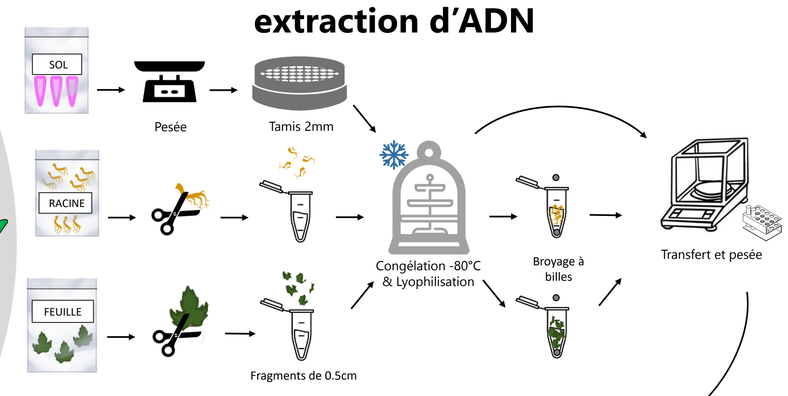
2. Echantillonnage des différents compartiments microbiens

6 Réplicats par parcelle





3. Préparation des échantillons et extraction d'ADN



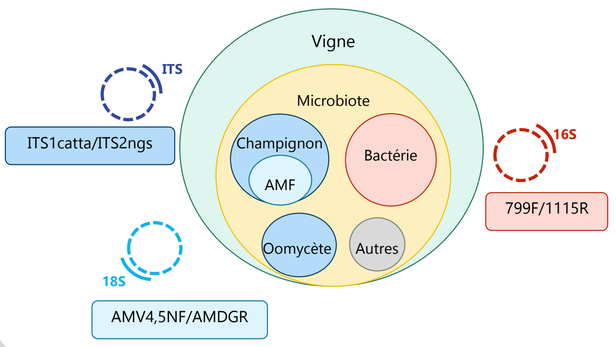
Méthodes d'extraction d'ADN optimisées

- Sols : Power Soil Pro kit
- Racines : Protocole CTAB
- Feuilles : Plant Dneasy Pro kit

4. Caractérisation des microbiotes par métabarcoding

Amplification → Séquençage → Prétraitement des données

Amorces sélectionnés encadrés





MiSeq Illumina
1 Run / marqueur

Pipe-line FROGS pour décontamination et clusterisation des données, puis assignation taxonomique afin d'obtenir les communautés microbienne associées à chaque échantillon (Table d'abondance relative des ASVs)

	Sample 1	Sample 2	Sample 3
ASV/Microorganism 1	2000	0	0
ASV/Microorganism 2	50	0	400
ASV/Microorganism 3	300	200	0
ASV/Microorganism 4	0	4000	3000
...			

5. Analyses de diversité et recherche de bioindicateurs microbiens

Trois approches complémentaires

- Comparaison de diversité : Caractéristiques de chaque communauté
- Analyse d'abondance différentielle : µorganismes bioindicateurs
- Algorithmes d'apprentissage supervisé : Prédiction



Avancement du projet et perspectives

A l'heure actuelle, les 10 paires des parcelles aux rendements contrastés ont été sélectionnées dans les bases de données d'historique de rendement puis des échantillons de sols, racines et feuilles ont été collectés dans six zones de chaque parcelles. Les échantillons ont été préparés et l'ADN environnemental, associé à chaque échantillon dans les différents compartiments de la vigne, a été extrait à l'aide de méthodes d'extraction d'ADN optimisées. Ces extraits ont fait l'objet d'amplification des marqueurs génétiques permettant l'identification des bactéries (16S), des champignons et oomycètes (ITS) et de champignons arbusculaires mychorhiziens (AMF – 18S). Le séquençage est en cours afin d'obtenir les communautés microbiennes associées à chaque échantillon. A court terme, trois approches complémentaires seront utilisées pour analyser la diversité et la richesse des communautés, identifier les micro-organismes ou groupe de micro-organismes bioindicateurs caractéristiques des parcelles viticoles à forte résilience du rendement, mais aussi prédire le potentiel agronomique de parcelles à l'aide d'algorithmes d'apprentissage supervisé. A plus long terme, ces bio-indicateurs microbiens permettront de développer programmes de bio-surveillance des écosystèmes viticoles et d'orienter les pratiques culturales, mais pourrait être aussi de bons candidats pour des approches de biocontrôle ou de biofertilisation.

Références

Fournier, P., Pellan, L., Barroso-Bergadà, D., Bohan, D. A., Candresse, T., Delmotte, F., ... & Vacher, C. (2022). The functional microbiome of grapevine throughout plant evolutionary history and lifetime. In Advances in Ecological Research (Vol. 67, pp. 27-99). Academic Press.

Djemiel, C., Dequiedt, S., Karimi, B., Cottin, A., Horrigue, W., Bailly, A., ... & Terrat, S. (2022). Potential of meta-omics to provide modern microbial indicators for monitoring soil quality and securing food production. *Frontiers in Microbiology, 13*, 889788.

La microbiologie du sol au service d'une agriculture durable : diagnostics et solutions innovantes

27 & 28 Juin 2023

Annexe n°4

Arbuscular mycorrhizal fungi as biomarkers of vineyard yield in Champagne.

Lucile Pellan[1], Paola Fournier[1], Marc Brevot[2], Emilie Chancerel[3], Erwan Guichoux[3], François Delmotte[1], Laurence Mercier[2] and Corinne Vacher[1].

[1] INRAE, Bordeaux Sciences Agro, ISVV, SAVE, Villenave-d'Ornon, France
[2] Centre de Recherche Robert-Jean de Vogüé, Moët-Henessy, Oiry, France
[3] INRAE, Univ Bordeaux, BioGeCo, 33610 Cestas, France

Abstract. Grapevines are colonized by a multitude of microorganisms (fungi, bacteria, oomycetes), mainly through roots in contact with the soil microbial reservoir. Some microorganisms cause disease and others have positive or negative effects on the plant (protection against pathogens, resistance to abiotic stress, improved nutrition). In addition to their functional roles, microorganisms respond rapidly to environmental changes (climate, cultivation practices), which could make them candidate biomarkers of the performance of the viticultural ecosystem. The aim of this study is (i) to test whether a positive relationship exists between microbial diversity and vineyard yield, (ii) to identify potential microorganisms that are biomarkers of overtime high and stable yields over time, and (iii) to test whether arbuscular mycorrhizal fungi (AMF) are over-represented among these biomarkers. Vine plots with long-term contrasted yields were selected in Champagne based on multi-year records of yield. We sampled the vine roots and characterized the microbiota using metabarcoding approaches targeting bacterial and fungal communities. Our analyses revealed no relationship between microbial taxonomic diversity and grape yield. Using differential abundance analyses and supervised machine learning algorithms, we identified microbial biomarkers of high versus low yield in the root compartment. We identified 58 fungal and oomycete biomarkers, among which there were several AMFs. These AMFs were all biomarkers of high-yielding plots, suggesting a direct role in vine growth and productivity. These microbial biomarkers of stable and high yields will enable the development of diagnostic programs for the functioning of viticultural ecosystems.

1 Introduction

Cropping systems worldwide are increasingly exposed to various disturbances from local to global scales, that can negatively affect yields, particularly within the current context of global climate change [1]. Grape production, in particular, faces challenges related to the development of resistant varieties within protected designations of origin (PDOs) [2]. It relies heavily on pesticides to control pathogens [3], [4], despite the growing political and societal demand to reduce the use of chemical pesticide and fertilizers because their detrimental effects on human health and the environment [5]. These combined challenges have led to issues such as lower yields, uprooting of plants (dieback) [6], [7], and reshaping landscape of viticulture. The year 2022 marks a new threshold, with the lowest global production since 1961 according to an analysis based on twenty-nine countries accounting for 94% of global production in 2022 [8]. This situation highlights the need for innovative strategies to sustain and revitalize viticultural landscapes.

The study of vineyard microbiota is an emerging field with the potential to improve vine adaptation to climate change and prevent pathogenic infections [9]. In particular, harnessing the functional microbiota could contribute to this transition. Plants and their associated microorganisms form a holobiont - a co-evolved community that includes bacterial, archaeal, and various eukaryotic species such as fungi. The health of the holobiont relies on beneficial interactions between the host and its microbiota, while microbial dysbioses are often associated with disease [10]. Plants are colonized by a multitude of microorganisms mainly through roots. The enrichment of bacterial and fungal endophytic and rhizospheric microorganisms through plant roots is not a random process, but rather a targeted one. Current models suggest that soil microorganisms serve as a reservoir [11], with microbes being attracted to roots by nutrients such as carbohydrates and amino acids, in addition to specific plant secondary metabolites [12], [13]. Furthermore, plant defense-signaling also influences this selective recruitment process.

The grapevine microbiota are implicated in a variety of functional roles in viticultural agrosystems [14]. Some have a negative effect on the plant, such as the pathogens *Plasmopara viticola* and *Erysiphe necator*, which are responsible for two major diseases, downy and powdery mildew respectively. These pathogens cause significant yield losses depending on the severity of the attacks [15], [16], [17]. Conversely, other microorganisms have beneficial effects on the plant [18], particularly microorganisms antagonistic to pathogens, such as *Bacillus subtilis* or *Pythium oligandrum*. These microorganisms act either directly—through mechanisms

like antibiosis, parasitism, or niche competition—or indirectly by inducing resistance, thereby limiting the development of bio-aggressors and enhancing the plant's resistance to biotic stress factors [19], [20], [21]. Plant growth promoter also colonize grapevines and are primarly localized in the roots, such as arbuscular mycorrhizal fungi (AMF, ex: *Rhizophagus irregularis*). These symbiotic organisms improve the grapevine hydric and mineral nutrition, resistance against abiotic stresses, and promote general plant fitness [22], [23]. Overall, the beneficial properties of these various microorganisms may even overlap and consequently contribute to increasing crop yield [24], [25], [26], [27].

The ability of complex microbial communities to resist pathogen invasion and enhance plant growth and productivity is closely linked to their diversity [28], [29]. A loss of key microbial species within these communities can engender disease outbreaks or result in sub-optimal plant yields [30]. Microbial communities with higher phylogenetic and taxonomic diversity not only produce a broader range of molecules that promote plant growth and health (such as biocontrol substances, phytohormones, and soil structuring compounds), but also support beneficial ecological processes such as microbial redundancy, complementarity and synergy [31]. In addition to these functional roles, microbiota respond rapidly to environmental changes (climate, cultivation practices), making them promising candidate biomarkers for assessing the performance of viticultural agrosystems [32], [33].

The aim of this study is to (i) determine whether a positive relationship exists between microbial diversity and vineyard plot yield, (ii) identify microorganisms that are root biomarkers of long-time high and stable yields over time, and (iii) assess whether arbuscular mycorrhizal fungi (AMF) are over-represented among these biomarkers. To test these hypotheses, we sampled vine roots from 20 plots in the Epernay region (Champagne, France) in June 2022. These plots, selected based on yield data collected over the last ten years, comprised 10 pairs with contrasted yields. We specifically sampled the roots, which serve as the entry point for microorganisms colonizing the vine and the preferred habitat for growth stimulators. This approach allowed us to capture the microbiota potentially involved in vine physiology and yield development, particularly those present in the most productive plot of each pair.

2 Material and methods

2.1 Selection of study sites based on annual yield database

The vineyard plots were selected from a database maintained and provided by the *Centre de recherche Robert-Jean de Vogüé* (Moët-Hennessy, Oiry, FRANCE). This database contains records of approximately 2000 vineyard plots in the Grand Est region of France, including details of plot characteristics, vine characteristics, vineyard management practices and yield history from 2009 to 2020. Based on this yield survey, we identified pairs of vineyard plots with contrasted yields (defined by the ability of the plot to produce above-average yields consistently over monitored years). To ensure fair comparisons, the plots were grouped into homogeneous categories based on geographical area, grape variety, rootstock, age range (production state, between 20 and 40 years), management and pruning method. Within these homogeneous groups, plots were each considered as good or bad yielding if their annual yield was either higher (high yield plot) or lower (low yield plot) than the homogeneous group's average annual yield for at least 80% of the years monitored. If several plots met these criteria, the plot pair was formed by combining the high yield and low yield plots separated by the shortest geographical distance. This selection process resulted in the selection of 10 pairs of plots.

2.2 Sampling design and sample processing

All biological samples were harvested in a single campaign spread over 9 days (June 28 to July 6 2022), corresponding to phenological stage of grapevine BBCH 73-75 (beginning of grape bunch formation). In every selected plot, a grid consisting of 6 sampling points distributed over two rows in the center of the plot were identified. In each of these six areas, we collected root composite samples from three adjacent visually healthy vines which were representative of the plot's general condition. At the base of vine trunk, the top 5-10 cm of soil was removed and the undersoil was carefully excavated to a depth of 25 cm to expose the roots of the vines. About 5 growing root fragments were harvested with disinfected tools from each vine plant. Samples were maintained on ice until arrival at the laboratory and were stored at -80°C.

Roots samples were taken one by one from -80°C freezer, and crushed by hand into their sampling bag to fragment the tissues. In a microbiological safety cabinet, the samples were cut into 1cm pieces, following which they were transferred to sterile tubes and freeze-dried, before grinding with steel beads in TissueLyser II (QIAGEN) : 4 rounds of 2 min 30 sec at 25 Hz interspersed with a 30 sec pause.

2.3 DNA extraction and metabarcoding

DNA from root samples were extracted with a CTAB chloroform/isoamyl alcohol protocol (250 mg of grounded and freeze-dried sample input) [34]. Amplification, library preparation and sequencing were carried out at the Genome Transcriptome Platform of Bordeaux (https://pgtb.fr/). First PCRs were performed with 5 µl of template DNA, 2 µl of each primer concentrated to 3µM, 4 µl of HOT FIREPol® MultiPlex Mix 10mM MgCl2 concentrated to 5X, and ultrapure water to 20 µl. The primer pair: 799F (5'-AACMGGATTAGATACCCKG-3') / 1115r (5'-AGGGTTGCGCTCGTTG-3') [35] was specifically chosen for the amplification of bacterial sequences because it excludes chloroplast DNA. The PCR

conditions comprised an initial denaturation step at 95°C for 15 min, 30 cycles of denaturation at 95°C for 30 sec, annealing at 47°C for 30 sec, and elongation at 72°C for 30 min, followed by a final extension step at 72°C for 5 min. Oomycete and fungal sequences were amplified using the primer pair : ITS1catta (5′-ACCWGCGGARGGATCATTA-3′) / ITS2ngs (5′-TTYRCKRCGTTCTTCATCG-3′) specific for the ITS regions of fungi and oomycetes [36]. The PCR conditions comprised an initial denaturation step at 95°C for 15 min, 35 cycles of denaturation at 95°C for 30 sec, annealing at 48°C for 30 s, and elongation at 72°C for 30 min, followed by a final extension step at 72°C for 5 min. DNA amplicon size and purity were evaluated with 1% agarose gel electrophoresis. Amplicons were purified to eliminate primer and primer dimers and then submitted to a second PCR for the Illumina specific sequence adaptator ligation and index (Nextera-XT combinatorial index). Sequencing was performed on a NextSeq 2000 system (Illumina) using P1 reagents and 301:10:10:301 cycles.

2.4 Sequencing data processing

Sequencing data processing was carried out with FROGS pipeline v4.1.0 [37] on the Galaxy France server (https://metabarcoding.usegalaxy.fr/) with separate analyses for each barcode region (16S, ITS). Sequencing data processing included dereplication, sequences clustering, removing chimera and filtration step, which results in the clustering of sequences into ASV, Amplicon Sequence Variant. Taxonomic assignments of 16S and ITS short reads were conducted using SILVA 138.1 [38] and UNITE Fungi 8.3 [39] reference databases, respectively. The assignments were performed with both the RDPClassifier [40] and BLASTn+ algorithms [41]. Finally, we used the *metabaR* v1.0.0 R package to decontaminate the datasets [42].

2.4 Statistics

All statistical analyses were performed using R v4.2.3 (R Core Team, 2023). Microbial community analyses were conducted using the R *phyloseq* package v1.42.0 [43] and figures were generated using the *ggplot2* package v3.5.1 [44]. To investigate whether the diversity of soil, root microbial assemblages was higher in vineyard plots with a high yield (H1), the α-diversity of microbial population was assessed through Inverse Simpson Index for each sample. To investigate if the yield levels were associated with a higher abundance of specific taxa, as biomarker taxa of high and low yield, we used a set of three complementary methods. First, we performed a differential abundance analysis with the *Maaslin 2* package v1.12.0 [45]. Second, we conducted an indicator species analysis using the *IndicSpecies* package v1.7.14 [46]. Finally, a Random Forest (RF) analysis was performed to identify the most important predictor ASVs of vineyard yield as biomarkers ASVs. To this end, we used the *microranger* package [47], which incorporates RF classification functions derived from the *ranger* package [48], specifically designed for microbial community classification.

3 Results and Discussion

3.1 Ten pairs of vineyard plots (with low vs high yield) were selected according to the annual yield database

Following the plot selection process, a total of twenty plots forming ten pairs of plots with contrasted yields (each pair comprising one high-yield plot and one low-yield plot) were selected to establish the experimental design. This specific experimental set-up was developed to study the effect of plot yield while minimizing potential confounding factors (Fournier and Pellan et al. 2022). Plot yield levels were determined by a long-term study over several years (2009-2019), and we selected pairs of plots with contrasted yields that were otherwise as similar as possible. Samples were collected at the start of grape cluster formation to highlight the microbiota present and potentially involved in this yield-forming phase. For each pair, the annual yield of the high-yield plot was always higher than that of the low-yield plot. These pairs of plots covered 9 geographical areas of the Champagne region, spread over three production zones (Vallée de la Marne, Montagne de Reims and Côte des blancs): Avize, Aÿ, Bouzy, Cramant, Hautvillers, Le Mesnil sur Oger, Oger, Romont and Vertus, with 1 pair per zone, except in Aÿ where two pairs were selected. The ten pairs of plots were planted with the same rootstock (41B), they were all in full production stage (between 20 and 40 years since plantation) and their management style was similar (conventional viticulture, HVE/Sustainable Viticulture certification) alongside minimized intra-pair plot distance. Six pairs out of ten were planted with Chardonnay variety (Chablis pruning method), while the remaining four were planted with Pinot Noir variety (Cordon pruning method).

3.2 Microbial diversity is not higher in grapevine plots with high yield

After sequencing and processing data of samples collected from the pairs of plots with contrasted yields, the final fungal dataset comprised 9,331,270 reads grouped into 473 ASVs, while the final bacterial dataset comprised 25,598,44 reads grouped into 1,097 ASVs. For bacteria, 19 phyla were identified in the root tissues. The bacterial community was dominated by Actinobacteria (38.7%), Proteobacteria (35.4%), and Chloroflexi (10.5%) (Figure 1), a composition similar to that reported in other studies characterizing the bacterial communities in grapevine roots [49], [50], [51]. In terms of fungal diversity, 10 phyla were detected in the root habitat, with Ascomycota representing the predominant phylum (92.4%), followed by Basidiomycota with 4% of the identified sequences. This is also consistent with previous studies on the fungal microbiota of grapevine roots [49], [52]. Interestingly, Glomeromycota ranked third, accounting for 2.6% of the sequences, and included arbuscular mycorrhizal fungi, which play a crucial role in water and nutrient absorption

in grapevines [23]. We also detected the presence of oomycetes represented by the phylum Stramenopila and accounting for 0.35% of the relative abundance.

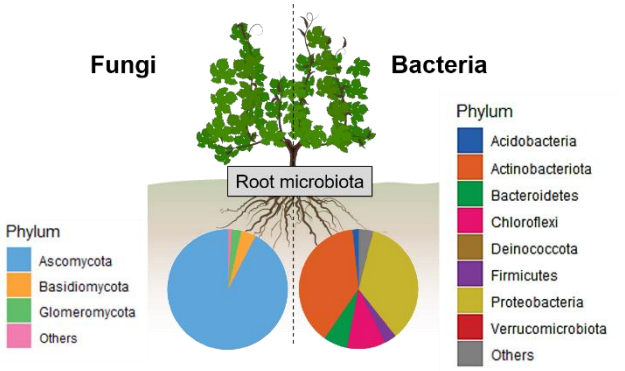


Figure 1. Microbial community profiles of grapevine roots. Each part of circular diagram represents the average proportion of sequences assigned to each phylum for all plots, based on the analysis of ITS and 16S metabarcoding for fungi and bacteria respectively. Figure displays only phyla that account for more than 1% of sequences; all other phyla are grouped in the "Others" category (Aphelidiomycota, Basidiobolomycota, Blastocladiomycota, Mucoromycota, Olpidiomycota, Rozellomycota for fungal phyla and Bdellovibrionota, Desulfobacterota, Entotheonellaeota, Gemmatimonadota, Halanaerobiaeota Methylomirabilota, Myxococcota, Nitrospirota, Patescibacteria, Planctomycetota, Spirochaetota for bacterial phyla).

In contrast with our hypothesis, we did not find any differences in diversity between the microbial assemblages associated with high-yield plots and those associated with low-yield plots for both bacterial and fungal communities (Figure 2). These findings suggest that strengthening specific key microbial taxa have a more significant impact on grapevine health and yield performance than the broader microbial diversity.

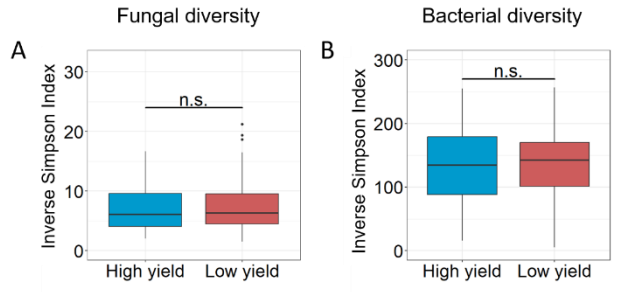


Figure 2. Diversity of microbial communities as a function of vineyard yield. Fungal (A) and bacterial (B) diversity index (Inverse Simpson Index) from high or low yield plot are presented. Pairwise Wilcoxon test was performed to identify statistical differences between diversity index from high or low yield plots (p-value > 0.05 : n.s.).

3.3 Some root fungal species are biomarkers of vineyard yield.

Our analyses identified 58 fungal ASVs that were significantly more abundant in plots with either low or high yields, as determined by at least one of three different analytical methods. The use of combined integrated approaches, which included differential abundance analysis, indicator species analysis, and machine learning methods, enabled a more precise identification of biomarkers from metabarcoding data [53].

In grapevine roots, some fungal ASVs were consistently more abundant in plots with high yield, including fungi belonging to the *Didymella* genus and the Glomeraceae family (Figure 3). Glomeraceae are a family of arbuscular mycorrhizal fungi that play a crucial role in water and nutrient absorption in grapevines [23]. Conversely, some ASVs were significantly more abundant in plots with low yield, such as the plant pathogenic oomycete *Pythium ultimum* and fungi from the *Laburnicola* genus and Helotiales order. *Pythium ultimum* is associated with damping-off and root rot diseases in hundreds of diverse plant hosts, including corn, soybean, wheat, potato, tomato, and perennial plants such as apple trees [54], [55], [56]. This pathogen has also been identified in the root microbiota of grapevines, particularly in studies focusing on vines in decline [57] or those affected by root rot [58], [59]. Its preferential presence in low-yield plots may lead to root system damage, reducing nutrient absorption capacity and partially explaining the decreased yield potential.

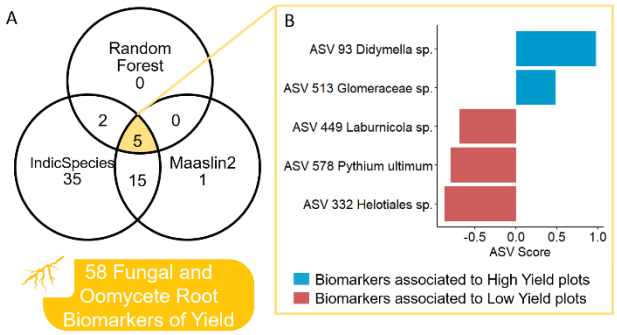


Figure 3. Root fungal and oomycete biomarkers of vineyard yield. **A.** Root fungal and oomycete ASV biomarkers were selected using three complementary methods: indicator species (Association coefficient with $p < 0.05$), differential abundance (Maaslin2 coefficient with $q < 0.1$) and random forest (Gini index with $p < 0.1$) analyses. This resulted in a final set of 58 ASVs. **B.** Root fungal and oomycete ASV biomarkers identified with the three different methods and associated ASV score.

3.4 Among fungal biomarkers of yield, arbuscular mycorrhizal fungi are associated with high yield.

Among the 58 fungal biomarkers associated with yield, 39 were associated to high yield and 19 to low yield (Figure 4). Within the high-yield biomarkers, arbuscular mycorrhizal fungi (Glomeraceae family) accounted for 8 of the 25 ASVs with an identified lifestyle (taxonomic affiliation sufficient to find a match in the FugalTraits database if the lifestyle of these fungi are known). By contrast, AMFs were not found among the fungal biomarkers of low-yield plots (Figure 4).

AMFs that were biomarkers of high yields primarily belonged to the genus *Glomus*, with two ASVs identified as *Rhizophagus irregularis*. The AMF group are the most prevalent mycorrhizae associated with grapevine roots,

with *Glomus* and *Rhizophagus* being among the most frequently recovered genera in grapevine root studies [60], [61]. These symbiotic fungi are actively recruited by grapevine roots during water and nutrient stress and are well-known for their plant growth-promoting capabilities [62]. Indeed, these fungi enhance soil exploration by proliferating extra-radicular hyphae, which play a crucial role in improving the uptake and transport of water from the bulk soil to the vine [63]. This mycelial network also provides phosphorus and nitrogen to plant root cells [64] and improves overall soil structure, reducing erosion [65]. In a study using non-targeted metabolomics and targeted transcriptomics, AMFs demonstrated their ability to reprogram primary metabolism, in line with the concept of nutrient exchanges between plants and mycorrhizal fungi. This includes a strong induction of Pathogenesis Related (PR) protein expression in roots and slight increased defense hormone levels in leaves [66]. Another study showed that pre-mycorrhizal inoculation of grapevines alters the expression of several *Plasmopara viticola* effectors, thus reducing downy mildew symptoms [67]. These findings suggest that, in addition to promoting vine growth and resistance to abiotic stress, AMFs may also confer enhanced resistance to grapevine pathogens and could play a significant role in the yield differences observed in the study plots.

Among the biomarkers associated with high yield, we also identified a higher number of saprotrophic fungi, particularly those from soil and litter environments. Saprotrophic fungi play a crucial role in ecosystem functions, including carbon and nitrogen cycling [68], [69], metal complexation, and the release of organic acids and solubilizing enzymes. These processes can alter soil minerals and make nutrients such as potassium, phosphate, magnesium, calcium, and iron bio-available to plants. Additionally, they contribute to soil particle rearrangement, which can improve water retention [70] and resistance to soil erosion [71]. The enhanced availability of water and nutrients may influence soil fertility and, consequently, the elaboration of yield. In a study by Ning et al. (2021) [72], the saprotrophic fungal communities were found to be strongly associated with a multifactorial soil fertility index, which is central to soil health and quality in agroecosystems.

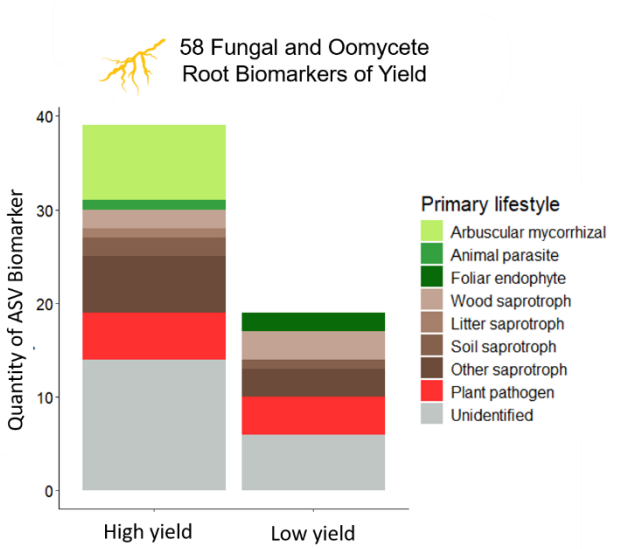


Figure 4. Primary lifestyle of all significant root fungi identified as biomarkers of high and low yield plots. The primary lifestyle of fungal biomarkers were inferred based on the FungalTraits database. Lifestyles associated with beneficial functions for the plant are in greens colors, lifestyles associated with indirect functions are in browns and lifestyles associated to nefast functions for the plant are in red.

4 Perspectives

After establishing a relationship between the presence of AMFs (among others) in the grapevine root compartment and improved long-term yield, we plan to sequence the extracted DNA using AMF-specific primers to better identify the AMF species associated with high yield. The choice of primer set is known to introduce taxonomic biases, particularly for Glomeromycota strains [49]. Therefore, we hypothesize that some species in this family may not have been detected due to primer limitations. To enhance taxonomic affiliation, we will re-sequence the root DNA using long-read technology to cover the entire 16S RNA sequence, which will enhance taxonomic resolution [73]. Additionally, we will conduct microbial community analyses of the soil compartment as a reservoir in the same plots, combined with soil physicochemical analyses, to determine the influence of soil type on microbiota distribution and better control of confounding factors [70], [74]. Finally, we will assess the predictive power of these microbial biomarkers using random forest algorithms [47], [53], [75]. Ultimately, we aim to develop a high-throughput detection tool for these biomarkers in vineyards using a microfluidic chip [76].

Funding: This work is funded by the Fondation Université Bordeaux and the French National Research Agency (ANR) under the grant 20-PCPA-0010 (VITAE project).

Références

1. E. A. Martin, B. Feit, F. Requier, H. Friberg, and M. Jonsson, Adv. Ecol. Res., **60**, 59–123, (2019)
2. R. Töpfer and O. Trapp, Theor. Appl. Genet., **135**, 3947–3960, (2022)
3. A. Nasehi, M. Nasr Esfahani, A. Nasr Esfahani, L. Mohammadbagheri, M. J. Yazdi, and M. Mohammadi, Ecol. Genet. Genomics, **29**, (2023)
4. Agreste, (2019). [Online]. Available: https://agreste.agriculture.gouv.fr/agreste-web/download/publication/publie/Chd2407/cd2024-7_PK-GC2021-IFT.pdf
5. N. Dhankhar and J. Kumar, Mater. Today Proc., (2023)
6. F. Bernizzoni, M. Gatti, S. Civardi, and S. Poni, Am. J. Enol. Vitic., **60**, 339–348, (2009)
7. K. Bou Nader, M. Stoll, D. Rauhut, C. D. Patz, R. Jung, O. Loehnertz, H. R. Schultz, G. Hilbert, C. Renaud, J. P. Roby, S. Delrot, and E. Gomès, Eur. J. Agron., **104**, 1–12, (2019)
8. OIV, (2022). [Online]. Available: https://www.oiv.int/sites/default/files/documents/OIV_State_of_the_world_Vine_and_Wine_sector_in_2022_2.pdf
9. R. Darriaut, V. Lailheugue, I. Masneuf-Pomarède, E. Marguerit, G. Martins, S. Compant, P. Ballestra, S. Upton, N. Ollat, and V. Lauvergeat, Hoticulture Res., **9**, (2022)
10. F. Mesny, S. Hacquard, and B. P. Thomma, EMBO Rep., **24**, (2023)
11. G. Santoyo, J. Adv. Res., **40**, 45–58, (2022)
12. C. E. Prescott, S. J. Grayston, H. S. Helmisaari, E. Kaštovská, C. Körner, H. Lambers, I. C. Meier, P. Millard, and I. Ostonen, Trends Ecol. Evol., **35**, 1110–1118, (2020)
13. V. Vives-Peris, C. de Ollas, A. Gómez-Cadenas, and R. M. Pérez-Clemente, Plant Cell Reports 2019 391, **39**, 3–17, (2019)
14. P. Fournier, L. Pellan, D. Barroso-Bergadà, D. A. Bohan, T. Candresse, F. Delmotte, M. C. Dufour, V. Lauvergeat, C. Le Marrec, A. Marais, G. Martins, I. Masneuf-Pomarède, P. Rey, D. Sherman, P. This, C. Frioux, S. Labarthe, and C. Vacher, Adv. Ecol. Res., **67**, 27–99, (2022)
15. F. Fabre, L. Delbac, C. Poeydebat, and M. Zaffaroni, bioRxiv, 1–31, (2024)
16. M. Jermini, P. Blaise, and C. Gessler, Vitis, **2**, 77–85, (2010).
17. S. Savary, L. Willocquet, S. J. Pethybridge, P. Esker, N. McRoberts, and A. Nelson, Nat. Ecol. Evol. 2019 33, **3**, 430–439, (2019)
18. G. Armijo, R. Schlechter, M. Agurto, D. Muñoz, C. Nuñez, and P. Arce-Johnson, Front. Plant Sci., **7**, (2016) Accessed: Aug. 05, 2022. [Online]. Available: https://www.frontiersin.org/articles/10.3389/fpls.2016.00382
19. R. S. Jayawardena, W. Purahong, W. Zhang, T. Wubet, X. H. Li, M. Liu, W. Zhao, K. D. Hyde, J. H. Liu, and J. Yan, *Biodiversity of fungi on Vitis vinifera L. revealed by traditional and high-resolution culture-independent approaches*, **90**. Springer Netherlands, 2018.
20. O. A. Boiu-Sicuia, R. C. Toma, C. F. Diguță, F. Matei, and C. P. Cornea, Plants 2023, Vol. 12, Page 2553, **12**, 2553, (2023)
21. P. Jeandet, P. Trotel-Aziz, C. Jacquard, C. Clément, C. Mohan, I. Morkunas, H. Khan, and A. Aziz, Agronomy, **13**, 2225, (2023)
22. P. A. Noceto, P. Bettenfeld, R. Boussageon, M. Hériché, A. Sportes, D. van Tuinen, P. E. Courty, and D. Wipf, Mycorrhiza, **31**, 655–669, (2021)
23. S. Trouvelot, L. Bonneau, D. Redecker, D. van Tuinen, M. Adrian, and D. Wipf, Agron. Sustain. Dev., **35**, 1449–1467, (2015)
24. M. Karoglan, T. Radić, M. Anić, Ž. Andabaka, D. Stupić, I. Tomaz, J. Mesić, T. Karažija, M. Petek, B. Lazarević, M. Poljak, and M. Osrečak, Agric. 2021, Vol. 11, Page 615, **11**, 615, (2021)
25. A. Raio and G. Puopolo, World J. Microbiol. Biotechnol., **37**, 1–8, (2021)
26. S. Zhang, A. Lehmann, W. Zheng, Z. You, and M. C. Rillig, New Phytol., **222**, 543–555, (2019)
27. A. Nawaz, M. Shahbaz, M. Asadullah, A. Imran, M. U. Marghoob, M. Imtiaz, and F. Mubeen, Front. Microbiol., **11**, (2020)
28. C. A. Mallon, J. D. Van Elsas, and J. F. Salles, Trends Microbiol., **23**, 719–729, (2015)
29. G. Berg, M. Köberl, D. Rybakova, H. Müller, R. Grosch, and K. Smalla, FEMS Microbiol. Ecol., **93**, 50, (2017)
30. M. J. Blaser, Cleve. Clin. J. Med., **85**, 928–930, (2018)
31. M. Saleem, J. Hu, and A. Jousset, Annu. Rev. Ecol. Evol. Syst, **50**, 145–168, (2019)
32. D. A. Nikitin, M. V. Semenov, T. I. Chernov, N. A. Ksenofontova, A. D. Zhelezova, E. A. Ivanova, N. B. Khitrov, and A. L. Stepanov, Eurasian Soil Sci., **55**, 221–234, (2022)
33. F. Ma, C. Wang, Y. Zhang, J. Chen, R. Xie, and Z. Sun, Int. J. Environ. Res. Public Health, **19**, 13888, (2022)
34. E. Bruez, J. Vallance, J. Gerbore, P. Lecomte, J.-P. Da Costa, L. Guerin-Dubrana, and P. Rey, PLoS One, **9**, (2014)
35. Chelius, M.K. and E. W. Triplett, Microb. Ecol., **41**, 252–263, (2001).
36. F. H. Behrens and M. Fischer, Phytobiomes J., 1–25, (2022)
37. F. Escudié, L. Auer, M. Bernard, M. Mariadassou, L. Cauquil, K. Vidal, S. Maman, G. Hernandez-Raquet, S. Combes, and G. Pascal, Bioinformatics, **34**, 1287–1294, (2018)
38. C. Quast, E. Pruesse, P. Yilmaz, J. Gerken, T. Schweer, P. Yarza, J. Peplies, and F. O. Glöckner, Nucleic Acids Res., **41**, 590–596, (2013)
39. R. H. Nilsson, K. H. Larsson, A. F. S. Taylor, J. Bengtsson-Palme, T. S. Jeppesen, D. Schigel, P. Kennedy, K. Picard, F. O. Glöckner, L. Tedersoo, I. Saar, U. Kõljalg, and K. Abarenkov, Nucleic Acids Res., **47**, 259–264, (2019)
40. Q. Wang, G. M. Garrity, J. M. Tiedje, and J. R.

Cole, Appl. Environ. Microbiol., **73**, 5261–5267, (2007)
41. C. Camacho, G. Coulouris, V. Avagyan, N. Ma, J. Papadopoulos, K. Bealer, and T. L. Madden, BMC Bioinformatics, **10**, 1–9, (2009)
42. L. Zinger, C. Lionnet, A. S. Benoiston, J. Donald, C. Mercier, and F. Boyer, Methods Ecol. Evol., **12**, 586–592, (2021)
43. P. J. McMurdie and S. Holmes, PLoS One, **8**, (2013)
44. H. Wickham, *ggplot2: Elegant Graphics for Data Analysis.* Springer-Verlag New York, 2016. Accessed: Sep. 05, 2024. [Online]. Available: https://ggplot2.tidyverse.org
45. H. Mallick *et al.*, PLOS Comput. Biol., **17**, (2021)
46. M. De Cáceres, P. Legendre, and M. Moretti, Oikos, **119**, 1674–1684, (2010)
47. M. C. Cambon, M. Trillat, I. Lesur-Kupin, R. Burlett, E. Chancerel, E. Guichoux, L. Piouceau, B. Castagneyrol, G. Le Provost, S. Robin, Y. Ritter, I. Van Halder, S. Delzon, D. A. Bohan, and C. Vacher, Mol. Ecol., **32**, 5944–5958, (2023)
48. M. N. Wright and A. Ziegler, J. Stat. Softw., **77**, (2015)
49. P. Bettenfeld, J. i Canals, L. Jacquens, O. Fernandez, F. Fontaine, E. van Schaik, P.-E. Courty, and S. Trouvelot, J. Adv. Res., (2021)
50. G. Novello, E. Gamalero, E. Bona, L. Boatti, F. Mignone, N. Massa, P. Cesaro, G. Lingua, and G. Berta, Front. Microbiol., **8**, 1–11, (2017)
51. L. Dries, S. Bussotti, C. Pozzi, R. Kunz, S. Schnell, O. Löhnertz, and A. Vortkamp, Microorganisms, **9**, 1–12, (2021)
52. D. Liu and K. Howell, Environ. Microbiol., **23**, 1842–1857, (2021)
53. S. Lutz, N. Bodenhausen, J. Hess, A. Valzano-Held, J. Waelchli, G. Deslandes-Hérold, K. Schlaeppi, and M. G. A. van der Heijden, Nat. Microbiol., **8**, 2277–2289, (2023)
54. M. Salman and R. Abuamsha, BioControl, **57**, 711–718, (2012)
55. A. E. Dorrance, S. A. Berry, P. E. Bowen, and P. E. Lipps, Plant Heal. Prog., **5**, (2004)
56. Y. Zhu, J. Shao, Z. Zhou, and R. E. Davis, Hortic. Res., **6**, (2019)
57. C. F. J. Spies, M. Mazzola, and A. McLeod, Eur. J. Plant Pathol., **131**, 103–119, (2011)
58. L. Chiarappa, Phytopathology, **49**, 510–519, (1959).
59. W. D. Gubler, K. Baumgartner, G. T. Browne, A. Eskalen, S. Rooney Latham, E. Petit, and L. A. Bayramian, Australas. Plant Pathol., **33**, 157–165, (2004)
60. R. Darriaut, L. Antonielli, G. Martins, P. Ballestra, P. Vivin, E. Marguerit, B. Mitter, I. Masneuf-Pomarède, S. Compant, N. Ollat, and V. Lauvergeat, Front. Microbiol., **13**, 1–21, (2022)
61. D. Liu and K. Howell, Environ. Microbiol., **23**, 1842–1857, (2021)
62. M. J. Carbone, S. Alaniz, P. Mondino, M. Gelabert, D. Tekielska, R. Bujanda, and D. Gramaje, J. Fungi, **7**, (2021)
63. R. Biasi, E. Brunori, S. Vanino, A. Bernardini, A. Catalani, R. Farina, A. Bruno, and G. Chilosi, Agric., **13**, 1051, (2023)
64. G. C. Popescu, Curr. Trends Nat. Sci., **5**, 107–116, (2016).
65. G. W. T. Wilson, C. W. Rice, M. C. Rillig, A. Springer, and D. C. Hartnett, Ecol. Lett., **12**, 452–461, (2009)
66. M. L. Goddard, L. Belval, I. R. Martin, L. Roth, H. Laloue, L. Deglène-Benbrahim, L. Valat, C. Bertsch, and J. Chong, Front. Plant Sci., **12**, (2021)
67. A. Cruz-Silva, A. Figueiredo, and M. Sebastiana, Sustainability, **13**, 1226, (2021)
68. S. Fontaine, C. Henault, A. Aamor, N. Bdioui, J. M. G. Bloor, V. Maire, B. Mary, S. Revaillot, and P. A. Maron, Soil Biol. Biochem., **43**, 86–96, (2011)
69. A. Van der Wal, T. D. Geydan, T. W. Kuyper, and W. De Boer, FEMS Microbiol. Rev., **37**, 477–494, (2013)
70. L. Philippot, C. Chenu, A. Kappler, M. C. Rillig, and N. Fierer, Nat. Rev. Microbiol., **22**, 226–239, (2023)
71. M. H. Beare, S. Hu, D. C. Coleman, and P. F. Hendrix, Appl. Soil Ecol., **5**, 211–219, (1997)
72. Q. Ning, L. Chen, C. Zhang, D. Ma, D. Li, X. Han, Z. Cai, S. Huang, and J. Zhang, Appl. Soil Ecol., **159**, 103843, (2021)
73. L. Tedersoo, M. Bahram, L. Zinger, H. Nilsson, P. Kennedy, T. Yang, S. Anslan, and V. Mikryukov, Authorea Prepr., 1–33, (2021).
74. W. Islam, A. Noman, H. Naveed, Z. Huang, and H. Y. H. Chen, Environ. Sci. Pollut. Res. 2020 2733, **27**, 41225–41247, (2020)
75. L. Anand, T. Gentimis, A. B. Downie, and C. M. R. Lopez, bioRxiv, (2024)
76. M. C. Dufour, N. Magnin, B. Dumas, S. Vergnes, and M. F. Corio-Costet, BMC Genomics, **17**, (2016)

Annexe n°5

Open Conference on Grapevine Physiology and Biotechnology
LOGROÑO - LA RIOJA
7-11 July 2024

Mining microbiome data to identify antagonists of grapevine downy mildew (*Plasmopara viticola*)

Authors: Paola Fournier[1,2,3]*, Lucile Pellan[1], Aarti Jaswa[1,4], Jessica Vallance[1], Emilie Chancerel[2], Olivier Bonnard[2], Marc Raynal[5], Christian Debord[5], Simon Labarthe[2], Laurent Deliere[1], François Delmotte[1], Patrice This[3], Corinne Vacher[2]

[1]*INRAE, Bordeaux Sciences Agro, ISVV, SAVE, 33140 Villenave-d'Ornon, France*
[2]*INRAE, Univ Bordeaux, BioGeCo, 33610 Cestas, France*
[3]*INRAE, CIRAD, Univ Montpellier, Institut AGRO, AGAP institut, 34398 Montpellier, France*
[4]*Univ Bordeaux, UMR oenologie, INRAE, Bx INP, Bordeaux Sciences Agro, ISVV, 33882 Villenave d'Ornon ,France*
[5]*IFV, 33290 Blanquefort, France*
[*]*Corresponding author: paola.fournier@inrae.fr*

Abstract (250 words)

Vineyards are home to a myriad of microorganisms that interact with each other and with the vines. Some microorganisms are plant pathogens, such as the oomycete *Plasmopara viticola*, causing grapevine downy mildew. Others have a positive effect on vine health, such as disease biocontrol agents. These beneficial plant-microbe and microbe-microbe interactions have gained more attention in recent years because they could represent an alternative to the use of fungicides in viticulture. The aim of the present study is to identify bacterial and fungal taxa naturally present in vineyard soil and grapevine leaves and significantly more abundant in plots with low susceptibility to downy mildew (DM), susceptibility being defined by the intensity and frequency of DM symptoms over several years. Seven pairs of vineyard plots with contrasting susceptibility to DM were selected on the basis of a long-term epidemiological survey conducted in the Bordeaux region by the IFV. In each plot, we sampled young leaves (at phenological stage of 2-3 spreading leaves) and surface soil (top 5 cm) before the first fungicide treatments of the growing season. We used metabarcoding approaches to explore the entire microbial community of the samples. Up to 1974 and 769 taxonomic units of bacteria and fungi respectively were identified. Using differential abundance analyses, we could identify taxa that were significantly more abundant in plots of vines with low susceptibility to DM. As perspectives, the antagonistic activity of these taxa will be studied experimentally to develop microbial biocontrol of downy mildew and move viticulture towards pesticide-free viticulture.

Keywords: *Plasmopara viticola*, phyllosphere, pest management, sustainable viticulture, grape-associated microorganisms

Annexe n° 6: Microbial ASVs significantly more abundant in asymptomatic versus symptomatic leaf tissue (Chapter n° 2).

Domain: ASV domain (Bacteria or Fungi), *Region*: Regional level of analysis (France as a whole, Aquitaine, Occitanie or Champagne region), *ASV:* ASV final taxonomic assignment (i.e. to the lowest known taxonomic level) followed by ASV number, *Score*: Average score across all methods that identified the ASV as significantly differentially abundant (LInDA, ZicoSeq, MaAsLin2 and ANCOM-BC2), *Asymptomatic count*: Number of methods that identified the ASV as significantly associated with asymptomatic leaf tissue, *Symptomatic count*: Number of methods that identified the ASV as significantly associated with symptomatic leaf tissue. In the column 'ASV', the prefix abbreviations are: p for phylum, c for class, o for order, f for family, g for genus, and s for species. The rows are sorted according to the ASV column in alphabetical order, starting with the ASVs for which the lowest known taxonomic level is species, then those for which it is genus, and so on. They are then sorted by region.

Kingdom	Region	ASV	Score	Asymptomatic count	Symptomatic count
Fungi	France	s__Alternaria metachromatica ASV10	0.7	3	0
Fungi	Aquitaine	s__Alternaria metachromatica ASV10	0.4	1	0
Fungi	France	s__Alternaria rosae ASV520	0.49	2	0
Fungi	Aquitaine	s__Alternaria rosae ASV520	0.63	3	0
Fungi	France	s__Angustimassarina acerina ASV638	0.54	3	0
Fungi	France	s__Bulleromyces albus ASV295	-0.79	0	2
Fungi	Aquitaine	s__Bulleromyces albus ASV295	-0.6	0	1
Fungi	France	s__Crocicreas cyathoideum ASV95	0.31	1	0
Fungi	Occitanie	s__Crocicreas cyathoideum ASV95	0.74	2	0
Fungi	France	s__Cryptococcus laurentii ASV622	-0.53	0	2
Fungi	Aquitaine	s__Cryptococcus laurentii ASV622	-1	0	1
Fungi	France	s__Curvibasidium cygneicollum ASV617	-0.52	0	1
Fungi	France	s__Cystofilobasidium macerans ASV317	-0.9	0	2
Fungi	Aquitaine	s__Cystofilobasidium macerans ASV317	-1	0	3
Fungi	France	s__Dioszegia hungarica ASV100	0.25	1	0
Fungi	Aquitaine	s__Itersonilia pannonica ASV91	-0.6	0	1
Fungi	France	s__Keissleriella phragmiticola ASV82	0.27	3	0
Fungi	Occitanie	s__Keissleriella phragmiticola ASV82	0.59	2	0
Fungi	Occitanie	s__Monographella nivalis ASV39	-0.6	0	1
Fungi	France	s__Mycosphaerella tassiana ASV1	0.25	1	0
Fungi	France	s__Pseudopithomyces rosae ASV327	0.61	3	0
Fungi	Aquitaine	s__Pseudopithomyces rosae ASV327	0.6	1	0
Fungi	France	s__Sporobolomyces patagonicus ASV252	-0.39	0	2
Fungi	Aquitaine	s__Sporobolomyces patagonicus ASV252	-0.54	0	2
Fungi	France	s__Sporobolomyces roseus ASV611	-0.46	0	1
Fungi	France	s__Sporobolomyces roseus ASV625	-0.98	0	2
Fungi	Aquitaine	s__Sporobolomyces roseus ASV625	-0.4	0	1
Fungi	Champagne	s__Sporobolomyces roseus ASV625	-1	0	2
Fungi	France	s__Sporobolomyces roseus ASV99	-0.99	0	2
Fungi	Occitanie	s__Sporobolomyces roseus ASV99	-0.6	0	1
Fungi	Aquitaine	s__Sporobolomyces roseus ASV99	-0.76	0	3
Fungi	Champagne	s__Sporobolomyces roseus ASV99	-0.76	0	3
Fungi	France	s__Stagonospora pseudovitensis ASV87	0.4	2	0

Annexes

Fungi	France	s__Stemphylium solani ASV52	0.56	3	0
Fungi	France	s__Udeniomyces pyricola ASV245	-0.54	0	1
Fungi	Aquitaine	s__Udeniomyces pyricola ASV245	-0.7	0	2
Fungi	France	s__Vishniacozyma victoriae ASV580	0.25	1	0
Fungi	France	g__Alternaria ASV189	0.5	1	0
Bacteria	Champagne	g__Bacillus ASV113	-0.81	0	3
Bacteria	Champagne	g__Bacillus ASV401	-0.65	0	2
Fungi	France	g__Bensingtonia ASV621	0.25	1	0
Fungi	France	g__Botrytis ASV208	0.88	4	0
Fungi	Occitanie	g__Botrytis ASV208	0.96	2	0
Fungi	Aquitaine	g__Botrytis ASV208	0.53	3	0
Fungi	France	g__Erysiphe ASV36	0.29	3	0
Fungi	Aquitaine	g__Erysiphe ASV36	0.42	2	0
Fungi	Occitanie	g__Filobasidium ASV60	-0.6	0	1
Bacteria	France	g__Frigoribacterium ASV112	-1	0	1
Bacteria	Occitanie	g__Frigoribacterium ASV112	-1	0	3
Bacteria	Occitanie	g__Massilia ASV13	-0.83	0	1
Bacteria	Occitanie	g__Massilia ASV888	-0.83	0	1
Bacteria	Occitanie	g__Methylobacterium-Methylorubrum ASV246	0.93	2	0
Bacteria	Occitanie	g__Methylobacterium-Methylorubrum ASV368	0.79	2	0
Fungi	France	g__Neoascochyta ASV147	0.88	2	0
Fungi	Occitanie	g__Neoascochyta ASV147	1	3	0
Fungi	France	g__Neoascochyta ASV274	0.95	2	0
Fungi	Occitanie	g__Neoascochyta ASV274	0.89	3	0
Fungi	France	g__Phaeosphaeria ASV632	0.45	3	0
Fungi	Occitanie	g__Phaeosphaeria ASV632	0.52	1	0
Bacteria	Occitanie	g__Pseudokineococcus ASV778	1	2	0
Fungi	France	g__Pyrenophora ASV629	0.6	2	0
Fungi	Aquitaine	g__Pyrenophora ASV629	0.75	3	0
Bacteria	France	g__Sphingomonas ASV1	-0.33	0	1
Bacteria	Occitanie	g__Sphingomonas ASV1	-0.67	0	1
Bacteria	France	g__Sphingomonas ASV556	-0.67	0	1
Fungi	Aquitaine	g__Sporobolomyces ASV140	-0.4	0	1
Bacteria	Champagne	g__Streptomyces ASV168	-1	0	4
Fungi	France	g__Vishniacozyma ASV356	-1	0	1
Fungi	Occitanie	g__Vishniacozyma ASV356	-1	0	1
Fungi	France	g__Vishniacozyma ASV396	0.25	1	0
Fungi	France	f___Dermateaceae ASV33	0.25	2	0
Fungi	Champagne	f___Nectriaceae ASV626	-0.83	0	3
Fungi	France	f___Phaeosphaeriaceae ASV101	0.25	1	0
Fungi	France	o___Dothideales ASV395	0.25	1	0
Fungi	Aquitaine	o___Dothideales ASV395	-0.53	0	2
Fungi	France	o___Pleosporales ASV633	0.62	2	0
Fungi	Aquitaine	o___Pleosporales ASV633	0.58	3	0
Fungi	France	c___Leotiomycetes ASV49	0.3	2	0

Annexes

Fungi	France	p___Ascomycota ASV112	0.65	3	0
Fungi	Aquitaine	p___Ascomycota ASV112	1	1	0
Fungi	France	p___Ascomycota ASV198	0.55	1	0
Fungi	Aquitaine	p___Ascomycota ASV198	0.85	4	0
Fungi	France	p___Ascomycota ASV416	0.25	1	0
Fungi	France	p___Ascomycota ASV97	0.32	3	0

Annexe n° 7: Fungal and bacterial ASVs indicating low and high *Plasmopara viticola* abundance in leaf (Chapter n° 2).

Domain: ASV domain (Bacteria or Fungi), *Region*: Regional level of analysis (France as a whole, Aquitaine, Occitanie or Champagne region), *ASV*: ASV final taxonomic assignment (i.e. to the lowest known taxonomic level) followed by ASV number, *TITAN res*: Result from TITAN indicating whether the ASV is an indicator of low or high value of *P. viticola* abundance in leaf, *TITAN zscore*: TITAN z score. In the column 'ASV', the prefix abbreviations are: p for phylum, c for class, o for order, f for family, g for genus, and s for species. The rows are sorted according to the ASV column in alphabetical order, starting with the ASVs for which the lowest known taxonomic level is species, then those for which it is genus, and so on. They are then sorted by region.

Kingdom	Region	ASV	TITAN res	TITAN zscore
Fungi	Aquitaine	s__Alternaria rosae ASV520	Low	6.13
Fungi	France	s__Angustimassarina acerina ASV638	Low	4.93
Fungi	France	s__Antrodia xantha ASV212	Low	6.61
Fungi	France	s__Bipolaris cynodontis ASV183	Low	3.62
Fungi	France	s__Blumeria graminis ASV310	Low	6.38
Fungi	France	s__Buckleyzyma aurantiaca ASV18	Low	5.78
Fungi	Aquitaine	s__Buckleyzyma salicina ASV119	High	4.61
Fungi	Champagne	s__Bullera crocea ASV628	High	3.04
Fungi	Aquitaine	s__Bulleromyces albus ASV295	High	4.4
Fungi	France	s__Cladosporium delicatulum ASV294	High	3.12
Fungi	Aquitaine	s__Claviceps arundinis ASV78	Low	5.2
Fungi	France	s__Coprinellus sclerocystidiosus ASV277	Low	3.16
Fungi	France	s__Coprinopsis radiata ASV184	Low	6.37
Fungi	Aquitaine	s__Coprinopsis radiata ASV184	Low	6.92
Fungi	France	s__Crocicreas cyathoideum ASV95	Low	5.11
Fungi	Occitanie	s__Crocicreas cyathoideum ASV95	Low	6.27
Fungi	France	s__Cryptococcus laurentii ASV622	High	2.95
Fungi	Aquitaine	s__Cryptococcus laurentii ASV622	High	3.11
Fungi	France	s__Curvibasidium cygneicollum ASV617	High	2.86
Fungi	Aquitaine	s__Curvibasidium cygneicollum ASV617	High	3.13
Fungi	France	s__Cystofilobasidium macerans ASV317	High	4.51
Fungi	Occitanie	s__Cystofilobasidium macerans ASV317	High	3.94
Fungi	Aquitaine	s__Cystofilobasidium macerans ASV317	High	4.66
Fungi	France	s__Cystofilobasidium macerans ASV55	High	6.66
Fungi	Champagne	s__Cystofilobasidium macerans ASV55	High	5.26
Fungi	France	s__Dioszegia buhagiarii ASV422	Low	7.37
Fungi	France	s__Erysiphe necator ASV66	Low	3.26
Fungi	France	s__Fomes fomentarius ASV239	Low	6.11
Fungi	Aquitaine	s__Fomes fomentarius ASV239	Low	4.33
Fungi	Champagne	s__Fomes fomentarius ASV239	Low	5.63
Fungi	France	s__Genolevuria amylolytica ASV227	Low	12.03
Fungi	Occitanie	s__Genolevuria amylolytica ASV227	Low	5.84
Fungi	France	s__Holtermanniella wattica ASV448	High	3.15
Fungi	France	s__Hyphodermella rosae ASV401	Low	7.62
Fungi	Occitanie	s__Hyphodermella rosae ASV401	Low	5.62

Annexes

Fungi	France	s__Itersonilia perplexans ASV47	Low	7.82
Fungi	Occitanie	s__Itersonilia perplexans ASV47	Low	7.36
Fungi	France	s__Keissleriella phragmiticola ASV82	Low	5.59
Fungi	Occitanie	s__Keissleriella phragmiticola ASV82	Low	5.26
Fungi	France	s__Kondoa aeria ASV190	Low	4.91
Fungi	France	s__Kondoa yuccicola ASV303	Low	4.04
Fungi	France	s__Monochaetia junipericola ASV365	Low	4.65
Fungi	Occitanie	s__Mycosphaerella tassiana ASV263	High	3.76
Fungi	France	s__Panaeolus papilionaceus ASV353	Low	4.62
Fungi	France	s__Periconia homothallica ASV284	Low	4.55
Fungi	Aquitaine	s__Periconia homothallica ASV284	Low	3.97
Fungi	France	s__Pseudopithomyces chartarum ASV104	Low	7.18
Fungi	Aquitaine	s__Pseudopithomyces chartarum ASV104	Low	6.61
Fungi	France	s__Pseudopithomyces rosae ASV327	Low	5.89
Fungi	Aquitaine	s__Rhodotorula babjevae ASV217	High	2.5
Fungi	France	s__Septoria cretae ASV29	High	3.78
Fungi	Occitanie	s__Septoria cretae ASV29	High	3.94
Fungi	Aquitaine	s__Sporobolomyces roseus ASV41	High	5.72
Fungi	France	s__Sporobolomyces roseus ASV611	High	4.09
Fungi	Aquitaine	s__Sporobolomyces roseus ASV611	High	6.2
Fungi	Aquitaine	s__Sporobolomyces roseus ASV625	High	7.78
Fungi	France	s__Sporobolomyces roseus ASV99	High	4.81
Fungi	Aquitaine	s__Sporobolomyces roseus ASV99	High	3.46
Fungi	Champagne	s__Sporobolomyces roseus ASV99	High	5.13
Fungi	France	s__Sporormiella intermedia ASV288	Low	15.19
Fungi	Occitanie	s__Stagonospora pseudovitensis ASV87	Low	5.73
Fungi	Occitanie	s__Stemphylium solani ASV52	Low	3.7
Fungi	Aquitaine	s__Stemphylium solani ASV52	Low	5.79
Fungi	France	s__Stereum hirsutum ASV503	Low	10.42
Fungi	France	s__Taphrina pruni ASV231	Low	10.43
Fungi	France	s__Torula acaciae ASV271	Low	4.6
Fungi	Aquitaine	s__Torula acaciae ASV271	Low	3.21
Fungi	Aquitaine	s__Torula herbarum ASV128	Low	3.51
Fungi	France	s__Udeniomyces pyricola ASV245	High	4.07
Fungi	Aquitaine	s__Udeniomyces pyricola ASV245	High	2.6
Fungi	Aquitaine	s__Vishniacozyma dimennae ASV635	High	8.12
Fungi	France	s__Vishniacozyma globispora ASV77	Low	5.46
Fungi	France	s__Vishniacozyma victoriae ASV144	Low	6.19
Fungi	France	s__Vishniacozyma victoriae ASV366	High	7.44
Bacteria	France	g__1174-901-12 ASV49	High	5.55
Bacteria	Aquitaine	g__1174-901-12 ASV49	High	6.43
Bacteria	France	g__Acidiphilium ASV54	High	8.14
Bacteria	France	g__Acidovorax ASV115	Low	4.52
Bacteria	Aquitaine	g__Acinetobacter ASV179	Low	3.14
Bacteria	France	g__Acinetobacter ASV4	Low	7.42
Bacteria	Champagne	g__Acinetobacter ASV4	Low	5.99

Annexes

Bacteria	France	g__Allorhizobium-Neorhizobium-Pararhizobium-Rhizobium ASV78	Low	4.23
Bacteria	Champagne	g__Allorhizobium-Neorhizobium-Pararhizobium-Rhizobium ASV78	Low	3.99
Bacteria	France	g__Altererythrobacter ASV567	Low	9.39
Fungi	France	g__Alternaria ASV189	Low	4.19
Fungi	Aquitaine	g__Alternaria ASV189	Low	4.19
Fungi	Champagne	g__Alternaria ASV189	Low	3.88
Fungi	France	g__Alternaria ASV437	Low	3.2
Fungi	France	g__Alternaria ASV476	Low	3.62
Fungi	France	g__Alternaria ASV72	Low	3.25
Bacteria	France	g__Aquipuribacter ASV281	High	4.59
Bacteria	France	g__Arthrobacter ASV203	High	3.24
Bacteria	Champagne	g__Arthrobacter ASV629	High	10.14
Bacteria	France	g__Bacillus ASV113	High	11.05
Bacteria	Champagne	g__Bacillus ASV113	High	6.42
Bacteria	France	g__Bacillus ASV184	High	7.77
Bacteria	Champagne	g__Bacillus ASV184	High	4.41
Bacteria	France	g__Bacillus ASV249	High	11.8
Bacteria	Champagne	g__Bacillus ASV38	Low	5.44
Bacteria	France	g__Bacillus ASV401	High	8.53
Bacteria	Champagne	g__Bacillus ASV401	High	5.46
Bacteria	France	g__Blastococcus ASV155	Low	6.14
Bacteria	Champagne	g__Blastococcus ASV197	Low	6
Fungi	France	g__Botrytis ASV208	Low	6.27
Fungi	Occitanie	g__Botrytis ASV208	Low	4.27
Fungi	Aquitaine	g__Botrytis ASV208	Low	5.54
Bacteria	France	g__Brevibacterium ASV575	Low	7.26
Bacteria	France	g__Clavibacter ASV512	Low	5.27
Fungi	France	g__Constantinomyces ASV297	Low	5.81
Fungi	France	g__Coprinopsis ASV172	Low	7.15
Fungi	Aquitaine	g__Coprinopsis ASV172	Low	6.05
Fungi	France	g__Coprinopsis ASV311	Low	6
Bacteria	France	g__Corynebacterium ASV291	Low	3.69
Bacteria	France	g__Corynebacterium ASV98	Low	6.87
Bacteria	France	g__Craurococcus-Caldovatus ASV925	High	8.61
Bacteria	France	g__Enhydrobacter ASV139	Low	6.67
Bacteria	France	g__Enhydrobacter ASV235	Low	7.95
Bacteria	Champagne	g__Enhydrobacter ASV235	Low	8.42
Fungi	France	g__Erysiphe ASV36	Low	5.36
Fungi	Aquitaine	g__Erysiphe ASV36	Low	4.86
Bacteria	France	g__Fictibacillus ASV531	High	14.21
Bacteria	Champagne	g__Fictibacillus ASV531	High	7.27
Fungi	France	g__Filobasidium ASV178	Low	2.63
Fungi	Occitanie	g__Filobasidium ASV60	High	3.17
Bacteria	France	g__Frigoribacterium ASV112	High	3.47
Bacteria	Occitanie	g__Frigoribacterium ASV112	High	5.43

Annexes

Bacteria	France	g__Frigoribacterium ASV201	Low	4.23
Bacteria	France	g__Frigoribacterium ASV35	High	4.35
Fungi	Aquitaine	g__Holtermanniella ASV12	High	3.35
Bacteria	France	g__Hymenobacter ASV105	Low	5.11
Bacteria	Aquitaine	g__Hymenobacter ASV68	High	5.78
Bacteria	France	g__Iamia ASV677	Low	7.08
Bacteria	France	g__Iamia ASV681	Low	5.24
Bacteria	France	g__Intrasporangium ASV753	Low	9.72
Bacteria	France	g__Janibacter ASV582	High	10.89
Bacteria	Champagne	g__Janibacter ASV582	High	5.76
Bacteria	France	g__Knoellia ASV669	Low	5.86
Bacteria	France	g__Kocuria ASV148	Low	4.11
Fungi	France	g__Kondoa ASV98	Low	5.93
Fungi	Occitanie	g__Kondoa ASV98	Low	6.32
Bacteria	France	g__Lactobacillus ASV374	Low	4.24
Bacteria	France	g__Marmoricola ASV285	Low	9.16
Bacteria	France	g__Marmoricola ASV872	Low	5.04
Bacteria	Champagne	g__Massilia ASV329	Low	5.62
Bacteria	France	g__Massilia ASV426	Low	5.86
Bacteria	France	g__Methylobacterium-Methylorubrum ASV22	High	6.07
Bacteria	Champagne	g__Methylobacterium-Methylorubrum ASV22	High	5.46
Bacteria	Occitanie	g__Methylobacterium-Methylorubrum ASV246	Low	5.92
Bacteria	France	g__Methylobacterium-Methylorubrum ASV357	High	5.51
Bacteria	France	g__Methylobacterium-Methylorubrum ASV600	Low	5.06
Bacteria	France	g__Microbacterium ASV622	Low	4.17
Bacteria	Aquitaine	g__Microbacterium ASV622	Low	4.7
Bacteria	Aquitaine	g__Micrococcus ASV678	Low	4.72
Fungi	France	g__Mycosphaerella ASV500	High	3.1
Fungi	Champagne	g__Mycosphaerella ASV500	High	2.99
Fungi	France	g__Neoascochyta ASV147	Low	4.35
Fungi	Occitanie	g__Neoascochyta ASV147	Low	6.23
Fungi	Aquitaine	g__Neoascochyta ASV147	Low	5.16
Fungi	France	g__Neoascochyta ASV274	Low	7.73
Fungi	Occitanie	g__Neoascochyta ASV274	Low	7.28
Fungi	France	g__Neoascochyta ASV89	High	5.51
Fungi	Champagne	g__Neoascochyta ASV89	High	7.48
Bacteria	Champagne	g__Nocardioides ASV147	High	6.81
Bacteria	France	g__Nocardioides ASV171	High	4.41
Bacteria	Champagne	g__Nocardioides ASV279	Low	8.32
Bacteria	France	g__Nocardioides ASV470	High	4.34
Bacteria	Champagne	g__Nocardioides ASV85	High	4.31
Bacteria	France	g__Okibacterium ASV33	High	10.76
Bacteria	Champagne	g__Okibacterium ASV33	High	5.66

Annexes

Bacteria	Occitanie	g__P3OB-42 ASV301	High	8.24
Bacteria	France	g__Paenarthrobacter ASV100	High	10.3
Bacteria	Champagne	g__Paenarthrobacter ASV100	High	5.63
Bacteria	France	g__Paenisporosarcina ASV577	High	8.59
Bacteria	Champagne	g__Paenisporosarcina ASV577	High	7.15
Bacteria	France	g__Pantoea ASV146	High	4.25
Bacteria	France	g__Pantoea ASV334	High	5.09
Bacteria	France	g__Pantoea ASV689	High	7.85
Bacteria	France	g__Paracoccus ASV966	Low	2.68
Fungi	France	g__Parasola ASV410	Low	3.67
Fungi	France	g__Parastagonospora ASV218	Low	4.4
Bacteria	France	g__Patulibacter ASV349	High	5.62
Fungi	France	g__Peniophora ASV135	Low	7.72
Fungi	Occitanie	g__Peniophora ASV135	Low	6.23
Fungi	France	g__Peniophora ASV358	Low	4.45
Fungi	France	g__Phaeosphaeria ASV632	Low	3.82
Bacteria	France	g__Phenylobacterium ASV594	Low	12.56
Bacteria	France	g__Pseudarthrobacter ASV259	High	4.56
Bacteria	France	g__Pseudarthrobacter ASV479	High	7.34
Bacteria	Champagne	g__Pseudarthrobacter ASV479	High	4.13
Bacteria	France	g__Pseudarthrobacter ASV557	High	7.94
Bacteria	Champagne	g__Pseudarthrobacter ASV557	High	4.38
Bacteria	France	g__Pseudomonas ASV322	Low	9.84
Bacteria	Aquitaine	g__Pseudomonas ASV322	Low	7.22
Bacteria	Occitanie	g__Pseudomonas ASV412	High	5.13
Bacteria	France	g__Pseudomonas ASV534	High	4.19
Bacteria	France	g__Pseudomonas ASV57	High	4.47
Bacteria	Occitanie	g__Pseudomonas ASV57	High	5.91
Bacteria	France	g__Pseudomonas ASV844	High	5.79
Bacteria	Occitanie	g__Pseudomonas ASV844	High	6.9
Fungi	France	g__Pseudopithomyces ASV634	Low	4.83
Fungi	Aquitaine	g__Pseudopithomyces ASV634	Low	3.29
Bacteria	France	g__Quadrisphaera ASV463	High	4.47
Bacteria	France	g__Rhodococcus ASV135	High	7.12
Bacteria	Champagne	g__Rhodococcus ASV335	High	3.88
Bacteria	Aquitaine	g__Rubellimicrobium ASV119	Low	5.94
Bacteria	France	g__Saccharopolyspora ASV707	Low	3.9
Bacteria	Occitanie	g__Salana ASV150	Low	4.69
Bacteria	France	g__Serinibacter ASV840	Low	7.81
Fungi	France	g__Sigarispora ASV507	Low	7.21
Bacteria	Aquitaine	g__Solirubrobacter ASV94	Low	3.28
Bacteria	France	g__Sphingomonas ASV341	Low	5.37
Bacteria	France	g__Sphingomonas ASV588	High	6.23
Bacteria	France	g__Sphingomonas ASV667	Low	5.08
Bacteria	France	g__Sphingomonas ASV957	High	7.54
Fungi	Aquitaine	g__Sporobolomyces ASV140	High	3.82

Annexes

Bacteria	France	g__Sporosarcina ASV369	High	7.95
Bacteria	France	g__Sporosarcina ASV786	High	11.81
Fungi	France	g__Stemphylium ASV624	Low	3.27
Bacteria	France	g__Streptomyces ASV168	High	12.64
Bacteria	Champagne	g__Streptomyces ASV168	High	7.76
Fungi	France	g__Symmetrospora ASV194	Low	4.55
Fungi	France	g__Symmetrospora ASV28	Low	7.77
Fungi	Occitanie	g__Symmetrospora ASV28	Low	6.02
Fungi	France	g__Taphrina ASV450	Low	7.47
Fungi	Occitanie	g__Taphrina ASV450	Low	5.09
Bacteria	France	g__Thermoactinomyces ASV88	Low	6.12
Bacteria	Champagne	g__Thermoactinomyces ASV88	Low	5.99
Fungi	Occitanie	g__Truncatella ASV169	Low	6.85
Fungi	France	g__Vishniacozyma ASV151	High	13.52
Fungi	Champagne	g__Vishniacozyma ASV151	High	7.83
Fungi	France	g__Vuilleminia ASV240	Low	8.42
Fungi	Occitanie	g__Vuilleminia ASV240	Low	6.69
Fungi	France	g__Vuilleminia ASV341	Low	5.89
Fungi	Occitanie	g__Vuilleminia ASV341	Low	6.6
Bacteria	France	g__Xanthomonas ASV320	High	7.5
Bacteria	Occitanie	g__Xanthomonas ASV320	High	8.96
Bacteria	France	f__67-14 ASV517	Low	3.54
Fungi	France	f__Cladosporiaceae ASV451	Low	3.12
Fungi	France	f__Dermateaceae ASV33	Low	7.47
Bacteria	France	f__Erwiniaceae ASV223	High	4.38
Bacteria	Occitanie	f__Erwiniaceae ASV223	High	6.18
Bacteria	France	f__Erwiniaceae ASV423	High	4.41
Bacteria	France	f__Ilumatobacteraceae ASV364	High	8.64
Bacteria	Champagne	f__Intrasporangiaceae ASV270	Low	6.25
Fungi	France	f__Kondoaceae ASV109	Low	2.89
Fungi	France	f__Kondoaceae ASV70	Low	5.16
Fungi	Occitanie	f__Kondoaceae ASV70	Low	4.3
Fungi	France	f__Lentitheciaceae ASV427	Low	5.77
Bacteria	France	f__Micrococcaceae ASV20	High	9.1
Bacteria	Champagne	f__Micrococcaceae ASV20	High	8.07
Fungi	France	f__Nectriaceae ASV31	High	3.08
Fungi	France	f__Nectriaceae ASV626	High	8.69
Fungi	Champagne	f__Nectriaceae ASV626	High	6.87
Fungi	France	f__Parmeliaceae ASV255	Low	2.91
Fungi	France	f__Phaeosphaeriaceae ASV101	Low	3.73
Bacteria	France	f__Solirubrobacteraceae ASV324	Low	4.08
Fungi	France	f__Sordariaceae ASV224	Low	4.18
Bacteria	France	f__Sphingobacteriaceae ASV48	High	4.32
Bacteria	Aquitaine	f__Sphingobacteriaceae ASV48	High	5.41
Bacteria	France	f__Sphingomonadaceae ASV144	Low	3.86
Fungi	Occitanie	o__Dothideales ASV395	High	3.08

Annexes

Fungi	Aquitaine	o__Dothideales ASV395	High	4.43
Bacteria	France	o__Frankiales ASV646	High	5.7
Bacteria	France	o__Frankiales ASV911	Low	6.42
Bacteria	Aquitaine	o__Frankiales ASV911	Low	5.66
Fungi	France	o__Helotiales ASV357	Low	6.05
Fungi	France	o__Helotiales ASV393	Low	4.98
Fungi	France	o__Helotiales ASV79	Low	7.81
Fungi	Occitanie	o__Helotiales ASV79	Low	4.78
Fungi	France	o__Pleosporales ASV266	Low	12.75
Fungi	Occitanie	o__Pleosporales ASV266	Low	9.11
Fungi	France	o__Pleosporales ASV633	Low	5.61
Fungi	Aquitaine	o__Pleosporales ASV633	Low	5.46
Fungi	France	o__Tremellales ASV26	High	6.61
Fungi	France	c__Leotiomycetes ASV49	Low	5.72
Fungi	France	p__Ascomycota ASV112	Low	9.85
Fungi	Occitanie	p__Ascomycota ASV112	Low	6.29
Fungi	Aquitaine	p__Ascomycota ASV112	Low	5.89
Fungi	Aquitaine	p__Ascomycota ASV198	Low	6.23
Fungi	France	p__Ascomycota ASV210	Low	3.24
Fungi	France	p__Ascomycota ASV325	Low	8.48
Fungi	France	p__Ascomycota ASV399	Low	4.17
Fungi	France	p__Ascomycota ASV495	Low	11.62
Fungi	France	p__Ascomycota ASV97	Low	7.9
Fungi	Occitanie	p__Ascomycota ASV97	Low	5.18
Bacteria	France	p__Proteobacteria ASV981	High	5.87

Annexe n°8 : Factors influencing the beta diversity of the microbiota.

Sampling Year : 2022												
		Fungi						Bacteria				
		Topsoil		Phyllosphere		Endosphere		Topsoil		Phyllosphere		Endosphere	
Group	Retained explanatory variables	Marginal effects of terms	p	Marginal effects of terms	p	Marginal effects of terms	p	Marginal effects of terms	p	Marginal effects of terms	p	Marginal effects of terms	p
Soil physical chemistry (*Soil*)	Clays	39.75	***	10.61	n.s.	9.62	*	42.82	**	31.28	**	1.283	**
	Sands	34.84	**					40.99	**				
	Silts									22.65	.		
	C/N	30.64	***					38.43	**	26.08	*		
	pH	38.37	***	13.14	*			63.00	***			0.999	.
	Organic matter	19.41	*					20.64	*	25.77	*		
	Total carbon	19.23	*	14.94	*					25.76	*		
	Total limestone	19.21	*	15.17	*	7.33	.	25.45	**	25.74	*		
	Total nitrogen	32.98	***	16.45	*			47.78	**	27.40	**		
	Total organic carbon							20.67	*				
	Vine variety	77.68	***	33.80	***	15.58	***	77.94	**	34.52	***	1.423	**
	Management			30.17	***	18.29	***	34.85	**				
	Whether fungicides were applied or not to the plot area the year before collect	17.87	*	16.35	*	6.93	.	18.39	*				
Position of the plot and position of the vine within the plot (*Space*)	PCNM1	45.19	***	30.21	***	18.00	***	33.84	**			1.192	*
	PCNM2							34.46	**	25.68	*		
	PCNM3	44.97	***	30.18	***	19.32	***	34.65	**	25.68	*	2.391	***
	PCNM4	45.15	***					34.92	**			1.851	***
	PCNM5	57.93	***	30.20	***			37.79	***	25.11	*	1.247	**
	Edge	34.36	***	13.18	.	7.58	.	32.99	**				
	Humidity at 5am on the day of sampling (%)							45.45	***				

Annexes

Weather during the month before sampling (Weather)	Temperature at 5am on the day of sampling (°C)		***							25.68	*		
	Humidity at 10pm on the day before sampling (%)			30.16	***								
	Temperature at 10am on the day before sampling (°C)					14.20	*						
	Temperature at 3pm on the day before sampling (°C)									25.66	*		
	Maximum temperature on day of sampling (°C)	45.05	***										
	Maximum insolation on day of sampling (hours)	45.06	***										
	Maximum humidity the day before sampling (%)									25.68	*		
	Total rainfall on the day before sampling (mm)			30.17	***								
	Average total rainfall for the 15 days prior to sampling (mm)			30.17	***								
	Average maximum insolation for the 30 days prior to sampling (hours)			30.17	***			33.99	**	25.66	*		
	Average total rainfall for the 30 days prior to sampling (mm)	45.07	***							25.66	*		
	Average maximum temperatures for the 30 days prior to sampling (°C)	45.08	***									1.370	**
Sampling Year : 2023													
		Fungi						Bacteria					
		Topsoil		Phyllosphere		Endosphere		Topsoil		Phyllosphere		Endosphere	
Group	Retained explanatory variables	Marginal effects of terms	p	Marginal effects of terms	p	Marginal effects of terms	p	Marginal effects of terms	p	Marginal effects of terms	p	Marginal effects of terms	p
Soil physical chemistry (*Soil*)	Clays	54.70	**										
	Sands	51.51	**							113.3	*		
	Silts							148.01	***				
	C/N	53.77	**	51.45	.	20.16	*	102.52	***				
	pH					34.49	**	128.62	***				
	Organic matter			51.55	.			63.76	**				
	Total carbon					31.12	***			105.6	.		
	Total limestone												

Annexes

	Total nitrogen	51.96	**					65.16	**				
	Total organic carbon	52.36	**	51.56	.								
	Vine variety	57.36	***	52.15	.			136.06	***	102.3	.		
	Management			51.40	.								
	Whether fungicides were applied or not to the plot area the year before collect												
Position of the plot and position of the vine within the plot (*Space*)	PCNM1							97.59	***				
	PCNM2												
	PCNM3											6.056	*
	PCNM4	55.66	**	51.50	.			95.93	***				
	PCNM5												
	Edge												
Weather during the month before sampling (Weather)	Humidity at 5am on the day of sampling (%)	51.74	**										
	Temperature at 10am on the day of sampling (°C)									106.7	.		
	Humidity at 5am on the day before sampling (%)							108.03	***				
	Humidity at 10am on the day before sampling (%)					40.86	***						
	Humidity at 10pm on the day before sampling (%)	60.04	***										
	Temperature at 5am on the day before sampling (°C)							91.59	***				
	Temperature at 10pm on the day before sampling (°C)			51.39	.								
	Rainfall at 10pm on the day before sampling (mm)					44.47	***						
	Maximum temperature on the day of sampling (°C)	59.53	***					91.80	***				
	Maximum humidity on the day of sampling (%)			51.38	.								
	Maximum humidity on the day before sampling (%)			51.36	.								
	Average maximum humidity for the 15 days preceding sampling (%)			51.40	.								
	Average total rainfall for the 15 days prior to sampling (mm)	54.42	**									6.188	*
	Average maximum insolation for the 30 days prior to sampling (hours)												

Annexes

	Average maximum temperatures for the 30 days prior to sampling (°C)					42.38	***						
	Average total rainfall for the 30 days prior to sampling (mm)			51.40	.					115.0	.		

Annex n° 9: Microbial ASVs significantly more abundant in plots with high versus low susceptibility to downy mildew (Chapter n° 3).

Domain: ASV domain (Bacteria or Fungi), *Habitat*: Microbial habitat in which the ASV was found (Topsoil, Phyllosphere, endosphere), *Year*: Sampling year, ASV: ASV final taxonomic assignment (i.e. to the lowest known taxonomic level) followed by ASV number, *Low count*: Number of methods that identified the ASV as significantly associated with plots with low susceptibility to downy mildew, *High count*: Number of methods that identified the ASV as significantly associated with plots with high susceptibility to downy mildew, *Score*: Average score across all methods that identified the ASV as significantly differentially abundant (LInDA, ZicoSeq, MaAsLin2 and ANCOM-BC2) or significantly discriminant (Random Forest), *%reads*: Relative abundance of the ASV for this combination of Habitat * Domain * Sampling Year and *Prev.*: Prevalence of the ASV for this combination of Habitat * Domain * Sampling Year. In the column 'ASV', the prefix abbreviations are: p for phylum, c for class, o for order, f for family, g for genus, and s for species. The rows are sorted according to the ASV column in alphabetical order, starting with the ASVs for which the lowest known taxonomic level is species, then those for which it is genus, and so on. They are then sorted by habitat and year.

Domain	Habitat	Year	ASV	Low count	High count	Score	%reads	Prev.
Bacteria	Topsoil	2022	s__[Brevibacterium] frigoritolerans ASV78	1	0	0.02	0.54	75.00
Fungi	Topsoil	2022	s__Acremonium furcatum ASV128	3	0	0.42	0.23	52.83
Fungi	Phyllosphere	2022	s__Acremonium fusidioides ASV417	0	1	-0.33	0.00	13.92
Fungi	Topsoil	2022	s__Acremonium fusidioides ASV417	0	3	-0.23	0.06	57.86
Fungi	Topsoil	2023	s__Acremonium fusidioides ASV417	0	3	-0.21	0.01	66.67
Fungi	Topsoil	2022	s__Acremonium persicinum ASV378	0	4	-0.41	0.05	45.91
Fungi	Topsoil	2023	s__Acremonium persicinum ASV378	0	4	-0.50	0.08	60.42
Fungi	Phyllosphere	2022	s__Acremonium sclerotigenum ASV782	0	3	-0.75	0.03	36.71
Fungi	Topsoil	2022	s__Acremonium sclerotigenum ASV782	0	3	-0.21	0.00	14.47
Fungi	Topsoil	2022	s__Acremonium spinosum ASV838	2	0	0.23	0.02	55.97
Bacteria	Topsoil	2022	s__Actinomycetales bacterium ASV133	4	0	0.51	0.09	80.00
Bacteria	Topsoil	2023	s__Actinomycetales bacterium ASV133	4	0	0.47	0.09	91.67
Bacteria	Topsoil	2022	s__Adhaeribacter terrae ASV639	0	3	-0.16	0.11	82.50
Bacteria	Topsoil	2023	s__Adhaeribacter terrae ASV639	0	4	-0.51	0.06	93.75
Bacteria	Topsoil	2022	s__Agromyces ramosus ASV49	1	0	0.04	0.85	78.13
Fungi	Topsoil	2022	s__Albifimbria verrucaria ASV78	1	0	0.28	0.36	71.70
Fungi	Phyllosphere	2022	s__Allocryptovalsa polyspora ASV394	1	0	0.35	0.01	20.25
Bacteria	Topsoil	2022	s__Alsobacter metallidurans ASV1208	3	0	0.14	0.02	77.50
Bacteria	Topsoil	2023	s__Alsobacter metallidurans ASV1208	3	0	0.39	0.05	83.33
Fungi	Phyllosphere	2022	s__Alternaria alternata ASV18	0	2	-0.59	0.70	91.77
Fungi	Topsoil	2023	s__Alternaria alternata ASV18	3	0	0.23	0.16	100
Fungi	Phyllosphere	2022	s__Alternaria infectoria ASV53	0	3	-0.49	0.19	94.30
Fungi	Phyllosphere	2022	s__Alternaria rosae ASV204	0	4	-0.70	0.01	69.62
Bacteria	Topsoil	2023	s__Amnibacterium kyonggiense ASV1923	1	0	0.31	0.04	58.33
Bacteria	Topsoil	2022	s__Amycolatopsis keratiniphila ASV947	2	0	0.10	0.01	21.88
Fungi	Phyllosphere	2022	s__Angustimassarina acerina ASV113	4	0	0.79	0.99	72.78
Bacteria	Topsoil	2023	s__Archangium gephyra ASV1087	0	3	-0.27	0.04	89.58
Bacteria	Topsoil	2022	s__Archangium gephyra ASV422	3	0	0.18	0.10	89.38
Bacteria	Topsoil	2023	s__Archangium gephyra ASV422	2	0	0.06	0.13	100
Fungi	Phyllosphere	2022	s__Arthrinium malaysianum ASV82	0	2	-0.30	0.03	76.58

Annexes

Fungi	Topsoil	2022	s__Arthrinium malaysianum ASV82	0	2	-0.32	0.44	64.15
Fungi	Topsoil	2023	s__Arthrinium malaysianum ASV82	0	2	-0.33	0.27	83.33
Fungi	Phyllosphere	2022	s__Arthrinium pseudosinense ASV792	0	1	-0.25	0.00	17.09
Fungi	Topsoil	2022	s__Arthrinium pseudosinense ASV792	0	3	-0.18	0.02	38.36
Fungi	Topsoil	2023	s__Arthrinium pseudosinense ASV792	0	2	-0.38	0.02	47.92
Bacteria	Topsoil	2022	s__Arthrobacter globiformis ASV1353	3	0	0.42	0.03	10.00
Bacteria	Topsoil	2023	s__Arthrobacter globiformis ASV1353	2	0	0.31	0.02	27.08
Bacteria	Topsoil	2022	s__Arthrobacter globiformis ASV281	3	0	0.28	0.16	80.63
Bacteria	Topsoil	2023	s__Arthrobacter globiformis ASV281	2	0	0.12	0.12	100
Bacteria	Topsoil	2022	s__Arthrobacter globiformis ASV50	4	0	0.43	0.49	80.63
Bacteria	Topsoil	2023	s__Arthrobacter globiformis ASV50	4	0	0.45	0.84	95.83
Bacteria	Topsoil	2022	s__Arthrobacter globiformis ASV64	3	0	0.22	0.62	81.88
Bacteria	Topsoil	2023	s__Arthrobacter globiformis ASV64	3	0	0.32	0.61	97.92
Bacteria	Phyllosphere	2022	s__Arthrobacter globiformis ASV791	1	0	0.23	0.01	10.00
Bacteria	Topsoil	2022	s__Arthrobacter globiformis ASV791	3	0	0.46	0.07	10.00
Bacteria	Topsoil	2023	s__Arthrobacter globiformis ASV791	3	0	0.41	0.03	37.50
Bacteria	Phyllosphere	2022	s__Arthrobacter oryzae ASV45	1	0	0.09	0.31	72.50
Bacteria	Topsoil	2022	s__Arthrobacter oryzae ASV45	3	0	0.23	0.89	91.88
Bacteria	Phyllosphere	2022	s__Arthrobacter pascens ASV307	2	0	0.23	0.04	43.75
Bacteria	Topsoil	2023	s__Arthrobacter pascens ASV307	4	0	0.59	0.11	91.67
Fungi	Phyllosphere	2022	s__Articulospora proliferata ASV156	0	3	-0.42	0.00	63.92
Fungi	Topsoil	2022	s__Articulospora proliferata ASV156	0	4	-0.35	0.27	77.99
Fungi	Topsoil	2022	s__Articulospora proliferata ASV791	3	0	0.22	0.01	40.88
Fungi	Topsoil	2022	s__Aspergillus alliaceus ASV693	3	0	0.24	0.00	11.95
Fungi	Endosphere	2022	s__Aspergillus insuetus ASV115	1	0	0.16	0.00	9.38
Fungi	Phyllosphere	2022	s__Aspergillus japonicus ASV399	0	1	-0.16	0.00	11.39
Fungi	Topsoil	2022	s__Aspergillus japonicus ASV399	0	4	-0.43	0.06	61.01
Fungi	Topsoil	2022	s__Aspergillus pseudodeflectus ASV284	4	0	0.51	0.06	58.49
Fungi	Topsoil	2023	s__Aspergillus pseudodeflectus ASV284	4	0	0.84	0.22	77.08
Fungi	Phyllosphere	2022	s__Aspergillus wentii ASV131	0	3	-0.29	0.00	34.81
Fungi	Phyllosphere	2022	s__Atrocalyx lignicola ASV151	3	0	0.59	0.28	43.67
Fungi	Phyllosphere	2022	s__Aureobasidium pullulans ASV2	3	0	0.43	11.24	94.30
Fungi	Topsoil	2022	s__Aureobasidium pullulans ASV2	0	1	-0.03	0.15	90.57
Fungi	Phyllosphere	2022	s__Auricularia mesenterica ASV571	1	0	0.32	0.05	65.19
Bacteria	Topsoil	2022	s__Azohydromonas australica ASV1060	4	0	0.40	0.02	62.50
Bacteria	Topsoil	2023	s__Azohydromonas australica ASV1060	4	0	0.64	0.04	83.33
Bacteria	Topsoil	2022	s__Bacillus litoralis ASV797	1	0	0.03	0.10	62.50
Bacteria	Topsoil	2022	s__Bacillus megaterium NBRC 15308 = ATCC 14581 ASV21	3	0	0.23	1.23	92.50
Bacteria	Topsoil	2022	s__Bacillus mycoides KBAB4 ASV250	0	3	-0.11	0.09	89.38
Bacteria	Topsoil	2023	s__Bacillus mycoides KBAB4 ASV250	0	1	-0.08	0.12	97.92
Bacteria	Topsoil	2022	s__Bacillus nealsonii ASV676	3	0	0.16	0.06	82.50
Bacteria	Phyllosphere	2022	s__Bacillus thermolactis ASV1089	1	0	0.16	0.05	24.38
Bacteria	Topsoil	2022	s__bacterium Ellin504 ASV1184	3	0	0.14	0.03	76.88
Bacteria	Topsoil	2023	s__bacterium Ellin504 ASV1184	2	0	0.18	0.04	81.25
Bacteria	Topsoil	2022	s__bacterium Ellin510 ASV1109	3	0	0.23	0.01	48.13
Bacteria	Topsoil	2023	s__bacterium Ellin510 ASV1109	4	0	0.54	0.00	39.58

Annexes

Bacteria	Topsoil	2023	s__bacterium Ellin6517 ASV297	3	0	0.32	0.10	64.58
Fungi	Phyllosphere	2022	s__Biatriospora antibiotica ASV338	0	3	-0.65	0.17	35.44
Fungi	Topsoil	2022	s__Biatriospora antibiotica ASV338	0	1	-0.09	0.03	45.91
Fungi	Topsoil	2022	s__Bionectria ralfsii ASV248	0	5	-0.56	0.10	37.11
Fungi	Topsoil	2023	s__Bionectria ralfsii ASV248	0	2	-0.39	0.11	60.42
Fungi	Phyllosphere	2022	s__Bjerkandera adusta ASV422	1	0	0.13	0.02	84.18
Fungi	Topsoil	2022	s__Bjerkandera adusta ASV422	2	0	0.10	0.00	15.72
Fungi	Topsoil	2023	s__Bjerkandera adusta ASV422	2	0	0.17	0.00	12.50
Fungi	Phyllosphere	2022	s__Blumeria graminis ASV132	3	0	0.39	0.01	48.73
Fungi	Topsoil	2022	s__Blumeria graminis ASV146	0	2	-0.07	0.00	25.16
Fungi	Topsoil	2022	s__Blumeria graminis ASV201	0	3	-0.12	0.00	25.16
Fungi	Phyllosphere	2022	s__Blumeria graminis ASV560	2	0	0.21	0.01	67.09
Fungi	Endosphere	2022	s__Blumeria graminis ASV59	0	2	-0.80	1.67	15.63
Fungi	Phyllosphere	2022	s__Blumeria graminis ASV59	0	2	-0.38	0.35	48.73
Fungi	Topsoil	2022	s__Boeremia exigua ASV33	0	2	-0.25	1.47	79.87
Fungi	Topsoil	2023	s__Boeremia exigua ASV33	4	0	0.41	0.45	97.92
Fungi	Topsoil	2023	s__Botryotrichum atrogriseum ASV198	0	1	-0.15	0.04	52.08
Fungi	Phyllosphere	2022	s__Botrytis cinerea ASV19	0	2	-0.32	2.42	92.41
Fungi	Topsoil	2022	s__Botrytis cinerea ASV19	0	3	-0.17	0.72	86.79
Fungi	Topsoil	2022	s__Bradymyces graniticola ASV647	4	0	0.42	0.02	11.95
Fungi	Topsoil	2023	s__Bradymyces graniticola ASV647	1	0	0.45	0.03	27.08
Fungi	Phyllosphere	2022	s__Buckleyzyma aurantiaca ASV245	5	0	0.76	0.18	73.42
Fungi	Topsoil	2022	s__Bullera alba ASV242	0	4	-0.29	0.05	52.83
Fungi	Topsoil	2023	s__Bullera alba ASV242	2	0	0.49	0.04	50.00
Fungi	Phyllosphere	2022	s__Cadophora luteo ASV180	0	3	-0.66	0.08	56.33
Fungi	Topsoil	2022	s__Cadophora luteo ASV180	0	1	-0.09	0.13	82.39
Bacteria	Topsoil	2022	s__Chelatococcus asaccharovorans ASV432	3	0	0.22	0.06	27.50
Fungi	Phyllosphere	2022	s__Chloridium aseptatum ASV459	0	1	-0.14	0.00	5.06
Fungi	Topsoil	2022	s__Chloridium aseptatum ASV459	0	4	-0.30	0.05	63.52
Fungi	Phyllosphere	2022	s__Cinereomyces lindbladii ASV851	1	0	0.18	0.00	37.97
Fungi	Phyllosphere	2022	s__Cladosporium allicinum ASV288	0	1	-0.42	0.09	86.71
Fungi	Phyllosphere	2022	s__Cladosporium allicinum ASV8	0	3	-0.48	6.71	93.67
Fungi	Topsoil	2022	s__Cladosporium allicinum ASV8	0	1	-0.10	0.94	89.31
Fungi	Phyllosphere	2022	s__Cladosporium cladosporiodes ASV5	0	4	-0.77	9.61	93.67
Fungi	Topsoil	2022	s__Cladosporium cladosporiodes ASV5	0	1	-0.03	4.54	95.60
Fungi	Topsoil	2023	s__Cladosporium cladosporiodes ASV5	2	0	0.16	1.26	100
Fungi	Topsoil	2022	s__Cladosporium cladosporiodes ASV680	1	0	0.10	0.02	96.23
Fungi	Topsoil	2023	s__Cladosporium cladosporiodes ASV680	3	0	0.16	0.01	95.83
Fungi	Topsoil	2022	s__Cladosporium langeronii ASV196	1	0	0.19	0.01	54.72
Fungi	Topsoil	2022	s__Clarireedia bennettii ASV1122	4	0	0.33	0.02	71.70
Fungi	Phyllosphere	2022	s__Clarireedia bennettii ASV579	0	3	-0.28	0.00	8.86
Fungi	Topsoil	2023	s__Clarireedia bennettii ASV579	1	0	0.41	0.10	58.33
Fungi	Topsoil	2022	s__Clarireedia bennettii ASV721	1	0	0.17	0.01	33.96
Fungi	Topsoil	2022	s__Claviceps arundinis ASV68	3	0	0.16	0.01	29.56
Fungi	Endosphere	2022	s__Clonostachys miodochialis ASV71	0	1	-0.18	0.00	33.13
Fungi	Phyllosphere	2022	s__Clonostachys rosea ASV34	0	1	-0.29	0.01	56.33

Annexes

Fungi	Topsoil	2022	s__Clonostachys rosea ASV34	0	3	-0.16	1.43	94.97
Fungi	Topsoil	2023	s__Clonostachys rosea ASV34	0	2	-0.12	1.20	100
Bacteria	Topsoil	2022	s__Clostridium magnum ASV2013	3	0	0.19	0.03	73.13
Bacteria	Topsoil	2022	s__Clostridium subterminale ASV1045	0	3	-0.08	0.04	79.38
Bacteria	Topsoil	2023	s__Clostridium subterminale ASV1045	0	3	-0.20	0.03	97.92
Fungi	Topsoil	2022	s__Coniochaeta fasciculata ASV347	5	0	0.82	0.11	69.18
Fungi	Topsoil	2023	s__Coniochaeta fasciculata ASV347	4	0	0.55	0.10	87.50
Fungi	Phyllosphere	2022	s__Coprinellus micaceus ASV1000	0	3	-0.35	0.00	19.62
Fungi	Phyllosphere	2022	s__Cordyceps bassiana ASV330	0	1	-0.36	0.05	27.85
Bacteria	Phyllosphere	2022	s__Corynebacterium stationis ASV1165	3	0	0.21	0.01	15.63
Bacteria	Phyllosphere	2022	s__Curtobacterium flaccumfaciens pv. flaccumfaciens ASV123	0	1	-0.86	0.49	70.00
Fungi	Topsoil	2022	s__Curvibasidium cygneicollum ASV42	0	4	-0.35	0.05	62.26
Fungi	Topsoil	2022	s__Cystobasidium slooffiae ASV216	1	0	0.08	0.00	6.29
Fungi	Phyllosphere	2022	s__Cystofilobasidium capitatum ASV181	3	0	0.52	0.24	55.70
Fungi	Phyllosphere	2022	s__Cystofilobasidium infirmominiatum ASV80	4	0	0.61	0.59	45.57
Fungi	Topsoil	2022	s__Cystofilobasidium infirmominiatum ASV80	2	0	0.22	0.11	40.25
Fungi	Endosphere	2022	s__Cystofilobasidium macerans ASV107	1	0	0.14	0.00	13.13
Fungi	Topsoil	2023	s__Cystofilobasidium macerans ASV48	2	0	0.44	0.08	91.67
Fungi	Topsoil	2022	s__Cystofilobasidium macerans ASV666	0	2	-0.12	0.01	19.50
Bacteria	Topsoil	2022	s__Cytophaga hutchinsonii ATCC 33406 ASV886	0	4	-0.31	0.05	69.38
Bacteria	Topsoil	2023	s__Cytophaga hutchinsonii ATCC 33406 ASV886	0	1	-0.29	0.02	89.58
Fungi	Phyllosphere	2022	s__Dactylonectria anthuriicola ASV511	0	1	-0.14	0.00	5.06
Fungi	Phyllosphere	2022	s__Dactylonectria estremocensis ASV81	0	2	-0.30	0.00	37.97
Fungi	Topsoil	2022	s__Dactylonectria estremocensis ASV81	0	3	-0.19	0.48	83.02
Fungi	Phyllosphere	2022	s__Daedaleopsis confragosa ASV880	4	0	0.23	0.00	48.73
Fungi	Phyllosphere	2022	s__Daldinia vanderguchtiae ASV100	1	0	0.11	0.06	72.78
Bacteria	Topsoil	2022	s__Deinococcus radioresistens ASV503	2	0	0.27	0.06	60.00
Bacteria	Topsoil	2023	s__Deinococcus radioresistens ASV503	3	0	0.34	0.03	58.33
Fungi	Topsoil	2022	s__Diaporthe cynaroidis ASV308	0	2	-0.13	0.00	18.24
Fungi	Phyllosphere	2022	s__Diatrype stigma ASV881	1	0	0.16	0.00	55.70
Fungi	Phyllosphere	2022	s__Didymella pomorum ASV24	4	0	0.88	0.93	82.91
Fungi	Topsoil	2022	s__Didymella pomorum ASV24	5	0	0.79	1.43	88.68
Fungi	Topsoil	2023	s__Didymella pomorum ASV24	3	0	0.31	0.93	97.92
Fungi	Phyllosphere	2022	s__Didymella pomorum ASV549	0	5	-0.72	0.00	21.52
Fungi	Topsoil	2022	s__Didymella pomorum ASV549	0	4	-0.39	0.03	11.95
Fungi	Phyllosphere	2022	s__Dioszegia butyracea ASV328	1	0	0.07	0.18	81.65
Fungi	Phyllosphere	2022	s__Dioszegia fristingensis ASV535	1	0	0.24	0.04	70.89
Fungi	Phyllosphere	2022	s__Dioszegia hungarica ASV103	1	0	0.16	0.57	92.41
Fungi	Topsoil	2022	s__Dioszegia hungarica ASV103	1	0	0.19	0.04	85.53
Fungi	Topsoil	2022	s__Diplodia seriata ASV26	1	0	0.19	0.01	75.47
Fungi	Topsoil	2022	s__Dissoconium eucalypti ASV472	4	0	0.34	0.01	61.64
Fungi	Topsoil	2022	s__Emericellopsis minima ASV351	0	3	-0.28	0.13	25.79
Fungi	Topsoil	2022	s__Endophoma elongata ASV141	1	0	0.05	0.24	40.25

Annexes

Fungi	Topsoil	2023	s__Endophoma elongata ASV141	1	0	0.13	0.30	72.92
Fungi	Phyllosphere	2022	s__Epicoccum nigrum ASV252	0	3	-0.62	0.09	51.90
Fungi	Topsoil	2023	s__Epicoccum nigrum ASV7	4	0	0.49	0.16	97.92
Fungi	Phyllosphere	2022	s__Erythrobasidium yunnanense ASV598	3	0	0.52	0.04	55.70
Fungi	Topsoil	2022	s__Erythrobasidium yunnanense ASV598	3	0	0.14	0.00	32.08
Fungi	Phyllosphere	2022	s__Exidia glandulosa ASV892	1	0	0.29	0.02	62.66
Bacteria	Topsoil	2022	s__Exiguobacterium sibiricum 255-15 ASV169	3	0	0.15	0.01	26.88
Bacteria	Topsoil	2023	s__Exiguobacterium sibiricum 255-15 ASV169	0	3	-0.43	0.00	22.92
Fungi	Phyllosphere	2022	s__Exophiala equina ASV202	0	1	-0.17	0.00	27.85
Fungi	Topsoil	2022	s__Exophiala equina ASV202	0	3	-0.13	0.03	45.28
Fungi	Topsoil	2023	s__Exophiala opportunistica ASV426	2	0	0.31	0.09	81.25
Fungi	Phyllosphere	2022	s__Filobasidium magnum ASV625	3	0	0.48	0.02	51.27
Fungi	Topsoil	2022	s__Filobasidium magnum ASV625	2	0	0.15	0.00	21.38
Fungi	Phyllosphere	2022	s__Filobasidium oeirense ASV524	4	0	0.52	0.02	68.35
Fungi	Topsoil	2022	s__Filobasidium oeirense ASV524	3	0	0.26	0.01	45.91
Fungi	Topsoil	2023	s__Filobasidium oeirense ASV524	3	0	0.49	0.02	68.75
Fungi	Phyllosphere	2022	s__Filobasidium wieringae ASV154	4	0	0.65	0.30	75.95
Bacteria	Phyllosphere	2022	s__Flavisolibacter tropicus ASV231	1	0	0.12	0.03	47.50
Bacteria	Topsoil	2022	s__Flavisolibacter tropicus ASV231	3	0	0.13	0.11	93.13
Bacteria	Topsoil	2022	s__Flavobacterium psychrophilum ASV1748	0	3	-0.17	0.03	78.75
Fungi	Phyllosphere	2022	s__Fomes inzengae ASV134	0	1	-0.15	0.03	89.87
Fungi	Topsoil	2023	s__Funneliformis geosporum ASV1403	0	4	-0.42	0.03	37.50
Fungi	Topsoil	2022	s__Fusarium avenaceum ASV25	0	4	-0.31	2.23	92.45
Fungi	Topsoil	2022	s__Fusarium avenaceum ASV946	0	1	-0.12	0.02	93.08
Fungi	Phyllosphere	2022	s__Fusarium brachygibbosum ASV46	1	0	0.38	0.02	36.71
Fungi	Topsoil	2022	s__Fusarium brachygibbosum ASV46	5	0	0.53	0.86	42.14
Fungi	Topsoil	2023	s__Fusarium brachygibbosum ASV46	1	0	0.25	1.11	85.42
Fungi	Topsoil	2022	s__Fusarium brachygibbosum ASV837	5	0	0.37	0.02	35.85
Fungi	Topsoil	2023	s__Fusarium brachygibbosum ASV837	4	0	0.41	0.02	68.75
Fungi	Topsoil	2022	s__Fusarium sporotrichioides ASV537	0	3	-0.23	0.03	39.62
Fungi	Topsoil	2023	s__Fusarium waltergamsii ASV229	0	4	-0.51	0.13	75.00
Fungi	Phyllosphere	2022	s__Fuscoporia ferruginosa ASV1009	0	3	-0.34	0.00	46.20
Fungi	Topsoil	2022	s__Fusicolla acetilerea ASV677	0	2	-0.10	0.02	24.53
Fungi	Phyllosphere	2022	s__Fusicolla aquaeductuum ASV29	0	3	-0.53	0.00	13.92
Fungi	Topsoil	2022	s__Fusicolla aquaeductuum ASV29	0	4	-0.34	0.51	69.81
Fungi	Topsoil	2023	s__Fusicolla aquaeductuum ASV29	0	3	-0.53	0.17	89.58
Fungi	Topsoil	2022	s__Fusicolla septimanifiniscientiae ASV92	0	1	-0.25	0.35	51.57
Fungi	Topsoil	2023	s__Fusicolla septimanifiniscientiae ASV92	0	1	-0.29	0.30	85.42
Bacteria	Topsoil	2022	s__Geodermatophilaceae bacterium URHB0048 ASV203	4	0	0.27	0.12	75.63
Bacteria	Topsoil	2023	s__Geodermatophilaceae bacterium URHB0048 ASV203	1	0	0.06	0.14	85.42
Fungi	Phyllosphere	2022	s__Gibberella intricans ASV16	1	0	0.18	0.06	59.49
Fungi	Topsoil	2022	s__Gibberella intricans ASV16	1	0	0.30	3.75	91.19
Fungi	Topsoil	2022	s__Gibberella intricans ASV587	3	0	0.12	0.02	92.45

Annexes

Fungi	Phyllosphere	2023	s__Gibberella intricans ASV806	2	0	0.46	0.00	19.15
Fungi	Topsoil	2022	s__Gliomastix roseogrisea ASV289	0	3	-0.18	0.08	86.16
Fungi	Topsoil	2023	s__Gliomastix roseogrisea ASV289	0	3	-0.20	0.08	95.83
Fungi	Endosphere	2022	s__Gnomonia virginianae ASV259	3	0	1.00	0.41	31.25
Fungi	Phyllosphere	2022	s__Gnomonia virginianae ASV259	3	0	0.28	0.00	29.11
Fungi	Phyllosphere	2022	s__Golovinomyces artemisiae ASV49	4	0	0.45	0.01	36.08
Fungi	Topsoil	2022	s__Hirsutella lecaniicola ASV52	4	0	0.38	0.00	16.98
Fungi	Topsoil	2022	s__Holtermanniella festucosa ASV86	0	1	-0.18	0.20	68.55
Fungi	Topsoil	2023	s__Holtermanniella festucosa ASV86	1	0	0.30	0.14	89.58
Fungi	Phyllosphere	2022	s__Hormonema macrosporum ASV596	3	0	0.41	0.00	68.35
Fungi	Endosphere	2022	s__Humicola grisea ASV89	2	0	0.16	0.00	10.00
Fungi	Topsoil	2022	s__Humicola olivacea ASV254	0	4	-0.43	0.11	41.51
Fungi	Topsoil	2023	s__Humicola olivacea ASV254	0	1	-0.46	0.13	70.83
Fungi	Topsoil	2022	s__Humicola olivacea ASV382	2	0	0.42	0.07	23.27
Fungi	Topsoil	2023	s__Humicola olivacea ASV382	0	3	-0.25	0.01	60.42
Bacteria	Topsoil	2023	s__Hymenobacter aquaticus ASV698	0	1	-0.11	0.00	6.25
Fungi	Phyllosphere	2022	s__Hypholoma fasciculare ASV1185	1	0	0.14	0.00	44.30
Fungi	Topsoil	2022	s__Hypholoma fasciculare ASV1185	1	0	0.15	0.01	69.18
Fungi	Endosphere	2022	s__Hypomyces microspermus ASV480	0	2	-0.13	0.00	7.50
Fungi	Phyllosphere	2022	s__Ilyonectria lusitanica ASV548	0	3	-0.30	0.00	6.33
Fungi	Topsoil	2022	s__Ilyonectria lusitanica ASV548	0	2	-0.15	0.03	47.17
Fungi	Phyllosphere	2022	s__Ilyonectria macrodidyma ASV76	0	1	-0.25	0.00	44.30
Fungi	Topsoil	2022	s__Ilyonectria macrodidyma ASV76	2	0	0.38	0.45	86.79
Bacteria	Topsoil	2022	s__Isoptericola variabilis ASV170	0	3	-0.12	0.00	17.50
Bacteria	Topsoil	2023	s__Isoptericola variabilis ASV170	0	3	-0.31	0.00	33.33
Fungi	Phyllosphere	2022	s__Itersonilia pannonica ASV14	1	0	0.10	6.90	79.11
Fungi	Phyllosphere	2022	s__Itersonilia perplexans ASV30	4	0	0.63	0.48	91.14
Fungi	Topsoil	2023	s__Itersonilia perplexans ASV30	2	0	0.51	0.17	91.67
Fungi	Phyllosphere	2022	s__Keissleriella cladophila ASV515	2	0	0.32	0.02	27.85
Fungi	Topsoil	2022	s__Keissleriella cladophila ASV515	1	0	0.12	0.00	19.50
Fungi	Phyllosphere	2022	s__Keissleriella rosarum ASV808	2	0	0.28	0.00	34.18
Fungi	Topsoil	2022	s__Keissleriella rosarum ASV808	3	0	0.23	0.00	37.11
Fungi	Topsoil	2023	s__Knufia tsunedae ASV463	2	0	0.42	0.19	72.92
Fungi	Phyllosphere	2022	s__Knufia tsunedae ASV617	0	1	-0.11	0.00	8.86
Fungi	Phyllosphere	2022	s__Kondoa aeria ASV555	0	1	-0.25	0.00	30.38
Bacteria	Topsoil	2022	s__Kouleothrix aurantiaca ASV407	3	0	0.14	0.07	65.00
Bacteria	Topsoil	2023	s__Kouleothrix aurantiaca ASV407	2	0	0.17	0.08	66.67
Bacteria	Topsoil	2023	s__Labilithrix luteola ASV361	0	3	-0.07	0.11	100
Fungi	Topsoil	2022	s__Lectera capsici ASV357	4	0	0.41	0.06	11.32
Fungi	Topsoil	2022	s__Lectera capsici ASV360	4	0	0.45	0.06	13.84
Fungi	Topsoil	2022	s__Lectera longa ASV431	2	0	0.21	0.05	43.40
Fungi	Phyllosphere	2022	s__Lectera longa ASV94	1	0	0.31	0.01	39.24
Fungi	Topsoil	2022	s__Lectera longa ASV94	4	0	0.71	0.36	40.25
Fungi	Topsoil	2023	s__Lectera longa ASV94	4	0	0.67	0.35	68.75
Fungi	Topsoil	2022	s__Leucosporidium fragarium ASV581	2	0	0.22	0.02	52.20
Fungi	Topsoil	2023	s__Leucosporidium fragarium ASV581	2	0	0.49	0.02	52.08

Annexes

Fungi	Phyllosphere	2022	s__Leucosporidium golubevii ASV211	0	5	-0.82	0.08	72.15
Fungi	Topsoil	2022	s__Leucosporidium golubevii ASV211	0	4	-0.37	0.12	70.44
Fungi	Phyllosphere	2022	s__Leucosporidium intermedium ASV278	0	3	-0.51	0.02	66.46
Fungi	Topsoil	2022	s__Leucosporidium intermedium ASV278	0	4	-0.65	0.08	71.70
Fungi	Phyllosphere	2022	s__Leucosporidium scottii ASV410	4	0	0.72	0.10	46.84
Fungi	Topsoil	2022	s__Leucosporidium scottii ASV410	1	0	0.15	0.01	41.51
Fungi	Topsoil	2022	s__Lophiostoma corticola ASV761	0	2	-0.12	0.02	34.59
Fungi	Topsoil	2023	s__Lophiostoma corticola ASV761	0	3	-0.29	0.02	43.75
Fungi	Topsoil	2022	s__Lycoperdon pratense ASV209	0	1	-0.08	0.09	35.85
Fungi	Topsoil	2023	s__Lycoperdon pratense ASV209	0	3	-0.65	0.40	77.08
Bacteria	Topsoil	2022	s__Massilia aurea ASV32	1	0	0.02	0.03	86.25
Bacteria	Topsoil	2023	s__Massilia aurea ASV32	3	0	0.29	0.01	83.33
Bacteria	Topsoil	2023	s__Massilia brevitalea ASV1339	3	0	0.29	0.00	25.00
Bacteria	Topsoil	2022	s__Massilia putida ASV917	3	0	0.16	0.04	71.25
Bacteria	Topsoil	2023	s__Massilia putida ASV917	1	0	0.09	0.06	72.92
Bacteria	Topsoil	2023	s__Massilia varians ASV2128	0	3	-0.23	0.01	79.17
Bacteria	Topsoil	2022	s__Massilia violaceinigra ASV59	4	0	0.42	0.76	90.00
Fungi	Phyllosphere	2022	s__Metacordyceps chlamydosporia ASV590	0	1	-0.13	0.00	3.80
Fungi	Topsoil	2022	s__Metacordyceps chlamydosporia ASV590	0	4	-0.20	0.03	60.38
Fungi	Topsoil	2023	s__Metacordyceps chlamydosporia ASV590	0	4	-0.49	0.02	75.00
Fungi	Topsoil	2022	s__Metarhizium marquandii ASV1067	0	3	-0.23	0.02	23.27
Fungi	Topsoil	2023	s__Metarhizium marquandii ASV1067	0	4	-0.61	0.01	29.17
Fungi	Phyllosphere	2022	s__Metarhizium marquandii ASV226	0	3	-0.30	0.00	8.23
Fungi	Topsoil	2022	s__Metarhizium marquandii ASV226	0	3	-0.31	0.13	40.25
Fungi	Topsoil	2023	s__Metarhizium marquandii ASV226	0	3	-0.51	0.07	56.25
Fungi	Topsoil	2022	s__Metarhizium marquandii ASV640	0	1	-0.19	0.03	32.70
Fungi	Topsoil	2023	s__Metarhizium marquandii ASV640	0	1	-0.41	0.02	31.25
Fungi	Topsoil	2022	s__Metarhizium marquandii ASV802	0	2	-0.18	0.02	38.36
Fungi	Topsoil	2023	s__Metarhizium marquandii ASV802	0	3	-0.26	0.00	25.00
Bacteria	Topsoil	2023	s__Methylobacterium adhaesivum ASV23	3	0	0.27	0.06	100
Bacteria	Topsoil	2023	s__Methylobacterium brachiatum ASV22	2	0	0.14	0.04	95.83
Bacteria	Topsoil	2023	s__Methylobacterium cerastii ASV207	1	0	0.19	0.00	39.58
Bacteria	Topsoil	2023	s__Methylobacterium cerastii ASV334	1	0	0.23	0.00	41.67
Bacteria	Topsoil	2022	s__Methylobacterium isbiliense ASV1222	3	0	0.16	0.02	77.50
Bacteria	Topsoil	2023	s__Methylobacterium marchantiae ASV471	3	0	0.36	0.01	83.33
Bacteria	Topsoil	2023	s__Methylobacterium phyllostachyos ASV466	3	0	0.23	0.00	35.42
Bacteria	Topsoil	2023	s__Methylobacterium soli ASV485	2	0	0.13	0.16	68.75
Bacteria	Topsoil	2023	s__Microbacterium arborescens ASV1239	0	3	-0.25	0.02	85.42
Bacteria	Topsoil	2022	s__Microbacterium oxydans ASV267	0	3	-0.15	0.10	88.75
Bacteria	Topsoil	2023	s__Microbacterium oxydans ASV267	0	1	-0.15	0.08	100
Bacteria	Topsoil	2022	s__Microbacterium saccharophilum ASV129	0	3	-0.25	0.45	88.13
Bacteria	Topsoil	2023	s__Microbacterium saccharophilum ASV129	0	4	-0.26	0.35	100

Annexes

Fungi	Phyllosphere	2022	s__Microsphaeropsis spartii-juncei ASV889	2	0	0.29	0.01	47.47
Bacteria	Topsoil	2022	s__Microvirga ossetica ASV91	0	3	-0.19	0.24	68.75
Bacteria	Topsoil	2023	s__Microvirga ossetica ASV91	0	4	-0.40	0.30	87.50
Bacteria	Topsoil	2022	s__Modestobacter marinus ASV228	1	0	0.01	0.07	80.00
Bacteria	Topsoil	2023	s__Modestobacter marinus ASV228	3	0	0.20	0.11	100
Bacteria	Topsoil	2023	s__Modestobacter versicolor ASV220	3	0	0.39	0.12	72.92
Fungi	Phyllosphere	2022	s__Monochaetia junipericola ASV821	3	0	0.37	0.02	43.67
Fungi	Phyllosphere	2022	s__Monocillium griseo-ochraceum ASV531	0	2	-0.16	0.00	6.96
Fungi	Topsoil	2022	s__Monocillium griseo-ochraceum ASV531	0	4	-0.45	0.05	65.41
Fungi	Topsoil	2023	s__Monocillium griseo-ochraceum ASV531	0	3	-0.35	0.02	64.58
Fungi	Topsoil	2022	s__Monocillium mucidum ASV163	0	1	-0.05	0.21	76.73
Fungi	Phyllosphere	2022	s__Monographella nivalis ASV652	3	0	0.38	0.01	58.23
Fungi	Topsoil	2022	s__Mortierella alpina ASV468	3	0	0.30	0.03	39.62
Fungi	Topsoil	2023	s__Mortierella alpina ASV483	0	1	-0.24	0.06	77.08
Fungi	Topsoil	2022	s__Mortierella amoeboidea ASV740	0	4	-0.33	0.01	25.16
Fungi	Topsoil	2023	s__Mortierella amoeboidea ASV740	0	1	-0.37	0.04	22.92
Fungi	Phyllosphere	2022	s__Mortierella elongata ASV50	1	0	0.11	0.01	50.63
Fungi	Topsoil	2022	s__Mortierella elongata ASV50	3	0	0.55	1.70	81.76
Fungi	Topsoil	2023	s__Mortierella elongata ASV50	2	0	0.24	1.28	100
Fungi	Topsoil	2022	s__Mortierella elongata ASV675	2	0	0.27	0.04	84.91
Fungi	Phyllosphere	2022	s__Mortierella exigua ASV157	0	4	-0.50	0.00	13.29
Fungi	Topsoil	2022	s__Mortierella exigua ASV157	2	0	0.12	0.37	49.69
Fungi	Phyllosphere	2022	s__Mortierella gamsii ASV117	0	3	-0.33	0.00	32.28
Fungi	Topsoil	2022	s__Mortierella gamsii ASV117	0	4	-0.53	0.29	62.26
Fungi	Topsoil	2023	s__Mortierella gamsii ASV117	0	4	-0.65	0.43	91.67
Fungi	Endosphere	2022	s__Mrakiella aquatica ASV379	1	0	0.12	0.00	4.38
Fungi	Topsoil	2022	s__Mrakiella aquatica ASV379	0	4	-0.37	0.03	40.88
Fungi	Topsoil	2022	s__Mrakiella aquatica ASV615	0	4	-0.32	0.01	51.57
Bacteria	Topsoil	2022	s__Mycobacterium asiaticum ASV417	3	0	0.19	0.05	83.75
Bacteria	Topsoil	2023	s__Mycobacterium asiaticum ASV417	3	0	0.18	0.08	75.00
Bacteria	Topsoil	2022	s__Mycobacterium psychrotolerans ASV53	0	4	-0.25	0.62	93.13
Bacteria	Topsoil	2023	s__Mycobacterium psychrotolerans ASV53	0	3	-0.20	1.00	97.92
Bacteria	Topsoil	2023	s__Mycobacterium tuberculosis ASV435	0	3	-0.15	0.13	97.92
Fungi	Phyllosphere	2022	s__Mycosphaerella punctiformis ASV234	3	0	0.43	0.17	83.54
Bacteria	Topsoil	2022	s__Naasia aerilata ASV880	4	0	0.36	0.02	65.00
Bacteria	Topsoil	2023	s__Naasia aerilata ASV880	4	0	0.57	0.05	68.75
Fungi	Phyllosphere	2022	s__Naganishia albida ASV593	2	0	0.26	0.00	32.91
Fungi	Topsoil	2022	s__Naganishia albida ASV593	1	0	0.14	0.00	40.88
Fungi	Phyllosphere	2022	s__Neoascochyta graminicola ASV342	2	0	0.39	0.01	41.77
Fungi	Phyllosphere	2022	s__Neocatenulostroma microsporum ASV766	0	1	-0.39	0.03	56.96
Fungi	Topsoil	2022	s__Neocosmospora rubicola ASV37	4	0	0.32	1.21	93.71
Fungi	Phyllosphere	2022	s__Neoerysiphe galeopsidis ASV282	0	3	-0.34	0.01	53.80
Fungi	Topsoil	2022	s__Neoerysiphe galeopsidis ASV282	0	2	-0.09	0.00	10.06
Fungi	Phyllosphere	2022	s__Neoerysiphe nevoi ASV64	4	0	0.55	0.03	56.96
Fungi	Topsoil	2022	s__Neofusicoccum parvum ASV641	0	1	-0.09	0.00	22.01
Fungi	Phyllosphere	2022	s__Neosetophoma italica ASV122	3	0	0.44	0.06	17.09

Annexes

Bacteria	Phyllosphere	2022	s__Nocardioides aquaticus ASV808	0	1	-0.65	0.06	52.50
Bacteria	Topsoil	2023	s__Nocardioides aquaticus ASV808	2	0	0.13	0.00	56.25
Bacteria	Phyllosphere	2022	s__Nocardioides cavernae ASV37	0	2	-0.45	0.36	81.88
Bacteria	Topsoil	2022	s__Nocardioides cavernae ASV37	1	0	0.02	0.81	92.50
Bacteria	Phyllosphere	2023	s__Nocardioides cavernae ASV37	1	0	0.24	0.31	95.74
Bacteria	Topsoil	2023	s__Nocardioides cavernae ASV37	0	2	-0.13	0.45	100
Bacteria	Phyllosphere	2022	s__Nocardioides sediminis ASV1725	0	2	-0.45	0.01	20.00
Bacteria	Topsoil	2022	s__Nocardioides sediminis ASV1725	0	5	-0.75	0.02	73.13
Bacteria	Topsoil	2023	s__Nocardioides sediminis ASV1725	0	4	-0.51	0.03	87.50
Bacteria	Topsoil	2023	s__Nocardioides tritolerans ASV1608	2	0	0.29	0.02	60.42
Fungi	Phyllosphere	2022	s__Olpidium brassicae ASV404	2	0	0.30	0.00	10.13
Fungi	Topsoil	2022	s__Olpidium brassicae ASV404	1	0	0.11	0.06	13.84
Fungi	Endosphere	2022	s__Operculomyces laminatus ASV620	0	1	-0.09	0.00	6.25
Fungi	Topsoil	2023	s__Operculomyces laminatus ASV620	0	3	-0.39	0.02	18.75
Bacteria	Topsoil	2022	s__Paenibacillus borealis ASV2861	4	0	0.24	0.03	79.38
Bacteria	Topsoil	2022	s__Paenibacillus crassostreae ASV2310	3	0	0.10	0.03	83.75
Fungi	Topsoil	2022	s__Papiliotrema flavescens ASV383	1	0	0.17	0.00	43.40
Fungi	Topsoil	2022	s__Papiliotrema frias ASV816	1	0	0.18	0.00	45.91
Fungi	Phyllosphere	2022	s__Papiliotrema laurentii ASV239	0	3	-0.33	0.00	23.42
Fungi	Phyllosphere	2022	s__Papiliotrema laurentii ASV316	3	0	0.29	0.00	20.89
Fungi	Topsoil	2022	s__Papiliotrema laurentii ASV316	5	0	0.46	0.06	57.86
Fungi	Topsoil	2022	s__Papiliotrema terrestris ASV88	4	0	0.50	0.40	62.89
Fungi	Topsoil	2023	s__Papiliotrema terrestris ASV88	4	0	0.55	0.21	91.67
Bacteria	Phyllosphere	2022	s__Paracoccus homiensis ASV882	0	2	-0.52	0.06	38.75
Fungi	Phyllosphere	2022	s__Paraconiothyrium brasiliense ASV456	3	0	0.38	0.04	48.10
Fungi	Topsoil	2023	s__Paraconiothyrium cyclothyrioides ASV801	0	1	-0.24	0.05	41.67
Fungi	Phyllosphere	2022	s__Paramycosphaerella intermedia ASV870	1	0	0.30	0.02	46.84
Fungi	Phyllosphere	2022	s__Paraphaeosphaeria minitans ASV155	2	0	0.15	0.00	31.01
Fungi	Topsoil	2023	s__Paraphaeosphaeria minitans ASV155	0	4	-0.31	0.45	79.17
Fungi	Topsoil	2022	s__Paraphaeosphaeria neglecta ASV174	0	3	-0.27	0.04	49.69
Fungi	Topsoil	2023	s__Paraphaeosphaeria neglecta ASV174	0	3	-0.53	0.01	64.58
Fungi	Phyllosphere	2022	s__Paraphoma pye ASV752	2	0	0.33	0.00	35.44
Fungi	Topsoil	2022	s__Paraphoma pye ASV752	5	0	0.61	0.02	47.80
Fungi	Topsoil	2023	s__Paraphoma pye ASV752	4	0	0.66	0.01	68.75
Fungi	Topsoil	2022	s__Paraphoma radicina ASV589	4	0	0.43	0.01	64.78
Fungi	Topsoil	2022	s__Penicillium bilaiae ASV474	4	0	0.38	0.05	42.77
Fungi	Topsoil	2022	s__Penicillium citreonigrum ASV584	3	0	0.30	0.04	21.38
Fungi	Phyllosphere	2022	s__Penicillium expansum ASV656	2	0	0.21	0.00	13.29
Fungi	Topsoil	2022	s__Penicillium expansum ASV656	0	4	-0.46	0.03	34.59
Fungi	Topsoil	2023	s__Penicillium expansum ASV656	0	3	-0.33	0.00	33.33
Fungi	Topsoil	2022	s__Penicillium jensenii ASV45	0	5	-0.89	0.83	67.92
Fungi	Topsoil	2023	s__Penicillium jensenii ASV45	0	4	-0.56	1.52	93.75
Fungi	Topsoil	2023	s__Penicillium kongii ASV199	0	4	-0.47	0.02	72.92
Fungi	Topsoil	2022	s__Penicillium roseopurpureum ASV470	0	4	-0.35	0.03	38.36
Fungi	Topsoil	2023	s__Penicillium roseopurpureum ASV470	0	3	-0.53	0.09	52.08

Annexes

Fungi	Topsoil	2022	s__Penicillium simplicissimum ASV428	0	5	-0.40	0.05	36.48
Fungi	Topsoil	2022	s__Penicillium solitum ASV144	0	1	-0.13	0.02	55.97
Fungi	Phyllosphere	2022	s__Penicillium solitum ASV768	0	1	-0.12	0.00	6.33
Fungi	Topsoil	2022	s__Penicillium solitum ASV768	0	1	-0.14	0.03	58.49
Fungi	Topsoil	2022	s__Penicillium solitum ASV898	0	1	-0.12	0.02	47.17
Fungi	Phyllosphere	2022	s__Peniophora lycii ASV886	0	2	-0.18	0.02	42.41
Fungi	Phyllosphere	2022	s__Peniophora rufomarginata ASV1498	3	0	0.20	0.02	50.00
Fungi	Topsoil	2022	s__Peniophora versicolor ASV165	2	0	0.14	0.00	61.64
Fungi	Phyllosphere	2022	s__Peniophora versicolor ASV492	2	0	0.14	0.04	44.94
Fungi	Topsoil	2022	s__Phaeomoniella chlamydospora ASV604	1	0	0.14	0.00	35.22
Fungi	Topsoil	2023	s__Phaeomoniella chlamydospora ASV604	0	4	-0.47	0.01	58.33
Fungi	Topsoil	2022	s__Phaeosphaeria ampeli ASV358	0	3	-0.17	0.13	76.73
Fungi	Topsoil	2023	s__Phaeosphaeria ampeli ASV358	0	3	-0.30	0.02	81.25
Fungi	Topsoil	2022	s__Phaeosphaeria lunariae ASV599	1	0	0.12	0.00	28.93
Fungi	Phyllosphere	2022	s__Phialocephala hiberna ASV514	1	0	0.10	0.00	10.13
Fungi	Topsoil	2022	s__Phialocephala humicola ASV477	0	4	-0.32	0.03	55.35
Fungi	Topsoil	2023	s__Phialocephala humicola ASV477	0	3	-0.45	0.05	58.33
Fungi	Phyllosphere	2022	s__Phialophora cyclaminis ASV367	0	3	-0.40	0.00	13.29
Fungi	Phyllosphere	2022	s__Plagiostoma dilatatum ASV377	1	0	0.15	0.00	28.48
Fungi	Topsoil	2022	s__Plectosphaerella cucumerina ASV31	0	3	-0.20	2.02	88.68
Fungi	Topsoil	2022	s__Plectosphaerella cucumerina ASV645	0	3	-0.14	0.04	89.31
Fungi	Phyllosphere	2022	s__Podosphaera xanthii ASV345	4	0	0.51	0.01	21.52
Fungi	Phyllosphere	2022	s__Protomyces macrosporus ASV437	0	3	-0.52	0.04	60.13
Bacteria	Topsoil	2023	s__Pseudarthrobacter defluvii ASV932	2	0	0.27	0.04	50.00
Bacteria	Topsoil	2023	s__Pseudarthrobacter defluvii ASV95	3	0	0.40	0.49	81.25
Bacteria	Phyllosphere	2022	s__Pseudarthrobacter equi ASV1234	1	0	0.16	0.01	20.00
Bacteria	Topsoil	2022	s__Pseudarthrobacter equi ASV1234	3	0	0.32	0.02	50.63
Bacteria	Topsoil	2023	s__Pseudarthrobacter equi ASV1234	4	0	0.78	0.02	43.75
Bacteria	Topsoil	2022	s__Pseudarthrobacter equi ASV90	2	0	0.36	0.16	78.13
Bacteria	Topsoil	2023	s__Pseudarthrobacter equi ASV90	2	0	0.12	0.18	89.58
Bacteria	Topsoil	2022	s__Pseudarthrobacter oxydans ASV138	4	0	0.45	0.26	53.13
Bacteria	Phyllosphere	2022	s__Pseudarthrobacter sulfonivorans ASV178	1	0	0.14	0.09	50.00
Bacteria	Topsoil	2022	s__Pseudarthrobacter sulfonivorans ASV178	4	0	0.63	0.16	63.75
Bacteria	Topsoil	2023	s__Pseudarthrobacter sulfonivorans ASV178	1	0	0.10	0.11	89.58
Fungi	Topsoil	2022	s__Pseudeurotium ovale ASV781	0	1	-0.21	0.02	62.89
Fungi	Topsoil	2023	s__Pseudeurotium ovale ASV781	0	1	-0.35	0.03	77.08
Fungi	Phyllosphere	2022	s__Pseudoidium neolycopersici ASV588	0	3	-0.44	0.00	15.82
Bacteria	Topsoil	2023	s__Pseudomonas azotoformans ASV76	2	0	0.30	0.01	70.83
Bacteria	Topsoil	2022	s__Pseudomonas graminis ASV47	3	0	0.19	0.06	45.63
Bacteria	Topsoil	2023	s__Pseudomonas graminis ASV47	3	0	0.38	0.01	39.58
Bacteria	Topsoil	2022	s__Pseudomonas rhizosphaerae ASV17	0	2	-0.10	0.01	65.63
Bacteria	Topsoil	2023	s__Pseudomonas rhizosphaerae ASV17	2	0	0.23	0.00	64.58
Bacteria	Topsoil	2022	s__Pseudomonas viridiflava ASV35	2	0	0.11	0.01	33.75
Fungi	Phyllosphere	2022	s__Pseudopeziza medicaginis ASV720	2	0	0.30	0.00	25.95

Annexes

Fungi	Phyllosphere	2023	s__Pseudopeziza medicaginis ASV720	2	0	1.00	0.02	29.79
Fungi	Endosphere	2022	s__Pyrenochaetopsis leptospora ASV85	0	2	-0.16	0.00	36.25
Fungi	Topsoil	2022	s__Pyrenochaetopsis leptospora ASV85	0	4	-0.65	0.50	75.47
Fungi	Topsoil	2023	s__Pyrenochaetopsis leptospora ASV85	0	4	-0.48	0.05	85.42
Fungi	Phyllosphere	2022	s__Pyrenochaetopsis tabarestanensis ASV381	0	3	-0.20	0.00	13.29
Fungi	Topsoil	2022	s__Pyrenochaetopsis tabarestanensis ASV381	0	4	-0.37	0.06	37.11
Fungi	Topsoil	2023	s__Pyrenochaetopsis tabarestanensis ASV381	0	3	-0.35	0.03	37.50
Fungi	Phyllosphere	2022	s__Pyrenophora dictyoides ASV344	0	2	-0.44	0.02	62.66
Fungi	Topsoil	2022	s__Pyrenophora dictyoides ASV344	0	3	-0.23	0.03	39.62
Fungi	Topsoil	2023	s__Pyxidiophora arvernensis ASV700	0	4	-0.51	0.03	81.25
Fungi	Phyllosphere	2022	s__Ramophialophora humicola ASV1111	0	1	-0.18	0.00	3.16
Bacteria	Phyllosphere	2022	s__Rathayibacter festucae ASV52	0	1	-0.88	0.77	82.50
Bacteria	Topsoil	2022	s__Rathayibacter festucae ASV52	1	0	0.04	0.07	90.63
Bacteria	Topsoil	2023	s__Rathayibacter festucae ASV52	3	0	0.35	0.05	100
Fungi	Phyllosphere	2022	s__Resinicium bicolor ASV188	1	0	0.14	0.00	68.35
Bacteria	Topsoil	2023	s__Rhizobium soli ASV96	2	0	0.25	0.01	81.25
Bacteria	Topsoil	2023	s__Rhodococcus fascians ASV1185	1	0	0.22	0.01	64.58
Bacteria	Topsoil	2022	s__Rhodococcus hoagii ASV611	0	2	-0.07	0.05	91.25
Bacteria	Topsoil	2023	s__Rhodococcus hoagii ASV611	0	4	-0.33	0.05	100
Fungi	Topsoil	2022	s__Rhodotorula babjevae ASV235	3	0	0.24	0.02	74.84
Fungi	Topsoil	2023	s__Rhodotorula babjevae ASV235	2	0	0.41	0.01	54.17
Fungi	Topsoil	2022	s__Rhodotorula nothofagi ASV420	0	1	-0.21	0.01	44.65
Fungi	Phyllosphere	2022	s__Rhodotorula nothofagi ASV503	4	0	0.91	0.06	36.08
Fungi	Topsoil	2022	s__Rhodotorula nothofagi ASV503	1	0	0.15	0.00	23.27
Fungi	Phyllosphere	2022	s__Robillarda sessilis ASV322	3	0	0.24	0.00	36.71
Fungi	Topsoil	2022	s__Robillarda sessilis ASV322	5	0	0.56	0.06	72.33
Bacteria	Topsoil	2023	s__Romboutsia hominis ASV975	0	3	-0.26	0.01	75.00
Fungi	Topsoil	2022	s__Sagenomella striatispora ASV543	3	0	0.25	0.04	29.56
Fungi	Topsoil	2023	s__Sagenomella striatispora ASV543	0	1	-0.29	0.01	39.58
Fungi	Topsoil	2022	s__Saitozyma podzolica ASV763	3	0	0.34	0.02	19.50
Fungi	Phyllosphere	2022	s__Sarocladium bactrocephalum ASV213	0	3	-0.58	0.02	60.76
Fungi	Topsoil	2022	s__Sarocladium bactrocephalum ASV213	0	4	-0.50	0.11	81.76
Fungi	Phyllosphere	2022	s__Schizophyllum commune ASV609	3	0	0.46	0.02	59.49
Fungi	Topsoil	2023	s__Sclerotinia sclerotiorum ASV454	1	0	0.12	0.00	14.58
Fungi	Phyllosphere	2022	s__Seimatosporium vitis ASV162	3	0	0.53	0.32	30.38
Fungi	Topsoil	2022	s__Seimatosporium vitis ASV162	3	0	0.13	0.00	28.93
Fungi	Topsoil	2023	s__Selenophoma mahoniae ASV556	1	0	0.31	0.02	35.42
Fungi	Phyllosphere	2022	s__Solicoccozyma phenolica ASV61	0	2	-0.28	0.01	52.53
Fungi	Topsoil	2022	s__Solicoccozyma terricola ASV120	0	1	-0.05	0.29	42.14
Fungi	Phyllosphere	2022	s__Sphaerulina amelanchier ASV400	5	0	0.54	0.08	81.01
Bacteria	Topsoil	2023	s__Sphingomonas aerolata ASV18	3	0	0.20	0.00	87.50
Bacteria	Phyllosphere	2022	s__Sphingomonas astaxanthinifaciens ASV511	0	1	-0.63	0.07	65.00
Bacteria	Topsoil	2022	s__Sphingomonas astaxanthinifaciens ASV511	3	0	0.15	0.02	84.38

Annexes

Bacteria	Phyllosphere	2022	s__Sphingomonas aurantiaca ASV85	0	1	-0.86	0.53	80.00
Bacteria	Topsoil	2022	s__Sphingomonas aurantiaca ASV85	3	0	0.18	0.01	59.38
Bacteria	Topsoil	2023	s__Sphingomonas aurantiaca ASV85	2	0	0.20	0.00	56.25
Bacteria	Phyllosphere	2022	s__Sphingomonas faeni ASV16	0	1	-0.92	3.87	86.88
Bacteria	Topsoil	2023	s__Sphingomonas limnosediminicola ASV1002	3	0	0.25	0.04	77.08
Bacteria	Phyllosphere	2022	s__Sphingomonas panni ASV596	0	3	-0.87	0.11	57.50
Bacteria	Topsoil	2022	s__Sphingomonas prati ASV311	0	3	-0.11	0.01	58.13
Bacteria	Topsoil	2022	s__Sphingomonas sediminicola ASV761	3	0	0.18	0.04	86.25
Bacteria	Topsoil	2023	s__Sphingomonas sediminicola ASV761	2	0	0.10	0.06	100
Bacteria	Topsoil	2022	s__Sphingomonas sediminicola ASV94	1	0	0.04	0.58	93.13
Bacteria	Topsoil	2023	s__Sphingomonas sediminicola ASV94	2	0	0.06	0.52	100
Bacteria	Topsoil	2023	s__Spirosoma aerophilum ASV1813	3	0	0.32	0.00	43.75
Fungi	Phyllosphere	2022	s__Sporobolomyces roseus ASV210	0	2	-0.71	0.22	82.91
Fungi	Topsoil	2022	s__Sporobolomyces roseus ASV210	0	4	-0.31	0.01	50.31
Bacteria	Topsoil	2022	s__Sporosarcina psychrophila ASV1873	2	0	0.19	0.03	73.13
Fungi	Phyllosphere	2022	s__Stagonosporopsis valerianellae ASV219	1	0	0.31	0.01	20.25
Fungi	Phyllosphere	2022	s__Stemphylium beticola ASV485	0	4	-0.74	0.00	22.78
Fungi	Phyllosphere	2022	s__Stemphylium lycii ASV558	0	2	-0.37	0.01	67.72
Fungi	Phyllosphere	2022	s__Stemphylium solani ASV54	0	4	-0.65	0.12	84.81
Fungi	Endosphere	2022	s__Stephanonectria keithii ASV304	2	0	0.23	0.00	8.13
Fungi	Phyllosphere	2022	s__Stephanonectria keithii ASV304	0	2	-0.22	0.00	13.92
Fungi	Topsoil	2022	s__Stephanonectria keithii ASV304	0	4	-0.40	0.09	56.60
Fungi	Topsoil	2023	s__Stephanonectria keithii ASV304	0	4	-0.71	0.08	64.58
Fungi	Phyllosphere	2022	s__Stereum hirsutum ASV484	4	0	0.49	0.06	70.25
Fungi	Topsoil	2022	s__Stereum hirsutum ASV484	1	0	0.07	0.00	25.79
Fungi	Phyllosphere	2022	s__Stereum sanguinolentum ASV407	1	0	0.04	0.02	55.70
Bacteria	Topsoil	2022	s__Streptomyces albidoflavus ASV875	3	0	0.21	0.02	66.25
Bacteria	Topsoil	2022	s__Streptomyces ambofaciens ASV915	3	0	0.21	0.02	69.38
Bacteria	Topsoil	2023	s__Streptomyces ambofaciens ASV915	1	0	0.13	0.04	97.92
Bacteria	Topsoil	2022	s__Streptomyces anulatus ASV221	0	3	-0.14	0.11	88.13
Bacteria	Topsoil	2023	s__Streptomyces anulatus ASV221	0	3	-0.17	0.10	100
Bacteria	Topsoil	2022	s__Streptomyces hygroscopicus ASV708	3	0	0.13	0.08	86.25
Bacteria	Topsoil	2023	s__Streptomyces lydicus ASV820	0	3	-0.36	0.06	91.67
Bacteria	Topsoil	2022	s__Streptomyces xinghaiensis S187 ASV383	3	0	0.13	0.00	12.50
Fungi	Topsoil	2022	s__Striaticonidium brachysporum ASV1207	0	4	-0.40	0.02	32.08
Fungi	Topsoil	2022	s__Striaticonidium cinctum ASV820	3	0	0.23	0.02	12.58
Fungi	Topsoil	2023	s__Striaticonidium cinctum ASV820	3	0	0.31	0.00	8.33
Fungi	Topsoil	2022	s__Symmetrospora coprosmae ASV60	0	1	-0.11	0.04	84.91
Fungi	Topsoil	2022	s__Talaromyces minioluteus ASV789	0	5	-0.66	0.02	33.96
Fungi	Topsoil	2023	s__Talaromyces minioluteus ASV789	0	4	-0.60	0.03	31.25
Fungi	Topsoil	2022	s__Talaromyces primulinus ASV746	0	3	-0.25	0.03	45.28
Fungi	Topsoil	2023	s__Talaromyces primulinus ASV746	0	2	-0.39	0.02	50.00
Fungi	Phyllosphere	2022	s__Taphrina inositophila ASV285	1	0	0.32	0.15	73.42
Fungi	Topsoil	2022	s__Taphrina inositophila ASV285	1	0	0.15	0.00	42.14
Fungi	Phyllosphere	2022	s__Taphrina inositophila ASV754	3	0	0.45	0.03	53.80

Annexes

Fungi	Phyllosphere	2022	s__Tausonia pullulans ASV533	3	0	0.50	0.02	37.34
Fungi	Phyllosphere	2022	s__Terana coerulea ASV562	3	0	0.25	0.07	63.29
Fungi	Phyllosphere	2022	s__Terana coerulea ASV923	1	0	0.10	0.02	58.23
Bacteria	Phyllosphere	2022	s__Terrabacter terrae ASV39	0	1	-0.22	0.13	73.13
Bacteria	Topsoil	2022	s__Terrabacter terrae ASV39	0	2	-0.20	0.69	91.25
Bacteria	Topsoil	2022	s__Terribacillus goriensis ASV1216	1	0	0.10	0.03	48.75
Fungi	Phyllosphere	2022	s__Thelonectria olida ASV354	0	1	-0.15	0.00	5.70
Fungi	Topsoil	2022	s__Thelonectria olida ASV354	0	3	-0.20	0.07	38.36
Fungi	Topsoil	2023	s__Thelonectria olida ASV354	0	3	-0.22	0.24	72.92
Bacteria	Topsoil	2023	s__Thermoactinomyces vulgaris ASV962	0	1	-0.17	0.01	66.67
Bacteria	Topsoil	2022	s__Thermobifida fusca YX ASV913	0	3	-0.19	0.01	23.13
Bacteria	Topsoil	2023	s__Thermobifida fusca YX ASV913	0	3	-0.32	0.01	22.92
Fungi	Phyllosphere	2022	s__Trametes versicolor ASV264	4	0	0.43	0.04	83.54
Fungi	Topsoil	2022	s__Trametes versicolor ASV264	1	0	0.09	0.00	27.67
Fungi	Topsoil	2023	s__Trichocladium opacum ASV525	0	2	-0.40	0.07	77.08
Fungi	Topsoil	2022	s__Trichoderma atroviride ASV96	0	4	-0.41	0.40	85.53
Fungi	Topsoil	2023	s__Trichoderma hamatum ASV299	0	2	-0.37	0.04	54.17
Fungi	Topsoil	2022	s__Trichoderma lixii ASV576	4	0	0.49	0.04	36.48
Fungi	Endosphere	2022	s__Trichoderma virens ASV1092	0	1	-0.10	0.00	2.50
Fungi	Topsoil	2022	s__Trichoderma virens ASV1092	4	0	0.45	0.02	23.27
Fungi	Topsoil	2022	s__Trichoderma virens ASV586	3	0	0.28	0.05	20.75
Fungi	Topsoil	2022	s__Truncatella angustata ASV545	3	0	0.32	0.04	21.38
Fungi	Topsoil	2023	s__Truncatella angustata ASV545	1	0	0.46	0.01	25.00
Bacteria	Topsoil	2022	s__Tumebacillus avium ASV1103	0	3	-0.25	0.05	65.63
Bacteria	Topsoil	2023	s__Tumebacillus avium ASV1103	0	3	-0.41	0.02	83.33
Fungi	Endosphere	2022	s__Udeniomyces pyricola ASV21	0	2	-0.47	0.80	10.00
Fungi	Phyllosphere	2022	s__Udeniomyces pyricola ASV21	0	1	-0.12	4.41	73.42
Fungi	Topsoil	2022	s__Udeniomyces pyricola ASV21	0	3	-0.24	0.13	45.28
Fungi	Topsoil	2022	s__Vishniacozyma carnescens ASV11	0	3	-0.19	0.22	86.16
Fungi	Topsoil	2022	s__Vishniacozyma carnescens ASV331	0	2	-0.09	0.00	73.58
Fungi	Topsoil	2023	s__Vishniacozyma dimennae ASV114	2	0	0.44	0.13	97.92
Fungi	Topsoil	2023	s__Vishniacozyma dimennae ASV79	1	0	0.28	0.22	97.92
Fungi	Topsoil	2022	s__Vishniacozyma globispora ASV421	0	1	-0.11	0.00	45.91
Fungi	Topsoil	2023	s__Vishniacozyma heimaeyensis ASV110	2	0	0.30	0.06	100
Fungi	Phyllosphere	2022	s__Vishniacozyma tephrensis ASV247	4	0	0.75	0.13	77.85
Fungi	Topsoil	2022	s__Vishniacozyma tephrensis ASV416	0	3	-0.23	0.02	61.64
Fungi	Topsoil	2023	s__Vishniacozyma tephrensis ASV416	2	0	0.33	0.00	45.83
Fungi	Topsoil	2022	s__Vishniacozyma victoriae ASV10	0	3	-0.45	3.07	85.53
Fungi	Topsoil	2023	s__Vishniacozyma victoriae ASV10	2	0	0.28	1.37	100
Fungi	Topsoil	2022	s__Vishniacozyma victoriae ASV126	0	3	-0.21	0.03	61.64
Fungi	Phyllosphere	2022	s__Vishniacozyma victoriae ASV283	0	3	-0.30	0.07	96.84
Fungi	Topsoil	2022	s__Vishniacozyma victoriae ASV283	0	3	-0.16	0.06	86.16
Fungi	Topsoil	2023	s__Vishniacozyma victoriae ASV283	1	0	0.29	0.03	93.75
Fungi	Topsoil	2022	s__Vishniacozyma victoriae ASV98	0	3	-0.23	0.10	66.04
Fungi	Phyllosphere	2022	s__Volucrispora graminea ASV785	0	1	-0.14	0.00	7.59
Fungi	Topsoil	2022	s__Volucrispora graminea ASV785	1	0	0.20	0.03	39.62

Annexes

Fungi	Topsoil	2023	s__Volucrispora graminea ASV785	0	1	-0.21	0.00	14.58
Fungi	Topsoil	2022	s__Volutella ciliata ASV73	5	0	0.71	0.37	68.55
Fungi	Topsoil	2023	s__Volutella ciliata ASV73	2	0	0.52	1.00	93.75
Fungi	Phyllosphere	2022	s__Wallemia muriae ASV450	1	0	0.15	0.04	64.56
Bacteria	Topsoil	2022	s__Williamsia faeni ASV528	0	1	-0.04	0.06	86.25
Bacteria	Topsoil	2023	s__Williamsia faeni ASV528	0	3	-0.20	0.05	100
Bacteria	Topsoil	2022	g__1174-901-12 sp ASV81	1	0	0.10	0.00	4.38
Bacteria	Topsoil	2023	g__Abditibacterium sp ASV434	2	0	0.22	0.00	70.83
Bacteria	Topsoil	2023	g__Abditibacterium sp ASV856	3	0	0.34	0.06	87.50
Bacteria	Topsoil	2022	g__Acidibacter sp ASV248	0	4	-0.28	0.25	75.00
Bacteria	Topsoil	2023	g__Acidibacter sp ASV248	0	4	-0.29	0.10	97.92
Bacteria	Topsoil	2022	g__Acidibacter sp ASV827	0	1	-0.02	0.10	91.25
Bacteria	Topsoil	2022	g__Actinocorallia sp ASV430	0	4	-0.30	0.09	58.13
Bacteria	Topsoil	2023	g__Actinocorallia sp ASV430	0	4	-0.49	0.04	60.42
Bacteria	Topsoil	2023	g__Actinomycetospora sp ASV197	0	3	-0.12	0.21	100
Bacteria	Topsoil	2022	g__Actinomycetospora sp ASV269	0	3	-0.30	0.02	70.63
Bacteria	Topsoil	2023	g__Actinomycetospora sp ASV269	0	1	-0.27	0.01	66.67
Bacteria	Topsoil	2022	g__Actinoplanes sp ASV2069	0	3	-0.09	0.03	90.63
Bacteria	Topsoil	2023	g__Actinoplanes sp ASV2069	0	2	-0.09	0.02	100
Bacteria	Topsoil	2022	g__Actinotalea sp ASV1068	5	0	0.61	0.03	42.50
Bacteria	Topsoil	2023	g__Actinotalea sp ASV1068	1	0	0.23	0.01	64.58
Bacteria	Topsoil	2022	g__Adhaeribacter sp ASV686	3	0	0.31	0.04	30.63
Bacteria	Topsoil	2023	g__Adhaeribacter sp ASV748	0	4	-0.39	0.03	85.42
Bacteria	Topsoil	2022	g__Adhaeribacter sp ASV993	0	3	-0.11	0.04	47.50
Bacteria	Topsoil	2023	g__Adhaeribacter sp ASV993	0	3	-0.26	0.04	47.92
Bacteria	Topsoil	2023	g__ADurb.Bin063-1 sp ASV386	2	0	0.13	0.13	95.83
Bacteria	Topsoil	2022	g__Aeromicrobium sp ASV1821	3	0	0.27	0.02	47.50
Bacteria	Topsoil	2023	g__Aeromicrobium sp ASV1821	1	0	0.10	0.04	77.08
Bacteria	Topsoil	2023	g__Aeromicrobium sp ASV618	3	0	0.17	0.05	97.92
Bacteria	Topsoil	2022	g__Agrococcus sp ASV671	1	0	0.09	0.04	47.50
Bacteria	Topsoil	2023	g__Agrococcus sp ASV671	0	1	-0.23	0.02	83.33
Bacteria	Topsoil	2022	g__Agromyces sp ASV1009	0	1	-0.03	0.08	69.38
Bacteria	Topsoil	2023	g__Agromyces sp ASV1009	0	3	-0.23	0.04	85.42
Bacteria	Topsoil	2022	g__Agromyces sp ASV253	1	0	0.02	0.20	83.13
Bacteria	Topsoil	2022	g__alphaI_cluster sp ASV1026	3	0	0.09	0.04	83.13
Bacteria	Topsoil	2023	g__alphaI_cluster sp ASV1026	2	0	0.09	0.04	100
Bacteria	Topsoil	2023	g__alphaI_cluster sp ASV420	0	1	-0.14	0.08	100
Bacteria	Topsoil	2022	g__Altererythrobacter sp ASV1791	0	3	-0.23	0.08	74.38
Bacteria	Topsoil	2023	g__Altererythrobacter sp ASV1791	0	4	-0.44	0.02	93.75
Bacteria	Phyllosphere	2022	g__Amaricoccus sp ASV663	0	3	-0.63	0.02	31.88
Bacteria	Topsoil	2022	g__Amaricoccus sp ASV663	0	4	-0.34	0.05	67.50
Bacteria	Topsoil	2023	g__Amaricoccus sp ASV663	0	4	-0.74	0.03	85.42
Bacteria	Topsoil	2022	g__Amaricoccus sp ASV788	0	3	-0.26	0.05	42.50
Bacteria	Topsoil	2023	g__Amaricoccus sp ASV788	0	4	-0.67	0.02	72.92
Bacteria	Topsoil	2022	g__Amaricoccus sp ASV984	0	3	-0.18	0.03	72.50
Bacteria	Topsoil	2023	g__Amaricoccus sp ASV984	0	4	-0.38	0.02	87.50

Annexes

Bacteria	Phyllosphere	2022	g__Amnibacterium sp ASV1629	2	0	0.20	0.00	18.75
Bacteria	Topsoil	2022	g__Amnibacterium sp ASV1629	3	0	0.21	0.01	41.25
Bacteria	Topsoil	2023	g__Amnibacterium sp ASV1629	3	0	0.42	0.04	45.83
Bacteria	Topsoil	2022	g__Amnibacterium sp ASV409	3	0	0.15	0.01	68.13
Bacteria	Topsoil	2023	g__Amnibacterium sp ASV409	2	0	0.24	0.02	64.58
Bacteria	Topsoil	2023	g__Anaeromyxobacter sp ASV1213	0	4	-0.39	0.03	52.08
Bacteria	Topsoil	2022	g__Anaeromyxobacter sp ASV1897	3	0	0.22	0.01	56.25
Bacteria	Topsoil	2023	g__Anaeromyxobacter sp ASV1897	2	0	0.27	0.03	58.33
Bacteria	Topsoil	2022	g__Anaeromyxobacter sp ASV2399	3	0	0.13	0.02	76.25
Bacteria	Topsoil	2022	g__Anaeromyxobacter sp ASV586	4	0	0.39	0.08	50.00
Bacteria	Phyllosphere	2022	g__Angustibacter sp ASV331	2	0	0.20	0.01	34.38
Bacteria	Topsoil	2022	g__Angustibacter sp ASV331	3	0	0.40	0.07	51.88
Bacteria	Topsoil	2023	g__Angustibacter sp ASV331	4	0	0.79	0.11	68.75
Bacteria	Topsoil	2022	g__Aquipuribacter sp ASV1174	4	0	0.43	0.03	66.25
Bacteria	Topsoil	2022	g__Arenimonas sp ASV1332	0	3	-0.13	0.06	86.88
Bacteria	Topsoil	2023	g__Arenimonas sp ASV1332	0	1	-0.07	0.01	85.42
Bacteria	Topsoil	2022	g__Arenimonas sp ASV2010	3	0	0.11	0.04	82.50
Bacteria	Topsoil	2023	g__Arenimonas sp ASV2010	0	3	-0.22	0.01	87.50
Bacteria	Topsoil	2023	g__Arenimonas sp ASV754	0	2	-0.14	0.02	100
Bacteria	Topsoil	2023	g__Arthrobacter sp ASV828	0	2	-0.42	0.03	66.67
Fungi	Topsoil	2022	g__Articulospora sp ASV145	0	3	-0.27	0.12	32.08
Fungi	Topsoil	2023	g__Articulospora sp ASV145	2	0	0.39	0.61	70.83
Fungi	Topsoil	2022	g__Articulospora sp ASV183	3	0	0.25	0.01	66.04
Fungi	Topsoil	2023	g__Articulospora sp ASV183	3	0	0.54	0.01	33.33
Fungi	Phyllosphere	2022	g__Articulospora sp ASV269	1	0	0.16	0.00	32.91
Fungi	Topsoil	2022	g__Articulospora sp ASV363	4	0	0.32	0.04	58.49
Fungi	Topsoil	2023	g__Articulospora sp ASV363	3	0	0.40	0.11	60.42
Fungi	Topsoil	2022	g__Articulospora sp ASV455	3	0	0.28	0.03	54.09
Fungi	Phyllosphere	2022	g__Articulospora sp ASV479	0	1	-0.16	0.00	13.29
Fungi	Topsoil	2022	g__Articulospora sp ASV479	0	4	-0.31	0.02	25.16
Fungi	Topsoil	2023	g__Articulospora sp ASV479	1	0	0.46	0.10	75.00
Fungi	Topsoil	2022	g__Ascobolus sp ASV601	0	1	-0.14	0.04	13.21
Fungi	Topsoil	2023	g__Ascobolus sp ASV601	0	3	-0.34	0.00	14.58
Fungi	Endosphere	2022	g__Aspergillus sp ASV161	2	0	0.20	0.00	12.50
Fungi	Phyllosphere	2022	g__Aspergillus sp ASV161	0	1	-0.17	0.00	24.05
Fungi	Phyllosphere	2022	g__Aspergillus sp ASV376	0	3	-0.28	0.00	6.96
Fungi	Topsoil	2022	g__Aspergillus sp ASV376	0	4	-0.41	0.04	39.62
Fungi	Topsoil	2023	g__Aspergillus sp ASV376	0	1	-0.26	0.10	66.67
Fungi	Topsoil	2022	g__Aspergillus sp ASV573	4	0	0.49	0.01	25.16
Fungi	Topsoil	2023	g__Aspergillus sp ASV573	3	0	0.61	0.14	37.50
Fungi	Phyllosphere	2022	g__Aspergillus sp ASV724	1	0	0.16	0.01	60.76
Fungi	Topsoil	2022	g__Aspergillus sp ASV724	0	3	-0.17	0.00	35.85
Fungi	Phyllosphere	2022	g__Aspergillus sp ASV77	4	0	0.77	0.17	58.86
Fungi	Topsoil	2022	g__Aspergillus sp ASV77	3	0	0.21	0.02	30.19
Fungi	Phyllosphere	2022	g__Atrocalyx sp ASV111	3	0	0.40	0.12	39.24
Bacteria	Topsoil	2022	g__Aurantisolimonas sp ASV1205	3	0	0.15	0.04	86.25

Annexes

Bacteria	Topsoil	2022	g__Aurantisolimonas sp ASV318	0	2	-0.12	0.00	19.38
Bacteria	Topsoil	2023	g__Aureimonas sp ASV287	1	0	0.10	0.01	91.67
Bacteria	Topsoil	2023	g__Aureimonas sp ASV450	2	0	0.21	0.00	18.75
Bacteria	Topsoil	2022	g__Bacillus sp ASV104	3	0	0.19	0.40	88.75
Bacteria	Phyllosphere	2022	g__Bacillus sp ASV1057	1	0	0.13	0.00	13.13
Bacteria	Topsoil	2022	g__Bacillus sp ASV1612	0	2	-0.10	0.04	61.25
Bacteria	Topsoil	2023	g__Bacillus sp ASV1612	0	1	-0.19	0.02	89.58
Bacteria	Phyllosphere	2022	g__Bacillus sp ASV262	0	2	-0.51	0.02	33.75
Bacteria	Topsoil	2022	g__Bacillus sp ASV262	0	3	-0.18	0.12	56.88
Bacteria	Topsoil	2023	g__Bacillus sp ASV262	0	2	-0.26	0.09	95.83
Bacteria	Phyllosphere	2022	g__Bacillus sp ASV317	0	3	-0.65	0.22	65.63
Bacteria	Topsoil	2022	g__Bacillus sp ASV317	0	3	-0.16	0.16	88.75
Bacteria	Phyllosphere	2022	g__Bacillus sp ASV484	4	0	0.26	0.01	21.25
Bacteria	Topsoil	2022	g__Bacillus sp ASV484	5	0	0.85	0.05	53.75
Bacteria	Topsoil	2023	g__Bacillus sp ASV484	4	0	0.87	0.07	70.83
Bacteria	Topsoil	2022	g__Bacillus sp ASV581	0	3	-0.19	0.11	38.75
Bacteria	Topsoil	2023	g__Bacillus sp ASV581	0	3	-0.42	0.03	89.58
Bacteria	Topsoil	2022	g__Bacillus sp ASV80	0	1	-0.05	0.41	82.50
Bacteria	Topsoil	2023	g__Bacillus sp ASV80	0	3	-0.24	0.34	97.92
Bacteria	Topsoil	2022	g__Belnapia sp ASV1228	3	0	0.17	0.01	77.50
Bacteria	Topsoil	2023	g__Belnapia sp ASV1228	2	0	0.20	0.03	79.17
Fungi	Topsoil	2022	g__Bensingtonia sp ASV101	0	1	-0.06	0.03	67.30
Fungi	Phyllosphere	2022	g__Bensingtonia sp ASV466	0	2	-0.21	0.03	88.61
Bacteria	Phyllosphere	2022	g__Blastococcus sp ASV46	1	0	0.05	0.22	71.25
Bacteria	Topsoil	2022	g__Blastococcus sp ASV46	3	0	0.22	0.94	93.75
Bacteria	Topsoil	2023	g__Blastococcus sp ASV46	3	0	0.17	0.88	100
Bacteria	Phyllosphere	2022	g__Blastococcus sp ASV662	2	0	0.16	0.01	18.13
Bacteria	Topsoil	2022	g__Blastococcus sp ASV662	1	0	0.18	0.05	40.00
Bacteria	Topsoil	2022	g__Blastococcus sp ASV70	2	0	0.11	0.70	91.88
Bacteria	Topsoil	2023	g__Blastococcus sp ASV70	0	1	-0.11	0.64	100
Bacteria	Topsoil	2022	g__Bradyrhizobium sp ASV122	1	0	0.01	0.42	90.63
Bacteria	Topsoil	2022	g__Bradyrhizobium sp ASV3357	2	0	0.17	0.01	61.25
Bacteria	Topsoil	2022	g__Bradyrhizobium sp ASV504	1	0	0.04	0.04	86.88
Bacteria	Topsoil	2023	g__Bradyrhizobium sp ASV504	3	0	0.25	0.11	93.75
Bacteria	Topsoil	2023	g__Bradyrhizobium sp ASV901	2	0	0.19	0.02	62.50
Bacteria	Topsoil	2023	g__Bradyrhizobium sp ASV996	0	3	-0.22	0.02	97.92
Bacteria	Topsoil	2022	g__Bryobacter sp ASV1011	1	0	0.03	0.02	84.38
Bacteria	Topsoil	2023	g__Bryobacter sp ASV1011	1	0	0.04	0.08	97.92
Bacteria	Topsoil	2022	g__Bryobacter sp ASV1443	3	0	0.14	0.03	75.00
Bacteria	Topsoil	2022	g__Bryobacter sp ASV990	1	0	0.05	0.03	58.13
Bacteria	Topsoil	2022	g__Caenimonas sp ASV1098	0	2	-0.09	0.03	92.50
Bacteria	Topsoil	2022	g__Caenimonas sp ASV1134	0	3	-0.16	0.03	91.25
Bacteria	Topsoil	2023	g__Caenimonas sp ASV1134	0	4	-0.36	0.01	95.83
Bacteria	Topsoil	2022	g__Caenimonas sp ASV545	0	1	-0.02	0.06	83.75
Bacteria	Phyllosphere	2022	g__Candidatus_Alysiosphaera sp ASV1497	0	1	-0.42	0.00	19.38
Bacteria	Topsoil	2022	g__Candidatus_Alysiosphaera sp ASV1497	0	3	-0.19	0.04	56.25

Annexes

Bacteria	Topsoil	2023	g__Candidatus_Alysiosphaera sp ASV1497	0	4	-0.49	0.02	77.08
Bacteria	Topsoil	2023	g__Candidatus_Alysiosphaera sp ASV358	0	3	-0.25	0.15	77.08
Bacteria	Topsoil	2023	g__Candidatus_Alysiosphaera sp ASV764	0	4	-0.25	0.03	100
Bacteria	Topsoil	2023	g__Candidatus_Alysiosphaera sp ASV925	0	3	-0.33	0.05	89.58
Bacteria	Topsoil	2022	g__Candidatus_Koribacter sp ASV1123	1	0	0.08	0.01	36.88
Bacteria	Topsoil	2023	g__Candidatus_Solibacter sp ASV1503	3	0	0.17	0.04	64.58
Bacteria	Topsoil	2022	g__Candidatus_Solibacter sp ASV438	4	0	0.26	0.09	83.75
Bacteria	Topsoil	2022	g__Candidatus_Solibacter sp ASV890	3	0	0.17	0.05	85.63
Bacteria	Topsoil	2023	g__Candidatus_Solibacter sp ASV890	1	0	0.03	0.08	97.92
Bacteria	Phyllosphere	2022	g__Candidatus_Udaeobacter sp ASV1838	1	0	0.20	0.01	19.38
Bacteria	Topsoil	2022	g__Candidatus_Udaeobacter sp ASV1838	2	0	0.10	0.05	54.38
Bacteria	Topsoil	2023	g__Cellulomonas sp ASV114	0	2	-0.09	0.14	100
Bacteria	Topsoil	2022	g__Cellulomonas sp ASV132	1	0	0.01	0.29	91.88
Bacteria	Topsoil	2022	g__Cellulomonas sp ASV929	4	0	0.39	0.04	24.38
Fungi	Phyllosphere	2022	g__Ceratobasidium sp ASV106	2	0	0.18	0.02	72.15
Fungi	Phyllosphere	2022	g__Ceratobasidium sp ASV253	3	0	0.27	0.01	63.29
Fungi	Endosphere	2022	g__Cercophora sp ASV189	2	0	0.23	0.00	19.38
Fungi	Phyllosphere	2022	g__Cercophora sp ASV189	0	3	-0.43	0.00	22.78
Fungi	Topsoil	2022	g__Cercophora sp ASV189	0	1	-0.14	0.30	78.62
Fungi	Topsoil	2022	g__Cercophora sp ASV582	0	3	-0.28	0.02	35.22
Fungi	Topsoil	2023	g__Chaetomium sp ASV368	0	3	-0.22	0.02	89.58
Fungi	Topsoil	2022	g__Chloridium sp ASV622	0	3	-0.20	0.03	33.33
Bacteria	Topsoil	2022	g__Chryseolinea sp ASV1368	0	3	-0.20	0.02	73.13
Bacteria	Topsoil	2023	g__Chryseolinea sp ASV1368	0	3	-0.24	0.01	87.50
Bacteria	Topsoil	2022	g__Chryseolinea sp ASV305	0	3	-0.28	0.13	75.63
Bacteria	Topsoil	2023	g__Chryseolinea sp ASV305	0	4	-0.63	0.07	77.08
Bacteria	Topsoil	2022	g__Chryseolinea sp ASV518	0	3	-0.15	0.06	81.25
Bacteria	Topsoil	2023	g__Chryseolinea sp ASV518	0	4	-0.38	0.06	95.83
Bacteria	Topsoil	2022	g__CL500-29_marine_group sp ASV576	0	2	-0.07	0.07	90.00
Bacteria	Topsoil	2023	g__CL500-29_marine_group sp ASV576	0	1	-0.14	0.04	100
Bacteria	Topsoil	2022	g__CL500-29_marine_group sp ASV696	2	0	0.18	0.05	81.88
Bacteria	Topsoil	2023	g__CL500-29_marine_group sp ASV696	1	0	0.26	0.04	75.00
Bacteria	Topsoil	2022	g__CL500-29_marine_group sp ASV898	0	3	-0.20	0.05	74.38
Bacteria	Topsoil	2023	g__CL500-29_marine_group sp ASV898	0	4	-0.53	0.02	81.25
Bacteria	Topsoil	2022	g__CL500-29_marine_group sp ASV919	0	3	-0.16	0.06	78.75
Bacteria	Topsoil	2023	g__CL500-29_marine_group sp ASV919	0	2	-0.25	0.05	91.67
Fungi	Topsoil	2022	g__Cladophialophora sp ASV866	0	4	-0.27	0.01	24.53
Fungi	Topsoil	2023	g__Cladophialophora sp ASV866	0	3	-0.34	0.07	27.08
Fungi	Topsoil	2022	g__Cladosporium sp ASV223	0	3	-0.24	0.01	56.60
Bacteria	Topsoil	2022	g__Clostridium_sensu_stricto_1 sp ASV1202	3	0	0.19	0.03	71.88
Bacteria	Topsoil	2022	g__Clostridium_sensu_stricto_1 sp ASV1376	4	0	0.26	0.03	72.50
Bacteria	Topsoil	2023	g__Clostridium_sensu_stricto_13 sp ASV315	0	1	-0.11	0.10	95.83
Bacteria	Topsoil	2022	g__Conexibacter sp ASV1073	0	3	-0.12	0.04	77.50
Bacteria	Topsoil	2022	g__Conexibacter sp ASV1307	4	0	0.29	0.03	89.38

Annexes

Bacteria	Topsoil	2023	g__Conexibacter sp ASV1307	3	0	0.19	0.04	100
Bacteria	Topsoil	2023	g__Conexibacter sp ASV834	2	0	0.12	0.05	100
Fungi	Topsoil	2022	g__Coniochaeta sp ASV323	3	0	0.19	0.06	64.15
Fungi	Phyllosphere	2022	g__Coniochaeta sp ASV683	1	0	0.16	0.00	16.46
Fungi	Topsoil	2022	g__Coniochaeta sp ASV683	2	0	0.11	0.02	42.77
Fungi	Topsoil	2022	g__Constantinomyces sp ASV968	1	0	0.10	0.00	18.24
Fungi	Topsoil	2022	g__Coprinellus sp ASV828	0	3	-0.12	0.00	10.69
Fungi	Topsoil	2022	g__Coprinopsis sp ASV1141	1	0	0.11	0.00	18.24
Bacteria	Topsoil	2022	g__Craurococcus-Caldovatus sp ASV693	1	0	0.08	0.05	43.75
Bacteria	Topsoil	2022	g__Crossiella sp ASV468	0	2	-0.16	0.04	46.25
Bacteria	Topsoil	2023	g__Defluviicoccus sp ASV921	0	3	-0.45	0.05	56.25
Bacteria	Topsoil	2023	g__Deinococcus sp ASV86	2	0	0.26	0.01	54.17
Bacteria	Topsoil	2023	g__Demequina sp ASV1645	0	4	-0.41	0.01	83.33
Fungi	Phyllosphere	2022	g__Diaporthe sp ASV776	3	0	0.43	0.00	40.51
Fungi	Phyllosphere	2022	g__Didymella sp ASV221	3	0	0.52	0.07	63.29
Fungi	Topsoil	2022	g__Didymella sp ASV221	4	0	0.44	0.07	57.86
Fungi	Topsoil	2023	g__Didymella sp ASV221	3	0	0.56	0.08	58.33
Bacteria	Topsoil	2023	g__Domibacillus sp ASV1266	0	2	-0.20	0.02	68.75
Bacteria	Topsoil	2023	g__Dongia sp ASV1257	0	3	-0.35	0.03	72.92
Bacteria	Topsoil	2022	g__Duganella sp ASV1986	3	0	0.15	0.04	88.75
Bacteria	Topsoil	2023	g__Duganella sp ASV1986	0	3	-0.18	0.02	97.92
Bacteria	Topsoil	2022	g__Duganella sp ASV634	4	0	0.28	0.07	85.63
Bacteria	Topsoil	2023	g__Duganella sp ASV634	3	0	0.38	0.04	95.83
Bacteria	Topsoil	2022	g__Duganella sp ASV685	3	0	0.17	0.02	74.38
Bacteria	Topsoil	2022	g__Edaphobaculum sp ASV3585	0	2	-0.13	0.03	80.00
Bacteria	Topsoil	2023	g__Edaphobaculum sp ASV3585	0	2	-0.12	0.02	91.67
Bacteria	Topsoil	2023	g__Ellin517 sp ASV1643	3	0	0.36	0.03	87.50
Bacteria	Topsoil	2023	g__Ellin517 sp ASV602	3	0	0.11	0.05	97.92
Bacteria	Topsoil	2022	g__Ellin517 sp ASV755	0	3	-0.20	0.05	81.25
Bacteria	Topsoil	2023	g__Ellin517 sp ASV755	0	3	-0.18	0.04	100
Bacteria	Topsoil	2022	g__Ellin517 sp ASV860	0	3	-0.12	0.04	84.38
Bacteria	Topsoil	2022	g__Ellin6067 sp ASV1627	0	2	-0.09	0.03	63.13
Bacteria	Topsoil	2023	g__Ellin6067 sp ASV1627	0	3	-0.36	0.02	68.75
Bacteria	Topsoil	2022	g__Ellin6067 sp ASV1742	3	0	0.19	0.04	75.00
Bacteria	Topsoil	2022	g__Ellin6067 sp ASV219	0	4	-0.23	0.17	78.13
Bacteria	Topsoil	2023	g__Ellin6067 sp ASV259	0	1	-0.19	0.09	97.92
Bacteria	Topsoil	2022	g__Ellin6067 sp ASV289	0	4	-0.32	0.16	87.50
Bacteria	Topsoil	2023	g__Ellin6067 sp ASV289	0	4	-0.39	0.05	93.75
Bacteria	Topsoil	2022	g__Ellin6067 sp ASV583	0	1	-0.03	0.17	81.88
Bacteria	Topsoil	2023	g__Ellin6067 sp ASV583	0	4	-0.45	0.06	93.75
Bacteria	Topsoil	2023	g__Ellin6067 sp ASV681	2	0	0.40	0.03	70.83
Fungi	Topsoil	2022	g__Emericellopsis sp ASV727	0	1	-0.16	0.04	15.72
Bacteria	Phyllosphere	2022	g__Exiguobacterium sp ASV260	0	1	-0.65	0.38	13.75
Bacteria	Topsoil	2022	g__Exiguobacterium sp ASV260	2	0	0.15	0.01	29.38
Bacteria	Topsoil	2023	g__Exiguobacterium sp ASV260	0	3	-0.35	0.01	27.08
Fungi	Endosphere	2022	g__Exophiala sp ASV561	0	1	-0.10	0.00	2.50

Annexes

Fungi	Phyllosphere	2022	g__Exophiala sp ASV561	0	1	-0.14	0.00	5.70
Fungi	Phyllosphere	2022	g__Exophiala sp ASV637	0	3	-0.60	0.02	20.25
Fungi	Phyllosphere	2022	g__Exophiala sp ASV777	0	1	-0.14	0.00	7.59
Fungi	Phyllosphere	2022	g__Exophiala sp ASV91	0	1	-0.24	0.00	33.54
Fungi	Topsoil	2022	g__Exophiala sp ASV91	0	4	-0.49	0.36	67.92
Fungi	Topsoil	2023	g__Exophiala sp ASV91	0	3	-0.43	0.41	81.25
Bacteria	Topsoil	2022	g__Ferruginibacter sp ASV1046	0	3	-0.12	0.03	83.75
Bacteria	Topsoil	2023	g__Ferruginibacter sp ASV1046	0	3	-0.25	0.02	91.67
Bacteria	Topsoil	2022	g__Ferruginibacter sp ASV1280	0	3	-0.14	0.04	88.13
Bacteria	Topsoil	2023	g__Ferruginibacter sp ASV1280	0	2	-0.27	0.03	91.67
Bacteria	Topsoil	2022	g__Ferruginibacter sp ASV1333	0	3	-0.16	0.03	75.00
Bacteria	Topsoil	2023	g__Ferruginibacter sp ASV1333	0	4	-0.60	0.01	66.67
Bacteria	Topsoil	2022	g__Ferruginibacter sp ASV1747	3	0	0.15	0.02	79.38
Bacteria	Topsoil	2023	g__Ferruginibacter sp ASV1747	1	0	0.19	0.01	89.58
Bacteria	Topsoil	2022	g__Ferruginibacter sp ASV1967	0	3	-0.17	0.03	86.25
Bacteria	Topsoil	2023	g__Ferruginibacter sp ASV1967	0	3	-0.24	0.01	77.08
Bacteria	Topsoil	2023	g__FFCH7168 sp ASV1345	3	0	0.26	0.03	58.33
Bacteria	Topsoil	2022	g__FFCH7168 sp ASV974	3	0	0.14	0.03	58.13
Bacteria	Phyllosphere	2022	g__Fictibacillus sp ASV961	0	1	-0.29	0.00	8.13
Bacteria	Topsoil	2022	g__Fictibacillus sp ASV961	0	4	-0.34	0.03	50.63
Bacteria	Topsoil	2023	g__Fictibacillus sp ASV961	0	3	-0.33	0.03	68.75
Bacteria	Phyllosphere	2022	g__Flavisolibacter sp ASV1179	0	1	-0.35	0.00	13.75
Bacteria	Topsoil	2023	g__Flavisolibacter sp ASV1179	3	0	0.22	0.02	66.67
Bacteria	Topsoil	2022	g__Flavisolibacter sp ASV1898	3	0	0.20	0.02	73.13
Bacteria	Topsoil	2023	g__Flavisolibacter sp ASV1898	2	0	0.28	0.02	89.58
Bacteria	Topsoil	2022	g__Flavisolibacter sp ASV493	0	1	-0.11	0.05	91.25
Bacteria	Topsoil	2023	g__Flavisolibacter sp ASV493	0	3	-0.10	0.07	100
Bacteria	Topsoil	2022	g__Flavisolibacter sp ASV629	1	0	0.02	0.08	90.63
Bacteria	Topsoil	2023	g__Flavisolibacter sp ASV629	3	0	0.17	0.10	100
Bacteria	Phyllosphere	2022	g__Flavisolibacter sp ASV678	2	0	0.20	0.01	29.38
Bacteria	Topsoil	2022	g__Flavisolibacter sp ASV678	3	0	0.20	0.10	83.13
Bacteria	Topsoil	2022	g__Flavisolibacter sp ASV902	3	0	0.18	0.03	88.13
Bacteria	Topsoil	2022	g__Friedmanniella sp ASV30	1	0	0.02	0.09	86.88
Bacteria	Topsoil	2023	g__Friedmanniella sp ASV30	2	0	0.18	0.09	100
Bacteria	Topsoil	2022	g__Frigoribacterium sp ASV43	1	0	0.05	0.03	88.13
Bacteria	Topsoil	2023	g__Frigoribacterium sp ASV43	2	0	0.30	0.01	85.42
Bacteria	Topsoil	2022	g__Frondihabitans sp ASV119	1	0	0.04	0.02	74.38
Fungi	Topsoil	2022	g__Fusarium sp ASV1127	0	1	-0.05	0.02	94.97
Fungi	Phyllosphere	2022	g__Fusarium sp ASV3	1	0	0.10	0.12	63.92
Fungi	Topsoil	2022	g__Fusarium sp ASV329	1	0	0.16	0.12	94.97
Fungi	Topsoil	2022	g__Fusarium sp ASV366	2	0	0.17	0.10	94.97
Fungi	Topsoil	2022	g__Fusarium sp ASV414	2	0	0.15	0.05	94.97
Fungi	Phyllosphere	2022	g__Fusarium sp ASV607	0	1	-0.13	0.00	37.97
Fungi	Topsoil	2022	g__Fusarium sp ASV607	1	0	0.10	0.03	96.86
Fungi	Topsoil	2022	g__Fusarium sp ASV738	0	1	-0.08	0.03	90.57
Fungi	Topsoil	2022	g__Fusarium sp ASV767	0	3	-0.25	0.02	10.06

Annexes

Fungi	Endosphere	2022	g__Fusicolla sp ASV750	1	0	0.09	0.00	2.50
Fungi	Topsoil	2022	g__Fusicolla sp ASV750	0	4	-0.36	0.02	33.33
Bacteria	Topsoil	2022	g__Gaiella sp ASV1001	4	0	0.33	0.06	58.13
Bacteria	Topsoil	2023	g__Gaiella sp ASV1001	4	0	0.38	0.01	81.25
Bacteria	Phyllosphere	2022	g__Gaiella sp ASV102	3	0	0.23	0.01	38.13
Bacteria	Topsoil	2022	g__Gaiella sp ASV102	3	0	0.25	0.23	75.00
Bacteria	Topsoil	2023	g__Gaiella sp ASV102	1	0	0.11	0.41	91.67
Bacteria	Phyllosphere	2022	g__Gaiella sp ASV1076	1	0	0.13	0.01	10.00
Bacteria	Topsoil	2022	g__Gaiella sp ASV1076	4	0	0.33	0.05	43.75
Bacteria	Topsoil	2023	g__Gaiella sp ASV1076	1	0	0.12	0.06	75.00
Bacteria	Topsoil	2022	g__Gaiella sp ASV1255	0	2	-0.09	0.04	46.88
Bacteria	Topsoil	2023	g__Gaiella sp ASV1255	0	3	-0.25	0.05	54.17
Bacteria	Topsoil	2022	g__Gaiella sp ASV136	0	1	-0.04	0.53	78.13
Bacteria	Topsoil	2023	g__Gaiella sp ASV136	0	1	-0.12	0.41	95.83
Bacteria	Topsoil	2023	g__Gaiella sp ASV1395	0	4	-0.63	0.01	52.08
Bacteria	Topsoil	2022	g__Gaiella sp ASV1454	0	3	-0.18	0.02	45.00
Bacteria	Topsoil	2022	g__Gaiella sp ASV172	0	1	-0.06	0.43	76.25
Bacteria	Topsoil	2023	g__Gaiella sp ASV172	0	2	-0.22	0.45	95.83
Bacteria	Phyllosphere	2022	g__Gaiella sp ASV1723	0	1	-0.37	0.00	15.63
Bacteria	Topsoil	2022	g__Gaiella sp ASV1723	0	3	-0.16	0.03	73.13
Bacteria	Topsoil	2023	g__Gaiella sp ASV1723	0	4	-0.32	0.03	66.67
Bacteria	Topsoil	2023	g__Gaiella sp ASV192	0	2	-0.25	0.21	85.42
Bacteria	Phyllosphere	2022	g__Gaiella sp ASV258	1	0	0.16	0.04	36.88
Bacteria	Topsoil	2023	g__Gaiella sp ASV258	1	0	0.08	0.12	95.83
Bacteria	Topsoil	2022	g__Gaiella sp ASV283	0	3	-0.19	0.24	71.25
Bacteria	Topsoil	2023	g__Gaiella sp ASV283	0	1	-0.21	0.14	85.42
Bacteria	Topsoil	2022	g__Gaiella sp ASV320	0	3	-0.17	0.19	50.00
Bacteria	Topsoil	2023	g__Gaiella sp ASV320	0	2	-0.31	0.07	81.25
Bacteria	Topsoil	2022	g__Gaiella sp ASV631	0	3	-0.32	0.06	45.00
Bacteria	Topsoil	2023	g__Gaiella sp ASV631	0	4	-0.66	0.04	62.50
Bacteria	Topsoil	2022	g__Gaiella sp ASV779	0	4	-0.43	0.04	32.50
Bacteria	Topsoil	2023	g__Gaiella sp ASV779	0	3	-0.48	0.05	47.92
Bacteria	Topsoil	2022	g__Gaiella sp ASV885	1	0	0.19	0.02	51.88
Bacteria	Topsoil	2023	g__Gaiella sp ASV885	4	0	0.37	0.05	70.83
Bacteria	Topsoil	2022	g__Gaiella sp ASV973	2	0	0.08	0.04	61.25
Bacteria	Topsoil	2023	g__Gaiella sp ASV973	3	0	0.20	0.02	68.75
Bacteria	Topsoil	2022	g__Galbitalea sp ASV322	1	0	0.01	0.09	93.13
Bacteria	Topsoil	2022	g__Galbitalea sp ASV655	0	2	-0.11	0.06	80.00
Bacteria	Topsoil	2023	g__Galbitalea sp ASV655	0	3	-0.23	0.03	97.92
Bacteria	Topsoil	2022	g__Geminicoccus sp ASV784	3	0	0.13	0.02	83.13
Bacteria	Topsoil	2023	g__Geminicoccus sp ASV784	1	0	0.03	0.03	100
Bacteria	Phyllosphere	2022	g__Gemmatimonas sp ASV1110	4	0	0.30	0.02	35.00
Bacteria	Topsoil	2022	g__Gemmatimonas sp ASV1110	5	0	0.61	0.05	79.38
Bacteria	Topsoil	2023	g__Gemmatimonas sp ASV1110	2	0	0.46	0.05	87.50
Bacteria	Topsoil	2022	g__Gemmatimonas sp ASV1293	0	2	-0.12	0.04	65.00
Bacteria	Topsoil	2023	g__Gemmatimonas sp ASV1293	0	4	-0.37	0.02	83.33

Annexes

Bacteria	Topsoil	2022	g__Gemmatimonas sp ASV1312	0	2	-0.16	0.04	82.50
Bacteria	Topsoil	2023	g__Gemmatimonas sp ASV1312	0	3	-0.17	0.03	97.92
Bacteria	Topsoil	2022	g__Gemmatimonas sp ASV1342	3	0	0.25	0.03	18.13
Bacteria	Phyllosphere	2022	g__Gemmatimonas sp ASV1351	1	0	0.18	0.01	23.75
Bacteria	Topsoil	2022	g__Gemmatimonas sp ASV1351	3	0	0.16	0.03	87.50
Bacteria	Topsoil	2023	g__Gemmatimonas sp ASV1394	2	0	0.38	0.05	60.42
Bacteria	Topsoil	2022	g__Gemmatimonas sp ASV153	3	0	0.12	0.22	89.38
Bacteria	Topsoil	2023	g__Gemmatimonas sp ASV153	0	3	-0.09	0.17	100
Bacteria	Topsoil	2022	g__Gemmatimonas sp ASV391	0	1	-0.02	0.11	90.00
Bacteria	Topsoil	2023	g__Gemmatimonas sp ASV391	0	3	-0.11	0.11	100
Bacteria	Phyllosphere	2022	g__Gemmatimonas sp ASV557	0	1	-0.56	0.01	23.13
Bacteria	Topsoil	2022	g__Gemmatimonas sp ASV557	0	1	-0.04	0.08	51.88
Bacteria	Topsoil	2022	g__Gemmatimonas sp ASV687	1	0	0.07	0.04	55.00
Bacteria	Topsoil	2023	g__Gemmatimonas sp ASV687	3	0	0.41	0.05	54.17
Bacteria	Topsoil	2022	g__Gemmatimonas sp ASV835	4	0	0.33	0.05	81.25
Bacteria	Topsoil	2023	g__Gemmatimonas sp ASV835	2	0	0.13	0.02	95.83
Bacteria	Topsoil	2022	g__Gemmatimonas sp ASV916	3	0	0.13	0.05	85.00
Fungi	Phyllosphere	2022	g__Genolevuria sp ASV793	0	3	-0.55	0.00	20.25
Fungi	Topsoil	2022	g__Genolevuria sp ASV793	0	4	-0.32	0.02	10.69
Bacteria	Topsoil	2023	g__Geodermatophilus sp ASV187	3	0	0.32	0.18	77.08
Bacteria	Topsoil	2022	g__Geodermatophilus sp ASV41	3	0	0.25	0.65	92.50
Bacteria	Topsoil	2023	g__Geodermatophilus sp ASV41	3	0	0.13	0.61	100
Fungi	Phyllosphere	2022	g__Golovinomyces sp ASV224	5	0	0.72	0.01	51.27
Fungi	Phyllosphere	2022	g__Golovinomyces sp ASV501	3	0	0.24	0.01	32.28
Bacteria	Topsoil	2022	g__Haliangium sp ASV1106	0	3	-0.15	0.03	65.63
Bacteria	Topsoil	2023	g__Haliangium sp ASV1106	0	4	-0.48	0.03	93.75
Bacteria	Topsoil	2023	g__Haliangium sp ASV1119	0	1	-0.05	0.03	89.58
Bacteria	Topsoil	2022	g__Haliangium sp ASV264	0	4	-0.26	0.15	71.88
Bacteria	Topsoil	2023	g__Haliangium sp ASV264	0	3	-0.21	0.08	100
Bacteria	Topsoil	2022	g__Hassallia sp ASV1177	0	1	-0.06	0.03	47.50
Bacteria	Topsoil	2022	g__Hassallia sp ASV497	0	4	-0.35	0.07	82.50
Bacteria	Topsoil	2023	g__Hassallia sp ASV497	0	3	-0.36	0.06	91.67
Bacteria	Topsoil	2022	g__Hassallia sp ASV627	0	4	-0.52	0.11	57.50
Bacteria	Topsoil	2023	g__Hassallia sp ASV627	0	3	-0.50	0.02	62.50
Bacteria	Topsoil	2022	g__Hassallia sp ASV910	0	4	-0.46	0.05	76.88
Bacteria	Topsoil	2023	g__Hassallia sp ASV910	0	4	-0.60	0.04	89.58
Bacteria	Topsoil	2022	g__Hassallia sp ASV999	0	3	-0.15	0.04	66.88
Fungi	Topsoil	2022	g__Helgardia sp ASV710	2	0	0.26	0.01	47.17
Fungi	Topsoil	2023	g__Helgardia sp ASV710	1	0	0.32	0.06	60.42
Fungi	Phyllosphere	2022	g__Herpotrichia sp ASV175	2	0	0.35	0.07	64.56
Fungi	Topsoil	2022	g__Herpotrichia sp ASV175	1	0	0.15	0.00	44.03
Fungi	Topsoil	2022	g__Humicola sp ASV771	4	0	0.47	0.02	29.56
Bacteria	Topsoil	2022	g__Hymenobacter sp ASV1118	2	0	0.09	0.00	32.50
Bacteria	Topsoil	2023	g__Hymenobacter sp ASV12	3	0	0.42	0.02	95.83
Bacteria	Topsoil	2023	g__Hymenobacter sp ASV19	3	0	0.27	0.01	95.83
Bacteria	Topsoil	2022	g__Hymenobacter sp ASV274	1	0	0.15	0.03	87.50

Annexes

Bacteria	Topsoil	2023	g__Hymenobacter sp ASV274	2	0	0.23	0.01	83.33
Bacteria	Topsoil	2023	g__Hymenobacter sp ASV279	2	0	0.27	0.00	33.33
Bacteria	Topsoil	2022	g__Hymenobacter sp ASV661	3	0	0.18	0.01	69.38
Bacteria	Topsoil	2023	g__Hymenobacter sp ASV725	3	0	0.35	0.00	50.00
Bacteria	Topsoil	2023	g__Hymenobacter sp ASV822	3	0	0.29	0.00	54.17
Bacteria	Topsoil	2023	g__Hymenobacter sp ASV839	1	0	0.26	0.00	39.58
Bacteria	Topsoil	2022	g__Hymenobacter sp ASV905	3	0	0.12	0.01	61.25
Bacteria	Topsoil	2023	g__Hymenobacter sp ASV905	3	0	0.31	0.01	72.92
Bacteria	Topsoil	2022	g__Iamia sp ASV284	0	4	-0.23	0.14	81.88
Bacteria	Topsoil	2023	g__Iamia sp ASV284	0	4	-0.26	0.08	100
Bacteria	Topsoil	2022	g__Iamia sp ASV609	0	4	-0.47	0.08	58.13
Bacteria	Topsoil	2023	g__Iamia sp ASV609	0	4	-0.55	0.04	72.92
Bacteria	Topsoil	2022	g__Iamia sp ASV636	0	3	-0.23	0.06	78.13
Bacteria	Topsoil	2023	g__Iamia sp ASV636	0	3	-0.26	0.04	91.67
Bacteria	Topsoil	2022	g__Iamia sp ASV849	0	3	-0.08	0.06	91.88
Bacteria	Topsoil	2023	g__Iamia sp ASV849	0	1	-0.08	0.05	100
Bacteria	Topsoil	2022	g__Iamia sp ASV936	0	3	-0.08	0.04	91.88
Bacteria	Topsoil	2023	g__Iamia sp ASV936	0	2	-0.15	0.03	93.75
Bacteria	Phyllosphere	2022	g__Ilumatobacter sp ASV164	0	2	-0.55	0.02	48.13
Bacteria	Topsoil	2022	g__Ilumatobacter sp ASV164	0	4	-0.34	0.24	73.13
Bacteria	Topsoil	2023	g__Ilumatobacter sp ASV164	0	4	-0.56	0.09	91.67
Bacteria	Topsoil	2022	g__Ilumatobacter sp ASV171	0	3	-0.13	0.21	81.88
Bacteria	Topsoil	2023	g__Ilumatobacter sp ASV171	0	4	-0.36	0.13	95.83
Bacteria	Topsoil	2023	g__Ilumatobacter sp ASV226	0	1	-0.10	0.12	100
Bacteria	Topsoil	2023	g__Ilumatobacter sp ASV883	0	1	-0.33	0.03	58.33
Bacteria	Topsoil	2023	g__IMCC26207 sp ASV1206	0	1	-0.05	0.03	97.92
Bacteria	Topsoil	2022	g__Intrasporangium sp ASV1044	0	3	-0.35	0.02	31.88
Bacteria	Topsoil	2023	g__Intrasporangium sp ASV1044	0	4	-0.50	0.05	47.92
Bacteria	Topsoil	2022	g__IS-44 sp ASV1137	0	3	-0.16	0.02	43.13
Bacteria	Topsoil	2022	g__IS-44 sp ASV931	0	2	-0.11	0.03	70.63
Bacteria	Topsoil	2023	g__IS-44 sp ASV931	0	3	-0.33	0.03	75.00
Bacteria	Topsoil	2022	g__Jatrophihabitans sp ASV121	4	0	0.41	0.21	90.00
Bacteria	Topsoil	2023	g__Jatrophihabitans sp ASV121	2	0	0.18	0.24	97.92
Bacteria	Topsoil	2023	g__Jatrophihabitans sp ASV465	3	0	0.29	0.09	64.58
Fungi	Topsoil	2022	g__Jattaea sp ASV722	3	0	0.11	0.00	8.81
Bacteria	Topsoil	2022	g__Kineococcus sp ASV42	3	0	0.12	0.01	87.50
Bacteria	Topsoil	2023	g__Kineococcus sp ASV42	3	0	0.35	0.01	85.42
Bacteria	Topsoil	2022	g__Kineosporia sp ASV1021	3	0	0.13	0.05	91.88
Bacteria	Topsoil	2023	g__Kineosporia sp ASV1021	3	0	0.21	0.04	100
Bacteria	Topsoil	2023	g__Klenkia sp ASV140	1	0	0.22	0.01	85.42
Bacteria	Phyllosphere	2022	g__Knoellia sp ASV691	0	3	-0.70	0.09	63.75
Bacteria	Topsoil	2022	g__Knoellia sp ASV691	3	0	0.16	0.02	79.38
Bacteria	Phyllosphere	2022	g__Kocuria sp ASV1267	0	3	-0.62	0.04	31.88
Bacteria	Topsoil	2022	g__Kocuria sp ASV1267	2	0	0.09	0.00	10.63
Bacteria	Phyllosphere	2022	g__Kouleothrix sp ASV1113	2	0	0.22	0.00	8.75
Bacteria	Topsoil	2022	g__Kouleothrix sp ASV1113	4	0	0.60	0.04	55.00

Annexes

Bacteria	Topsoil	2023	g__Kouleothrix sp ASV1113	1	0	0.33	0.02	70.83
Bacteria	Topsoil	2022	g__Kouleothrix sp ASV1225	0	2	-0.16	0.02	45.63
Bacteria	Topsoil	2022	g__Kouleothrix sp ASV239	0	2	-0.24	0.16	50.63
Bacteria	Topsoil	2023	g__Kouleothrix sp ASV239	3	0	0.19	0.18	70.83
Bacteria	Topsoil	2023	g__Kouleothrix sp ASV538	2	0	0.20	0.05	64.58
Bacteria	Topsoil	2022	g__Kouleothrix sp ASV568	3	0	0.16	0.07	70.63
Bacteria	Topsoil	2022	g__Kouleothrix sp ASV612	0	2	-0.15	0.04	48.13
Bacteria	Topsoil	2023	g__Kouleothrix sp ASV612	2	0	0.13	0.06	54.17
Bacteria	Topsoil	2022	g__Kouleothrix sp ASV690	1	0	0.06	0.06	56.88
Bacteria	Topsoil	2022	g__Kouleothrix sp ASV941	1	0	0.06	0.01	30.00
Bacteria	Topsoil	2022	g__Kribbella sp ASV392	0	3	-0.12	0.07	91.88
Bacteria	Topsoil	2023	g__Kribbella sp ASV392	0	1	-0.14	0.08	100
Bacteria	Topsoil	2022	g__Lapillicoccus sp ASV1648	4	0	0.47	0.03	61.25
Bacteria	Topsoil	2023	g__Lapillicoccus sp ASV1648	4	0	0.40	0.03	95.83
Bacteria	Topsoil	2022	g__Lapillicoccus sp ASV238	0	4	-0.31	0.13	85.63
Bacteria	Topsoil	2023	g__Lapillicoccus sp ASV238	0	3	-0.24	0.12	91.67
Bacteria	Topsoil	2022	g__Lapillicoccus sp ASV721	0	4	-0.45	0.03	74.38
Bacteria	Topsoil	2023	g__Lapillicoccus sp ASV721	0	4	-0.47	0.06	79.17
Fungi	Phyllosphere	2022	g__Leptodiscella sp ASV773	0	3	-0.22	0.00	5.70
Fungi	Topsoil	2022	g__Leptodiscella sp ASV773	4	0	0.29	0.02	54.72
Fungi	Phyllosphere	2022	g__Leptospora sp ASV464	0	1	-0.12	0.03	88.61
Fungi	Topsoil	2022	g__Leptospora sp ASV464	0	2	-0.12	0.00	16.35
Bacteria	Topsoil	2022	g__Longimicrobium sp ASV1549	0	2	-0.14	0.02	54.38
Bacteria	Topsoil	2023	g__Longimicrobium sp ASV1549	0	1	-0.30	0.02	72.92
Bacteria	Topsoil	2022	g__Luedemannella sp ASV868	0	3	-0.14	0.07	77.50
Bacteria	Topsoil	2023	g__Luedemannella sp ASV868	0	3	-0.27	0.06	97.92
Bacteria	Topsoil	2022	g__Lysinimonas sp ASV1284	0	3	-0.08	0.05	88.75
Bacteria	Topsoil	2023	g__Lysinimonas sp ASV1284	0	3	-0.13	0.03	100
Bacteria	Topsoil	2023	g__Marmoricola sp ASV126	0	2	-0.15	0.32	100
Bacteria	Topsoil	2022	g__Marmoricola sp ASV1298	4	0	0.25	0.01	68.13
Bacteria	Topsoil	2023	g__Marmoricola sp ASV1475	0	2	-0.14	0.02	79.17
Bacteria	Topsoil	2022	g__Marmoricola sp ASV740	4	0	0.32	0.03	83.75
Bacteria	Topsoil	2023	g__Marmoricola sp ASV740	4	0	0.49	0.05	91.67
Bacteria	Topsoil	2022	g__Massilia sp ASV1034	4	0	0.33	0.06	85.63
Bacteria	Topsoil	2023	g__Massilia sp ASV1034	1	0	0.04	0.06	100
Bacteria	Topsoil	2022	g__Massilia sp ASV1319	1	0	0.04	0.03	72.50
Bacteria	Topsoil	2022	g__Massilia sp ASV1425	3	0	0.21	0.03	82.50
Bacteria	Topsoil	2022	g__Massilia sp ASV36	4	0	0.29	0.03	87.50
Bacteria	Topsoil	2023	g__Massilia sp ASV36	1	0	0.07	0.01	95.83
Bacteria	Topsoil	2022	g__Massilia sp ASV362	2	0	0.21	0.05	83.75
Bacteria	Topsoil	2022	g__Massilia sp ASV425	2	0	0.25	0.04	80.63
Bacteria	Topsoil	2023	g__Massilia sp ASV490	0	3	-0.35	0.07	91.67
Bacteria	Topsoil	2022	g__Massilia sp ASV529	2	0	0.08	0.03	73.13
Bacteria	Topsoil	2023	g__Massilia sp ASV801	3	0	0.22	0.02	54.17
Bacteria	Topsoil	2022	g__Massilia sp ASV864	1	0	0.19	0.07	70.00
Fungi	Phyllosphere	2022	g__Metarhizium sp ASV69	1	0	0.29	0.01	48.73

Annexes

Fungi	Topsoil	2023	g__Metarhizium sp ASV69	1	0	0.26	0.62	83.33
Bacteria	Topsoil	2023	g__Methylobacterium-Methylorubrum sp ASV158	2	0	0.14	0.01	75.00
Bacteria	Topsoil	2022	g__Methylobacterium-Methylorubrum sp ASV310	3	0	0.15	0.01	61.88
Bacteria	Topsoil	2023	g__Methylobacterium-Methylorubrum sp ASV310	2	0	0.16	0.01	64.58
Bacteria	Phyllosphere	2022	g__Methylobacterium-Methylorubrum sp ASV380	0	4	-0.79	0.13	48.75
Bacteria	Topsoil	2022	g__Methylobacterium-Methylorubrum sp ASV380	0	1	-0.10	0.01	55.00
Bacteria	Topsoil	2023	g__Methylobacterium-Methylorubrum sp ASV380	3	0	0.24	0.01	83.33
Bacteria	Topsoil	2022	g__Methylorosula sp ASV303	3	0	0.21	0.06	88.13
Bacteria	Topsoil	2023	g__Methylorosula sp ASV303	2	0	0.18	0.12	97.92
Bacteria	Topsoil	2022	g__Methylotenera sp ASV587	0	3	-0.18	0.07	80.63
Bacteria	Topsoil	2022	g__Microbacterium sp ASV175	0	2	-0.14	0.21	84.38
Bacteria	Topsoil	2023	g__Microbacterium sp ASV175	0	3	-0.18	0.13	100
Bacteria	Topsoil	2022	g__Microbacterium sp ASV327	0	1	-0.01	0.11	86.88
Bacteria	Topsoil	2023	g__Microbacterium sp ASV327	0	3	-0.10	0.10	100
Bacteria	Topsoil	2022	g__Microbacterium sp ASV942	0	3	-0.10	0.04	83.13
Bacteria	Topsoil	2023	g__Microbacterium sp ASV942	0	3	-0.21	0.02	95.83
Fungi	Phyllosphere	2022	g__Microdochium sp ASV702	0	1	-0.23	0.00	18.35
Fungi	Topsoil	2022	g__Microdochium sp ASV702	0	3	-0.34	0.03	55.35
Bacteria	Topsoil	2022	g__Microlunatus sp ASV180	0	3	-0.14	0.19	95.00
Bacteria	Topsoil	2023	g__Microlunatus sp ASV180	0	3	-0.08	0.12	100
Bacteria	Phyllosphere	2022	g__Microlunatus sp ASV209	5	0	0.53	0.03	40.63
Bacteria	Topsoil	2022	g__Microlunatus sp ASV209	5	0	0.77	0.13	48.75
Bacteria	Topsoil	2023	g__Microlunatus sp ASV209	4	0	0.97	0.11	81.25
Bacteria	Phyllosphere	2022	g__Microlunatus sp ASV440	5	0	0.41	0.01	27.50
Bacteria	Topsoil	2022	g__Microlunatus sp ASV440	5	0	0.39	0.04	32.50
Bacteria	Topsoil	2023	g__Microlunatus sp ASV440	4	0	0.89	0.08	39.58
Bacteria	Phyllosphere	2022	g__Microlunatus sp ASV823	0	2	-0.66	0.01	20.63
Bacteria	Phyllosphere	2022	g__Micromonospora sp ASV1156	0	5	-0.92	0.02	34.38
Bacteria	Topsoil	2022	g__Micromonospora sp ASV1156	0	3	-0.20	0.04	73.13
Bacteria	Topsoil	2023	g__Micromonospora sp ASV1156	0	4	-0.36	0.06	93.75
Bacteria	Topsoil	2022	g__Micromonospora sp ASV1379	1	0	0.14	0.02	71.88
Bacteria	Topsoil	2023	g__Micromonospora sp ASV1379	0	1	-0.14	0.03	100
Bacteria	Phyllosphere	2022	g__Micromonospora sp ASV2911	0	1	-0.41	0.01	21.88
Bacteria	Topsoil	2022	g__Micromonospora sp ASV2911	0	3	-0.15	0.02	75.63
Bacteria	Topsoil	2023	g__Micromonospora sp ASV2911	0	4	-0.58	0.03	87.50
Bacteria	Phyllosphere	2022	g__Micropruina sp ASV1452	0	3	-0.76	0.02	32.50
Bacteria	Topsoil	2022	g__Micropruina sp ASV1452	0	4	-0.50	0.04	65.00
Bacteria	Topsoil	2023	g__Micropruina sp ASV1452	0	4	-0.58	0.02	81.25
Bacteria	Topsoil	2022	g__Microvirga sp ASV1107	1	0	0.04	0.03	71.25
Bacteria	Topsoil	2023	g__Microvirga sp ASV1107	0	1	-0.23	0.05	91.67
Bacteria	Topsoil	2022	g__Microvirga sp ASV1276	3	0	0.33	0.02	26.88
Bacteria	Topsoil	2023	g__Microvirga sp ASV1276	3	0	0.29	0.03	58.33

Annexes

Bacteria	Topsoil	2022	g__Microvirga sp ASV1480	4	0	0.32	0.02	60.00
Bacteria	Topsoil	2022	g__Microvirga sp ASV314	3	0	0.17	0.07	86.25
Bacteria	Topsoil	2022	g__Microvirga sp ASV476	3	0	0.13	0.07	71.88
Bacteria	Topsoil	2022	g__Microvirga sp ASV559	0	3	-0.14	0.06	83.75
Bacteria	Topsoil	2023	g__Microvirga sp ASV559	0	4	-0.27	0.07	100
Bacteria	Topsoil	2023	g__Microvirga sp ASV599	0	3	-0.20	0.06	85.42
Bacteria	Topsoil	2022	g__Microvirga sp ASV747	1	0	0.06	0.09	64.38
Bacteria	Topsoil	2022	g__Microvirga sp ASV825	3	0	0.27	0.03	51.25
Bacteria	Topsoil	2023	g__Microvirga sp ASV922	0	3	-0.20	0.05	79.17
Bacteria	Topsoil	2022	g__Microvirga sp ASV945	0	3	-0.08	0.03	90.00
Bacteria	Topsoil	2022	g__Microvirga sp ASV957	0	1	-0.14	0.03	64.38
Bacteria	Topsoil	2023	g__Microvirga sp ASV957	0	3	-0.22	0.04	89.58
Bacteria	Topsoil	2022	g__mle1-7 sp ASV1354	3	0	0.23	0.03	78.75
Bacteria	Topsoil	2023	g__mle1-7 sp ASV1354	4	0	0.53	0.03	70.83
Bacteria	Topsoil	2022	g__MND1 sp ASV1022	0	4	-0.22	0.04	72.50
Bacteria	Topsoil	2023	g__MND1 sp ASV1022	0	3	-0.21	0.05	95.83
Bacteria	Topsoil	2022	g__MND1 sp ASV1153	0	4	-0.26	0.09	81.88
Bacteria	Topsoil	2023	g__MND1 sp ASV1153	0	4	-0.48	0.07	97.92
Bacteria	Topsoil	2022	g__MND1 sp ASV1214	3	0	0.12	0.02	87.50
Bacteria	Topsoil	2023	g__MND1 sp ASV1214	2	0	0.12	0.04	97.92
Bacteria	Topsoil	2022	g__MND1 sp ASV1226	0	3	-0.18	0.03	63.13
Bacteria	Topsoil	2023	g__MND1 sp ASV1226	0	3	-0.40	0.02	70.83
Bacteria	Topsoil	2022	g__MND1 sp ASV1230	0	1	-0.14	0.03	87.50
Bacteria	Topsoil	2022	g__MND1 sp ASV1248	0	4	-0.36	0.02	82.50
Bacteria	Topsoil	2023	g__MND1 sp ASV1248	0	3	-0.21	0.04	95.83
Bacteria	Topsoil	2022	g__MND1 sp ASV1900	3	0	0.16	0.03	80.63
Bacteria	Topsoil	2023	g__MND1 sp ASV346	0	1	-0.08	0.11	87.50
Bacteria	Topsoil	2022	g__MND1 sp ASV669	0	4	-0.26	0.06	66.88
Bacteria	Topsoil	2023	g__MND1 sp ASV669	0	4	-0.34	0.03	89.58
Bacteria	Topsoil	2022	g__Modestobacter sp ASV751	5	0	0.58	0.04	33.75
Bacteria	Topsoil	2023	g__Modestobacter sp ASV751	4	0	0.83	0.03	54.17
Fungi	Phyllosphere	2022	g__Mollisia sp ASV639	0	1	-0.18	0.00	19.62
Fungi	Phyllosphere	2022	g__Mollisia sp ASV803	2	0	0.26	0.03	75.32
Fungi	Phyllosphere	2022	g__Mortierella sp ASV109	0	3	-0.42	0.00	15.19
Fungi	Endosphere	2022	g__Mortierella sp ASV203	0	2	-0.17	0.00	22.50
Fungi	Phyllosphere	2022	g__Mortierella sp ASV203	0	3	-0.27	0.00	13.92
Fungi	Topsoil	2022	g__Mortierella sp ASV203	0	2	-0.27	0.16	52.83
Fungi	Topsoil	2023	g__Mortierella sp ASV203	0	3	-0.54	0.05	52.08
Fungi	Topsoil	2022	g__Mortierella sp ASV227	0	1	-0.21	0.10	62.89
Fungi	Topsoil	2023	g__Mortierella sp ASV258	0	3	-0.32	0.12	70.83
Fungi	Phyllosphere	2022	g__Mortierella sp ASV301	0	3	-0.38	0.00	24.05
Fungi	Topsoil	2023	g__Mortierella sp ASV301	3	0	0.47	0.06	70.83
Fungi	Endosphere	2022	g__Mortierella sp ASV303	0	2	-0.19	0.00	20.00
Fungi	Phyllosphere	2022	g__Mortierella sp ASV303	0	3	-0.33	0.00	8.23
Fungi	Phyllosphere	2022	g__Mortierella sp ASV373	0	3	-0.32	0.00	14.56
Fungi	Topsoil	2022	g__Mortierella sp ASV373	4	0	0.57	0.05	27.67

Annexes

Fungi	Topsoil	2023	g__Mortierella sp ASV373	4	0	0.68	0.08	52.08
Fungi	Topsoil	2022	g__Mortierella sp ASV475	0	1	-0.04	0.07	55.35
Fungi	Topsoil	2023	g__Mortierella sp ASV475	4	0	0.36	0.05	64.58
Fungi	Topsoil	2022	g__Mortierella sp ASV627	3	0	0.29	0.03	11.95
Fungi	Phyllosphere	2022	g__Mortierella sp ASV704	0	2	-0.16	0.00	6.96
Fungi	Topsoil	2022	g__Mortierella sp ASV704	3	0	0.25	0.02	37.11
Fungi	Topsoil	2023	g__Mortierella sp ASV704	1	0	0.50	0.02	33.33
Bacteria	Topsoil	2022	g__Mucilaginibacter sp ASV443	3	0	0.16	0.01	66.88
Bacteria	Topsoil	2022	g__Mycetocola sp ASV1486	1	0	0.05	0.03	67.50
Bacteria	Topsoil	2023	g__Mycetocola sp ASV1486	3	0	0.20	0.03	85.42
Bacteria	Phyllosphere	2022	g__Mycobacterium sp ASV1358	0	2	-0.55	0.01	21.88
Bacteria	Topsoil	2022	g__Mycobacterium sp ASV1358	0	5	-0.53	0.04	41.25
Bacteria	Topsoil	2023	g__Mycobacterium sp ASV1358	0	4	-0.62	0.03	45.83
Bacteria	Topsoil	2022	g__Mycobacterium sp ASV1594	2	0	0.11	0.03	66.25
Bacteria	Topsoil	2022	g__Mycobacterium sp ASV57	0	2	-0.19	0.29	86.88
Bacteria	Topsoil	2022	g__Mycobacterium sp ASV615	0	2	-0.18	0.04	56.88
Bacteria	Topsoil	2023	g__Mycobacterium sp ASV615	0	3	-0.30	0.02	64.58
Bacteria	Topsoil	2022	g__Mycobacterium sp ASV62	0	3	-0.12	0.13	92.50
Fungi	Phyllosphere	2022	g__Mycocentrospora sp ASV488	1	0	0.27	0.03	34.81
Fungi	Phyllosphere	2022	g__Myrmecridium sp ASV359	1	0	0.19	0.00	22.15
Fungi	Topsoil	2022	g__Naganishia sp ASV90	2	0	0.35	0.23	61.01
Bacteria	Phyllosphere	2022	g__Nakamurella sp ASV1272	0	4	-0.61	0.01	23.13
Bacteria	Topsoil	2022	g__Nakamurella sp ASV1272	0	4	-0.33	0.03	66.88
Bacteria	Topsoil	2023	g__Nakamurella sp ASV1272	0	3	-0.21	0.01	79.17
Bacteria	Topsoil	2022	g__Nakamurella sp ASV1380	4	0	0.23	0.01	51.25
Bacteria	Topsoil	2023	g__Nakamurella sp ASV1380	3	0	0.26	0.02	54.17
Bacteria	Phyllosphere	2022	g__Nakamurella sp ASV145	0	3	-0.63	0.08	66.88
Bacteria	Topsoil	2022	g__Nakamurella sp ASV145	0	4	-0.36	0.28	88.13
Bacteria	Topsoil	2023	g__Nakamurella sp ASV145	0	3	-0.26	0.23	93.75
Bacteria	Topsoil	2022	g__Nakamurella sp ASV268	3	0	0.12	0.04	92.50
Bacteria	Topsoil	2023	g__Nakamurella sp ASV268	4	0	0.50	0.06	100
Bacteria	Topsoil	2022	g__Nakamurella sp ASV54	0	4	-0.27	0.60	91.88
Bacteria	Topsoil	2023	g__Nakamurella sp ASV54	0	3	-0.18	0.54	97.92
Fungi	Topsoil	2022	g__Neobulgaria sp ASV433	4	0	0.39	0.05	40.88
Bacteria	Phyllosphere	2022	g__Nitrospira sp ASV1231	1	0	0.17	0.00	19.38
Bacteria	Topsoil	2022	g__Nitrospira sp ASV1231	3	0	0.19	0.04	73.13
Bacteria	Topsoil	2023	g__Nitrospira sp ASV1231	1	0	0.08	0.05	85.42
Bacteria	Topsoil	2022	g__Nitrospira sp ASV1384	3	0	0.19	0.06	86.25
Bacteria	Topsoil	2023	g__Nitrospira sp ASV1384	3	0	0.17	0.05	100
Bacteria	Topsoil	2023	g__Nitrospira sp ASV167	0	1	-0.07	0.18	75.00
Bacteria	Topsoil	2022	g__Nitrospira sp ASV498	1	0	0.02	0.19	83.13
Bacteria	Topsoil	2022	g__Nitrospira sp ASV706	3	0	0.15	0.04	81.88
Bacteria	Topsoil	2022	g__Nocardioides sp ASV101	0	1	-0.03	0.31	85.63
Bacteria	Topsoil	2023	g__Nocardioides sp ASV101	0	1	-0.17	0.26	97.92
Bacteria	Topsoil	2022	g__Nocardioides sp ASV1117	0	2	-0.07	0.07	91.25
Bacteria	Topsoil	2023	g__Nocardioides sp ASV1117	0	3	-0.21	0.03	100

Annexes

Bacteria	Phyllosphere	2022	g__Nocardioides sp ASV113	0	1	-0.38	0.03	60.63
Bacteria	Topsoil	2022	g__Nocardioides sp ASV1140	1	0	0.12	0.02	32.50
Bacteria	Topsoil	2023	g__Nocardioides sp ASV1140	4	0	0.44	0.02	47.92
Bacteria	Topsoil	2022	g__Nocardioides sp ASV1171	0	3	-0.15	0.01	13.13
Bacteria	Topsoil	2023	g__Nocardioides sp ASV1171	1	0	0.30	0.04	18.75
Bacteria	Topsoil	2023	g__Nocardioides sp ASV1209	0	3	-0.12	0.02	97.92
Bacteria	Topsoil	2022	g__Nocardioides sp ASV1254	0	2	-0.18	0.04	92.50
Bacteria	Topsoil	2023	g__Nocardioides sp ASV1254	0	2	-0.12	0.02	93.75
Bacteria	Topsoil	2022	g__Nocardioides sp ASV1294	0	3	-0.15	0.03	88.75
Bacteria	Topsoil	2023	g__Nocardioides sp ASV1294	0	4	-0.29	0.01	97.92
Bacteria	Topsoil	2023	g__Nocardioides sp ASV1399	3	0	0.57	0.02	45.83
Bacteria	Topsoil	2022	g__Nocardioides sp ASV141	1	0	0.05	0.22	81.88
Bacteria	Topsoil	2023	g__Nocardioides sp ASV141	0	1	-0.07	0.31	97.92
Bacteria	Topsoil	2022	g__Nocardioides sp ASV146	1	0	0.03	0.24	68.75
Bacteria	Topsoil	2022	g__Nocardioides sp ASV149	1	0	0.08	0.24	81.88
Bacteria	Topsoil	2023	g__Nocardioides sp ASV149	1	0	0.06	0.21	89.58
Bacteria	Topsoil	2023	g__Nocardioides sp ASV1518	1	0	0.25	0.03	39.58
Bacteria	Topsoil	2023	g__Nocardioides sp ASV154	0	2	-0.18	0.12	89.58
Bacteria	Topsoil	2023	g__Nocardioides sp ASV1798	0	3	-0.17	0.02	87.50
Bacteria	Topsoil	2022	g__Nocardioides sp ASV2350	0	3	-0.18	0.04	76.88
Bacteria	Topsoil	2023	g__Nocardioides sp ASV2350	0	4	-0.24	0.03	85.42
Bacteria	Topsoil	2022	g__Nocardioides sp ASV2373	1	0	0.02	0.02	79.38
Bacteria	Phyllosphere	2022	g__Nocardioides sp ASV282	0	4	-0.80	0.05	67.50
Bacteria	Topsoil	2022	g__Nocardioides sp ASV282	0	4	-0.21	0.10	94.38
Bacteria	Topsoil	2023	g__Nocardioides sp ASV282	0	4	-0.36	0.07	100
Bacteria	Topsoil	2022	g__Nocardioides sp ASV290	0	2	-0.11	0.00	35.63
Bacteria	Topsoil	2023	g__Nocardioides sp ASV290	0	1	-0.20	0.00	25.00
Bacteria	Topsoil	2023	g__Nocardioides sp ASV312	0	1	-0.13	0.08	91.67
Bacteria	Topsoil	2022	g__Nocardioides sp ASV368	3	0	0.17	0.11	76.88
Bacteria	Topsoil	2023	g__Nocardioides sp ASV368	1	0	0.17	0.06	95.83
Bacteria	Topsoil	2022	g__Nocardioides sp ASV372	3	0	0.21	0.08	85.00
Bacteria	Topsoil	2023	g__Nocardioides sp ASV372	4	0	0.43	0.12	91.67
Bacteria	Phyllosphere	2022	g__Nocardioides sp ASV412	3	0	0.21	0.01	31.88
Bacteria	Topsoil	2022	g__Nocardioides sp ASV412	3	0	0.23	0.08	81.88
Bacteria	Topsoil	2023	g__Nocardioides sp ASV412	4	0	0.31	0.06	97.92
Bacteria	Topsoil	2022	g__Nocardioides sp ASV421	0	4	-0.29	0.09	81.25
Bacteria	Topsoil	2023	g__Nocardioides sp ASV421	0	3	-0.24	0.05	91.67
Bacteria	Topsoil	2022	g__Nocardioides sp ASV428	1	0	0.12	0.11	45.63
Bacteria	Topsoil	2023	g__Nocardioides sp ASV428	0	3	-0.29	0.02	43.75
Bacteria	Topsoil	2022	g__Nocardioides sp ASV464	0	2	-0.16	0.07	91.88
Bacteria	Topsoil	2023	g__Nocardioides sp ASV464	0	3	-0.22	0.03	100
Bacteria	Topsoil	2022	g__Nocardioides sp ASV495	1	0	0.08	0.06	81.25
Bacteria	Topsoil	2023	g__Nocardioides sp ASV495	0	3	-0.25	0.02	91.67
Bacteria	Phyllosphere	2022	g__Nocardioides sp ASV507	1	0	0.17	0.02	20.63
Bacteria	Topsoil	2022	g__Nocardioides sp ASV507	4	0	0.41	0.08	23.75
Bacteria	Topsoil	2023	g__Nocardioides sp ASV507	1	0	0.25	0.02	39.58

Annexes

Bacteria	Topsoil	2022	g__Nocardioides sp ASV51	0	3	-0.22	0.59	91.88
Bacteria	Phyllosphere	2022	g__Nocardioides sp ASV540	0	2	-0.58	0.02	46.25
Bacteria	Topsoil	2022	g__Nocardioides sp ASV540	0	4	-0.39	0.12	80.63
Bacteria	Topsoil	2023	g__Nocardioides sp ASV540	0	4	-0.47	0.06	89.58
Bacteria	Topsoil	2022	g__Nocardioides sp ASV548	0	4	-0.40	0.11	63.75
Bacteria	Topsoil	2023	g__Nocardioides sp ASV548	0	3	-0.39	0.05	83.33
Bacteria	Topsoil	2022	g__Nocardioides sp ASV553	3	0	0.12	0.07	90.63
Bacteria	Topsoil	2023	g__Nocardioides sp ASV553	0	1	-0.17	0.04	100
Bacteria	Topsoil	2022	g__Nocardioides sp ASV603	0	3	-0.24	0.06	60.63
Bacteria	Topsoil	2023	g__Nocardioides sp ASV603	0	3	-0.26	0.04	75.00
Bacteria	Topsoil	2022	g__Nocardioides sp ASV63	0	1	-0.02	0.60	95.63
Bacteria	Topsoil	2023	g__Nocardioides sp ASV63	0	3	-0.14	0.43	100
Bacteria	Phyllosphere	2022	g__Nocardioides sp ASV726	0	2	-0.45	0.01	20.63
Bacteria	Topsoil	2022	g__Nocardioides sp ASV726	0	4	-0.27	0.06	78.13
Bacteria	Topsoil	2023	g__Nocardioides sp ASV726	0	1	-0.21	0.04	91.67
Bacteria	Topsoil	2022	g__Nocardioides sp ASV809	0	2	-0.16	0.05	73.75
Bacteria	Topsoil	2023	g__Nocardioides sp ASV809	0	1	-0.18	0.03	79.17
Bacteria	Topsoil	2022	g__Nocardioides sp ASV966	0	4	-0.42	0.04	42.50
Bacteria	Topsoil	2023	g__Nocardioides sp ASV966	0	4	-0.52	0.02	43.75
Bacteria	Topsoil	2022	g__Noviherbaspirillum sp ASV1468	4	0	0.24	0.02	88.13
Bacteria	Topsoil	2023	g__Noviherbaspirillum sp ASV1468	3	0	0.19	0.03	100
Bacteria	Topsoil	2022	g__Noviherbaspirillum sp ASV1935	5	0	0.55	0.02	43.75
Bacteria	Topsoil	2023	g__Noviherbaspirillum sp ASV1935	4	0	0.83	0.02	52.08
Bacteria	Topsoil	2022	g__Noviherbaspirillum sp ASV286	4	0	0.37	0.10	79.38
Bacteria	Topsoil	2023	g__Noviherbaspirillum sp ASV286	4	0	0.46	0.17	97.92
Bacteria	Topsoil	2022	g__Noviherbaspirillum sp ASV308	4	0	0.31	0.09	81.88
Bacteria	Phyllosphere	2022	g__Noviherbaspirillum sp ASV335	1	0	0.10	0.10	63.75
Bacteria	Topsoil	2022	g__Noviherbaspirillum sp ASV335	4	0	0.40	0.08	86.25
Bacteria	Topsoil	2023	g__Noviherbaspirillum sp ASV335	2	0	0.14	0.13	100
Bacteria	Topsoil	2022	g__Noviherbaspirillum sp ASV836	3	0	0.14	0.02	57.50
Bacteria	Topsoil	2023	g__Noviherbaspirillum sp ASV836	3	0	0.28	0.05	60.42
Bacteria	Phyllosphere	2022	g__Novosphingobium sp ASV1899	0	1	-0.40	0.01	23.13
Bacteria	Topsoil	2022	g__Novosphingobium sp ASV415	2	0	0.08	0.02	88.75
Bacteria	Topsoil	2023	g__Novosphingobium sp ASV415	1	0	0.12	0.03	89.58
Bacteria	Topsoil	2022	g__Ohtaekwangia sp ASV1508	0	4	-0.25	0.07	85.63
Bacteria	Topsoil	2023	g__Ohtaekwangia sp ASV1508	0	3	-0.14	0.05	100
Bacteria	Topsoil	2023	g__Ohtaekwangia sp ASV1510	0	3	-0.27	0.02	91.67
Bacteria	Topsoil	2022	g__OLB12 sp ASV408	0	4	-0.55	0.11	63.75
Bacteria	Topsoil	2023	g__OLB12 sp ASV408	0	4	-0.82	0.04	62.50
Bacteria	Topsoil	2023	g__Oligoflexus sp ASV1653	0	3	-0.26	0.03	97.92
Fungi	Phyllosphere	2022	g__Ophiognomonia sp ASV310	5	0	0.50	0.01	79.75
Fungi	Topsoil	2022	g__Ophiognomonia sp ASV310	3	0	0.17	0.00	16.35
Bacteria	Topsoil	2023	g__P3OB-42 sp ASV997	0	2	-0.09	0.03	100
Bacteria	Topsoil	2022	g__Paenarthrobacter sp ASV249	4	0	0.31	0.08	80.63
Bacteria	Topsoil	2023	g__Paenarthrobacter sp ASV249	3	0	0.30	0.09	95.83
Bacteria	Topsoil	2022	g__Paenibacillus sp ASV1684	3	0	0.18	0.02	80.63

Annexes

Bacteria	Topsoil	2022	g__Paenibacillus sp ASV1687	0	2	-0.08	0.05	79.38
Bacteria	Topsoil	2023	g__Paenibacillus sp ASV1687	0	3	-0.10	0.03	100
Bacteria	Topsoil	2023	g__Paenibacillus sp ASV1700	0	1	-0.13	0.03	100
Bacteria	Topsoil	2023	g__Paenibacillus sp ASV2109	0	1	-0.19	0.02	95.83
Bacteria	Topsoil	2023	g__Paenibacillus sp ASV3019	0	3	-0.18	0.02	97.92
Bacteria	Topsoil	2022	g__Paenibacillus sp ASV660	0	2	-0.11	0.00	13.75
Bacteria	Phyllosphere	2022	g__Paenibacillus sp ASV766	1	0	0.15	0.00	23.75
Bacteria	Topsoil	2022	g__Paenibacillus sp ASV766	3	0	0.14	0.05	88.13
Bacteria	Topsoil	2023	g__Paenibacillus sp ASV766	2	0	0.09	0.05	100
Bacteria	Topsoil	2023	g__Paenibacillus sp ASV786	0	1	-0.09	0.07	100
Bacteria	Topsoil	2022	g__Paenibacillus sp ASV930	0	3	-0.16	0.05	64.38
Bacteria	Topsoil	2023	g__Paenibacillus sp ASV930	0	3	-0.28	0.03	93.75
Bacteria	Topsoil	2023	g__Pajaroellobacter sp ASV1314	0	3	-0.16	0.03	100
Bacteria	Topsoil	2023	g__Pantoea sp ASV353	2	0	0.22	0.00	43.75
Fungi	Phyllosphere	2022	g__Papiliotrema sp ASV903	3	0	0.37	0.02	54.43
Bacteria	Topsoil	2022	g__Parafilimonas sp ASV1115	3	0	0.19	0.05	50.00
Bacteria	Topsoil	2023	g__Parafilimonas sp ASV1115	3	0	0.52	0.04	56.25
Bacteria	Topsoil	2022	g__Parafilimonas sp ASV969	0	4	-0.34	0.04	77.50
Bacteria	Topsoil	2023	g__Parafilimonas sp ASV969	0	4	-0.37	0.03	91.67
Bacteria	Topsoil	2022	g__Paucibacter sp ASV1331	0	3	-0.31	0.04	65.63
Bacteria	Topsoil	2023	g__Paucibacter sp ASV1331	0	1	-0.31	0.01	75.00
Bacteria	Topsoil	2022	g__Pedobacter sp ASV445	0	3	-0.28	0.01	43.13
Bacteria	Topsoil	2023	g__Pedobacter sp ASV713	1	0	0.20	0.01	70.83
Bacteria	Topsoil	2022	g__Pedobacter sp ASV783	0	3	-0.12	0.01	75.63
Bacteria	Topsoil	2022	g__Pedobacter sp ASV848	0	1	-0.08	0.00	12.50
Bacteria	Topsoil	2023	g__Pedococcus-Phycicoccus sp ASV546	3	0	0.27	0.08	64.58
Bacteria	Topsoil	2023	g__Pedomicrobium sp ASV1315	0	3	-0.35	0.04	81.25
Bacteria	Topsoil	2023	g__Pedomicrobium sp ASV1848	0	1	-0.10	0.03	91.67
Fungi	Topsoil	2022	g__Penicillium sp ASV1373	0	2	-0.12	0.01	69.81
Fungi	Topsoil	2023	g__Penicillium sp ASV1373	0	2	-0.29	0.00	52.08
Fungi	Phyllosphere	2022	g__Penicillium sp ASV193	0	1	-0.18	0.00	12.66
Fungi	Topsoil	2022	g__Penicillium sp ASV193	0	4	-0.30	0.19	52.83
Fungi	Topsoil	2023	g__Penicillium sp ASV193	0	3	-0.45	0.01	54.17
Fungi	Topsoil	2022	g__Penicillium sp ASV197	0	5	-0.75	0.24	78.62
Fungi	Topsoil	2023	g__Penicillium sp ASV197	0	3	-0.37	0.06	83.33
Fungi	Topsoil	2022	g__Penicillium sp ASV432	4	0	0.39	0.10	29.56
Fungi	Phyllosphere	2022	g__Peniophora sp ASV1275	2	0	0.16	0.01	53.80
Fungi	Phyllosphere	2022	g__Peniophora sp ASV490	2	0	0.13	0.05	45.57
Fungi	Phyllosphere	2022	g__Peniophora sp ASV955	0	2	-0.15	0.04	45.57
Fungi	Phyllosphere	2022	g__Periconia sp ASV643	0	2	-0.31	0.01	57.59
Fungi	Phyllosphere	2022	g__Pestalotiopsis sp ASV580	0	3	-0.34	0.03	14.56
Fungi	Phyllosphere	2022	g__Phaeoacremonium sp ASV696	0	1	-0.19	0.00	10.76
Fungi	Topsoil	2022	g__Phaeoacremonium sp ASV696	0	3	-0.25	0.03	35.22
Fungi	Topsoil	2023	g__Phaeoacremonium sp ASV696	0	3	-0.43	0.03	27.08
Fungi	Phyllosphere	2022	g__Phaeococcomyces sp ASV1109	1	0	0.27	0.01	40.51
Fungi	Phyllosphere	2022	g__Phaeosphaeria sp ASV387	0	2	-0.51	0.02	89.24

Annexes

Fungi	Phyllosphere	2022	g__Phaeosphaeria sp ASV530	0	1	-0.22	0.01	84.18
Fungi	Topsoil	2023	g__Phaeosphaeria sp ASV530	0	1	-0.22	0.00	31.25
Fungi	Phyllosphere	2022	g__Phaeosphaeria sp ASV574	3	0	0.38	0.03	71.52
Fungi	Topsoil	2023	g__Phaeosphaeria sp ASV574	1	0	0.17	0.00	14.58
Fungi	Topsoil	2022	g__Phaeotremella sp ASV938	0	1	-0.09	0.02	33.96
Bacteria	Topsoil	2023	g__Phenylobacterium sp ASV1162	0	1	-0.17	0.02	100
Bacteria	Phyllosphere	2022	g__Phenylobacterium sp ASV1302	1	0	0.17	0.01	15.00
Bacteria	Topsoil	2022	g__Phenylobacterium sp ASV558	3	0	0.19	0.07	88.13
Bacteria	Topsoil	2023	g__Phenylobacterium sp ASV558	2	0	0.08	0.09	100
Fungi	Topsoil	2022	g__Pilidium sp ASV129	1	0	0.31	0.28	74.84
Bacteria	Topsoil	2023	g__Piscinibacter sp ASV857	2	0	0.17	0.04	91.67
Bacteria	Topsoil	2023	g__Plantibacter sp ASV815	2	0	0.28	0.01	72.92
Fungi	Phyllosphere	2022	g__Podosphaera sp ASV164	2	0	0.24	0.00	34.18
Fungi	Phyllosphere	2022	g__Podosphaera sp ASV698	1	0	0.36	0.01	49.37
Fungi	Endosphere	2022	g__Podosphaera sp ASV74	0	1	-0.64	1.63	10.00
Fungi	Phyllosphere	2022	g__Podosphaera sp ASV74	0	3	-0.63	0.08	28.48
Bacteria	Topsoil	2022	g__Polaromonas sp ASV920	0	1	-0.02	0.05	88.13
Bacteria	Topsoil	2023	g__possible_genus_04 sp ASV831	0	2	-0.17	0.06	100
Bacteria	Topsoil	2022	g__Pseudarthrobacter sp ASV111	4	0	0.51	0.29	10.63
Bacteria	Topsoil	2023	g__Pseudarthrobacter sp ASV111	1	0	0.20	0.13	79.17
Bacteria	Phyllosphere	2022	g__Pseudarthrobacter sp ASV48	3	0	0.31	0.84	61.25
Bacteria	Topsoil	2022	g__Pseudarthrobacter sp ASV48	3	0	0.29	1.30	88.13
Bacteria	Topsoil	2023	g__Pseudarthrobacter sp ASV48	4	0	0.28	1.40	100
Bacteria	Topsoil	2022	g__Pseudarthrobacter sp ASV895	4	0	0.34	0.03	15.63
Bacteria	Topsoil	2022	g__Pseudolabrys sp ASV1236	0	3	-0.09	0.07	85.63
Bacteria	Topsoil	2022	g__Pseudolabrys sp ASV549	1	0	0.02	0.09	54.38
Bacteria	Topsoil	2022	g__Pseudolabrys sp ASV846	3	0	0.24	0.06	30.63
Bacteria	Topsoil	2023	g__Pseudolabrys sp ASV846	1	0	0.26	0.02	33.33
Bacteria	Topsoil	2023	g__Pseudonocardia sp ASV1199	1	0	0.20	0.02	64.58
Bacteria	Phyllosphere	2022	g__Pseudonocardia sp ASV1224	0	3	-0.70	0.02	38.13
Bacteria	Topsoil	2022	g__Pseudonocardia sp ASV1224	0	3	-0.23	0.02	66.25
Bacteria	Topsoil	2023	g__Pseudonocardia sp ASV1224	0	2	-0.17	0.02	89.58
Bacteria	Phyllosphere	2022	g__Pseudonocardia sp ASV1398	0	1	-0.40	0.00	11.25
Bacteria	Topsoil	2022	g__Pseudonocardia sp ASV1398	0	5	-0.30	0.01	51.25
Bacteria	Topsoil	2023	g__Pseudonocardia sp ASV1398	0	1	-0.22	0.03	58.33
Bacteria	Topsoil	2022	g__Pseudonocardia sp ASV2499	0	2	-0.15	0.01	68.13
Bacteria	Topsoil	2022	g__Pseudonocardia sp ASV292	0	1	-0.06	0.12	78.75
Bacteria	Topsoil	2023	g__Pseudonocardia sp ASV292	0	3	-0.18	0.14	100
Bacteria	Phyllosphere	2022	g__Pseudonocardia sp ASV431	0	1	-0.44	0.01	35.63
Bacteria	Topsoil	2022	g__Pseudonocardia sp ASV431	0	3	-0.13	0.05	78.75
Bacteria	Topsoil	2022	g__Pseudonocardia sp ASV500	0	2	-0.17	0.04	68.75
Bacteria	Topsoil	2023	g__Pseudonocardia sp ASV500	1	0	0.20	0.07	83.33
Bacteria	Topsoil	2022	g__Pseudonocardia sp ASV541	3	0	0.16	0.05	91.88
Bacteria	Topsoil	2022	g__Pseudonocardia sp ASV550	0	1	-0.09	0.03	41.25
Bacteria	Topsoil	2023	g__Pseudonocardia sp ASV550	3	0	0.39	0.06	45.83
Bacteria	Topsoil	2022	g__Pseudonocardia sp ASV946	0	3	-0.20	0.02	37.50

Annexes

Bacteria	Topsoil	2023	g__Pseudonocardia sp ASV946	0	4	-0.42	0.05	56.25
Bacteria	Topsoil	2022	g__Pseudonocardia sp ASV977	3	0	0.20	0.07	89.38
Bacteria	Topsoil	2023	g__Pseudonocardia sp ASV977	2	0	0.15	0.06	100
Fungi	Phyllosphere	2022	g__Pseudopithomyces sp ASV260	0	2	-0.41	0.01	51.90
Fungi	Topsoil	2022	g__Pseudopithomyces sp ASV260	4	0	0.54	0.03	67.30
Fungi	Topsoil	2022	g__Pseudopithomyces sp ASV825	4	0	0.30	0.00	51.57
Bacteria	Topsoil	2022	g__Pseudorhodoplanes sp ASV944	0	3	-0.17	0.04	81.88
Bacteria	Topsoil	2023	g__Pseudorhodoplanes sp ASV944	0	3	-0.27	0.02	93.75
Bacteria	Topsoil	2022	g__Psychrobacillus sp ASV1646	4	0	0.21	0.02	85.63
Bacteria	Topsoil	2023	g__Psychrobacillus sp ASV1646	0	2	-0.14	0.02	100
Bacteria	Phyllosphere	2022	g__Psychroglaciecola sp ASV1232	0	3	-0.47	0.01	18.13
Bacteria	Topsoil	2023	g__Psychroglaciecola sp ASV1232	0	3	-0.14	0.05	43.75
Bacteria	Topsoil	2023	g__Psychroglaciecola sp ASV1274	3	0	0.35	0.03	79.17
Fungi	Phyllosphere	2022	g__Pyrenochaetopsis sp ASV385	0	3	-0.36	0.00	8.86
Fungi	Topsoil	2022	g__Pyrenochaetopsis sp ASV385	0	4	-0.36	0.06	16.98
Bacteria	Topsoil	2022	g__Quadrisphaera sp ASV1042	1	0	0.07	0.00	13.13
Fungi	Phyllosphere	2022	g__Rachicladosporium sp ASV717	3	0	0.32	0.02	40.51
Fungi	Topsoil	2022	g__Rachicladosporium sp ASV717	1	0	0.09	0.00	13.21
Bacteria	Topsoil	2023	g__Ramlibacter sp ASV521	2	0	0.12	0.10	95.83
Bacteria	Topsoil	2023	g__Ramlibacter sp ASV649	3	0	0.45	0.03	77.08
Bacteria	Topsoil	2023	g__Ramlibacter sp ASV873	3	0	0.44	0.04	95.83
Fungi	Phyllosphere	2022	g__Ramularia sp ASV644	3	0	0.34	0.03	76.58
Fungi	Phyllosphere	2022	g__Ramularia sp ASV65	1	0	0.12	1.56	89.24
Bacteria	Topsoil	2022	g__RB41 sp ASV1381	3	0	0.10	0.06	45.00
Bacteria	Topsoil	2022	g__RB41 sp ASV1657	1	0	0.07	0.02	52.50
Bacteria	Topsoil	2022	g__RB41 sp ASV1826	0	3	-0.18	0.04	62.50
Bacteria	Topsoil	2022	g__RB41 sp ASV2200	1	0	0.12	0.03	64.38
Bacteria	Topsoil	2023	g__RB41 sp ASV326	0	2	-0.09	0.16	100
Bacteria	Topsoil	2023	g__RB41 sp ASV3661	3	0	0.26	0.01	62.50
Bacteria	Topsoil	2022	g__RB41 sp ASV369	3	0	0.24	0.23	85.00
Bacteria	Phyllosphere	2022	g__RB41 sp ASV377	1	0	0.14	0.02	33.13
Bacteria	Topsoil	2022	g__RB41 sp ASV377	3	0	0.18	0.13	83.75
Bacteria	Topsoil	2023	g__RB41 sp ASV377	3	0	0.29	0.09	97.92
Bacteria	Topsoil	2022	g__RB41 sp ASV865	2	0	0.22	0.06	83.75
Bacteria	Topsoil	2023	g__RB41 sp ASV865	3	0	0.26	0.05	95.83
Bacteria	Topsoil	2023	g__Reyranella sp ASV1529	0	4	-0.31	0.02	66.67
Bacteria	Topsoil	2022	g__Reyranella sp ASV1568	1	0	0.13	0.06	77.50
Bacteria	Topsoil	2022	g__Reyranella sp ASV1590	3	0	0.09	0.03	83.75
Bacteria	Topsoil	2023	g__Reyranella sp ASV1590	0	3	-0.16	0.02	89.58
Bacteria	Topsoil	2023	g__Reyranella sp ASV298	0	1	-0.09	0.12	100
Bacteria	Topsoil	2022	g__Reyranella sp ASV3224	0	3	-0.09	0.03	81.88
Bacteria	Topsoil	2023	g__Reyranella sp ASV3224	0	3	-0.11	0.02	97.92
Fungi	Phyllosphere	2022	g__Rhinocladiella sp ASV748	3	0	0.29	0.00	34.81
Fungi	Topsoil	2022	g__Rhinocladiella sp ASV748	3	0	0.15	0.00	26.42
Bacteria	Topsoil	2022	g__Rhizobacter sp ASV1437	1	0	0.11	0.02	86.88
Bacteria	Topsoil	2023	g__Rhizobacter sp ASV1437	2	0	0.14	0.01	85.42

Annexes

Bacteria	Topsoil	2023	g__Rhizobacter sp ASV1980	2	0	0.18	0.02	93.75
Bacteria	Topsoil	2022	g__Rhizobacter sp ASV296	0	2	-0.08	0.28	93.75
Bacteria	Topsoil	2023	g__Rhizobacter sp ASV296	0	1	-0.10	0.15	100
Bacteria	Topsoil	2022	g__Rhizobacter sp ASV400	3	0	0.12	0.09	91.88
Bacteria	Topsoil	2023	g__Rhizobacter sp ASV400	2	0	0.08	0.05	100
Bacteria	Topsoil	2022	g__Rhizobacter sp ASV653	3	0	0.11	0.06	90.63
Bacteria	Topsoil	2023	g__Rhizobacter sp ASV653	3	0	0.12	0.03	100
Bacteria	Topsoil	2022	g__Rhodoplanes sp ASV1372	3	0	0.19	0.03	75.63
Bacteria	Topsoil	2022	g__Rhodoplanes sp ASV1419	3	0	0.18	0.02	60.63
Bacteria	Topsoil	2023	g__Rhodoplanes sp ASV1419	1	0	0.21	0.03	81.25
Bacteria	Topsoil	2022	g__Rhodoplanes sp ASV859	0	3	-0.20	0.08	88.13
Bacteria	Phyllosphere	2022	g__Rhodovastum sp ASV1663	1	0	0.25	0.03	35.63
Bacteria	Topsoil	2022	g__Rhodovastum sp ASV1663	2	0	0.07	0.00	48.13
Bacteria	Topsoil	2022	g__Romboutsia sp ASV1934	0	3	-0.28	0.01	22.50
Bacteria	Topsoil	2023	g__Romboutsia sp ASV1934	0	2	-0.31	0.01	31.25
Bacteria	Topsoil	2023	g__Roseimicrobium sp ASV1479	0	3	-0.15	0.04	100
Bacteria	Topsoil	2023	g__Roseimicrobium sp ASV1651	0	3	-0.26	0.02	91.67
Bacteria	Topsoil	2023	g__Roseomonas sp ASV1790	0	3	-0.24	0.04	83.33
Bacteria	Topsoil	2023	g__Roseomonas sp ASV658	1	0	0.18	0.00	77.08
Bacteria	Topsoil	2022	g__Rubellimicrobium sp ASV1085	3	0	0.21	0.01	16.25
Bacteria	Phyllosphere	2022	g__Rubellimicrobium sp ASV1477	0	1	-0.55	0.02	33.75
Bacteria	Topsoil	2022	g__Rubellimicrobium sp ASV1477	3	0	0.18	0.01	51.25
Bacteria	Topsoil	2022	g__Rubellimicrobium sp ASV339	4	0	0.34	0.04	78.75
Bacteria	Topsoil	2023	g__Rubellimicrobium sp ASV339	3	0	0.19	0.07	87.50
Bacteria	Topsoil	2022	g__Rubellimicrobium sp ASV390	1	0	0.04	0.04	61.25
Bacteria	Topsoil	2022	g__Rubellimicrobium sp ASV826	3	0	0.08	0.00	26.88
Bacteria	Topsoil	2022	g__Rubrobacter sp ASV1086	3	0	0.16	0.02	17.50
Bacteria	Topsoil	2023	g__Rubrobacter sp ASV1086	2	0	0.36	0.03	8.33
Bacteria	Topsoil	2022	g__Rubrobacter sp ASV13	1	0	0.04	2.55	68.75
Bacteria	Topsoil	2022	g__Rubrobacter sp ASV159	0	3	-0.24	0.15	50.00
Bacteria	Topsoil	2023	g__Rubrobacter sp ASV159	0	3	-0.25	0.27	70.83
Bacteria	Topsoil	2022	g__Rubrobacter sp ASV1636	3	0	0.11	0.02	66.25
Bacteria	Topsoil	2023	g__Rubrobacter sp ASV176	0	1	-0.07	0.40	75.00
Bacteria	Phyllosphere	2022	g__Rubrobacter sp ASV190	0	2	-0.49	0.01	30.00
Bacteria	Topsoil	2022	g__Rubrobacter sp ASV190	0	3	-0.23	0.19	66.88
Bacteria	Topsoil	2023	g__Rubrobacter sp ASV190	0	1	-0.08	0.36	85.42
Bacteria	Topsoil	2022	g__Rubrobacter sp ASV2082	2	0	0.06	0.03	69.38
Bacteria	Phyllosphere	2022	g__Rubrobacter sp ASV452	1	0	0.12	0.02	18.75
Bacteria	Topsoil	2022	g__Rubrobacter sp ASV452	3	0	0.37	0.07	35.63
Bacteria	Topsoil	2023	g__Rubrobacter sp ASV452	3	0	0.38	0.09	77.08
Bacteria	Phyllosphere	2022	g__Rubrobacter sp ASV522	1	0	0.12	0.00	13.75
Bacteria	Topsoil	2022	g__Rubrobacter sp ASV522	3	0	0.33	0.06	16.88
Bacteria	Topsoil	2022	g__Rubrobacter sp ASV552	3	0	0.21	0.05	53.13
Bacteria	Topsoil	2022	g__Rubrobacter sp ASV782	3	0	0.31	0.03	30.00
Fungi	Endosphere	2022	g__Schizothecium sp ASV687	0	2	-0.11	0.00	6.88
Fungi	Topsoil	2022	g__Schizothecium sp ASV687	3	0	0.17	0.04	30.19

Annexes

Bacteria	Topsoil	2023	g__Segetibacter sp ASV1130	3	0	0.26	0.05	56.25
Bacteria	Topsoil	2022	g__Segetibacter sp ASV1211	2	0	0.19	0.03	68.13
Bacteria	Topsoil	2022	g__Segetibacter sp ASV1788	1	0	0.03	0.02	87.50
Bacteria	Topsoil	2023	g__Segetibacter sp ASV1788	3	0	0.15	0.03	100
Bacteria	Topsoil	2022	g__Segetibacter sp ASV1865	1	0	0.05	0.02	64.38
Bacteria	Topsoil	2023	g__Segetibacter sp ASV1865	3	0	0.36	0.05	62.50
Bacteria	Topsoil	2023	g__Segetibacter sp ASV1924	3	0	0.34	0.04	79.17
Bacteria	Topsoil	2023	g__Segetibacter sp ASV539	3	0	0.34	0.10	60.42
Bacteria	Phyllosphere	2022	g__Segetibacter sp ASV814	1	0	0.18	0.01	25.00
Bacteria	Topsoil	2022	g__Segetibacter sp ASV814	3	0	0.14	0.02	74.38
Bacteria	Topsoil	2023	g__Segetibacter sp ASV814	3	0	0.32	0.04	83.33
Bacteria	Topsoil	2022	g__Segetibacter sp ASV943	3	0	0.13	0.01	45.63
Bacteria	Topsoil	2023	g__Segetibacter sp ASV943	3	0	0.25	0.05	50.00
Bacteria	Phyllosphere	2022	g__Segetibacter sp ASV954	1	0	0.12	0.00	15.63
Bacteria	Topsoil	2022	g__Segetibacter sp ASV954	3	0	0.14	0.03	88.13
Fungi	Topsoil	2022	g__Septoglomus sp ASV1040	0	1	-0.16	0.02	19.50
Fungi	Topsoil	2023	g__Septoglomus sp ASV1040	0	3	-0.46	0.05	43.75
Bacteria	Topsoil	2023	g__SH-PL14 sp ASV577	0	3	-0.14	0.07	100
Bacteria	Topsoil	2023	g__Singulisphaera sp ASV2588	0	1	-0.15	0.07	100
Bacteria	Topsoil	2023	g__Skermanella sp ASV1238	2	0	0.08	0.08	100
Bacteria	Topsoil	2023	g__Skermanella sp ASV1327	0	2	-0.13	0.05	89.58
Bacteria	Topsoil	2023	g__Skermanella sp ASV205	0	3	-0.17	0.23	97.92
Bacteria	Topsoil	2022	g__Skermanella sp ASV2957	3	0	0.14	0.01	76.25
Bacteria	Topsoil	2023	g__Skermanella sp ASV341	0	3	-0.18	0.15	95.83
Bacteria	Topsoil	2022	g__Skermanella sp ASV444	3	0	0.19	0.15	84.38
Bacteria	Topsoil	2022	g__Skermanella sp ASV980	1	0	0.05	0.01	51.25
Bacteria	Topsoil	2023	g__Skermanella sp ASV980	1	0	0.06	0.05	81.25
Bacteria	Topsoil	2023	g__Solibacillus sp ASV1215	0	3	-0.22	0.01	95.83
Fungi	Phyllosphere	2022	g__Solicoccozyma sp ASV190	0	1	-0.13	0.00	18.99
Fungi	Topsoil	2022	g__Solicoccozyma sp ASV190	2	0	0.26	0.14	83.02
Fungi	Topsoil	2023	g__Solicoccozyma sp ASV190	1	0	0.27	0.23	95.83
Fungi	Topsoil	2022	g__Solicoccozyma sp ASV632	0	3	-0.24	0.02	25.79
Fungi	Topsoil	2022	g__Solicoccozyma sp ASV9	2	0	0.30	5.15	80.50
Fungi	Topsoil	2023	g__Solicoccozyma sp ASV9	1	0	0.38	8.80	95.83
Bacteria	Topsoil	2022	g__Solirubrobacter sp ASV1053	1	0	0.02	0.04	90.63
Bacteria	Topsoil	2023	g__Solirubrobacter sp ASV1053	3	0	0.14	0.06	100
Bacteria	Topsoil	2022	g__Solirubrobacter sp ASV1337	3	0	0.17	0.04	61.88
Bacteria	Topsoil	2023	g__Solirubrobacter sp ASV1337	1	0	0.18	0.02	66.67
Bacteria	Topsoil	2023	g__Solirubrobacter sp ASV1887	0	3	-0.17	0.03	89.58
Bacteria	Topsoil	2022	g__Solirubrobacter sp ASV2007	0	4	-0.30	0.03	74.38
Bacteria	Topsoil	2023	g__Solirubrobacter sp ASV2007	0	3	-0.30	0.02	72.92
Bacteria	Phyllosphere	2022	g__Solirubrobacter sp ASV300	0	4	-0.51	0.01	25.00
Bacteria	Phyllosphere	2022	g__Solirubrobacter sp ASV388	0	1	-0.54	0.02	45.00
Bacteria	Topsoil	2022	g__Solirubrobacter sp ASV388	0	3	-0.14	0.08	91.25
Bacteria	Topsoil	2023	g__Solirubrobacter sp ASV388	0	3	-0.14	0.08	100
Bacteria	Topsoil	2022	g__Solirubrobacter sp ASV454	1	0	0.01	0.04	86.25

Annexes

Bacteria	Topsoil	2023	g__Solirubrobacter sp ASV454	2	0	0.12	0.08	95.83
Bacteria	Topsoil	2022	g__Solirubrobacter sp ASV65	1	0	0.02	0.51	87.50
Bacteria	Topsoil	2022	g__Solirubrobacter sp ASV665	3	0	0.13	0.05	80.63
Bacteria	Topsoil	2022	g__Solirubrobacter sp ASV677	0	3	-0.15	0.03	44.38
Bacteria	Topsoil	2023	g__Solirubrobacter sp ASV677	0	3	-0.21	0.07	60.42
Bacteria	Topsoil	2022	g__Solirubrobacter sp ASV772	0	1	-0.04	0.02	41.88
Bacteria	Topsoil	2023	g__Solirubrobacter sp ASV772	0	3	-0.21	0.06	56.25
Bacteria	Topsoil	2023	g__Solirubrobacter sp ASV903	3	0	0.27	0.05	62.50
Bacteria	Topsoil	2022	g__Sphingomonas sp ASV10	3	0	0.13	0.02	89.38
Bacteria	Topsoil	2023	g__Sphingomonas sp ASV10	3	0	0.29	0.01	91.67
Bacteria	Topsoil	2022	g__Sphingomonas sp ASV1149	0	1	-0.14	0.09	83.75
Bacteria	Topsoil	2022	g__Sphingomonas sp ASV139	4	0	0.36	0.21	81.25
Bacteria	Topsoil	2023	g__Sphingomonas sp ASV139	3	0	0.37	0.25	93.75
Bacteria	Topsoil	2022	g__Sphingomonas sp ASV1420	3	0	0.11	0.00	24.38
Bacteria	Topsoil	2023	g__Sphingomonas sp ASV1420	3	0	0.23	0.00	27.08
Bacteria	Topsoil	2022	g__Sphingomonas sp ASV1626	3	0	0.21	0.02	80.00
Bacteria	Topsoil	2023	g__Sphingomonas sp ASV1626	2	0	0.30	0.01	77.08
Bacteria	Phyllosphere	2022	g__Sphingomonas sp ASV181	1	0	0.07	0.10	71.25
Bacteria	Topsoil	2022	g__Sphingomonas sp ASV181	1	0	0.04	0.50	90.63
Bacteria	Topsoil	2022	g__Sphingomonas sp ASV1947	4	0	0.37	0.02	55.00
Bacteria	Topsoil	2022	g__Sphingomonas sp ASV2	1	0	0.04	0.01	66.88
Bacteria	Topsoil	2023	g__Sphingomonas sp ASV217	1	0	0.02	0.25	100
Bacteria	Topsoil	2022	g__Sphingomonas sp ASV252	1	0	0.06	0.00	31.25
Bacteria	Topsoil	2022	g__Sphingomonas sp ASV3098	3	0	0.20	0.01	36.88
Bacteria	Topsoil	2022	g__Sphingomonas sp ASV379	3	0	0.15	0.09	74.38
Bacteria	Topsoil	2023	g__Sphingomonas sp ASV379	2	0	0.16	0.10	87.50
Bacteria	Topsoil	2023	g__Sphingomonas sp ASV448	3	0	0.38	0.01	79.17
Bacteria	Topsoil	2022	g__Sphingomonas sp ASV467	0	2	-0.12	0.01	55.00
Bacteria	Topsoil	2023	g__Sphingomonas sp ASV467	4	0	0.49	0.00	60.42
Bacteria	Topsoil	2023	g__Sphingomonas sp ASV469	3	0	0.27	0.00	16.67
Bacteria	Topsoil	2022	g__Sphingomonas sp ASV647	3	0	0.19	0.06	71.25
Bacteria	Topsoil	2023	g__Sphingomonas sp ASV647	3	0	0.35	0.06	79.17
Bacteria	Topsoil	2022	g__Sphingomonas sp ASV710	3	0	0.24	0.13	83.13
Bacteria	Topsoil	2023	g__Sphingomonas sp ASV746	2	0	0.14	0.05	77.08
Bacteria	Topsoil	2022	g__Sphingomonas sp ASV847	1	0	0.12	0.00	21.88
Bacteria	Topsoil	2022	g__Sphingomonas sp ASV909	1	0	0.14	0.01	75.00
Bacteria	Topsoil	2023	g__Sphingomonas sp ASV909	1	0	0.19	0.01	81.25
Bacteria	Topsoil	2023	g__Spirosoma sp ASV222	2	0	0.22	0.00	39.58
Bacteria	Topsoil	2022	g__Spirosoma sp ASV619	3	0	0.14	0.00	15.00
Bacteria	Topsoil	2023	g__Spirosoma sp ASV892	3	0	0.31	0.00	50.00
Bacteria	Topsoil	2023	g__Sporacetigenium sp ASV1814	0	3	-0.21	0.03	79.17
Fungi	Phyllosphere	2022	g__Sporobolomyces sp ASV552	0	3	-0.59	0.01	53.80
Fungi	Topsoil	2022	g__Sporobolomyces sp ASV552	0	3	-0.22	0.04	40.88
Fungi	Phyllosphere	2022	g__Stagonosporopsis sp ASV139	2	0	0.45	0.04	24.05
Fungi	Topsoil	2022	g__Stagonosporopsis sp ASV139	3	0	0.37	0.10	38.99
Fungi	Topsoil	2023	g__Stagonosporopsis sp ASV139	1	0	0.42	0.12	70.83

Annexes

Bacteria	Topsoil	2022	g__Steroidobacter sp ASV1539	0	3	-0.20	0.05	72.50
Bacteria	Topsoil	2023	g__Steroidobacter sp ASV1539	0	3	-0.27	0.05	83.33
Bacteria	Topsoil	2023	g__Streptomyces sp ASV1334	0	3	-0.26	0.03	91.67
Bacteria	Topsoil	2022	g__Streptomyces sp ASV179	3	0	0.14	0.15	94.38
Bacteria	Topsoil	2023	g__Streptomyces sp ASV179	0	2	-0.13	0.19	100
Bacteria	Topsoil	2022	g__Streptomyces sp ASV2448	0	3	-0.15	0.01	62.50
Bacteria	Topsoil	2022	g__Streptomyces sp ASV344	0	2	-0.17	0.06	71.25
Bacteria	Topsoil	2023	g__Streptomyces sp ASV344	0	2	-0.48	0.13	79.17
Bacteria	Topsoil	2023	g__Streptomyces sp ASV525	0	1	-0.19	0.00	10.42
Bacteria	Topsoil	2023	g__Streptomyces sp ASV536	0	1	-0.13	0.12	100
Bacteria	Topsoil	2022	g__Streptomyces sp ASV642	0	3	-0.24	0.05	66.88
Bacteria	Topsoil	2023	g__Streptomyces sp ASV642	0	4	-0.56	0.07	91.67
Bacteria	Phyllosphere	2022	g__Streptomyces sp ASV674	2	0	0.18	0.01	22.50
Bacteria	Topsoil	2022	g__Streptomyces sp ASV674	1	0	0.06	0.05	70.00
Bacteria	Topsoil	2023	g__Streptomyces sp ASV674	1	0	0.13	0.05	95.83
Bacteria	Phyllosphere	2022	g__Streptomyces sp ASV720	1	0	0.13	0.01	35.63
Bacteria	Topsoil	2022	g__Streptomyces sp ASV720	3	0	0.14	0.08	91.25
Bacteria	Topsoil	2023	g__Streptomyces sp ASV720	2	0	0.06	0.10	100
Bacteria	Topsoil	2023	g__Streptomyces sp ASV729	2	0	0.21	0.07	83.33
Bacteria	Topsoil	2023	g__Streptomyces sp ASV89	0	1	-0.14	0.37	100
Bacteria	Topsoil	2022	g__Streptosporangium sp ASV1126	0	4	-0.25	0.04	85.63
Bacteria	Topsoil	2023	g__Streptosporangium sp ASV1126	0	3	-0.25	0.05	100
Bacteria	Topsoil	2022	g__Streptosporangium sp ASV591	0	4	-0.25	0.06	71.88
Bacteria	Topsoil	2022	g__Subgroup_10 sp ASV1273	0	1	-0.04	0.03	63.13
Bacteria	Topsoil	2023	g__Subgroup_10 sp ASV1523	0	3	-0.29	0.04	68.75
Bacteria	Topsoil	2023	g__Subgroup_10 sp ASV812	3	0	0.41	0.07	64.58
Bacteria	Topsoil	2022	g__Subgroup_10 sp ASV881	0	3	-0.20	0.04	71.25
Bacteria	Topsoil	2023	g__Subgroup_10 sp ASV881	0	1	-0.27	0.04	68.75
Fungi	Topsoil	2022	g__Talaromyces sp ASV281	1	0	0.24	0.10	64.78
Fungi	Topsoil	2023	g__Talaromyces sp ASV281	1	0	0.29	0.09	79.17
Fungi	Topsoil	2022	g__Talaromyces sp ASV332	1	0	0.21	0.03	36.48
Fungi	Topsoil	2022	g__Talaromyces sp ASV93	2	0	0.21	0.04	48.43
Bacteria	Topsoil	2022	g__Terrimonas sp ASV1344	0	4	-0.25	0.07	91.25
Bacteria	Topsoil	2022	g__Terrimonas sp ASV829	0	1	-0.01	0.06	94.38
Fungi	Topsoil	2022	g__Tetracladium sp ASV121	3	0	0.38	0.53	92.45
Fungi	Phyllosphere	2022	g__Tetracladium sp ASV191	0	1	-0.20	0.00	31.65
Fungi	Phyllosphere	2022	g__Tetracladium sp ASV280	0	1	-0.17	0.00	17.72
Fungi	Topsoil	2022	g__Tetracladium sp ASV280	0	1	-0.18	0.08	75.47
Fungi	Phyllosphere	2022	g__Tetracladium sp ASV41	0	3	-0.36	0.00	43.67
Fungi	Topsoil	2022	g__Tetracladium sp ASV41	0	1	-0.05	0.89	66.67
Fungi	Topsoil	2022	g__Tetracladium sp ASV412	1	0	0.23	0.05	67.30
Fungi	Topsoil	2023	g__Tetracladium sp ASV412	3	0	0.51	0.07	58.33
Fungi	Topsoil	2022	g__Tetracladium sp ASV519	2	0	0.18	0.03	27.67
Fungi	Topsoil	2022	g__Thelonectria sp ASV135	0	3	-0.16	0.26	80.50
Fungi	Topsoil	2023	g__Thelonectria sp ASV135	0	3	-0.19	0.23	93.75
Fungi	Topsoil	2022	g__Thelonectria sp ASV491	0	1	-0.06	0.06	76.73

Annexes

Fungi	Topsoil	2023	g__Thelonectria sp ASV491	1	0	0.19	0.11	87.50
Bacteria	Topsoil	2023	g__TM7a sp ASV1456	0	2	-0.19	0.01	75.00
Bacteria	Topsoil	2022	g__TM7a sp ASV473	0	3	-0.34	0.09	52.50
Fungi	Endosphere	2022	g__Tremellomycetes sp ASV63	0	1	-0.23	0.01	21.25
Fungi	Topsoil	2022	g__Tremellomycetes sp ASV63	0	1	-0.11	0.43	84.28
Fungi	Topsoil	2023	g__Tremellomycetes sp ASV63	1	0	0.30	0.18	100
Fungi	Phyllosphere	2022	g__Tricharina sp ASV566	0	3	-0.30	0.00	9.49
Fungi	Topsoil	2022	g__Tricharina sp ASV566	3	0	0.31	0.05	45.28
Fungi	Phyllosphere	2022	g__Trichoderma sp ASV630	0	2	-0.15	0.00	6.33
Fungi	Topsoil	2022	g__Trichoderma sp ASV630	0	5	-0.47	0.03	39.62
Bacteria	Topsoil	2022	g__Truepera sp ASV1188	3	0	0.25	0.03	33.13
Bacteria	Topsoil	2023	g__Truepera sp ASV1188	1	0	0.34	0.02	47.92
Bacteria	Topsoil	2022	g__Truepera sp ASV837	4	0	0.34	0.03	20.00
Bacteria	Topsoil	2022	g__Tumebacillus sp ASV1489	0	3	-0.19	0.03	63.75
Bacteria	Topsoil	2023	g__Tumebacillus sp ASV1489	0	2	-0.21	0.03	60.42
Bacteria	Topsoil	2022	g__Tumebacillus sp ASV211	0	4	-0.35	0.21	75.00
Bacteria	Topsoil	2023	g__Tumebacillus sp ASV211	0	4	-0.47	0.17	93.75
Bacteria	Topsoil	2022	g__Tundrisphaera sp ASV1000	2	0	0.06	0.05	91.88
Bacteria	Topsoil	2022	g__Turicibacter sp ASV1260	0	3	-0.20	0.00	12.50
Bacteria	Topsoil	2023	g__Turicibacter sp ASV1260	0	3	-0.41	0.00	14.58
Bacteria	Topsoil	2022	g__Uliginosibacterium sp ASV650	0	3	-0.16	0.07	68.75
Bacteria	Topsoil	2023	g__Uliginosibacterium sp ASV650	0	2	-0.30	0.03	81.25
Fungi	Topsoil	2022	g__Valsonectria sp ASV306	0	1	-0.18	0.07	40.88
Fungi	Topsoil	2023	g__Valsonectria sp ASV306	0	3	-0.22	0.08	64.58
Fungi	Topsoil	2022	g__Valsonectria sp ASV690	0	3	-0.16	0.03	55.35
Bacteria	Topsoil	2023	g__Variovorax sp ASV143	3	0	0.30	0.00	58.33
Fungi	Phyllosphere	2022	g__Vishniacozyma sp ASV133	1	0	0.20	0.18	72.15
Fungi	Topsoil	2022	g__Volutella sp ASV692	0	4	-0.32	0.02	59.75
Fungi	Phyllosphere	2022	g__Vuilleminia sp ASV104	2	0	0.44	0.34	69.62
Fungi	Topsoil	2022	g__Vuilleminia sp ASV104	0	1	-0.07	0.00	37.11
Fungi	Phyllosphere	2022	g__Vuilleminia sp ASV1557	3	0	0.32	0.02	61.39
Fungi	Phyllosphere	2022	g__Vuilleminia sp ASV62	2	0	0.42	0.69	70.89
Fungi	Topsoil	2022	g__Vuilleminia sp ASV62	0	1	-0.05	0.00	45.28
Bacteria	Phyllosphere	2022	g__YC-ZSS-LKJ147 sp ASV2024	1	0	0.13	0.00	11.88
Bacteria	Topsoil	2023	g__YC-ZSS-LKJ147 sp ASV2024	3	0	0.21	0.03	89.58
Bacteria	Topsoil	2022	g__YC-ZSS-LKJ147 sp ASV480	3	0	0.11	0.08	89.38
Bacteria	Topsoil	2023	g__YC-ZSS-LKJ147 sp ASV694	0	2	-0.30	0.07	85.42
Bacteria	Phyllosphere	2022	f__67-14 sp ASV107	2	0	0.18	0.01	30.63
Bacteria	Topsoil	2022	f__67-14 sp ASV107	1	0	0.07	0.29	73.13
Bacteria	Topsoil	2022	f__67-14 sp ASV1151	0	2	-0.10	0.04	76.88
Bacteria	Topsoil	2022	f__67-14 sp ASV1152	0	3	-0.28	0.00	23.75
Bacteria	Topsoil	2023	f__67-14 sp ASV1152	0	4	-0.34	0.06	43.75
Bacteria	Topsoil	2022	f__67-14 sp ASV1288	0	3	-0.27	0.03	44.38
Bacteria	Topsoil	2023	f__67-14 sp ASV1288	0	4	-0.51	0.04	56.25
Bacteria	Topsoil	2022	f__67-14 sp ASV1289	3	0	0.21	0.03	66.25
Bacteria	Topsoil	2023	f__67-14 sp ASV1289	4	0	0.37	0.02	75.00

Annexes

Bacteria	Topsoil	2023	f__67-14 sp ASV1304	0	1	-0.21	0.02	83.33
Bacteria	Topsoil	2023	f__67-14 sp ASV1325	0	3	-0.28	0.04	81.25
Bacteria	Topsoil	2023	f__67-14 sp ASV1389	0	1	-0.08	0.02	100
Bacteria	Topsoil	2022	f__67-14 sp ASV1438	0	3	-0.21	0.02	45.00
Bacteria	Topsoil	2023	f__67-14 sp ASV1438	0	3	-0.42	0.05	68.75
Bacteria	Topsoil	2022	f__67-14 sp ASV163	4	0	0.27	0.15	83.13
Bacteria	Topsoil	2023	f__67-14 sp ASV163	3	0	0.23	0.25	91.67
Bacteria	Phyllosphere	2022	f__67-14 sp ASV1766	0	1	-0.33	0.00	11.88
Bacteria	Topsoil	2022	f__67-14 sp ASV1766	0	3	-0.26	0.02	58.75
Bacteria	Topsoil	2023	f__67-14 sp ASV1766	0	4	-0.47	0.03	77.08
Bacteria	Topsoil	2022	f__67-14 sp ASV1931	3	0	0.15	0.03	70.00
Bacteria	Topsoil	2023	f__67-14 sp ASV1931	1	0	0.13	0.01	89.58
Bacteria	Phyllosphere	2022	f__67-14 sp ASV225	0	1	-0.55	0.02	30.63
Bacteria	Topsoil	2022	f__67-14 sp ASV225	0	4	-0.28	0.16	87.50
Bacteria	Topsoil	2023	f__67-14 sp ASV225	0	3	-0.32	0.19	97.92
Bacteria	Topsoil	2022	f__67-14 sp ASV2308	0	4	-0.40	0.02	25.00
Bacteria	Topsoil	2023	f__67-14 sp ASV2308	0	4	-0.62	0.02	41.67
Bacteria	Topsoil	2023	f__67-14 sp ASV2336	0	3	-0.33	0.02	60.42
Bacteria	Topsoil	2022	f__67-14 sp ASV2464	4	0	0.26	0.01	58.13
Bacteria	Topsoil	2023	f__67-14 sp ASV2464	4	0	0.34	0.04	58.33
Bacteria	Phyllosphere	2022	f__67-14 sp ASV276	1	0	0.18	0.02	29.38
Bacteria	Topsoil	2022	f__67-14 sp ASV276	3	0	0.27	0.14	65.63
Bacteria	Topsoil	2023	f__67-14 sp ASV393	1	0	0.10	0.07	100
Bacteria	Phyllosphere	2022	f__67-14 sp ASV483	3	0	0.21	0.01	12.50
Bacteria	Topsoil	2022	f__67-14 sp ASV483	4	0	0.44	0.08	33.13
Bacteria	Topsoil	2023	f__67-14 sp ASV483	1	0	0.17	0.05	85.42
Bacteria	Topsoil	2022	f__67-14 sp ASV510	0	1	-0.07	0.07	53.75
Bacteria	Topsoil	2023	f__67-14 sp ASV510	0	3	-0.35	0.18	85.42
Bacteria	Topsoil	2023	f__67-14 sp ASV542	0	1	-0.07	0.11	95.83
Bacteria	Topsoil	2023	f__67-14 sp ASV544	1	0	0.04	0.09	81.25
Bacteria	Topsoil	2022	f__67-14 sp ASV607	0	3	-0.33	0.05	60.63
Bacteria	Topsoil	2023	f__67-14 sp ASV607	0	4	-0.76	0.06	72.92
Bacteria	Phyllosphere	2022	f__67-14 sp ASV623	0	1	-0.30	0.00	8.13
Bacteria	Topsoil	2022	f__67-14 sp ASV623	0	5	-0.37	0.05	73.13
Bacteria	Topsoil	2023	f__67-14 sp ASV623	0	3	-0.21	0.04	91.67
Bacteria	Topsoil	2022	f__67-14 sp ASV67	0	3	-0.27	0.30	89.38
Bacteria	Topsoil	2023	f__67-14 sp ASV67	0	4	-0.34	0.52	100
Bacteria	Topsoil	2022	f__67-14 sp ASV689	0	3	-0.22	0.02	49.38
Bacteria	Topsoil	2023	f__67-14 sp ASV689	0	3	-0.27	0.08	75.00
Bacteria	Topsoil	2022	f__67-14 sp ASV753	0	1	-0.15	0.04	88.13
Bacteria	Topsoil	2023	f__67-14 sp ASV753	0	1	-0.29	0.07	95.83
Bacteria	Topsoil	2023	f__67-14 sp ASV767	1	0	0.21	0.04	64.58
Bacteria	Topsoil	2023	f__67-14 sp ASV787	0	3	-0.26	0.14	72.92
Bacteria	Phyllosphere	2022	f__67-14 sp ASV87	0	1	-0.43	0.02	41.25
Bacteria	Topsoil	2022	f__67-14 sp ASV87	0	3	-0.13	0.36	86.25
Bacteria	Topsoil	2023	f__67-14 sp ASV87	0	3	-0.15	0.40	100

Annexes

Bacteria	Topsoil	2022	f__67-14 sp ASV92	3	0	0.18	0.40	78.75
Bacteria	Topsoil	2023	f__67-14 sp ASV976	4	0	0.45	0.07	68.75
Bacteria	Topsoil	2022	f__A21b sp ASV833	0	3	-0.16	0.05	70.00
Bacteria	Topsoil	2023	f__A21b sp ASV833	0	1	-0.22	0.03	83.33
Bacteria	Topsoil	2023	f__Acetobacteraceae sp ASV1108	3	0	0.42	0.03	41.67
Bacteria	Topsoil	2022	f__Acetobacteraceae sp ASV1223	3	0	0.13	0.01	70.00
Bacteria	Topsoil	2023	f__Acetobacteraceae sp ASV1223	2	0	0.18	0.04	75.00
Bacteria	Topsoil	2023	f__Acetobacteraceae sp ASV1413	2	0	0.24	0.05	58.33
Bacteria	Topsoil	2022	f__Acetobacteraceae sp ASV58	4	0	0.27	0.22	90.00
Bacteria	Topsoil	2022	f__Acetobacteraceae sp ASV970	2	0	0.07	0.01	41.25
Bacteria	Topsoil	2023	f__Acetobacteraceae sp ASV970	3	0	0.27	0.06	47.92
Bacteria	Topsoil	2023	f__AKIW781 sp ASV1251	2	0	0.21	0.04	58.33
Bacteria	Topsoil	2022	f__AKIW781 sp ASV1467	0	2	-0.13	0.01	41.25
Bacteria	Topsoil	2022	f__AKYG1722 sp ASV1414	4	0	0.26	0.02	64.38
Bacteria	Topsoil	2022	f__AKYH767 sp ASV906	0	3	-0.13	0.04	85.63
Bacteria	Topsoil	2023	f__AKYH767 sp ASV906	0	3	-0.16	0.04	97.92
Bacteria	Topsoil	2022	f__AKYH767 sp ASV949	0	4	-0.25	0.05	85.63
Bacteria	Topsoil	2023	f__AKYH767 sp ASV949	0	3	-0.24	0.02	97.92
Bacteria	Topsoil	2023	f__Alcaligenaceae sp ASV759	0	1	-0.09	0.00	2.08
Fungi	Endosphere	2022	f__Amphisphaeriaceae sp ASV27	1	0	0.42	4.89	36.25
Fungi	Phyllosphere	2022	f__Amphisphaeriaceae sp ASV27	4	0	0.78	0.03	67.09
Fungi	Endosphere	2023	f__Amphisphaeriaceae sp ASV27	0	1	-1.00	3.62	56.25
Fungi	Topsoil	2023	f__Ascobolaceae sp ASV494	0	3	-0.32	0.01	14.58
Bacteria	Topsoil	2023	f__Beijerinckiaceae sp ASV1210	0	1	-0.13	0.00	6.25
Bacteria	Phyllosphere	2022	f__Beijerinckiaceae sp ASV418	1	0	0.18	0.01	16.25
Bacteria	Topsoil	2022	f__Beijerinckiaceae sp ASV418	4	0	0.38	0.05	43.13
Bacteria	Topsoil	2023	f__Beijerinckiaceae sp ASV418	3	0	0.38	0.08	58.33
Bacteria	Topsoil	2022	f__Beijerinckiaceae sp ASV579	3	0	0.19	0.06	71.88
Bacteria	Topsoil	2023	f__Beijerinckiaceae sp ASV579	4	0	0.41	0.06	91.67
Bacteria	Topsoil	2022	f__Beijerinckiaceae sp ASV610	4	0	0.40	0.03	78.75
Bacteria	Topsoil	2023	f__Beijerinckiaceae sp ASV610	3	0	0.30	0.07	93.75
Bacteria	Topsoil	2022	f__Beijerinckiaceae sp ASV817	0	4	-0.34	0.02	33.13
Bacteria	Topsoil	2023	f__Beijerinckiaceae sp ASV817	0	3	-0.30	0.06	43.75
Fungi	Phyllosphere	2022	f__Bionectriaceae sp ASV185	0	1	-0.14	0.00	6.96
Fungi	Topsoil	2023	f__Bionectriaceae sp ASV185	0	2	-0.50	0.11	75.00
Bacteria	Topsoil	2022	f__Caldilineaceae sp ASV1892	0	3	-0.18	0.02	53.13
Bacteria	Topsoil	2023	f__Caldilineaceae sp ASV1892	0	3	-0.21	0.04	89.58
Bacteria	Topsoil	2022	f__Caldilineaceae sp ASV2904	0	3	-0.15	0.04	79.38
Bacteria	Topsoil	2023	f__Caldilineaceae sp ASV2904	0	4	-0.32	0.03	95.83
Bacteria	Topsoil	2022	f__Chitinophagaceae sp ASV1100	0	2	-0.10	0.03	81.88
Bacteria	Topsoil	2023	f__Chitinophagaceae sp ASV1100	0	4	-0.29	0.03	93.75
Bacteria	Topsoil	2022	f__Chitinophagaceae sp ASV1321	0	3	-0.09	0.03	93.13
Bacteria	Phyllosphere	2022	f__Chitinophagaceae sp ASV1476	2	0	0.19	0.01	21.88
Bacteria	Topsoil	2022	f__Chitinophagaceae sp ASV1476	3	0	0.32	0.03	58.75
Bacteria	Topsoil	2022	f__Chitinophagaceae sp ASV161	0	2	-0.13	0.32	73.75
Bacteria	Topsoil	2023	f__Chitinophagaceae sp ASV161	0	1	-0.12	0.12	85.42

Annexes

Bacteria	Topsoil	2022	f__Chitinophagaceae sp ASV1635	1	0	0.16	0.03	81.88
Bacteria	Topsoil	2022	f__Chitinophagaceae sp ASV1655	0	3	-0.19	0.01	78.13
Bacteria	Topsoil	2023	f__Chitinophagaceae sp ASV1655	0	2	-0.18	0.02	91.67
Bacteria	Topsoil	2022	f__Chitinophagaceae sp ASV349	0	3	-0.11	0.08	89.38
Bacteria	Topsoil	2023	f__Chitinophagaceae sp ASV349	0	3	-0.25	0.07	97.92
Bacteria	Topsoil	2022	f__Chitinophagaceae sp ASV598	3	0	0.18	0.04	90.63
Bacteria	Topsoil	2023	f__Chitinophagaceae sp ASV598	3	0	0.13	0.08	100
Bacteria	Topsoil	2023	f__Chitinophagaceae sp ASV638	0	4	-0.42	0.03	91.67
Bacteria	Phyllosphere	2022	f__Chitinophagaceae sp ASV670	2	0	0.19	0.01	35.00
Bacteria	Topsoil	2023	f__Chitinophagaceae sp ASV896	3	0	0.13	0.05	100
Bacteria	Topsoil	2022	f__Clostridiaceae sp ASV1142	1	0	0.12	0.03	71.25
Bacteria	Topsoil	2023	f__Clostridiaceae sp ASV1142	0	1	-0.06	0.03	93.75
Bacteria	Topsoil	2022	f__Comamonadaceae sp ASV1029	0	2	-0.08	0.05	91.25
Bacteria	Topsoil	2022	f__Comamonadaceae sp ASV1035	0	4	-0.22	0.03	88.13
Bacteria	Topsoil	2022	f__Comamonadaceae sp ASV1147	3	0	0.12	0.01	74.38
Bacteria	Topsoil	2023	f__Comamonadaceae sp ASV1147	4	0	0.41	0.04	68.75
Bacteria	Topsoil	2023	f__Comamonadaceae sp ASV1286	2	0	0.11	0.02	95.83
Bacteria	Topsoil	2023	f__Comamonadaceae sp ASV130	2	0	0.24	0.00	52.08
Bacteria	Phyllosphere	2022	f__Comamonadaceae sp ASV1317	0	1	-0.58	0.02	30.63
Bacteria	Topsoil	2023	f__Comamonadaceae sp ASV1317	2	0	0.10	0.02	100
Bacteria	Topsoil	2023	f__Comamonadaceae sp ASV1499	0	3	-0.19	0.02	97.92
Bacteria	Topsoil	2022	f__Comamonadaceae sp ASV411	3	0	0.18	0.12	93.13
Bacteria	Topsoil	2023	f__Comamonadaceae sp ASV411	2	0	0.10	0.10	100
Bacteria	Topsoil	2022	f__Comamonadaceae sp ASV456	3	0	0.19	0.05	80.63
Bacteria	Topsoil	2023	f__Comamonadaceae sp ASV456	3	0	0.30	0.10	91.67
Fungi	Endosphere	2022	f__Didymellaceae sp ASV22	0	3	-0.84	13.93	23.13
Fungi	Phyllosphere	2022	f__Didymellaceae sp ASV22	1	0	0.52	0.10	44.94
Bacteria	Topsoil	2022	f__Entotheonellaceae sp ASV1543	0	3	-0.28	0.01	21.25
Bacteria	Topsoil	2023	f__Entotheonellaceae sp ASV1543	0	3	-0.34	0.04	33.33
Bacteria	Topsoil	2022	f__Entotheonellaceae sp ASV1589	0	3	-0.27	0.01	31.25
Bacteria	Topsoil	2023	f__Entotheonellaceae sp ASV1589	0	4	-0.49	0.07	54.17
Bacteria	Topsoil	2022	f__Entotheonellaceae sp ASV965	0	1	-0.11	0.07	45.63
Bacteria	Topsoil	2023	f__Entotheonellaceae sp ASV965	0	2	-0.16	0.13	81.25
Bacteria	Topsoil	2022	f__env.OPS_17 sp ASV1910	0	4	-0.24	0.02	86.25
Bacteria	Topsoil	2023	f__env.OPS_17 sp ASV1910	0	2	-0.13	0.03	97.92
Bacteria	Topsoil	2022	f__env.OPS_17 sp ASV2155	0	3	-0.13	0.03	81.25
Bacteria	Topsoil	2023	f__env.OPS_17 sp ASV2155	0	3	-0.18	0.03	95.83
Bacteria	Phyllosphere	2023	f__Frankiaceae sp ASV704	4	0	1.00	0.04	38.30
Bacteria	Topsoil	2023	f__Frankiaceae sp ASV704	2	0	0.12	0.11	93.75
Bacteria	Topsoil	2022	f__Gemmatimonadaceae sp ASV1032	0	1	-0.14	0.03	64.38
Bacteria	Topsoil	2023	f__Gemmatimonadaceae sp ASV1032	0	3	-0.30	0.07	87.50
Bacteria	Topsoil	2023	f__Gemmatimonadaceae sp ASV1041	3	0	0.19	0.03	77.08
Bacteria	Topsoil	2023	f__Gemmatimonadaceae sp ASV1121	3	0	0.30	0.03	60.42
Bacteria	Topsoil	2022	f__Gemmatimonadaceae sp ASV1144	4	0	0.37	0.04	13.13
Bacteria	Topsoil	2023	f__Gemmatimonadaceae sp ASV1144	1	0	0.24	0.01	18.75
Bacteria	Topsoil	2022	f__Gemmatimonadaceae sp ASV1145	0	3	-0.16	0.04	79.38

Annexes

Bacteria	Topsoil	2022	f__Gemmatimonadaceae sp ASV1264	4	0	0.33	0.03	75.00
Bacteria	Topsoil	2022	f__Gemmatimonadaceae sp ASV127	1	0	0.04	0.30	90.63
Bacteria	Topsoil	2023	f__Gemmatimonadaceae sp ASV1308	2	0	0.14	0.02	64.58
Bacteria	Topsoil	2022	f__Gemmatimonadaceae sp ASV1330	0	2	-0.13	0.02	41.25
Bacteria	Topsoil	2022	f__Gemmatimonadaceae sp ASV1374	3	0	0.14	0.04	69.38
Bacteria	Topsoil	2022	f__Gemmatimonadaceae sp ASV1393	3	0	0.16	0.03	63.75
Bacteria	Topsoil	2023	f__Gemmatimonadaceae sp ASV1393	2	0	0.18	0.01	62.50
Bacteria	Topsoil	2022	f__Gemmatimonadaceae sp ASV1719	3	0	0.31	0.04	38.75
Bacteria	Topsoil	2023	f__Gemmatimonadaceae sp ASV1719	1	0	0.16	0.01	62.50
Bacteria	Topsoil	2022	f__Gemmatimonadaceae sp ASV1955	3	0	0.18	0.04	24.38
Bacteria	Topsoil	2023	f__Gemmatimonadaceae sp ASV2092	0	2	-0.33	0.02	60.42
Bacteria	Topsoil	2022	f__Gemmatimonadaceae sp ASV215	4	0	0.29	0.18	88.13
Bacteria	Topsoil	2022	f__Gemmatimonadaceae sp ASV245	3	0	0.18	0.13	89.38
Bacteria	Topsoil	2022	f__Gemmatimonadaceae sp ASV508	4	0	0.50	0.10	11.25
Bacteria	Topsoil	2023	f__Gemmatimonadaceae sp ASV508	2	0	0.34	0.02	18.75
Bacteria	Phyllosphere	2022	f__Gemmatimonadaceae sp ASV571	1	0	0.11	0.00	9.38
Bacteria	Topsoil	2022	f__Gemmatimonadaceae sp ASV571	4	0	0.48	0.09	13.13
Bacteria	Topsoil	2023	f__Gemmatimonadaceae sp ASV571	1	0	0.32	0.02	25.00
Bacteria	Topsoil	2022	f__Gemmatimonadaceae sp ASV785	4	0	0.31	0.04	80.00
Bacteria	Topsoil	2023	f__Gemmatimonadaceae sp ASV785	1	0	0.02	0.05	97.92
Bacteria	Topsoil	2022	f__Gemmatimonadaceae sp ASV819	0	2	-0.16	0.03	55.63
Bacteria	Topsoil	2023	f__Gemmatimonadaceae sp ASV819	2	0	0.34	0.06	68.75
Bacteria	Topsoil	2022	f__Gemmatimonadaceae sp ASV912	4	0	0.30	0.06	75.00
Bacteria	Topsoil	2023	f__Gemmatimonadaceae sp ASV912	3	0	0.29	0.03	91.67
Bacteria	Topsoil	2022	f__Gemmatimonadaceae sp ASV988	3	0	0.14	0.03	72.50
Bacteria	Topsoil	2023	f__Gemmatimonadaceae sp ASV988	3	0	0.32	0.03	68.75
Bacteria	Topsoil	2022	f__Geodermatophilaceae sp ASV72	4	0	0.36	0.40	87.50
Bacteria	Topsoil	2023	f__Geodermatophilaceae sp ASV72	3	0	0.23	0.39	100
Bacteria	Topsoil	2022	f__Geodermatophilaceae sp ASV983	3	0	0.19	0.02	76.25
Bacteria	Phyllosphere	2022	f__Geodermatophilaceae sp ASV987	0	1	-0.46	0.01	38.13
Bacteria	Topsoil	2022	f__Geodermatophilaceae sp ASV987	3	0	0.11	0.03	90.63
Fungi	Phyllosphere	2022	f__Gnomoniaceae sp ASV430	4	0	0.24	0.00	42.41
Fungi	Phyllosphere	2022	f__Gnomoniaceae sp ASV628	4	0	0.48	0.00	58.86
Fungi	Phyllosphere	2022	f__Gnomoniaceae sp ASV674	3	0	0.32	0.00	12.66
Fungi	Phyllosphere	2022	f__Helotiaceae sp ASV670	2	0	0.26	0.00	15.19
Fungi	Topsoil	2022	f__Helotiaceae sp ASV670	0	1	-0.12	0.03	13.84
Fungi	Topsoil	2022	f__Helotiales_fam_Incertae_sedis sp ASV583	0	4	-0.32	0.03	44.65
Fungi	Topsoil	2022	f__Helotiales_fam_Incertae_sedis sp ASV664	0	1	-0.09	0.03	59.75
Fungi	Topsoil	2022	f__Herpotrichiellaceae sp ASV353	0	3	-0.20	0.08	33.33
Fungi	Topsoil	2022	f__Hypocreales_fam_Incertae_sedis sp ASV542	0	4	-0.35	0.01	52.83
Bacteria	Phyllosphere	2022	f__Ilumatobacteraceae sp ASV1017	0	1	-0.32	0.00	10.00
Bacteria	Topsoil	2022	f__Ilumatobacteraceae sp ASV1017	0	3	-0.28	0.04	48.75
Bacteria	Topsoil	2023	f__Ilumatobacteraceae sp ASV1017	0	4	-0.53	0.02	54.17
Bacteria	Topsoil	2022	f__Ilumatobacteraceae sp ASV1071	0	3	-0.33	0.03	40.63

Annexes

Bacteria	Topsoil	2023	f__Ilumatobacteraceae sp ASV1071	0	4	-0.64	0.04	45.83
Bacteria	Topsoil	2022	f__Ilumatobacteraceae sp ASV128	0	4	-0.25	0.23	81.25
Bacteria	Topsoil	2023	f__Ilumatobacteraceae sp ASV128	0	4	-0.35	0.25	97.92
Bacteria	Topsoil	2022	f__Ilumatobacteraceae sp ASV1509	0	3	-0.10	0.04	86.88
Bacteria	Topsoil	2023	f__Ilumatobacteraceae sp ASV1509	0	3	-0.20	0.02	97.92
Bacteria	Phyllosphere	2022	f__Ilumatobacteraceae sp ASV406	0	4	-0.62	0.01	23.13
Bacteria	Topsoil	2022	f__Ilumatobacteraceae sp ASV406	0	4	-0.29	0.07	81.25
Bacteria	Topsoil	2023	f__Ilumatobacteraceae sp ASV406	0	4	-0.34	0.07	97.92
Bacteria	Topsoil	2022	f__Ilumatobacteraceae sp ASV477	0	4	-0.26	0.10	52.50
Bacteria	Topsoil	2023	f__Ilumatobacteraceae sp ASV477	0	4	-0.38	0.04	89.58
Bacteria	Topsoil	2022	f__Ilumatobacteraceae sp ASV479	0	3	-0.35	0.06	32.50
Bacteria	Topsoil	2023	f__Ilumatobacteraceae sp ASV479	0	4	-0.56	0.10	50.00
Bacteria	Topsoil	2022	f__Intrasporangiaceae sp ASV1054	0	4	-0.46	0.03	25.00
Bacteria	Topsoil	2023	f__Intrasporangiaceae sp ASV1054	0	4	-0.69	0.02	27.08
Bacteria	Topsoil	2022	f__Intrasporangiaceae sp ASV162	0	2	-0.19	0.11	86.25
Bacteria	Topsoil	2023	f__Intrasporangiaceae sp ASV162	0	2	-0.20	0.27	91.67
Bacteria	Topsoil	2022	f__Intrasporangiaceae sp ASV232	0	4	-0.31	0.16	48.75
Bacteria	Topsoil	2023	f__Intrasporangiaceae sp ASV232	0	2	-0.50	0.10	62.50
Bacteria	Topsoil	2022	f__Intrasporangiaceae sp ASV263	0	3	-0.18	0.17	71.88
Bacteria	Topsoil	2023	f__Intrasporangiaceae sp ASV263	0	3	-0.35	0.07	91.67
Bacteria	Topsoil	2022	f__Intrasporangiaceae sp ASV275	0	3	-0.14	0.23	88.13
Bacteria	Topsoil	2023	f__Intrasporangiaceae sp ASV275	0	3	-0.23	0.16	100
Bacteria	Phyllosphere	2022	f__Intrasporangiaceae sp ASV345	0	5	-0.86	0.03	56.25
Bacteria	Topsoil	2022	f__Intrasporangiaceae sp ASV345	0	3	-0.15	0.11	69.38
Bacteria	Topsoil	2023	f__Intrasporangiaceae sp ASV345	0	4	-0.40	0.20	95.83
Bacteria	Topsoil	2022	f__Intrasporangiaceae sp ASV494	4	0	0.38	0.06	73.13
Bacteria	Topsoil	2023	f__Intrasporangiaceae sp ASV494	1	0	0.15	0.03	77.08
Bacteria	Topsoil	2023	f__Isosphaeraceae sp ASV1287	0	3	-0.13	0.05	97.92
Bacteria	Topsoil	2022	f__Isosphaeraceae sp ASV1291	2	0	0.12	0.06	83.13
Bacteria	Topsoil	2023	f__Isosphaeraceae sp ASV1291	0	1	-0.10	0.06	100
Bacteria	Topsoil	2022	f__JG30-KF-CM45 sp ASV1025	4	0	0.51	0.08	17.50
Bacteria	Topsoil	2023	f__JG30-KF-CM45 sp ASV1025	2	0	0.37	0.05	52.08
Bacteria	Topsoil	2023	f__JG30-KF-CM45 sp ASV1065	3	0	0.26	0.02	66.67
Bacteria	Topsoil	2022	f__JG30-KF-CM45 sp ASV1138	0	3	-0.16	0.05	73.75
Bacteria	Topsoil	2023	f__JG30-KF-CM45 sp ASV1138	0	4	-0.43	0.03	91.67
Bacteria	Topsoil	2022	f__JG30-KF-CM45 sp ASV1167	3	0	0.15	0.05	47.50
Bacteria	Topsoil	2023	f__JG30-KF-CM45 sp ASV1167	1	0	0.19	0.01	52.08
Bacteria	Topsoil	2022	f__JG30-KF-CM45 sp ASV1246	3	0	0.20	0.07	53.13
Bacteria	Topsoil	2022	f__JG30-KF-CM45 sp ASV125	3	0	0.14	0.31	78.13
Bacteria	Topsoil	2023	f__JG30-KF-CM45 sp ASV125	2	0	0.30	0.39	91.67
Bacteria	Phyllosphere	2022	f__JG30-KF-CM45 sp ASV1440	3	0	0.30	0.00	10.63
Bacteria	Topsoil	2022	f__JG30-KF-CM45 sp ASV1440	4	0	0.53	0.04	15.00
Bacteria	Topsoil	2023	f__JG30-KF-CM45 sp ASV1440	3	0	0.44	0.01	14.58
Bacteria	Topsoil	2022	f__JG30-KF-CM45 sp ASV1656	3	0	0.24	0.03	30.63
Bacteria	Topsoil	2022	f__JG30-KF-CM45 sp ASV1736	0	4	-0.33	0.02	31.88
Bacteria	Topsoil	2023	f__JG30-KF-CM45 sp ASV1736	0	3	-0.47	0.03	56.25

Annexes

Bacteria	Topsoil	2022	f__JG30-KF-CM45 sp ASV1804	1	0	0.07	0.02	38.75
Bacteria	Topsoil	2022	f__JG30-KF-CM45 sp ASV1835	3	0	0.15	0.02	77.50
Bacteria	Topsoil	2022	f__JG30-KF-CM45 sp ASV1847	4	0	0.27	0.03	81.88
Bacteria	Topsoil	2023	f__JG30-KF-CM45 sp ASV1847	3	0	0.18	0.02	93.75
Bacteria	Topsoil	2022	f__JG30-KF-CM45 sp ASV2337	0	4	-0.41	0.01	26.88
Bacteria	Topsoil	2023	f__JG30-KF-CM45 sp ASV2337	0	4	-0.53	0.05	43.75
Bacteria	Topsoil	2022	f__JG30-KF-CM45 sp ASV3702	0	2	-0.16	0.02	68.75
Bacteria	Topsoil	2023	f__JG30-KF-CM45 sp ASV3702	0	4	-0.57	0.02	72.92
Bacteria	Topsoil	2022	f__JG30-KF-CM45 sp ASV441	0	4	-0.47	0.08	79.38
Bacteria	Topsoil	2023	f__JG30-KF-CM45 sp ASV441	0	4	-0.58	0.13	89.58
Bacteria	Phyllosphere	2022	f__JG30-KF-CM45 sp ASV60	1	0	0.13	0.11	56.25
Bacteria	Topsoil	2022	f__JG30-KF-CM45 sp ASV60	3	0	0.33	0.72	83.13
Bacteria	Topsoil	2023	f__JG30-KF-CM45 sp ASV60	3	0	0.24	0.44	95.83
Bacteria	Phyllosphere	2022	f__JG30-KF-CM45 sp ASV622	0	3	-0.62	0.01	27.50
Bacteria	Topsoil	2022	f__JG30-KF-CM45 sp ASV622	0	5	-0.47	0.08	71.88
Bacteria	Topsoil	2023	f__JG30-KF-CM45 sp ASV622	0	4	-0.37	0.07	91.67
Bacteria	Phyllosphere	2022	f__JG30-KF-CM45 sp ASV714	2	0	0.23	0.02	19.38
Bacteria	Topsoil	2022	f__JG30-KF-CM45 sp ASV714	3	0	0.37	0.09	21.25
Bacteria	Topsoil	2022	f__JG30-KF-CM45 sp ASV813	3	0	0.25	0.07	88.75
Bacteria	Topsoil	2023	f__JG30-KF-CM45 sp ASV813	3	0	0.21	0.06	97.92
Bacteria	Phyllosphere	2022	f__JG30-KF-CM45 sp ASV816	0	1	-0.43	0.01	20.63
Bacteria	Phyllosphere	2022	f__JG30-KF-CM45 sp ASV871	0	2	-0.37	0.00	13.75
Bacteria	Topsoil	2022	f__JG30-KF-CM45 sp ASV871	0	5	-0.50	0.04	41.25
Bacteria	Topsoil	2023	f__JG30-KF-CM45 sp ASV871	0	4	-0.69	0.07	58.33
Bacteria	Phyllosphere	2022	f__JG30-KF-CM45 sp ASV960	1	0	0.19	0.01	24.38
Bacteria	Topsoil	2022	f__JG30-KF-CM45 sp ASV960	1	0	0.17	0.01	40.00
Bacteria	Topsoil	2023	f__JG30-KF-CM45 sp ASV960	2	0	0.28	0.08	70.83
Bacteria	Topsoil	2023	f__KF-JG30-B3 sp ASV1525	0	3	-0.38	0.04	81.25
Fungi	Phyllosphere	2022	f__Lasiosphaeriaceae sp ASV374	0	1	-0.14	0.00	12.66
Fungi	Topsoil	2022	f__Lasiosphaeriaceae sp ASV600	4	0	0.29	0.07	30.82
Fungi	Topsoil	2022	f__Lasiosphaeriaceae sp ASV835	0	1	-0.18	0.02	28.30
Fungi	Topsoil	2023	f__Lasiosphaeriaceae sp ASV835	0	3	-0.42	0.02	25.00
Fungi	Topsoil	2022	f__Lasiosphaeriaceae sp ASV874	3	0	0.24	0.04	21.38
Fungi	Topsoil	2023	f__Lasiosphaeriaceae sp ASV874	0	4	-0.41	0.00	22.92
Fungi	Topsoil	2022	f__Lentitheciaceae sp ASV298	0	4	-0.39	0.07	62.26
Fungi	Topsoil	2023	f__Lentitheciaceae sp ASV298	0	3	-0.34	0.11	79.17
Bacteria	Topsoil	2022	f__Longimicrobiaceae sp ASV1400	0	2	-0.14	0.03	71.88
Bacteria	Topsoil	2023	f__Longimicrobiaceae sp ASV1400	0	3	-0.23	0.04	77.08
Fungi	Topsoil	2022	f__Magnaporthaceae sp ASV460	3	0	0.22	0.04	44.03
Bacteria	Topsoil	2023	f__Methyloligellaceae sp ASV537	0	3	-0.27	0.04	97.92
Bacteria	Topsoil	2023	f__Methyloligellaceae sp ASV796	0	2	-0.23	0.05	97.92
Bacteria	Topsoil	2022	f__Microbacteriaceae sp ASV255	1	0	0.05	0.03	83.13
Bacteria	Topsoil	2023	f__Microbacteriaceae sp ASV255	2	0	0.19	0.01	97.92
Bacteria	Topsoil	2022	f__Microbacteriaceae sp ASV775	3	0	0.13	0.06	90.63
Bacteria	Topsoil	2022	f__Microbacteriaceae sp ASV924	1	0	0.04	0.02	67.50
Bacteria	Topsoil	2023	f__Microbacteriaceae sp ASV924	2	0	0.12	0.04	68.75

Annexes

Bacteria	Topsoil	2022	f__Micrococcaceae sp ASV1075	0	3	-0.27	0.02	14.38
Bacteria	Phyllosphere	2022	f__Micrococcaceae sp ASV1212	1	0	0.19	0.01	21.25
Bacteria	Topsoil	2022	f__Micrococcaceae sp ASV1212	4	0	0.35	0.02	18.13
Bacteria	Topsoil	2022	f__Micrococcaceae sp ASV356	3	0	0.25	0.04	42.50
Bacteria	Topsoil	2023	f__Micrococcaceae sp ASV356	4	0	0.45	0.11	52.08
Bacteria	Topsoil	2022	f__Micromonosporaceae sp ASV1701	0	1	-0.07	0.02	53.13
Bacteria	Topsoil	2023	f__Micromonosporaceae sp ASV1701	0	4	-0.42	0.03	81.25
Bacteria	Topsoil	2022	f__Micromonosporaceae sp ASV855	0	3	-0.07	0.01	70.00
Bacteria	Topsoil	2023	f__Micromonosporaceae sp ASV855	0	3	-0.21	0.01	93.75
Bacteria	Topsoil	2022	f__Microscillaceae sp ASV1049	0	4	-0.30	0.05	38.75
Bacteria	Topsoil	2023	f__Microscillaceae sp ASV1049	0	3	-0.39	0.01	35.42
Bacteria	Topsoil	2022	f__Microscillaceae sp ASV1876	0	3	-0.23	0.03	51.88
Bacteria	Topsoil	2023	f__Microscillaceae sp ASV1876	0	3	-0.49	0.02	60.42
Bacteria	Topsoil	2022	f__Microscillaceae sp ASV423	0	4	-0.36	0.11	57.50
Bacteria	Topsoil	2023	f__Microscillaceae sp ASV423	0	3	-0.49	0.04	60.42
Bacteria	Topsoil	2022	f__Microscillaceae sp ASV666	0	4	-0.53	0.11	67.50
Bacteria	Topsoil	2023	f__Microscillaceae sp ASV666	0	4	-0.55	0.08	91.67
Bacteria	Topsoil	2022	f__Microscillaceae sp ASV776	0	2	-0.13	0.04	61.88
Bacteria	Topsoil	2023	f__Microscillaceae sp ASV776	0	3	-0.37	0.05	60.42
Bacteria	Topsoil	2022	f__Microscillaceae sp ASV807	0	5	-0.70	0.12	68.13
Bacteria	Topsoil	2023	f__Microscillaceae sp ASV807	0	4	-1.00	0.11	87.50
Bacteria	Topsoil	2022	f__Microtrichaceae sp ASV1082	0	2	-0.05	0.03	93.13
Bacteria	Topsoil	2023	f__Microtrichaceae sp ASV1082	0	1	-0.05	0.03	95.83
Fungi	Topsoil	2022	f__Mycosphaerellaceae sp ASV214	0	3	-0.26	0.05	24.53
Fungi	Phyllosphere	2022	f__Mycosphaerellaceae sp ASV262	0	1	-0.29	0.05	55.06
Fungi	Topsoil	2022	f__Mycosphaerellaceae sp ASV262	0	1	-0.19	0.04	20.13
Fungi	Topsoil	2022	f__Mycosphaerellaceae sp ASV293	0	1	-0.22	0.03	33.33
Fungi	Phyllosphere	2022	f__Mycosphaerellaceae sp ASV595	0	4	-0.77	0.02	46.20
Fungi	Topsoil	2022	f__Mycosphaerellaceae sp ASV595	0	4	-0.30	0.01	20.13
Bacteria	Topsoil	2022	f__Myxococcaceae sp ASV1084	3	0	0.11	0.04	84.38
Bacteria	Topsoil	2023	f__Myxococcaceae sp ASV1084	0	1	-0.09	0.07	100
Bacteria	Topsoil	2022	f__Myxococcaceae sp ASV1346	0	3	-0.18	0.03	74.38
Bacteria	Topsoil	2023	f__Myxococcaceae sp ASV1371	0	2	-0.08	0.03	100
Bacteria	Topsoil	2023	f__Myxococcaceae sp ASV2572	0	1	-0.05	0.04	91.67
Bacteria	Topsoil	2022	f__Nannocystaceae sp ASV1157	0	3	-0.13	0.03	81.88
Bacteria	Topsoil	2023	f__Nannocystaceae sp ASV1157	0	3	-0.26	0.03	95.83
Fungi	Phyllosphere	2022	f__Nectriaceae sp ASV1029	0	1	-0.09	0.00	2.53
Fungi	Topsoil	2022	f__Nectriaceae sp ASV1029	0	4	-0.36	0.02	56.60
Fungi	Topsoil	2023	f__Nectriaceae sp ASV1029	0	4	-0.36	0.01	54.17
Fungi	Endosphere	2022	f__Nectriaceae sp ASV147	0	3	-0.48	0.00	27.50
Fungi	Topsoil	2022	f__Nectriaceae sp ASV147	4	0	0.35	0.25	64.78
Fungi	Phyllosphere	2022	f__Nectriaceae sp ASV271	0	3	-0.33	0.00	6.33
Fungi	Topsoil	2022	f__Nectriaceae sp ASV271	0	4	-0.38	0.11	38.99
Fungi	Topsoil	2022	f__Nectriaceae sp ASV35	0	4	-0.59	2.03	53.46
Fungi	Topsoil	2023	f__Nectriaceae sp ASV35	0	4	-0.55	0.70	83.33
Fungi	Endosphere	2022	f__Nectriaceae sp ASV391	2	0	0.14	0.00	6.25

Annexes

Fungi	Phyllosphere	2022	f__Nectriaceae sp ASV391	0	2	-0.18	0.00	10.76
Fungi	Topsoil	2023	f__Nectriaceae sp ASV391	3	0	0.60	0.05	52.08
Fungi	Topsoil	2023	f__Nectriaceae sp ASV409	0	4	-0.29	0.19	70.83
Fungi	Topsoil	2022	f__Nectriaceae sp ASV529	1	0	0.12	0.03	95.60
Fungi	Topsoil	2022	f__Nectriaceae sp ASV830	0	4	-0.37	0.03	55.97
Fungi	Topsoil	2023	f__Nectriaceae sp ASV830	0	4	-0.36	0.02	54.17
Bacteria	Topsoil	2022	f__Nitrosomonadaceae sp ASV1023	1	0	0.02	0.02	74.38
Bacteria	Topsoil	2023	f__Nitrosomonadaceae sp ASV1023	1	0	0.06	0.04	77.08
Bacteria	Topsoil	2022	f__Nocardiaceae sp ASV460	0	3	-0.18	0.02	86.25
Bacteria	Topsoil	2022	f__Nocardioidaceae sp ASV1263	3	0	0.21	0.02	47.50
Bacteria	Topsoil	2022	f__Nocardioidaceae sp ASV2417	0	2	-0.16	0.02	80.63
Fungi	Phyllosphere	2022	f__Olpidiaceae sp ASV564	0	3	-0.50	0.00	8.86
Fungi	Phyllosphere	2022	f__Olpidiaceae sp ASV691	0	1	-0.17	0.00	12.03
Fungi	Topsoil	2022	f__Olpidiaceae sp ASV691	0	4	-0.28	0.03	25.16
Fungi	Topsoil	2023	f__Olpidiaceae sp ASV691	0	3	-0.47	0.01	22.92
Fungi	Topsoil	2022	f__Ophiocordycipitaceae sp ASV905	0	3	-0.16	0.01	30.82
Bacteria	Topsoil	2022	f__Oxalobacteraceae sp ASV1078	4	0	0.30	0.03	81.88
Bacteria	Topsoil	2022	f__Oxalobacteraceae sp ASV1160	3	0	0.12	0.00	50.00
Bacteria	Topsoil	2023	f__Oxalobacteraceae sp ASV1160	0	2	-0.17	0.00	54.17
Bacteria	Topsoil	2022	f__Oxalobacteraceae sp ASV1227	1	0	0.18	0.04	85.63
Bacteria	Phyllosphere	2022	f__Oxalobacteraceae sp ASV1306	3	0	0.28	0.00	11.25
Bacteria	Topsoil	2022	f__Oxalobacteraceae sp ASV1306	1	0	0.23	0.01	38.13
Bacteria	Topsoil	2023	f__Oxalobacteraceae sp ASV1306	4	0	0.86	0.03	43.75
Bacteria	Topsoil	2022	f__Oxalobacteraceae sp ASV1432	4	0	0.39	0.03	76.88
Bacteria	Phyllosphere	2022	f__Oxalobacteraceae sp ASV1487	2	0	0.22	0.02	30.00
Bacteria	Topsoil	2022	f__Oxalobacteraceae sp ASV1487	3	0	0.22	0.02	76.25
Bacteria	Topsoil	2023	f__Oxalobacteraceae sp ASV1487	2	0	0.26	0.04	89.58
Bacteria	Topsoil	2022	f__Oxalobacteraceae sp ASV1588	3	0	0.10	0.02	83.13
Bacteria	Topsoil	2022	f__Oxalobacteraceae sp ASV202	1	0	0.04	0.07	53.13
Bacteria	Topsoil	2023	f__Oxalobacteraceae sp ASV202	4	0	0.43	0.23	62.50
Bacteria	Topsoil	2022	f__Oxalobacteraceae sp ASV2437	3	0	0.11	0.04	91.88
Bacteria	Topsoil	2022	f__Oxalobacteraceae sp ASV365	2	0	0.25	0.15	60.63
Bacteria	Topsoil	2023	f__Oxalobacteraceae sp ASV365	3	0	0.32	0.05	68.75
Bacteria	Phyllosphere	2022	f__Oxalobacteraceae sp ASV491	1	0	0.34	0.06	45.00
Bacteria	Topsoil	2022	f__Oxalobacteraceae sp ASV491	4	0	0.31	0.07	84.38
Bacteria	Topsoil	2023	f__Oxalobacteraceae sp ASV491	2	0	0.19	0.03	95.83
Bacteria	Topsoil	2022	f__Oxalobacteraceae sp ASV800	3	0	0.29	0.04	24.38
Bacteria	Topsoil	2022	f__Oxalobacteraceae sp ASV877	3	0	0.17	0.03	57.50
Bacteria	Topsoil	2023	f__Oxalobacteraceae sp ASV877	4	0	0.43	0.06	72.92
Bacteria	Topsoil	2022	f__Oxalobacteraceae sp ASV889	3	0	0.20	0.05	88.75
Bacteria	Topsoil	2023	f__Pedosphaeraceae sp ASV1077	2	0	0.17	0.06	60.42
Bacteria	Topsoil	2022	f__Pedosphaeraceae sp ASV1150	0	3	-0.10	0.04	72.50
Bacteria	Topsoil	2023	f__Pedosphaeraceae sp ASV1150	0	3	-0.15	0.02	95.83
Bacteria	Topsoil	2023	f__Pedosphaeraceae sp ASV1341	3	0	0.18	0.05	97.92
Bacteria	Topsoil	2022	f__Pedosphaeraceae sp ASV1387	3	0	0.10	0.02	86.88
Bacteria	Topsoil	2022	f__Pedosphaeraceae sp ASV1450	0	3	-0.15	0.02	78.75

Annexes

Bacteria	Topsoil	2023	f__Pedosphaeraceae sp ASV1450	0	3	-0.16	0.02	95.83
Bacteria	Topsoil	2022	f__Pedosphaeraceae sp ASV1496	0	1	-0.03	0.03	44.38
Bacteria	Topsoil	2023	f__Pedosphaeraceae sp ASV1496	0	4	-0.46	0.03	68.75
Bacteria	Topsoil	2022	f__Pedosphaeraceae sp ASV378	0	3	-0.12	0.10	75.63
Bacteria	Topsoil	2022	f__Pedosphaeraceae sp ASV543	0	4	-0.22	0.09	87.50
Bacteria	Topsoil	2023	f__Pedosphaeraceae sp ASV543	0	3	-0.10	0.10	100
Bacteria	Topsoil	2022	f__Pedosphaeraceae sp ASV953	0	1	-0.04	0.04	59.38
Bacteria	Topsoil	2023	f__Pedosphaeraceae sp ASV953	0	4	-0.59	0.05	66.67
Bacteria	Topsoil	2023	f__Peptostreptococcaceae sp ASV1015	0	3	-0.46	0.03	70.83
Bacteria	Topsoil	2022	f__Peptostreptococcaceae sp ASV1752	0	3	-0.15	0.03	78.13
Bacteria	Topsoil	2023	f__Peptostreptococcaceae sp ASV1752	0	3	-0.25	0.04	97.92
Fungi	Topsoil	2023	f__Pezizaceae sp ASV867	2	0	0.51	0.04	39.58
Fungi	Phyllosphere	2022	f__Phaeosphaeriaceae sp ASV457	1	0	0.41	0.05	80.38
Fungi	Phyllosphere	2022	f__Phaeosphaeriaceae sp ASV736	2	0	0.21	0.00	39.87
Fungi	Topsoil	2022	f__Phaeosphaeriaceae sp ASV817	1	0	0.27	0.02	49.06
Fungi	Topsoil	2022	f__Plectosphaerellaceae sp ASV772	0	3	-0.17	0.02	29.56
Bacteria	Topsoil	2023	f__Polyangiaceae sp ASV1802	0	3	-0.09	0.06	100
Bacteria	Topsoil	2022	f__Rhizobiales_Incertae_Sedis sp ASV1908	2	0	0.14	0.02	86.25
Bacteria	Topsoil	2022	f__Roseiflexaceae sp ASV1006	3	0	0.28	0.02	31.88
Bacteria	Topsoil	2023	f__Roseiflexaceae sp ASV1006	4	0	0.34	0.04	45.83
Bacteria	Topsoil	2023	f__Roseiflexaceae sp ASV1099	2	0	0.34	0.01	10.42
Bacteria	Topsoil	2022	f__Roseiflexaceae sp ASV1127	3	0	0.26	0.02	35.63
Bacteria	Topsoil	2023	f__Roseiflexaceae sp ASV1127	2	0	0.18	0.02	52.08
Bacteria	Topsoil	2023	f__Roseiflexaceae sp ASV1180	1	0	0.21	0.05	68.75
Bacteria	Topsoil	2022	f__Roseiflexaceae sp ASV1194	3	0	0.21	0.02	36.25
Bacteria	Topsoil	2023	f__Roseiflexaceae sp ASV1194	3	0	0.22	0.06	43.75
Bacteria	Topsoil	2022	f__Roseiflexaceae sp ASV1196	3	0	0.31	0.04	50.00
Bacteria	Topsoil	2022	f__Roseiflexaceae sp ASV1249	1	0	0.16	0.04	75.63
Bacteria	Topsoil	2023	f__Roseiflexaceae sp ASV1249	1	0	0.06	0.02	97.92
Bacteria	Topsoil	2022	f__Roseiflexaceae sp ASV1285	1	0	0.11	0.02	52.50
Bacteria	Topsoil	2022	f__Roseiflexaceae sp ASV1338	1	0	0.05	0.04	33.75
Bacteria	Topsoil	2022	f__Roseiflexaceae sp ASV1409	3	0	0.22	0.04	40.00
Bacteria	Topsoil	2022	f__Roseiflexaceae sp ASV182	4	0	0.41	0.44	83.13
Bacteria	Topsoil	2023	f__Roseiflexaceae sp ASV182	3	0	0.24	0.33	95.83
Bacteria	Topsoil	2023	f__Roseiflexaceae sp ASV2106	3	0	0.45	0.03	47.92
Bacteria	Topsoil	2022	f__Roseiflexaceae sp ASV2179	0	3	-0.18	0.02	46.25
Bacteria	Topsoil	2023	f__Roseiflexaceae sp ASV218	1	0	0.04	0.10	89.58
Bacteria	Phyllosphere	2022	f__Roseiflexaceae sp ASV227	3	0	0.26	0.04	26.25
Bacteria	Topsoil	2022	f__Roseiflexaceae sp ASV227	3	0	0.17	0.13	78.13
Bacteria	Topsoil	2023	f__Roseiflexaceae sp ASV227	4	0	0.43	0.13	83.33
Bacteria	Topsoil	2022	f__Roseiflexaceae sp ASV244	4	0	0.33	0.15	29.38
Bacteria	Topsoil	2022	f__Roseiflexaceae sp ASV2551	3	0	0.22	0.04	76.88
Bacteria	Topsoil	2023	f__Roseiflexaceae sp ASV2551	3	0	0.41	0.02	75.00
Bacteria	Phyllosphere	2022	f__Roseiflexaceae sp ASV347	1	0	0.17	0.01	20.63
Bacteria	Topsoil	2022	f__Roseiflexaceae sp ASV347	4	0	0.45	0.12	56.25
Bacteria	Topsoil	2023	f__Roseiflexaceae sp ASV347	3	0	0.44	0.05	85.42

Annexes

Bacteria	Topsoil	2022	f__Roseiflexaceae sp ASV354	1	0	0.04	0.06	60.63
Bacteria	Topsoil	2023	f__Roseiflexaceae sp ASV354	3	0	0.27	0.07	58.33
Bacteria	Phyllosphere	2022	f__Roseiflexaceae sp ASV385	2	0	0.20	0.01	25.00
Bacteria	Topsoil	2022	f__Roseiflexaceae sp ASV385	1	0	0.11	0.09	69.38
Bacteria	Topsoil	2023	f__Roseiflexaceae sp ASV385	3	0	0.38	0.10	75.00
Bacteria	Topsoil	2022	f__Roseiflexaceae sp ASV427	3	0	0.22	0.06	40.63
Bacteria	Topsoil	2023	f__Roseiflexaceae sp ASV427	3	0	0.19	0.09	43.75
Bacteria	Topsoil	2022	f__Roseiflexaceae sp ASV436	0	2	-0.29	0.08	39.38
Bacteria	Topsoil	2023	f__Roseiflexaceae sp ASV436	1	0	0.07	0.06	50.00
Bacteria	Topsoil	2023	f__Roseiflexaceae sp ASV451	0	3	-0.48	0.02	35.42
Bacteria	Topsoil	2023	f__Roseiflexaceae sp ASV505	3	0	0.24	0.02	29.17
Bacteria	Topsoil	2023	f__Roseiflexaceae sp ASV520	1	0	0.19	0.06	43.75
Bacteria	Topsoil	2022	f__Roseiflexaceae sp ASV527	3	0	0.25	0.08	20.63
Bacteria	Topsoil	2022	f__Roseiflexaceae sp ASV547	1	0	0.08	0.03	40.00
Bacteria	Topsoil	2023	f__Roseiflexaceae sp ASV547	3	0	0.20	0.06	54.17
Bacteria	Topsoil	2023	f__Roseiflexaceae sp ASV554	4	0	0.60	0.09	58.33
Bacteria	Topsoil	2022	f__Roseiflexaceae sp ASV561	3	0	0.33	0.07	70.63
Bacteria	Topsoil	2023	f__Roseiflexaceae sp ASV592	2	0	0.15	0.04	68.75
Bacteria	Topsoil	2022	f__Roseiflexaceae sp ASV595	0	3	-0.23	0.18	46.88
Bacteria	Topsoil	2023	f__Roseiflexaceae sp ASV595	0	3	-0.56	0.09	79.17
Bacteria	Phyllosphere	2022	f__Roseiflexaceae sp ASV628	1	0	0.13	0.01	16.88
Bacteria	Topsoil	2022	f__Roseiflexaceae sp ASV628	3	0	0.26	0.06	56.25
Bacteria	Topsoil	2022	f__Roseiflexaceae sp ASV668	0	3	-0.16	0.02	21.25
Bacteria	Topsoil	2023	f__Roseiflexaceae sp ASV724	2	0	0.21	0.06	62.50
Bacteria	Topsoil	2022	f__Roseiflexaceae sp ASV732	1	0	0.04	0.03	48.75
Bacteria	Topsoil	2022	f__Roseiflexaceae sp ASV735	0	1	-0.15	0.05	76.88
Bacteria	Topsoil	2022	f__Roseiflexaceae sp ASV760	4	0	0.34	0.09	82.50
Bacteria	Topsoil	2023	f__Roseiflexaceae sp ASV760	3	0	0.21	0.05	91.67
Bacteria	Topsoil	2022	f__Roseiflexaceae sp ASV811	3	0	0.27	0.04	66.25
Bacteria	Topsoil	2023	f__Roseiflexaceae sp ASV811	4	0	0.73	0.04	70.83
Bacteria	Topsoil	2022	f__Roseiflexaceae sp ASV844	0	2	-0.19	0.04	48.75
Bacteria	Topsoil	2023	f__Roseiflexaceae sp ASV844	1	0	0.08	0.04	54.17
Bacteria	Topsoil	2022	f__Roseiflexaceae sp ASV851	3	0	0.32	0.03	49.38
Bacteria	Topsoil	2023	f__Roseiflexaceae sp ASV851	4	0	0.39	0.03	56.25
Bacteria	Phyllosphere	2022	f__Roseiflexaceae sp ASV858	2	0	0.15	0.00	8.75
Bacteria	Topsoil	2022	f__Roseiflexaceae sp ASV858	1	0	0.08	0.02	30.63
Bacteria	Topsoil	2023	f__Roseiflexaceae sp ASV858	4	0	0.48	0.05	50.00
Bacteria	Topsoil	2023	f__Roseiflexaceae sp ASV862	2	0	0.35	0.06	12.50
Bacteria	Topsoil	2022	f__Roseiflexaceae sp ASV879	3	0	0.21	0.04	71.25
Bacteria	Topsoil	2023	f__Roseiflexaceae sp ASV879	3	0	0.47	0.06	72.92
Bacteria	Topsoil	2023	f__Roseiflexaceae sp ASV956	4	0	0.45	0.04	58.33
Bacteria	Topsoil	2022	f__Roseiflexaceae sp ASV978	1	0	0.05	0.04	54.38
Bacteria	Topsoil	2022	f__Roseiflexaceae sp ASV985	5	0	0.60	0.07	63.13
Bacteria	Topsoil	2023	f__Roseiflexaceae sp ASV985	3	0	0.40	0.04	85.42
Bacteria	Topsoil	2022	f__Sandaracinaceae sp ASV1193	2	0	0.11	0.04	80.63
Bacteria	Topsoil	2023	f__Sandaracinaceae sp ASV1193	0	3	-0.22	0.04	100

Annexes

Bacteria	Topsoil	2022	f__Sandaracinaceae sp ASV1311	0	1	-0.04	0.04	64.38
Bacteria	Topsoil	2023	f__Sandaracinaceae sp ASV1311	0	3	-0.29	0.04	89.58
Bacteria	Topsoil	2023	f__Sandaracinaceae sp ASV803	0	3	-0.29	0.04	97.92
Bacteria	Topsoil	2023	f__SC-I-84 sp ASV1027	2	0	0.17	0.05	60.42
Bacteria	Topsoil	2022	f__SC-I-84 sp ASV1036	0	3	-0.17	0.04	89.38
Bacteria	Topsoil	2023	f__SC-I-84 sp ASV1036	0	3	-0.23	0.02	100
Bacteria	Topsoil	2023	f__SC-I-84 sp ASV1178	0	1	-0.02	0.02	77.08
Bacteria	Topsoil	2022	f__SC-I-84 sp ASV319	0	4	-0.34	0.15	80.63
Bacteria	Topsoil	2023	f__SC-I-84 sp ASV319	0	4	-0.37	0.13	97.92
Bacteria	Topsoil	2023	f__SC-I-84 sp ASV718	3	0	0.31	0.06	58.33
Bacteria	Topsoil	2023	f__SC-I-84 sp ASV838	0	3	-0.15	0.04	85.42
Bacteria	Topsoil	2022	f__Solirubrobacteraceae sp ASV1062	4	0	0.25	0.02	81.88
Bacteria	Topsoil	2023	f__Solirubrobacteraceae sp ASV1062	2	0	0.10	0.04	100
Bacteria	Topsoil	2022	f__Solirubrobacteraceae sp ASV1424	1	0	0.11	0.02	85.00
Bacteria	Topsoil	2023	f__Solirubrobacteraceae sp ASV1424	1	0	0.17	0.02	97.92
Bacteria	Topsoil	2023	f__Solirubrobacteraceae sp ASV185	3	0	0.50	0.38	97.92
Bacteria	Topsoil	2022	f__Solirubrobacteraceae sp ASV330	0	3	-0.16	0.11	78.13
Bacteria	Topsoil	2023	f__Solirubrobacteraceae sp ASV3663	2	0	0.10	0.03	100
Bacteria	Topsoil	2023	f__Solirubrobacteraceae sp ASV695	4	0	0.43	0.06	91.67
Bacteria	Topsoil	2022	f__Solirubrobacteraceae sp ASV810	3	0	0.16	0.10	86.25
Bacteria	Topsoil	2023	f__Sphingomonadaceae sp ASV1169	1	0	0.22	0.03	95.83
Bacteria	Topsoil	2023	f__Sphingomonadaceae sp ASV575	1	0	0.24	0.05	97.92
Bacteria	Topsoil	2023	f__Sphingomonadaceae sp ASV900	3	0	0.26	0.04	89.58
Bacteria	Topsoil	2022	f__Sporichthyaceae sp ASV186	3	0	0.22	0.16	86.25
Bacteria	Topsoil	2023	f__Sporichthyaceae sp ASV186	0	3	-0.13	0.17	100
Bacteria	Topsoil	2022	f__Sporichthyaceae sp ASV291	1	0	0.15	0.10	72.50
Bacteria	Topsoil	2023	f__Sporichthyaceae sp ASV291	3	0	0.32	0.10	60.42
Bacteria	Topsoil	2022	f__Sporichthyaceae sp ASV453	3	0	0.18	0.06	86.88
Bacteria	Topsoil	2023	f__Sporichthyaceae sp ASV453	2	0	0.16	0.06	97.92
Fungi	Topsoil	2022	f__Sporormiaceae sp ASV594	3	0	0.21	0.00	15.72
Bacteria	Topsoil	2022	f__Steroidobacteraceae sp ASV1072	1	0	0.10	0.04	61.25
Bacteria	Topsoil	2022	f__Steroidobacteraceae sp ASV1318	0	2	-0.12	0.03	56.88
Bacteria	Topsoil	2023	f__Steroidobacteraceae sp ASV1318	0	2	-0.14	0.02	83.33
Bacteria	Topsoil	2022	f__Steroidobacteraceae sp ASV2033	0	2	-0.07	0.05	78.75
Bacteria	Topsoil	2023	f__Steroidobacteraceae sp ASV2033	0	3	-0.13	0.02	100
Bacteria	Topsoil	2022	f__Steroidobacteraceae sp ASV2574	2	0	0.07	0.03	57.50
Bacteria	Topsoil	2023	f__Steroidobacteraceae sp ASV342	0	3	-0.20	0.09	97.92
Bacteria	Topsoil	2022	f__Steroidobacteraceae sp ASV893	0	3	-0.09	0.04	34.38
Bacteria	Topsoil	2023	f__Steroidobacteraceae sp ASV893	0	3	-0.28	0.03	47.92
Bacteria	Topsoil	2022	f__Sutterellaceae sp ASV1141	0	1	-0.15	0.02	26.88
Bacteria	Topsoil	2023	f__Sutterellaceae sp ASV1390	0	1	-0.05	0.02	72.92
Bacteria	Topsoil	2023	f__Sutterellaceae sp ASV2295	0	1	-0.33	0.02	64.58
Bacteria	Topsoil	2022	f__Sutterellaceae sp ASV472	0	3	-0.14	0.07	41.25
Bacteria	Topsoil	2023	f__Sutterellaceae sp ASV472	0	3	-0.31	0.10	62.50
Fungi	Topsoil	2022	f__Tetraplosphaeriaceae sp ASV747	0	3	-0.23	0.02	50.94
Fungi	Phyllosphere	2022	f__Thyridariaceae sp ASV123	0	2	-0.39	0.00	42.41

Annexes

Fungi	Topsoil	2022	f__Thyridariaceae sp ASV123	0	4	-0.43	0.26	75.47
Fungi	Topsoil	2023	f__Thyridariaceae sp ASV123	0	4	-0.58	0.29	89.58
Fungi	Phyllosphere	2022	f__Thyridariaceae sp ASV246	0	1	-0.23	0.00	23.42
Fungi	Topsoil	2022	f__Thyridariaceae sp ASV246	1	0	0.06	0.09	44.03
Bacteria	Topsoil	2022	f__TRA3-20 sp ASV1101	0	3	-0.11	0.04	78.75
Bacteria	Topsoil	2023	f__TRA3-20 sp ASV1101	0	3	-0.15	0.01	91.67
Bacteria	Topsoil	2022	f__TRA3-20 sp ASV1670	0	4	-0.24	0.04	80.00
Bacteria	Topsoil	2023	f__TRA3-20 sp ASV1670	0	3	-0.25	0.01	79.17
Bacteria	Topsoil	2022	f__TRA3-20 sp ASV1761	0	3	-0.28	0.03	60.00
Bacteria	Topsoil	2023	f__TRA3-20 sp ASV1761	0	4	-0.64	0.02	64.58
Bacteria	Topsoil	2023	f__TRA3-20 sp ASV246	2	0	0.06	0.10	100
Bacteria	Topsoil	2022	f__TRA3-20 sp ASV399	0	3	-0.09	0.10	81.88
Bacteria	Topsoil	2023	f__TRA3-20 sp ASV399	0	1	-0.03	0.08	97.92
Bacteria	Topsoil	2023	f__TRA3-20 sp ASV697	0	3	-0.09	0.04	100
Bacteria	Topsoil	2022	f__TRA3-20 sp ASV774	0	2	-0.15	0.08	62.50
Bacteria	Topsoil	2023	f__TRA3-20 sp ASV774	0	2	-0.22	0.03	75.00
Fungi	Endosphere	2022	f__Trichosporonaceae sp ASV528	0	2	-0.12	0.00	8.75
Fungi	Phyllosphere	2022	f__Valsaceae sp ASV152	4	0	0.61	0.34	35.44
Fungi	Topsoil	2022	f__Valsaceae sp ASV152	1	0	0.07	0.00	33.33
Fungi	Topsoil	2022	f__Valsaceae sp ASV256	0	2	-0.11	0.00	22.64
Fungi	Topsoil	2022	f__Venturiaceae sp ASV415	2	0	0.27	0.05	47.80
Fungi	Topsoil	2023	f__Venturiaceae sp ASV415	4	0	0.41	0.04	62.50
Bacteria	Topsoil	2022	f__Verrucomicrobiaceae sp ASV853	0	1	-0.02	0.05	80.00
Bacteria	Topsoil	2023	f__Verrucomicrobiaceae sp ASV853	0	4	-0.50	0.05	95.83
Bacteria	Topsoil	2022	f__WWH38 sp ASV935	0	3	-0.23	0.05	31.25
Bacteria	Topsoil	2023	f__Xanthobacteraceae sp ASV109	0	3	-0.20	0.33	100
Bacteria	Topsoil	2022	f__Xanthobacteraceae sp ASV1168	0	4	-0.27	0.03	68.75
Bacteria	Topsoil	2023	f__Xanthobacteraceae sp ASV1168	0	4	-0.38	0.02	87.50
Bacteria	Topsoil	2023	f__Xanthobacteraceae sp ASV1615	0	3	-0.23	0.02	91.67
Bacteria	Topsoil	2022	f__Xanthobacteraceae sp ASV230	4	0	0.24	0.17	85.63
Bacteria	Topsoil	2022	f__Xanthobacteraceae sp ASV2333	0	3	-0.22	0.03	40.00
Bacteria	Topsoil	2023	f__Xanthobacteraceae sp ASV2333	0	4	-0.45	0.02	58.33
Bacteria	Topsoil	2022	f__Xanthobacteraceae sp ASV601	0	3	-0.13	0.10	75.63
Bacteria	Topsoil	2023	f__Xanthobacteraceae sp ASV601	0	4	-0.30	0.06	100
Bacteria	Topsoil	2023	f__Xanthobacteraceae sp ASV719	0	3	-0.38	0.06	85.42
Bacteria	Topsoil	2022	f__Xanthobacteraceae sp ASV799	0	3	-0.17	0.04	86.88
Bacteria	Topsoil	2023	f__Xanthobacteraceae sp ASV799	0	3	-0.17	0.05	100
Bacteria	Topsoil	2022	f__Xanthobacteraceae sp ASV850	1	0	0.11	0.07	33.13
Bacteria	Topsoil	2022	f__Xanthomonadaceae sp ASV1066	5	0	0.29	0.05	38.75
Bacteria	Topsoil	2022	f__Xanthomonadaceae sp ASV778	0	3	-0.15	0.07	80.63
Bacteria	Topsoil	2023	f__Xanthomonadaceae sp ASV778	0	4	-0.33	0.02	97.92
Bacteria	Topsoil	2023	f__Xanthomonadaceae sp ASV891	2	0	0.14	0.03	64.58
Bacteria	Topsoil	2023	f__Xanthomonadaceae sp ASV948	0	4	-0.52	0.01	77.08
Bacteria	Topsoil	2023	o__0319-6G20 sp ASV1170	2	0	0.08	0.04	100
Bacteria	Topsoil	2023	o__0319-6G20 sp ASV4311	2	0	0.07	0.04	100
Bacteria	Topsoil	2022	o__Actinomarinales sp ASV299	0	4	-0.64	0.07	20.00

Annexes

Bacteria	Topsoil	2023	o__Actinomarinales sp ASV299	0	4	-0.69	0.16	50.00
Bacteria	Topsoil	2022	o__Actinomarinales sp ASV743	1	0	0.20	0.06	31.88
Bacteria	Topsoil	2022	o__Bacillales sp ASV2253	0	3	-0.17	0.02	59.38
Bacteria	Topsoil	2023	o__Bacillales sp ASV2253	0	1	-0.18	0.02	75.00
Bacteria	Topsoil	2022	o__C0119 sp ASV1548	3	0	0.19	0.02	41.88
Bacteria	Phyllosphere	2022	o__C0119 sp ASV199	0	1	-0.35	0.01	10.63
Bacteria	Topsoil	2022	o__C0119 sp ASV199	0	4	-0.65	0.19	63.75
Bacteria	Topsoil	2023	o__C0119 sp ASV199	0	4	-0.65	0.10	83.33
Bacteria	Topsoil	2022	o__C0119 sp ASV486	0	1	-0.10	0.03	38.75
Bacteria	Phyllosphere	2022	o__C0119 sp ASV982	0	1	-0.27	0.01	8.75
Bacteria	Topsoil	2023	o__C0119 sp ASV982	1	0	0.17	0.04	41.67
Fungi	Phyllosphere	2022	o__Cantharellales sp ASV440	3	0	0.23	0.02	73.42
Fungi	Topsoil	2022	o__Cantharellales sp ASV440	2	0	0.11	0.00	15.72
Fungi	Phyllosphere	2022	o__Cantharellales sp ASV563	4	0	0.43	0.00	56.33
Fungi	Topsoil	2022	o__Capnodiales sp ASV678	0	1	-0.20	0.03	17.61
Fungi	Topsoil	2023	o__Capnodiales sp ASV678	0	3	-0.30	0.01	8.33
Bacteria	Topsoil	2022	o__CCD24 sp ASV531	0	4	-0.29	0.09	71.25
Bacteria	Topsoil	2023	o__CCD24 sp ASV531	0	4	-0.46	0.07	97.92
Fungi	Topsoil	2022	o__Chaetothyriales sp ASV1013	0	3	-0.17	0.01	17.61
Fungi	Topsoil	2022	o__Chaetothyriales sp ASV441	0	3	-0.22	0.02	26.42
Fungi	Phyllosphere	2022	o__Chaetothyriales sp ASV99	3	0	0.32	0.00	10.13
Fungi	Topsoil	2022	o__Chaetothyriales sp ASV99	4	0	0.62	0.34	11.32
Fungi	Topsoil	2023	o__Chaetothyriales sp ASV99	1	0	0.44	0.42	45.83
Bacteria	Phyllosphere	2022	o__Elsterales sp ASV313	1	0	0.12	0.02	39.38
Bacteria	Topsoil	2022	o__Elsterales sp ASV313	4	0	0.31	0.13	90.00
Bacteria	Topsoil	2023	o__Elsterales sp ASV313	3	0	0.10	0.42	100
Fungi	Topsoil	2022	o__Erythrobasidiales sp ASV418	0	4	-0.28	0.02	81.76
Fungi	Phyllosphere	2022	o__Filobasidiales sp ASV205	2	0	0.45	0.18	46.84
Bacteria	Topsoil	2022	o__Frankiales sp ASV1182	3	0	0.25	0.02	75.63
Bacteria	Topsoil	2023	o__Frankiales sp ASV1182	4	0	0.35	0.01	81.25
Bacteria	Topsoil	2022	o__Frankiales sp ASV738	3	0	0.21	0.01	70.63
Bacteria	Topsoil	2023	o__Frankiales sp ASV738	4	0	0.53	0.02	83.33
Bacteria	Topsoil	2022	o__Frankiales sp ASV805	0	3	-0.17	0.04	75.00
Bacteria	Topsoil	2022	o__Frankiales sp ASV843	3	0	0.15	0.04	75.00
Bacteria	Topsoil	2023	o__Frankiales sp ASV843	3	0	0.32	0.04	75.00
Bacteria	Topsoil	2023	o__Gaiellales sp ASV1061	1	0	0.11	0.06	97.92
Bacteria	Topsoil	2023	o__Gaiellales sp ASV1080	2	0	0.35	0.02	14.58
Bacteria	Topsoil	2022	o__Gaiellales sp ASV1181	1	0	0.05	0.05	35.63
Bacteria	Topsoil	2023	o__Gaiellales sp ASV1181	1	0	0.15	0.01	35.42
Bacteria	Topsoil	2022	o__Gaiellales sp ASV1201	3	0	0.20	0.04	25.63
Bacteria	Topsoil	2022	o__Gaiellales sp ASV1265	3	0	0.31	0.04	16.25
Bacteria	Topsoil	2023	o__Gaiellales sp ASV1265	2	0	0.27	0.00	8.33
Bacteria	Topsoil	2022	o__Gaiellales sp ASV1361	5	0	0.33	0.04	34.38
Bacteria	Topsoil	2022	o__Gaiellales sp ASV1378	3	0	0.23	0.05	53.75
Bacteria	Topsoil	2023	o__Gaiellales sp ASV1378	3	0	0.37	0.03	72.92
Bacteria	Topsoil	2023	o__Gaiellales sp ASV1417	0	2	-0.42	0.01	56.25

Annexes

Bacteria	Topsoil	2022	o__Gaiellales sp ASV1494	0	3	-0.24	0.03	38.75
Bacteria	Topsoil	2023	o__Gaiellales sp ASV1494	0	3	-0.42	0.02	43.75
Bacteria	Topsoil	2023	o__Gaiellales sp ASV1662	1	0	0.23	0.03	31.25
Bacteria	Topsoil	2022	o__Gaiellales sp ASV200	0	3	-0.18	0.23	45.00
Bacteria	Topsoil	2022	o__Gaiellales sp ASV2298	1	0	0.05	0.03	84.38
Bacteria	Topsoil	2022	o__Gaiellales sp ASV257	0	3	-0.29	0.08	40.63
Bacteria	Topsoil	2023	o__Gaiellales sp ASV257	0	3	-0.35	0.17	72.92
Bacteria	Phyllosphere	2022	o__Gaiellales sp ASV266	0	1	-0.32	0.00	9.38
Bacteria	Topsoil	2022	o__Gaiellales sp ASV266	0	3	-0.29	0.10	45.63
Bacteria	Topsoil	2023	o__Gaiellales sp ASV266	0	3	-0.48	0.17	66.67
Bacteria	Topsoil	2022	o__Gaiellales sp ASV304	0	4	-0.42	0.13	26.25
Bacteria	Topsoil	2023	o__Gaiellales sp ASV304	0	4	-0.57	0.28	58.33
Bacteria	Topsoil	2022	o__Gaiellales sp ASV376	0	3	-0.27	0.07	31.88
Bacteria	Topsoil	2023	o__Gaiellales sp ASV376	0	4	-0.49	0.11	68.75
Bacteria	Topsoil	2022	o__Gaiellales sp ASV433	3	0	0.21	0.06	26.25
Bacteria	Topsoil	2023	o__Gaiellales sp ASV475	0	3	-0.29	0.09	47.92
Bacteria	Topsoil	2022	o__Gaiellales sp ASV487	4	0	0.41	0.07	27.50
Bacteria	Topsoil	2023	o__Gaiellales sp ASV487	2	0	0.24	0.06	41.67
Bacteria	Topsoil	2022	o__Gaiellales sp ASV516	0	3	-0.26	0.05	31.25
Bacteria	Topsoil	2023	o__Gaiellales sp ASV516	0	4	-0.58	0.08	64.58
Bacteria	Topsoil	2022	o__Gaiellales sp ASV564	3	0	0.15	0.09	29.38
Bacteria	Topsoil	2023	o__Gaiellales sp ASV564	2	0	0.29	0.05	31.25
Bacteria	Topsoil	2022	o__Gaiellales sp ASV570	0	4	-0.23	0.12	90.00
Bacteria	Topsoil	2023	o__Gaiellales sp ASV570	0	3	-0.12	0.11	100
Bacteria	Topsoil	2022	o__Gaiellales sp ASV613	3	0	0.24	0.09	31.88
Bacteria	Topsoil	2023	o__Gaiellales sp ASV613	3	0	0.29	0.03	56.25
Bacteria	Topsoil	2022	o__Gaiellales sp ASV707	0	3	-0.33	0.06	40.63
Bacteria	Topsoil	2023	o__Gaiellales sp ASV707	0	4	-0.56	0.03	62.50
Bacteria	Topsoil	2022	o__Gaiellales sp ASV728	0	4	-0.35	0.02	27.50
Bacteria	Topsoil	2023	o__Gaiellales sp ASV728	0	3	-0.52	0.07	39.58
Bacteria	Topsoil	2022	o__Gaiellales sp ASV731	0	4	-0.43	0.02	31.25
Bacteria	Topsoil	2023	o__Gaiellales sp ASV731	0	4	-0.42	0.10	58.33
Bacteria	Topsoil	2022	o__Gaiellales sp ASV750	2	0	0.14	0.04	49.38
Bacteria	Topsoil	2023	o__Gaiellales sp ASV750	3	0	0.41	0.05	56.25
Bacteria	Topsoil	2023	o__Gaiellales sp ASV866	3	0	0.33	0.04	83.33
Bacteria	Topsoil	2022	o__Gaiellales sp ASV934	0	3	-0.34	0.01	21.25
Bacteria	Topsoil	2023	o__Gaiellales sp ASV934	0	3	-0.35	0.06	43.75
Fungi	Topsoil	2022	o__GS11 sp ASV619	0	4	-0.27	0.03	10.06
Fungi	Topsoil	2023	o__GS11 sp ASV619	1	0	0.42	0.00	8.33
Fungi	Topsoil	2022	o__GS11 sp ASV629	0	3	-0.17	0.05	22.01
Fungi	Topsoil	2023	o__GS11 sp ASV629	3	0	0.37	0.00	14.58
Fungi	Topsoil	2022	o__GS11 sp ASV631	0	3	-0.18	0.05	13.84
Fungi	Phyllosphere	2022	o__Helotiales sp ASV116	0	1	-0.24	0.00	48.73
Fungi	Topsoil	2023	o__Helotiales sp ASV116	3	0	0.36	0.61	85.42
Fungi	Phyllosphere	2022	o__Helotiales sp ASV130	1	0	0.23	0.29	85.44
Fungi	Topsoil	2022	o__Helotiales sp ASV136	0	1	-0.10	0.26	75.47

Annexes

Fungi	Topsoil	2022	o__Helotiales sp ASV325	4	0	0.44	0.08	50.31
Fungi	Topsoil	2023	o__Helotiales sp ASV591	0	3	-0.30	0.01	41.67
Fungi	Topsoil	2022	o__Helotiales sp ASV916	0	3	-0.20	0.02	23.90
Fungi	Topsoil	2023	o__Helotiales sp ASV916	0	1	-0.41	0.01	16.67
Fungi	Topsoil	2022	o__Hypocreales sp ASV465	0	3	-0.23	0.01	23.27
Fungi	Topsoil	2022	o__Hypocreales sp ASV794	0	1	-0.06	0.00	6.92
Bacteria	Topsoil	2022	o__IMCC26256 sp ASV1038	0	2	-0.06	0.04	80.00
Bacteria	Topsoil	2023	o__IMCC26256 sp ASV1038	0	3	-0.15	0.02	85.42
Bacteria	Topsoil	2022	o__IMCC26256 sp ASV1048	0	3	-0.20	0.10	86.88
Bacteria	Topsoil	2023	o__IMCC26256 sp ASV1048	0	3	-0.13	0.05	100
Bacteria	Topsoil	2023	o__IMCC26256 sp ASV1159	2	0	0.19	0.04	100
Bacteria	Topsoil	2022	o__IMCC26256 sp ASV1197	0	2	-0.07	0.04	70.00
Bacteria	Topsoil	2023	o__IMCC26256 sp ASV1197	0	3	-0.19	0.04	93.75
Bacteria	Topsoil	2022	o__IMCC26256 sp ASV147	0	3	-0.19	0.23	89.38
Bacteria	Topsoil	2023	o__IMCC26256 sp ASV147	0	1	-0.23	0.17	95.83
Bacteria	Topsoil	2022	o__IMCC26256 sp ASV309	3	0	0.11	0.08	87.50
Bacteria	Topsoil	2023	o__IMCC26256 sp ASV309	4	0	0.39	0.13	95.83
Bacteria	Topsoil	2022	o__IMCC26256 sp ASV462	0	3	-0.23	0.08	73.13
Bacteria	Topsoil	2023	o__IMCC26256 sp ASV462	0	3	-0.29	0.09	95.83
Bacteria	Topsoil	2022	o__IMCC26256 sp ASV489	0	3	-0.12	0.05	76.25
Bacteria	Topsoil	2023	o__IMCC26256 sp ASV597	0	2	-0.21	0.05	89.58
Bacteria	Topsoil	2022	o__IMCC26256 sp ASV802	0	3	-0.23	0.01	49.38
Bacteria	Topsoil	2022	o__Kapabacteriales sp ASV1455	3	0	0.11	0.03	84.38
Bacteria	Topsoil	2023	o__Kapabacteriales sp ASV1455	0	1	-0.14	0.02	100
Bacteria	Phyllosphere	2022	o__Microtrichales sp ASV1058	0	1	-0.41	0.01	21.88
Bacteria	Topsoil	2022	o__Microtrichales sp ASV1058	0	1	-0.08	0.05	51.25
Bacteria	Topsoil	2023	o__Microtrichales sp ASV1058	0	1	-0.09	0.12	75.00
Bacteria	Topsoil	2022	o__Microtrichales sp ASV1067	3	0	0.07	0.03	95.00
Bacteria	Topsoil	2023	o__Microtrichales sp ASV1067	1	0	0.13	0.02	100
Bacteria	Topsoil	2022	o__Microtrichales sp ASV1297	0	3	-0.16	0.04	45.63
Bacteria	Topsoil	2023	o__Microtrichales sp ASV1297	0	1	-0.17	0.01	37.50
Bacteria	Topsoil	2022	o__Microtrichales sp ASV1357	0	3	-0.16	0.03	63.13
Bacteria	Topsoil	2023	o__Microtrichales sp ASV1357	0	3	-0.22	0.03	91.67
Bacteria	Topsoil	2022	o__Microtrichales sp ASV1895	0	3	-0.19	0.03	69.38
Bacteria	Topsoil	2023	o__Microtrichales sp ASV1895	0	4	-0.39	0.02	89.58
Bacteria	Topsoil	2022	o__Microtrichales sp ASV328	3	0	0.21	0.11	81.88
Bacteria	Topsoil	2023	o__Microtrichales sp ASV328	2	0	0.17	0.10	97.92
Bacteria	Topsoil	2022	o__Microtrichales sp ASV366	0	3	-0.15	0.09	83.75
Bacteria	Topsoil	2023	o__Microtrichales sp ASV366	0	4	-0.25	0.08	95.83
Bacteria	Topsoil	2023	o__Microtrichales sp ASV756	0	3	-0.15	0.03	97.92
Bacteria	Topsoil	2023	o__Microtrichales sp ASV806	0	3	-0.17	0.04	100
Bacteria	Topsoil	2023	o__Microtrichales sp ASV904	0	3	-0.21	0.05	62.50
Fungi	Topsoil	2023	o__Monoblepharidales sp ASV799	0	1	-0.10	0.03	81.25
Fungi	Phyllosphere	2022	o__Pleosporales sp ASV112	0	2	-0.29	0.00	38.61
Fungi	Topsoil	2022	o__Pleosporales sp ASV112	0	4	-0.35	0.42	54.09
Fungi	Topsoil	2023	o__Pleosporales sp ASV112	0	1	-0.16	0.23	77.08

Annexes

Fungi	Topsoil	2022	o__Pleosporales sp ASV119	0	1	-0.13	0.01	56.60
Fungi	Phyllosphere	2022	o__Pleosporales sp ASV184	0	3	-0.39	0.00	18.99
Fungi	Topsoil	2022	o__Pleosporales sp ASV184	0	4	-0.36	0.18	61.64
Fungi	Topsoil	2023	o__Pleosporales sp ASV184	0	3	-0.30	0.07	79.17
Fungi	Phyllosphere	2022	o__Pleosporales sp ASV195	0	2	-0.18	0.00	7.59
Fungi	Topsoil	2022	o__Pleosporales sp ASV195	0	3	-0.17	0.05	68.55
Fungi	Topsoil	2023	o__Pleosporales sp ASV195	0	3	-0.38	0.45	62.50
Fungi	Phyllosphere	2022	o__Pleosporales sp ASV207	4	0	0.63	0.17	15.82
Fungi	Phyllosphere	2022	o__Pleosporales sp ASV236	0	1	-0.21	0.00	34.18
Fungi	Topsoil	2023	o__Pleosporales sp ASV236	0	2	-0.17	0.12	97.92
Fungi	Topsoil	2023	o__Pleosporales sp ASV274	0	2	-0.39	0.13	91.67
Fungi	Endosphere	2022	o__Pleosporales sp ASV287	0	3	-0.37	0.00	16.25
Fungi	Topsoil	2022	o__Pleosporales sp ASV287	3	0	0.18	0.08	54.09
Fungi	Topsoil	2023	o__Pleosporales sp ASV287	0	3	-0.24	0.05	77.08
Fungi	Topsoil	2022	o__Pleosporales sp ASV302	4	0	0.36	0.07	75.47
Fungi	Phyllosphere	2022	o__Pleosporales sp ASV313	1	0	0.24	0.03	48.73
Fungi	Phyllosphere	2022	o__Pleosporales sp ASV343	0	1	-0.21	0.00	32.91
Fungi	Topsoil	2022	o__Pleosporales sp ASV343	0	1	-0.05	0.06	70.44
Fungi	Topsoil	2022	o__Pleosporales sp ASV348	0	3	-0.17	0.08	66.67
Fungi	Topsoil	2022	o__Pleosporales sp ASV427	5	0	0.47	0.04	47.17
Fungi	Topsoil	2023	o__Pleosporales sp ASV427	3	0	0.34	0.06	81.25
Fungi	Topsoil	2022	o__Pleosporales sp ASV516	4	0	0.52	0.03	35.85
Fungi	Topsoil	2023	o__Pleosporales sp ASV516	2	0	0.50	0.04	62.50
Fungi	Phyllosphere	2022	o__Pleosporales sp ASV655	2	0	0.36	0.00	8.86
Fungi	Topsoil	2022	o__Pleosporales sp ASV655	5	0	0.75	0.03	32.70
Fungi	Topsoil	2023	o__Pleosporales sp ASV655	3	0	0.43	0.02	31.25
Bacteria	Topsoil	2023	o__PLTA13 sp ASV1556	0	2	-0.35	0.02	54.17
Bacteria	Phyllosphere	2022	o__PLTA13 sp ASV265	1	0	0.15	0.00	15.00
Bacteria	Topsoil	2022	o__PLTA13 sp ASV265	1	0	0.19	0.19	32.50
Bacteria	Topsoil	2023	o__PLTA13 sp ASV458	0	3	-0.27	0.07	64.58
Bacteria	Topsoil	2022	o__Rhizobiales sp ASV188	4	0	0.22	0.16	66.25
Bacteria	Topsoil	2022	o__Rhizobiales sp ASV680	1	0	0.03	0.03	50.00
Bacteria	Topsoil	2023	o__Rhizobiales sp ASV680	0	2	-0.29	0.04	72.92
Fungi	Topsoil	2022	o__Rhizophlyctidales sp ASV963	0	1	-0.07	0.03	54.09
Fungi	Topsoil	2023	o__Rhizophlyctidales sp ASV963	0	1	-0.39	0.03	54.17
Fungi	Topsoil	2022	o__Rhizophydiales sp ASV401	0	1	-0.12	0.06	61.64
Fungi	Topsoil	2023	o__Rhizophydiales sp ASV401	0	1	-0.22	0.04	64.58
Fungi	Topsoil	2022	o__Rhizophydiales sp ASV497	0	1	-0.07	0.04	58.49
Fungi	Topsoil	2023	o__Rhizophydiales sp ASV497	0	4	-0.42	0.01	60.42
Fungi	Phyllosphere	2022	o__Rhizophydiales sp ASV728	0	1	-0.10	0.00	5.06
Fungi	Topsoil	2022	o__Rhizophydiales sp ASV728	0	1	-0.03	0.02	69.18
Fungi	Topsoil	2023	o__Rhizophydiales sp ASV728	0	3	-0.19	0.02	75.00
Bacteria	Topsoil	2022	o__S085 sp ASV1074	0	3	-0.23	0.02	40.00
Bacteria	Topsoil	2023	o__S085 sp ASV1074	0	4	-0.53	0.06	58.33
Bacteria	Topsoil	2022	o__S085 sp ASV1262	3	0	0.16	0.03	59.38
Bacteria	Topsoil	2023	o__S085 sp ASV1262	0	1	-0.34	0.04	81.25

Annexes

Bacteria	Topsoil	2022	o__S085 sp ASV1324	0	3	-0.20	0.04	26.25
Bacteria	Topsoil	2023	o__S085 sp ASV1324	0	3	-0.38	0.02	45.83
Bacteria	Topsoil	2022	o__S085 sp ASV1383	0	4	-0.26	0.03	81.25
Bacteria	Topsoil	2023	o__S085 sp ASV1383	0	4	-0.38	0.05	95.83
Bacteria	Topsoil	2023	o__S085 sp ASV1669	0	3	-0.36	0.03	62.50
Bacteria	Topsoil	2022	o__S085 sp ASV235	0	3	-0.16	0.16	55.63
Bacteria	Topsoil	2023	o__S085 sp ASV235	0	3	-0.27	0.14	100
Bacteria	Topsoil	2022	o__S085 sp ASV261	0	4	-0.24	0.18	83.75
Bacteria	Topsoil	2023	o__S085 sp ASV261	0	1	-0.24	0.15	95.83
Bacteria	Topsoil	2022	o__S085 sp ASV768	3	0	0.17	0.05	58.75
Bacteria	Topsoil	2023	o__S085 sp ASV768	0	1	-0.31	0.03	77.08
Bacteria	Topsoil	2022	o__Saccharimonadales sp ASV1292	0	3	-0.16	0.03	83.13
Bacteria	Topsoil	2023	o__Saccharimonadales sp ASV1292	0	1	-0.26	0.03	95.83
Bacteria	Topsoil	2023	o__Saccharimonadales sp ASV1492	0	3	-0.30	0.03	83.33
Bacteria	Topsoil	2022	o__Saccharimonadales sp ASV370	0	4	-0.39	0.12	78.13
Bacteria	Topsoil	2023	o__Saccharimonadales sp ASV370	0	3	-0.16	0.04	97.92
Bacteria	Topsoil	2022	o__Saccharimonadales sp ASV447	0	2	-0.17	0.06	84.38
Fungi	Phyllosphere	2022	o__Sebacinales sp ASV852	0	1	-0.13	0.00	3.16
Fungi	Topsoil	2022	o__Sebacinales sp ASV852	3	0	0.20	0.01	37.11
Fungi	Topsoil	2023	o__Sebacinales sp ASV852	2	0	0.35	0.13	60.42
Fungi	Topsoil	2022	o__Sebacinales sp ASV865	0	3	-0.14	0.02	43.40
Bacteria	Phyllosphere	2022	o__Solirubrobacterales sp ASV1163	2	0	0.13	0.00	9.38
Bacteria	Topsoil	2022	o__Solirubrobacterales sp ASV1163	1	0	0.07	0.01	59.38
Bacteria	Topsoil	2023	o__Solirubrobacterales sp ASV1163	4	0	0.47	0.03	58.33
Bacteria	Topsoil	2022	o__Solirubrobacterales sp ASV1191	0	4	-0.41	0.02	41.88
Bacteria	Topsoil	2023	o__Solirubrobacterales sp ASV1191	0	4	-0.61	0.03	60.42
Bacteria	Topsoil	2022	o__Solirubrobacterales sp ASV1219	4	0	0.26	0.03	58.13
Bacteria	Topsoil	2023	o__Solirubrobacterales sp ASV523	2	0	0.44	0.11	70.83
Bacteria	Topsoil	2023	o__Solirubrobacterales sp ASV621	0	3	-0.08	0.11	100
Bacteria	Topsoil	2022	o__Solirubrobacterales sp ASV656	4	0	0.35	0.04	82.50
Bacteria	Topsoil	2023	o__Solirubrobacterales sp ASV656	4	0	0.38	0.07	97.92
Fungi	Topsoil	2022	o__Sordariales sp ASV790	0	4	-0.28	0.02	12.58
Fungi	Topsoil	2023	o__Sordariales sp ASV790	0	2	-0.24	0.01	12.50
Bacteria	Topsoil	2023	o__Subgroup_7 sp ASV1014	0	3	-0.28	0.03	89.58
Bacteria	Topsoil	2022	o__Subgroup_7 sp ASV1242	4	0	0.46	0.01	31.25
Bacteria	Topsoil	2023	o__Subgroup_7 sp ASV1242	3	0	0.43	0.04	33.33
Bacteria	Topsoil	2023	o__Subgroup_7 sp ASV1465	0	3	-0.30	0.04	56.25
Bacteria	Topsoil	2022	o__Subgroup_7 sp ASV1738	0	3	-0.21	0.04	23.75
Bacteria	Topsoil	2022	o__Subgroup_7 sp ASV1944	3	0	0.22	0.05	67.50
Bacteria	Topsoil	2023	o__Subgroup_7 sp ASV1944	0	3	-0.21	0.04	83.33
Bacteria	Topsoil	2023	o__Subgroup_7 sp ASV229	0	3	-0.29	0.10	83.33
Bacteria	Topsoil	2022	o__Subgroup_7 sp ASV588	0	2	-0.18	0.09	83.13
Bacteria	Topsoil	2023	o__Subgroup_7 sp ASV832	0	3	-0.33	0.01	72.92
Bacteria	Topsoil	2022	o__Subgroup_7 sp ASV878	0	3	-0.16	0.07	65.00
Fungi	Phyllosphere	2022	o__Tremellales sp ASV148	1	0	0.11	0.67	91.77
Fungi	Topsoil	2022	o__Tremellales sp ASV148	0	3	-0.20	0.08	88.68

Annexes

Bacteria	Topsoil	2023	o__Vicinamibacterales sp ASV2749	0	1	-0.12	0.01	100
Fungi	Topsoil	2022	o__Xylariales sp ASV856	2	0	0.26	0.02	59.75
Bacteria	Topsoil	2022	c__Acidimicrobiia sp ASV874	0	3	-0.09	0.04	89.38
Bacteria	Topsoil	2023	c__Acidimicrobiia sp ASV874	1	0	0.10	0.04	100
Bacteria	Phyllosphere	2022	c__Actinobacteria sp ASV1326	3	0	0.20	0.00	12.50
Bacteria	Topsoil	2022	c__Actinobacteria sp ASV1326	4	0	0.55	0.03	16.25
Bacteria	Topsoil	2023	c__Actinobacteria sp ASV1326	3	0	0.53	0.02	22.92
Bacteria	Topsoil	2022	c__Alphaproteobacteria sp ASV1271	0	3	-0.13	0.01	24.38
Bacteria	Topsoil	2023	c__Alphaproteobacteria sp ASV1271	0	3	-0.30	0.04	43.75
Bacteria	Topsoil	2022	c__bacteriap25 sp ASV1698	3	0	0.23	0.03	42.50
Bacteria	Topsoil	2022	c__bacteriap25 sp ASV535	0	1	-0.06	0.10	43.13
Bacteria	Topsoil	2023	c__bacteriap25 sp ASV535	0	1	-0.14	0.19	68.75
Fungi	Topsoil	2023	c__Dothideomycetes sp ASV462	1	0	0.40	0.04	20.83
Fungi	Topsoil	2022	c__Dothideomycetes sp ASV811	1	0	0.07	0.00	13.84
Bacteria	Topsoil	2022	c__Gammaproteobacteria sp ASV950	3	0	0.32	0.07	51.25
Fungi	Topsoil	2022	c__GS37 sp ASV396	0	4	-0.44	0.05	36.48
Fungi	Topsoil	2023	c__GS37 sp ASV396	0	1	-0.31	0.05	41.67
Fungi	Topsoil	2022	c__GS37 sp ASV714	3	0	0.31	0.02	19.50
Fungi	Topsoil	2023	c__GS37 sp ASV714	3	0	0.48	0.02	29.17
Bacteria	Topsoil	2022	c__JG30-KF-CM66 sp ASV1019	1	0	0.12	0.03	73.75
Bacteria	Topsoil	2022	c__JG30-KF-CM66 sp ASV1028	0	2	-0.11	0.01	42.50
Bacteria	Topsoil	2023	c__JG30-KF-CM66 sp ASV1028	0	3	-0.35	0.05	64.58
Bacteria	Topsoil	2022	c__JG30-KF-CM66 sp ASV1064	4	0	0.40	0.04	11.25
Bacteria	Topsoil	2023	c__JG30-KF-CM66 sp ASV1064	1	0	0.31	0.01	31.25
Bacteria	Topsoil	2022	c__JG30-KF-CM66 sp ASV1279	0	1	-0.10	0.01	33.13
Bacteria	Topsoil	2023	c__JG30-KF-CM66 sp ASV1279	1	0	0.02	0.04	35.42
Bacteria	Topsoil	2022	c__JG30-KF-CM66 sp ASV1402	0	3	-0.21	0.02	41.88
Bacteria	Topsoil	2023	c__JG30-KF-CM66 sp ASV1402	0	3	-0.31	0.05	68.75
Bacteria	Topsoil	2022	c__JG30-KF-CM66 sp ASV1544	0	2	-0.14	0.02	35.63
Bacteria	Topsoil	2023	c__JG30-KF-CM66 sp ASV1544	0	3	-0.25	0.02	58.33
Bacteria	Topsoil	2022	c__JG30-KF-CM66 sp ASV1824	0	3	-0.22	0.01	51.25
Bacteria	Topsoil	2022	c__JG30-KF-CM66 sp ASV306	0	3	-0.16	0.01	30.00
Bacteria	Topsoil	2023	c__JG30-KF-CM66 sp ASV306	0	3	-0.27	0.22	50.00
Bacteria	Topsoil	2023	c__JG30-KF-CM66 sp ASV374	0	2	-0.11	0.08	100
Bacteria	Topsoil	2022	c__JG30-KF-CM66 sp ASV589	1	0	0.02	0.07	70.00
Bacteria	Topsoil	2023	c__JG30-KF-CM66 sp ASV589	2	0	0.19	0.04	66.67
Bacteria	Topsoil	2023	c__JG30-KF-CM66 sp ASV744	3	0	0.42	0.07	50.00
Bacteria	Topsoil	2022	c__JG30-KF-CM66 sp ASV780	3	0	0.14	0.07	71.25
Bacteria	Topsoil	2023	c__JG30-KF-CM66 sp ASV780	0	1	-0.06	0.05	87.50
Bacteria	Topsoil	2023	c__KD4-96 sp ASV1043	0	3	-0.27	0.04	79.17
Bacteria	Topsoil	2023	c__KD4-96 sp ASV1295	0	3	-0.15	0.03	97.92
Bacteria	Topsoil	2022	c__KD4-96 sp ASV1512	0	4	-0.36	0.04	40.63
Bacteria	Topsoil	2023	c__KD4-96 sp ASV1512	0	3	-0.44	0.02	58.33
Bacteria	Topsoil	2022	c__KD4-96 sp ASV1823	3	0	0.11	0.01	78.13
Bacteria	Topsoil	2023	c__KD4-96 sp ASV1823	3	0	0.18	0.03	85.42
Bacteria	Topsoil	2023	c__KD4-96 sp ASV2229	0	3	-0.32	0.02	70.83

Annexes

Bacteria	Topsoil	2023	c__KD4-96 sp ASV790	0	3	-0.13	0.05	100
Fungi	Topsoil	2022	c__Leotiomycetes sp ASV689	4	0	0.65	0.03	20.13
Fungi	Topsoil	2023	c__Leotiomycetes sp ASV689	3	0	0.41	0.01	33.33
Bacteria	Topsoil	2022	c__MB-A2-108 sp ASV118	0	2	-0.22	0.15	52.50
Bacteria	Topsoil	2023	c__MB-A2-108 sp ASV118	0	3	-0.43	0.40	75.00
Bacteria	Topsoil	2023	c__MB-A2-108 sp ASV206	0	1	-0.15	0.06	60.42
Bacteria	Topsoil	2022	c__MB-A2-108 sp ASV410	0	2	-0.13	0.08	58.13
Bacteria	Topsoil	2022	c__MB-A2-108 sp ASV424	0	3	-0.16	0.11	46.25
Bacteria	Topsoil	2023	c__MB-A2-108 sp ASV424	0	3	-0.37	0.13	72.92
Bacteria	Phyllosphere	2022	c__MB-A2-108 sp ASV455	0	1	-0.32	0.00	8.13
Bacteria	Topsoil	2022	c__MB-A2-108 sp ASV455	0	4	-0.39	0.08	63.75
Bacteria	Topsoil	2023	c__MB-A2-108 sp ASV455	0	3	-0.34	0.06	77.08
Bacteria	Topsoil	2022	c__MB-A2-108 sp ASV515	3	0	0.13	0.16	43.13
Bacteria	Phyllosphere	2022	c__MB-A2-108 sp ASV637	1	0	0.16	0.00	19.38
Bacteria	Topsoil	2022	c__MB-A2-108 sp ASV637	3	0	0.13	0.02	63.75
Bacteria	Topsoil	2023	c__MB-A2-108 sp ASV637	4	0	0.49	0.09	50.00
Bacteria	Topsoil	2022	c__MB-A2-108 sp ASV841	3	0	0.27	0.07	22.50
Bacteria	Topsoil	2022	c__OLB14 sp ASV166	0	3	-0.14	0.22	81.25
Bacteria	Topsoil	2023	c__S0134_terrestrial_group sp ASV1040	0	1	-0.13	0.03	85.42
Fungi	Topsoil	2022	c__Sordariomycetes sp ASV314	0	4	-0.32	0.04	15.09
Fungi	Topsoil	2023	c__Sordariomycetes sp ASV314	0	3	-0.38	0.16	29.17
Fungi	Topsoil	2022	c__Sordariomycetes sp ASV321	0	4	-0.33	0.10	61.01
Fungi	Topsoil	2023	c__Sordariomycetes sp ASV321	0	3	-0.39	0.07	79.17
Fungi	Topsoil	2022	c__Sordariomycetes sp ASV324	0	4	-0.57	0.06	68.55
Fungi	Topsoil	2023	c__Sordariomycetes sp ASV324	0	4	-0.67	0.04	83.33
Fungi	Topsoil	2022	c__Sordariomycetes sp ASV536	0	3	-0.20	0.03	33.96
Fungi	Topsoil	2023	c__Sordariomycetes sp ASV536	0	2	-0.19	0.04	58.33
Fungi	Topsoil	2022	c__Sordariomycetes sp ASV55	0	3	-0.22	0.77	91.19
Bacteria	Topsoil	2022	c__Subgroup_5 sp ASV2163	0	1	-0.06	0.03	60.63
Bacteria	Topsoil	2023	c__Subgroup_5 sp ASV2163	0	3	-0.36	0.02	68.75
Bacteria	Topsoil	2023	c__Thermoleophilia sp ASV1018	0	2	-0.12	0.03	89.58
Bacteria	Topsoil	2022	c__Thermoleophilia sp ASV1020	2	0	0.09	0.05	80.00
Bacteria	Topsoil	2022	c__Thermoleophilia sp ASV1360	0	3	-0.18	0.03	69.38
Bacteria	Topsoil	2023	c__Thermoleophilia sp ASV1360	0	3	-0.26	0.02	81.25
Bacteria	Topsoil	2023	c__Thermoleophilia sp ASV2111	0	3	-0.28	0.01	56.25
Bacteria	Topsoil	2023	c__Thermoleophilia sp ASV582	0	1	-0.04	0.10	81.25
Bacteria	Topsoil	2022	c__Thermoleophilia sp ASV955	2	0	0.13	0.04	67.50
Bacteria	Topsoil	2022	c__TK10 sp ASV1016	1	0	0.21	0.04	26.88
Bacteria	Topsoil	2022	c__TK10 sp ASV1031	0	4	-0.46	0.03	21.88
Bacteria	Topsoil	2023	c__TK10 sp ASV1031	0	3	-0.49	0.03	39.58
Bacteria	Topsoil	2022	c__TK10 sp ASV1037	3	0	0.31	0.08	23.75
Bacteria	Topsoil	2022	c__TK10 sp ASV1039	0	2	-0.12	0.02	76.25
Bacteria	Topsoil	2023	c__TK10 sp ASV1290	0	2	-0.25	0.02	47.92
Bacteria	Topsoil	2023	c__TK10 sp ASV1355	0	1	-0.18	0.04	97.92
Bacteria	Topsoil	2022	c__TK10 sp ASV1366	3	0	0.24	0.05	29.38
Bacteria	Topsoil	2023	c__TK10 sp ASV1366	2	0	0.28	0.01	16.67

Annexes

Bacteria	Topsoil	2022	c__TK10 sp ASV144	1	0	0.02	0.18	68.13
Bacteria	Topsoil	2023	c__TK10 sp ASV144	3	0	0.32	0.27	81.25
Bacteria	Topsoil	2022	c__TK10 sp ASV1446	4	0	0.38	0.03	71.88
Bacteria	Topsoil	2023	c__TK10 sp ASV1446	1	0	0.07	0.03	81.25
Bacteria	Topsoil	2022	c__TK10 sp ASV152	2	0	0.20	0.27	56.88
Bacteria	Topsoil	2023	c__TK10 sp ASV1744	2	0	0.09	0.03	60.42
Bacteria	Topsoil	2022	c__TK10 sp ASV1894	0	2	-0.18	0.02	66.25
Bacteria	Topsoil	2023	c__TK10 sp ASV1894	0	1	-0.35	0.04	89.58
Bacteria	Topsoil	2022	c__TK10 sp ASV191	0	1	-0.09	0.18	58.13
Bacteria	Topsoil	2023	c__TK10 sp ASV191	0	3	-0.42	0.12	79.17
Bacteria	Topsoil	2022	c__TK10 sp ASV2081	3	0	0.23	0.04	44.38
Bacteria	Topsoil	2023	c__TK10 sp ASV2081	3	0	0.28	0.00	45.83
Bacteria	Topsoil	2022	c__TK10 sp ASV254	3	0	0.24	0.16	72.50
Bacteria	Topsoil	2022	c__TK10 sp ASV2631	4	0	0.38	0.02	76.25
Bacteria	Topsoil	2023	c__TK10 sp ASV2631	3	0	0.45	0.02	81.25
Bacteria	Topsoil	2022	c__TK10 sp ASV363	4	0	0.29	0.11	31.88
Bacteria	Topsoil	2022	c__TK10 sp ASV397	1	0	0.15	0.06	76.88
Bacteria	Topsoil	2023	c__TK10 sp ASV397	3	0	0.28	0.08	87.50
Bacteria	Topsoil	2022	c__TK10 sp ASV401	4	0	0.47	0.10	37.50
Bacteria	Topsoil	2023	c__TK10 sp ASV401	1	0	0.24	0.05	64.58
Bacteria	Topsoil	2023	c__TK10 sp ASV449	3	0	0.20	0.08	64.58
Bacteria	Topsoil	2022	c__TK10 sp ASV519	0	3	-0.30	0.10	41.88
Bacteria	Topsoil	2023	c__TK10 sp ASV519	0	4	-0.56	0.14	68.75
Bacteria	Topsoil	2022	c__TK10 sp ASV572	0	1	-0.02	0.08	69.38
Bacteria	Topsoil	2022	c__TK10 sp ASV604	0	4	-0.26	0.06	40.00
Bacteria	Topsoil	2023	c__TK10 sp ASV604	0	3	-0.32	0.10	62.50
Bacteria	Topsoil	2022	c__TK10 sp ASV614	0	3	-0.28	0.01	23.13
Bacteria	Topsoil	2023	c__TK10 sp ASV614	0	2	-0.44	0.10	47.92
Bacteria	Topsoil	2022	c__TK10 sp ASV635	4	0	0.40	0.15	65.00
Bacteria	Topsoil	2022	c__TK10 sp ASV657	3	0	0.12	0.07	32.50
Bacteria	Topsoil	2022	c__TK10 sp ASV667	4	0	0.34	0.05	71.25
Bacteria	Topsoil	2023	c__TK10 sp ASV667	3	0	0.20	0.06	87.50
Bacteria	Topsoil	2022	c__TK10 sp ASV789	0	3	-0.23	0.10	57.50
Bacteria	Topsoil	2023	c__TK10 sp ASV789	0	4	-0.66	0.03	75.00
Bacteria	Topsoil	2022	c__TK10 sp ASV852	4	0	0.31	0.06	26.88
Bacteria	Topsoil	2023	c__TK10 sp ASV852	2	0	0.25	0.00	8.33
Bacteria	Topsoil	2022	c__TK10 sp ASV870	3	0	0.25	0.03	46.88
Bacteria	Topsoil	2023	c__TK10 sp ASV870	4	0	0.93	0.04	45.83
Bacteria	Phyllosphere	2022	c__TK10 sp ASV911	2	0	0.15	0.00	12.50
Bacteria	Topsoil	2022	c__TK10 sp ASV911	4	0	0.40	0.03	64.38
Bacteria	Topsoil	2023	c__TK10 sp ASV911	4	0	0.38	0.05	60.42
Bacteria	Phyllosphere	2022	c__TK10 sp ASV937	2	0	0.15	0.00	9.38
Bacteria	Topsoil	2023	c__TK10 sp ASV937	4	0	0.49	0.07	60.42
Bacteria	Topsoil	2023	c__TK10 sp ASV963	0	3	-0.32	0.01	60.42
Bacteria	Topsoil	2022	p__Armatimonadota sp ASV2796	3	0	0.10	0.03	66.88
Fungi	Topsoil	2022	p__Ascomycota sp ASV176	0	1	-0.06	0.07	74.84

Annexes

Fungi	Topsoil	2022	p__Ascomycota sp ASV356	0	3	-0.25	0.07	57.86
Fungi	Topsoil	2023	p__Ascomycota sp ASV356	0	3	-0.36	0.02	62.50
Fungi	Phyllosphere	2022	p__Ascomycota sp ASV372	0	1	-0.11	0.00	8.86
Fungi	Topsoil	2023	p__Ascomycota sp ASV487	0	3	-0.41	0.05	45.83
Fungi	Topsoil	2022	p__Ascomycota sp ASV606	0	4	-0.33	0.02	20.13
Fungi	Topsoil	2022	p__Ascomycota sp ASV667	3	0	0.29	0.02	54.72
Fungi	Topsoil	2022	p__Ascomycota sp ASV707	0	4	-0.41	0.03	44.65
Fungi	Topsoil	2023	p__Ascomycota sp ASV707	0	4	-0.39	0.06	66.67
Fungi	Topsoil	2022	p__Ascomycota sp ASV732	2	0	0.17	0.04	26.42
Fungi	Topsoil	2023	p__Ascomycota sp ASV732	3	0	0.36	0.02	10.42
Fungi	Phyllosphere	2022	p__Ascomycota sp ASV780	2	0	0.40	0.02	25.32
Fungi	Phyllosphere	2022	p__Ascomycota sp ASV920	0	3	-0.37	0.01	16.46
Fungi	Topsoil	2022	p__Ascomycota sp ASV920	0	2	-0.14	0.00	10.69
Fungi	Topsoil	2022	p__Ascomycota sp ASV954	0	3	-0.26	0.02	49.69
Fungi	Topsoil	2023	p__Ascomycota sp ASV954	0	2	-0.47	0.02	47.92
Bacteria	Topsoil	2022	p__Chloroflexi sp ASV1282	3	0	0.23	0.02	31.88
Bacteria	Topsoil	2023	p__Chloroflexi sp ASV1282	2	0	0.28	0.02	60.42
Bacteria	Topsoil	2022	p__Chloroflexi sp ASV640	1	0	0.18	0.07	31.88
Bacteria	Topsoil	2022	p__Chloroflexi sp ASV651	1	0	0.12	0.03	43.13
Bacteria	Phyllosphere	2022	p__Chloroflexi sp ASV672	2	0	0.19	0.00	8.75
Bacteria	Topsoil	2022	p__Chloroflexi sp ASV672	3	0	0.28	0.09	76.88
Bacteria	Topsoil	2022	p__Chloroflexi sp ASV715	3	0	0.20	0.07	60.63
Bacteria	Topsoil	2023	p__Chloroflexi sp ASV84	0	3	-0.43	0.27	66.67
Bacteria	Topsoil	2023	p__Chloroflexi sp ASV979	0	1	-0.12	0.05	100.0
Bacteria	Topsoil	2022	p__Desulfobacterota sp ASV2690	0	1	-0.08	0.02	79.38
Bacteria	Topsoil	2023	p__Desulfobacterota sp ASV2690	0	1	-0.08	0.03	87.50
Bacteria	Topsoil	2022	p__RCP2-54 sp ASV1458	1	0	0.14	0.03	77.50
Bacteria	Topsoil	2023	p__RCP2-54 sp ASV1458	0	4	-0.31	0.02	89.58
Bacteria	Phyllosphere	2022	p__RCP2-54 sp ASV348	1	0	0.13	0.01	38.13
Bacteria	Topsoil	2022	p__RCP2-54 sp ASV348	2	0	0.23	0.32	80.00
Bacteria	Topsoil	2022	p__RCP2-54 sp ASV644	0	3	-0.35	0.09	31.88
Bacteria	Topsoil	2023	p__RCP2-54 sp ASV644	0	3	-0.48	0.03	60.42

Annexe n° 10: Fungal and bacterial ASVs indicating low and high *Plasmopara viticola* DNA concentrations in topsoil (Chapter n° 3).

Domain: ASV domain (Bacteria or Fungi), *Habitat*: Microbial habitat in which the ASV was found (Topsoil, Phyllosphere, endosphere), *Year*: Sampling year, *ASV*: ASV final taxonomic assignment (i.e. to the lowest known taxonomic level) followed by ASV number, *TITAN res*: Result from TITAN indicating whether the ASV is an indicator of low or high value of P. viticola DNA concentration in topsoil, *TITAN zscore*: TITAN z score, *%reads*: Relative abundance of the ASV for this combination of Habitat * Domain * Sampling Year and *Prev.*: Prevalence of the ASV for this combination of Habitat * Domain * Sampling Year. In the column 'ASV', the prefix abbreviations are: p for phylum, c for class, o for order, f for family, g for genus, and s for species. The rows are sorted according to the ASV column in alphabetical order, starting with the ASVs for which the lowest known taxonomic level is species, then those for which it is genus, and so on. They are then sorted by habitat and year.

Domain	Habitat	Year	ASV	TITAN res	TITAN zscore	%reads	Prev.
Bacteria	Topsoil	2022	s__[Brevibacterium] frigoritolerans ASV78	Low	4.53	0.54	75.00
Bacteria	Phyllosphere	2023	s__Acetobacteraceae bacterium ASV1090	Low	4.83	0.04	27.66
Fungi	Phyllosphere	2023	s__Acremonium sclerotigenum ASV782	High	6.07	0.00	8.51
Bacteria	Topsoil	2022	s__Actinomycetales bacterium ASV133	Low	4.93	0.09	80.00
Bacteria	Topsoil	2022	s__Adhaeribacter terrae ASV639	High	6.23	0.11	82.50
Bacteria	Phyllosphere	2022	s__Agromyces ramosus ASV49	Low	4.64	0.09	53.13
Fungi	Topsoil	2022	s__Albifimbria verrucaria ASV78	High	4.73	0.36	71.70
Fungi	Topsoil	2022	s__Alternaria alternata ASV18	Low	4.3	0.30	90.57
Fungi	Topsoil	2023	s__Alternaria alternata ASV18	Low	3.46	0.16	100
Fungi	Phyllosphere	2022	s__Alternaria rosae ASV204	High	3.81	0.01	69.62
Fungi	Phyllosphere	2023	s__Alternaria rosae ASV204	High	3.1	0.02	38.30
Bacteria	Topsoil	2022	s__Amnibacterium kyonggiense ASV1923	Low	4.1	0.01	51.25
Bacteria	Topsoil	2022	s__Amycolatopsis keratiniphila ASV947	Low	3.81	0.01	21.88
Fungi	Topsoil	2022	s__Arthrinium malaysianum ASV82	High	3.69	0.44	64.15
Bacteria	Topsoil	2022	s__Arthrobacter globiformis ASV1353	Low	5.11	0.03	10.00
Bacteria	Phyllosphere	2022	s__Arthrobacter globiformis ASV1353	Low	6.38	0.00	8.75
Bacteria	Topsoil	2022	s__Arthrobacter globiformis ASV281	Low	5.69	0.16	80.63
Bacteria	Phyllosphere	2022	s__Arthrobacter globiformis ASV281	Low	7.45	0.03	38.75
Bacteria	Topsoil	2022	s__Arthrobacter globiformis ASV64	Low	5.57	0.62	81.88
Bacteria	Phyllosphere	2023	s__Arthrobacter globiformis ASV64	Low	3.43	0.10	65.96
Bacteria	Topsoil	2022	s__Arthrobacter globiformis ASV791	Low	5.19	0.07	10.00
Bacteria	Phyllosphere	2022	s__Arthrobacter globiformis ASV791	Low	6.59	0.01	10.00
Bacteria	Topsoil	2022	s__Arthrobacter oryzae ASV45	Low	4.97	0.89	91.88
Bacteria	Phyllosphere	2022	s__Arthrobacter pascens ASV307	Low	5.3	0.04	43.75
Bacteria	Topsoil	2023	s__Arthrobacter pascens ASV307	Low	4.04	0.11	91.67
Fungi	Topsoil	2022	s__Articulospora proliferata ASV669	Low	2.95	0.02	63.52
Fungi	Topsoil	2023	s__Articulospora proliferata ASV669	Low	3.96	0.02	62.50
Fungi	Topsoil	2022	s__Ascochyta medicaginicola var. macrospora ASV350	Low	4.63	0.05	20.75
Fungi	Phyllosphere	2022	s__Ascochyta medicaginicola var. macrospora ASV350	Low	3.24	0.02	43.04
Fungi	Topsoil	2022	s__Aspergillus pseudodeflectus ASV284	Low	3.42	0.06	58.49
Fungi	Topsoil	2023	s__Aspergillus pseudodeflectus ASV284	Low	3.72	0.22	77.08
Fungi	Phyllosphere	2022	s__Aureobasidium pullulans ASV2	Low	3.4	11.24	94.30

Annexes

Bacteria	Topsoil	2022	s__Azohydromonas australica ASV1060	Low	4.11	0.02	62.50
Fungi	Topsoil	2022	s__Bacidia chloroticula ASV597	Low	3.48	0.00	18.24
Bacteria	Phyllosphere	2023	s__Bacillus coagulans ASV233	Low	4.17	0.13	89.36
Bacteria	Topsoil	2023	s__Bacillus cytotoxicus ASV765	High	3.64	0.04	93.75
Bacteria	Phyllosphere	2023	s__Bacillus drentensis ASV177	Low	4.87	0.04	46.81
Bacteria	Topsoil	2022	s__Bacillus litoralis ASV797	Low	4.92	0.10	62.50
Bacteria	Topsoil	2022	s__Bacillus megaterium NBRC 15308 = ATCC 14581 ASV21	Low	6.72	1.23	92.50
Bacteria	Phyllosphere	2022	s__Bacillus megaterium NBRC 15308 = ATCC 14581 ASV21	Low	4.2	0.19	80.00
Bacteria	Phyllosphere	2022	s__Bacillus mycoides KBAB4 ASV250	Low	4.85	0.04	41.25
Bacteria	Topsoil	2023	s__Bacillus mycoides KBAB4 ASV250	High	3.37	0.12	97.92
Bacteria	Topsoil	2022	s__Bacillus nealsonii ASV676	Low	4.07	0.06	82.50
Bacteria	Phyllosphere	2022	s__Bacillus thermolactis ASV1089	Low	3.21	0.05	24.38
Bacteria	Phyllosphere	2023	s__Bacillus thermolactis ASV1089	High	4.06	0.02	19.15
Fungi	Topsoil	2022	s__Biatriospora antibiotica ASV338	High	3.83	0.03	45.91
Fungi	Phyllosphere	2022	s__Biatriospora antibiotica ASV338	High	3.12	0.17	35.44
Fungi	Endosphere	2023	s__Botrytis cinerea ASV19	High	3.32	0.53	58.33
Fungi	Topsoil	2022	s__Bradymyces graniticola ASV647	Low	5.45	0.02	11.95
Fungi	Phyllosphere	2022	s__Bullera alba ASV242	Low	4.04	0.17	83.54
Fungi	Phyllosphere	2022	s__Caloplaca obscurella ASV565	High	9.49	0.00	4.43
Fungi	Topsoil	2022	s__Catenulostroma hermanusense ASV255	Low	3.53	0.00	27.67
Bacteria	Phyllosphere	2022	s__Caulobacter vibrioides ASV1261	Low	5.93	0.01	13.75
Bacteria	Topsoil	2022	s__Chelatococcus asaccharovorans ASV432	Low	4.14	0.06	27.50
Fungi	Topsoil	2023	s__Cladosporium allicinum ASV8	Low	3.85	0.10	100
Fungi	Phyllosphere	2023	s__Cladosporium allicinum ASV8	High	4.06	2.08	76.60
Fungi	Topsoil	2023	s__Cladosporium cladosporiodes ASV5	Low	3.65	1.26	100
Fungi	Phyllosphere	2023	s__Cladosporium cladosporiodes ASV5	High	4.42	3.18	91.49
Fungi	Topsoil	2023	s__Cladosporium cladosporiodes ASV680	Low	3.31	0.01	95.83
Fungi	Endosphere	2022	s__Clonostachys miodochialis ASV71	High	4.04	0.00	33.13
Bacteria	Phyllosphere	2022	s__Clostridium magnum ASV2013	Low	8.73	0.00	8.13
Bacteria	Topsoil	2023	s__Clostridium magnum ASV2013	High	2.76	0.02	95.83
Bacteria	Phyllosphere	2022	s__Corynebacterium xerosis ASV584	Low	2.71	0.00	13.13
Fungi	Phyllosphere	2022	s__Curvularia hawaiiensis ASV326	Low	5.73	0.00	25.32
Fungi	Topsoil	2022	s__Curvularia inaequalis ASV662	High	4.22	0.02	51.57
Fungi	Phyllosphere	2022	s__Cystobasidium pinicola ASV569	Low	3.03	0.03	53.16
Fungi	Topsoil	2022	s__Cystofilobasidium infirmominiatum ASV80	Low	3.64	0.11	40.25
Fungi	Phyllosphere	2022	s__Cystofilobasidium infirmominiatum ASV80	Low	2.39	0.59	45.57
Fungi	Topsoil	2022	s__Cystofilobasidium macerans ASV48	Low	3.34	0.23	72.33
Fungi	Phyllosphere	2022	s__Cystofilobasidium macerans ASV48	Low	3.4	1.04	89.24
Fungi	Phyllosphere	2023	s__Cystofilobasidium macerans ASV666	High	3.97	0.03	21.28
Bacteria	Topsoil	2023	s__Cytophaga hutchinsonii ATCC 33406 ASV886	High	3.3	0.02	89.58
Fungi	Phyllosphere	2022	s__Cytospora prunicola ASV575	Low	5.34	0.01	26.58
Fungi	Topsoil	2022	s__Dactylaria dimorphospora ASV671	High	5.3	0.03	38.99
Fungi	Topsoil	2023	s__Dactylaria dimorphospora ASV671	High	5.87	0.00	20.83
Fungi	Topsoil	2022	s__Dactylonectria estremocensis ASV81	High	3.69	0.48	83.02
Fungi	Phyllosphere	2022	s__Daldinia vanderguchtiae ASV100	Low	3.1	0.06	72.78

Annexes

Fungi	Topsoil	2022	s__Diaporthe cynaroidis ASV308	High	5.88	0.00	18.24
Fungi	Topsoil	2022	s__Dioszegia butyracea ASV328	High	6.05	0.00	54.72
Fungi	Topsoil	2022	s__Dissoconium eucalypti ASV472	High	4.63	0.01	61.64
Fungi	Topsoil	2022	s__Emericellopsis minima ASV351	Low	5.3	0.13	25.79
Fungi	Topsoil	2023	s__Epicoccum nigrum ASV7	Low	3.91	0.16	97.92
Fungi	Phyllosphere	2023	s__Exidia glandulosa ASV892	High	3.98	0.02	42.55
Bacteria	Topsoil	2022	s__Exiguobacterium sibiricum 255-15 ASV169	Low	7.08	0.01	26.88
Fungi	Endosphere	2022	s__Exophiala attenuata ASV225	High	4.97	0.43	35.00
Fungi	Phyllosphere	2022	s__Filobasidium stepposum ASV13	High	5.11	5.24	93.04
Fungi	Phyllosphere	2022	s__Filobasidium stepposum ASV319	High	4.82	0.07	95.57
Bacteria	Phyllosphere	2022	s__Flavisolibacter tropicus ASV231	Low	4.53	0.03	47.50
Fungi	Topsoil	2022	s__Funneliformis geosporum ASV1403	High	4.09	0.03	23.90
Fungi	Phyllosphere	2022	s__Fusarium avenaceum ASV25	Low	2.87	0.31	86.71
Fungi	Topsoil	2022	s__Fusarium avenaceum ASV946	Low	2.73	0.02	93.08
Fungi	Topsoil	2022	s__Fusarium brachygibbosum ASV46	Low	4.07	0.86	42.14
Fungi	Endosphere	2022	s__Fusarium brachygibbosum ASV46	Low	4.59	0.00	16.88
Fungi	Topsoil	2022	s__Fusarium brachygibbosum ASV837	Low	3.32	0.02	35.85
Fungi	Topsoil	2022	s__Fusarium waltergamsii ASV229	High	4.1	0.10	45.28
Fungi	Topsoil	2023	s__Fusicolla aquaeductuum ASV29	High	3.47	0.17	89.58
Fungi	Phyllosphere	2023	s__Ganoderma pfeifferi ASV610	High	5.25	0.08	63.83
Fungi	Phyllosphere	2023	s__Gibberella intricans ASV806	Low	4.32	0.00	19.15
Fungi	Topsoil	2022	s__Gliomastix roseogrisea ASV289	Low	3.13	0.08	86.16
Fungi	Phyllosphere	2022	s__Hormonema macrosporum ASV596	Low	5.32	0.00	68.35
Fungi	Topsoil	2022	s__Humicola grisea ASV89	Low	3.07	0.19	65.41
Fungi	Topsoil	2022	s__Humicola olivacea ASV254	High	5.94	0.11	41.51
Bacteria	Phyllosphere	2023	s__Hymenobacter aquaticus ASV698	High	6.63	0.11	12.77
Bacteria	Phyllosphere	2022	s__Hymenobacter nivis ASV1516	Low	4.27	0.03	43.13
Fungi	Topsoil	2022	s__Hypomyces microspermus ASV480	High	6.58	0.05	8.18
Fungi	Topsoil	2022	s__Itersonilia pannonica ASV14	High	3.02	0.06	86.16
Fungi	Endosphere	2022	s__Itersonilia perplexans ASV30	High	4.49	2.29	19.38
Fungi	Topsoil	2022	s__Laccaria laccata ASV723	Low	3.96	0.03	9.43
Fungi	Phyllosphere	2022	s__Lecanora sambuci ASV1179	Low	2.55	0.00	28.48
Fungi	Topsoil	2022	s__Lectera capsici ASV357	Low	4.43	0.06	11.32
Fungi	Topsoil	2022	s__Lectera capsici ASV360	Low	4.07	0.06	13.84
Fungi	Topsoil	2022	s__Lectera longa ASV431	Low	3.31	0.05	43.40
Fungi	Topsoil	2022	s__Lectera longa ASV94	Low	4.15	0.36	40.25
Fungi	Topsoil	2023	s__Lycoperdon pratense ASV209	High	3.12	0.40	77.08
Fungi	Endosphere	2022	s__Malassezia restricta ASV932	Low	3.91	0.03	18.75
Fungi	Topsoil	2022	s__Mariannaea punicea ASV744	High	6.23	0.02	38.36
Fungi	Topsoil	2023	s__Mariannaea punicea ASV744	High	4.9	0.00	14.58
Bacteria	Topsoil	2023	s__Massilia aurea ASV32	Low	3.39	0.01	83.33
Bacteria	Phyllosphere	2022	s__Massilia putida ASV917	Low	2.9	0.03	50.63
Fungi	Topsoil	2023	s__Metacordyceps chlamydosporia ASV590	High	4.22	0.02	75.00
Fungi	Topsoil	2023	s__Metarhizium marquandii ASV802	High	4.45	0.00	25.00
Bacteria	Phyllosphere	2022	s__Methylobacterium isbiliense ASV1222	Low	6.61	0.01	26.25
Bacteria	Phyllosphere	2022	s__Methylobacterium soli ASV485	Low	3.56	0.05	56.25

Annexes

Bacteria	Topsoil	2023	s__Microbacterium saccharophilum ASV129	High	4.73	0.35	100
Bacteria	Topsoil	2022	s__Microvirga ossetica ASV91	High	3.45	0.24	68.75
Fungi	Topsoil	2023	s__Monocillium griseo-ochraceum ASV531	High	6	0.02	64.58
Fungi	Topsoil	2022	s__Monocillium mucidum ASV163	High	4.89	0.21	76.73
Fungi	Topsoil	2022	s__Mortierella amoeboidea ASV740	High	4.83	0.01	25.16
Bacteria	Topsoil	2022	s__Mycobacterium psychrotolerans ASV53	High	3.66	0.62	93.13
Bacteria	Topsoil	2022	s__Naasia aerilata ASV880	Low	4.82	0.02	65.00
Fungi	Topsoil	2022	s__Neocosmospora rubicola ASV37	Low	5.96	1.21	93.71
Fungi	Phyllosphere	2023	s__Neoerysiphe nevoi ASV64	High	3.55	0.06	65.96
Fungi	Topsoil	2022	s__Neofusicoccum parvum ASV641	High	4.54	0.00	22.01
Fungi	Topsoil	2022	s__Neosetophoma italica ASV122	High	3.32	0.00	11.95
Bacteria	Topsoil	2023	s__Nocardioides sediminis ASV1725	High	4.35	0.03	87.50
Bacteria	Topsoil	2022	s__Nocardioides tritolerans ASV1608	High	4.42	0.03	63.75
Fungi	Phyllosphere	2022	s__Olpidium brassicae ASV404	Low	3.11	0.00	10.13
Bacteria	Topsoil	2022	s__Paenibacillus borealis ASV2861	Low	4.03	0.03	79.38
Bacteria	Phyllosphere	2022	s__Paenibacillus borealis ASV2861	Low	3.23	0.00	16.25
Bacteria	Topsoil	2022	s__Paenibacillus crassostreae ASV2310	Low	4.63	0.03	83.75
Fungi	Phyllosphere	2022	s__Papiliotrema flavescens ASV383	High	3.88	0.05	72.15
Fungi	Phyllosphere	2023	s__Paraconiothyrium brasiliense ASV456	High	3.78	0.07	57.45
Fungi	Topsoil	2022	s__Paraconiothyrium cyclothyrioides ASV801	High	5.18	0.01	30.19
Fungi	Topsoil	2022	s__Paraphoma pye ASV752	Low	4.8	0.02	47.80
Fungi	Topsoil	2023	s__Paraphoma pye ASV752	Low	4.99	0.01	68.75
Fungi	Topsoil	2022	s__Paraphoma radicina ASV589	Low	4.46	0.01	64.78
Fungi	Topsoil	2022	s__Penicillium decumbens ASV66	Low	5.8	0.56	75.47
Fungi	Phyllosphere	2022	s__Penicillium dierckxii ASV861	Low	4.02	0.00	6.96
Fungi	Topsoil	2022	s__Penicillium jensenii ASV45	High	4.73	0.83	67.92
Fungi	Topsoil	2023	s__Penicillium jensenii ASV45	High	3.78	1.52	93.75
Fungi	Topsoil	2023	s__Penicillium kongii ASV199	High	3.82	0.02	72.92
Fungi	Phyllosphere	2023	s__Peniophora versicolor ASV165	Low	3.2	0.79	85.11
Fungi	Phyllosphere	2023	s__Pestalotiopsis rosea ASV504	High	7.07	0.00	10.64
Fungi	Topsoil	2022	s__Phaeosphaeria lunariae ASV741	High	4.17	0.00	15.72
Fungi	Phyllosphere	2022	s__Phaeosphaeria lunariae ASV741	High	3.96	0.03	20.25
Fungi	Topsoil	2022	s__Phialocephala humicola ASV477	High	6.89	0.03	55.35
Fungi	Topsoil	2023	s__Phialocephala humicola ASV477	High	5.55	0.05	58.33
Fungi	Phyllosphere	2022	s__Plagiostoma pulchellum ASV784	Low	5.96	0.00	27.85
Fungi	Phyllosphere	2022	s__Plectosphaerella cucumerina ASV31	Low	4.02	0.04	71.52
Fungi	Phyllosphere	2022	s__Plectosphaerella cucumerina ASV645	Low	5.87	0.00	32.28
Fungi	Topsoil	2022	s__Protomyces macrosporus ASV437	High	6.07	0.02	43.40
Fungi	Phyllosphere	2022	s__Protomyces macrosporus ASV437	High	5.37	0.04	60.13
Bacteria	Topsoil	2022	s__Pseudarthrobacter equi ASV1234	Low	5.29	0.02	50.63
Bacteria	Topsoil	2022	s__Pseudarthrobacter oxydans ASV138	Low	4.91	0.26	53.13
Bacteria	Topsoil	2022	s__Pseudarthrobacter sulfonivorans ASV178	Low	3.43	0.16	63.75
Bacteria	Phyllosphere	2022	s__Pseudarthrobacter sulfonivorans ASV178	Low	4.08	0.09	50.00
Fungi	Topsoil	2022	s__Pseudeurotium bakeri ASV159	Low	4.68	0.13	69.18
Bacteria	Topsoil	2022	s__Pseudomonas rhizosphaerae ASV17	High	3.98	0.01	65.63
Bacteria	Phyllosphere	2022	s__Pseudomonas rhodesiae ASV66	Low	2.99	0.35	66.88

Annexes

Fungi	Phyllosphere	2022	s__Pseudopeziza medicaginis ASV720	Low	3.43	0.00	25.95
Fungi	Topsoil	2022	s__Pyrenochaetopsis leptospora ASV85	High	5.69	0.50	75.47
Fungi	Topsoil	2022	s__Pyrenochaetopsis tabarestanensis ASV381	High	5.31	0.06	37.11
Fungi	Topsoil	2023	s__Pyxidiophora arvernensis ASV700	High	4.38	0.03	81.25
Bacteria	Topsoil	2023	s__Rhizobium soli ASV96	Low	3.06	0.01	81.25
Bacteria	Topsoil	2023	s__Rhodococcus hoagii ASV611	High	4.68	0.05	100
Fungi	Topsoil	2022	s__Rhodotorula babjevae ASV235	Low	3.59	0.02	74.84
Fungi	Topsoil	2023	s__Saitozyma podzolica ASV763	High	4.11	0.00	12.50
Fungi	Topsoil	2022	s__Sarocladium bactrocephalum ASV213	High	2.92	0.11	81.76
Fungi	Topsoil	2022	s__Seimatosporium rosicola ASV230	High	6.68	0.01	21.38
Bacteria	Topsoil	2023	s__Sphingomonas aerolata ASV18	Low	3.53	0.00	87.50
Bacteria	Topsoil	2022	s__Sphingomonas astaxanthinifaciens ASV511	Low	4.82	0.02	84.38
Bacteria	Phyllosphere	2022	s__Sphingomonas faeni ASV512	High	3.61	0.11	56.88
Bacteria	Topsoil	2023	s__Sphingomonas limnosediminicola ASV1002	Low	4.74	0.04	77.08
Bacteria	Phyllosphere	2022	s__Sphingomonas sediminicola ASV761	Low	4.61	0.02	40.00
Bacteria	Phyllosphere	2022	s__Sphingomonas sediminicola ASV94	Low	4	0.12	71.25
Fungi	Topsoil	2023	s__Spizellomyces pseudodichotomus ASV815	Low	4.02	0.09	35.42
Bacteria	Topsoil	2022	s__Sporosarcina psychrophila ASV1873	Low	3.75	0.03	73.13
Fungi	Topsoil	2022	s__Stemphylium lycii ASV558	High	4.27	0.00	40.88
Fungi	Topsoil	2023	s__Stemphylium solani ASV54	Low	3.73	0.01	89.58
Fungi	Topsoil	2023	s__Stephanonectria keithii ASV304	High	4.57	0.08	64.58
Fungi	Phyllosphere	2023	s__Stereum sanguinolentum ASV407	Low	4.32	0.23	74.47
Bacteria	Phyllosphere	2022	s__Streptococcus oralis ASV1602	Low	5	0.07	31.25
Bacteria	Topsoil	2022	s__Streptomyces albidoflavus ASV875	Low	6.05	0.02	66.25
Bacteria	Phyllosphere	2022	s__Streptomyces albidoflavus ASV875	Low	5.15	0.01	26.25
Bacteria	Topsoil	2023	s__Streptomyces albidoflavus ASV875	Low	3.13	0.04	100
Bacteria	Topsoil	2022	s__Streptomyces ambofaciens ASV915	Low	6.73	0.02	69.38
Bacteria	Phyllosphere	2022	s__Streptomyces ambofaciens ASV915	Low	4.02	0.01	16.88
Bacteria	Phyllosphere	2022	s__Streptomyces anulatus ASV221	Low	4.62	0.03	47.50
Fungi	Topsoil	2022	s__Symmetrospora coprosmae ASV60	High	3.8	0.04	84.91
Fungi	Phyllosphere	2023	s__Taphrina pruni ASV499	High	4.1	0.17	46.81
Bacteria	Phyllosphere	2022	s__Terrabacter terrae ASV39	Low	2.55	0.13	73.13
Bacteria	Phyllosphere	2022	s__Terribacillus goriensis ASV1216	Low	7.48	0.01	7.50
Bacteria	Phyllosphere	2022	s__Thermobifida fusca YX ASV913	Low	3.19	0.06	42.50
Bacteria	Phyllosphere	2023	s__Thermobifida fusca YX ASV913	High	4.35	0.03	19.15
Fungi	Endosphere	2022	s__Tomentella galzinii ASV265	High	6.47	0.00	4.38
Fungi	Phyllosphere	2022	s__Torula acaciae ASV805	Low	3.83	0.01	53.16
Fungi	Phyllosphere	2023	s__Torula acaciae ASV805	High	7.34	0.02	21.28
Fungi	Phyllosphere	2022	s__Tremella phaeophysciae ASV523	Low	5.27	0.03	49.37
Fungi	Topsoil	2023	s__Trichocladium opacum ASV525	High	4.12	0.07	77.08
Fungi	Topsoil	2022	s__Trichoderma hamatum ASV299	Low	4.56	0.09	43.40
Fungi	Topsoil	2022	s__Trichothecium roseum ASV218	High	6.83	0.00	6.29
Fungi	Topsoil	2023	s__Truncatella angustata ASV32	High	4.19	1.66	100
Fungi	Phyllosphere	2022	s__Truncatella angustata ASV545	High	4.8	0.00	17.09
Fungi	Topsoil	2023	s__Truncatella angustata ASV545	Low	4.46	0.01	25.00
Fungi	Topsoil	2022	s__Tuber maculatum ASV813	High	9.14	0.02	4.40

Annexes

Fungi	Topsoil	2022	s__Vishniacozyma dimennae ASV114	Low	3.22	0.18	79.87
Fungi	Phyllosphere	2022	s__Vishniacozyma dimennae ASV114	High	3.08	0.25	83.54
Fungi	Topsoil	2023	s__Vishniacozyma dimennae ASV114	Low	3.1	0.13	97.92
Fungi	Endosphere	2022	s__Vishniacozyma dimennae ASV79	Low	3.19	0.00	13.75
Fungi	Phyllosphere	2023	s__Vishniacozyma globispora ASV421	Low	3.44	0.11	27.66
Fungi	Phyllosphere	2022	s__Vishniacozyma tephrensis ASV416	High	4.49	0.09	73.42
Fungi	Phyllosphere	2022	s__Vishniacozyma victoriae ASV283	High	2.98	0.07	96.84
Fungi	Topsoil	2022	s__Volutella ciliata ASV73	Low	4.8	0.37	68.55
Fungi	Topsoil	2022	s__Wallemia muriae ASV450	High	4.87	0.00	25.16
Fungi	Topsoil	2022	s__Zymoseptoria verkleyi ASV795	High	5.38	0.00	37.74
Fungi	Phyllosphere	2022	s__Zymoseptoria verkleyi ASV795	High	3.89	0.06	62.03
Bacteria	Phyllosphere	2022	g__1174-901-12 sp ASV1329	Low	4.94	0.03	21.25
Bacteria	Phyllosphere	2022	g__1174-901-12 sp ASV288	Low	4.33	0.10	60.00
Bacteria	Topsoil	2022	g__Abditibacterium sp ASV856	Low	3.18	0.02	76.25
Bacteria	Topsoil	2023	g__Actinomycetospora sp ASV269	High	5.4	0.01	66.67
Bacteria	Topsoil	2022	g__Actinotalea sp ASV1068	Low	7.63	0.03	42.50
Bacteria	Phyllosphere	2022	g__Actinotalea sp ASV1068	Low	2.81	0.02	39.38
Bacteria	Topsoil	2022	g__Adhaeribacter sp ASV686	Low	4.03	0.04	30.63
Bacteria	Phyllosphere	2022	g__Adhaeribacter sp ASV686	Low	4.15	0.01	23.13
Bacteria	Topsoil	2022	g__Adhaeribacter sp ASV748	High	4.05	0.07	81.25
Bacteria	Topsoil	2022	g__Aeromicrobium sp ASV1821	Low	4.18	0.02	47.50
Bacteria	Topsoil	2023	g__Aeromicrobium sp ASV1821	Low	2.91	0.04	77.08
Bacteria	Topsoil	2022	g__Agrococcus sp ASV671	Low	3.18	0.04	47.50
Bacteria	Phyllosphere	2022	g__Agromyces sp ASV253	Low	4.75	0.02	40.63
Bacteria	Phyllosphere	2022	g__alphaI_cluster sp ASV420	Low	3.62	0.01	28.13
Fungi	Topsoil	2022	g__Alternaria sp ASV388	High	3.83	0.03	66.04
Bacteria	Topsoil	2022	g__Amaricoccus sp ASV984	High	3.77	0.03	72.50
Bacteria	Topsoil	2023	g__Amaricoccus sp ASV984	High	4.73	0.02	87.50
Bacteria	Topsoil	2022	g__Amnibacterium sp ASV1629	Low	3.02	0.01	41.25
Bacteria	Topsoil	2023	g__Amnibacterium sp ASV1629	Low	4.37	0.04	45.83
Bacteria	Phyllosphere	2022	g__Amnibacterium sp ASV409	Low	4.61	0.08	74.38
Bacteria	Phyllosphere	2022	g__Anaeromyxobacter sp ASV586	Low	7.5	0.01	15.63
Bacteria	Phyllosphere	2022	g__Angustibacter sp ASV331	Low	4.35	0.01	34.38
Fungi	Topsoil	2022	g__Apiotrichum sp ASV309	High	5.12	0.09	41.51
Bacteria	Topsoil	2023	g__Arenimonas sp ASV1332	High	5.18	0.01	85.42
Bacteria	Topsoil	2023	g__Arenimonas sp ASV2010	High	4.52	0.01	87.50
Bacteria	Phyllosphere	2022	g__Arenimonas sp ASV673	Low	8.53	0.00	15.00
Bacteria	Topsoil	2022	g__Arenimonas sp ASV754	High	2.94	0.10	86.25
Bacteria	Phyllosphere	2022	g__Arthrobacter sp ASV828	Low	8	0.01	20.63
Fungi	Phyllosphere	2022	g__Articulospora sp ASV269	Low	3.84	0.00	32.91
Fungi	Topsoil	2022	g__Articulospora sp ASV455	Low	5.5	0.03	54.09
Fungi	Topsoil	2023	g__Articulospora sp ASV455	Low	4.88	0.11	39.58
Fungi	Topsoil	2022	g__Articulospora sp ASV479	High	4.02	0.02	25.16
Fungi	Topsoil	2022	g__Aspergillus sp ASV161	Low	2.99	0.14	68.55
Fungi	Topsoil	2022	g__Aspergillus sp ASV376	High	3.11	0.04	39.62
Fungi	Topsoil	2022	g__Aspergillus sp ASV573	Low	4.27	0.01	25.16

Annexes

Fungi	Endosphere	2022	g__Aspergillus sp ASV623	Low	4.57	0.22	10.00
Fungi	Topsoil	2022	g__Aspergillus sp ASV724	High	5.08	0.00	35.85
Fungi	Phyllosphere	2022	g__Aspergillus sp ASV77	Low	2.99	0.17	58.86
Fungi	Topsoil	2022	g__Atrocalyx sp ASV111	Low	6.34	0.11	28.30
Bacteria	Phyllosphere	2022	g__Aurantisolimonas sp ASV1205	Low	4.25	0.02	36.25
Bacteria	Topsoil	2023	g__Aureimonas sp ASV157	Low	4.72	0.00	60.42
Fungi	Phyllosphere	2022	g__Aureobasidium sp ASV375	High	3.57	0.06	80.38
Bacteria	Topsoil	2022	g__Bacillus sp ASV104	Low	4.07	0.40	88.75
Bacteria	Phyllosphere	2022	g__Bacillus sp ASV104	Low	3.37	0.13	72.50
Bacteria	Phyllosphere	2023	g__Bacillus sp ASV104	Low	4.01	0.15	91.49
Bacteria	Phyllosphere	2022	g__Bacillus sp ASV1057	Low	4.97	0.00	13.13
Bacteria	Topsoil	2022	g__Bacillus sp ASV135	Low	5.62	0.15	93.13
Bacteria	Topsoil	2022	g__Bacillus sp ASV317	Low	3.36	0.16	88.75
Bacteria	Topsoil	2022	g__Bacillus sp ASV484	Low	7	0.05	53.75
Bacteria	Phyllosphere	2022	g__Bacillus sp ASV958	Low	2.53	0.01	21.25
Bacteria	Topsoil	2022	g__Blastococcus sp ASV46	Low	4.22	0.94	93.75
Bacteria	Phyllosphere	2022	g__Blastococcus sp ASV46	Low	3.24	0.22	71.25
Bacteria	Topsoil	2022	g__Blastococcus sp ASV662	Low	4.23	0.05	40.00
Bacteria	Phyllosphere	2022	g__Blastococcus sp ASV662	Low	2.92	0.01	18.13
Bacteria	Topsoil	2022	g__Blastococcus sp ASV70	Low	4.69	0.70	91.88
Bacteria	Phyllosphere	2022	g__Blastococcus sp ASV70	Low	3.38	0.29	73.13
Bacteria	Phyllosphere	2022	g__Bradyrhizobium sp ASV996	Low	4.23	0.01	23.75
Bacteria	Topsoil	2022	g__Caenimonas sp ASV1134	High	3.38	0.03	91.25
Bacteria	Topsoil	2022	g__Caenimonas sp ASV545	High	4.43	0.06	83.75
Bacteria	Phyllosphere	2022	g__Candidatus_Alysiosphaera sp ASV925	Low	3.8	0.00	21.25
Bacteria	Topsoil	2022	g__Candidatus_Koribacter sp ASV1123	Low	5.29	0.01	36.88
Bacteria	Phyllosphere	2022	g__Candidatus_Koribacter sp ASV1123	Low	8.16	0.01	11.25
Bacteria	Phyllosphere	2022	g__Candidatus_Koribacter sp ASV1912	Low	7.94	0.01	10.00
Bacteria	Phyllosphere	2022	g__Candidatus_Solibacter sp ASV1613	Low	8.17	0.00	11.25
Bacteria	Phyllosphere	2022	g__Candidatus_Solibacter sp ASV643	Low	4.09	0.02	27.50
Bacteria	Topsoil	2022	g__Candidatus_Solibacter sp ASV890	Low	6.96	0.05	85.63
Bacteria	Topsoil	2022	g__Cellulomonas sp ASV929	Low	3.34	0.04	24.38
Bacteria	Phyllosphere	2022	g__Cellulomonas sp ASV929	Low	3.85	0.01	24.38
Fungi	Endosphere	2022	g__Cercophora sp ASV189	Low	4.11	0.00	19.38
Fungi	Topsoil	2023	g__Cercophora sp ASV189	High	3.2	0.16	79.17
Fungi	Topsoil	2022	g__Cercophora sp ASV582	High	4.65	0.02	35.22
Bacteria	Topsoil	2022	g__Chryseolinea sp ASV1368	High	4.87	0.02	73.13
Bacteria	Topsoil	2023	g__Chryseolinea sp ASV305	High	3.45	0.07	77.08
Bacteria	Topsoil	2022	g__Chryseolinea sp ASV518	High	4.11	0.06	81.25
Bacteria	Phyllosphere	2022	g__CL500-29_marine_group sp ASV576	Low	4.22	0.00	26.25
Bacteria	Phyllosphere	2022	g__CL500-29_marine_group sp ASV696	Low	5.31	0.00	18.75
Bacteria	Topsoil	2022	g__CL500-29_marine_group sp ASV898	High	4.85	0.05	74.38
Bacteria	Topsoil	2023	g__CL500-29_marine_group sp ASV898	High	6.23	0.02	81.25
Bacteria	Topsoil	2022	g__CL500-29_marine_group sp ASV919	High	4.32	0.06	78.75
Fungi	Topsoil	2022	g__Cladophialophora sp ASV866	High	5.8	0.01	24.53
Fungi	Topsoil	2022	g__Cladosporium sp ASV223	High	2.95	0.01	56.60

Annexes

Bacteria	Topsoil	2022	g__Clostridium_sensu_stricto_1 sp ASV1376	Low	4.13	0.03	72.50
Bacteria	Phyllosphere	2022	g__Clostridium_sensu_stricto_13 sp ASV315	Low	2.47	0.01	28.75
Bacteria	Topsoil	2023	g__Clostridium_sensu_stricto_13 sp ASV315	High	3.88	0.10	95.83
Bacteria	Topsoil	2022	g__Conexibacter sp ASV1307	Low	5.76	0.03	89.38
Bacteria	Topsoil	2022	g__Conexibacter sp ASV834	Low	3.86	0.05	88.13
Fungi	Topsoil	2022	g__Coniochaeta sp ASV323	Low	3.68	0.06	64.15
Fungi	Topsoil	2022	g__Coniochaeta sp ASV683	Low	3.47	0.02	42.77
Fungi	Phyllosphere	2022	g__Constantinomyces sp ASV968	High	3.77	0.01	55.70
Fungi	Topsoil	2022	g__Coprinopsis sp ASV1141	High	4.84	0.00	18.24
Bacteria	Phyllosphere	2022	g__Craurococcus-Caldovatus sp ASV693	Low	5.27	0.01	20.00
Bacteria	Topsoil	2022	g__Defluviicoccus sp ASV921	High	5.03	0.03	29.38
Bacteria	Topsoil	2022	g__Deinococcus sp ASV86	High	4.82	0.01	55.63
Bacteria	Topsoil	2022	g__Demequina sp ASV1645	High	4.63	0.04	69.38
Bacteria	Topsoil	2023	g__Demequina sp ASV1645	High	5.36	0.01	83.33
Fungi	Phyllosphere	2022	g__Diaporthe sp ASV776	Low	4.97	0.00	40.51
Bacteria	Topsoil	2023	g__Duganella sp ASV634	Low	2.75	0.04	95.83
Bacteria	Phyllosphere	2023	g__Dyadobacter sp ASV1537	Low	3.53	0.02	17.02
Bacteria	Topsoil	2022	g__Edaphobaculum sp ASV1229	High	5.6	0.03	77.50
Bacteria	Topsoil	2022	g__Edaphobaculum sp ASV3585	High	4.97	0.03	80.00
Bacteria	Topsoil	2022	g__Ellin517 sp ASV755	High	3.31	0.05	81.25
Bacteria	Topsoil	2022	g__Ellin6055 sp ASV1365	High	3.76	0.03	66.25
Bacteria	Topsoil	2022	g__Ellin6067 sp ASV1742	Low	4.52	0.04	75.00
Bacteria	Phyllosphere	2022	g__Ellin6067 sp ASV259	Low	3.23	0.00	22.50
Bacteria	Topsoil	2022	g__Ellin6067 sp ASV289	High	5.89	0.16	87.50
Bacteria	Phyllosphere	2022	g__Ellin6067 sp ASV289	Low	3.68	0.00	18.13
Bacteria	Topsoil	2022	g__Exiguobacterium sp ASV260	Low	5.98	0.01	29.38
Fungi	Topsoil	2022	g__Exophiala sp ASV91	High	2.91	0.36	67.92
Fungi	Phyllosphere	2022	g__Exophiala sp ASV91	High	3.89	0.00	33.54
Bacteria	Topsoil	2022	g__Ferruginibacter sp ASV1046	High	3.85	0.03	83.75
Bacteria	Phyllosphere	2022	g__Ferruginibacter sp ASV1046	Low	6.17	0.01	26.25
Bacteria	Topsoil	2023	g__Ferruginibacter sp ASV1046	High	4.44	0.02	91.67
Bacteria	Topsoil	2022	g__Ferruginibacter sp ASV1280	High	4.01	0.04	88.13
Bacteria	Phyllosphere	2022	g__Ferruginibacter sp ASV1280	Low	5.62	0.01	25.00
Bacteria	Topsoil	2022	g__Ferruginibacter sp ASV1333	High	4.7	0.03	75.00
Bacteria	Topsoil	2023	g__Ferruginibacter sp ASV1333	High	4.35	0.01	66.67
Bacteria	Phyllosphere	2022	g__Ferruginibacter sp ASV1747	Low	4.71	0.01	33.75
Bacteria	Topsoil	2022	g__Ferruginibacter sp ASV1967	High	4.87	0.03	86.25
Bacteria	Topsoil	2023	g__Ferruginibacter sp ASV1967	High	4.13	0.01	77.08
Bacteria	Topsoil	2022	g__FFCH7168 sp ASV1345	High	4	0.02	63.13
Bacteria	Topsoil	2022	g__Flavisolibacter sp ASV1179	High	5.85	0.01	66.25
Bacteria	Topsoil	2022	g__Flavisolibacter sp ASV1668	High	6.43	0.03	81.25
Bacteria	Phyllosphere	2022	g__Flavisolibacter sp ASV1668	Low	4.74	0.00	18.75
Bacteria	Phyllosphere	2023	g__Flavisolibacter sp ASV1668	Low	5.07	0.01	8.51
Bacteria	Phyllosphere	2022	g__Flavisolibacter sp ASV493	Low	6.56	0.02	41.25
Bacteria	Phyllosphere	2022	g__Flavisolibacter sp ASV629	Low	5.13	0.02	37.50
Bacteria	Phyllosphere	2022	g__Flavisolibacter sp ASV678	Low	4.27	0.01	29.38

Annexes

Fungi	Topsoil	2022	g__Fusarium sp ASV1127	Low	3.78	0.02	94.97
Fungi	Topsoil	2023	g__Fusarium sp ASV1127	Low	3.45	0.01	97.92
Fungi	Topsoil	2022	g__Fusarium sp ASV366	High	3.26	0.10	94.97
Fungi	Topsoil	2023	g__Fusicolla sp ASV750	High	3.72	0.01	27.08
Bacteria	Topsoil	2023	g__Gaiella sp ASV102	Low	4.83	0.41	91.67
Bacteria	Topsoil	2022	g__Gaiella sp ASV1076	Low	4.07	0.05	43.75
Bacteria	Phyllosphere	2022	g__Gaiella sp ASV1076	Low	6.1	0.01	10.00
Bacteria	Phyllosphere	2022	g__Gaiella sp ASV112	Low	2.72	0.04	58.75
Bacteria	Phyllosphere	2022	g__Gaiella sp ASV172	Low	3.01	0.03	43.75
Bacteria	Phyllosphere	2022	g__Gaiella sp ASV192	Low	2.92	0.01	32.50
Bacteria	Phyllosphere	2022	g__Gaiella sp ASV258	Low	3.26	0.04	36.88
Bacteria	Phyllosphere	2022	g__Gaiella sp ASV283	Low	4.14	0.01	35.00
Bacteria	Topsoil	2022	g__Gaiella sp ASV617	High	2.81	0.09	45.63
Bacteria	Topsoil	2023	g__Gaiella sp ASV885	Low	4.19	0.05	70.83
Bacteria	Phyllosphere	2023	g__Gaiella sp ASV885	Low	4.52	0.01	14.89
Bacteria	Phyllosphere	2023	g__Gaiella sp ASV973	High	6.57	0.00	10.64
Bacteria	Topsoil	2023	g__Galbitalea sp ASV655	High	5.57	0.03	97.92
Bacteria	Topsoil	2022	g__Gemmatimonas sp ASV1110	Low	5.93	0.05	79.38
Bacteria	Phyllosphere	2022	g__Gemmatimonas sp ASV1110	Low	5.97	0.02	35.00
Bacteria	Phyllosphere	2022	g__Gemmatimonas sp ASV1258	Low	6.17	0.00	15.63
Bacteria	Topsoil	2022	g__Gemmatimonas sp ASV1293	High	3.91	0.04	65.00
Bacteria	Topsoil	2022	g__Gemmatimonas sp ASV1312	High	3	0.04	82.50
Bacteria	Topsoil	2022	g__Gemmatimonas sp ASV1342	Low	5.07	0.03	18.13
Bacteria	Phyllosphere	2022	g__Gemmatimonas sp ASV1351	Low	5.28	0.01	23.75
Bacteria	Topsoil	2022	g__Gemmatimonas sp ASV557	High	5	0.08	51.88
Bacteria	Phyllosphere	2022	g__Gemmatimonas sp ASV835	Low	5.73	0.01	25.00
Bacteria	Topsoil	2022	g__Geodermatophilus sp ASV41	Low	4.7	0.65	92.50
Bacteria	Topsoil	2023	g__Geodermatophilus sp ASV41	Low	3.58	0.61	100
Fungi	Phyllosphere	2022	g__Golovinomyces sp ASV501	Low	2.92	0.01	32.28
Bacteria	Topsoil	2022	g__Hassallia sp ASV497	High	5.42	0.07	82.50
Bacteria	Topsoil	2022	g__Hassallia sp ASV627	High	4.78	0.11	57.50
Bacteria	Topsoil	2022	g__Hassallia sp ASV910	High	3.76	0.05	76.88
Bacteria	Topsoil	2023	g__Hassallia sp ASV910	High	5.05	0.04	89.58
Bacteria	Topsoil	2022	g__Hassallia sp ASV999	High	3.89	0.04	66.88
Fungi	Topsoil	2022	g__Helgardia sp ASV449	Low	4.05	0.04	46.54
Fungi	Topsoil	2022	g__Helgardia sp ASV710	Low	3.12	0.01	47.17
Fungi	Topsoil	2022	g__Humicola sp ASV771	High	5.12	0.02	29.56
Bacteria	Phyllosphere	2022	g__Hymenobacter sp ASV1118	Low	3.46	0.04	37.50
Bacteria	Topsoil	2022	g__Hymenobacter sp ASV578	Low	4.17	0.00	44.38
Bacteria	Phyllosphere	2022	g__Hymenobacter sp ASV905	Low	2.48	0.06	55.00
Bacteria	Topsoil	2023	g__Hymenobacter sp ASV905	Low	4.91	0.01	72.92
Bacteria	Phyllosphere	2022	g__Iamia sp ASV284	Low	3.78	0.01	20.63
Bacteria	Topsoil	2022	g__Iamia sp ASV609	High	4.76	0.08	58.13
Bacteria	Phyllosphere	2022	g__Iamia sp ASV849	Low	3.83	0.01	26.25
Bacteria	Topsoil	2022	g__Ilumatobacter sp ASV164	High	4.34	0.24	73.13
Bacteria	Topsoil	2023	g__Ilumatobacter sp ASV164	High	6.09	0.09	91.67

Annexes

Bacteria	Topsoil	2022	g__Ilumatobacter sp ASV171	High	3.55	0.21	81.88
Bacteria	Phyllosphere	2022	g__Ilumatobacter sp ASV226	Low	5.73	0.01	43.13
Bacteria	Phyllosphere	2023	g__Ilumatobacter sp ASV883	High	3.74	0.00	10.64
Bacteria	Phyllosphere	2022	g__IMCC26207 sp ASV1206	Low	5.71	0.00	11.88
Bacteria	Topsoil	2022	g__Intrasporangium sp ASV1044	High	4.27	0.02	31.88
Bacteria	Topsoil	2022	g__IS-44 sp ASV1137	Low	4.1	0.02	43.13
Bacteria	Phyllosphere	2022	g__Jatrophihabitans sp ASV1192	Low	4.14	0.05	37.50
Bacteria	Topsoil	2022	g__Jatrophihabitans sp ASV121	Low	5.5	0.21	90.00
Fungi	Phyllosphere	2022	g__Jattaea sp ASV722	Low	8.98	0.03	9.49
Bacteria	Topsoil	2022	g__Kineosporia sp ASV1021	Low	4.26	0.05	91.88
Bacteria	Phyllosphere	2022	g__Kineosporia sp ASV585	Low	4.11	0.01	34.38
Bacteria	Topsoil	2022	g__Knoellia sp ASV691	Low	4.29	0.02	79.38
Bacteria	Topsoil	2022	g__Kouleothrix sp ASV1113	Low	3.99	0.04	55.00
Bacteria	Phyllosphere	2022	g__Kouleothrix sp ASV1113	Low	5.21	0.00	8.75
Bacteria	Topsoil	2022	g__Kouleothrix sp ASV538	High	4.17	0.06	65.00
Bacteria	Phyllosphere	2022	g__Kouleothrix sp ASV690	Low	5.12	0.01	13.13
Bacteria	Topsoil	2023	g__Kribbella sp ASV392	Low	4.43	0.08	100
Bacteria	Phyllosphere	2022	g__Lapillicoccus sp ASV1648	Low	4.9	0.00	11.88
Bacteria	Topsoil	2022	g__Lapillicoccus sp ASV721	High	4.03	0.03	74.38
Fungi	Topsoil	2022	g__Leptodiscella sp ASV471	High	3.53	0.03	47.17
Bacteria	Topsoil	2022	g__Longimicrobium sp ASV1549	Low	2.69	0.02	54.38
Fungi	Topsoil	2023	g__Lophiostoma sp ASV841	High	4.64	0.02	54.17
Bacteria	Topsoil	2022	g__Marmoricola sp ASV1298	Low	3.97	0.01	68.13
Bacteria	Topsoil	2022	g__Marmoricola sp ASV1475	Low	3.3	0.02	68.75
Bacteria	Topsoil	2022	g__Marmoricola sp ASV740	Low	5.65	0.03	83.75
Bacteria	Phyllosphere	2022	g__Marmoricola sp ASV740	Low	4.57	0.01	25.63
Bacteria	Topsoil	2022	g__Massilia sp ASV1034	Low	4.79	0.06	85.63
Bacteria	Topsoil	2022	g__Massilia sp ASV1319	Low	5.18	0.03	72.50
Bacteria	Topsoil	2022	g__Massilia sp ASV1425	Low	4.33	0.03	82.50
Bacteria	Topsoil	2023	g__Massilia sp ASV36	Low	3.62	0.01	95.83
Bacteria	Topsoil	2022	g__Massilia sp ASV362	Low	3.75	0.05	83.75
Bacteria	Topsoil	2023	g__Massilia sp ASV425	Low	3.93	0.02	93.75
Bacteria	Phyllosphere	2022	g__Methylotenera sp ASV587	Low	4.45	0.00	13.13
Bacteria	Topsoil	2023	g__Microbacterium sp ASV175	High	4.19	0.13	100
Fungi	Topsoil	2022	g__Microdochium sp ASV702	High	7.1	0.03	55.35
Bacteria	Topsoil	2022	g__Microlunatus sp ASV209	Low	7.29	0.13	48.75
Bacteria	Phyllosphere	2022	g__Microlunatus sp ASV209	Low	6.98	0.03	40.63
Bacteria	Topsoil	2022	g__Microlunatus sp ASV440	Low	3.85	0.04	32.50
Bacteria	Topsoil	2023	g__Microlunatus sp ASV440	Low	6.69	0.08	39.58
Bacteria	Topsoil	2022	g__Micromonospora sp ASV1379	Low	4.08	0.02	71.88
Bacteria	Topsoil	2023	g__Micromonospora sp ASV2911	High	3.22	0.03	87.50
Bacteria	Phyllosphere	2023	g__Micropruina sp ASV1452	High	5.56	0.00	10.64
Bacteria	Topsoil	2022	g__Microvirga sp ASV1276	Low	4.33	0.02	26.88
Bacteria	Phyllosphere	2022	g__Microvirga sp ASV314	Low	4.12	0.03	51.88
Bacteria	Phyllosphere	2022	g__Microvirga sp ASV476	Low	3.62	0.02	40.00
Bacteria	Topsoil	2022	g__Microvirga sp ASV559	High	4.75	0.06	83.75

Annexes

Bacteria	Topsoil	2022	g__Microvirga sp ASV825	Low	3.63	0.03	51.25
Bacteria	Phyllosphere	2022	g__Microvirga sp ASV922	Low	3.95	0.01	16.88
Bacteria	Topsoil	2022	g__Microvirga sp ASV957	High	5.59	0.03	64.38
Bacteria	Topsoil	2022	g__mle1-7 sp ASV1354	Low	4.89	0.03	78.75
Bacteria	Phyllosphere	2022	g__mle1-7 sp ASV1354	Low	5.62	0.00	15.63
Bacteria	Phyllosphere	2022	g__MND1 sp ASV1230	Low	9.88	0.00	8.75
Bacteria	Topsoil	2022	g__MND1 sp ASV669	High	3.86	0.06	66.88
Bacteria	Topsoil	2022	g__Modestobacter sp ASV751	Low	4.11	0.04	33.75
Bacteria	Phyllosphere	2022	g__Modestobacter sp ASV751	Low	4.14	0.01	31.88
Fungi	Topsoil	2022	g__Mollisia sp ASV639	Low	4.65	0.06	39.62
Fungi	Topsoil	2022	g__Mortierella sp ASV203	High	6.58	0.16	52.83
Fungi	Endosphere	2022	g__Mortierella sp ASV303	High	5.61	0.00	20.00
Bacteria	Topsoil	2022	g__Mycobacterium sp ASV1358	High	7.17	0.04	41.25
Bacteria	Topsoil	2022	g__Mycobacterium sp ASV615	High	6.34	0.04	56.88
Bacteria	Topsoil	2022	g__Mycobacterium sp ASV62	High	4.09	0.13	92.50
Bacteria	Topsoil	2022	g__Nakamurella sp ASV1272	High	3.91	0.03	66.88
Bacteria	Topsoil	2023	g__Nakamurella sp ASV1272	High	3.86	0.01	79.17
Bacteria	Topsoil	2022	g__Nakamurella sp ASV1380	Low	3.81	0.01	51.25
Bacteria	Phyllosphere	2022	g__Nitrosospira sp ASV703	Low	6.57	0.00	18.13
Bacteria	Topsoil	2022	g__Nitrospira sp ASV1231	Low	5.47	0.04	73.13
Bacteria	Phyllosphere	2022	g__Nitrospira sp ASV1231	Low	5.37	0.00	19.38
Bacteria	Topsoil	2023	g__Nitrospira sp ASV1231	Low	2.8	0.05	85.42
Bacteria	Phyllosphere	2022	g__Nitrospira sp ASV1384	Low	4.78	0.01	21.88
Bacteria	Phyllosphere	2022	g__Nitrospira sp ASV167	Low	5.31	0.01	18.75
Bacteria	Topsoil	2022	g__Nitrospira sp ASV706	Low	6.17	0.04	81.88
Bacteria	Phyllosphere	2022	g__Nitrospira sp ASV706	Low	7.09	0.00	14.38
Bacteria	Phyllosphere	2022	g__Nocardioides sp ASV141	Low	3.75	0.06	59.38
Bacteria	Phyllosphere	2022	g__Nocardioides sp ASV154	Low	3.69	0.01	40.00
Bacteria	Topsoil	2022	g__Nocardioides sp ASV2350	High	4.08	0.04	76.88
Bacteria	Topsoil	2022	g__Nocardioides sp ASV282	High	4.67	0.10	94.38
Bacteria	Phyllosphere	2022	g__Nocardioides sp ASV312	Low	6.19	0.02	38.13
Bacteria	Topsoil	2023	g__Nocardioides sp ASV312	High	3.96	0.08	91.67
Bacteria	Topsoil	2022	g__Nocardioides sp ASV412	Low	4.09	0.08	81.88
Bacteria	Phyllosphere	2022	g__Nocardioides sp ASV412	Low	4.06	0.01	31.88
Bacteria	Topsoil	2022	g__Nocardioides sp ASV421	High	3.7	0.09	81.25
Bacteria	Topsoil	2022	g__Nocardioides sp ASV464	High	3.41	0.07	91.88
Bacteria	Topsoil	2022	g__Nocardioides sp ASV495	Low	3.85	0.06	81.25
Bacteria	Topsoil	2022	g__Nocardioides sp ASV507	Low	4.38	0.08	23.75
Bacteria	Phyllosphere	2022	g__Nocardioides sp ASV507	Low	5.91	0.02	20.63
Bacteria	Topsoil	2022	g__Nocardioides sp ASV540	High	4.42	0.12	80.63
Bacteria	Topsoil	2022	g__Nocardioides sp ASV679	Low	2.93	0.05	48.75
Bacteria	Topsoil	2022	g__Nocardioides sp ASV726	High	4.13	0.06	78.13
Bacteria	Phyllosphere	2022	g__Nonomuraea sp ASV840	Low	2.93	0.00	17.50
Bacteria	Topsoil	2022	g__Noviherbaspirillum sp ASV1468	Low	3.74	0.02	88.13
Bacteria	Topsoil	2022	g__Noviherbaspirillum sp ASV1935	Low	6.49	0.02	43.75
Bacteria	Topsoil	2022	g__Noviherbaspirillum sp ASV286	Low	5.97	0.10	79.38

Annexes

Bacteria	Phyllosphere	2022	g__Noviherbaspirillum sp ASV286	Low	3.4	0.13	70.63
Bacteria	Topsoil	2023	g__Noviherbaspirillum sp ASV286	Low	4.29	0.17	97.92
Bacteria	Topsoil	2022	g__Noviherbaspirillum sp ASV335	Low	4.48	0.08	86.25
Bacteria	Topsoil	2023	g__Noviherbaspirillum sp ASV335	Low	3.6	0.13	100
Bacteria	Topsoil	2022	g__Novosphingobium sp ASV415	Low	4.54	0.02	88.75
Bacteria	Phyllosphere	2022	g__Ohtaekwangia sp ASV1508	Low	4.25	0.00	11.25
Bacteria	Phyllosphere	2022	g__Ohtaekwangia sp ASV1510	Low	7.67	0.00	10.63
Bacteria	Topsoil	2022	g__OLB12 sp ASV408	High	4.7	0.11	63.75
Bacteria	Topsoil	2023	g__OLB12 sp ASV408	High	3.48	0.04	62.50
Bacteria	Phyllosphere	2022	g__Oligoflexus sp ASV1653	Low	7.1	0.01	12.50
Bacteria	Topsoil	2023	g__P3OB-42 sp ASV997	High	4.75	0.03	100
Bacteria	Topsoil	2022	g__Paenarthrobacter sp ASV249	Low	5.16	0.08	80.63
Bacteria	Topsoil	2023	g__Paenarthrobacter sp ASV249	Low	3.28	0.09	95.83
Bacteria	Topsoil	2022	g__Paenibacillus sp ASV1684	Low	4.96	0.02	80.63
Bacteria	Phyllosphere	2022	g__Paenibacillus sp ASV1684	Low	7.22	0.00	9.38
Bacteria	Phyllosphere	2022	g__Paenibacillus sp ASV1700	Low	4.51	0.00	12.50
Bacteria	Topsoil	2023	g__Paenibacillus sp ASV1700	High	3.92	0.03	100
Bacteria	Topsoil	2022	g__Paenibacillus sp ASV2837	Low	3.88	0.02	86.25
Bacteria	Topsoil	2023	g__Paenibacillus sp ASV3019	High	4.82	0.02	97.92
Bacteria	Topsoil	2022	g__Paenibacillus sp ASV766	Low	3.59	0.05	88.13
Bacteria	Phyllosphere	2022	g__Paenibacillus sp ASV766	Low	6.44	0.00	23.75
Bacteria	Topsoil	2022	g__Paenibacillus sp ASV786	Low	5.59	0.08	87.50
Bacteria	Phyllosphere	2022	g__Paenibacillus sp ASV786	Low	6.25	0.01	25.63
Bacteria	Topsoil	2023	g__Pajaroellobacter sp ASV1314	High	4.24	0.03	100
Fungi	Phyllosphere	2022	g__Papiliotrema sp ASV903	Low	3.63	0.02	54.43
Bacteria	Topsoil	2022	g__Parafilimonas sp ASV969	High	5.4	0.04	77.50
Bacteria	Topsoil	2022	g__Parviterribacter sp ASV414	Low	4.11	0.10	79.38
Bacteria	Phyllosphere	2022	g__Parviterribacter sp ASV414	Low	6.36	0.01	30.00
Bacteria	Topsoil	2022	g__Pedobacter sp ASV1146	High	5.06	0.00	41.25
Bacteria	Phyllosphere	2022	g__Pedobacter sp ASV713	High	5.21	0.06	41.88
Bacteria	Topsoil	2022	g__Pedobacter sp ASV848	Low	4.18	0.00	12.50
Bacteria	Topsoil	2022	g__Pedococcus-Phycicoccus sp ASV777	High	5.56	0.04	81.25
Bacteria	Topsoil	2022	g__Pedomicrobium sp ASV1600	High	3.36	0.03	70.63
Fungi	Topsoil	2023	g__Penicillium sp ASV193	High	4.5	0.01	54.17
Fungi	Topsoil	2022	g__Penicillium sp ASV197	High	3.26	0.24	78.62
Fungi	Topsoil	2023	g__Penicillium sp ASV197	High	3.92	0.06	83.33
Fungi	Topsoil	2023	g__Penicillium sp ASV432	High	3.38	0.04	43.75
Fungi	Topsoil	2022	g__Penicillium sp ASV685	Low	2.72	0.02	25.16
Fungi	Phyllosphere	2022	g__Pestalotiopsis sp ASV580	High	4.56	0.03	14.56
Fungi	Topsoil	2023	g__Phaeoacremonium sp ASV696	High	4.27	0.03	27.08
Fungi	Phyllosphere	2022	g__Phaeococcomyces sp ASV1109	Low	3.88	0.01	40.51
Fungi	Topsoil	2022	g__Phaeosphaeria sp ASV530	High	4.97	0.00	42.14
Bacteria	Phyllosphere	2022	g__Phenylobacterium sp ASV1092	Low	4.32	0.00	11.25
Bacteria	Phyllosphere	2022	g__Phenylobacterium sp ASV1302	Low	7.05	0.01	15.00
Bacteria	Phyllosphere	2022	g__Phenylobacterium sp ASV558	Low	3.9	0.01	35.00
Bacteria	Phyllosphere	2022	g__Phenylobacterium sp ASV745	Low	3.96	0.02	42.50

Annexes

Bacteria	Phyllosphere	2022	g__Planifilum sp ASV1463	Low	4.8	0.02	30.00
Bacteria	Phyllosphere	2022	g__Planifilum sp ASV1840	Low	4.05	0.04	34.38
Bacteria	Phyllosphere	2022	g__Plantibacter sp ASV815	High	5.55	0.07	29.38
Fungi	Topsoil	2022	g__Podosphaera sp ASV108	High	5.7	0.00	14.47
Fungi	Endosphere	2022	g__Podosphaera sp ASV108	High	4.31	0.89	6.88
Fungi	Phyllosphere	2022	g__Podosphaera sp ASV164	Low	3.24	0.00	34.18
Fungi	Phyllosphere	2022	g__Podosphaera sp ASV461	Low	3.53	0.00	18.99
Bacteria	Topsoil	2022	g__possible_genus_04 sp ASV831	High	3.2	0.03	78.75
Bacteria	Topsoil	2022	g__Pseudarthrobacter sp ASV111	Low	4.92	0.29	10.63
Bacteria	Topsoil	2022	g__Pseudarthrobacter sp ASV48	Low	4.02	1.30	88.13
Bacteria	Phyllosphere	2022	g__Pseudarthrobacter sp ASV48	Low	3.86	0.84	61.25
Bacteria	Topsoil	2022	g__Pseudarthrobacter sp ASV895	Low	3.95	0.03	15.63
Bacteria	Topsoil	2022	g__Pseudonocardia sp ASV1224	High	4.25	0.02	66.25
Bacteria	Topsoil	2023	g__Pseudonocardia sp ASV2499	Low	2.94	0.02	89.58
Bacteria	Phyllosphere	2022	g__Pseudonocardia sp ASV292	Low	3.34	0.03	57.50
Bacteria	Topsoil	2023	g__Pseudonocardia sp ASV500	Low	3.71	0.07	83.33
Bacteria	Topsoil	2023	g__Pseudonocardia sp ASV534	High	4.4	0.19	100
Bacteria	Phyllosphere	2022	g__Pseudonocardia sp ASV541	Low	6.73	0.01	30.00
Bacteria	Topsoil	2023	g__Pseudonocardia sp ASV541	High	3.92	0.06	100
Bacteria	Phyllosphere	2022	g__Pseudonocardia sp ASV550	Low	4.72	0.01	29.38
Bacteria	Topsoil	2023	g__Pseudonocardia sp ASV550	Low	4.06	0.06	45.83
Bacteria	Topsoil	2022	g__Pseudonocardia sp ASV977	Low	4.64	0.07	89.38
Bacteria	Phyllosphere	2022	g__Pseudonocardia sp ASV977	Low	4.65	0.02	49.38
Bacteria	Topsoil	2022	g__Psychrobacillus sp ASV1646	Low	4.66	0.02	85.63
Bacteria	Topsoil	2022	g__Psychroglaciecola sp ASV1274	Low	3.99	0.01	50.00
Fungi	Topsoil	2022	g__Pyrenochaetopsis sp ASV385	High	4.87	0.06	16.98
Bacteria	Phyllosphere	2022	g__Ramlibacter sp ASV521	Low	6.37	0.01	25.63
Bacteria	Topsoil	2022	g__Ramlibacter sp ASV649	High	4.6	0.06	67.50
Bacteria	Phyllosphere	2022	g__RB41 sp ASV1124	Low	6.44	0.00	11.25
Bacteria	Phyllosphere	2022	g__RB41 sp ASV1203	Low	5.6	0.01	20.63
Bacteria	Topsoil	2022	g__RB41 sp ASV1281	High	3.19	0.04	73.75
Bacteria	Phyllosphere	2022	g__RB41 sp ASV1281	Low	4.65	0.01	16.88
Bacteria	Topsoil	2022	g__RB41 sp ASV1349	Low	4.88	0.04	83.75
Bacteria	Phyllosphere	2022	g__RB41 sp ASV1349	Low	3.89	0.00	13.75
Bacteria	Topsoil	2022	g__RB41 sp ASV2200	Low	4.4	0.03	64.38
Bacteria	Phyllosphere	2022	g__RB41 sp ASV326	Low	3.86	0.03	40.63
Bacteria	Phyllosphere	2022	g__RB41 sp ASV3661	Low	7.89	0.00	10.00
Bacteria	Topsoil	2022	g__RB41 sp ASV369	Low	5.6	0.23	85.00
Bacteria	Phyllosphere	2022	g__RB41 sp ASV369	Low	4.6	0.03	35.63
Bacteria	Topsoil	2022	g__RB41 sp ASV377	Low	3.64	0.13	83.75
Bacteria	Phyllosphere	2022	g__RB41 sp ASV377	Low	5.5	0.02	33.13
Bacteria	Topsoil	2023	g__Reyranella sp ASV3224	High	3.98	0.02	97.92
Fungi	Topsoil	2023	g__Rhinocladiella sp ASV748	Low	3.2	0.01	43.75
Bacteria	Topsoil	2022	g__Rhizobacter sp ASV3011	Low	4.33	0.02	86.25
Bacteria	Phyllosphere	2022	g__Rhizobacter sp ASV3011	Low	5.07	0.01	31.25
Bacteria	Phyllosphere	2022	g__Rhizobacter sp ASV400	Low	4.48	0.03	54.38

Annexes

Bacteria	Phyllosphere	2022	g__Rickettsiella sp ASV142	High	4.61	0.50	17.50
Bacteria	Topsoil	2023	g__Roseimicrobium sp ASV1651	High	5.8	0.02	91.67
Bacteria	Phyllosphere	2022	g__Roseomonas sp ASV1790	Low	2.89	0.01	17.50
Bacteria	Topsoil	2023	g__Roseomonas sp ASV580	Low	4.19	0.01	81.25
Bacteria	Topsoil	2022	g__Rubellimicrobium sp ASV1085	Low	4.3	0.01	16.25
Bacteria	Topsoil	2022	g__Rubellimicrobium sp ASV390	Low	3.83	0.04	61.25
Bacteria	Phyllosphere	2023	g__Rubellimicrobium sp ASV826	High	4.05	0.05	42.55
Bacteria	Phyllosphere	2022	g__Rubrobacter sp ASV13	Low	4.85	0.15	58.75
Bacteria	Phyllosphere	2022	g__Rubrobacter sp ASV176	Low	5.41	0.01	23.75
Bacteria	Topsoil	2022	g__Rubrobacter sp ASV452	Low	4.6	0.07	35.63
Bacteria	Phyllosphere	2022	g__Rubrobacter sp ASV452	Low	5.65	0.02	18.75
Bacteria	Topsoil	2022	g__Rubrobacter sp ASV522	Low	4.85	0.06	16.88
Bacteria	Phyllosphere	2022	g__Rubrobacter sp ASV522	Low	4.34	0.00	13.75
Bacteria	Topsoil	2022	g__Rubrobacter sp ASV552	Low	5.34	0.05	53.13
Bacteria	Phyllosphere	2022	g__Rubrobacter sp ASV552	Low	2.86	0.01	25.63
Bacteria	Topsoil	2022	g__Rubrobacter sp ASV782	Low	3.81	0.03	30.00
Bacteria	Phyllosphere	2022	g__Rubrobacter sp ASV782	Low	5.53	0.01	19.38
Bacteria	Phyllosphere	2022	g__Rubrobacter sp ASV989	Low	6.23	0.00	14.38
Bacteria	Topsoil	2022	g__Segetibacter sp ASV1218	High	4.44	0.02	92.50
Bacteria	Phyllosphere	2022	g__Segetibacter sp ASV1865	Low	4.02	0.01	23.75
Bacteria	Topsoil	2022	g__Segetibacter sp ASV539	Low	4.65	0.02	58.13
Bacteria	Topsoil	2023	g__Segetibacter sp ASV814	Low	4.62	0.04	83.33
Bacteria	Phyllosphere	2022	g__Segetibacter sp ASV943	Low	7.11	0.00	16.25
Bacteria	Topsoil	2023	g__Segetibacter sp ASV943	Low	3.98	0.05	50.00
Bacteria	Phyllosphere	2022	g__Segetibacter sp ASV954	Low	3.82	0.00	15.63
Bacteria	Topsoil	2022	g__SH-PL14 sp ASV577	High	3.2	0.08	90.63
Bacteria	Phyllosphere	2022	g__Skermanella sp ASV1352	Low	7.59	0.01	21.88
Bacteria	Phyllosphere	2022	g__Skermanella sp ASV1963	Low	2.9	0.00	15.00
Bacteria	Phyllosphere	2022	g__Skermanella sp ASV341	Low	4.05	0.02	35.00
Bacteria	Phyllosphere	2022	g__Skermanella sp ASV444	Low	3.18	0.06	51.25
Bacteria	Phyllosphere	2022	g__Skermanella sp ASV734	Low	5.47	0.01	28.75
Bacteria	Phyllosphere	2022	g__Skermanella sp ASV980	Low	6.1	0.00	12.50
Bacteria	Topsoil	2023	g__Skermanella sp ASV980	Low	4.8	0.05	81.25
Bacteria	Topsoil	2023	g__Solirubrobacter sp ASV1114	Low	4.99	0.04	91.67
Bacteria	Phyllosphere	2022	g__Solirubrobacter sp ASV1676	Low	5.98	0.00	6.88
Bacteria	Topsoil	2022	g__Solirubrobacter sp ASV2007	High	3.8	0.03	74.38
Bacteria	Phyllosphere	2022	g__Solirubrobacter sp ASV454	Low	3.31	0.01	30.63
Bacteria	Phyllosphere	2022	g__Solirubrobacter sp ASV65	Low	4.26	0.06	62.50
Bacteria	Topsoil	2022	g__Solirubrobacter sp ASV665	Low	4.05	0.05	80.63
Bacteria	Phyllosphere	2022	g__Solirubrobacter sp ASV665	Low	4.18	0.01	29.38
Bacteria	Phyllosphere	2022	g__Solirubrobacter sp ASV903	Low	6.14	0.00	16.25
Bacteria	Topsoil	2023	g__Sphingomonas sp ASV10	Low	3.78	0.01	91.67
Bacteria	Phyllosphere	2023	g__Sphingomonas sp ASV1033	High	3.18	0.03	34.04
Bacteria	Phyllosphere	2022	g__Sphingomonas sp ASV181	Low	4.41	0.10	71.25
Bacteria	Topsoil	2022	g__Sphingomonas sp ASV1947	Low	4.24	0.02	55.00
Bacteria	Topsoil	2022	g__Sphingomonas sp ASV252	Low	5.1	0.00	31.25

Annexes

Bacteria	Topsoil	2022	g__Sphingomonas sp ASV3098	Low	4.02	0.01	36.88
Bacteria	Topsoil	2022	g__Sphingomonas sp ASV647	Low	6.89	0.06	71.25
Bacteria	Phyllosphere	2022	g__Sphingomonas sp ASV647	Low	6.05	0.00	26.25
Bacteria	Phyllosphere	2022	g__Sphingomonas sp ASV847	Low	3.01	0.09	29.38
Bacteria	Topsoil	2022	g__Sphingomonas sp ASV99	Low	3.69	0.01	61.88
Bacteria	Topsoil	2022	g__Spirosoma sp ASV892	High	4.32	0.00	34.38
Fungi	Topsoil	2022	g__Stagonosporopsis sp ASV139	Low	3.43	0.10	38.99
Fungi	Phyllosphere	2022	g__Stagonosporopsis sp ASV139	Low	4.38	0.04	24.05
Bacteria	Phyllosphere	2022	g__Staphylococcus sp ASV1340	Low	3.59	0.05	37.50
Bacteria	Topsoil	2022	g__Streptomyces sp ASV194	Low	4.58	0.16	88.13
Bacteria	Phyllosphere	2022	g__Streptomyces sp ASV536	Low	4.7	0.01	36.25
Bacteria	Topsoil	2022	g__Streptomyces sp ASV674	Low	7.64	0.05	70.00
Bacteria	Phyllosphere	2022	g__Streptomyces sp ASV729	Low	3.99	0.01	23.13
Bacteria	Phyllosphere	2022	g__Subgroup_10 sp ASV1237	Low	4.48	0.00	7.50
Bacteria	Topsoil	2022	g__Subgroup_10 sp ASV1273	High	2.36	0.03	63.13
Bacteria	Topsoil	2023	g__Subgroup_10 sp ASV1386	Low	3.06	0.05	100
Bacteria	Topsoil	2022	g__Subgroup_10 sp ASV881	High	5.22	0.04	71.25
Fungi	Topsoil	2022	g__Talaromyces sp ASV281	Low	4.18	0.10	64.78
Fungi	Topsoil	2022	g__Talaromyces sp ASV93	Low	3.9	0.04	48.43
Bacteria	Phyllosphere	2022	g__Terrimonas sp ASV1059	Low	6.98	0.00	13.75
Bacteria	Topsoil	2022	g__Terrimonas sp ASV1344	High	6.8	0.07	91.25
Bacteria	Topsoil	2022	g__Terrimonas sp ASV829	High	4.32	0.06	94.38
Bacteria	Phyllosphere	2022	g__Terrimonas sp ASV829	Low	2.88	0.01	23.75
Fungi	Endosphere	2022	g__Tetracladium sp ASV41	Low	4.84	0.01	42.50
Fungi	Topsoil	2023	g__Tetracladium sp ASV519	Low	4.16	0.04	31.25
Bacteria	Topsoil	2022	g__TM7a sp ASV473	High	4.84	0.09	52.50
Bacteria	Topsoil	2023	g__TM7a sp ASV717	Low	4.92	0.04	97.92
Bacteria	Topsoil	2022	g__Truepera sp ASV1188	Low	4.75	0.03	33.13
Bacteria	Topsoil	2022	g__Truepera sp ASV120	Low	3.74	0.03	60.00
Bacteria	Topsoil	2022	g__Truepera sp ASV837	Low	3.34	0.03	20.00
Bacteria	Topsoil	2022	g__Turicibacter sp ASV1260	High	3.57	0.00	12.50
Fungi	Topsoil	2022	g__Valsonectria sp ASV306	High	2.92	0.07	40.88
Fungi	Topsoil	2022	g__Valsonectria sp ASV690	High	5.66	0.03	55.35
Fungi	Phyllosphere	2022	g__Vishniacozyma sp ASV133	High	4.73	0.18	72.15
Fungi	Topsoil	2022	g__Vishniacozyma sp ASV212	High	5.23	0.00	24.53
Bacteria	Phyllosphere	2022	g__YC-ZSS-LKJ147 sp ASV2024	Low	2.83	0.00	11.88
Bacteria	Topsoil	2022	f__67-14 sp ASV1152	High	4.68	0.00	23.75
Bacteria	Phyllosphere	2022	f__67-14 sp ASV1389	Low	3.43	0.00	6.88
Bacteria	Phyllosphere	2022	f__67-14 sp ASV163	Low	3.46	0.00	20.63
Bacteria	Topsoil	2022	f__67-14 sp ASV2464	Low	3.31	0.01	58.13
Bacteria	Topsoil	2022	f__67-14 sp ASV276	Low	3.84	0.14	65.63
Bacteria	Phyllosphere	2022	f__67-14 sp ASV276	Low	6.48	0.02	29.38
Bacteria	Phyllosphere	2022	f__67-14 sp ASV393	Low	3.85	0.01	26.25
Bacteria	Topsoil	2022	f__67-14 sp ASV483	Low	3.36	0.08	33.13
Bacteria	Phyllosphere	2022	f__67-14 sp ASV483	Low	4.53	0.01	12.50
Bacteria	Phyllosphere	2022	f__67-14 sp ASV542	Low	3.18	0.01	35.63

Annexes

Bacteria	Phyllosphere	2022	f__67-14 sp ASV560	Low	4.33	0.01	28.13
Bacteria	Topsoil	2022	f__67-14 sp ASV623	High	5.31	0.05	73.13
Bacteria	Phyllosphere	2022	f__67-14 sp ASV753	Low	3.67	0.01	21.25
Bacteria	Phyllosphere	2022	f__67-14 sp ASV92	Low	4.95	0.04	45.63
Bacteria	Topsoil	2022	f__A21b sp ASV833	High	3.66	0.05	70.00
Bacteria	Topsoil	2022	f__Acetobacteraceae sp ASV1223	Low	4.6	0.01	70.00
Bacteria	Phyllosphere	2022	f__Acetobacteraceae sp ASV1413	High	3.36	0.00	6.88
Bacteria	Phyllosphere	2022	f__Acetobacteraceae sp ASV876	Low	4.31	0.07	9.38
Bacteria	Topsoil	2022	f__AKIW781 sp ASV1467	High	5.57	0.01	41.25
Bacteria	Topsoil	2022	f__AKYG1722 sp ASV1414	Low	3.53	0.02	64.38
Bacteria	Phyllosphere	2022	f__AKYG1722 sp ASV1414	Low	5.96	0.01	23.75
Bacteria	Topsoil	2022	f__AKYH767 sp ASV906	High	3.4	0.04	85.63
Bacteria	Topsoil	2022	f__AKYH767 sp ASV949	High	5.41	0.05	85.63
Fungi	Phyllosphere	2022	f__Amphisphaeriaceae sp ASV27	Low	5.08	0.03	67.09
Fungi	Topsoil	2022	f__Ascobolaceae sp ASV944	Low	5.22	0.02	10.06
Bacteria	Topsoil	2022	f__Beijerinckiaceae sp ASV579	Low	3.51	0.06	71.88
Bacteria	Phyllosphere	2022	f__Beijerinckiaceae sp ASV579	Low	6.4	0.00	22.50
Bacteria	Topsoil	2023	f__Beijerinckiaceae sp ASV579	Low	4.22	0.06	91.67
Bacteria	Phyllosphere	2022	f__Beijerinckiaceae sp ASV610	Low	7.23	0.01	30.00
Bacteria	Topsoil	2023	f__Beijerinckiaceae sp ASV610	Low	4.42	0.07	93.75
Bacteria	Phyllosphere	2022	f__BIrii41 sp ASV1007	High	6.51	0.00	8.13
Fungi	Topsoil	2022	f__Chaetomiaceae sp ASV97	High	3.98	0.22	49.69
Fungi	Topsoil	2023	f__Chaetomiaceae sp ASV97	Low	3.36	1.36	89.58
Bacteria	Phyllosphere	2022	f__Chitinophagaceae sp ASV1100	Low	4.94	0.01	23.13
Bacteria	Topsoil	2022	f__Chitinophagaceae sp ASV1364	High	5.24	0.03	80.63
Bacteria	Topsoil	2023	f__Chitinophagaceae sp ASV1364	High	3.92	0.01	89.58
Bacteria	Topsoil	2022	f__Chitinophagaceae sp ASV161	High	4.7	0.32	73.75
Bacteria	Phyllosphere	2022	f__Chitinophagaceae sp ASV161	Low	4.28	0.00	13.75
Bacteria	Phyllosphere	2022	f__Chitinophagaceae sp ASV1635	Low	4.09	0.01	33.75
Bacteria	Topsoil	2023	f__Chitinophagaceae sp ASV1635	Low	3.88	0.04	95.83
Bacteria	Topsoil	2022	f__Chitinophagaceae sp ASV1655	High	3.62	0.01	78.13
Bacteria	Topsoil	2023	f__Chitinophagaceae sp ASV598	Low	4.24	0.08	100
Bacteria	Topsoil	2022	f__Chitinophagaceae sp ASV625	High	3.28	0.05	83.75
Bacteria	Phyllosphere	2022	f__Chitinophagaceae sp ASV638	Low	4.69	0.01	23.75
Bacteria	Phyllosphere	2022	f__Chitinophagaceae sp ASV670	Low	6.8	0.01	35.00
Bacteria	Topsoil	2022	f__Comamonadaceae sp ASV1029	High	4.33	0.05	91.25
Bacteria	Topsoil	2023	f__Comamonadaceae sp ASV130	Low	3.72	0.00	52.08
Bacteria	Topsoil	2022	f__Comamonadaceae sp ASV351	High	3.28	0.12	91.88
Bacteria	Phyllosphere	2022	f__Comamonadaceae sp ASV411	Low	6.07	0.01	39.38
Bacteria	Topsoil	2022	f__Entotheonellaceae sp ASV1543	High	3.49	0.01	21.25
Bacteria	Topsoil	2022	f__env.OPS_17 sp ASV1910	High	5.86	0.02	86.25
Bacteria	Topsoil	2022	f__env.OPS_17 sp ASV2155	High	6.91	0.03	81.25
Bacteria	Topsoil	2022	f__Gemmatimonadaceae sp ASV1032	Low	3.85	0.03	64.38
Bacteria	Topsoil	2022	f__Gemmatimonadaceae sp ASV1041	Low	4.2	0.03	80.00
Bacteria	Phyllosphere	2022	f__Gemmatimonadaceae sp ASV1121	Low	8.35	0.00	16.25
Bacteria	Topsoil	2022	f__Gemmatimonadaceae sp ASV1144	Low	5.2	0.04	13.13

Annexes

Bacteria	Topsoil	2022	f__Gemmatimonadaceae sp ASV127	Low	3.73	0.30	90.63
Bacteria	Phyllosphere	2022	f__Gemmatimonadaceae sp ASV127	Low	3.79	0.03	58.75
Bacteria	Topsoil	2022	f__Gemmatimonadaceae sp ASV1374	Low	3.49	0.04	69.38
Bacteria	Topsoil	2023	f__Gemmatimonadaceae sp ASV1375	Low	4.27	0.02	85.42
Bacteria	Topsoil	2022	f__Gemmatimonadaceae sp ASV1955	Low	3.95	0.04	24.38
Bacteria	Phyllosphere	2022	f__Gemmatimonadaceae sp ASV1955	Low	3.25	0.00	9.38
Bacteria	Phyllosphere	2022	f__Gemmatimonadaceae sp ASV2092	Low	3	0.00	6.88
Bacteria	Phyllosphere	2022	f__Gemmatimonadaceae sp ASV215	Low	4.04	0.01	34.38
Bacteria	Topsoil	2022	f__Gemmatimonadaceae sp ASV245	Low	4.75	0.13	89.38
Bacteria	Topsoil	2022	f__Gemmatimonadaceae sp ASV508	Low	4.5	0.10	11.25
Bacteria	Phyllosphere	2022	f__Gemmatimonadaceae sp ASV508	Low	3.25	0.00	8.13
Bacteria	Topsoil	2022	f__Gemmatimonadaceae sp ASV571	Low	4.03	0.09	13.13
Bacteria	Phyllosphere	2022	f__Gemmatimonadaceae sp ASV571	Low	6.55	0.00	9.38
Bacteria	Phyllosphere	2022	f__Gemmatimonadaceae sp ASV785	Low	5.76	0.01	25.63
Bacteria	Topsoil	2022	f__Gemmatimonadaceae sp ASV912	Low	3.31	0.06	75.00
Bacteria	Phyllosphere	2022	f__Gemmatimonadaceae sp ASV988	Low	6.1	0.01	25.63
Bacteria	Topsoil	2022	f__Geodermatophilaceae sp ASV72	Low	5.7	0.40	87.50
Bacteria	Topsoil	2022	f__Geodermatophilaceae sp ASV983	Low	4.45	0.02	76.25
Bacteria	Phyllosphere	2023	f__Geodermatophilaceae sp ASV983	Low	4.88	0.01	14.89
Bacteria	Topsoil	2022	f__Geodermatophilaceae sp ASV987	Low	5.26	0.03	90.63
Fungi	Phyllosphere	2022	f__Gnomoniaceae sp ASV674	Low	3.75	0.00	12.66
Fungi	Endosphere	2022	f__Gnomoniaceae sp ASV674	High	5.11	0.11	10.63
Fungi	Topsoil	2022	f__Herpotrichiellaceae sp ASV353	High	3.52	0.08	33.33
Fungi	Topsoil	2022	f__Hypocreales_fam_Incertae_sedis sp ASV542	High	3.83	0.01	52.83
Bacteria	Phyllosphere	2022	f__Intrasporangiaceae sp ASV162	Low	3.32	0.04	57.50
Bacteria	Topsoil	2023	f__Intrasporangiaceae sp ASV232	High	5.53	0.10	62.50
Bacteria	Topsoil	2022	f__Intrasporangiaceae sp ASV263	High	4.99	0.17	71.88
Bacteria	Topsoil	2022	f__Intrasporangiaceae sp ASV275	High	3.97	0.23	88.13
Bacteria	Topsoil	2022	f__Intrasporangiaceae sp ASV494	Low	3.75	0.06	73.13
Bacteria	Phyllosphere	2022	f__Isosphaeraceae sp ASV1291	Low	3.8	0.02	38.13
Bacteria	Phyllosphere	2022	f__Isosphaeraceae sp ASV4451	Low	3.21	0.00	18.13
Bacteria	Topsoil	2022	f__JG30-KF-CM45 sp ASV1025	Low	5.45	0.08	17.50
Bacteria	Phyllosphere	2022	f__JG30-KF-CM45 sp ASV1025	Low	6.62	0.01	18.13
Bacteria	Topsoil	2022	f__JG30-KF-CM45 sp ASV1125	Low	3.2	0.07	44.38
Bacteria	Phyllosphere	2022	f__JG30-KF-CM45 sp ASV1125	Low	3.96	0.01	26.25
Bacteria	Phyllosphere	2023	f__JG30-KF-CM45 sp ASV1125	Low	5.23	0.02	17.02
Bacteria	Topsoil	2022	f__JG30-KF-CM45 sp ASV1440	Low	5.73	0.04	15.00
Bacteria	Phyllosphere	2022	f__JG30-KF-CM45 sp ASV1440	Low	5.96	0.00	10.63
Bacteria	Topsoil	2022	f__JG30-KF-CM45 sp ASV1656	Low	3.51	0.03	30.63
Bacteria	Phyllosphere	2022	f__JG30-KF-CM45 sp ASV3702	Low	5.29	0.01	20.00
Bacteria	Phyllosphere	2022	f__JG30-KF-CM45 sp ASV429	Low	5.87	0.01	25.63
Bacteria	Phyllosphere	2022	f__JG30-KF-CM45 sp ASV60	Low	3.9	0.11	56.25
Bacteria	Topsoil	2022	f__JG30-KF-CM45 sp ASV714	Low	4.35	0.09	21.25
Bacteria	Phyllosphere	2022	f__JG30-KF-CM45 sp ASV714	Low	5.3	0.02	19.38
Bacteria	Topsoil	2022	f__JG30-KF-CM45 sp ASV813	Low	5.42	0.07	88.75
Bacteria	Topsoil	2023	f__JG30-KF-CM45 sp ASV813	Low	3.38	0.06	97.92

Annexes

Bacteria	Topsoil	2022	f__JG30-KF-CM45 sp ASV816	High	3.55	0.07	60.00
Bacteria	Topsoil	2023	f__JG30-KF-CM45 sp ASV960	Low	3.8	0.08	70.83
Bacteria	Phyllosphere	2022	f__Kineosporiaceae sp ASV482	High	2.97	0.08	51.25
Fungi	Topsoil	2022	f__Lasiosphaeriaceae sp ASV374	High	3.51	0.03	62.26
Bacteria	Phyllosphere	2022	f__Longimicrobiaceae sp ASV1400	Low	6.42	0.00	22.50
Fungi	Topsoil	2022	f__Magnaporthaceae sp ASV460	High	3.4	0.04	44.03
Bacteria	Topsoil	2022	f__Microbacteriaceae sp ASV775	Low	3.53	0.06	90.63
Bacteria	Phyllosphere	2022	f__Micrococcaceae sp ASV1075	High	4.8	0.01	15.63
Bacteria	Topsoil	2022	f__Micrococcaceae sp ASV1212	Low	3.75	0.02	18.13
Bacteria	Topsoil	2022	f__Micrococcaceae sp ASV356	Low	5.04	0.04	42.50
Bacteria	Topsoil	2023	f__Micrococcaceae sp ASV356	Low	4.53	0.11	52.08
Bacteria	Phyllosphere	2023	f__Micrococcaceae sp ASV61	Low	3.82	0.32	93.62
Bacteria	Topsoil	2023	f__Micromonosporaceae sp ASV855	High	3.34	0.01	93.75
Bacteria	Topsoil	2022	f__Microscillaceae sp ASV1049	High	3.44	0.05	38.75
Bacteria	Topsoil	2023	f__Microscillaceae sp ASV1049	High	4.57	0.01	35.42
Bacteria	Topsoil	2023	f__Microscillaceae sp ASV423	High	3.24	0.04	60.42
Bacteria	Topsoil	2023	f__Microscillaceae sp ASV666	High	3.09	0.08	91.67
Bacteria	Topsoil	2022	f__Microscillaceae sp ASV807	High	5.05	0.12	68.13
Bacteria	Topsoil	2023	f__Microscillaceae sp ASV807	High	4.89	0.11	87.50
Fungi	Topsoil	2022	f__Mycosphaerellaceae sp ASV293	High	4.89	0.03	33.33
Fungi	Phyllosphere	2022	f__Mycosphaerellaceae sp ASV293	High	5.83	0.09	53.80
Fungi	Topsoil	2022	f__Mycosphaerellaceae sp ASV595	High	3.35	0.01	20.13
Bacteria	Topsoil	2022	f__Myxococcaceae sp ASV1084	Low	3.48	0.04	84.38
Bacteria	Phyllosphere	2022	f__Myxococcaceae sp ASV1084	Low	9.55	0.00	11.88
Bacteria	Phyllosphere	2022	f__Myxococcaceae sp ASV1371	Low	4.31	0.00	11.25
Fungi	Topsoil	2022	f__Nectriaceae sp ASV1029	High	5.25	0.02	56.60
Fungi	Endosphere	2022	f__Nectriaceae sp ASV271	High	4.12	0.00	12.50
Fungi	Topsoil	2022	f__Nectriaceae sp ASV35	High	4.33	2.03	53.46
Fungi	Topsoil	2022	f__Nectriaceae sp ASV830	High	5.11	0.03	55.97
Bacteria	Topsoil	2022	f__Nitrosomonadaceae sp ASV569	Low	3.71	0.07	40.63
Bacteria	Phyllosphere	2022	f__Nitrosomonadaceae sp ASV569	Low	7.03	0.00	7.50
Bacteria	Topsoil	2023	f__Nocardiaceae sp ASV460	Low	2.96	0.05	95.83
Bacteria	Topsoil	2022	f__Nocardioidaceae sp ASV1263	Low	3.34	0.02	47.50
Bacteria	Phyllosphere	2022	f__Nocardioidaceae sp ASV1263	Low	7.8	0.00	9.38
Bacteria	Phyllosphere	2022	f__Nocardioidaceae sp ASV214	Low	3.1	0.02	43.75
Fungi	Topsoil	2022	f__Olpidiaceae sp ASV564	High	3.94	0.06	45.91
Bacteria	Phyllosphere	2022	f__Oxalobacteraceae sp ASV1078	Low	3.33	0.03	38.75
Bacteria	Topsoil	2022	f__Oxalobacteraceae sp ASV1227	Low	4.88	0.04	85.63
Bacteria	Phyllosphere	2022	f__Oxalobacteraceae sp ASV1227	Low	3.7	0.03	38.75
Bacteria	Topsoil	2022	f__Oxalobacteraceae sp ASV1306	Low	4.59	0.01	38.13
Bacteria	Phyllosphere	2022	f__Oxalobacteraceae sp ASV1306	Low	3.62	0.00	11.25
Bacteria	Phyllosphere	2022	f__Oxalobacteraceae sp ASV1432	Low	2.77	0.04	52.50
Bacteria	Topsoil	2023	f__Oxalobacteraceae sp ASV1487	Low	4.19	0.04	89.58
Bacteria	Phyllosphere	2023	f__Oxalobacteraceae sp ASV365	Low	2.98	0.09	40.43
Bacteria	Topsoil	2023	f__Oxalobacteraceae sp ASV491	Low	3.77	0.03	95.83
Bacteria	Topsoil	2022	f__Oxalobacteraceae sp ASV800	Low	4.26	0.04	24.38

Annexes

Bacteria	Phyllosphere	2022	f__Oxalobacteraceae sp ASV800	Low	5.11	0.01	21.25
Bacteria	Topsoil	2023	f__Oxalobacteraceae sp ASV877	Low	3.41	0.06	72.92
Bacteria	Topsoil	2022	f__Pedosphaeraceae sp ASV1150	High	3.26	0.04	72.50
Bacteria	Topsoil	2022	f__Pedosphaeraceae sp ASV1186	High	3.69	0.06	71.25
Bacteria	Phyllosphere	2022	f__Pedosphaeraceae sp ASV1186	Low	6.01	0.00	6.25
Bacteria	Phyllosphere	2022	f__Pedosphaeraceae sp ASV1387	Low	7.06	0.00	8.13
Bacteria	Topsoil	2023	f__Peptostreptococcaceae sp ASV1015	High	4.3	0.03	70.83
Bacteria	Topsoil	2023	f__Peptostreptococcaceae sp ASV1752	High	5.16	0.04	97.92
Fungi	Topsoil	2023	f__Pezizaceae sp ASV233	Low	2.79	0.42	79.17
Fungi	Phyllosphere	2022	f__Phaeomoniellaceae sp ASV493	Low	9.05	0.00	5.06
Fungi	Phyllosphere	2022	f__Phaeosphaeriaceae sp ASV457	Low	3.67	0.05	80.38
Fungi	Topsoil	2022	f__Phaeosphaeriaceae sp ASV517	Low	3.23	0.05	50.31
Fungi	Phyllosphere	2022	f__Phaeosphaeriaceae sp ASV517	Low	5.26	0.00	25.95
Fungi	Phyllosphere	2023	f__Phaeosphaeriaceae sp ASV665	Low	3.05	0.11	46.81
Fungi	Topsoil	2022	f__Phaeosphaeriaceae sp ASV817	High	3.59	0.02	49.06
Fungi	Phyllosphere	2022	f__Pseudeurotiaceae sp ASV831	High	7.36	0.03	30.38
Bacteria	Phyllosphere	2022	f__Rhizobiales_Incertae_Sedis sp ASV1908	Low	5.91	0.00	16.88
Bacteria	Topsoil	2023	f__Roseiflexaceae sp ASV1194	Low	4.79	0.06	43.75
Bacteria	Phyllosphere	2022	f__Roseiflexaceae sp ASV1409	Low	5.85	0.01	10.00
Bacteria	Phyllosphere	2022	f__Roseiflexaceae sp ASV182	Low	5.78	0.08	38.13
Bacteria	Topsoil	2022	f__Roseiflexaceae sp ASV2179	High	3.3	0.02	46.25
Bacteria	Phyllosphere	2022	f__Roseiflexaceae sp ASV227	Low	2.9	0.04	26.25
Bacteria	Topsoil	2022	f__Roseiflexaceae sp ASV2551	Low	5.03	0.04	76.88
Bacteria	Phyllosphere	2022	f__Roseiflexaceae sp ASV2551	Low	7.19	0.01	10.00
Bacteria	Topsoil	2022	f__Roseiflexaceae sp ASV347	Low	3.67	0.12	56.25
Bacteria	Phyllosphere	2022	f__Roseiflexaceae sp ASV347	Low	4.26	0.01	20.63
Bacteria	Phyllosphere	2022	f__Roseiflexaceae sp ASV385	Low	4.14	0.01	25.00
Bacteria	Phyllosphere	2022	f__Roseiflexaceae sp ASV427	Low	6.87	0.01	21.25
Bacteria	Topsoil	2022	f__Roseiflexaceae sp ASV451	High	3.87	0.10	43.13
Bacteria	Topsoil	2022	f__Roseiflexaceae sp ASV505	Low	5.53	0.01	37.50
Bacteria	Topsoil	2022	f__Roseiflexaceae sp ASV527	Low	3.17	0.08	20.63
Bacteria	Phyllosphere	2022	f__Roseiflexaceae sp ASV527	Low	5.26	0.01	7.50
Bacteria	Topsoil	2023	f__Roseiflexaceae sp ASV547	Low	4.8	0.06	54.17
Bacteria	Topsoil	2022	f__Roseiflexaceae sp ASV561	Low	4.51	0.07	70.63
Bacteria	Phyllosphere	2022	f__Roseiflexaceae sp ASV561	Low	6.05	0.01	15.63
Bacteria	Topsoil	2023	f__Roseiflexaceae sp ASV735	Low	3.62	0.06	93.75
Bacteria	Topsoil	2023	f__Roseiflexaceae sp ASV760	Low	4.7	0.05	91.67
Bacteria	Topsoil	2022	f__Roseiflexaceae sp ASV811	Low	5.28	0.04	66.25
Bacteria	Phyllosphere	2022	f__Roseiflexaceae sp ASV851	Low	4.63	0.01	17.50
Bacteria	Topsoil	2022	f__Roseiflexaceae sp ASV858	Low	3.07	0.02	30.63
Bacteria	Phyllosphere	2022	f__Roseiflexaceae sp ASV858	Low	4.16	0.00	8.75
Bacteria	Topsoil	2022	f__Roseiflexaceae sp ASV879	Low	4.13	0.04	71.25
Bacteria	Topsoil	2022	f__Roseiflexaceae sp ASV985	Low	4.76	0.07	63.13
Bacteria	Topsoil	2022	f__Roseiflexaceae sp ASV994	High	4.17	0.05	28.13
Bacteria	Topsoil	2023	f__Roseiflexaceae sp ASV994	High	3.71	0.00	20.83
Bacteria	Topsoil	2023	f__Sandaracinaceae sp ASV803	High	4.82	0.04	97.92

Annexes

Bacteria	Phyllosphere	2023	f__Sandaracinaceae sp ASV803	High	4.27	0.01	17.02
Bacteria	Topsoil	2022	f__SC-I-84 sp ASV1036	High	4.9	0.04	89.38
Bacteria	Topsoil	2022	f__SC-I-84 sp ASV319	High	4.93	0.15	80.63
Bacteria	Phyllosphere	2022	f__SC-I-84 sp ASV838	Low	3.99	0.00	15.63
Bacteria	Topsoil	2022	f__Solirubrobacteraceae sp ASV1062	Low	3.61	0.02	81.88
Bacteria	Phyllosphere	2022	f__Solirubrobacteraceae sp ASV1424	Low	4.51	0.01	16.88
Bacteria	Topsoil	2022	f__Solirubrobacteraceae sp ASV695	Low	3.12	0.04	85.63
Bacteria	Phyllosphere	2022	f__Solirubrobacteraceae sp ASV810	Low	4.66	0.01	33.13
Bacteria	Phyllosphere	2022	f__Sphingomonadaceae sp ASV1243	Low	4.99	0.00	6.25
Bacteria	Topsoil	2022	f__Sphingomonadaceae sp ASV1270	High	4.54	0.04	86.25
Bacteria	Phyllosphere	2022	f__Sphingomonadaceae sp ASV2277	Low	3.77	0.00	12.50
Bacteria	Phyllosphere	2022	f__Steroidobacteraceae sp ASV1072	Low	8.07	0.00	13.13
Bacteria	Phyllosphere	2022	f__Steroidobacteraceae sp ASV1318	Low	7.82	0.00	18.13
Fungi	Topsoil	2022	f__Tetraplosphaeriaceae sp ASV747	High	9.64	0.02	50.94
Fungi	Topsoil	2023	f__Tetraplosphaeriaceae sp ASV747	High	4.25	0.01	35.42
Fungi	Topsoil	2022	f__Thyridariaceae sp ASV123	High	3.96	0.26	75.47
Fungi	Topsoil	2023	f__Thyridariaceae sp ASV123	High	4.31	0.29	89.58
Fungi	Topsoil	2022	f__Thyridariaceae sp ASV246	High	3.63	0.09	44.03
Fungi	Phyllosphere	2022	f__Thyridariaceae sp ASV246	High	6.34	0.00	23.42
Bacteria	Phyllosphere	2022	f__TRA3-20 sp ASV1101	Low	6.35	0.01	14.38
Bacteria	Topsoil	2023	f__TRA3-20 sp ASV1670	High	3.69	0.01	79.17
Bacteria	Phyllosphere	2022	f__TRA3-20 sp ASV246	Low	5.32	0.01	42.50
Fungi	Topsoil	2022	f__Trichosporonaceae sp ASV528	High	3.77	0.03	26.42
Fungi	Topsoil	2022	f__Venturiaceae sp ASV415	Low	5.28	0.05	47.80
Bacteria	Topsoil	2022	f__Verrucomicrobiaceae sp ASV853	High	3.8	0.05	80.00
Bacteria	Topsoil	2023	f__Verrucomicrobiaceae sp ASV853	High	3.95	0.05	95.83
Bacteria	Phyllosphere	2023	f__Xanthobacteraceae sp ASV109	High	6.16	0.04	53.19
Bacteria	Phyllosphere	2022	f__Xanthobacteraceae sp ASV1168	Low	3.84	0.00	4.38
Bacteria	Topsoil	2022	f__Xanthobacteraceae sp ASV1615	High	3.57	0.03	80.63
Bacteria	Topsoil	2022	f__Xanthobacteraceae sp ASV2333	High	3.71	0.03	40.00
Bacteria	Topsoil	2022	f__Xanthomonadaceae sp ASV778	High	5.54	0.07	80.63
Bacteria	Topsoil	2022	f__Xanthomonadaceae sp ASV891	High	3.99	0.04	70.63
Bacteria	Topsoil	2022	o__0319-6G20 sp ASV4311	Low	4.99	0.02	85.63
Bacteria	Topsoil	2022	o__Actinomarinales sp ASV743	Low	5.03	0.06	31.88
Bacteria	Phyllosphere	2022	o__Actinomarinales sp ASV743	Low	10.62	0.00	11.88
Bacteria	Topsoil	2022	o__C0119 sp ASV199	High	6.27	0.19	63.75
Fungi	Topsoil	2022	o__Capnodiales sp ASV678	High	5.44	0.03	17.61
Fungi	Topsoil	2022	o__Chaetothyriales sp ASV1013	High	5.21	0.01	17.61
Fungi	Topsoil	2022	o__Chaetothyriales sp ASV441	High	4.04	0.02	26.42
Fungi	Topsoil	2022	o__Chaetothyriales sp ASV99	Low	5.89	0.34	11.32
Fungi	Phyllosphere	2022	o__Chaetothyriales sp ASV99	Low	3.75	0.00	10.13
Fungi	Topsoil	2022	o__Coniochaetales sp ASV371	High	3.72	0.06	40.25
Fungi	Topsoil	2023	o__Coniochaetales sp ASV371	High	4.64	0.03	37.50
Bacteria	Topsoil	2022	o__Elsterales sp ASV313	Low	5.19	0.13	90.00
Bacteria	Phyllosphere	2022	o__Elsterales sp ASV313	Low	3.66	0.02	39.38
Bacteria	Topsoil	2023	o__Frankiales sp ASV738	Low	4.75	0.02	83.33

Annexes

Bacteria	Topsoil	2022	o__Gaiellales sp ASV1265	Low	3.82	0.04	16.25
Bacteria	Topsoil	2023	o__Gaiellales sp ASV1417	High	5.13	0.01	56.25
Bacteria	Topsoil	2022	o__Gaiellales sp ASV1566	High	4.77	0.02	51.88
Bacteria	Topsoil	2022	o__Gaiellales sp ASV1662	Low	4.15	0.09	29.38
Bacteria	Topsoil	2022	o__Gaiellales sp ASV2298	Low	6.87	0.03	84.38
Bacteria	Topsoil	2022	o__Gaiellales sp ASV304	High	4.3	0.13	26.25
Bacteria	Topsoil	2022	o__Gaiellales sp ASV475	High	4.36	0.04	30.00
Bacteria	Topsoil	2022	o__Gaiellales sp ASV516	High	3.58	0.05	31.25
Bacteria	Phyllosphere	2022	o__Gaiellales sp ASV705	High	3.03	0.00	8.75
Bacteria	Topsoil	2023	o__Gaiellales sp ASV866	Low	3.87	0.04	83.33
Bacteria	Topsoil	2022	o__Gaiellales sp ASV934	High	6.1	0.01	21.25
Fungi	Endosphere	2022	o__Helotiales sp ASV116	Low	5.81	0.00	11.88
Fungi	Topsoil	2022	o__Helotiales sp ASV325	Low	2.63	0.08	50.31
Fungi	Topsoil	2022	o__Helotiales sp ASV591	High	4.17	0.04	61.64
Fungi	Topsoil	2022	o__Hypocreales sp ASV465	High	8.56	0.01	23.27
Bacteria	Topsoil	2022	o__IMCC26256 sp ASV309	Low	4.78	0.08	87.50
Bacteria	Phyllosphere	2022	o__IMCC26256 sp ASV309	Low	3.68	0.00	10.63
Bacteria	Topsoil	2022	o__IMCC26256 sp ASV802	High	5.9	0.01	49.38
Bacteria	Topsoil	2022	o__Microtrichales sp ASV1297	High	3.79	0.04	45.63
Bacteria	Topsoil	2022	o__Microtrichales sp ASV328	Low	3.41	0.11	81.88
Bacteria	Phyllosphere	2022	o__Microtrichales sp ASV328	Low	3.91	0.01	33.13
Bacteria	Phyllosphere	2022	o__Microtrichales sp ASV904	Low	4.87	0.00	13.13
Fungi	Topsoil	2022	o__Monoblepharidales sp ASV799	High	3.98	0.02	70.44
Fungi	Topsoil	2023	o__Pleosporales sp ASV119	High	3.99	0.00	52.08
Fungi	Topsoil	2022	o__Pleosporales sp ASV142	High	4.31	0.21	70.44
Fungi	Phyllosphere	2022	o__Pleosporales sp ASV184	High	3.71	0.00	18.99
Fungi	Topsoil	2022	o__Pleosporales sp ASV195	High	6.26	0.05	68.55
Fungi	Topsoil	2023	o__Pleosporales sp ASV195	High	3.64	0.45	62.50
Fungi	Topsoil	2022	o__Pleosporales sp ASV236	High	7.26	0.10	81.13
Fungi	Phyllosphere	2022	o__Pleosporales sp ASV274	High	4.38	0.03	58.23
Fungi	Endosphere	2022	o__Pleosporales sp ASV274	High	5.17	0.12	5.63
Fungi	Topsoil	2023	o__Pleosporales sp ASV287	High	4.55	0.05	77.08
Fungi	Phyllosphere	2022	o__Pleosporales sp ASV343	High	3.29	0.00	32.91
Fungi	Topsoil	2023	o__Pleosporales sp ASV343	High	3.2	0.06	77.08
Fungi	Topsoil	2022	o__Pleosporales sp ASV427	Low	4.67	0.04	47.17
Fungi	Topsoil	2023	o__Pleosporales sp ASV427	Low	5.67	0.06	81.25
Fungi	Topsoil	2022	o__Pleosporales sp ASV516	Low	4.11	0.03	35.85
Fungi	Topsoil	2022	o__Pleosporales sp ASV655	Low	3.1	0.03	32.70
Bacteria	Topsoil	2022	o__PLTA13 sp ASV265	Low	3.62	0.19	32.50
Bacteria	Phyllosphere	2022	o__PLTA13 sp ASV265	Low	3.11	0.00	15.00
Bacteria	Phyllosphere	2022	o__PLTA13 sp ASV458	Low	3.99	0.01	13.13
Fungi	Topsoil	2022	o__Rhizophlyctidales sp ASV963	High	3.62	0.03	54.09
Fungi	Topsoil	2022	o__Rhizophydiales sp ASV578	Low	2.97	0.04	55.35
Bacteria	Topsoil	2022	o__S085 sp ASV1262	Low	3.12	0.03	59.38
Bacteria	Topsoil	2022	o__S085 sp ASV235	Low	4.1	0.16	55.63
Bacteria	Topsoil	2023	o__Saccharimonadales sp ASV1269	Low	5.06	0.05	89.58

Annexes

Bacteria	Topsoil	2022	o__Saccharimonadales sp ASV370	High	5.21	0.12	78.13
Fungi	Topsoil	2023	o__Sebacinales sp ASV852	Low	3.78	0.13	60.42
Bacteria	Phyllosphere	2022	o__Solirubrobacterales sp ASV1163	Low	6.54	0.00	9.38
Bacteria	Topsoil	2023	o__Solirubrobacterales sp ASV523	Low	5.04	0.11	70.83
Bacteria	Topsoil	2023	o__Solirubrobacterales sp ASV656	Low	4.06	0.07	97.92
Bacteria	Topsoil	2023	o__Subgroup_7 sp ASV1382	High	3.43	0.00	16.67
Bacteria	Topsoil	2022	o__Subgroup_7 sp ASV461	Low	4.42	0.05	77.50
Fungi	Topsoil	2022	o__Tremellales sp ASV148	High	3.35	0.08	88.68
Bacteria	Phyllosphere	2022	o__Vicinamibacterales sp ASV2749	Low	4.96	0.00	15.63
Fungi	Topsoil	2023	o__Xylariales sp ASV486	Low	5.04	0.01	60.42
Fungi	Topsoil	2022	o__Xylariales sp ASV856	Low	3.46	0.02	59.75
Fungi	Topsoil	2023	o__Xylariales sp ASV856	Low	4.71	0.01	54.17
Bacteria	Topsoil	2022	c__Actinobacteria sp ASV1326	Low	4.83	0.03	16.25
Bacteria	Phyllosphere	2022	c__Actinobacteria sp ASV1326	Low	5.4	0.00	12.50
Bacteria	Topsoil	2022	c__Alphaproteobacteria sp ASV1271	High	6.49	0.01	24.38
Bacteria	Topsoil	2022	c__bacteriap25 sp ASV1698	Low	4.17	0.03	42.50
Bacteria	Phyllosphere	2022	c__bacteriap25 sp ASV1698	Low	6.16	0.00	15.00
Fungi	Phyllosphere	2022	c__Cystobasidiomycetes sp ASV443	Low	4.21	0.04	45.57
Fungi	Topsoil	2022	c__Dothideomycetes sp ASV462	Low	6.24	0.04	9.43
Fungi	Topsoil	2022	c__Eurotiomycetes sp ASV930	Low	6.53	0.06	9.43
Bacteria	Phyllosphere	2022	c__Gammaproteobacteria sp ASV950	Low	5.76	0.01	15.63
Fungi	Topsoil	2022	c__GS37 sp ASV714	Low	3.39	0.02	19.50
Bacteria	Topsoil	2022	c__JG30-KF-CM66 sp ASV1019	Low	5.07	0.03	73.75
Bacteria	Topsoil	2022	c__JG30-KF-CM66 sp ASV1064	Low	5.97	0.04	11.25
Bacteria	Topsoil	2022	c__JG30-KF-CM66 sp ASV1367	Low	4.11	0.01	82.50
Bacteria	Topsoil	2023	c__JG30-KF-CM66 sp ASV1367	Low	3.7	0.04	91.67
Bacteria	Phyllosphere	2022	c__KD4-96 sp ASV1043	Low	3.77	0.01	16.25
Bacteria	Topsoil	2022	c__KD4-96 sp ASV1823	Low	4.68	0.01	78.13
Bacteria	Phyllosphere	2022	c__KD4-96 sp ASV1823	Low	3.03	0.01	25.00
Bacteria	Phyllosphere	2022	c__KD4-96 sp ASV790	Low	3.25	0.01	34.38
Bacteria	Topsoil	2023	c__KD4-96 sp ASV790	High	6.58	0.05	100
Fungi	Topsoil	2022	c__Leotiomycetes sp ASV689	Low	4.38	0.03	20.13
Bacteria	Phyllosphere	2022	c__MB-A2-108 sp ASV285	Low	4.6	0.01	34.38
Bacteria	Topsoil	2022	c__MB-A2-108 sp ASV455	High	3.88	0.08	63.75
Bacteria	Topsoil	2022	c__MB-A2-108 sp ASV637	Low	3.37	0.02	63.75
Bacteria	Phyllosphere	2022	c__MB-A2-108 sp ASV637	Low	3.7	0.00	19.38
Bacteria	Topsoil	2022	c__MB-A2-108 sp ASV841	Low	3.65	0.07	22.50
Bacteria	Topsoil	2023	c__MB-A2-108 sp ASV841	High	4.56	0.00	16.67
Bacteria	Topsoil	2022	c__S0134_terrestrial_group sp ASV1040	High	2.86	0.05	80.63
Bacteria	Topsoil	2022	c__S0134_terrestrial_group sp ASV971	High	4.12	0.05	79.38
Fungi	Topsoil	2023	c__Sordariomycetes sp ASV321	High	4.35	0.07	79.17
Fungi	Topsoil	2022	c__Sordariomycetes sp ASV324	High	5.39	0.06	68.55
Fungi	Topsoil	2023	c__Sordariomycetes sp ASV324	High	4.01	0.04	83.33
Fungi	Topsoil	2022	c__Sordariomycetes sp ASV536	High	4.16	0.03	33.96
Bacteria	Topsoil	2022	c__Thermoleophilia sp ASV1020	Low	4.41	0.05	80.00
Bacteria	Phyllosphere	2022	c__Thermoleophilia sp ASV1020	Low	4.69	0.00	19.38

Annexes

Bacteria	Topsoil	2022	c__Thermoleophilia sp ASV1360	High	5.29	0.03	69.38
Bacteria	Topsoil	2022	c__Thermoleophilia sp ASV2111	High	5.4	0.03	38.13
Bacteria	Topsoil	2022	c__Thermoleophilia sp ASV582	High	3.87	0.02	56.25
Bacteria	Phyllosphere	2022	c__Thermoleophilia sp ASV955	Low	6.04	0.00	15.00
Bacteria	Topsoil	2022	c__TK10 sp ASV1016	Low	5.1	0.04	26.88
Bacteria	Phyllosphere	2022	c__TK10 sp ASV1016	Low	9.01	0.00	6.88
Bacteria	Topsoil	2023	c__TK10 sp ASV1037	High	3.92	0.02	16.67
Bacteria	Topsoil	2022	c__TK10 sp ASV1039	High	4.32	0.02	76.25
Bacteria	Topsoil	2023	c__TK10 sp ASV1055	High	5.64	0.02	81.25
Bacteria	Phyllosphere	2022	c__TK10 sp ASV1446	Low	5.65	0.00	14.38
Bacteria	Topsoil	2023	c__TK10 sp ASV1534	High	3.22	0.03	37.50
Bacteria	Topsoil	2022	c__TK10 sp ASV1744	High	3.73	0.02	67.50
Bacteria	Topsoil	2022	c__TK10 sp ASV191	High	3.46	0.18	58.13
Bacteria	Phyllosphere	2022	c__TK10 sp ASV254	Low	3.3	0.01	11.88
Bacteria	Topsoil	2022	c__TK10 sp ASV2631	Low	5.14	0.02	76.25
Bacteria	Phyllosphere	2022	c__TK10 sp ASV2631	Low	8.07	0.00	13.13
Bacteria	Topsoil	2022	c__TK10 sp ASV397	Low	3.19	0.06	76.88
Bacteria	Topsoil	2022	c__TK10 sp ASV401	Low	3.04	0.10	37.50
Bacteria	Topsoil	2022	c__TK10 sp ASV614	High	4	0.01	23.13
Bacteria	Phyllosphere	2022	c__TK10 sp ASV616	Low	7.02	0.01	18.75
Bacteria	Topsoil	2023	c__TK10 sp ASV616	Low	4.96	0.20	89.58
Bacteria	Phyllosphere	2022	c__TK10 sp ASV635	Low	4.58	0.01	20.00
Bacteria	Topsoil	2023	c__TK10 sp ASV657	High	4.03	0.03	33.33
Bacteria	Phyllosphere	2022	c__TK10 sp ASV667	Low	6.77	0.01	18.75
Bacteria	Topsoil	2022	c__TK10 sp ASV789	High	3.7	0.10	57.50
Bacteria	Phyllosphere	2022	c__TK10 sp ASV789	High	6.6	0.00	8.13
Bacteria	Topsoil	2022	c__TK10 sp ASV963	High	2.95	0.05	46.25
Bacteria	Topsoil	2022	p__Armatimonadota sp ASV2796	Low	3.19	0.03	66.88
Fungi	Topsoil	2022	p__Ascomycota sp ASV176	High	5.16	0.07	74.84
Fungi	Topsoil	2022	p__Ascomycota sp ASV606	High	6.05	0.02	20.13
Fungi	Topsoil	2022	p__Ascomycota sp ASV954	High	4.7	0.02	49.69
Fungi	Topsoil	2023	p__Ascomycota sp ASV954	High	5.72	0.02	47.92
Bacteria	Topsoil	2022	p__Chloroflexi sp ASV1282	Low	3.15	0.02	31.88
Bacteria	Topsoil	2022	p__Chloroflexi sp ASV640	Low	3.79	0.07	31.88
Bacteria	Phyllosphere	2022	p__Chloroflexi sp ASV640	Low	5.49	0.01	13.13
Bacteria	Topsoil	2022	p__Chloroflexi sp ASV672	Low	4.15	0.09	76.88
Bacteria	Phyllosphere	2022	p__Chloroflexi sp ASV672	Low	6.09	0.00	8.75
Bacteria	Topsoil	2022	p__Chloroflexi sp ASV715	Low	4.14	0.07	60.63
Bacteria	Topsoil	2022	p__RCP2-54 sp ASV1458	Low	3.33	0.03	77.50
Bacteria	Phyllosphere	2022	p__RCP2-54 sp ASV348	Low	5.74	0.01	38.13

Titre : Vers une viticulture sans pesticide: analyse du microbiome de la vigne et des sols viticoles pour développer le biocontrôle microbien du mildiou

Résumé : Les vignes et les sols viticoles hébergent une grande diversité de micro-organismes, qui forment collectivement le microbiote. Certains micro-organismes sont des agents pathogènes, comme l'oomycète *Plasmopara viticola*, responsable du mildiou. D'autres, tels que les promoteurs de croissance et les antagonistes des pathogènes, ont une influence positive sur la santé de la vigne. Ces interactions plante-microbe et microbe-microbe ont fait l'objet d'une attention accrue ces dernières années car leur compréhension pourrait constituer une piste pour sortir des pesticides. Le programme de recherche VITAE (2020-26) combine plusieurs approches de gestion innovantes pour réduire l'utilisation des fongicides en viticulture. L'une de ces approches est la gestion du microbiote de la vigne et des sols viticoles pour contrôler les maladies foliaires, dont le mildiou. L'objectif de cette thèse est d'identifier des micro-organismes, qu'il s'agisse de bactéries ou de champignons, susceptibles de contribuer au biocontrôle du mildiou. Le premier chapitre est une synthèse bibliographique sur la dynamique des interactions entre la vigne et son microbiote, au cours de l'histoire évolutive et au cours de la vie de la plante. Le deuxième chapitre compare le microbiote de tissus foliaires asymptomatiques avec le microbiote associé aux lésions du mildiou. Il montre que les lésions du mildiou hébergent des levures basidiomycètes (*Sporobolomyces patagonicus*, *S. roseus*, *Cryptococcus laurentii* et *Udeniomyces pyricola*) et des bactéries (*Bacillales*, *Streptomycetales*), la plupart connues pour leurs propriétés de biocontrôle. En revanche, les tissus foliaires asymptomatiques sont plutôt associés à d'autres agents pathogènes aériens (oïdium, botrytis). Ces résultats suggèrent que la feuille recrute localement certains taxons microbiens ayant une activité de biocontrôle lors de l'infection par le mildiou. Le troisième chapitre analyse le microbiote foliaire et le microbiote du sol superficiel dans des parcelles choisies en fonction de relevés épidémiologiques. Il montre que certains taxons microbiens fongiques (par exemple, *Buckleyzyma aurantiaca*, *Bullera alba*, *Trichoderma virens* et *Trichoderma hamatum*) et bactériens (par exemple, les genres *Streptomyces* et *Bacillus*) sont systématiquement plus abondants dans les parcelles historiquement moins sensibles au mildiou. Ces taxons sont nombreux dans la couche superficielle du sol, où les oospores (forme dormante du pathogène) passent l'hiver, et ils sont présents dans la phyllosphère, où les zoospores (spores biflagellées, forme responsable de l'infection) infectent les feuilles. En revanche, l'endosphère foliaire, où se développe le mycélium du pathogène, contient peu de taxons microbiens liés aux données épidémiologiques. Ce troisième chapitre montre aussi que la composition du microbiote du sol superficiel permet de prédire la sensibilité d'une parcelle au mildiou. Le quatrième chapitre explore le rôle du microbiote foliaire dans la résistance au mildiou de deux espèces de vigne américaines (*Vitis aestivalis* et *V. labrusca*). Ce chapitre s'appuie sur une campagne d'échantillonnage menée sur la côte est des États-Unis. Les données sont en cours d'analyse. En conclusion, la thèse a révélé l'existence de consortia microbiens naturellement présents dans les vignobles, qui constituent des candidats prometteurs pour le biocontrôle du mildiou. Ces micro-organismes sont présents dans la phyllosphère et dans le sol superficiel en début de saison végétative et semblent ensuite augmenter en abondance dans les lésions de la maladie. Les perspectives majeures sont : (i) l'isolement des candidats microbiens et l'évaluation expérimentale de leur activité de biocontrôle, seuls ou combinés en communautés synthétiques, (ii) l'identification des pratiques agronomiques favorisant les consortia microbiens identifiés et (iii) le développement d'outils de prédiction de la sensibilité au mildiou basés sur le microbiote.

Mots-clés : Microbiome, écologie microbienne, agroécologie, biocontrôle, métagénomique environnementale, vigne

---

Title: Towards pesticide-free viticulture: analysing the microbiome of grapevines and vineyard soils to develop microbial biocontrol of downy mildew

Abstract: Grapevines and viticultural soils host a great diversity of microorganisms that collectively form the microbiota. Some microorganisms are pathogens, such as the oomycete *Plasmopara viticola*, which causes downy mildew. Others, such as growth promoters and pathogen antagonists, are beneficial to grapevine health. These plant-microbe and microbe-microbe interactions have received increased attention in recent years because understanding them could provide a way to reduce the use of pesticides. The VITAE research programme (2020-26) combines several innovative management approaches to reduce fungicide use in viticulture. One of these approaches is the management of vine microbiota and vineyard soils to control foliar diseases, including downy mildew. The aim of this thesis is to identify microorganisms, whether bacteria or fungi, that may contribute to the biocontrol of downy mildew. The first chapter is a literature review on the dynamics of interactions between the vine and its microbiota throughout the evolutionary history and life of the plant. The second chapter compares the microbiota of asymptomatic leaf tissues with the microbiota associated with downy mildew lesions. It shows that downy mildew lesions harbor basidiomycete yeasts (*Sporobolomyces patagonicus*, *S. roseus*, *Cryptococcus laurentii*, and *Udeniomyces pyricola*) and bacteria (*Bacillales*, *Streptomycetales*), most of which are known for their biocontrol properties. In contrast, asymptomatic leaf tissues are more associated with other aerial pathogens (powdery mildew, Botrytis). These results suggest that the leaf locally recruits certain microbial taxa with biocontrol activity during downy mildew infection. The third chapter analyses the leaf and surface soil microbiota in plots selected on the basis of epidemiological surveys. It shows that certain fungal microbial taxa (for example, *Buckleyzyma aurantiaca*, *Bullera alba*, *Trichoderma virens*, and *Trichoderma hamatum*) and bacterial taxa (for example, the genera *Streptomyces* and *Bacillus*) are systematically more abundant in historically less downy mildew-susceptible plots. These taxa are abundant in the soil surface layer, where the oospores (the dormant form of the pathogen) overwinter, and in the phyllosphere, where the zoospores (flagellated spores, the form responsible for infection) infect the leaves. In contrast, the leaf endosphere, where the pathogen's mycelium develops, contains few microbial taxa linked to epidemiological data. This third chapter also shows that the composition of the surface soil microbiota allows for the prediction of a plot's susceptibility to downy mildew. The fourth chapter examines the role of leaf microbiota in downy mildew resistance of two American grapevine species (*Vitis aestivalis* and *V. labrusca*). This chapter is based on a sampling campaign carried out on the east coast of the United States. The data are currently being analysed. In conclusion, the thesis revealed the existence of microbial consortia naturally present in vineyards, which are promising candidates for the biocontrol of downy mildew. These microorganisms are present in the phyllosphere and in the surface soil at the beginning of the growing season and then seem to increase in abundance in the disease lesions. The main perspectives are: (i) the isolation of microbial candidates and the experimental evaluation of their biocontrol activity, either alone or combined in synthetic communities, (ii) the identification of agronomic practices that favour the identified microbial consortia, and (iii) the development of microbiota-based predictive tools for downy mildew susceptibility.

Keywords: Microbiome, microbial ecology, agroecology, biocontrol, environmental metagenomics, grapevine

---

Unité de recherche: UMR Santé et Agroécologie du Vignoble (SAVE) 1065, INRAE Bordeaux-Aquitaine, 71 Avenue Edouard Bourlaux, 33882 Villenave d'Ornon, France